FINAL REPORT Date: March 2019

Contract Title:

Development of a Test Method for Assessing the Performance of Vehicular Traffic Signal Assemblies during Hurricane Force Winds

Contract No.: BDV29 977-20

FINAL REPORT BDV29 977-20

SUBMITTED TO:

Florida Department of Transportation Research Center

Project Manager: Jeff Morgan

SUBMITTED BY:

Wall of Wind Research Facility

International Hurricane Research Center

Florida International University

Principal Investigator: Ioannis Zisis, Ph.D.

Co-Principal Investigator: Peter Irwin, Ph.D.

Arindam Chowdhury, Ph.D.

Atorod Azizinamini, Ph.D.

Graduate Research Assistant: Manuel Matus, M.S

Benito A. Berlanga, P.E.

Ziad Azzi, EIT

Johnny Estephan, M.S.

Disclaimer

The opinions, findings, and conclusions expressed in this publication are those of the authors and not necessarily those of the State of Florida Department of Transportation.

Metric Conversion Table

Symbol	*When You Know*	*Multiply by*	*To Find*	*Symbol*
Length				
in	inches	25.4	millimeters	mm
ft.	feet	0.305	meters	m
Area				
in^2	square inches	645.2	square millimeters	mm^2
$ft.^2$	square feet	0.093	square meters	m^2
Force				
lbf	pound-force	4.45	Newton	N

Technical Report Documentation Page

1. Report No. BDV29 TWO 977-20	2. Government Accession No.	3. Recipient's Catalog No.
4. Title and Subtitle Development of a Test Method for Assessing the Performance of Vehicular Traffic Signal Assemblies During Hurricane Force Winds		5. Revised Report Date March 2019 6. Performing Organization Code
7. Author(s) I. Zisis, P. Irwin, A. Chowdhury and A. Azizinamini		8. Performing Organization Report No.
9. Performing Organization Name and Address Florida International University Department of Civil & Environmental Engineering 10555 W. Flagler Street Miami, Florida 33174		10. Work Unit No. (TRAIS) 11. Contract or Grant No. BDV29 TWO 977-20
12. Sponsoring Agency Name and Address Florida Department of Transportation 605 Suwannee Street, MS 30 Tallahassee, FL 32399		13. Type of Report and Period Covered Final Report Nov. 2014 – March 2019 14. Sponsoring Agency Code
15. Supplementary Notes		

16. Abstract

The performance of span-wire mounted traffic signals during past hurricane seasons indicated to FDOT the need to explore new methods to improve traffic signal assembly survivability during hurricane force winds. FDOT and FIU embarked on a collaborative research program to study the performance of span-wire traffic signal systems subjected to extreme winds with the goal to enhance their resiliency and survivability and potentially find a methodology that could be utilized to certify the different products used in span-wire traffic signal assemblies.

The tasks under this research project included full and model scale testing, numerical simulation studies, development of a test methodology that could be used for certifying vehicular traffic signal assemblies, identification of potential active and passive mitigation measures and investigation of the feasibility of designing/building a mechanical or wind-based test apparatus that could be operated by FDOT to verify compliance with future test standards.

The execution of the different tasks generated a plethora of experimentally and numerically derived outcomes. The findings from the current research project are of great value and significance since it was the first time that these systems were tested at full-scale in a controlled and realistic environment. The aerodynamic instability that has been observed in the field was identified and quantified for the very first time in a laboratory setting. Numerous recommendations have been generated following the findings of this research that will assist FDOT to enhance the survivability of span-wire traffic signals during extreme wind events.

17. Key Word traffic signal, cable support, wind, cable systems, signal supports, hangers, hurricanes, wind resistant design	18. Distribution Statement No restrictions		
19. Security Classif. (of this report) Unclassified	20. Security Classif. (of this page) Unclassified	21. No. of Pages	22. Price

Acknowledgements

The authors would like to thank the Florida Department of Transportation (FDOT) for providing the funds for this project. The FDOT State Traffic Engineering and Operations Office, Traffic Engineering Research Lab assisted in acquiring the necessary traffic signal assemblies and components for full-scale tests and organized the donation of necessary equipment from various traffic hardware manufacturers. We thank the manufacturers that sent the donated equipment and took the time to attend test days. The authors also thank Horsepower Electric Inc. electrical contractors for their unlimited support by providing experienced teams for the installation of traffic signals and changing equipment between tests. Their hard work and patience is greatly appreciated. Finally, thanks are given to all of our fellow researchers and technical team at the Wall of Wind Research Facility who gave their time to this project to ensure the installation of various instrumentations and assure they worked smoothly.

Executive Summary

The performance of span-wire mounted traffic signals during past hurricane seasons indicated to FDOT the need to explore new methods to improve traffic signal assembly survivability during hurricane force winds. Prior research determined that to further improve the safety of signalized intersections during and after hurricane conditions and to reduce the cost of damage to the State's traffic control infrastructure, serviceability of the traffic signal assembly required additional research. FDOT and FIU embarked on a collaborative research program to study the performance of span-wire traffic signal systems subjected to extreme winds with the goal to enhance their resiliency and survivability and potentially find a methodology that could be utilized to certify the different products used in span-wire traffic signal assemblies.

The tasks of this research project included: Task 1 - Determine the nature of wind loading and system response of wire supported traffic signal assemblies for winds up to 150 MPH. This was achieved through full and model scale testing as well as by conducting numerical studies to better comprehend the problem; Task 2 - Develop a test methodology that could be used for certifying vehicular traffic signal assemblies with different attachment and/or reinforcement configurations. This was achieved utilizing the findings from Task 1 and by carrying out a detailed parametric study to evaluate several installation parameters on the overall performance of the system; Task 3 - Explore improvements to existing designs that will help mitigate wind response and enhance survivability and serviceability of wire supported traffic signal systems; and Task 4 - Investigate the feasibility of designing/building a mechanical or wind based test apparatus that would simulate the wind action experienced during this research and that could be operated by FDOT to verify compliance with future test standards.

The execution of the different tasks generated a plethora of experimentally and numerically derived outcomes. Among others, the full- and small-scale tests revealed that depending on the rigidity of the hanger, the traffic signal assembly is more susceptible to aerodynamic instabilities in the form of galloping. Flexible hangers have a tendency to undergo higher along-wind inclinations at lower wind speeds which appeared to trigger this instability at lower wind speeds (about 70 mph) than a rigid hanger, while for the rigid hanger the instability appears when the extension bars severely bend (about 110 mph). The 5-section signal has been found to be

susceptible to damage regardless of the type of hanger used. This may be due to its increased weight as well as the increased surface area compared to the 3-section signal. It is recommended to find an alternative to replace usage of 5-section signal. A common failure observed was with the 72-tooth serrated edge connection between the adjustable-hanger and the disconnect-box and also between the disconnect-box to signal-housing point. The failure mode with this connection point was when the serrated edge would shear, allowing the connection to turn. A resilient connection at these points should be considered to enhance the survivability of the signal under wind induced loads. Moreover, it was determined that Florida DOT specified aluminum alloy 535 should be continued due to its outstanding performance during testing and maximum overlap at tri-stud adjustable-hanger and extension-bar connection points should be used (top and bottom portions/connections).

The full-scale mitigation tests showed that when a fin was installed at the back of the signal housing, the bending of the extension bar was considerably lower than other cases, thus avoiding the appearance of aerodynamic instabilities due to the lower inclinations induced on the traffic signals. This mitigation device is ideal since it contains neither movable nor mechanical parts and the retrofitting of this device is relatively easy. Finally, the feasibility study concluded that a mechanical test rig is achievable if the blow back angle does not exceed about 60 degrees, whereas replication of the aerodynamic instabilities (i.e. galloping and/or flutter) in a purely mechanical rig will not be feasible.

The above findings are of great value and significance since it was the first time that these systems were tested at full-scale in a controlled and realistic environment. The aerodynamic instability that has been observed in the field was identified and quantified for the very first time in a laboratory setting. Numerous recommendations have been generated following the findings of this research that will assist FDOT to enhance the survivability of span-wire traffic lights during extreme wind events.

Table of Content

List of Figures

List of Tables

Chapter 1 - Introduction

The extensive vehicular traffic signal damage during past hurricane seasons has compelled FDOT to investigate new methods to improve vehicular traffic signal assembly survivability during hurricane force winds. Prior research performed in this area determined that to further improve the safety of signalized intersections during hurricane conditions and to reduce the cost associated with damage to the State's intersection traffic control infrastructure, serviceability of vehicular traffic signal assemblies should be investigated. In this case, serviceability is defined as ensuring the signal assembly (from catenary wire to bottom of signal) is capable of withstanding hurricane level wind speeds without structural damage that would prevent the signal from functioning properly and remaining properly aligned with approaching motorists as originally installed.

The tasks involved and discussed in this report are as follows:

Task 1 (Chapters 2-13): Determine the nature of wind loading and system response of wire supported traffic signal assemblies for winds up to 150 MPH. This was achieved through full and model scale testing in the Wall of Wind (WOW) Research Facility at Florida International University (FIU) as well as by conducting numerical studies to better comprehend the problem.

Task 2 (Chapter 14): Develop test methodology that could be used for certifying vehicular traffic signal assemblies with different attachment and/or reinforcement configurations. This was achieved utilizing the findings from Task 1 and by carrying out a detailed parametric study to evaluate several installation parameters on the overall performance of the system.

Task 3 (Chapter 15): Explore improvements to existing designs that will help mitigate wind response and enhance survivability and serviceability of wire supported traffic signal systems.

Task 4 (Chapter 16): Investigate the feasibility of designing/building a mechanical or wind based test apparatus that would simulate the wind action experienced during this research and that could be operated by FDOT to verify compliance with future test standards.

1.1. Test Setup for Task 1a to Task 3

Traffic signals to be tested were installed on a special test rig with a span of 21 ft 11 in. The test rig was designed using SAP2000 finite element based structural analysis and design software and drafted on AutoCAD 2014. There were two different hollow structural sections (HSS) that were utilized, HSS 10" x 6"x 3/8" and HSS 6" x 6" x 3/8". The total length of the test rig is 24 ft and the width is 7 ft and 6 in. The two support columns are 15 ft 6 in tall supported on top of HSS 10" x 6" x 3" sections. Total weight of the test rig is approximately 4,100 Ibs. A plan view of the test rig is shown in Figure 1, a profile elevation view is shown in Figure 2, and an end elevation view is shown in Figure 3. *For Case 10 of Task 1a, Task 2 and Task 3, the same short-span test rig (described above) was reinforced with an I-beam at the top of the two columns (see Figure 4 to Figure 6).*

The natural frequency for this full-scale system of signals for horizontal motions normal to the plane of the wires was determined to be approximately 0.5 cycles per second in zero wind. The natural frequency was determined through measurements and agreed with estimates based on small deflection theory. The system was also modeled on SAP2000 finite element software to determine its natural frequency.

A ½-inch diameter catenary cable was connected to an eyebolt on either end of the test rig span. The eyebolt was welded to the top plate of the loadcell which was attached to the test rig column. The center of the circular loadcell was located 6 in from the top of the column.

The catenary cable was configured to represent 5% sag in the field, per FDOT Standard Specifications for Road and Bridge Construction, Section 634. Therefore, for a typical 80-foot span in the field the sag length is 4 ft. The test rig is approximately ¼ of the typical 80 ft span. Therefore, four times the sag ratio was required for the catenary wire used on the test rig to maintain the same lateral stiffness, which resulted in a sag length of 4 ft in the rig.

Initially a ½-inch diameter messenger cable was also connected to an eyebolt on either end of the test rig span but due to elevated tension and stiffness it was decided to replace the ½-inch diameter cable with a 3/8-inch diameter cable. The eyebolt was also welded to the top plate of the loadcell which was attached to the test rig column. The center of the circular loadcell at either end of the messenger cable was located approximately 7 ft below the top catenary loadcells. The

messenger cable was tensioned to approximately 140 Ibs (unless specified differently in the test-setup section of each chapter). Per FDOT Standard Specifications for Road and Bridge Construction, Section 634, ½ inch diameter messenger wires are to be installed with wire tension of 645 Ibs/100 ft, linearly prorating cable tensions for other lengths. Following initial trials, the loadcells that were connected to the messenger cable were indicating high tensions when wind was applied. To lessen the tension readings on the loadcells a decision was made to replace the ½ inch diameter messenger cable with a 3/8-inch diameter cable instead. The initial tension placed on this cable was approximately 75 Ibs. Note that after observing the high tensions generated in the messenger wire it was realized that the extensibility of the wires needed to be exaggerated in the relatively short span of the test rig, 21.9 ft., so as to replicate extension effects in typical field spans, 50 ft. to 180 ft. or more. Appendix A describes the rationale for use of springs in the test rig. The length between the catenary and messenger cables at the lowest point of the catenary cable where the hanger assemblies were installed was approximately 3 ft.

1.2. Instrumentation for Task 1 to Task 2

The instruments used during testing included four 6-degree of freedom loadcells that measured x, y, z, force and moment components at the ends of the catenary and messenger cables. The loadcells had 1500 Ibs capacity. Picture of the loadcell is shown in Figure 7. Tri-axial accelerometers were installed in the traffic signals to measure rms of accelerations. Inclinometers were also installed on each signal to measure the inclination of the signals during wind exposure. The inclinometers measured inclination in two directions, one relative to an axis parallel to the wind direction and another relative to an axis perpendicular to the wind direction. The location of the loadcells, accelerometers and inclinometer may vary from case to case and thus they are shown in each case under the Instrumentation section.

Failure was considered when a component of the assembly failed causing the signal assembly to stop functioning properly: for example, the signal did not remain powered and/or properly aligned with approaching motorists as originally installed. Any breach of the housing, any damage to the hanger assembly or if catenary or messenger wires ruptured, any damage to visors where

LED signals cannot be seen was also considered a failure. Damage to back plates was not considered a failure.

All tests took place at Florida International University Wall of Wind Research Facility. This facility is comprised of a series of 12 fans able to produce winds in excess of 150 mph. The facility includes a 16 ft. 6 in. diameter turntable which allows the test structure to be rotated to different angles of exposure to the wind field.

For the reader's convenience, the different parts used in the span-wire traffic assembly are identified in Figure 8.

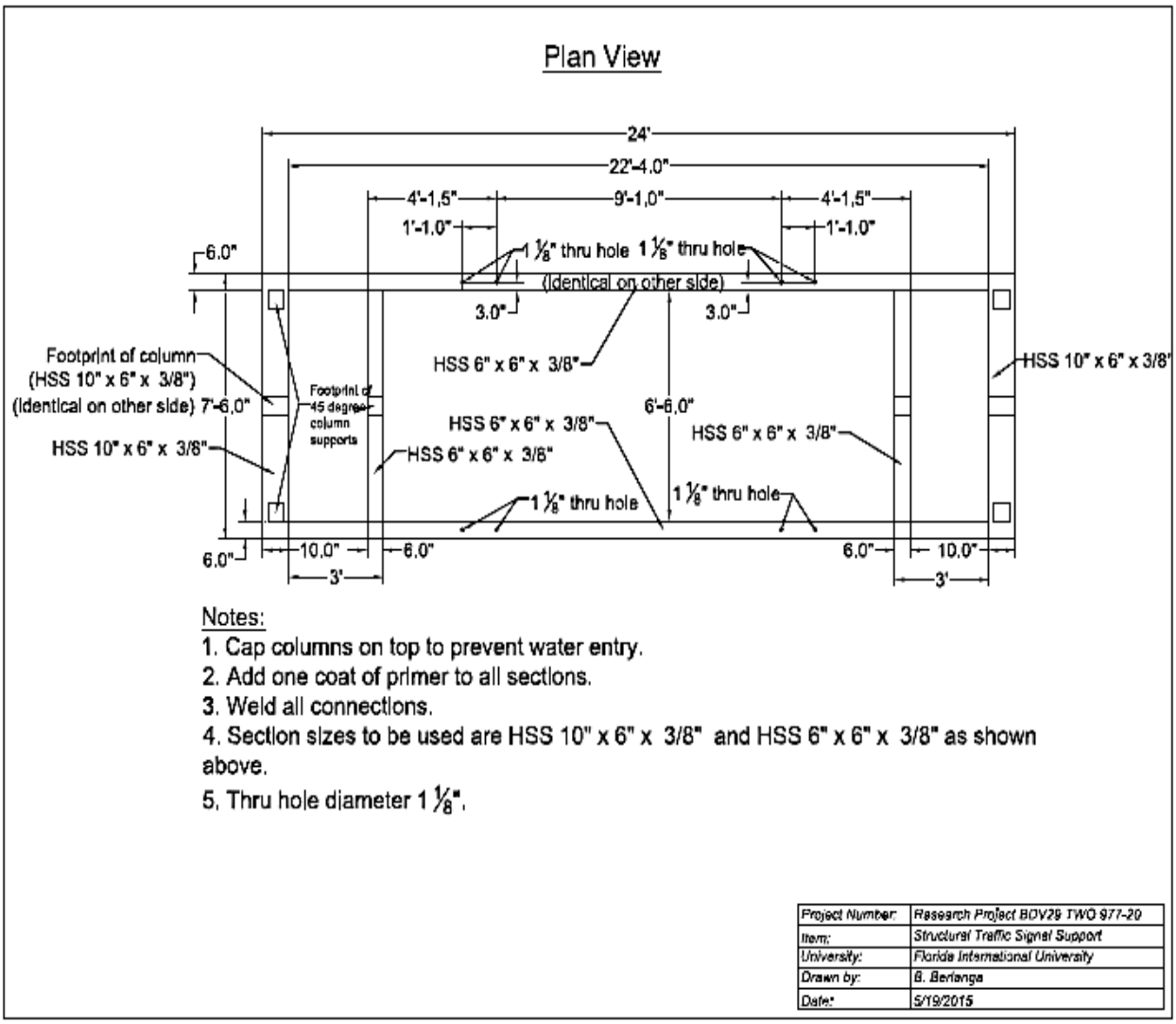

Figure 1: Plan view of test rig

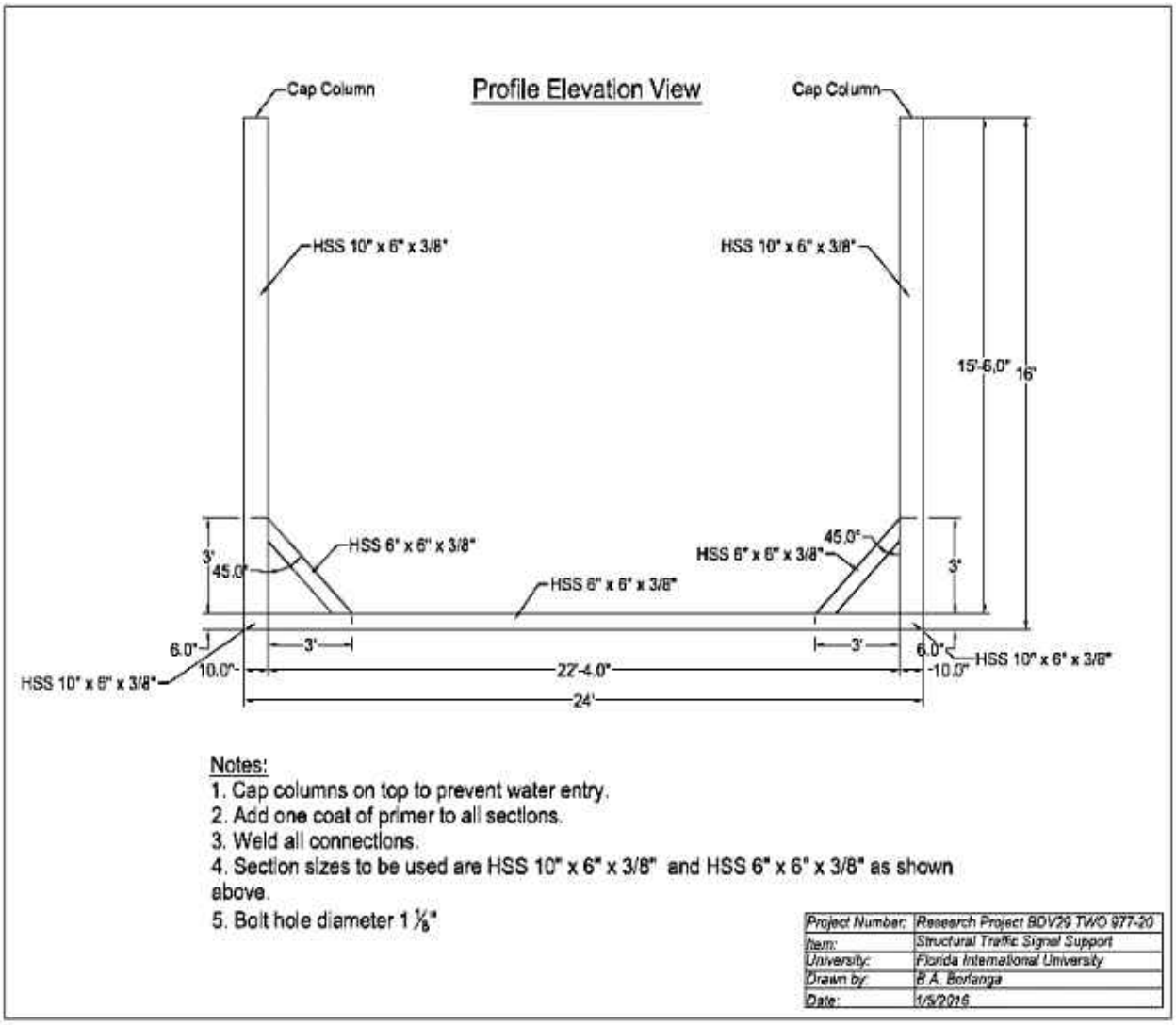

Figure 2: Profile Elevation View of test rig

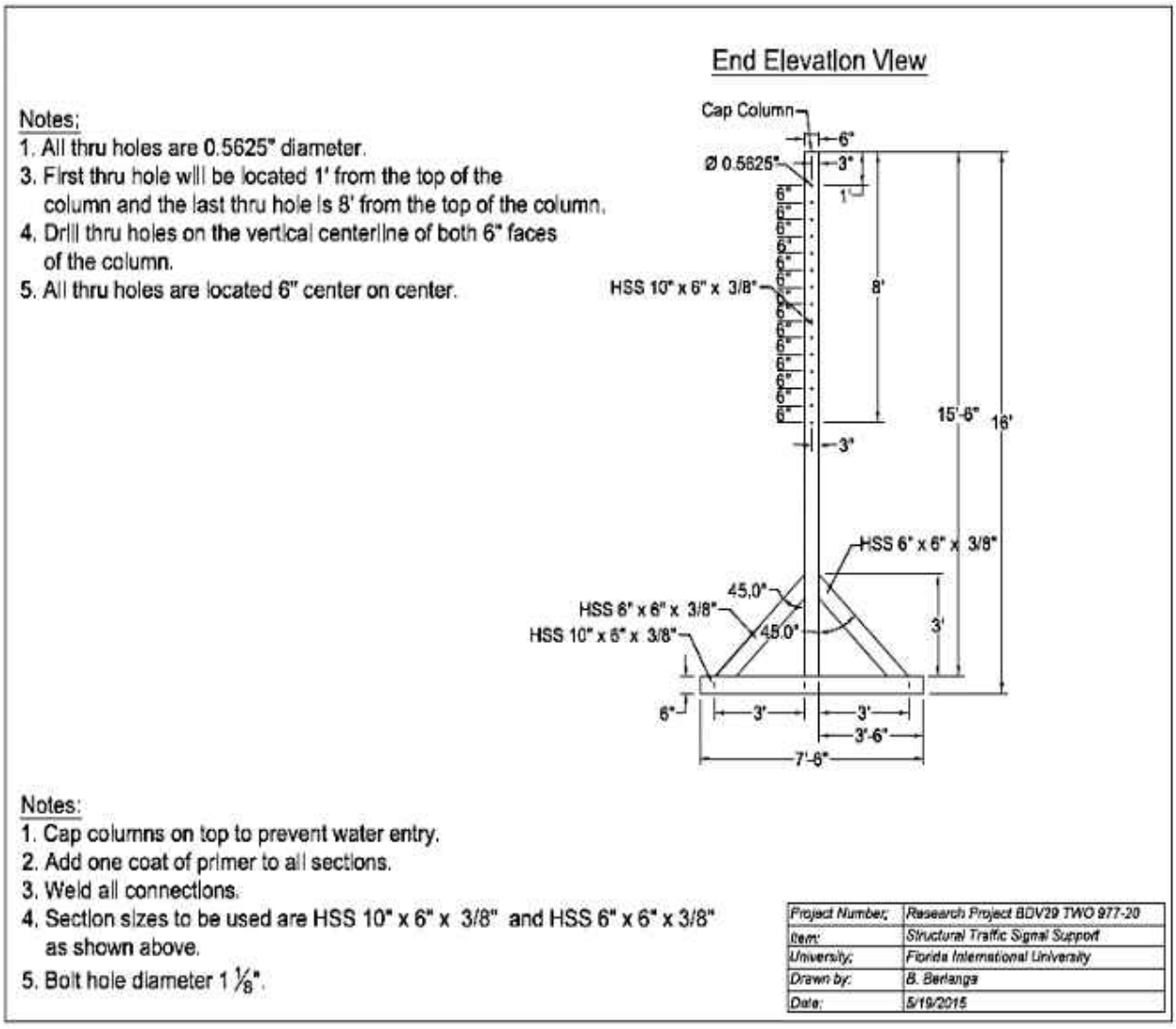

Figure 3: End Elevation of View of test rig

Plan View

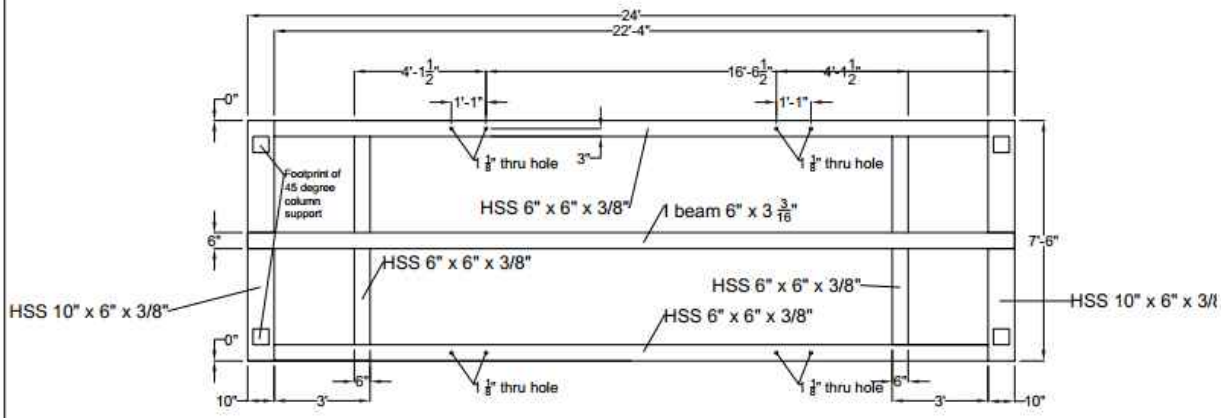

Item:	Structural Traffic Signal Support
University:	Florida International University
Drawn by:	B. Berlanga
Updated by:	M. Matus
Date:	3/9/2018

Notes:

1. Cap columns on top to prevent water entry
2. Add one coat of primer to all sections
3. Weld all connections
4. Section sizes to be used are HSS 10" x 6" x 3/8" and HSS 6" x 6" x 3/8" as shown above
5. Thru hole diameter 1 1/8"
6. I beam on top of columns for reinforcement

Figure 4: Plan view of reinforced test rig

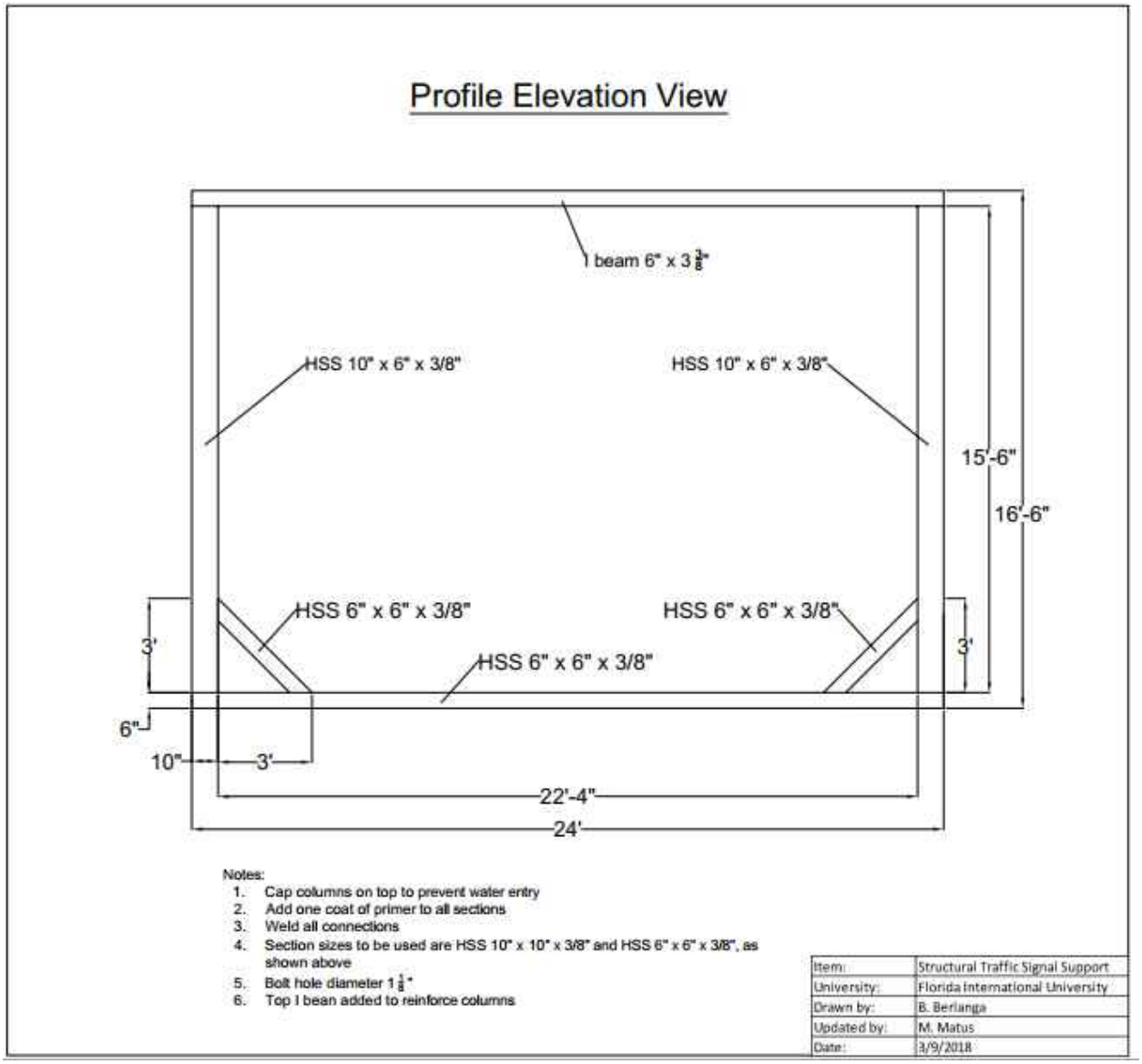

Figure 5: Profile elevation view of reinforced test rig

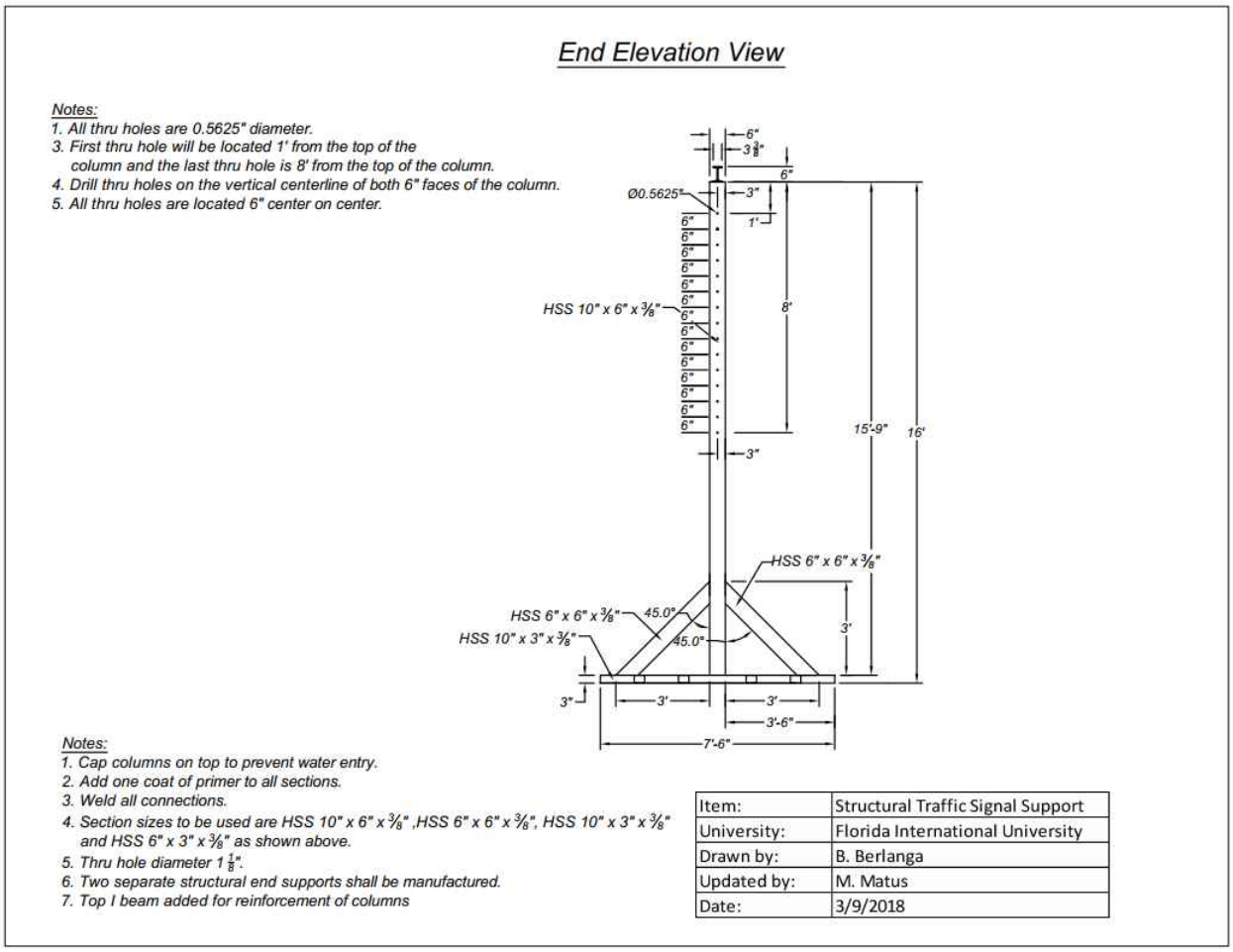

Figure 6: End elevation view of reinforced test rig

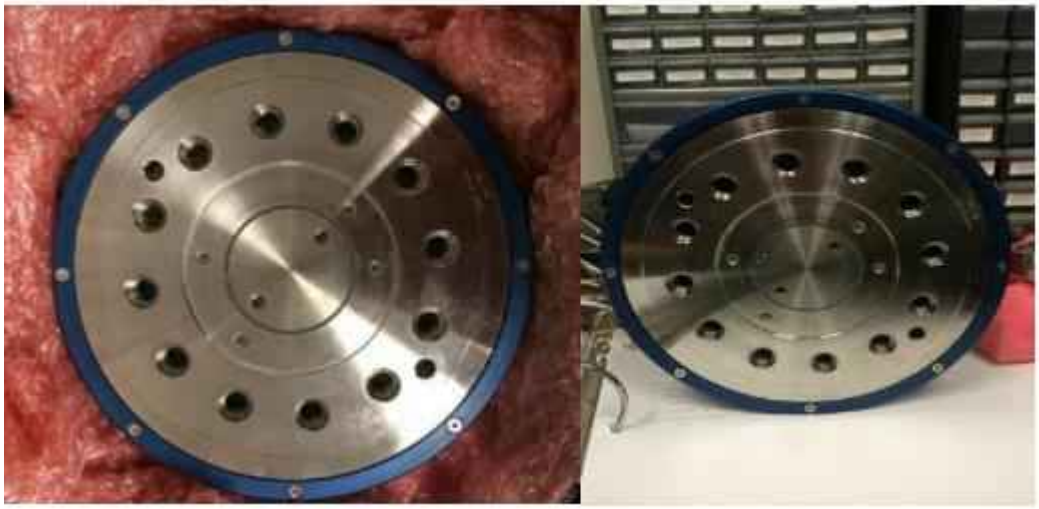

Figure 7: Picture of -degree of freedom loadcells

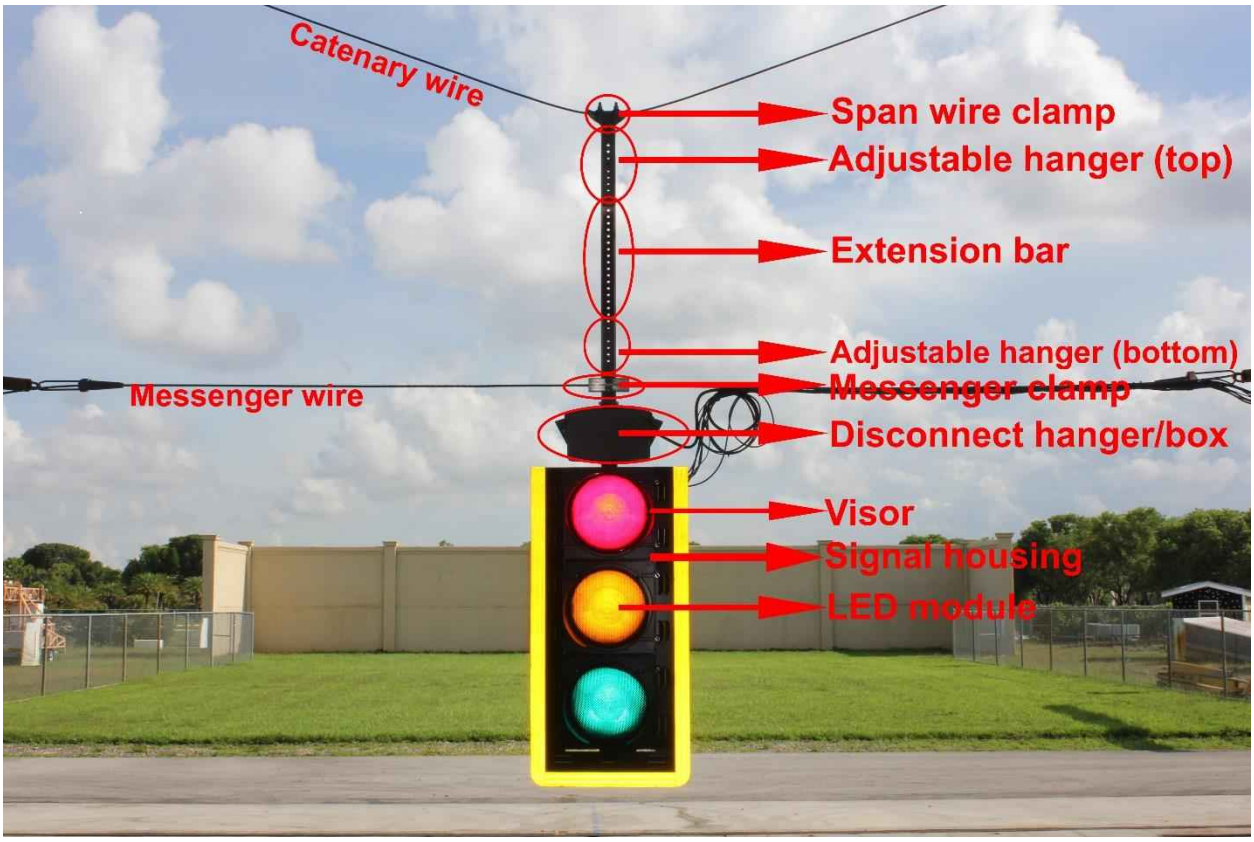

Figure 8: Span-wire traffic signal assembly components

Chapter 2 - Task 1a: FULL SCALE TESTING - Case 1

2.1. Introduction

The main objective of the tests discussed in this chapter was to determine a base condition configuration to utilize for future hanger assembly tests. Two configurations were evaluated. The first configuration (case 1) tested included one aluminum 5-section and one aluminum 3-section traffic signal. The second configuration (case 2) tested included one aluminum 4-section and two aluminum 3-section traffic signals. Both configurations utilized standard tri-stud adjustable hangers. The more vulnerable of the two will be considered the "**base condition"** scenario and will be used for testing the remaining signal hangers. In this chapter, results from case 1 are presented in detail. The results showed that there were higher messenger cable tensions and rotations in this configuration. Subsequently, FDOT requested to add a second 3-section signal to the base condition scenario.

2.2. Methodology

2.2.1. Test Setup

Case 1 consisted of one 3-section vertical and one 5-section traffic signal. Both signals were placed with a 5 ft center to center separation at approximately mid span of the test rig. There was a distance of approximately 8 ft 6 in from the outside edge of the 3-section signal to the front face of the steel column as shown in the sketch of the first signal combination setup, Figure 9 . The bottom of all signals for case 1 was at approximately 4 ft 6 in above the concrete floor. A picture of the test rig is shown in Figure 10.

All the signals were made of aluminum and included louvered back plates and visors. Standard tri-stud adjustable hangers were used for both signal combinations.

Case 1 was only tested at 0° direction for all speeds. This direction corresponds to the front face of the signals facing the approaching wind. Traffic signals for case 1 were planned to be exposed to wind speeds starting at 10 mph followed by 20 mph, 70 mph, 100 mph, 130 mph and

maximum or until failure of one of the traffic signal assemblies as shown in test protocol, Table 1. The components used for each test, with the respective manufacturers, is shown in Table 2.

2.2.2.Instrumentation

The directions of the x, y and z components for each loadcell are shown in Figure 11. Loadcells number 2 and 5 were located at either end of the messenger cable and loadcells number 1 and 4 located at either end of the catenary cable.

There was one accelerometer placed on the center top of the signal, Accel5, another placed on the bottom right side, Accel002, and a third placed on the bottom left side, Accel003 for the 5-section signal as shown in Figure 12. Accelerometer Accel007, was installed on the top center, accelerometer Accel004, was installed on the bottom left side and accelerometer Accel006, was installed on the bottom right side of the 3-section signal as shown in Figure 13.

There was one inclinometer installed on the top center of the signal, Inc4, and another on the bottom center of the signal, Inc3, for the 5-section signal as shown in Figure 12. Inclinometer, Inc2, was installed on the top center and inclinometer, Inc1, was installed on the bottom center of the of the 3-section signal as shown Figure 13.

Wind speeds in three component directions (u,v,w) were also recorded by the Wall of Wind sensors.

2.2.3.Test Method

Both of the tested signal combinations utilized standard tri-stud adjustable hangers. The purpose was to determine the more vulnerable of the two combinations to be used for future tests. The more vulnerable was determined to be the signal combination that sustained the most damage and failed the earliest.

Table 1: Test protocol (Task 1a: Case 1)

Signal Combination 1 and 2			
Wind Speed (mph)	**Direction**	**Duration (min)**	**Total Duration (min)**
10	0	1	2
Adj.		2	4
20	0	1	6
Adj.		2	8
40	0	1	10
Adj.		2	12
70	0	1	14
Adj.		2	16
100	0	1	18
Adj.		2	20
130	0	1	22
Adj.		2	24
Max	0	1	26
TOTAL			**26**

Table 2: Signal assembly components and manufacturers (Task 1a: Case 1)

Component	**Manufacturer**
Span wire clamp	Pelco
Adjustable hanger	Pelco
Extension bar	Pelco
Messenger clamp	Pelco
Disconnect Hanger	Pelco
Signal Assembly	McCain
Backplate	TCS
Visor	McCain
LED Modules	GE - Dialight - Duralight

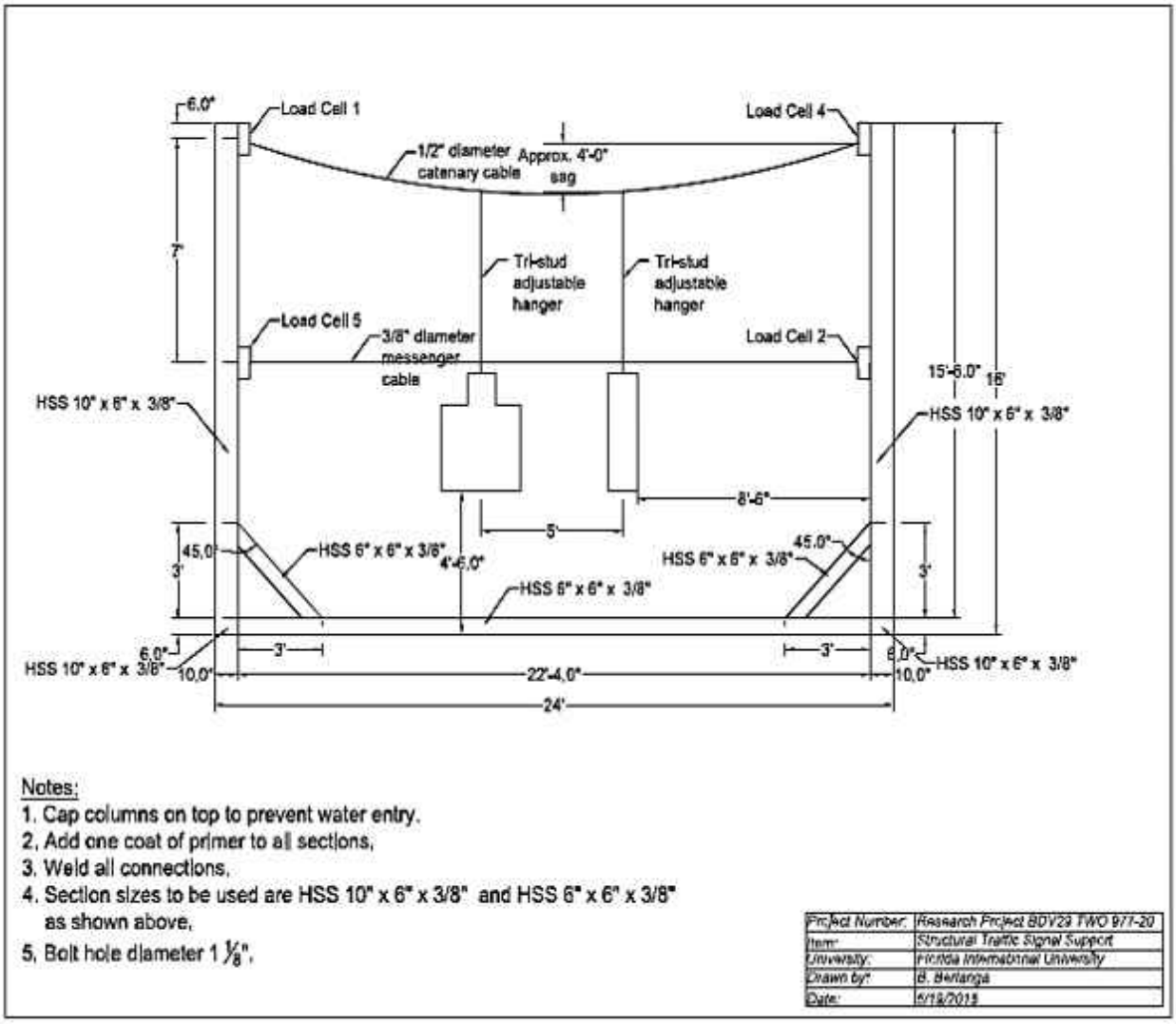

Notes:

1. Cap columns on top to prevent water entry.
2. Add one coat of primer to all sections.
3. Weld all connections.
4. Section sizes to be used are HSS 10" x 6" x 3/8" and HSS 6" x 6" x 3/8" as shown above.
5. Bolt hole diameter 1 1/8".

Project Number:	Research Project BDV23 TWO 977-20
Item:	Structural Traffic Signal Support
University:	Florida International University
Drawn by:	B. Berlanga
Date:	5/15/2015

Figure 9: First signal combination setup of one 3-section and one 5-section (case 1)

Figure 10: Picture of test rig frame

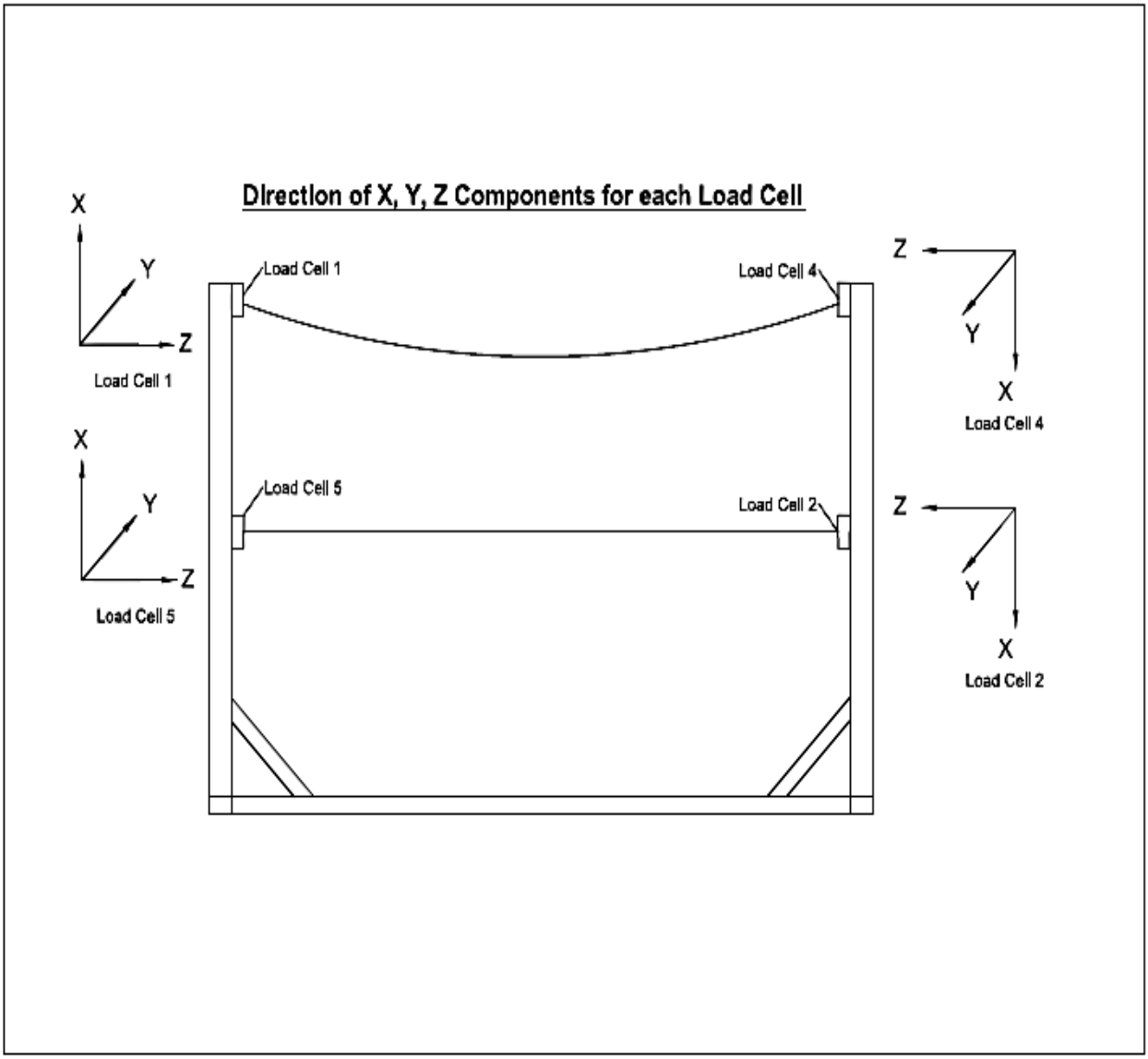

Figure 11: Direction of x, y, z components for each loadcell

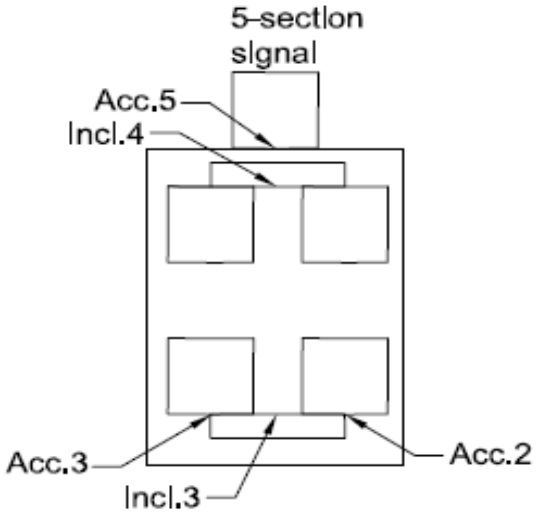

Figure 12: Location of accelerometers and inclinometers in 5-section signal for case 1

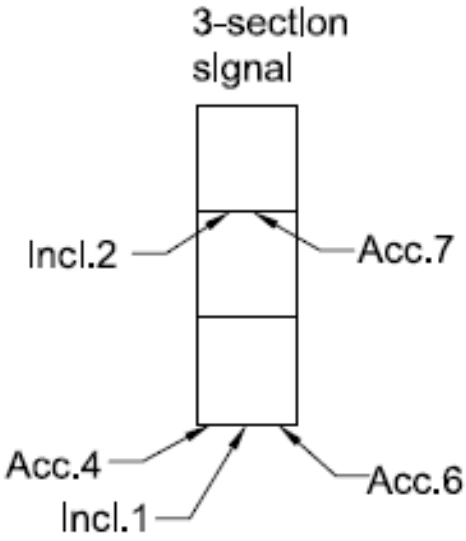

Figure 13: Location of accelerometers and inclinometers in 3-section signal for case 1

2.3. Test Results

Tests to determine base condition scenario were performed on July 28, 2015 and July 29, 2015. Representatives from the Florida Department of Transportation (FDOT) Traffic Engineering and Operations Office, Transportation Control Systems, manufacturer and distributer of the traffic signals and assemblies being tested, installation technicians from Horsepower Electric Inc. and advisor, Dr. Peter Irwin, Wall of Wind Laboratory Manager Walter Conklin and Research Scientist Roy Liu-Marques from Florida International University were present for the testing. Data was collected for catenary and messenger wire forces and traffic signal accelerations and inclinations.

In case 1 there was an increase in tension in the messenger cable as it shifted backwards and a decrease in tension in the catenary cable as it shifted forward as wind speed increased. This created excessive bending in the tri-stud adjustable hangers eventually causing a fracture. Case 1 consisting of one 3-section and one 5-section was exposed to a maximum wind speed of approximately 70 mph. At this point the standard tri-stud adjustable hangers broke just above the messenger wire and the test was stopped.

2.3.1. Cable Tensions, Lift, Drag and Span Forces

In case 1 where one 5-section and one 3-section combination was tested, it was observed as wind velocity increased the tensions recorded on both loadcells on the catenary wire increased slightly up to a certain point. When wind velocity reached approximately 48 mph both loadcells revealed a drop in catenary tension from the previous reading, this was the beginning of a downward trend in tension in the catenary cable recorded on loadcell 1 and 4 as seen in Figure 14 and Figure 15. As the wind load increases, drag force increases on the front surface area of the signals pushing back on the messenger cable and forward on the catenary cable, relieving the tension on the catenary. Data also indicates that as wind load increases lift force decreases the tension in the catenary cable. For instance, at 48 mph, loadcell 1 recorded a tension of 584 Ibs and loadcell 4 recorded a tension of 429 Ibs. While at 64 mph, loadcell 1 indicated tension of 570 Ibs and loadcell 4 indicated a resultant mean tension of 418 Ibs. Catenary cable tensions for Test

1 experienced an initial increase in tension with increasing wind speeds, followed by a reduction in the tensions for loadcells 1 and 4 as shown in Figure 16 and Figure 17 respectively.

The reverse is the case for the messenger cable, as wind velocity increased, the tension in the messenger cable increased. Tensions recorded on loadcell 5 and loadcell 2 increased as wind speed increased. For instance, in Test 1, the tension on loadcell 5 at 32 mph was 611 Ibs. and for loadcell 2 it was 636 Ibs. At 64 mph, right before ending the test, the tension recorded on loadcell 5 was 1112 Ibs. and for loadcell 2 it was 1134 Ibs. There was a steady increase of tension on the messenger cable from the beginning of Test 1 to the end as shown in Figure 18 and Figure 19. As an example, comparison of messenger cable tensions as wind speed increases for Test 1 & 2 are shown on Figure 20. In both cases the tensions increase with increase in wind speed. A detailed report incorporating the results for case 2 will be presented later. Figure 21 also shows the increase in tensions with increasing wind speeds on loadcell 2 for case 1.

Data for each component (Fx, Fy, Fz) of tension was collected by the loadcells. The direction of each component for each loadcell is shown in Figure 11. Force in the x direction (Fx) is due to lift, force in the y direction (Fy) is due to drag and force in the z direction (Fz) is due to span wise forces. Data indicates that lift force generally contribute to reducing the tension in the catenary cable as wind speed increases. Drag force initially contributed to an increase in tension in the catenary after which there is a decline in tension as wind speed increases. Span wire force also initially contributes to an increase in tension in the catenary cable followed by a decline in tension as wind speed increases. Tension behavior in the catenary cable was similar in both tests conducted.

Data shows that lift force initially contributes to an increase in tension in the messenger cable up to a certain wind speed following a decline in tension as wind speed increases. Drag force contribute to a gradual increase in tension in the messenger cable as wind speed increases. Span wire force contributes to a steady increase in tension in the messenger cable as wind speed increases.

Moments were recorded by the loadcells but are not discussed in this report.

2.3.2. Signal Accelerations

Data collected from the accelerometers installed in the 3-section signals revealed that there were higher rms accelerations on the bottom right corner of the signal as opposed to the bottom left corner or top center. In point of fact, from the onset of the test at very low speeds the bottom right corner accelerometer was recording higher rms accelerations than the other two. All three accelerometers indicated rms accelerations to be increasing as wind speed increased. This behavior was similarly observed in 3-section traffic signals for Test 1 as shown in Figure 22.

Data collected from the accelerometers installed in the 5-section signal is shown in Figure 23. The bottom right and left corners have similar rms accelerations. The top center of the signal had similar rms accelerations early on but decreased slightly later in the test. The difference in accelerations between the three locations was not nearly as dispersed as seen in the 3-sections signals.

2.3.3. Signal Inclinations

Data collected from the inclinometers installed in the 3-section signal for Test 1 revealed that there appeared to be similar inclinations, at approximately 64 mph, of 35 degrees relative to the perpendicular axis to the wind and recorded for both bottom and top center inclinometers Inc1-2 and Inc2-2, respectively as shown in Figure 24 and Figure 25. Inclinations recorded by the bottom center inclinometer Inc1-1, relative to the axis parallel to the wind, revealed the bottom part of the 3-section signal veered slightly to the left and up to approximately 32 mph after which it began veering to the right as shown in Figure 24. On the other hand, inclinations relative to the axis parallel to the wind recorded by the top center inclinometer Inc2-1, indicated the top portion of the 3-section signal veered to the right from the onset of the test at approximately 1.5 degrees at 24 mph to the end of the test as shown in Figure 25.

Data gathered from the inclinometers installed in the 5-section signal for Test 1 revealed that there were similar inclinations, at approximately 64 mph, of 35 degrees relative to the axis perpendicular to the wind recorded for both bottom and top center inclinometers Inc3-2 and Inc4-2, respectively as shown in Figure 26 and Figure 27. Inclinations recorded by the bottom center inclinometer Inc3-1, relative to the axis parallel to the wind, revealed the bottom part of

the 5-section signal veered to the left from the onset of the test at approximately 0.3 degrees to approximately 2 degrees as shown in Figure 26. On the other hand, inclinations, relative to the axis parallel to the wind, recorded by the top center inclinometer Inc4-1, indicated the top portion of the 5-section signal veered to the right to approximately 0.2 degrees at the beginning of the test after which it then began to veer in the opposite direction at 24 mph until the end of the test as shown in Figure 27.

As is self-evident, observations in the data revealed that much higher inclinations occurred relative to the axis perpendicular to the wind than relative to the axis parallel to the wind for all traffic signals utilized in both tests.

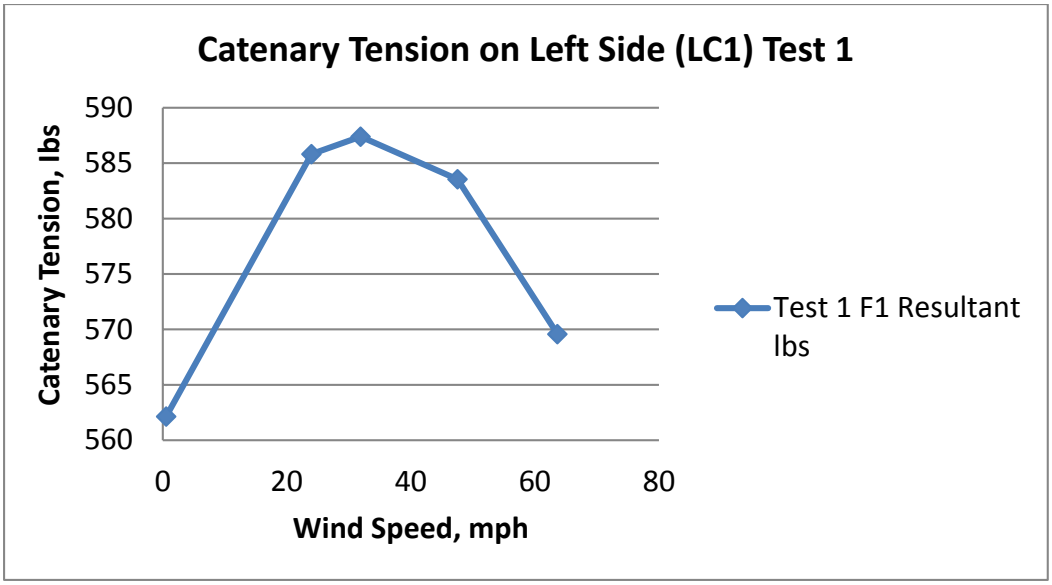

Figure 14: Downward trend in tension in the catenary cable for Test 1 at approximately 48 mph for loadcell 1

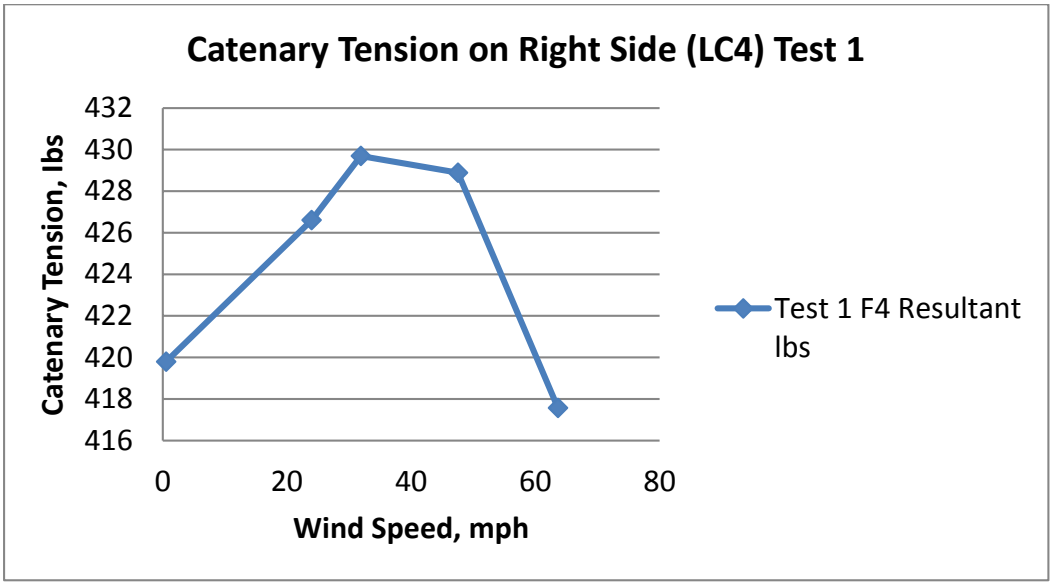

Figure 15: Downward trend in tension in the catenary cable for Test 1 at approximately 48 mph for loadcell 4

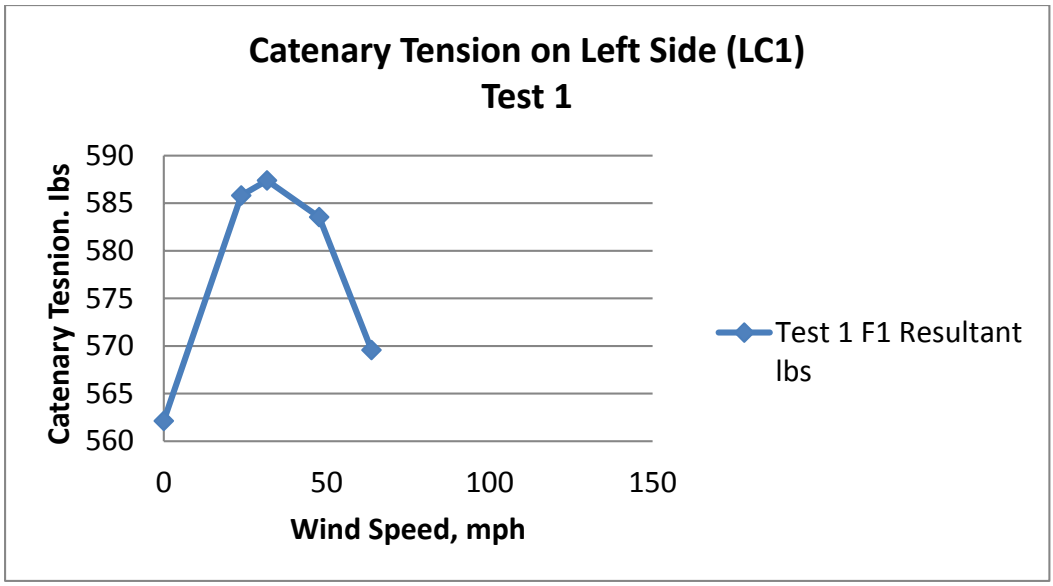

Figure 16: Catenary cable tensions for Test 1 as wind speed increases for loadcell 1

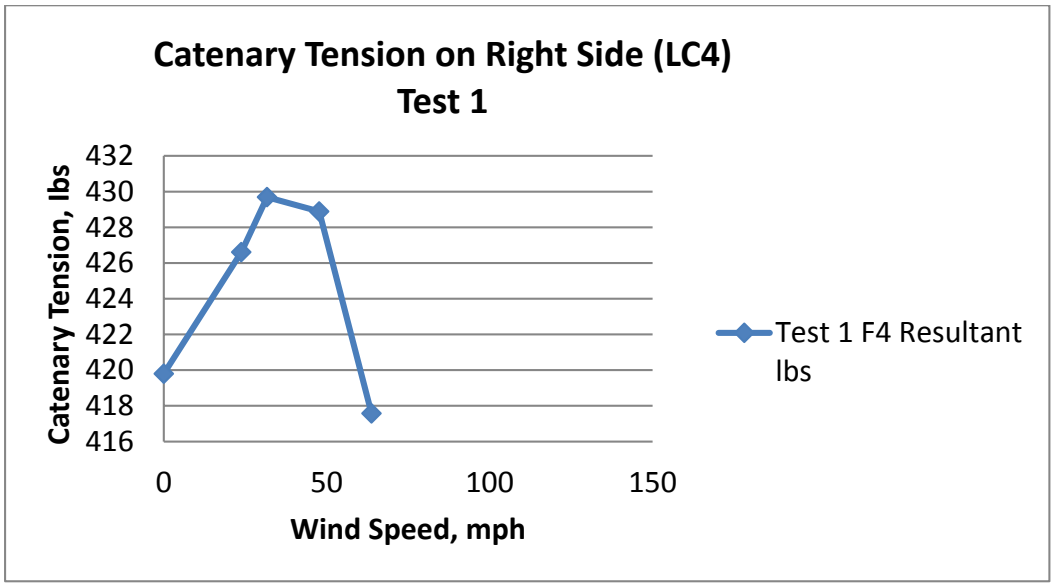

Figure 17: Catenary cable tensions for Test 1 as wind speed increases for loadcell 4

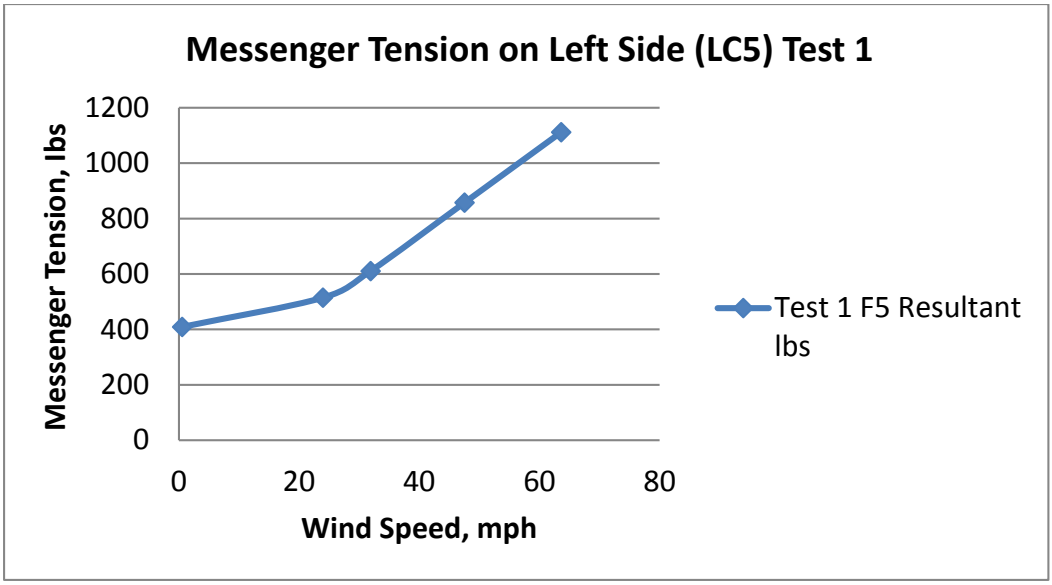

Figure 18: Tension in the messenger cable as wind speed increases for Test 1 loadcell 5

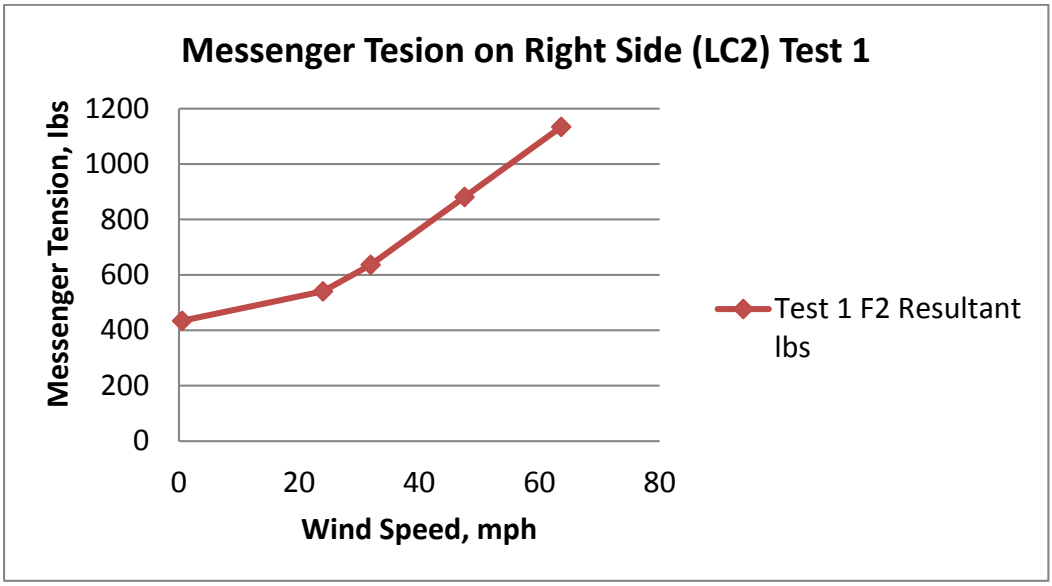

Figure 19: Tension in the messenger cable as wind speed increases for Test 1 loadcell 2

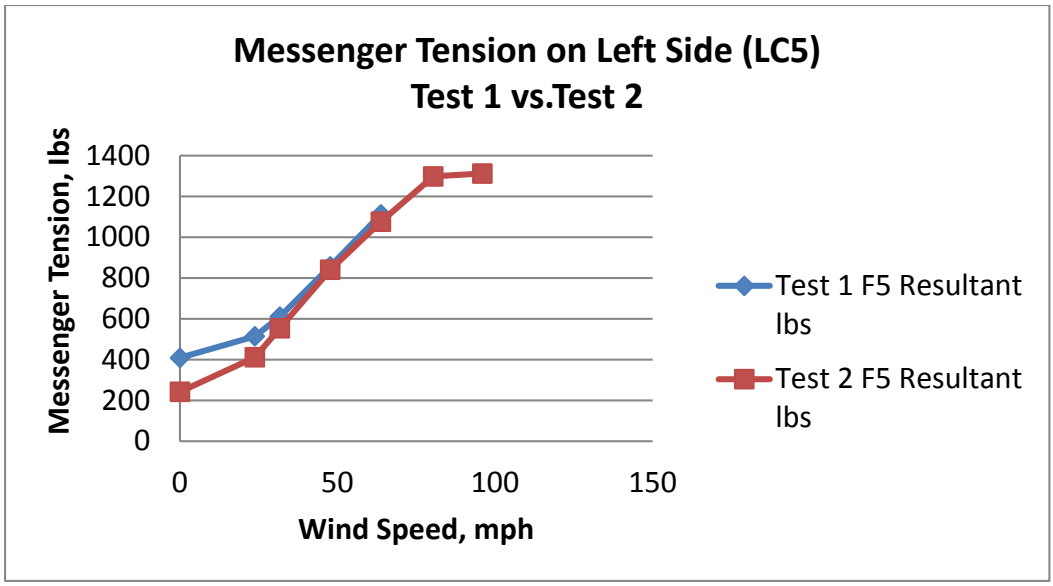

Figure 20: Comparison of messenger cable tensions for Test 1 vs Test 2 as wind speed increases for loadcell 5

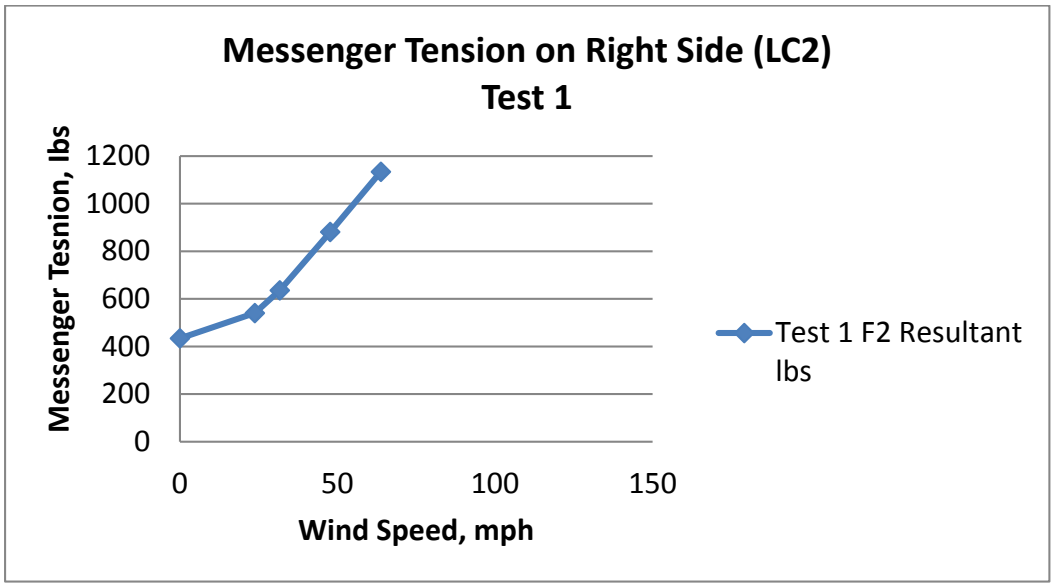

Figure 21: Messenger cable tensions for Test 1 as wind speed increases for loadcell 2

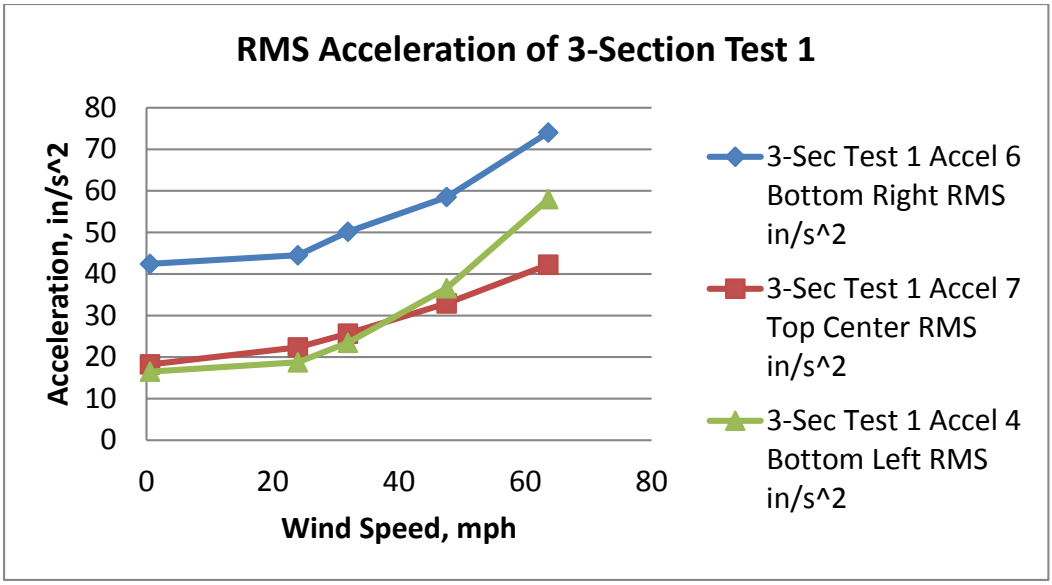

Figure 22: Acceleration of 3-section traffic signal for Test 1

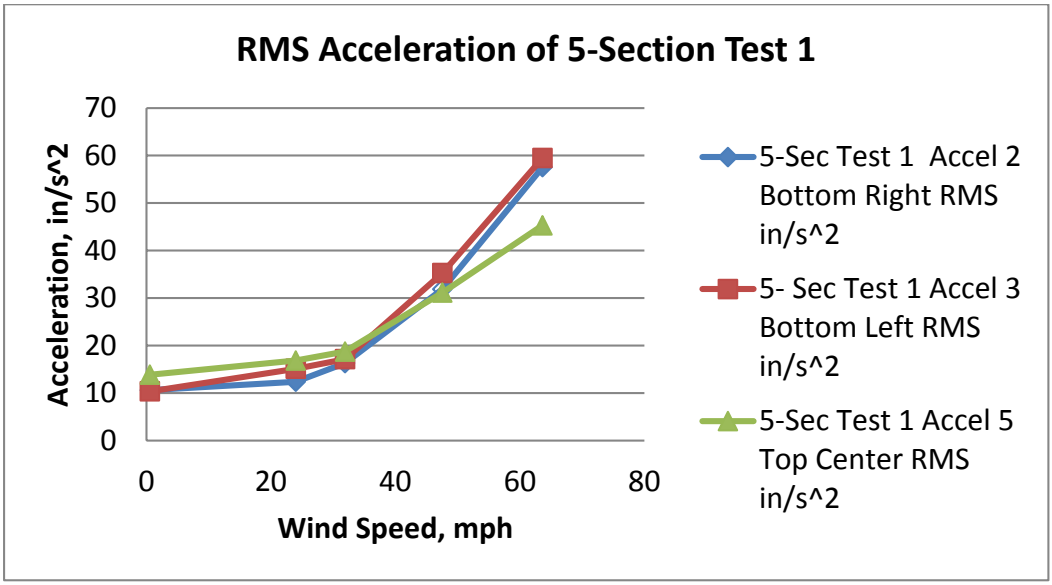

Figure 23: Acceleration of 5-section traffic signal for Test 1

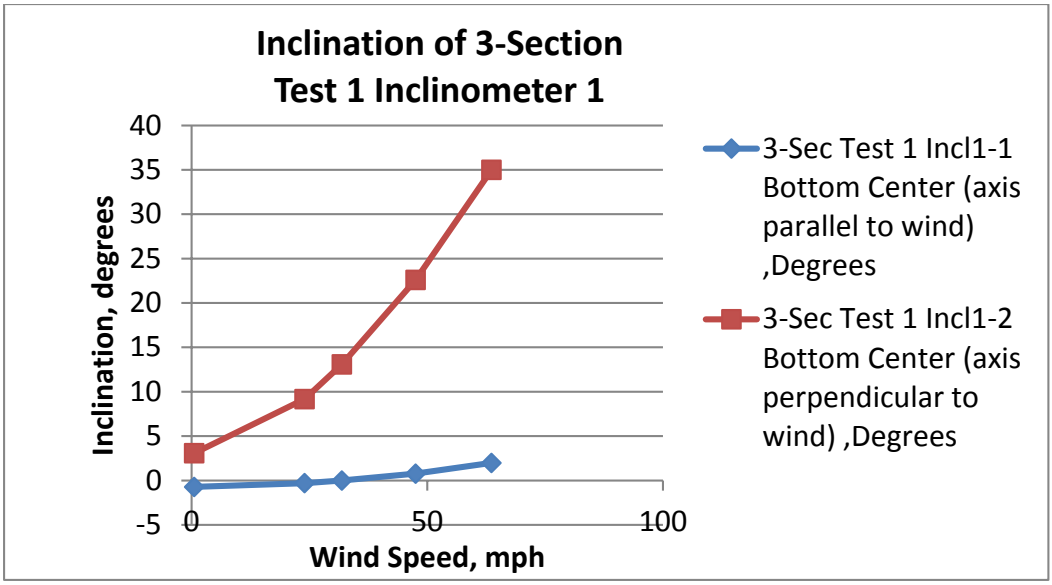

Figure 24: Inclination of 3-section traffic signal for Test 1 Inclinometer 1

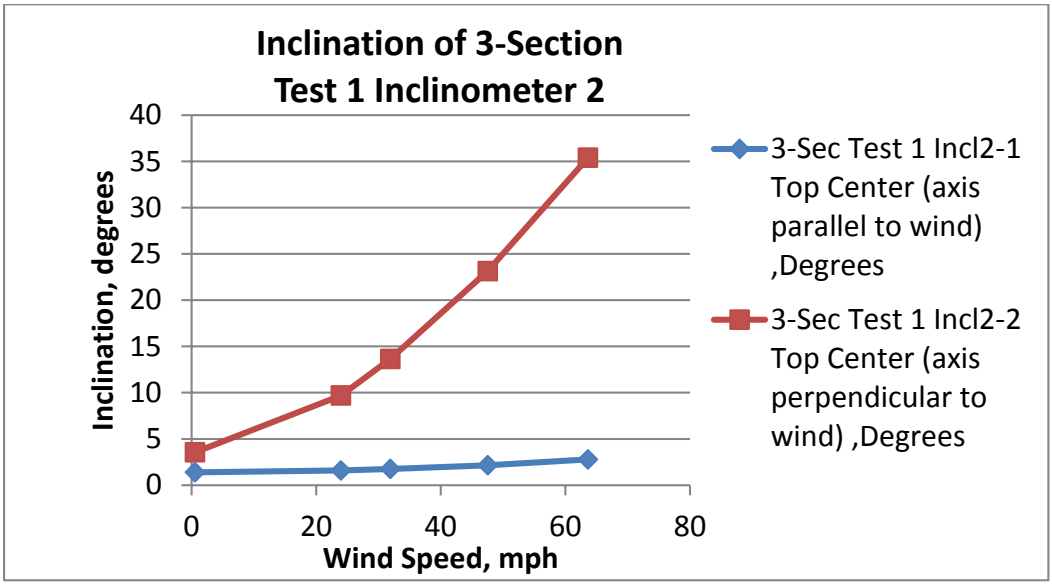

Figure 25: Inclination of 3-section traffic signal for Test 1 Inclinometer 2

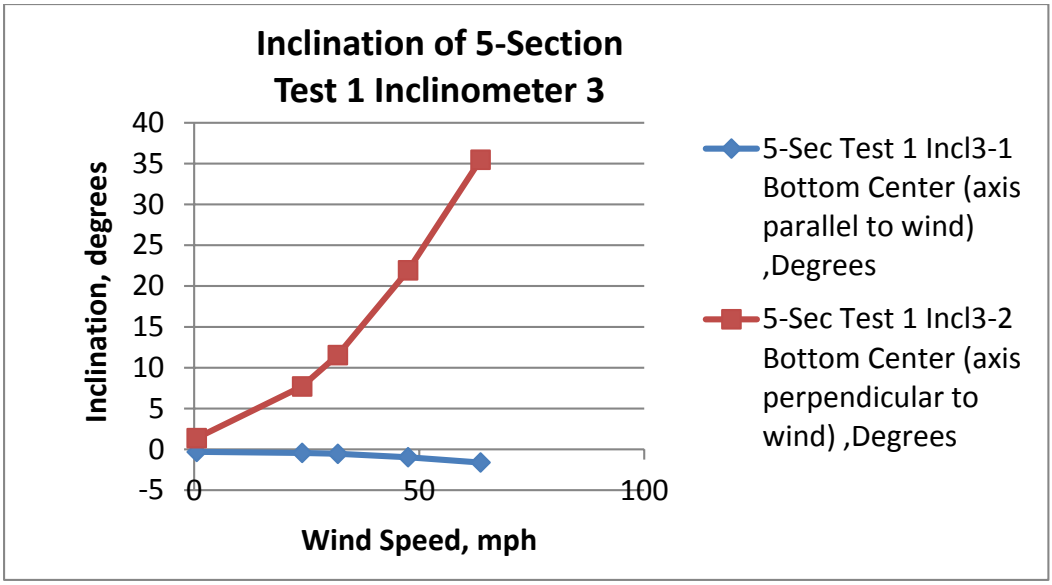

Figure 26: Inclination of 5-section traffic signal for Test 1 Inclinometer 3

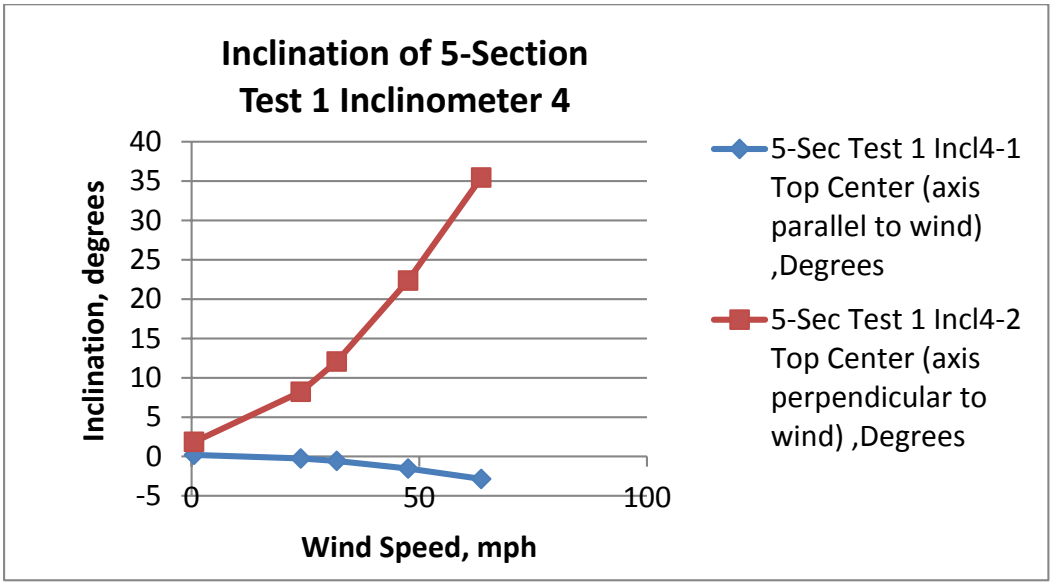

Figure 27: Inclination of 5-section traffic signal for Test 1 Inclinometer 4

2.4. Performance of Equipment and Hardware

As previously discussed, in these tests there were two alternative traffic signal configurations that were tested, and this chapter is dedicated to test 1. The first configuration tested was one 3-section traffic signal on the right side and one 5-section signal on the left side. All traffic signals consisted of sand cast aluminum disconnect boxes and standard sand cast aluminum tri-stud adjustable hangers. It should be noted that the standard tri-stud adjustable signal hangers used in these tests were unable to be identified as FDOT approved products. Before the tests the tri-stud adjustable hangers were inspected and did not provide any evidence that the material met FDOT requirements. The disconnect boxes for the 3-section and the 5-section traffic signal did not sustain any damage during Test 1 as shown in Figure 28 and Figure 29, respectively. There was no damage to the serrated teeth connection between the tri-stud bracket and the top of the disconnect box for none of the signals tested as shown in Figure 30.

The 3-section and 5-section signals, including visors, did not sustain any damage during Test 1 as shown in Figure 31 and Figure 32, respectively. The backplates sustained minor damage as they were slightly bent backwards.

The only damage that occurred during Test 1 originated from the standard tri-stud adjustable hanger assembly utilized. These hangers were sheared off at the proximity of the connection brackets that are attached to the top of the disconnect box.

Based on manufacturer's recommendations the overlap of the long extension brackets on the bottom bracket was three thru holes down from the top of the bottom bracket with bolts inserted on the top two thru holes.

There was no noticeable damage to the aluminum messenger clamps attached to the connection brackets. This is shown in Figure 33 for Test 1.

There was no notable damage observed to the span wire clamps attached to the catenary cables as shown in Figure 34.

Figure 28: Disconnect box for 3-section signal after Test 1 showing no noticeable damage

Figure 29: Disconnect box for 5-section signal after Test 1 showing no noticeable damage

Figure 30: Serrated teeth connection between the bracket and the top of the disconnect box with no noticeable damage

Figure 31: 3-section signal with visors after Test 1 showing no noticeable damage

Figure 32: 5-section signal with visors after Test 1 showing no noticeable damage

Figure 33: Tri-stud adjustable hanger after Test 1 showing location of damage. No noticeable damage to the extruded aluminum messenger wire clamp

Figure 34: Span wire clamp attached to the catenary cable with no noticeable damage

2.5. Summary, Conclusions and Recommendations

2.5.1. Summary

Two different traffic signal combinations were tested to determine the more susceptible of the two combinations. This chapter only summarizes the results of test case 1 which consisted of a 3-section and a 5-section traffic signal. All traffic signals were installed with aluminum tri-stud adjustable signal hangers and were tested at zero degrees. Cable tensions, accelerations and traffic signal inclinations were compared to assess the behavior of each signal combination. It was determined that there were higher cable tensions in the one 5-section and one 3-section signal combination causing failure at a lower wind speed, thus the more susceptible of the two signal combinations. This signal combination was decided on for future testing. Afterwards FDOT requested an additional 3-section signal to the base condition to reflect typical field installations more accurately. Therefore, the base condition will consist of one 5-section and two 3-section signals.

2.5.2. Conclusions

Test results revealed tension decreased in the catenary cable for the traffic signal combinations tested as wind velocity increased. There is initially a minor increase in the catenary cable tension up to a certain wind velocity but afterwards tension proceeds to decline. One important observation was that tension in the messenger cable increased as wind velocity increased. Furthermore, the traffic signals showed larger deflection angles backwards than sideways as expected.

2.5.3. Recommendations

Following the review of the data acquired from test case 1, it was found necessary to assess the behavior of test case 2, which is elaborately described in another chapter. In general, test case 1 showed that tension in the catenary and messenger cables were excessive and under these test conditions the traffic signals were not behaving in the manner that they would be in the field under similar wind conditions. Attempting to lessen the excessive tension in the cables and

simulate more realistic traffic signal behavior, springs with a stiffness of 50 Ibs/in were used in an independent test conducted on August 3, 2015. After examining the data, it was found that the tension in the cables was reduced and traffic signal behavior was more in tune with field conditions. Following an analysis, it was determined that in order to simulate a typical span of 80 ft in the field with 3/8-inch diameter catenary cable and 7/16-inch diameter messenger cable, springs with a stiffness of 100 Ibs/in and 145 Ibs/in respectively should be used in future tests.

Chapter 3 - Task 1a: FULL SCALE TESTING – Case 2

3.1. Introduction

The main objective of the tests discussed in this chapter was to determine a base condition configuration to utilize for future hanger assembly tests. Two configurations were evaluated. The first configuration consisted of one aluminum 5-section and one aluminum 3-section traffic signal, and the results for this test case are available in chapter 2. The main focus of this report is the second configuration (test case 2) that included one aluminum 4-section and two aluminum 3-section traffic signals. Both configurations utilized standard tri-stud adjustable hangers. The more vulnerable of the two will be considered the base condition scenario and will be used for testing the remaining signal hangers. Following these tests, the data that was obtained was analyzed and it was determined that the more vulnerable of the two configurations was one 5-section and one 3-section (see chapter 2). Subsequently, FDOT requested to add a second 3-section signal to the base condition (test case 1) scenario. Methodology

3.1.1. Test Setup

The second signal combination (test case 2) consisted of two 3-section and one 4-section. Signals were placed with a 4 ft center to center separation at mid-span of the test rig. There was a distance of approximately 6 ft 11 ½ in from the outside edge of the two outer signals to the front face of the steel column as shown in sketch of second signal combination setup in Figure 35. The bottom of all signals tested was at approximately 4 ft 6 in above the concrete floor. All signals were aluminum and included louvered back plates and visors. Standard tri-stud adjustable hangers were used for both signal combinations. A picture of the test rig is shown in Figure 36.

Test case 2 was only tested at 0° direction for all speeds. This direction corresponds to the front face of the signals facing the approaching wind. Traffic signals for test case 2 were planned to be exposed to wind speeds starting at 10 mph followed by 20 mph, 70 mph, 100 mph, 130 mph and maximum or until failure of one of the traffic signal assemblies as shown in test protocol Table 3. Table 4 shows the list of components and manufacturers used for each test.

3.1.2. Instrumentation

The directions of the x, y and z components for each loadcell are shown in Figure 37. The loadcells had one thousand five hundred lbs capacity. Loadcells 2 and 5 were located at either end of the messenger cable, while loadcells number 1 and 4 located at either end of the catenary cable.

The locations of the accelerometers and inclinometers are shown in Figure 38 and Figure 39. Wind speeds in three component directions (u,v,w) were also recorded by the Wall of Wind sensors.

3.1.3. Test Method

Both of the tested signal combinations utilized standard tri-stud adjustable hangers. The purpose was to determine the more vulnerable of the two combinations to be used for future tests. The more vulnerable was determined to be the signal combination that sustained the most damage and failed the earliest.

Table 3: Test protocol (Task 1a: Case 2)

Signal Combination 1 and 2			
Wind Speed (mph)	Direction	Duration (min)	Total Duration (min)
10	0	1	2
Adj.		2	4
20	0	1	6
Adj.		2	8
40	0	1	10
Adj.		2	12
70	0	1	14
Adj.		2	16
100	0	1	18
Adj.		2	20
130	0	1	22
Adj.		2	24
Max	0	1	26
TOTAL			26

Table 4: Signal assembly components and manufacturers (Task 1a: Case 2)

Component	Manufacturer
Span wire clamp	Pelco
Adjustable hanger	Pelco
Extension bar	Pelco
Messenger clamp	Pelco
Disconnect Hanger	Pelco
Signal Assembly	McCain
Backplate	TCS
Visor	McCain
LED Modules	GE - Dialight - Duralight

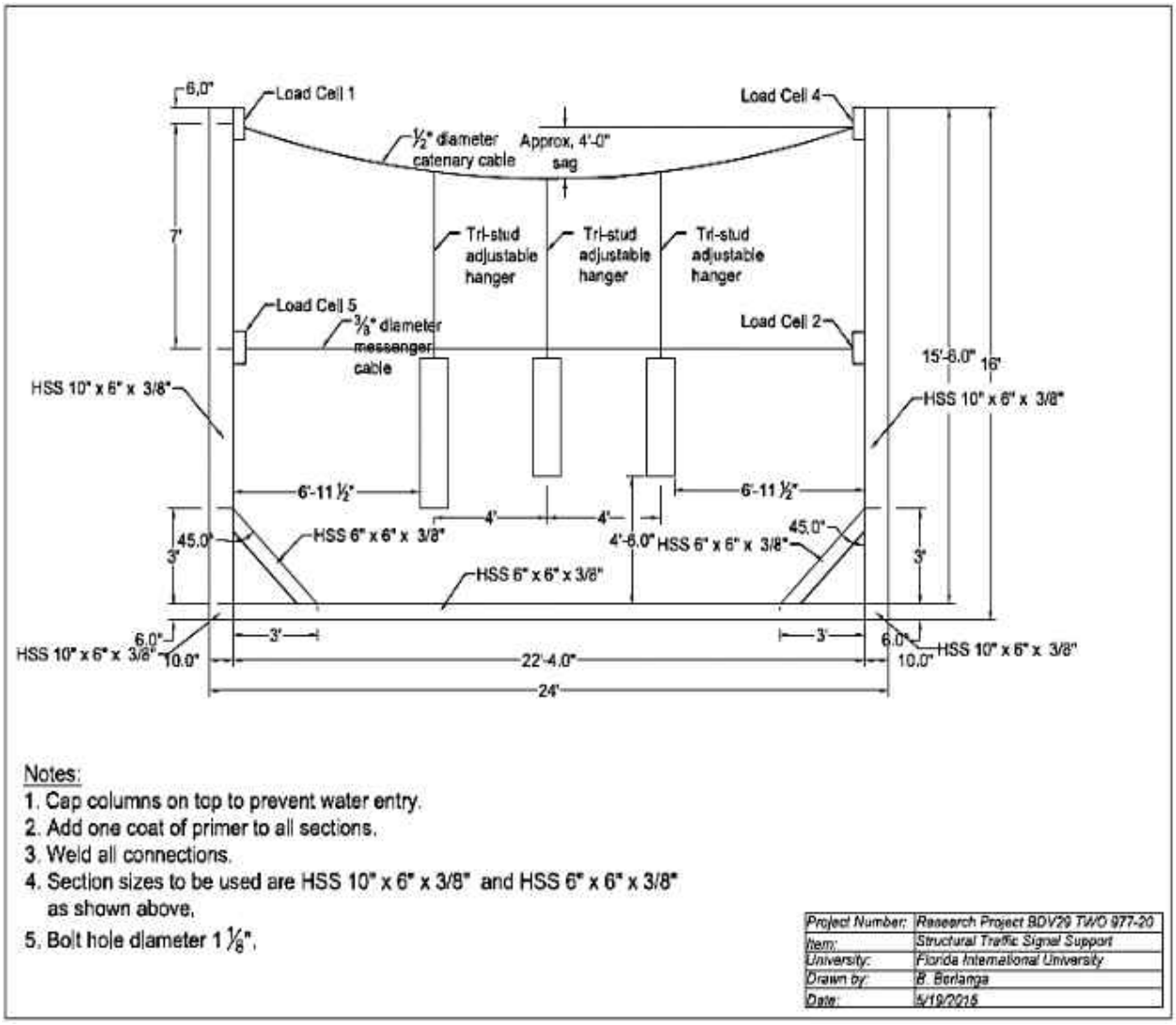

Notes:

1. Cap columns on top to prevent water entry.
2. Add one coat of primer to all sections.
3. Weld all connections.
4. Section sizes to be used are HSS 10" x 6" x 3/8" and HSS 6" x 6" x 3/8" as shown above.
5. Bolt hole diameter 1 ⅛".

Project Number:	Research Project BDV29 TWO 977-20
Item:	Structural Traffic Signal Support
University:	Florida International University
Drawn by:	B. Berlanga
Date:	5/19/2015

Figure 35: Second signal combination setup (test case 2) of two 3-section and one 4-section traffic signals

Figure 36: Picture of test rig frame

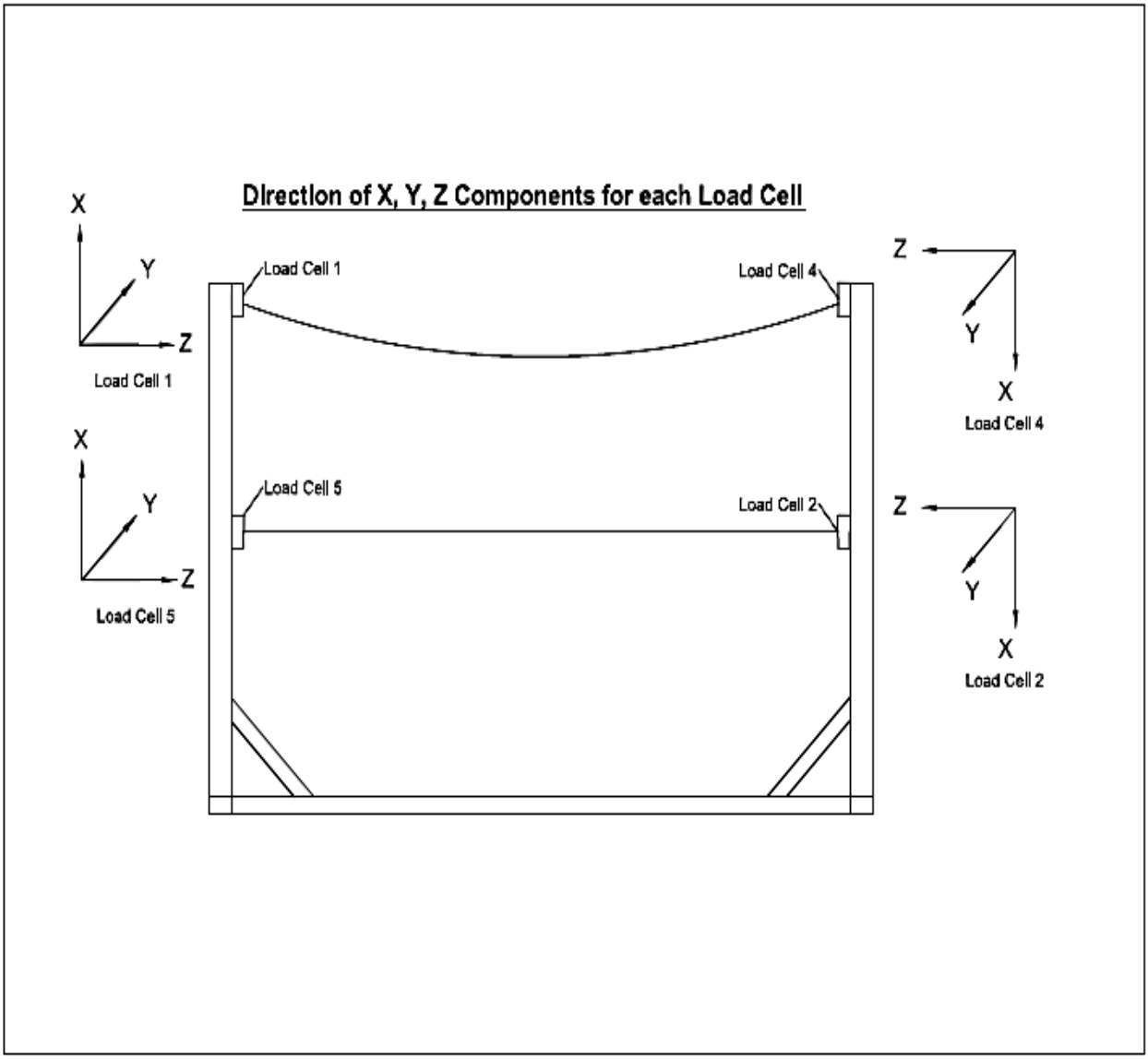

Figure 37: Direction of x, y, z components for each loadcell

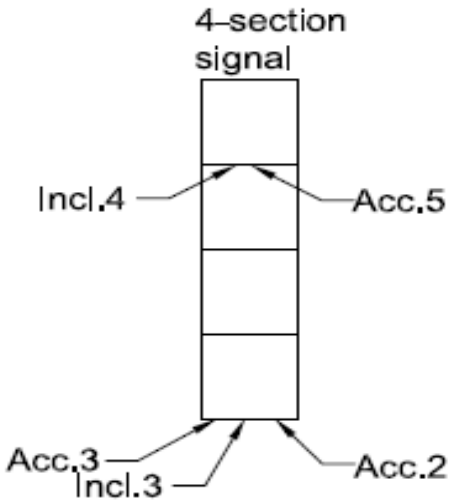

Figure 38: Location of accelerometers and inclinometers in 4-section signal

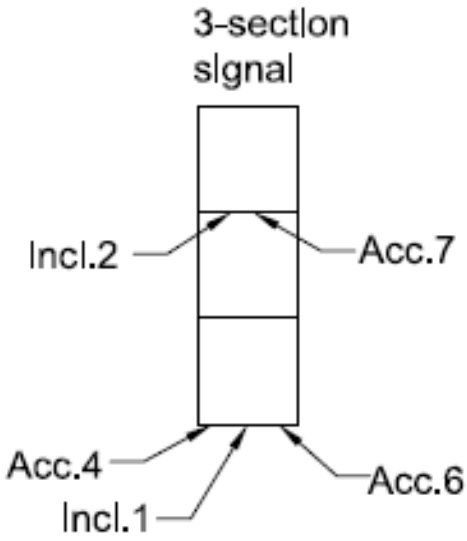

Figure 39: Location of accelerometers and inclinometers in 3-section signal

3.2. Test Results

Tests to determine base condition scenario were performed on July 28, 2015 and July 29, 2015. Representatives from the Florida Department of Transportation (FDOT) Traffic Engineering and Operations Office, Transportation Control Systems, manufacturer and distributer of the traffic signals and assemblies being tested, installation technicians from Horsepower Electric Inc. and advisor, Dr. Peter Irwin, Wall of Wind Laboratory Manager Walter Conklin and Research Scientist Roy Liu-Marques from Florida International University were present for the testing. Data was collected for catenary and messenger wire forces and traffic signal accelerations and inclinations.

In test case 2, the messenger cable experienced an increase in tension as it shifted backwards and a decrease in tension in the catenary cable as it shifted forward as wind speed increased. This created excessive bending in the tri-stud adjustable hangers eventually causing a fracture. Test case 2 consisting of two 3-sections and one 4-section was exposed to a maximum wind speed of approximately 105 mph. At this point the standard tri-stud adjustable hangers again broke just above the messenger wire and the test was stopped.

3.2.1. Cable Tensions, Lift, Drag and Span Forces

Although the previous chapter provides a detailed description of test case 1, a few selected results from test 1 are compared to test 2. It may be recalled that Case-1 consisted of one 5-section and one 3-section signal combination. The catenary tension for test cases 1 and 2 are compared for loadcell 1 in Figure 40. In general, for both cases, results show that with increasing wind speed the tension initially increases, but beyond 40 mph, there is a gradual decrease in catenary tension. However, in case 2 the tensions reduce rapidly as compared to test case 1. Similar observations were made for loadcell 4 as shown in Figure 41. As the wind load increases, drag force increases on the front surface area of the signals pushing back on the messenger cable and forward on the catenary cable, relieving the tension on the catenary. Data also indicates that as wind load increases lift force decreases the tension in the catenary cable.

The reverse is the case for the messenger cable, as wind velocity increased, the tension in the

messenger cable increased. Tensions recorded on loadcell 5 and loadcell 2 increased as wind speed increased, as shown in Figure 42 and Figure 43 respectively. For instance, in Test 2, the tension on loadcell 5 at 32 mph was 554 Ibs and for loadcell 2 it was 587Ibs. While at 96 mph, right before ending the test, the tension recorded on loadcell 5 was 1312 Ibs and for loadcell 2 it was 1320 Ibs.

Data for each component (Fx, Fy, Fz) of tension was collected by the loadcells. The direction of each component for each loadcell is shown in Figure 37. Force in the x direction (Fx) is due to lift, force in the y direction (Fy) is due to drag and force in the z direction (Fz) is due to spanwise forces. Data indicates that lift force generally contribute to reducing the tension in the catenary cable as wind speed increases. Drag force initially contributed to an increase in tension in the catenary wire after which there is a decline in tension as wind speed increases. Spanwise force also initially contributes to an increase in tension in the catenary cable followed by a decline in tension as wind speed increases. Tension behavior in the catenary cable was similar in both tests conducted. Furthermore, the lift force initially contributes to an increase in tension in the messenger cable up to a certain wind speed following a decline in tension as wind speed increases. Drag forces contribute to a gradual increase in tension in the messenger cable as wind speed increases. Spanwise force contributes to a steady increase in tension in the messenger cable as wind speed increases. Tension behavior in the messenger cable was similar in both tests conducted.

Moments were recorded by the loadcells but are not discussed in this report.

3.2.2.Signal Accelerations

Data collected from the accelerometers installed in the 3-section signals revealed that there were higher rms accelerations on the bottom right corner of the signal as opposed to the bottom left corner or top center. In point of fact, from the onset of the test at very low speeds the bottom right corner accelerometer was recording higher rms accelerations than the other two. All three accelerometers indicated rms accelerations to be increasing as wind speed increased. This behavior was similarly observed in 3-section traffic signal for Test 2 as shown in Figure 44 and Figure 45. Accelerometers 6 and 4 (Figure 44) produced accelerations that had similar trends,

although the magnitude of the rms acceleration was somewhat less from accelerometer 7.

Data collected from the accelerometers installed in the 4-section signal (Figure 45) revealed that, the bottom right and left corners appeared to have similar rms accelerations throughout the test. The top center of the signal had similar rms accelerations initially but decreased slightly later in the test.

3.2.3. Signal Inclinations

Figure 46 shows the inclinations recorded by the bottom center inclinometer Inc1-1, relative to the axis parallel to the wind, revealed the bottom part of the 3-section signal veered to the left up to approximately 32 mph after which it began veering to the right. On the other hand, inclinations relative to the axis parallel to the wind, recorded by the top center inclinometer Inc2-1 (Figure 47), indicated similar behavior to the bottom center inclinometer, veering to the left up to approximately 32 mph and then began to veer to the right. Data compiled from the inclinometers installed in the 3-section signal for Test 2 revealed that there was greater backward inclination of approximately 53 degrees at 96 mph relative to the axis perpendicular to the wind recorded for the top center inclinometer Inc2-2 as compared with the bottom center inclinometer Inc1-2, where it indicated a backward inclination of approximately 40 degrees at 96 mph.

There was a greater difference observed in backward inclinations relative to the axis perpendicular to the wind of the 3-section signal between the top and bottom center inclinometer in Test 2 as compared to Test 1 (see Chapter 2). Data indicated that as wind speed increased, the difference in backward inclination between the top and bottom center of the signal increased in Test 2. Inclinations recorded by the bottom center inclinometer Inc1-1, relative to the axis parallel to the wind, revealed the bottom part of the 3-section signal veered to the left up to approximately 32 mph after which it began veering to the right.

Data collected from the inclinometers installed in the 4-section signal for Test 2 revealed that there was slightly greater backward inclinations relative to the axis perpendicular to the wind as speed increased starting at 80 mph for the top center inclinometer Inc4-2 compared to the bottom center inclinometer Inc3-2 as shown in Figure 48 and Figure 49. Inclinations, relative to the axis parallel to the wind, recorded by the bottom center inclinometer Inc3-1 revealed the

bottom part of the 4-section signal veered to the left to 3 degrees at 15 mph from the onset of the test until approximately 73 mph after which it began to veer to the right to 0.3 degrees at 80 mph and increased to approximately 4 degrees at 96 mph as shown in Figure 48.

Inclinations relative to the axis parallel to the wind recorded by the top center inclinometer Inc4-1, indicated the top portion of the 4-section signal veered to the left from the onset of the test at approximately 3.3 degrees at 15 mph until the end of the test at approximately 0.2 degrees at 96 mph. In general, higher inclinations occurred relative to the axis perpendicular to the wind than relative to the axis parallel to the wind for all traffic signals utilized in both tests.

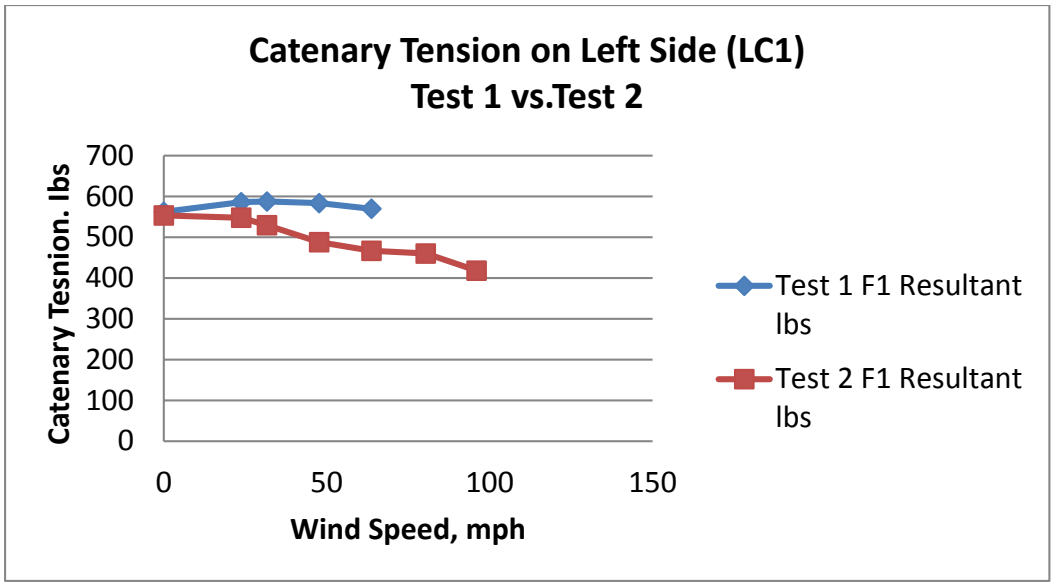

Figure 40: Comparison of catenary cable tensions for Test 1 vs Test 2

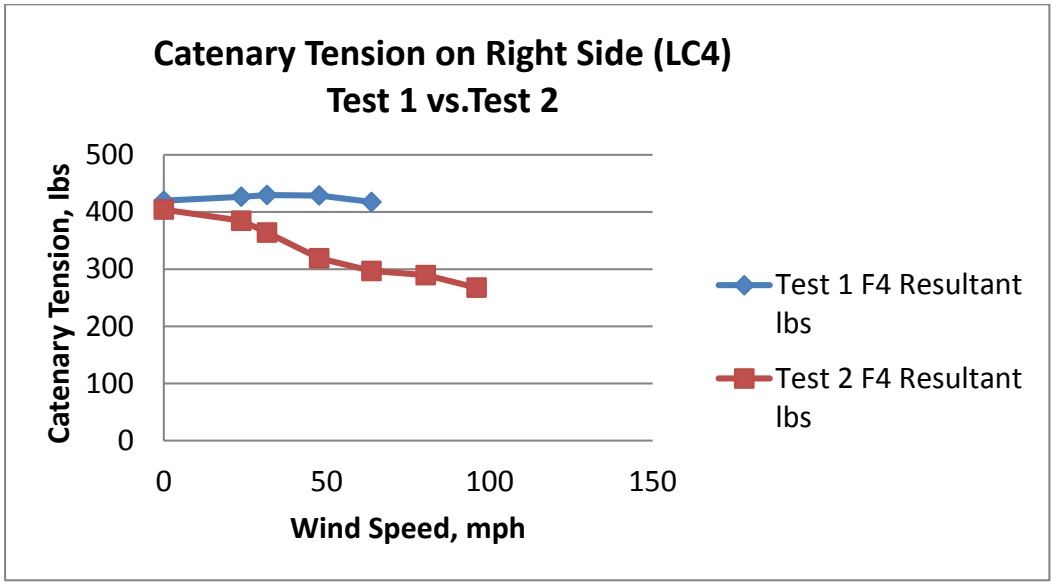

Figure 41: Comparison of catenary cable tensions for Test 1 vs Test 2

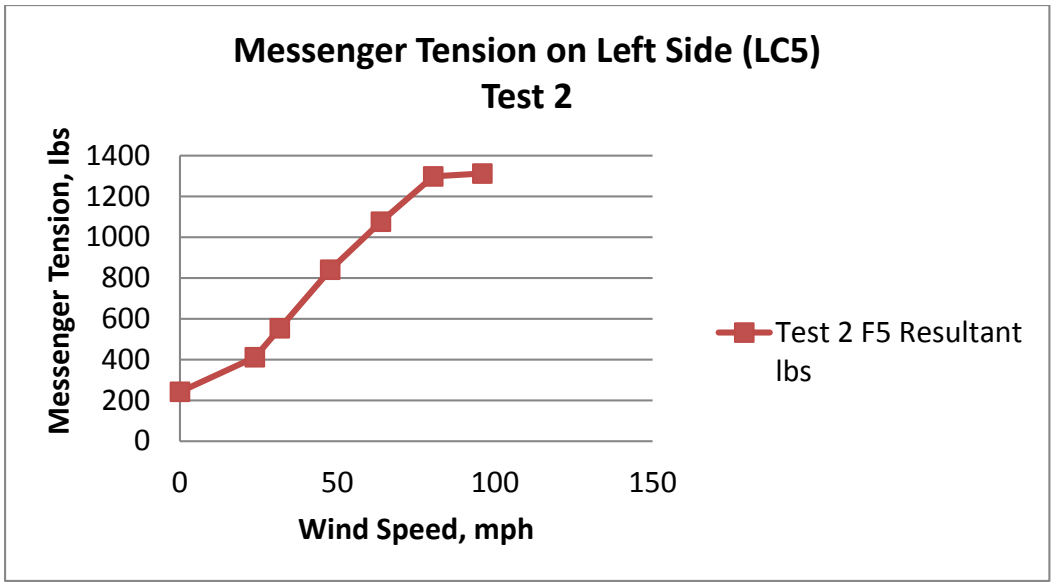

Figure 42: Messenger cable tension for Test 2 as wind speed increases for loadcell 5

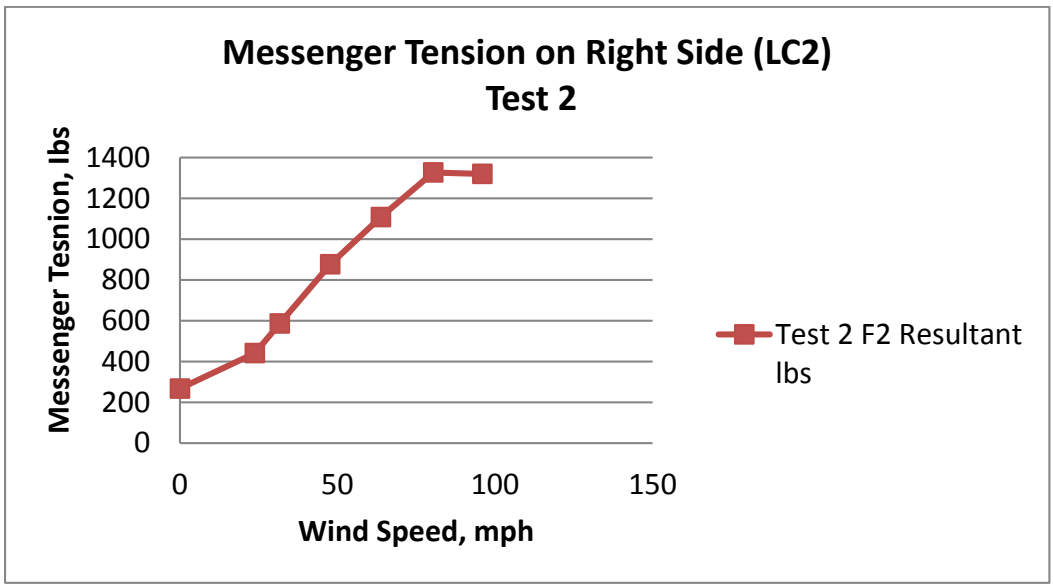

Figure 43: Messenger cable tensions for Test 2 as wind speed increases for loadcell 2

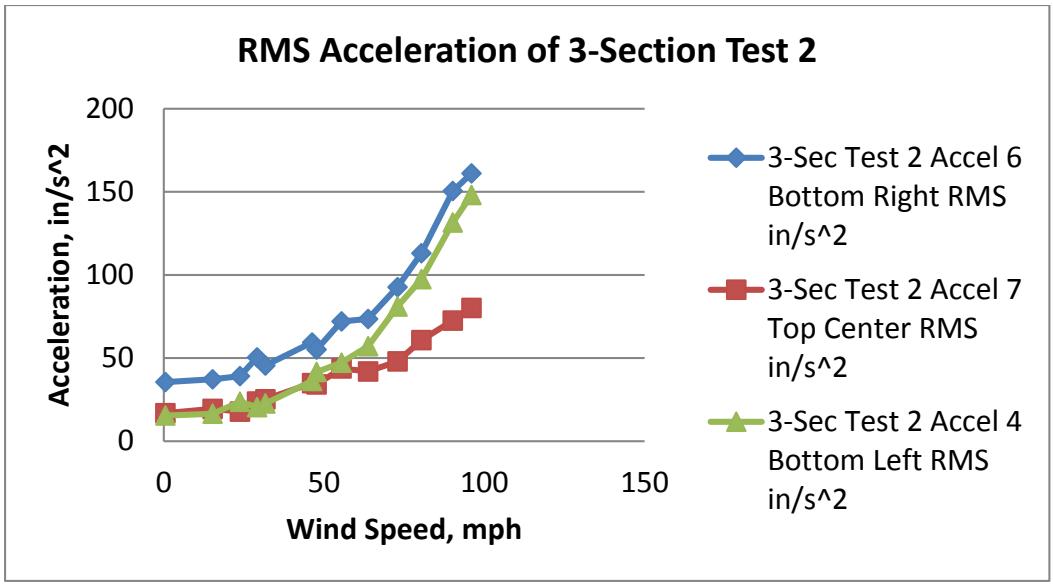

Figure 44: Acceleration of 3-section traffic signal for Test 2

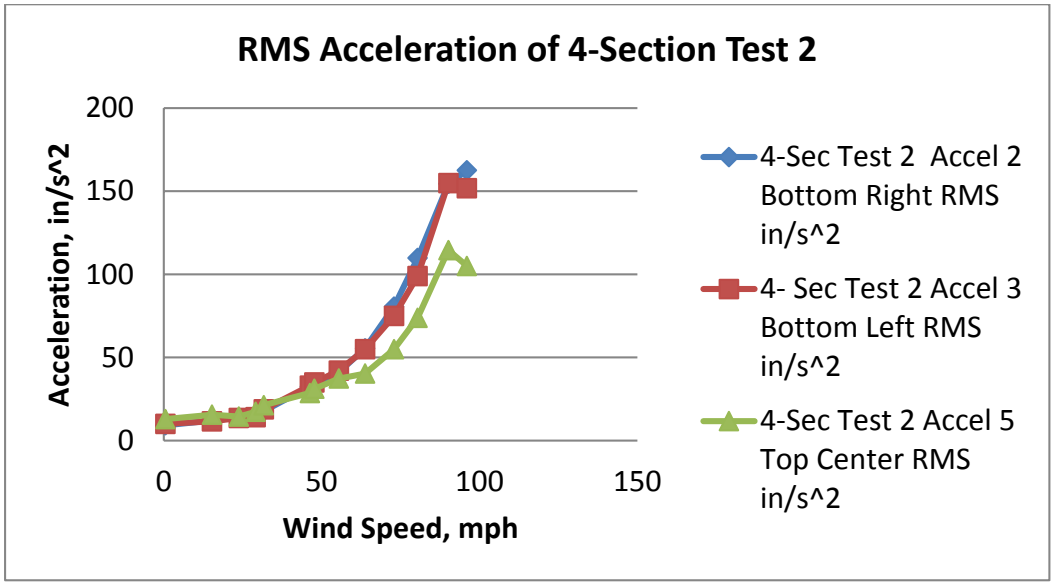

Figure 45: Acceleration of 4-section traffic signal for Test 2

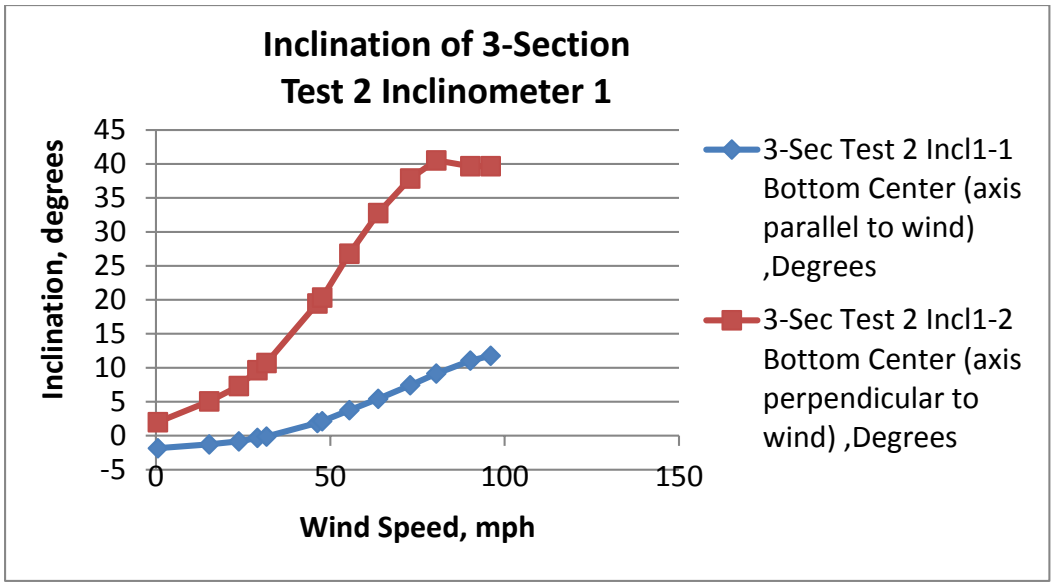

Figure 46: Inclination of 3-section traffic signal for Test 2 Inclinometer 1

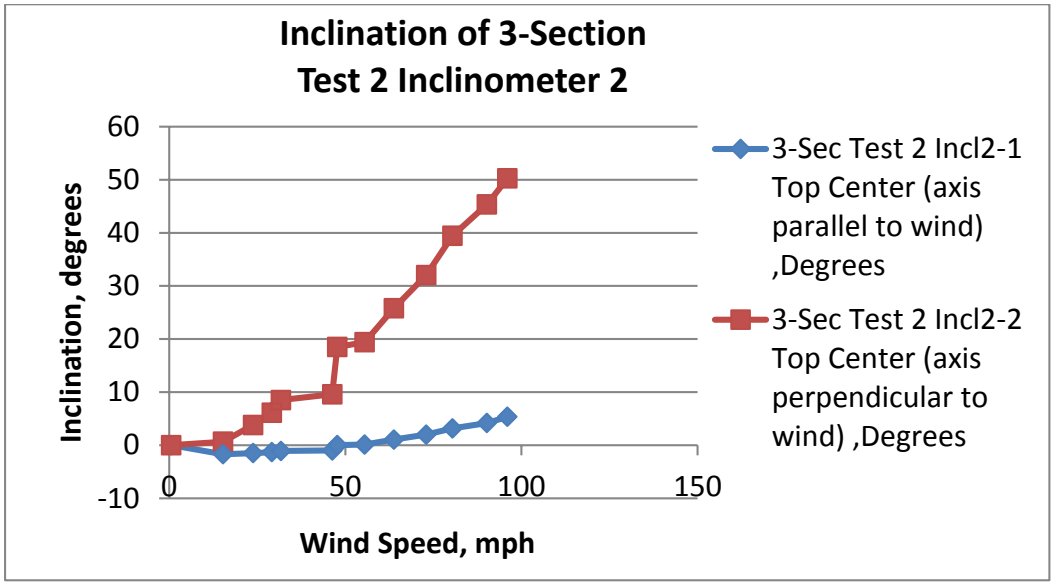

Figure 47: Inclination of 3-section traffic signal for Test 2 Inclinometer 2

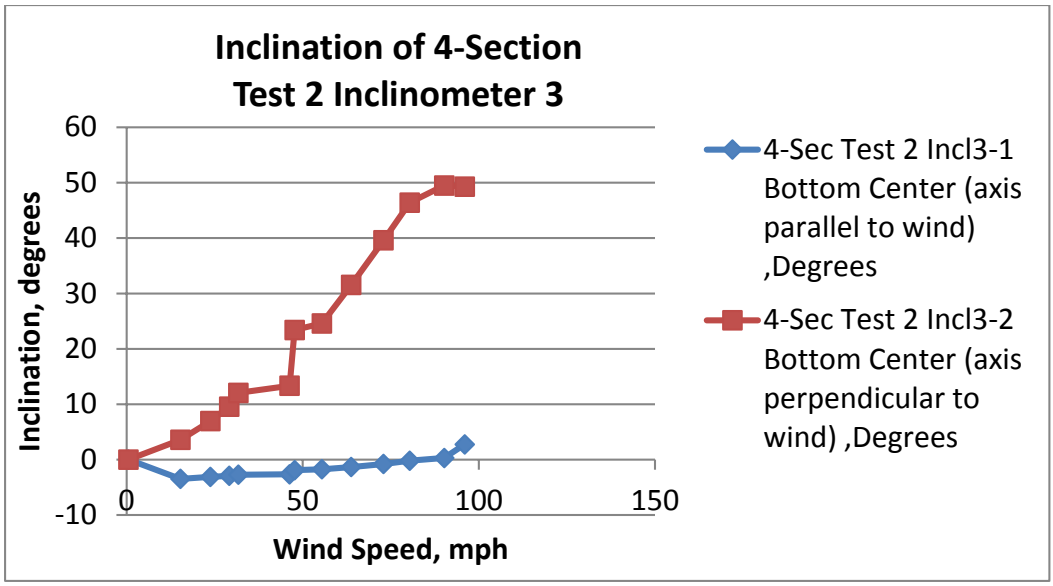

Figure 48: Inclination of 4-section traffic signal for Test 2 Inclinometer 3

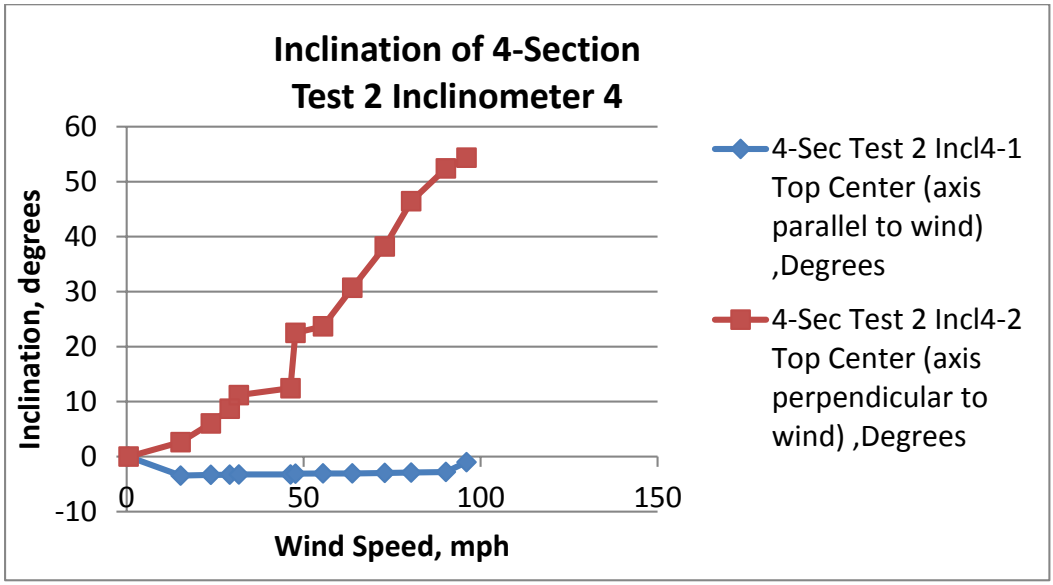

Figure 49: Inclination of 4-section traffic signal for Test 2 Inclinometer 4

3.3. Performance of Equipment and Hardware

As previously specified, in these tests there were two alternative traffic signal configurations that were tested. The first configuration tested was one 3-section traffic signal on the right side and one 5-section signal on the left side. The second configuration tested was one 3-section traffic signal on the right side and another in the center and one 4-section traffic signal on the left side. All traffic signals for both test configurations consisted of sand cast aluminum disconnect boxes and standard sand cast aluminum tri-stud adjustable hangers. It should be noted that the standard tri-stud adjustable signal hangers used in these tests were unable to be identified as FDOT/APL approved products. Before the tests the tri-stud adjustable hangers were inspected and they did not provide any evidence that the material met FDOT requirements. The disconnect boxes for the 3-sections and the 4-section traffic signals did not sustain any damage during Test 2 as shown in Figure 50 and Figure 51, respectively. Similarly, the 3-sections and the 4-section signals, including visors, did not sustain any noticeable damage during Test 2.

The only damage that occurred during Test 1 and Test 2 originated from the standard tri-stud adjustable hanger assembly utilized (Figure 52). These hangers were sheared off at the proximity of the connection brackets that are attached to the top of the disconnect box.

Based on manufacturer's recommendations the overlap of the long extension brackets on the bottom bracket was three thru holes down from the top of the bottom bracket with bolts inserted on the top two thru holes. The manufacturer recommended overlap resulted in the adjustable hanger failing sooner than when a maximum overlap was used in a "common sense" test conducted following test 2. Analysis and detailed results of this test will not be further reported here.

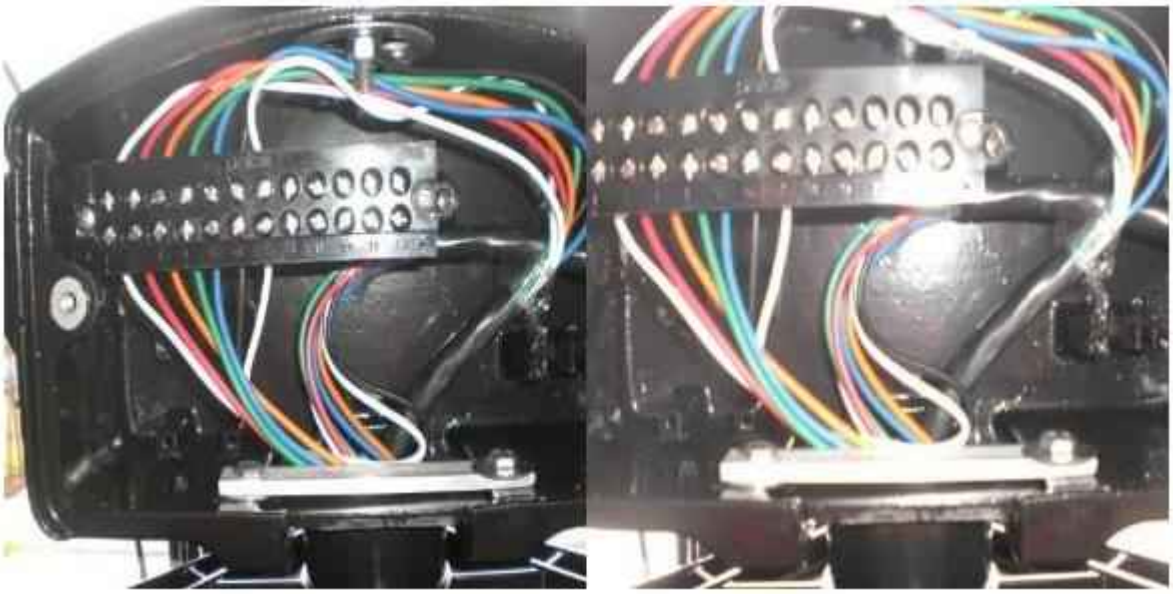

Figure 50: Disconnect box for 3-section signal after Test 2 showing no noticeable damage

Figure 51: Disconnect box for 4-section signal after Test 2 showing no noticeable damage

Figure 52: Tri-stud adjustable hanger after Test 2 showing location of damage. No noticeable damage to the aluminum messenger clamp. Sections of the bottom bracket that were sheared off

3.4. Discussion of Test Rig Performance and Future Enhancements

Following the test case 1 (see chapter 2) and test case 2 reported here, it was concluded that very high tensions were being generated in the messenger wire. This was attributed to the relatively short span of the test rig, 21.9 ft. The 21.9 ft span was selected so as to enable the entire rig to be mounted on the 16 ft diameter turntable and rotated to any desired angle without interference with surrounding WOW structure. In the field, where the span would be much longer the extensibility of the span wire plays a relatively larger role than in the rig and results in less tension increase. Therefore, a theoretical analysis of the relationship between lateral deflections of the span wires and the forces at the points of connection of the signals and hangers was undertaken. As a result of this analysis, which is provided in Appendix A, it was concluded that the same deflection-versus-force relationships as found in the field can be obtained by inserting springs of appropriate stiffness into the rig span-wires. It is to be noted that the deflection-versus-force relationships for the span wires are in general non-linear and are a function of the extensible stiffness of the wires. For example, at the mid-point of the messenger wire the relationship is

$$F_n = 4\frac{T_0}{L}x_n + 8\frac{EA}{L^3}x_n^3$$

where F_n = lateral force, T_0 = pretension of messenger wire, L = span length, E = modulus of elasticity for the wire, A = effective cross-sectional area of the wire, and x_n = lateral deflection at point of action of the force. In the test rig this same relationship is maintained if the coefficients of x_n and x_n^3 are kept the same. The coefficient of x_n is kept the same by reducing the initial tension T_0 in proportion to the span L. The coefficient of x_n^3 can be kept the same by introducing springs that have the same effect as reducing EA in proportion to L^3. For rig spans L_{RIG} that are much smaller than the span L_{FIELD} in the field (e.g. by a factor of 4), it is shown in Appendix A that to engineering accuracy the required spring stiffness k is given by

$$k = 2\left(\frac{L_{RIG}}{L_{FIELD}}\right)^3 \frac{EA_{FIELD}}{L_{RIG}}$$

where EA_{FIELD} is the EA value in the field.

Preliminary tests were undertaken with springs that were on hand using the second configuration of signals (one four signal unit and two three signal units). With the 50 lb/in springs that were on hand, it was calculated that a field span of 106 ft was simulated. The results confirmed the feasibility of using springs in the rig set-up. The rate of increase of messenger wire tensions with speed was considerably reduced and dynamic phenomena not seen before were revealed. Since the introduction of springs was not the initial objective of these tests the detailed results of the preliminary tests with springs will not be further reported here. However, a video recording of the dynamic response of the signals was provided to FDOT and it was decided to use springs in the future testing.

3.5. Summary, Conclusions and Recommendations

3.5.1. Summary

Two different traffic signal combinations were tested to determine the more susceptible of the two combinations. All traffic signals for both combinations were installed with aluminum tri-stud adjustable signal hangers. Both traffic signal combinations were tested at zero degrees. Cable tensions, accelerations and traffic signal inclinations were compared to assess the behavior of each signal combination. It was determined that there were higher cable tensions in the one 5-section and one 3-section signal combination causing failure at a lower wind speed, thus the more susceptible of the two signal combinations. This signal combination was decided on for future testing. Afterwards FDOT requested an additional 3-section signal to the base condition to reflect typical field installations more accurately. Therefore, the base condition will consist of one 5-section and two 3-section signals.

3.5.2. Conclusions

Test results revealed tension decreased in the catenary cable for test case 2 as wind velocity increased. There is initially a minor increase in the catenary cable tension up to a certain wind velocity but afterwards tension proceeds to decline. One observed difference in behavior between both signal combinations was that the second traffic signal combination tested experienced a decline in tension in the catenary cable sooner at a lower wind velocity. The opposite is the case for the messenger cable. Tension increased as wind velocity increased. Another difference between both signal combinations was that the second traffic signal combination experienced a greater magnitude in the final tension, before the end of the test, primarily because it resisted a larger wind velocity (see chapter 2 for results for 'test case 1'). All traffic signals showed larger deflection angles backwards than sideways as expected.

3.5.3. Recommendations

Following the review of the data acquired from both signal combinations tested, it was determined that tension in the catenary and messenger cables were excessive and under these test conditions the traffic signals were not behaving in the manner that they would be in the field under similar wind conditions. Attempting to lessen the excessive tension in the cables and simulate more realistic traffic signal behavior, springs with a stiffness of 50 Ibs/in were used in an independent test conducted on August 3, 2015. After examining the data, it was found that the tension in the cables was reduced and traffic signal behavior was more in tune with field conditions. Following an analysis, it was determined that in order to simulate a typical span of 80 ft in the field with 3/8-inch diameter catenary cable and 7/16-inch diameter messenger cable, springs with a stiffness of 100 Ibs/in and 145 Ibs/in respectively should be used in future tests.

Chapter 4 - Task 1a: FULL SCALE TESTING - Case 3

"Pivotal Adjustable Hanger Assembly with Disconnect Hanger/Signal Head Reinforcement Plates and with Aluminum Signal Housing" (vendor: Signal Safe) - Test Date: 11/17/2015

4.1. Introduction

In the first tasks of the current project a 'base' configuration was identified consisting of a 21.9 ft long section with two 3-section and one 5-section traffic signals (Task 1a – Cases 1 and 2). As a continuation of the study, FDOT tested the span wire traffic signal configurations connected to the catenary and messenger wires via a **"pivotal adjustable hanger assembly with disconnect hanger/signal head reinforcement plates, without reinforcement rod and with aluminum signal housing" (vendor: Signal Safe)**. The tests were carried out at wind directions ranging from 0 to 180 degrees and wind speeds ranging from 40 to 150 mph. The instruments consisted of loadcells to measure wind forces, accelerometers to measure accelerations, and inclinometers to measure the inclinations of the traffic signals.

This chapter presents the results from the tests conducted on the traffic signal assembly with **"pivotal adjustable hanger assembly with disconnect hanger/signal head reinforcement plates, without reinforcement rod and with aluminum signal housing" (vendor: Signal Safe)** at the WOW.

4.2. Methodology

4.2.1. Test Setup

The 3-3-5 signal assembly was installed on a short-span rig by means of a "pivotal adjustable hanger assembly with disconnect hanger/signal head reinforcement plates, without reinforcement rod and with aluminum signal housing" (vendor: Signal Safe). Figure 53 and Figure 54 show the signal assembly set up.

The test protocol is presented in Table 5 while the list of components and manufacturers used for this assembly are shown in Table 6.

4.2.2. Instrumentation

The directions of the x, y and z components for each loadcell are shown in Figure 55. The loadcells had 1500 lb capacity. Loadcells number 2 and 5 were located at either end of the messenger cable and loadcells number 1 and 4 located at either end of the catenary cable.

Tri-axial accelerometers were installed in the traffic signals to measure accelerations. There was one accelerometer placed on the center top of the signal, Accel5, another placed on the bottom right side, Accel002, and a third placed on the bottom left side, Accel003 for the 5-section signal as shown in Figure 56. Accelerometer Accel007, was installed on the top center, accelerometer Accel004, was installed on the bottom left side and accelerometer Accel006, was installed on the bottom right side of the 3-section signal as shown in Figure 57.

There was one inclinometer installed on the top center of the signal, Inc4, and another on the bottom center of the signal, Inc3, for the 5-section signal as shown in Figure 56. Inclinometer, Inc2, was installed on the top center and inclinometer, Inc1, was installed on the bottom center of the of the 3-section signal as shown Figure 57.

Wind speeds in three component directions (u,v,w) were also recorded by the Wall of Wind velocity sensors.

4.2.3. Test Method

The test set up was first tested for ‘zero wind’ conditions, and the values of the various ‘quantities’ (forces, accelerations and inclinations) obtained were later deducted from quantities obtained for different wind speeds (also known as “zero drift removal” process). Although erratic behavior, such as aerodynamic fluttering, may not cause an initial failure of the signal equipment, it may lead to additional testing to confirm this behavior will not cause failure of the equipment when experienced for long-term.

Table 5: Test protocol (Task 1a: Case 3)

Wind Speed (mph)	Wind Direction	Total Duration (min)
40	0, 45, 80, 100, 135, 180	6
70	0, 45, 80, 100, 135, 180	6
100	0, 45, 80, 100, 135, 180	6
110	0	1
120	0	1
130	0, 45, 80, 100, 135	5
150	0, 45, 80, 100, 135, 180	6
TOTAL		**31**

Table 6: Signal assembly components (Task 1a: Case 3)

Component	Manufacturer
Span wire clamp	Signal safe
Adjustable hanger	Signal safe
Extension bar	Pelco
Messenger clamp	Signal safe
Disconnect Hanger	Pelco
Signal Assembly	Signal safe
Backplate	Signal safe
Visor	Signal safe
LED Modules	Unknown

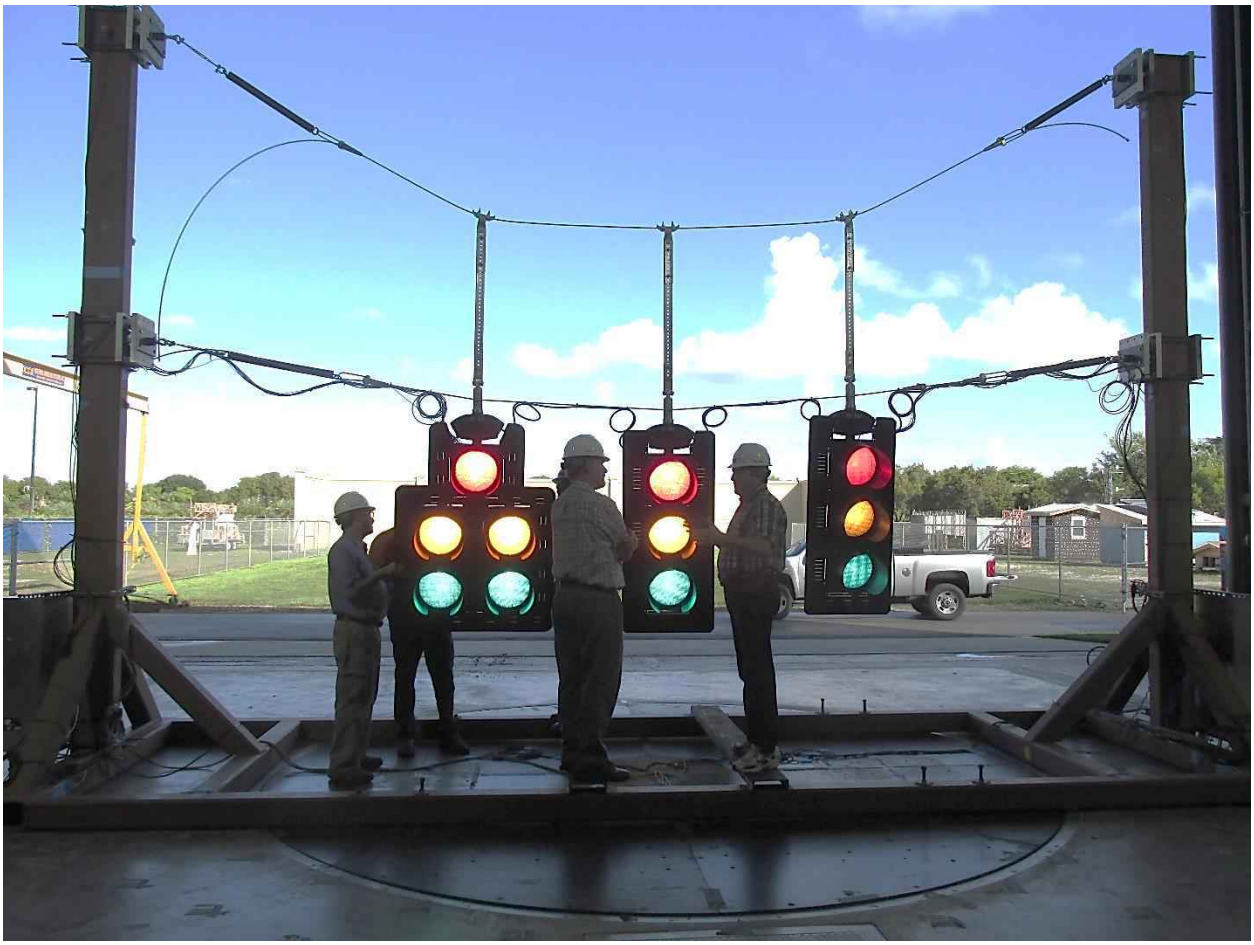

Figure 53: Picture of test rig frame with the signals

a)

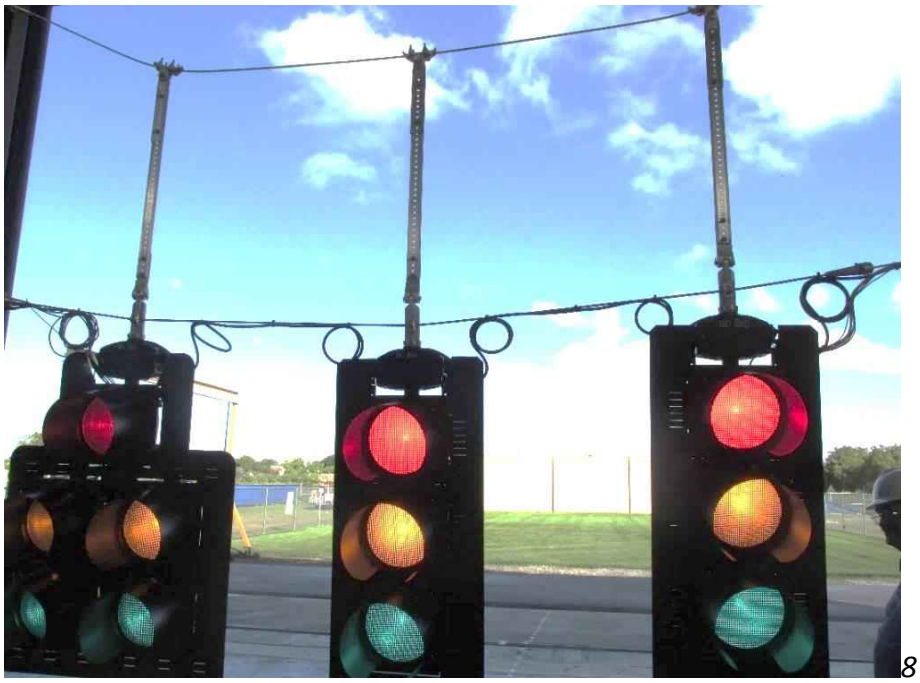

b)

Figure 54: Traffic signal set up: a) 3-section signal showing the pivotal adjustable hanger assembly with disconnect hanger/signal head reinforcement plates; b) traffic signal assembly facing the wind

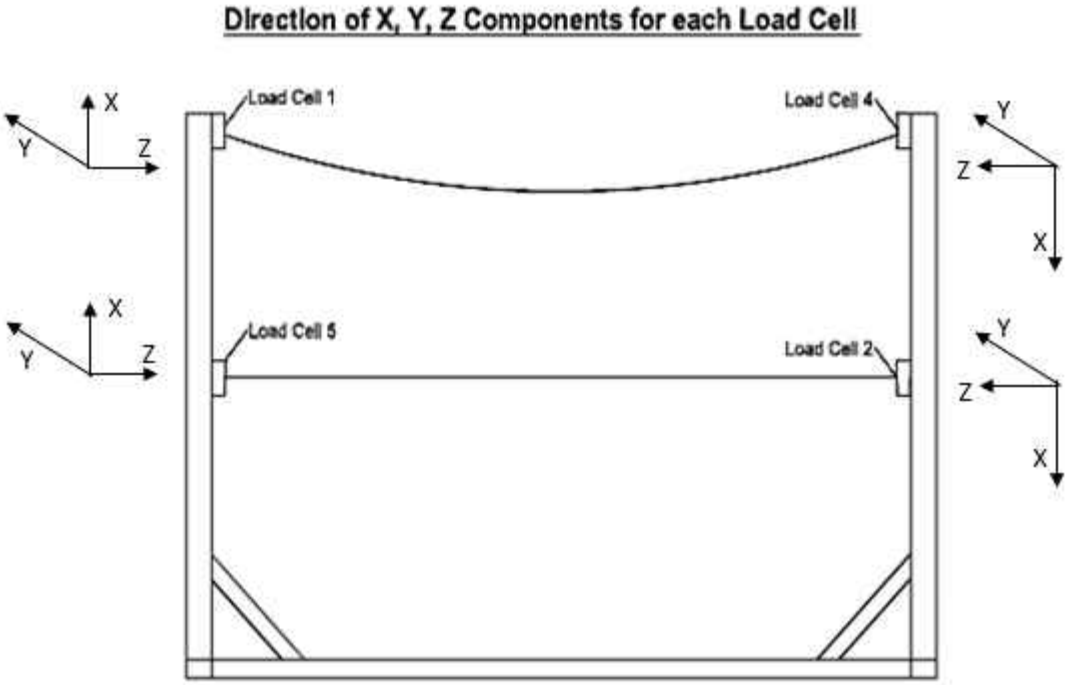

Figure 55: Direction of x, y, z components for each loadcell (direction of each axis shown represents 'positive direction')

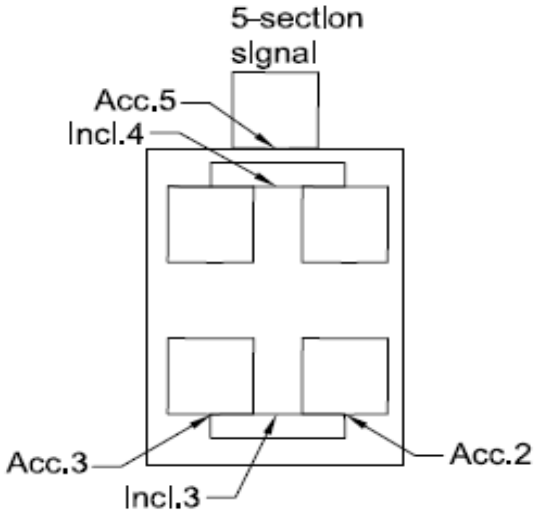

Figure 56: Location of accelerometers and inclinometers in 5-section signal

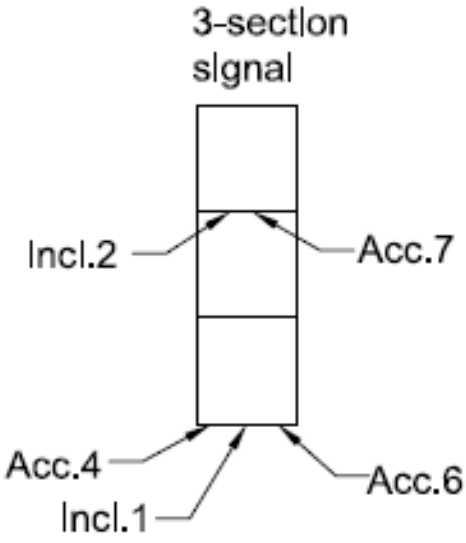

Figure 57: Location of accelerometers and inclinometers in 3-section signal

4.3. Test Results

The tests at the WOW were performed in the presence of the representatives from the Florida Department of Transportation (FDOT) Traffic Engineering and Operations Office and Traffic Engineering Research Lab (TERL), representatives from Signal Safe, installation technicians from Horsepower Electric Inc. and members of the WOW technical team. The results in this chapter are restricted to 0 degrees wind direction, with results for additional wind directions presented in appendix B.

4.3.1. Cable Tensions, Lift, Drag and Span Forces

The directions of the forces are shown in Figure 55. The mean and peak forces obtained at various wind speeds are discussed in this section. Figure 58 presents the wind induced mean forces on loadcell 2 (messenger wire) and loadcell 4 (catenary wire) at 0 degrees wind direction, for increasing wind speeds. It may be noted that the 'y' and 'z' components of the forces correspond to the 'drag' and 'cable tensions' respectively, while the 'x' component represents the uplift forces.

Data show that the along wind forces (Fy) increase with increasing wind speed at loadcell 2 (messenger wire), while Fy at loadcell 4 (catenary wire) experiences minimal change with increasing wind speeds. The highest along wind force of 220 lb was found at loadcell 2 at 150 mph. Similarly, the tension on loadcell 2 (Fz) increases in magnitude with increase in wind speed, although negligible change in tension on loadcell 4 for increasing wind speed was observed. This shows that the messenger wire experiences higher tension and drag than the catenary wire for increasing wind speeds. The uplift forces (Fx) on loadcell 2 (messenger wire) increases in magnitude with increase in wind speed. However negligible change in Fx on loadcell 4 (catenary wire) with increasing wind speed was observed.

Similar observations were made for loadcell 5 (messenger) and loadcell 1 (catenary) as shown in Figure 59. For instance, Fz (cable tension) and Fy (drag) increase with increasing wind speed on loadcell 5 (messenger wire). Fx on loadcell 5 also increases initially, but decreases slightly beyond 100 mph. A slight increase in Fy and Fx were observed at increasing wind speeds on loadcell 1 (catenary).

The peak forces at 0 degrees wind direction for loadcell 2 and loadcell 4 are shown in Figure 60. In this chapter, the highest magnitude of the peak forces is reported for a given wind speed, since this peak is critical for the safe wind design of the traffic signals. The peak forces of Fx, Fy and Fz on loadcell 2 increase with increasing wind speeds up to 100 mph, beyond which the peaks are somewhat reduced. Loadcell 4 also experienced an increase in forces for all components with increasing wind speed, but beyond 100 mph a slight decrease in forces were observed. In general, the messenger wire experienced higher peak forces than the catenary wire at a given wind speed. It may be noted that the 'positive direction' of 'Fx' component on loadcells 2 and 4 is 'downwards' (see Figure 55). Figure 61 presents results for loadcell 5 (messenger) and loadcell 1 (catenary). Fx (lift), Fy (drag) and Fz (cable tensions) on loadcell 5 (messenger wire) increase with increasing wind speeds up to 100 mph, beyond which the peaks reduce slightly. Results for additional wind directions are presented in appendix B.

Figure 62 (a) presents the 'total' mean drag and lift forces on the traffic signals. Results show that the drag on the traffic signals increase with an increase in wind speed – highest mean drag force of 545 lb was obtained at 150 mph at 0 degrees wind direction. The lift forces increase initially with increase in wind speed, although beyond 100 mph a nearly constant force of approximately 124 lb was obtained. The peak drag, and lift are shown in Figure 62 (b). Both the peak drag and lift forces increase with increasing wind speed up to 100 mph, beyond which the peak forces reduce.

4.3.2.Signal Accelerations

The root mean square (rms) of accelerations are presented in Figure 63. Accelerometers 4, 6 and 7 were located on the 3-section signal, while accelerometers 2, 3 and 5 were located on the 5-section signal (see Figure 56 and Figure 57). In general, the rms of accelerations obtained from all the accelerometers increase gradually with an increase in wind speed. Beyond 120 mph the accelerometers were removed to avoid damage due to violent oscillations.

4.3.3.Signal Inclinations

Figure 64 a) shows the mean inclinations, while peak inclinations are shown in Figure 64 for inclinations obtained from inclinometer 1 (3-section) and inclinometer 3 (5-section) at 0 degrees wind direction. It may be noted that for inclinometer 1, '1-1' refers to the component of inclination perpendicular to the wind, while '1-2' refers to the component of inclination in the direction of wind. Mean and peak components of inclination '1-2' at 40 mph were found to be 35 degrees and 45 degrees, respectively. The values of inclinations were negligible for 1-1 and 3-1 components. Beyond 70 mph, an erratic movement of the traffic signals (aerodynamic flutter) was observed, resulting in a wide range of inclinations.

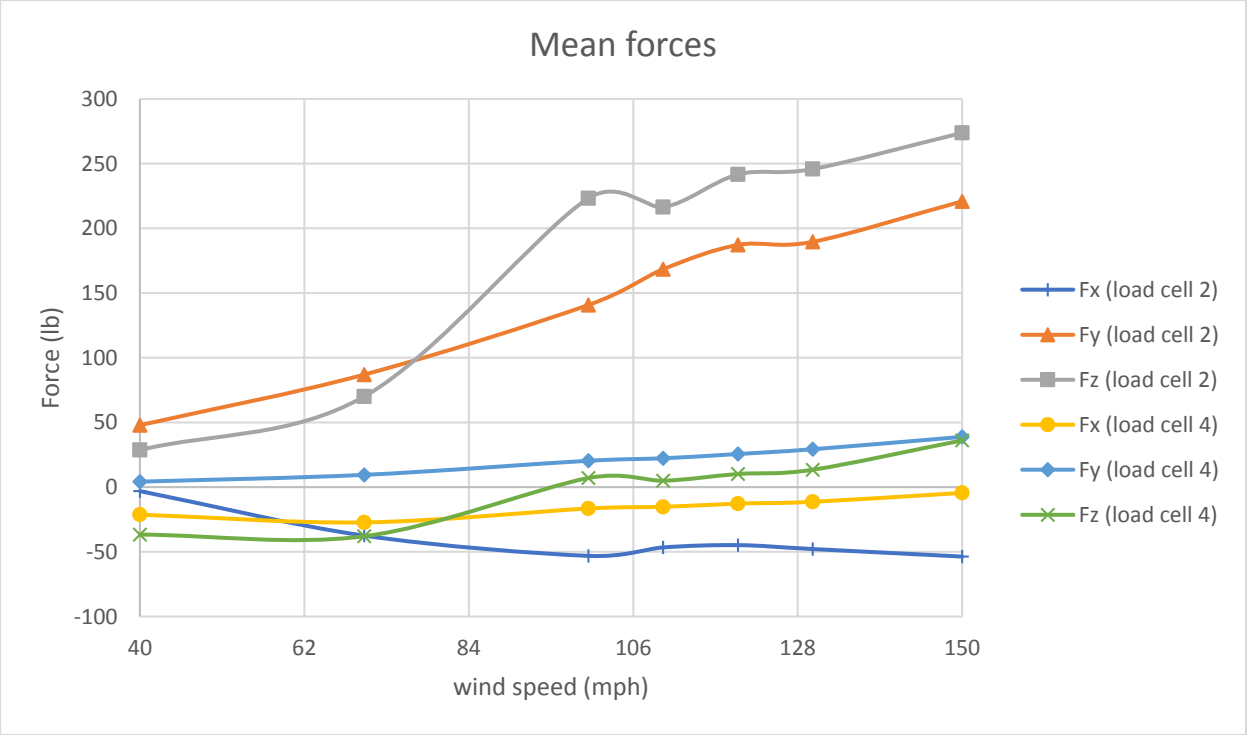

Figure 58: Mean forces on loadcells 2 (messenger wire) and 4 (catenary wire) at 0 degrees wind direction

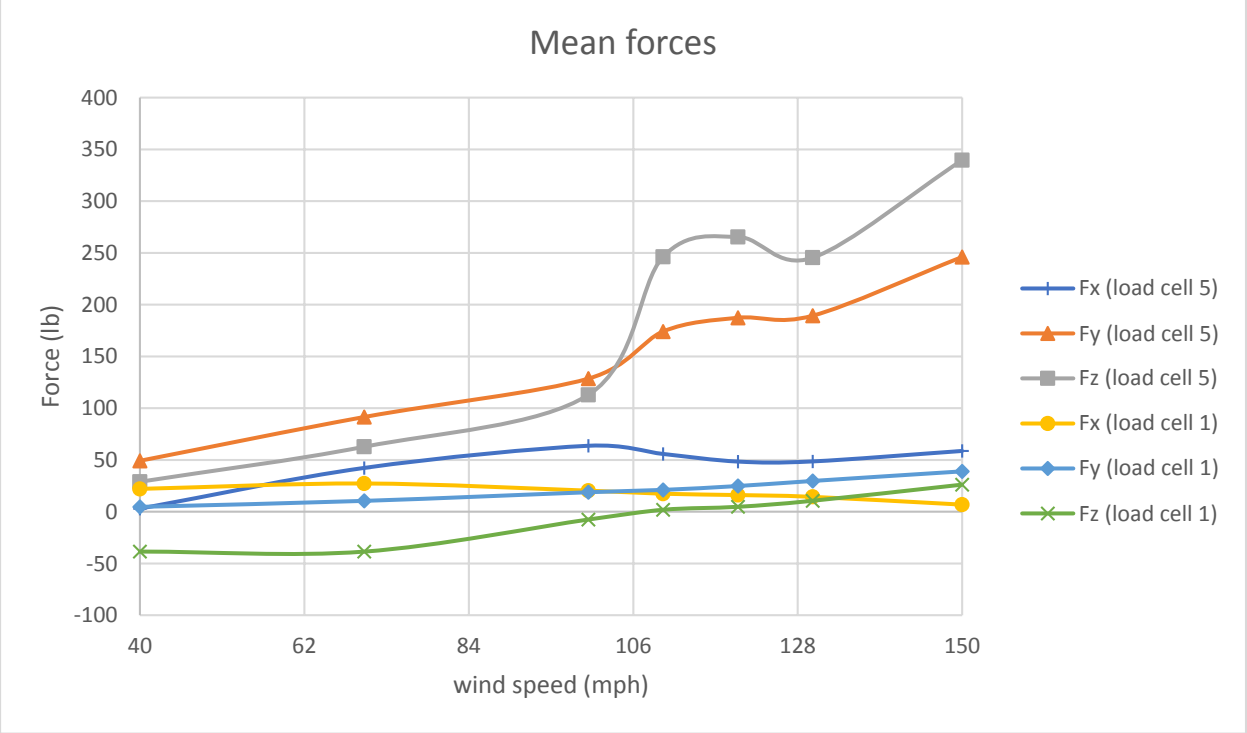

Figure 59: Mean forces on loadcells 1 (catenary wire) and 5 (messenger wire) at 0 degrees wind direction

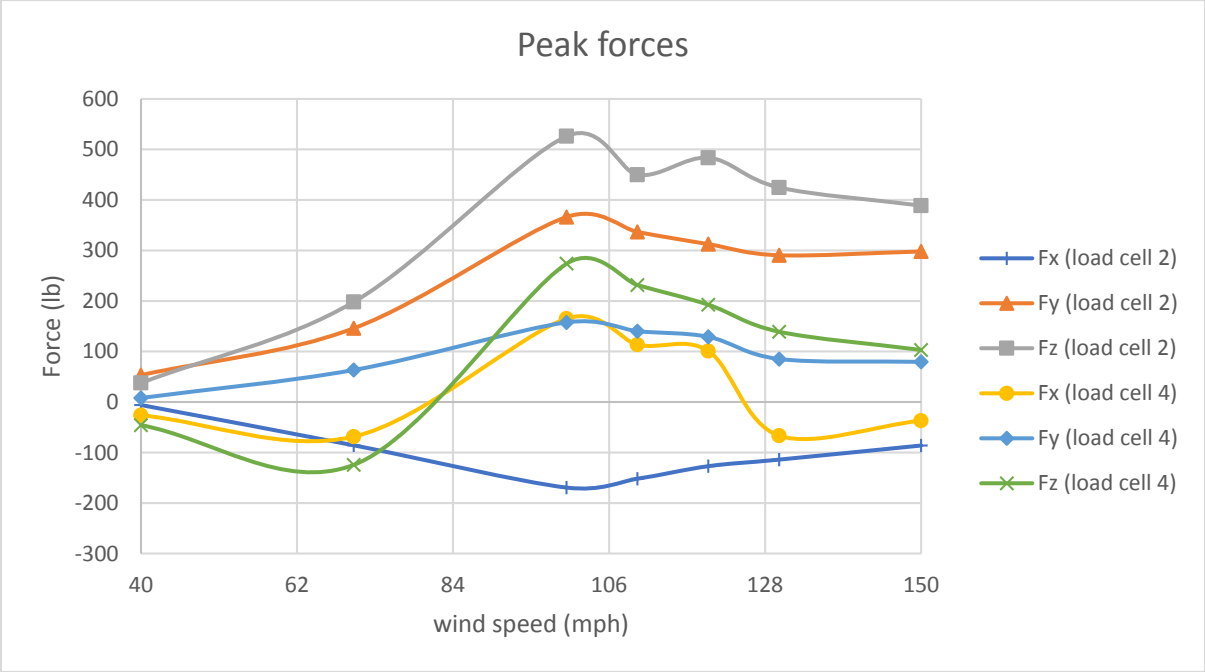

Figure 60: Peak forces at 0 degrees wind direction on loadcells 2 (messenger wire) and 4 (catenary wire)

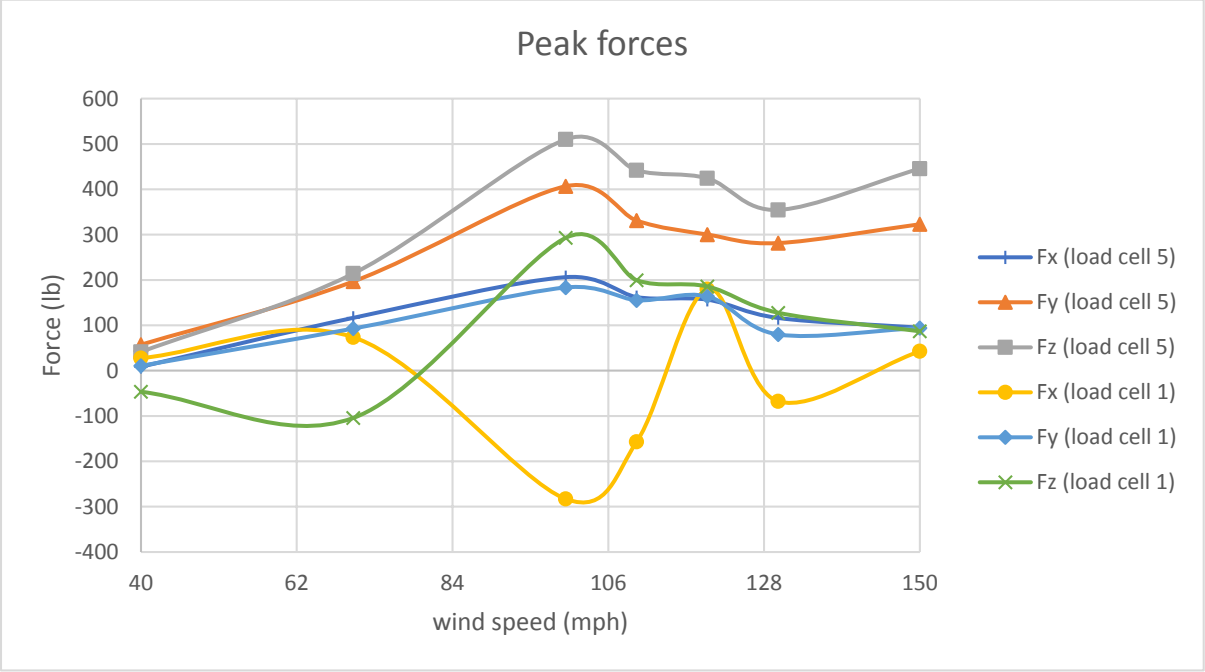

Figure 61: Peak forces at 0 degrees wind direction on loadcells 1 (catenary wire) and 5 (messenger wire)

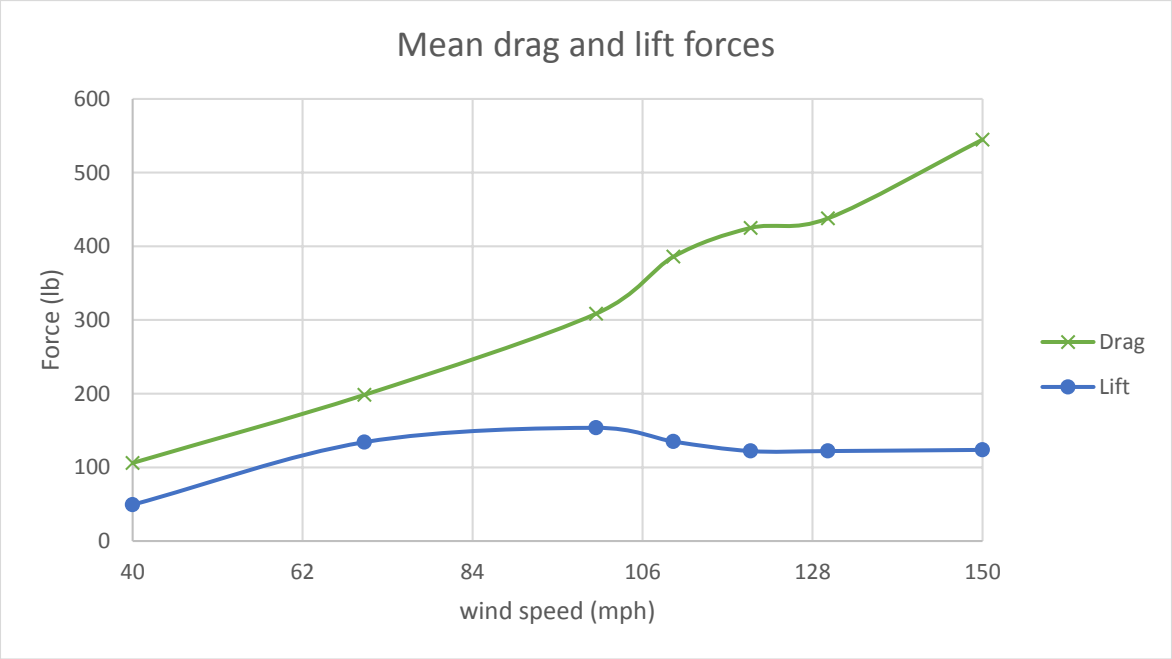

a)

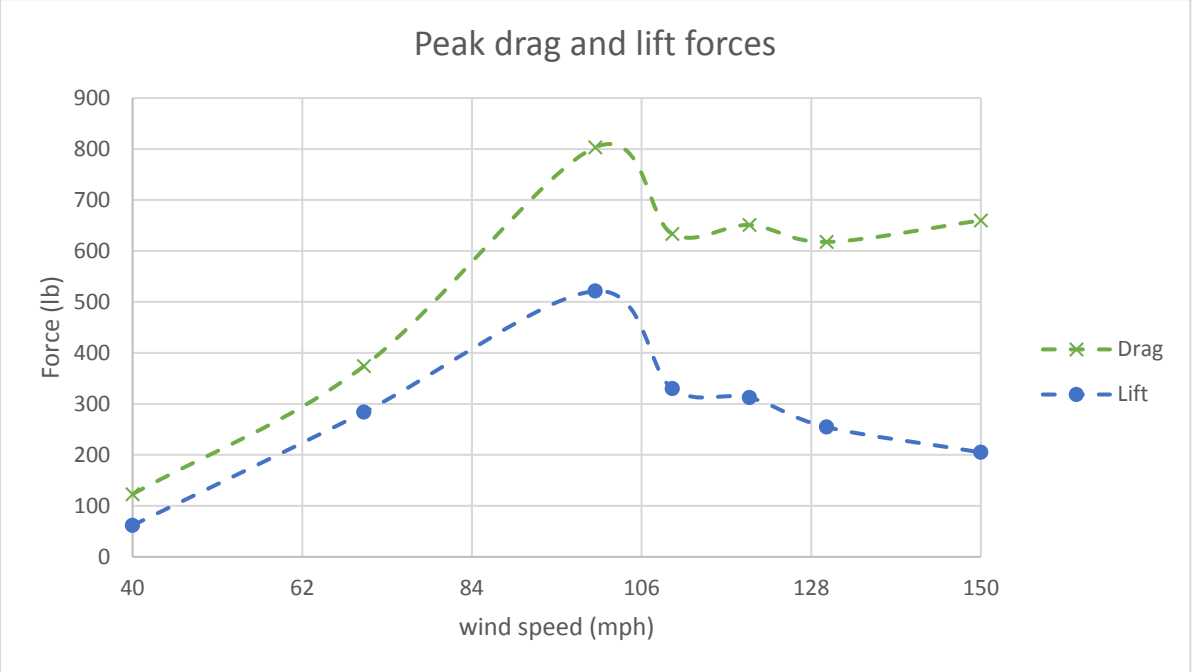

b)

Figure 62: Drag (Fy) and lift (Fx) forces on the traffic signals at 0 degrees: a) Mean; b) Peak

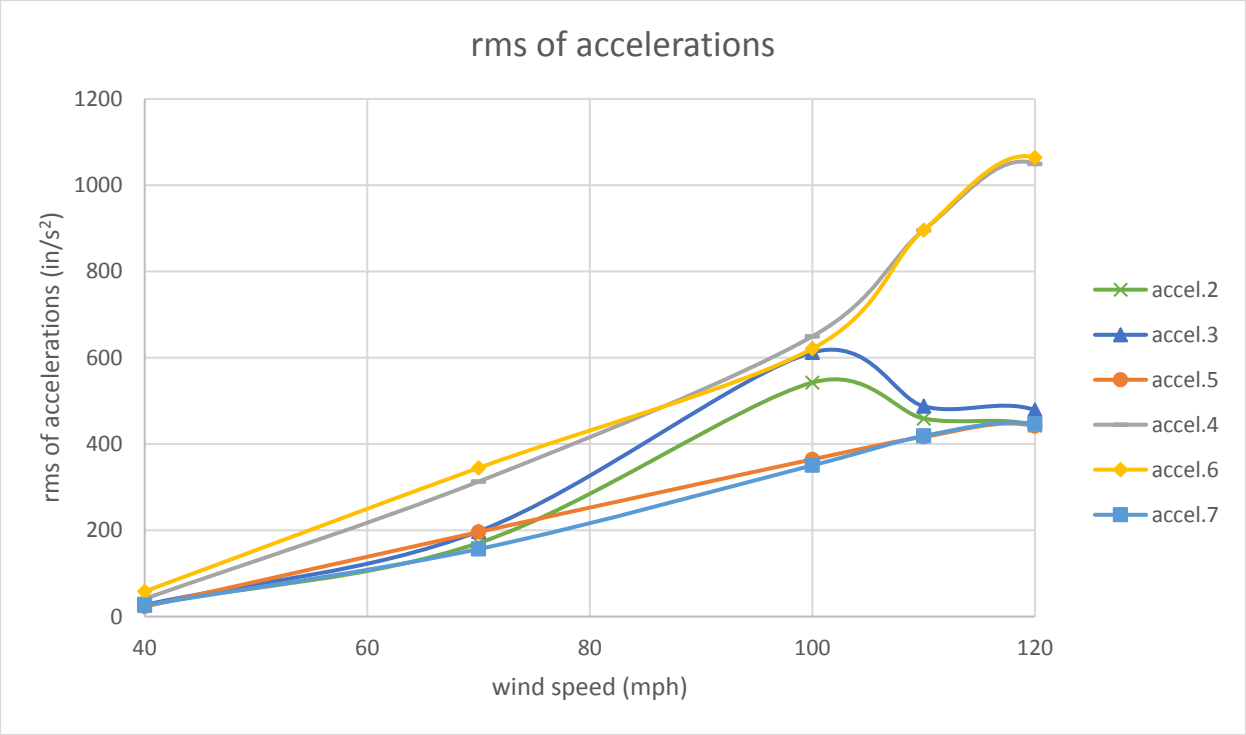

Figure 63: rms of accelerations on the 3-section and 5-section signals at 0 degrees

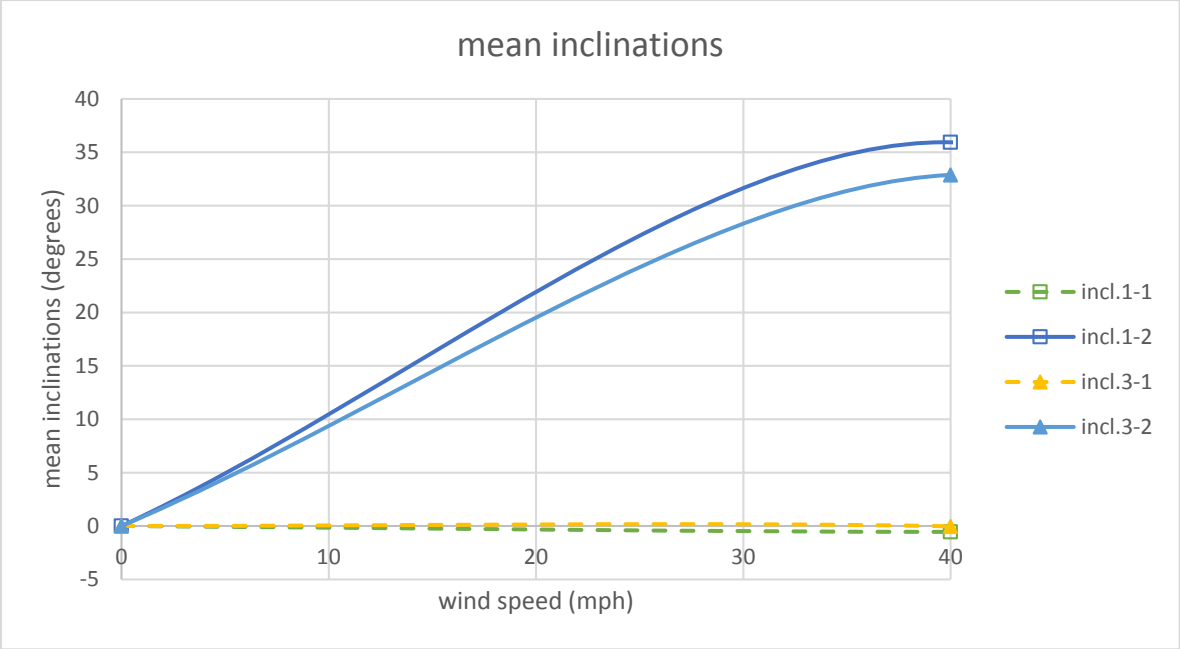

a)

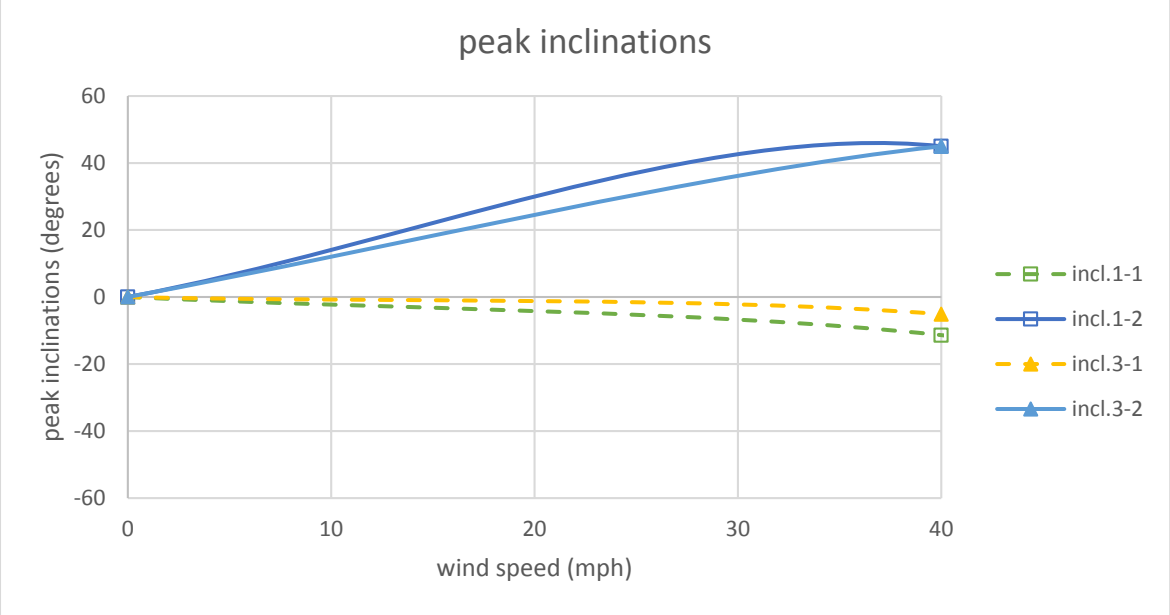

b)

Figure 64: Inclinations obtained at 0º for inclinometers 1 and 3: a) mean; b) peak

4.4. Performance of traffic signals during the tests

This test utilized two 3-section and one 5-section aluminum traffic signals installed in a span wire configuration connected to the catenary and messenger wires by means of a **"pivotal adjustable hanger assembly with disconnect hanger/signal head reinforcement plates, without reinforcement rod and with aluminum signal housing" (vendor: Signal Safe)**.

At 40 and 70 mph there was flexible bending of the pivotal portion of the adjustable hanger assembly but once the wind subsided the pivotal hanger assembly recovered from its bent position. At approximately 70 mph an erratic motion (aerodynamic flutter) of the traffic signals was observed.

More intense aerodynamic flutter was seen to occur at 100 mph. At this point the upper portions of the inside 3-section traffic signal back plate began to detach from the signal casing. At 100 mph and 45 degrees wind direction the 100 Ibs spring attached to the catenary wire came undone and test was temporarily stopped to reattach the spring and catenary wire to the support steel column. Once attached test was resumed at 100 mph and 80 degrees and finalized at 180 degrees. Following continuation of the test the upper portions of the back plates began to detach from the signal housings of both the 5-section and 3-section signals. At this point all visors remained attached.

Test continued to 130 mph through the full range of wind directions and the 5-section and 3-section signal back plates continued to detach from the signal housing and eventually flew away from the 5-section signal housing. It is important to note that at 130 mph and 0 degrees the 5-section signal began to rotate about the pivotal adjustable hanger assembly. It was later observed that the serrated teeth on the bracket connected above the disconnect box, as well at the serrated teeth on the disconnect box, was worn away allowing the rotation of the 5-section signal. This is seen in Figure 65 and Figure 66. A picture of the disconnect box is shown in Figure 67. Permanent bending also occurred right above the pivotal section of the 5-section signal hanger assembly at approximately 130 mph.

The disconnect box z portion of the hanger as seen in Figure 68. A summary of the observed damages is as follows:

- Damage to signal hanger: pivotal adjustable hanger assembly sheared off.
- Damage to disconnect hanger (box): serrated teeth on the bracket connected above the disconnect box, as well at the serrated teeth on the disconnect box, was worn away No other permanent visual damage observed.
- Damage to signal housing assembly: Damage to visors and back plate.

Figure 65: Bracket above disconnect teeth

Figure 66: Disconnect box with worn way serrated box with worn away serrated teeth

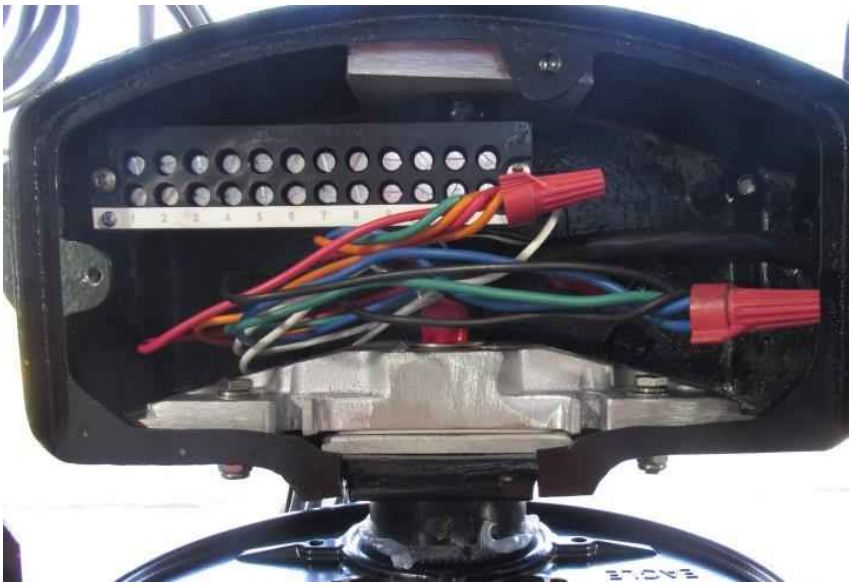

Figure 67: Disconnect box after test

Figure 68: Pivotal adjustable hanger sheared off above pivotal portion

4.5. Conclusions

This chapter summarizes the results of a test conducted at WOW at FIU for a span wire traffic signal assembly consisting of two 3-section and a 5-section traffic signal, connected using **"pivotal adjustable hanger assembly with disconnect hanger/signal head reinforcement plates, without reinforcement rod and with aluminum signal housing" (vendor: Signal Safe)**. Wind speeds were varied from 40 to 150 mph and wind directions were varied from 0 to 180 degrees. The various instruments used for this test include: loadcells to measure forces, accelerometers to measure accelerations and inclinometers to measure the inclinations. This study reports the data for different wind directions, in terms of: wind induced forces (drag (y-component), lift (x-component) and cable tension (z-component)), rms of accelerations and inclinations. Results for 0 degrees wind direction indicate that the total mean drag increases with increasing wind speed. The total mean lift increases initially with increasing wind speed, but becomes nearly constant beyond 100 mph. For any given wind speed, the messenger wire experienced higher cable tensions and drag than the catenary wire. The rms of accelerations increased with increasing wind speed from 40 mph to 120 mph. Similar observations were made for other wind directions (see appendix B). The magnitudes of the peak drag/lift forces increased with increasing wind speeds from 40 to 100 mph, beyond which the forces dropped. A mean inclination of 35 degrees and peak inclination of 45 degrees was observed at 40 mph. Beyond 70 mph, an erratic movement of the signals was observed (aerodynamic flutter). A failure was observed with the 5-section signal at 130 mph and 0 degrees, where the signal began to rotate about the pivotal hanger assembly vertical axis. It was later seen that what caused the rotation was worn away serrated teeth on the bracket above the disconnect box as well as on the disconnect box. Damage was also observed on the pivotal adjustable hanger assembly as it sheared off just above the pivotal portion of the hanger at 150 mph. Portions of back plates began to detach from the signal housing at around 100 mph subsequently worsening as speeds increased.

Chapter 5 - Task 1a: FULL SCALE TESTING - Case 4

"Pivotal Adjustable Hanger Assembly with Disconnect Hanger Reinforcement Rod, Disconnect Hanger/Signal Head Reinforcement Plates and with Aluminum Signal Housing" (vendor: Signal Safe) - Test Date: 11/17/2015

5.1. Introduction

In the first tasks of the current project a 'base' configuration was identified consisting of a 21.9 ft long section with two 3-section and one 5-section traffic signals (Task 1a – Cases 1 and 2). As a continuation of the study, FDOT tested the span wire traffic signal configurations connected to the catenary and messenger wires via a **"pivotal adjustable hanger assembly with disconnect hanger reinforcement rod, disconnect hanger/signal head reinforcement plates and with aluminum signal housing" (vendor: Signal Safe)**. The tests were carried out at wind directions ranging from 0 to 180 degrees and wind speeds ranging from 40 to 150 mph. The instruments consisted of loadcells to measure wind forces, accelerometers to measure accelerations, and inclinometers to measure the inclinations of the traffic signals.

This chapter presents the results from the tests conducted on the traffic signal assembly using a **"pivotal adjustable hanger assembly with disconnect hanger reinforcement rod, disconnect hanger/signal head reinforcement plates and with aluminum signal housing" (vendor: Signal Safe)** at the WOW. Additional results are presented in appendix C.

5.2. Experimental methodology

5.2.1. Test Setup

The 3-3-5 signal assembly was installed on a short-span rig by means of a "pivotal adjustable hanger assembly with disconnect hanger reinforcement rod, disconnect hanger/signal head reinforcement plates and with aluminum signal housing" (vendor: Signal Safe). Figure 69 and Figure 70 show the traffic signal assembly as well as the pivotal adjustable hanger assembly.

The test protocol is presented in Table 7. Table 8 shows the list of components used for this signal assembly.

5.2.2. Instrumentation

The directions of the x, y and z components for each loadcell are shown in Figure 71. Loadcells number 2 and 5 were located at either end of the messenger cable and loadcells number 1 and 4 located at either end of the catenary cable.

Tri-axial accelerometers were installed in the traffic signals to measure accelerations. There was one accelerometer placed on the center top of the signal, Accel5, another placed on the bottom right side, Accel002, and a third placed on the bottom left side, Accel003 for the 5-section signal as shown in Figure 72. Accelerometer Accel007, was installed on the top center, accelerometer Accel004, was installed on the bottom left side and accelerometer Accel006, was installed on the bottom right side of the 3-section signal as shown in Figure 73.

There was one inclinometer installed on the top center of the signal, Inc4, and another on the bottom center of the signal, Inc3, for the 5-section signal as shown in Figure 72. Inclinometer, Inc2, was installed on the top center and inclinometer, Inc1, was installed on the bottom center of the of the 3-section signal as shown Figure 73.

Wind speeds in three component directions (u,v,w) were also recorded by the Wall of Wind velocity sensors.

5.2.3. Test Method

The test set up was first tested for ‘zero wind’ conditions, and the values of the various ‘quantities’ (forces, accelerations and inclinations) obtained were later deducted from quantities obtained for different wind speeds (also known as “zero drift removal” process). Although erratic behavior, such as aerodynamic fluttering, may not cause an initial failure of the signal equipment, it may lead to additional testing to confirm this behavior will not cause failure of the equipment when experienced for long-term.

Table 7: Test protocol (Task 1a: Case 4)

Wind Speed (mph)	Wind Direction	Total Duration (min)
40	0, 45, 80, 100, 135, 180	6
70	0, 45, 80, 100, 135, 180	6
100	0, 45, 80, 100, 135, 180	6
130	0, 45, 80, 100, 135, 180	6
150	0, 45, 80, 100	4
TOTAL		**28**

Table 8: Components of signal assembly (Task 1a: Case 4)

Component	Manufacturer
Span wire clamp	Signal safe
Adjustable hanger	Signal safe
Extension bar	Pelco
Messenger clamp	Signal safe
Disconnect Hanger	Pelco
Signal Assembly	Signal safe
Backplate	Signal safe
Visor	Signal safe
LED Modules	Unknown

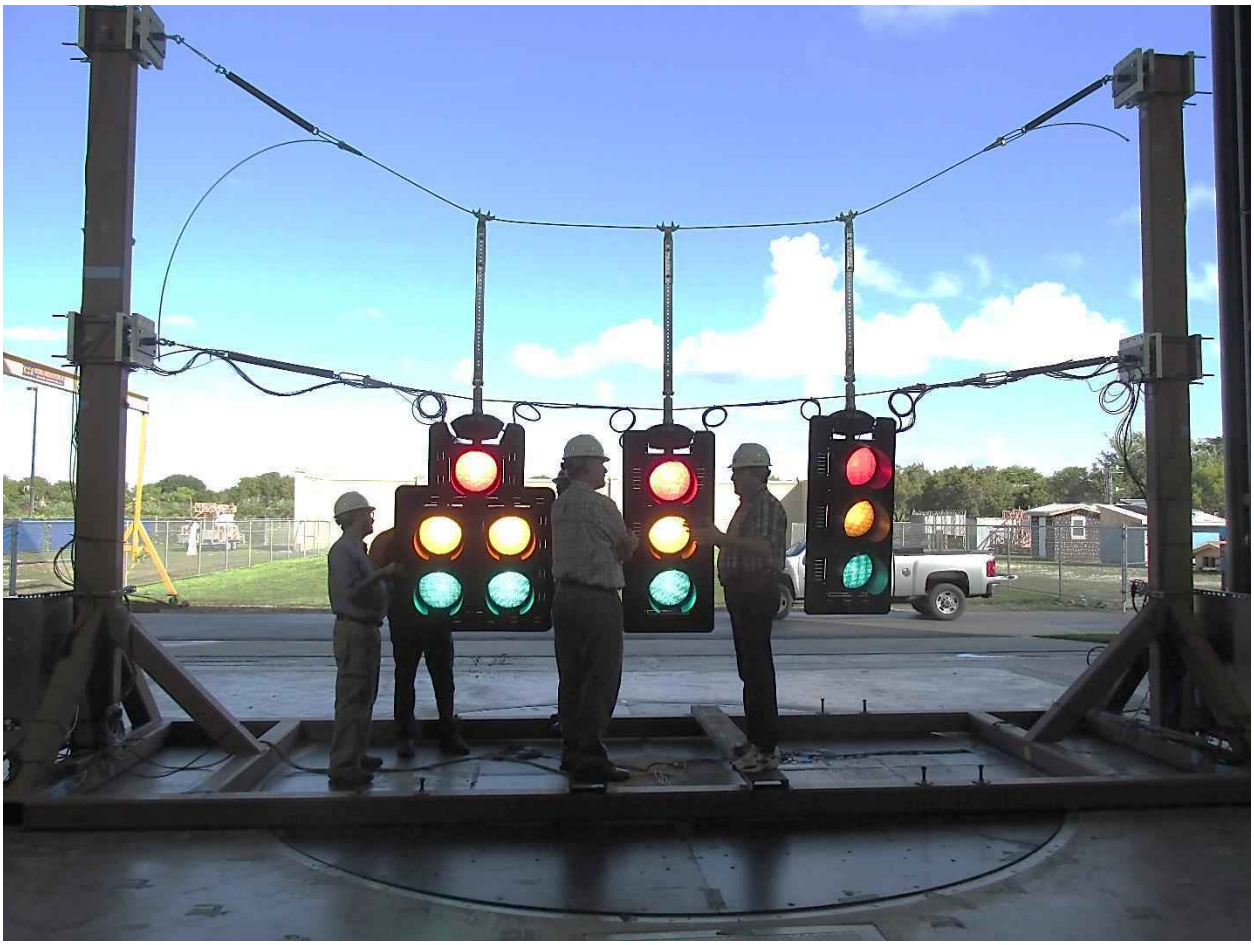

Figure 69: Picture of test rig frame with the signals

a)

b)

Figure 70: Traffic signal set up: a) 3-section signal showing the pivotal adjustable hanger assembly with disconnect hanger reinforcement rod and disconnect hanger/signal head reinforcement plates; b) traffic signal assembly facing the wind

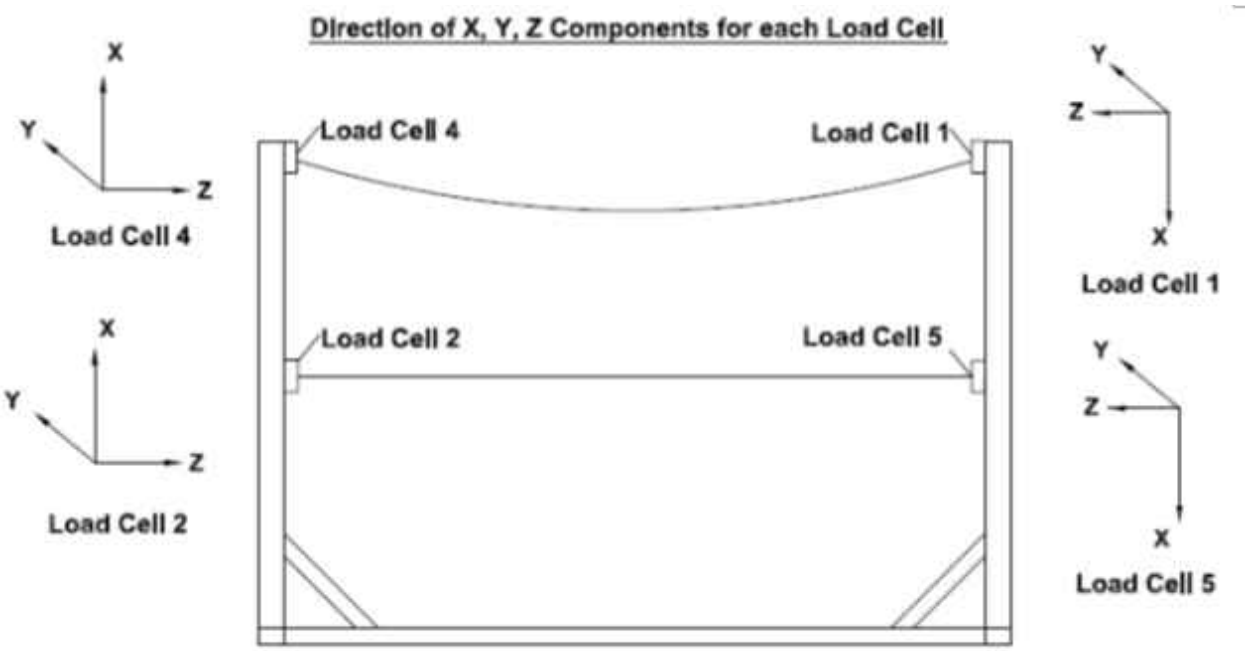

Figure 71: Direction of x, y, z components for each loadcell (direction of each axis shown represents 'positive direction')

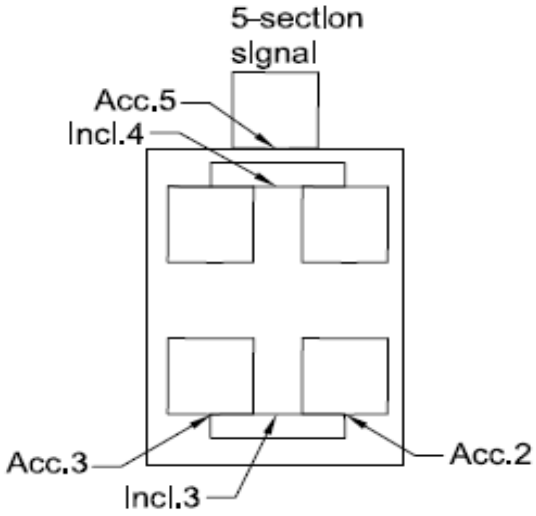

Figure 72: Location of accelerometers and inclinometers in 5-section signal

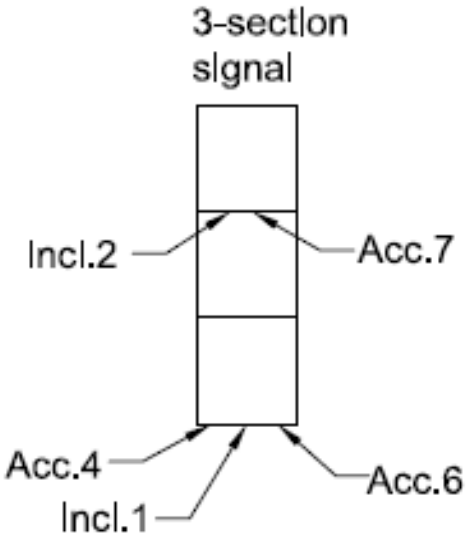

Figure 73: Location of accelerometers and inclinometers in 3-section signal

5.3. Results and discussion

The tests at the WOW were performed in the presence of the representatives from the Florida Department of Transportation (FDOT) Traffic Engineering and Operations Office and Traffic Engineering Research Lab (TERL), representatives from Signal Safe, installation technicians from Horsepower Electric Inc. and members of the WOW technical team. The results in this chapter are restricted to 0 degrees wind direction, with results for additional wind directions presented in appendix C.

5.3.1. Wind induced forces

The directions of the forces are shown in Figure 71. The mean and peak forces obtained at various wind speeds are discussed in this section. Figure 74 presents the wind induced mean forces on loadcell 2 (messenger wire) and loadcell 4 (catenary wire) at 0 degrees wind direction, for increasing wind speeds. It may be noted that the 'y' and 'z' components of the forces correspond to the 'drag' and 'cable tensions' respectively, while the 'x' component represents the uplift forces.

Data show that the along wind forces (Fy) increase with increasing wind speed at loadcell 2 (messenger wire), while Fy at loadcell 4 (catenary wire) experiences minimal change with increasing wind speeds. The highest along wind force of 267 lb was found at loadcell 2 at 150 mph. Similarly, the tension on loadcell 2 (Fz) increases with an increase in wind speed, although negligible change in tension on loadcell 4 (catenary wire) for increasing wind speed was observed. This shows that the messenger wire experiences higher tension and drag than the catenary wire for increasing wind speeds. The uplift forces (Fx) on loadcell 2 (messenger wire) increases in magnitude with increase in wind speed. However negligible change in Fx on loadcell 4 (catenary wire) with increasing wind speed was observed.

Similar observations were made for loadcell 5 (messenger) and loadcell 1 (catenary) as shown in Figure 75. For instance, Fz (cable tension) and Fy (drag) increase with increasing wind speed on loadcell 5 (messenger wire). Fx on loadcell 5 also remains relatively constant at wind speeds greater than 100 mph. Negligible changes in Fx, Fy and Fz were observed for increasing wind speeds on loadcell 1 (catenary).

The peak forces at 0 degrees wind direction for loadcell 2 and loadcell 4 are shown in Figure 76. It may be mentioned that only the highest magnitudes of peak forces for a given wind speed are reported since these values are needed for the safe wind design. The peak forces of Fz on loadcell 2 increases with increasing wind speeds up to 130 mph, beyond which it drops slightly. The peak forces of Fz on loadcell 4 also increases with increasing wind speed, but reduces slightly beyond 130 mph. The peak forces of Fy and Fx on loadcell 2 increases with an increase in wind speed, but decreases slightly beyond wind speed of 130 mph. The forces in the messenger wire are generally higher than the catenary wire at a given wind speed. Figure 77 presents results for loadcell 5 (messenger) and loadcell 1 (catenary). Fz (cable tension) on loadcell 5 increases with increasing wind speeds, although Fz on loadcell 1 experiences an increase beyond 100 mph. Fx and Fy on loadcell 5 (messenger) increase with increasing wind speed up to wind speed of 130 mph, beyond which the forces drop slightly.

Results for additional wind directions are presented in appendix C. Figure 78 (a) presents the 'total' mean drag and lift forces on the traffic signals. Results show that the drag and the lift on the traffic signals increase with an increase in wind speed up to 130 mph; beyond wind speed of 130 mph the lift force is nearly constant. The peak drag and lift are shown in Figure 78 (b). Both the peak drag and lift forces increase with increasing wind speeds, although beyond 130 mph both the drag and lift forces drop slightly.

5.3.2. rms of accelerations

The root mean squares (rms) of accelerations are presented in Figure 79. Accelerometers 4, 6 and 7 were located on the 3-section signal, while accelerometers 2, 3 and 5 were located on the 5-section signal (see Figure 72 and Figure 73). In general, the rms of accelerations obtained from all the accelerometers increase gradually with an increase in wind speed. Beyond 100 mph the sensors were removed to avoid damage.

5.3.3. Inclinations of the traffic signals

Figure 80 shows the inclinations (mean and peak) obtained from various inclinometers at 0 degrees wind direction. It may be noted that '1-1' refers to the component of inclination perpendicular to the wind, while '1-2' refers to the component of inclination in the direction of

wind. At 40 mph, the highest mean inclination of 40 degrees and highest peak inclination of 45 degrees was recorded. The values of inclinations were negligible for components of inclination perpendicular to wind, in the wind speed range of 0-40 mph. At 70 mph and beyond, an erratic movement of the traffic signals (aerodynamic flutter) was observed, resulting in a wide range of inclinations.

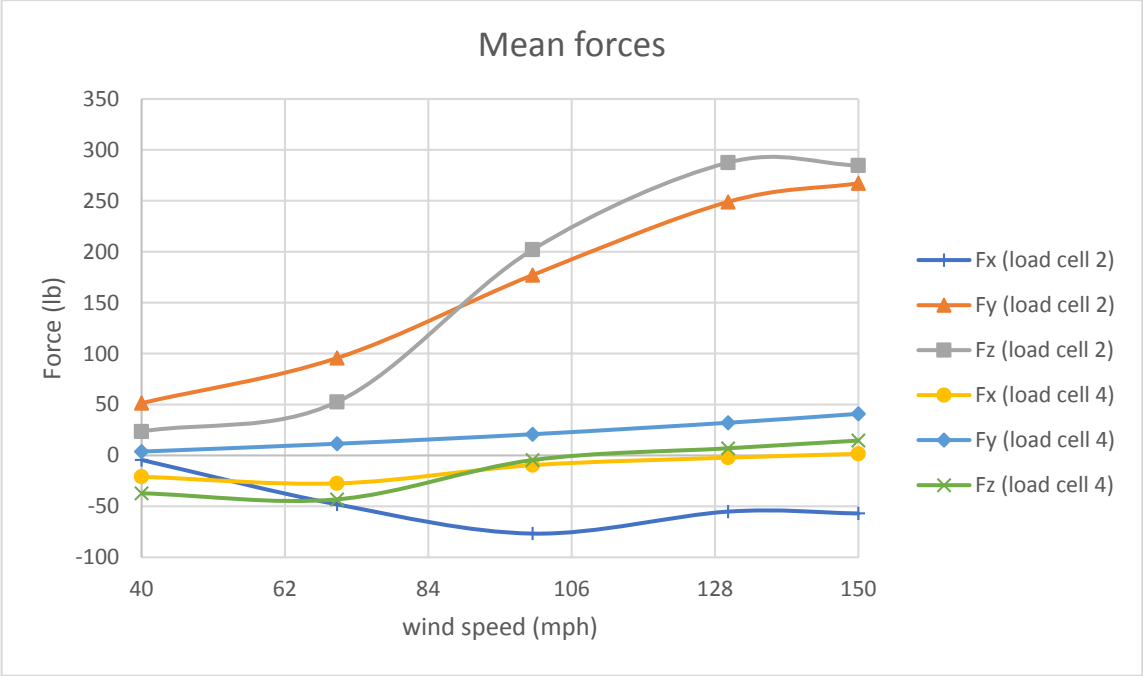

Figure 74: Mean forces on loadcells 2 (messenger wire) and 4 (catenary wire) at 0 degrees wind direction

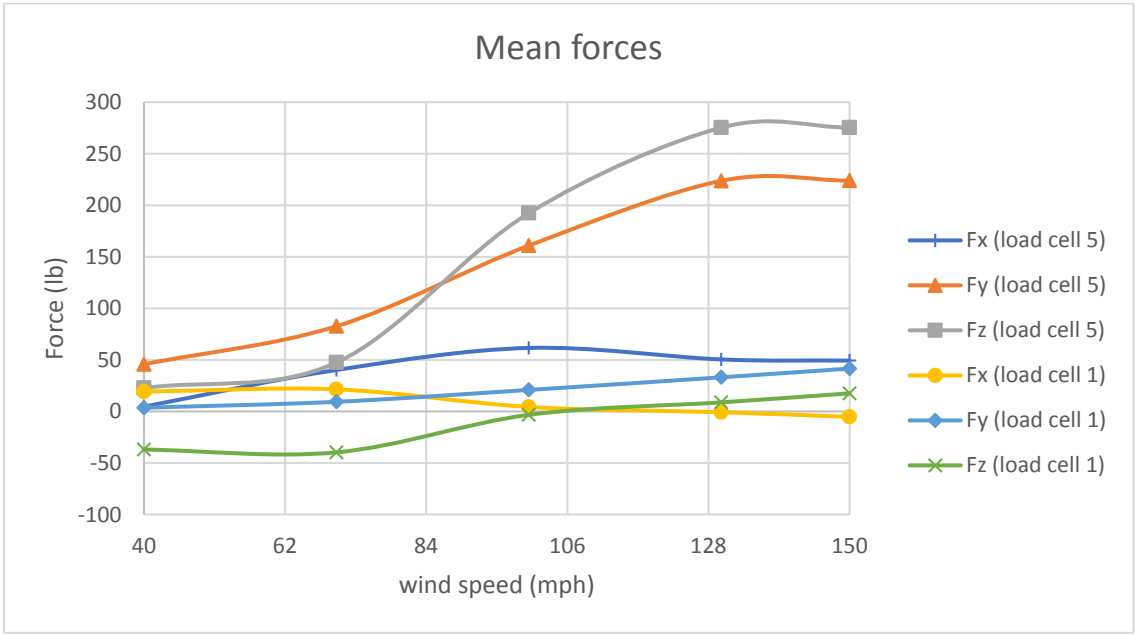

Figure 75: Mean forces on loadcells 1 (catenary wire) and 5 (messenger wire) at 0 degrees wind direction

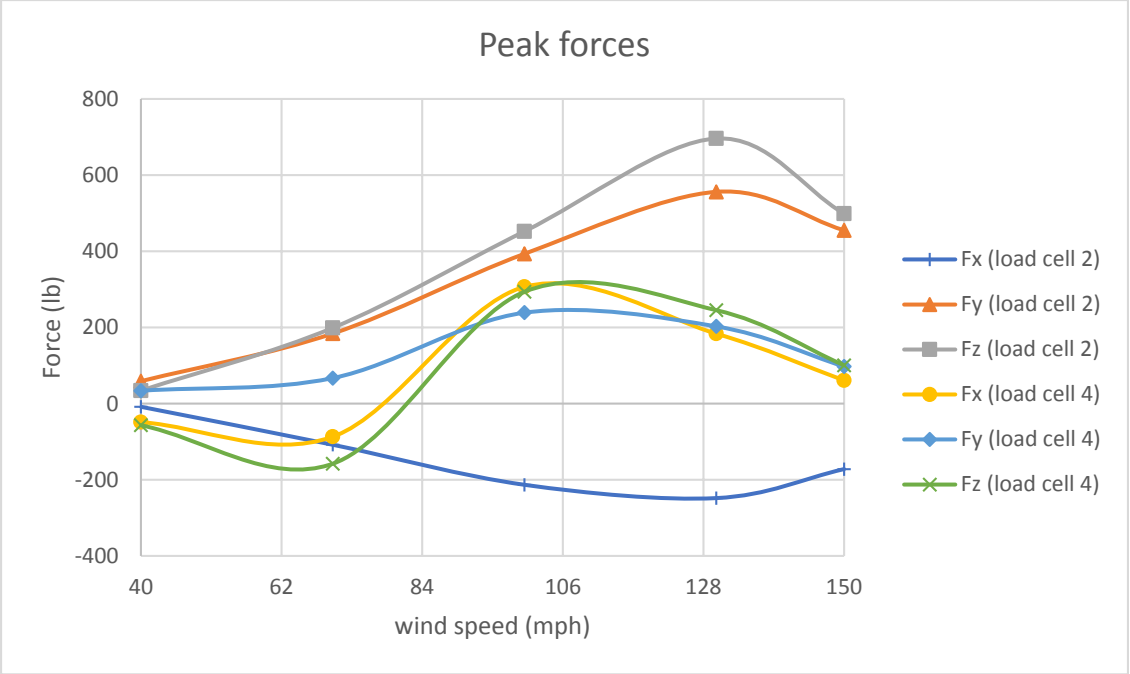

Figure 76: Peak forces at 0 degrees wind direction on loadcells 2 (messenger wire) and 4 (catenary wire)

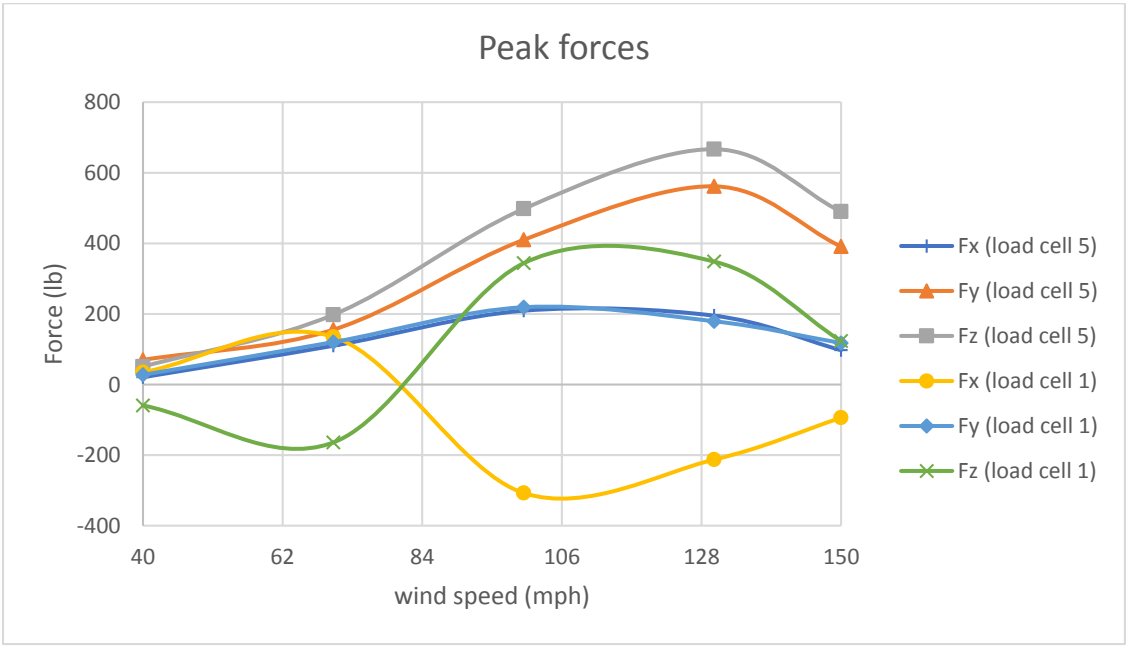

Figure 77: Peak forces at 0 degrees wind direction on loadcells 1 (catenary wire) and 5 (messenger wire)

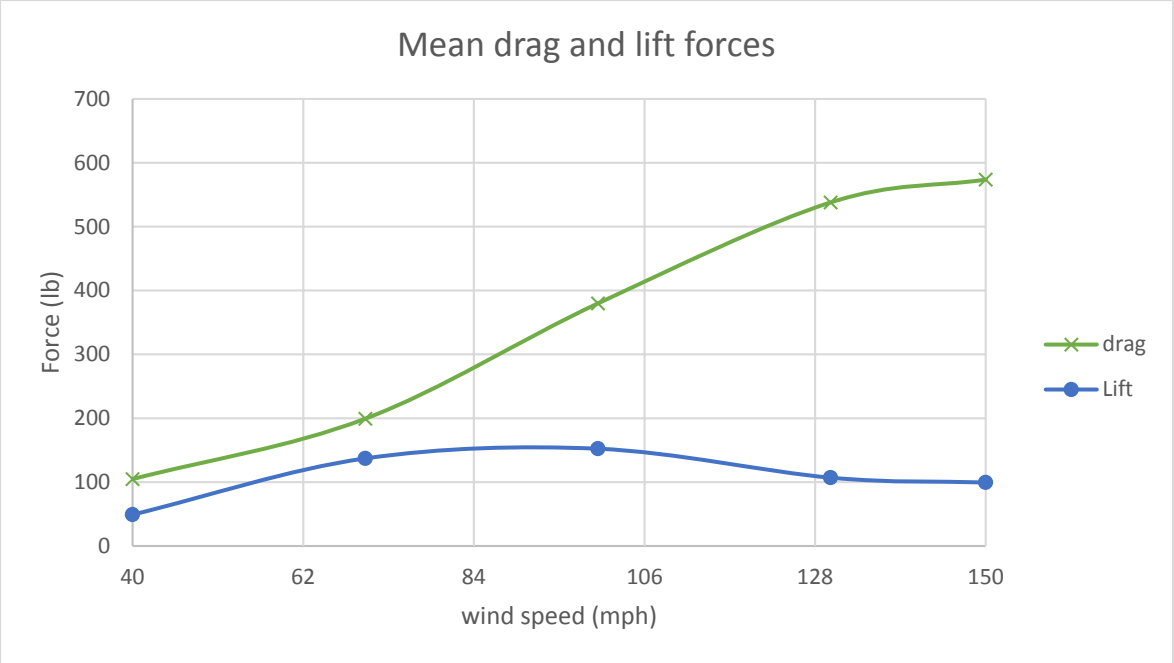

a)

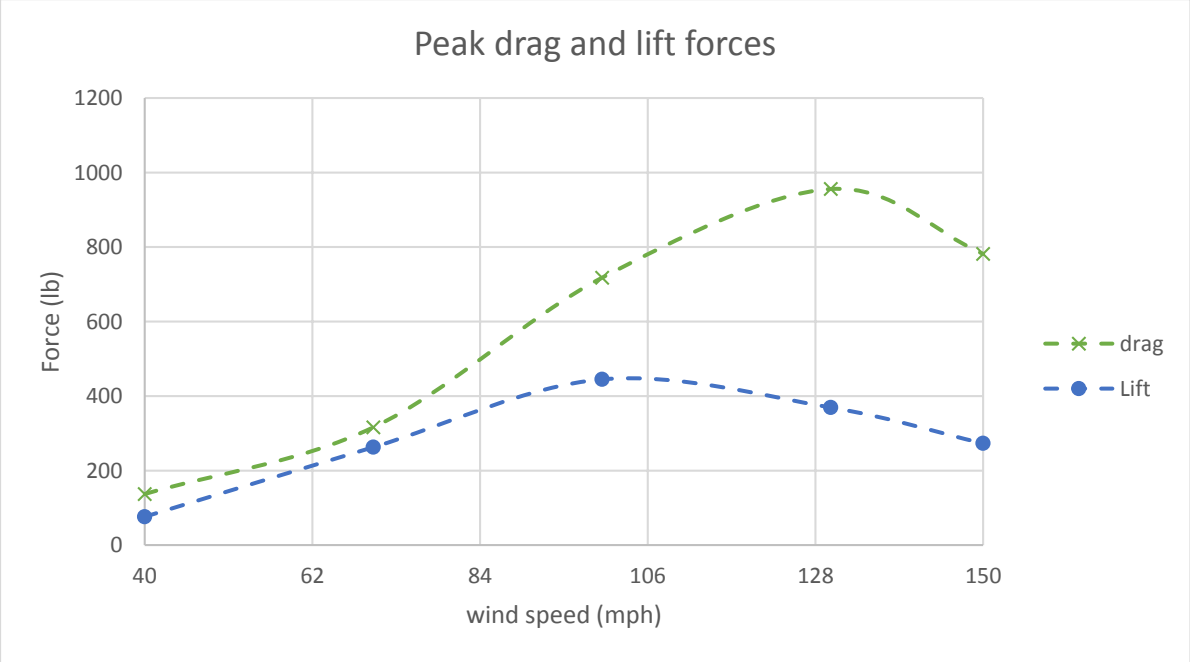

b)

Figure 78: Drag (Fy) and lift (Fx) forces on the traffic signals at 0 degrees: a) Mean; b) Peak

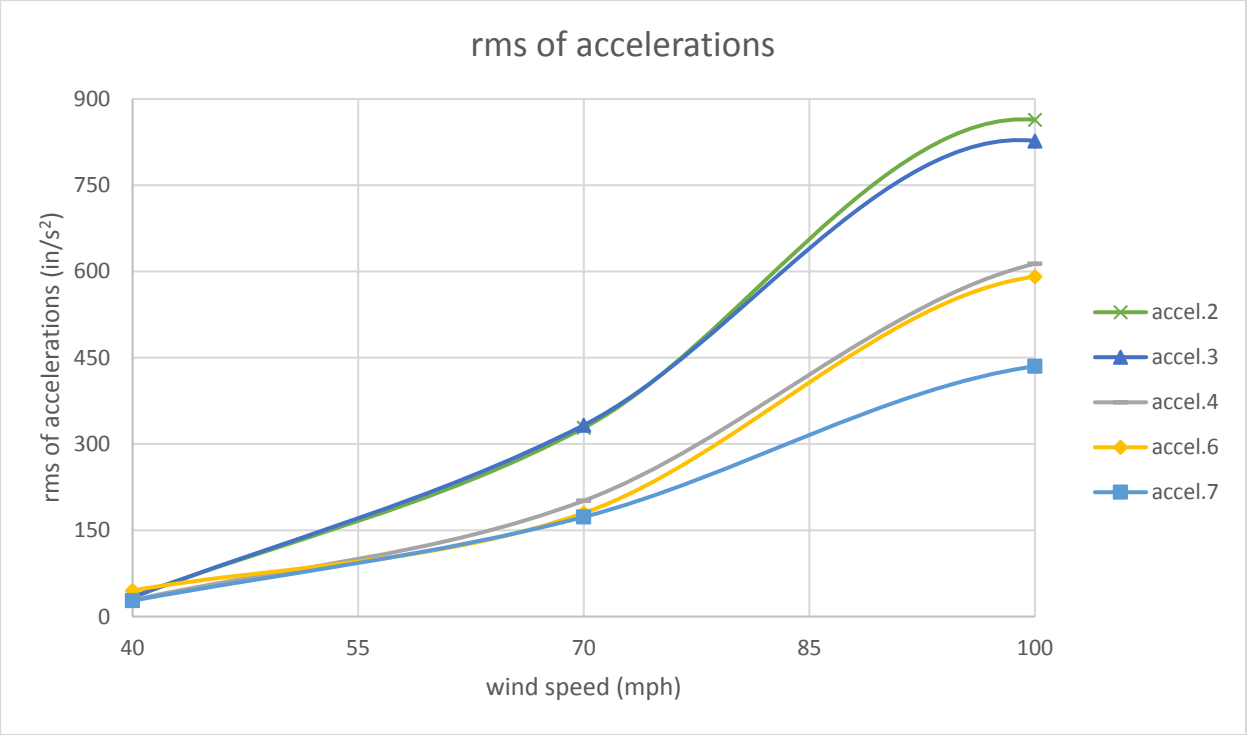

Figure 79: rms of accelerations on the 3-section and 5-section signals at 0 degrees

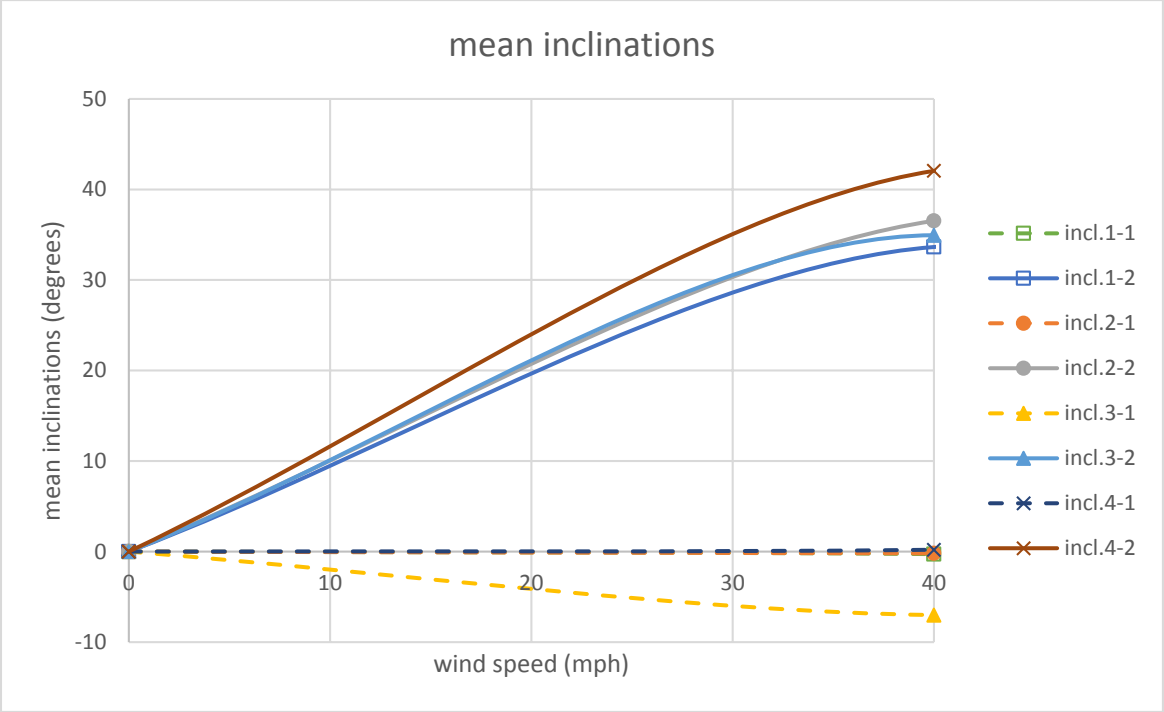

a)

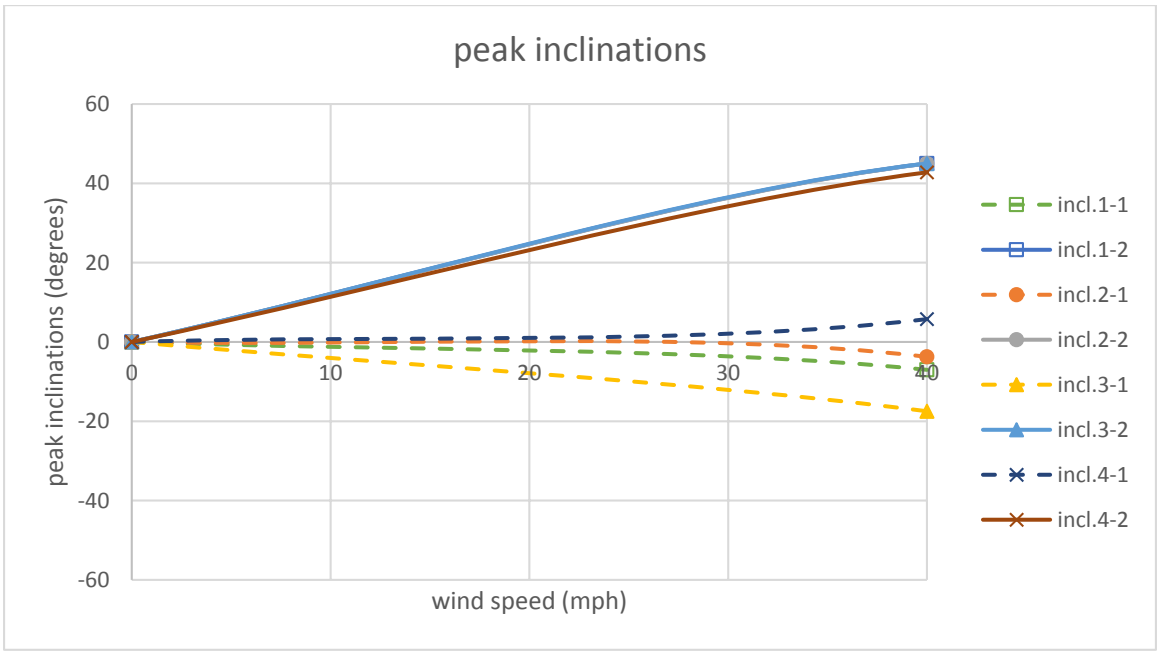

b)

Figure 80: Inclinations obtained at 0 degrees from inclinometers: a) mean; b) peak

5.4. Performance of traffic signals during the tests

This test utilized two 3-section and one 5-section aluminum traffic signals installed in a span wire configuration connected to the catenary and messenger wires by means of a **"pivotal adjustable hanger assembly with disconnect hanger reinforcement rod, disconnect hanger/signal head reinforcement plates and with aluminum signal housing" (vendor: Signal Safe)**.

At 40 and 70 mph there was bending, backward and forward position for all wind directions except at 80 and 100 degrees, of the pivotal segment of the hanger assembly but once the wind subsided the pivotal hanger recovered from its bent position and traffic signal returned to its original vertical position. Although¸ at approximately 70 mph an erratic motion (aerodynamic flutter), with a higher intensity at 0- and 180-degree wind direction, of the traffic signals was observed.

More intense aerodynamic flutter was seen to occur at 100 mph. At this point the upper portions of the 5-section and center 3-section traffic signal back plates began to detach from the signal housing. At 100 mph and 180-degree wind direction, the lower portion of the 5-section signal, consisting of four LED lights, rotated about the vertical center axis. Afterwards it was observed that the lower rotation of the signal was caused by depleted serrated teeth at the connection of the tri-stud elbow and upper LED light.

Test continued to 130 mph through the full range of wind directions and the 5-section and 3-section signal back plates continued to detach from the signal housing and eventually flew away. Aerodynamic flutter of the signals and rotation of the lower section of the 5-section signal was more powerful to a point where the 5-section and the 3-section signal began to collide with each other. Also, at 130 mph and 0-degree wind direction it is first noticed that there was twisting about the longitudinal axis of the adjustable extension hanger, presumably caused by the violent rotation of the lower portion of the 5-section signal. This is seen in Figure 81. Figure 82 shows signal assembly after full wind speed test.

The 5-section signal disconnect box exhibited a crack at the lower section of the box after the full range of wind speed test. Disconnect box for 5-section signal after the completion of the full test is shown in Figure 83. A summary of the observed damages is as follows:

- Damage to signal hanger: Twisted adjustable extension hanger for 5-section signal.
- Damage to disconnect hanger (box): A crack was observed at the lower section of the box.
- Damage to signal housing assembly: Damage to visors and back plate. No other permanent visual damage observed.

Figure 81: Twisted adjustable extension hanger for 5-section signal

Figure 82: Signal assembly after full wind speed test

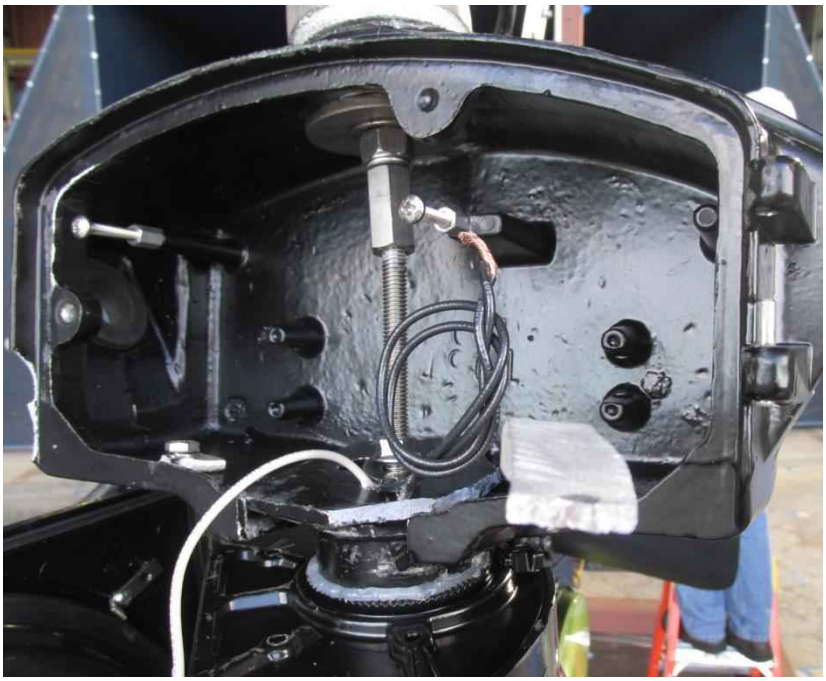

Figure 83: Disconnect box for 5-section signal after the completion of test

5.5. Conclusions

This chapter summarizes the results of a test conducted at WOW at FIU for a span wire traffic signal assembly consisting of two 3-section and a 5-section traffic signal, connected using a **"pivotal adjustable hanger assembly with disconnect hanger reinforcement rod, disconnect hanger/signal head reinforcement plates and with aluminum signal housing" (vendor: Signal Safe)**. Wind speeds were varied from 40 to 150 mph and wind directions were varied from 0 to 180 degrees. The various instruments used for this test include: loadcells to measure forces, accelerometers to measure accelerations and inclinometers to measure the inclinations. This study reports the data for different wind directions, in terms of: wind induced forces (drag (y-component), lift (x-component) and cable tension (z-component)), rms of accelerations and inclinations. Results for 0 degrees wind direction indicate that along wind forces (drag) and cable tensions generally increase in the messenger wire with increase in wind speed. The lift on the messenger wire increases only marginally with increasing wind speeds at 0 degrees. The catenary wire experiences only a minor increase of all three components of wind forces with increase in wind speed. At any given wind speed the messenger wire experiences higher tension forces than the catenary wire. In general, the rms of accelerations increased with increasing wind speeds. Similar observations were made for other wind directions (see appendix C). In the range of 0-40 mph for 0 degrees wind direction, the highest mean inclination in the along wind direction was found to be 40 degrees, while the highest peak inclination was found to be 45 degrees. Beyond 70 mph, an erratic movement of the signals was observed (aerodynamic flutter). A failure was observed with the 5-section signal at 100 mph and 180-degree wind direction, whereby the lower sector of the signal, which incorporates the four lower LED lights, was rotating about the longitudinal axis of the signal. It was later seen that it was attributed to deteriorated serrated teeth at the junction of the tri-stud elbow and upper LED light. Damage was also first observed on the adjustable extension hanger at 130 mph and 0-degree wind direction, when it twisted about the longitudinal axis of the hanger. This was apparently caused by violent rotation of the lower segment of the 5-section signal. The lower section of the disconnect box for the 5-section signal was observed to have sustained a crack when observed at the end of the test.

Chapter 6 - Task 1a: FULL SCALE TESTING - Case 5

"Steel Cable Hanger Assembly with Reinforced Disconnect Hanger and with Aluminum Signal Housing" (vendor: Engineered Castings) - Test Date: 3/1/2016

6.1. Introduction

In the first tasks of the current project a 'base' configuration was identified consisting of a 21.9 ft. long section with two 3-section and one 5-section traffic signals (Task 1a – Cases 1 and 2). As a continuation of the study, FDOT tested the span wire traffic signal configurations connected to the catenary and messenger wires via a **"steel cable hanger assembly with reinforced disconnect hanger and with aluminum signal housing" (vendor: Engineered Castings).** The tests were carried out at wind directions ranging from 0 to 180 degrees and wind speeds ranging from 40 to 150 mph. The instruments consisted of loadcells to measure wind forces, accelerometers to measure accelerations, and inclinometers to measure the inclinations of the traffic signals.

It may be noted that beyond 70 mph, there was no data recorded by accelerometers and inclinometers. A decision was made to disconnect and remove accelerometers and inclinometers for fear of damaging equipment due to violent motion of the traffic signals. There was no data recorded by loadcells as well.

This chapter presents the results from the tests conducted on the traffic signal assembly using a **"steel cable hanger assembly with reinforced disconnect hanger and with aluminum signal housing" (vendor: Engineered Castings)** at the WOW. Additional results are presented in appendix D.

6.2. Experimental methodology

6.2.1. Test Setup

The 3-3-5 signal assembly was installed on a short-span rig (refer to Chapter 1) by means of a "steel cable hanger assembly with reinforced disconnect hanger and with aluminum signal housing" (vendor: Engineered Castings). Figure 84 and Figure 85 show the traffic signal assembly

as well as the steel cable hanger assembly. Signals were made of either aluminum or polycarbonate and included louvered back plates and visors.

The test protocol is presented in Table 9. Table 10 shows the list of components with manufacturers used for this signal assembly.

6.2.2. Instrumentation

The directions of the x, y, z components for each loadcell are shown in Figure 86. Loadcells number 2 and 5 were located at either end of the messenger cable and loadcells number 1 and 4 located at either end of the catenary cable.

Tri-axial accelerometers were installed in the traffic signals to measure accelerations. There was one accelerometer placed on the center top of the signal, Accel005, another placed on the bottom right side, Accel002, and a third placed on the bottom left side, Accel003 for the 5-section signal as shown in Figure 87. Accelerometer Accel007, was installed on the top center, accelerometer Accel004, was installed on the bottom left side and accelerometer Accel006, was installed on the bottom right side of the 3-section signal as shown in Figure 88.

There was one inclinometer installed on the top center of the signal, Inc4, and another on the bottom center of the signal, Inc3, for the 5-section signal as shown in Figure 87. Inclinometer, Inc2, was installed on the top center and inclinometer, Inc1, was installed on the bottom center of the of the 3-section signal as shown Figure 88.

Wind speeds in three component directions (u, v, w) were also recorded by the Wall of Wind velocity sensors.

6.2.3. Test Method

The test set up was first tested for ‘zero wind’ conditions, and the values of the various ‘quantities’ (forces, accelerations and inclinations) obtained were later deducted from quantities obtained for different wind speeds (also known as “zero drift removal” process). Although erratic behavior, such as aerodynamic fluttering, may not cause an initial failure of the signal equipment, it may lead to additional testing to confirm this behavior will not cause failure of the equipment when experienced for long-term.

Table 9: Test protocol (Task 1a: Case 5)

Wind Speed (mph)	Wind Direction	Total Duration (min)
40	0, 45, 80, 100, 135, 180	6
70	0, 45, 80, 100, 135, 180	6
100	0, 45, 80, 100, 135, 180	6
130	0, 45, 80, 100, 135, 180	6
150	0, 45, 80, 100, 135, 180	6
TOTAL		**30**

Table 10: Components and manufacturers of signal assembly (Task 1a: Case 5)

Component	Manufacturer
Span wire clamp	Pelco
Adjustable hanger	Pelco
Extension bar	No extension bar
Messenger clamp	Pelco
Disconnect Hanger	Engineered Castings
Signal Assembly	McCain
Backplate	TCS
Visor	McCain
LED Modules	GE - Dialight - Duralight

Figure 84: Picture of test rig frame with the signals and the steel cable hanger assembly

a)

b)

Figure 85: Traffic signal set up: a) 3-section signal showing the steel cable hanger assembly with reinforced disconnect hanger (vendor: Engineered Castings); b) traffic signal assembly facing the wind

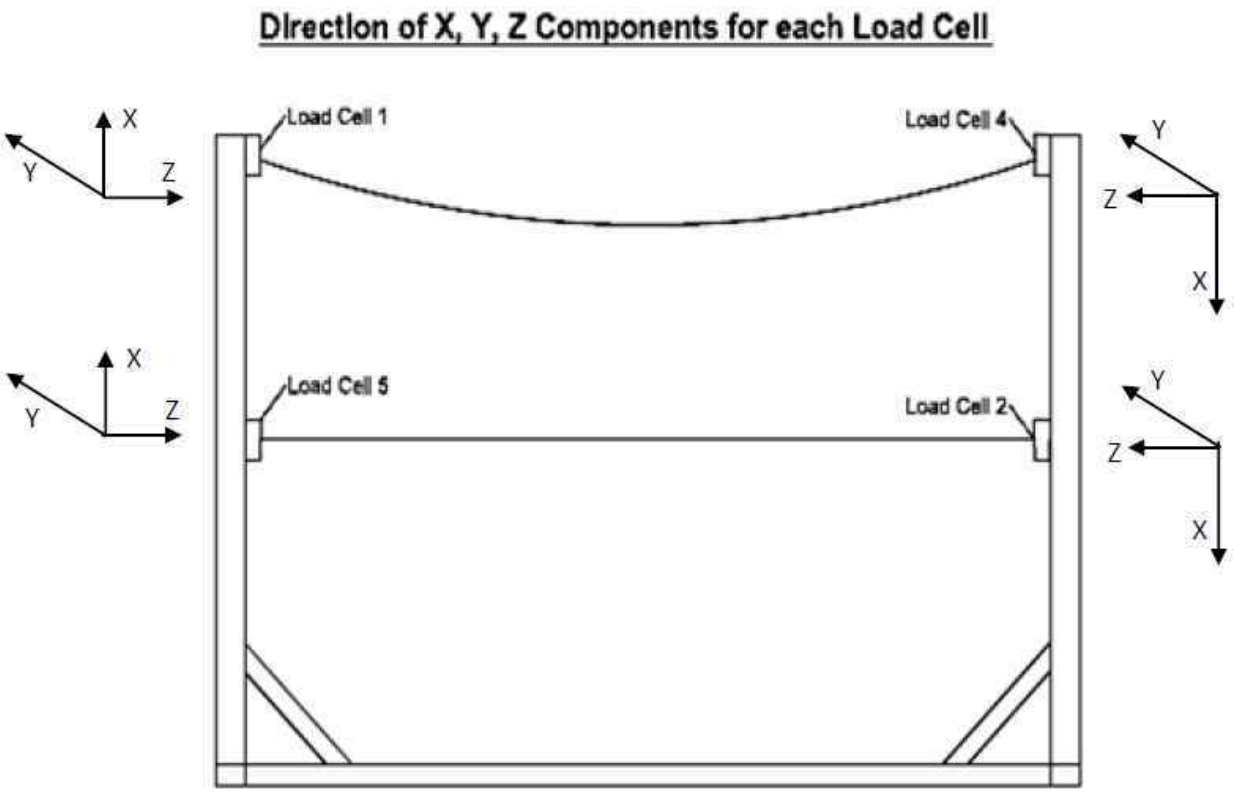

Figure 86: Direction of x, y, z components for each loadcell (direction of each axis shown represents 'positive direction')

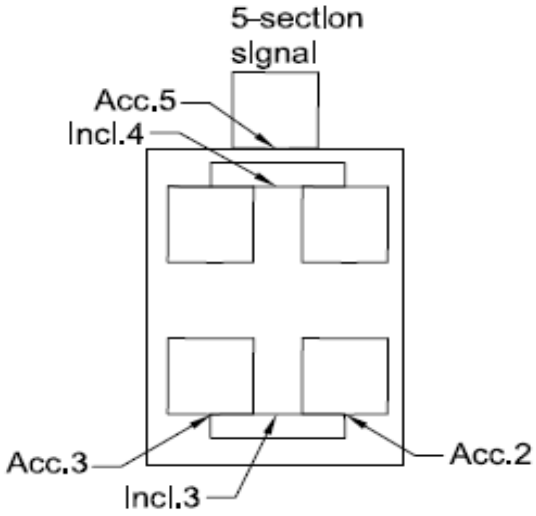

Figure 87: Location of accelerometers and inclinometers in 5-section signal

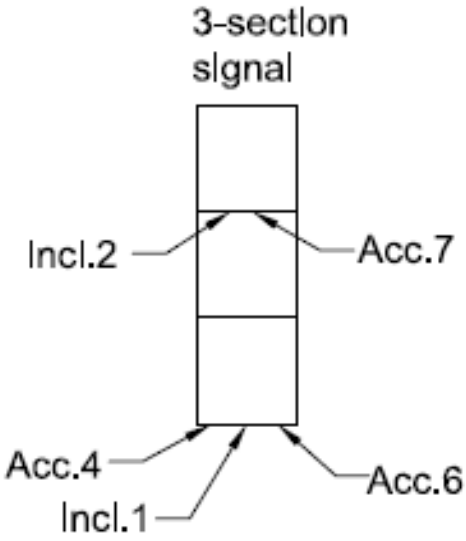

Figure 88: Location of accelerometers and inclinometers in 3-section signal

6.3. Results and discussion

The tests at the WOW were performed in the presence of the representatives from the Florida Department of Transportation (FDOT) Traffic Engineering and Operations Office and Traffic Engineering Research Lab (TERL), installation technicians from Horsepower Electric Inc., manufacturer and distributer of the steel cable hanger assembly with reinforced disconnect hanger and members of the WOW technical team. The results in this chapter are restricted to 0-degree wind direction, with results for additional wind directions presented in appendix D.

6.3.1. Wind induced forces

The directions of the forces are shown in Figure 86. The mean and peak forces obtained at various wind speeds are discussed in this section. Figure 89 presents the wind induced mean forces on loadcell 2 (messenger wire) and loadcell 4 (catenary wire) at 0-degrees wind direction, for increasing wind speeds. It may be noted that the 'y' and 'z' components of the forces correspond to the 'drag' and 'cable tensions' respectively, while the 'x' component represents the uplift forces. As specified earlier in this chapter, forces recorded pertain to 40 mph through 70 mph wind speeds.

Data show that the along wind forces (Fy) increase with increasing wind speed at loadcell 2 (messenger wire), while Fy at loadcell 4 (catenary wire) experiences minimal increase with increasing wind speeds. The highest along wind force of 82 lbs. was found at loadcell 2 at 70 mph. Similarly, the tension on loadcell 2 (Fz) increases with an increase in wind speed, although a small decrease in tension on loadcell 4 (catenary wire) for increasing wind speed was observed. This shows that the messenger wire experiences higher tension and drag than the catenary wire for increasing wind speed. The uplift forces (Fx) on loadcell 2 (messenger wire) slightly decreases in magnitude with increase in wind speed. A decrease in Fx on loadcell 4 (catenary wire) with increasing wind speed was observed. Similar observations were made for loadcell 5 (messenger) and loadcell 1 (catenary) as shown in Figure 90. For instance, Fz (cable tension) and Fy (drag) increase with increasing wind speed on loadcell 5 (messenger wire). Fx on loadcell 5 decreases at wind speeds of 40 mph through 70 mph.

The peak forces at 0-degrees wind direction for loadcell 2 and loadcell 4 are shown in Figure 91. The peak forces of Fz on loadcell 2 increases with increasing wind speeds up to 70 mph. The peak forces of Fz on loadcell 4 decreases slightly for 40-70 mph wind speed range. The peak forces of Fy on loadcell 2 increase with an increase in wind speed. The peak forces of Fy on loadcell 4 increase slightly with increasing wind speeds for 40-70 mph wind speed range. It may be noted that the 'positive direction' of 'Fx' component on loadcells 2 and 4 is 'downwards' (see Figure 86). The magnitude of the peak force Fx on loadcell 2 slightly decreases with an increase in wind speed from 40 mph to 70 mph, although Fx on loadcell 4 decreases despite an increase in wind speed. Figure 92 presents result for loadcell 5 (messenger) and loadcell 1 (catenary). Fz (cable tension) on loadcell 5 increases with increasing wind speeds, although Fz on loadcell 1 decreases despite increasing wind speeds. Fy on loadcells 5 and 1 both increase with increasing wind speeds. Fx (lift) on loadcell 5 (messenger) and loadcell 1 (catenary) decrease slightly for increasing wind speeds. Results for additional wind directions are presented in appendix D.

Figure 93 (a) presents the 'total' mean drag and lift forces on the traffic signals. Results show that the drag on the traffic signals increase with an increase in wind speed. A value of 104 lbs. was obtained at 40 mph - at 0-degrees wind direction - which was increased to 181 lbs. at 70 mph. Lift forces decrease when the wind speed is increased to 70 mph. The peak drag and lift are shown in Figure 93 (b). The peak drag increase with increasing wind speeds (116 lbs. to 211 lbs.) and the peak lift demonstrates a decrease with increasing wind speeds (140 lbs. to 72 lbs.).

6.3.2. rms of accelerations

The root mean squares (rms) of accelerations are presented in Figure 94. Accelerometers 4, 6 and 7 were located on the 3-section signal, while accelerometers 2, 3 and 5 were located on the 5-section signal (see Figure 87 and Figure 88). In general, the rms of accelerations obtained from all the accelerometers increase gradually with an increase in wind speed – highest rms value of 117 in/s2 was recorded at wind speed of 70 mph by accelerometer 4 located on the 3-section signal.

6.3.3. Inclinations of the traffic signals

Figure 95 shows the inclinations (mean and peak) obtained from inclinometer 1 (3-section) and inclinometer 3 (5-section) at 0-degrees wind direction. It may be noted that for inclinometer 1, '1-1' refers to the component of inclination perpendicular to the wind, while '1-2' refers to the component of inclination in the direction of wind. For inclinometers 1 and 3, the mean components '1-2' and '3-2' are generally in the range of 26 to 35 degrees for 40-70 mph wind speed range. Similarly, the maximum value of about 42-degrees was obtained at a wind speed of 70 mph for the inclinometer component 3-2. The values of inclinations were negligible for 1-1 and 3-1 components in the wind speed range of 40-70 mph. Beyond 70 mph, an erratic movement of the traffic signals (aerodynamic flutter) was observed. There was no data recorded beyond 70 mph.

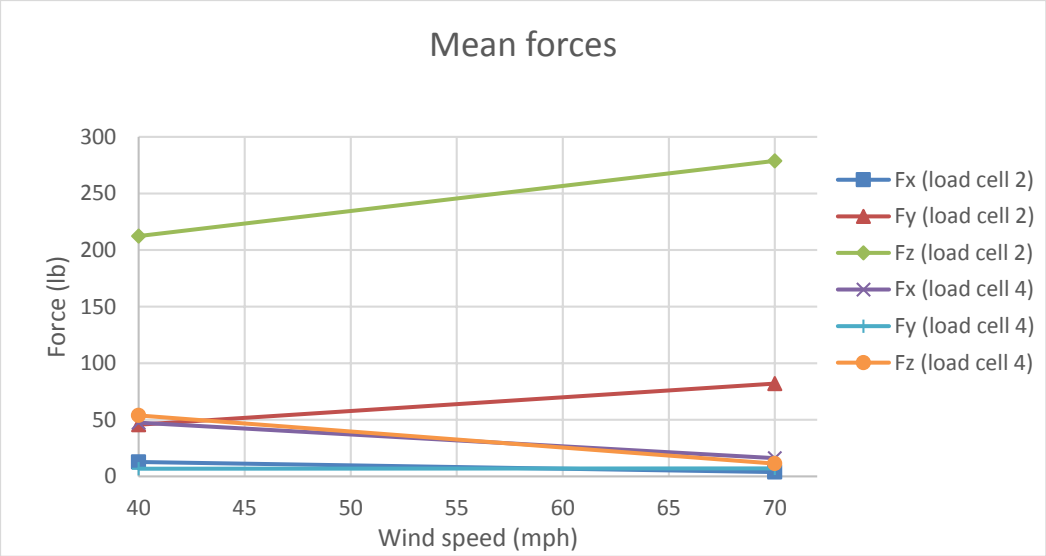

Figure 89: Mean forces on loadcells 2 (messenger wire) and 4 (catenary wire) at 0-degrees wind direction

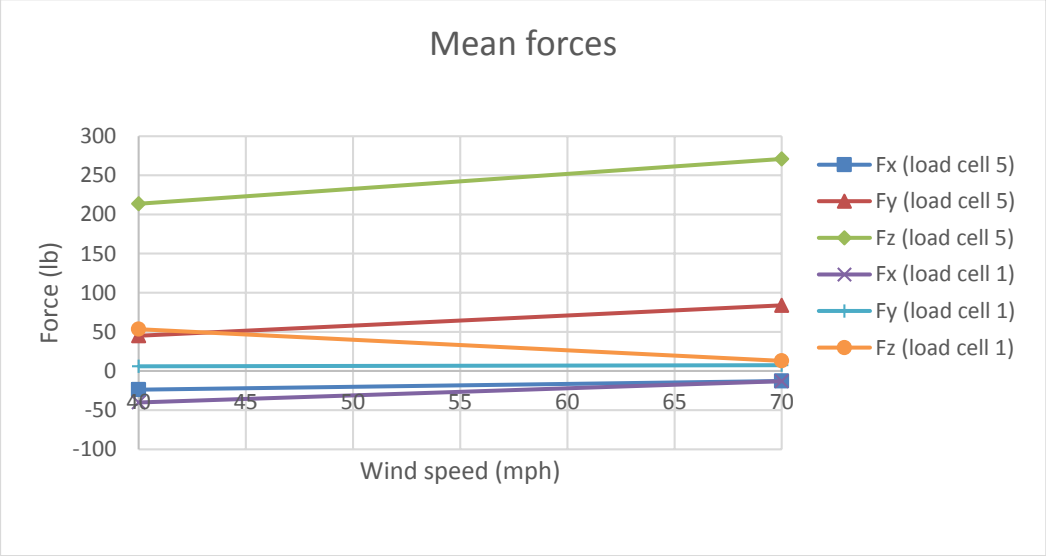

Figure 90: Mean forces on loadcells 1 (catenary wire) and 5 (messenger wire) at 0-degrees wind direction

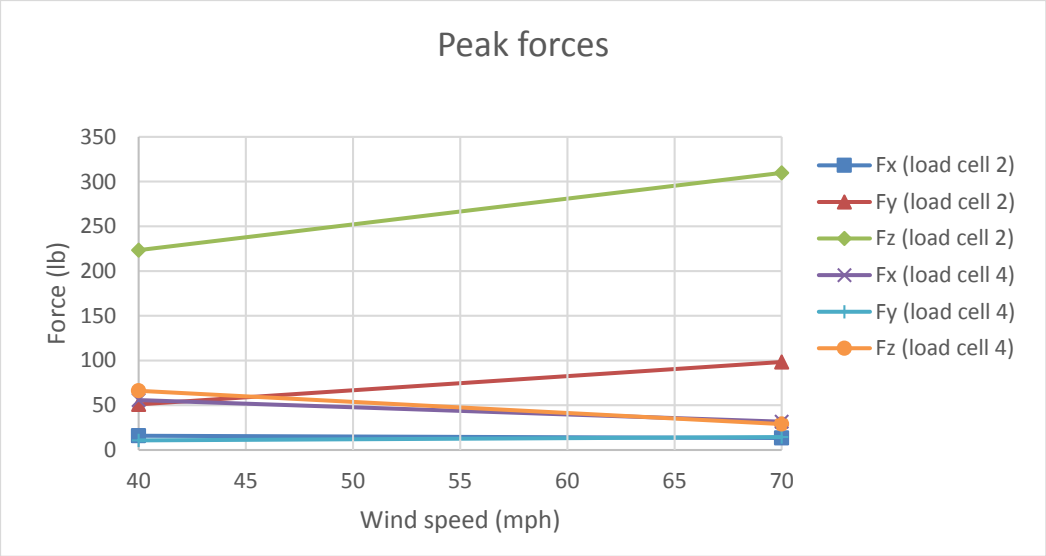

Figure 91: Peak forces at 0-degrees wind direction on loadcells 2 (messenger wire) and 4 (catenary wire)

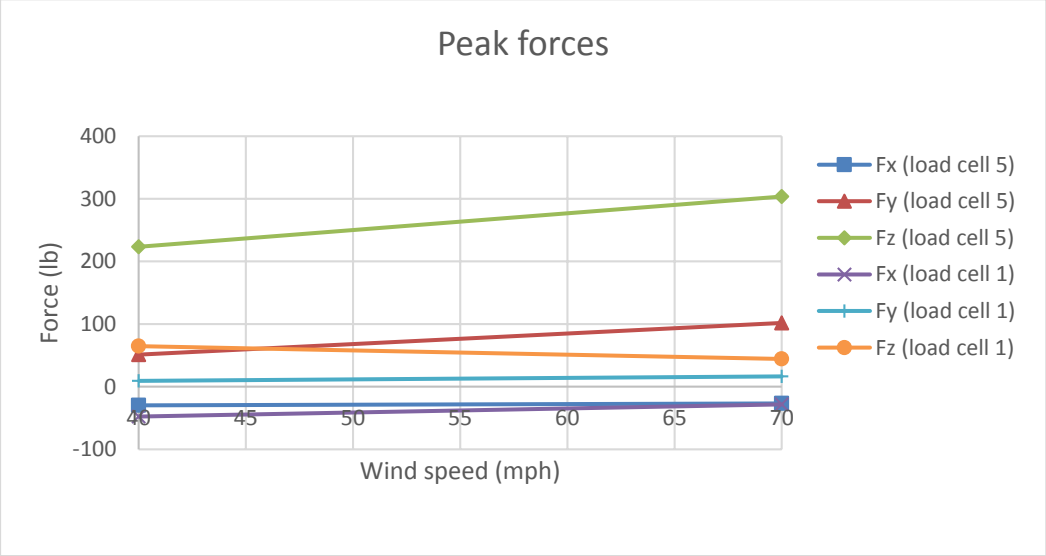

Figure 92: Peak forces at 0-degrees wind direction on loadcells 1 (catenary wire) and 5 (messenger wire)

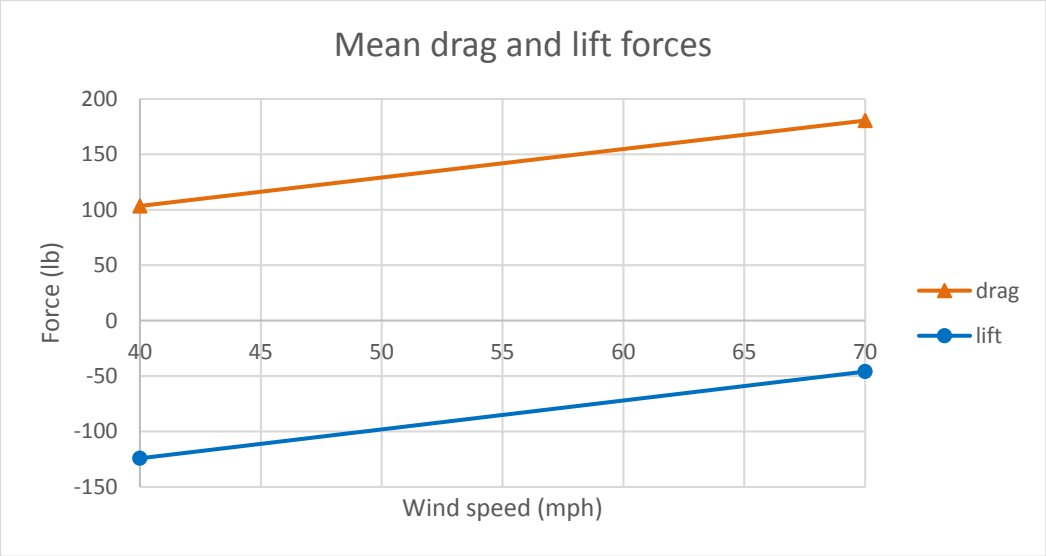

a)

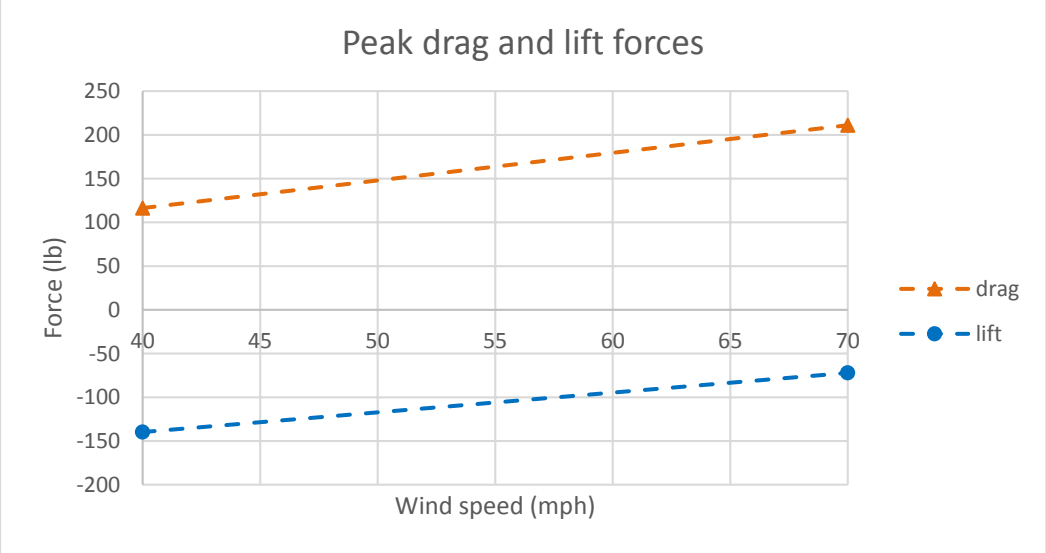

b)

Figure 93: Drag (Fy) and lift (Fx) forces on the traffic signals at 0-degrees: a) Mean; b) Peak

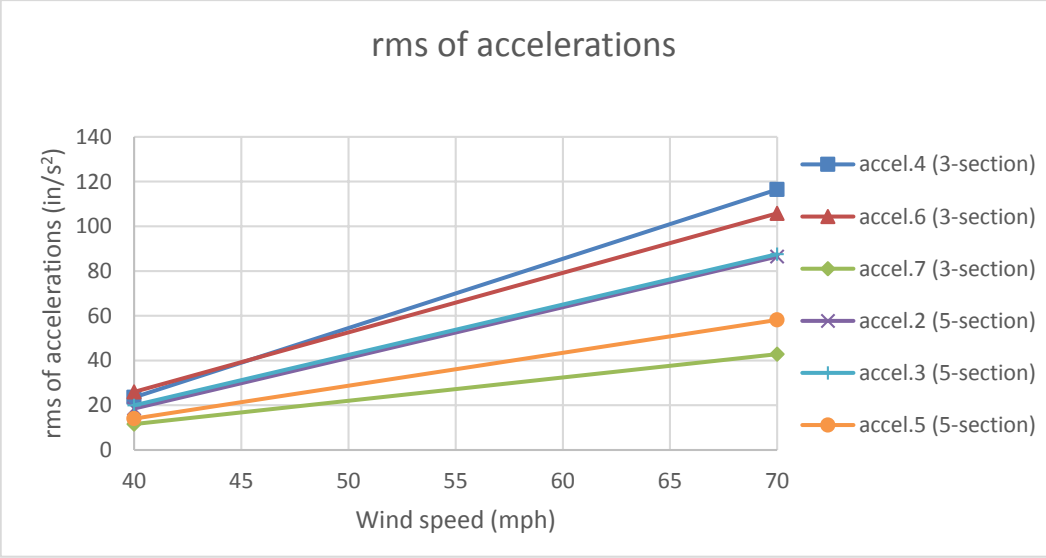

Figure 94: rms of accelerations on the 3-section and 5-section signals at 0-degrees

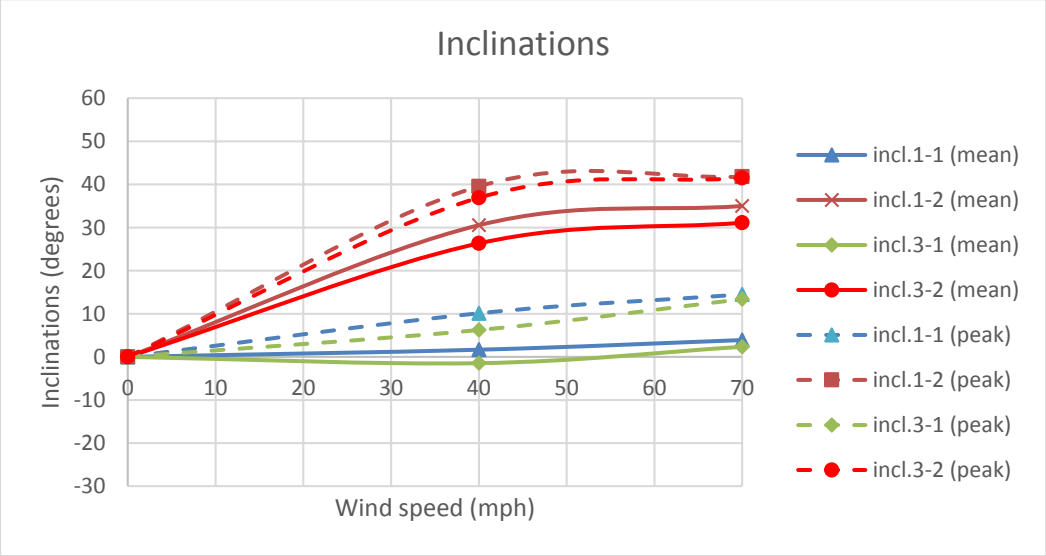

Figure 95: Inclinations (mean and peak) obtained at 0-degrees from inclinometers 1 and 3

6.4. Performance of traffic signals during the tests

This test utilized two 3-section and one 5-section aluminum traffic signals span wire configuration connected to the catenary and messenger wires by means of a **"steel cable hanger assembly with reinforced disconnect hanger and with aluminum signal housing" (vendor: Engineered Castings)**.

At 40 mph, and all wind directions, there was no damage observed to any of the traffic signals nor hanger assemblies. At 70 mph, 0-degrees, the upper right portion of the 5-section signal backplate comes undone and bends. Starting at 70 mph and 180-degrees traffic signals began to exhibit aerodynamic instability (flutter). At this point in time the disconnect box along with the attached 5-section signal sheared off from the steel cable hanger assembly and flew away. It was later observed that the aluminum hook attached to the top of the disconnect box had cracked, as shown in Figure 96. It was also observed that inside the disconnect box the lower aluminum clamp was cracked and torn away, as is shown in Figure 97. **It may be noted that beyond 70 mph due to the strong aerodynamic instability (flutter), a decision was made to remove the instrumentation for fear of damaging equipment.**

At 100 mph and 180-degree wind direction, the center 3-section signal rotated, facing towards the outer 3-section signal. It was later observed that the serrated teeth located on the bottom of the disconnect box had skipped its original placement from the serrated teeth located on the top of the upper LED signal. At 130 mph visors begin to detach and some fly away from the 3-section signals. The outer 3-section signal has lost all back plate while the center 3-section signal has portions of the back plate remaining. After 150 mph, all back plates are missing for both 3-section signals. The center 3-section signal had all visors missing while the outer 3-section signal remained with all its visors.

The 3-section signal disconnect box had no observed damage as shown in Figure 98. The three steel cable hanger assemblies were observed to have some bending after the full wind speed test was conducted as is depicted in Figure 99.

A summary of the observed damages is as follows:

- Damage to signal hanger: The three steel cable hanger assemblies were observed to have some bending.
- Damage to disconnect hanger (box): Cracked hook on top of 5-section signal disconnect box. Cracked lower clamp inside 5-section disconnect box. The 3-section signal disconnect box had no observed damage
- Damage to signal housing assembly: The 5-section signal flew away at 70mph. For the 3-section signal, visors and back plates were completely detached.

Figure 96: Cracked hook on top of 5-section signal disconnect box

Figure 97: Cracked lower clamp inside 5-section disconnect box

Figure 98: Disconnect box for 3-section signal with no observed damage

Figure 99: Steel cable hangers after full wind test

6.5. Conclusions

This chapter summarizes the results of a test conducted at WOW at FIU for a span wire traffic signal assembly consisting of two 3-section and a 5-section traffic signal, connected using a **"steel cable hanger assembly with reinforced disconnect hanger and with aluminum signal housing" (vendor: Engineered Castings)**. Wind speeds were varied from 40 to 150 mph, **although no data was recorded beyond 70 mph**, and wind directions were varied from 0 to 180 degrees. The various instruments used for this test include: loadcells to measure forces, accelerometers to measure accelerations and inclinometers to measure the inclinations. This study reports the data for different wind directions, in terms of: wind induced forces (drag (y-component), lift (x-component) and cable tension (z-component)), rms of accelerations and inclinations. Results for 0-degrees wind direction indicate that along wind forces (drag) and cable tensions generally increase in the messenger wire with increase in wind speed. The lift on the messenger wire decreases marginally with increasing wind speeds at 0-degrees. The catenary wire experiences a decrease in lift and tension and negligible increase in drag wind forces with increase in wind speed. At any given wind speed, the messenger wire experiences higher tension forces than the catenary wire. Similar observations were made for other wind directions (see appendix D). In general, the rms of accelerations increased with increasing wind speeds. In the range of 40 to 70 mph for 0-degrees wind direction, the mean inclinations in the along wind direction varied from 26 to 35 degrees, with a maximum value of about 42-degrees observed at 70 mph for inclinometer component 3-2. Beginning at 70 mph, 180 degrees and beyond an erratic movement of the signals was observed (aerodynamic flutter). No data was recorded beyond 70 mph. A failure was observed at 70 mph and 180-degrees, whereby the 5-section signal disconnect box broke off from the steel cable assembly and drifted away along with the 5-section signal. Afterwards it was detected that the aluminum hook at the top of the disconnect box had fractured. It was also noticed that the lower aluminum clamp located on the inside of the 5-section disconnect box had ruptured.

Chapter 7 - Task 1a: FULL SCALE TESTING - Case 6

"Adjustable Hanger Assembly with Cable Dampener, Reinforced Disconnect Hanger and Aluminum Signal Housing" (vendor: Pelco Products) - Test Date: 11/19/2015

7.1. Introduction

In the first tasks of the current project a 'base' configuration was identified consisting of a 21.9 ft long section with two 3-section and one 5-section traffic signals (Task 1a – Cases 1 and 2). As a continuation of the study, FDOT tested the span wire traffic signal configurations connected to the catenary and messenger wires via an **"adjustable hanger assembly with cable dampener, reinforced disconnect hanger and aluminum signal housing" (vendor: Pelco Products)**. The tests were carried out at wind directions ranging from 0 to 180 degrees and wind speeds ranging from 40 to 150 mph. The instruments consisted of loadcells to measure wind loads, accelerometers to measure accelerations, and inclinometers to measure the inclinations of the traffic signals.

This chapter presents the results from the tests conducted on the traffic signal assembly with the **"adjustable hanger assembly with cable dampener, reinforced disconnect hanger and aluminum signal housing" (vendor: Pelco Products)** at the WOW. Additional results are presented in appendix E.

7.2. Experimental methodology

7.2.1. Test Setup

The 3-3-5 signal assembly was installed on a short-span rig (described in Chapter 1) by means of an "adjustable hanger assembly with cable dampener, reinforced disconnect hanger and aluminum signal housing" (vendor: Pelco Products). Figure 100 and Figure 101 show the traffic signal assembly as well as the Pelco adjustable hanger assembly with cable dampener connection. All the signals were made of aluminum and included louvered back plates and visors. The test protocol is presented in Table 11. Table 12 shows the signal assembly components.

7.2.2. Instrumentation

The directions of the x, y and z components for each loadcell are shown in Figure 102. Loadcells number 2 and 5 were located at either end of the messenger cable and loadcells number 1 and 4 located at either end of the catenary cable.

Tri-axial accelerometers were installed in the traffic signals to measure accelerations. There was one accelerometer placed on the center top of the signal, Accel5, another placed on the bottom right side, Accel002, and a third placed on the bottom left side, Accel003 for the 5-section signal as shown in Figure 103. Accelerometer Accel007, was installed on the top center, accelerometer Accel004, was installed on the bottom left side and accelerometer Accel006, was installed on the bottom right side of the 3-section signal as shown in Figure 104.

There was one inclinometer installed on the top center of the signal, Inc4, and another on the bottom center of the signal, Inc3, for the 5-section signal as shown in Figure 103. Inclinometer, Inc2, was installed on the top center and inclinometer, Inc1, was installed on the bottom center of the of the 3-section signal as shown Figure 104.

Wind speeds in three component directions (u,v,w) were also recorded by the Wall of Wind velocity sensors.

7.2.3. Test Method

The test set up was first tested for ‘no wind’ conditions, and the values of the various ‘quantities’ (forces, accelerations and inclinations) obtained were later deducted from quantities obtained for different wind speeds (also known as “zero drift removal” process). Although erratic behavior, such as aerodynamic fluttering, may not cause an initial failure of the signal equipment, it may lead to additional testing to confirm this behavior will not cause failure of the equipment when experienced for long-term.

Table 11: Test protocol (Task 1a: Case 6)

Wind Speed (mph)	Wind Direction	Total Duration (min)
40	0, 45, 80, 100, 135, 180	6
70	0, 45, 80, 100, 135, 180	6
100	0, 45, 80, 100, 135, 180	6
130	0, 45, 80, 100, 135, 180	6
150	0, 45, 80, 100, 135, 180	6
TOTAL		**30**

Table 12: Components of signal assembly (Task 1a: Case 6)

Component	Manufacturer
Span wire clamp	Pelco
Adjustable hanger	Pelco
Extension bar	Pelco
Messenger clamp	Pelco
Disconnect Hanger	Pelco
Signal Assembly	McCain
Backplate	TCS
Visor	McCain
LED Modules	GE - Dialight - Duralight

Figure 100: Picture showing a portion of the test rig frame with the 3-section traffic signals

a)

b)

c)

Figure 101: Adjustable hanger assembly with cable dampener and reinforced disconnect hanger: a) signal setup for the test; b) magnified view of the connection; c) complete view of connection

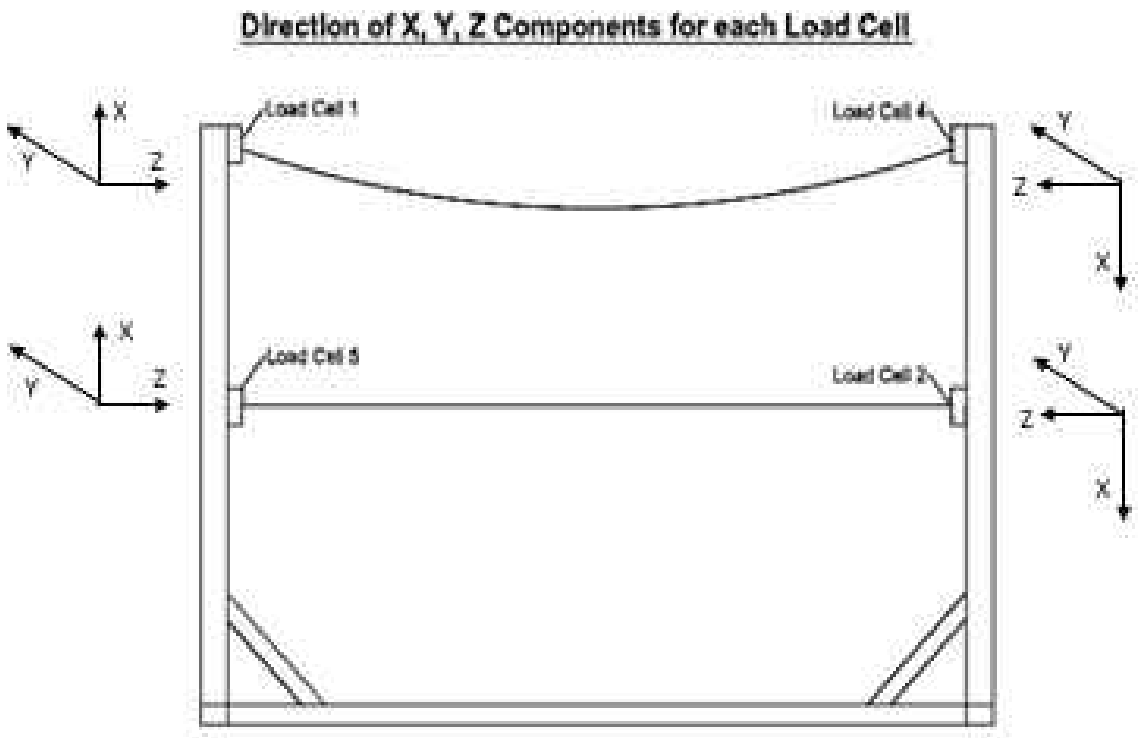

Figure 102: Direction of x, y, z components for each loadcell (direction of each axis shown represents 'positive direction')

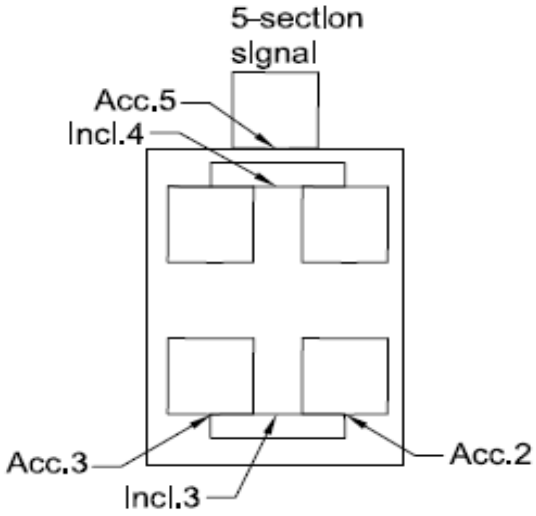

Figure 103: Location of accelerometers and inclinometers in 5-section signal

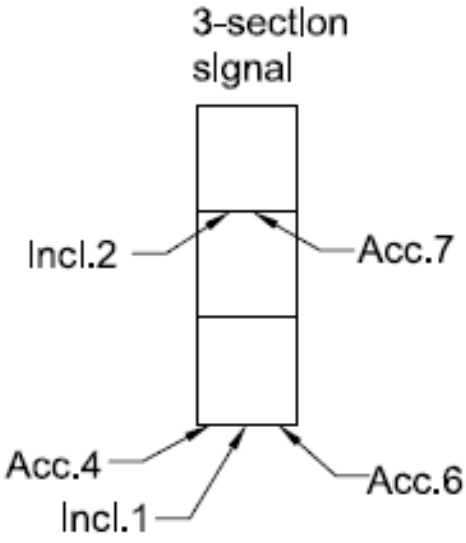

Figure 104: Location of accelerometers and inclinometers in 3-section signal

7.3. Results and discussion

The tests at the WOW were performed in the presence of the representatives from the Florida Department of Transportation (FDOT) Traffic Engineering and Operations Office and Traffic Engineering Research Lab (TERL), representatives from Pelco Products, installation technicians from Horsepower Electric Inc. and members of the WOW technical team. The results in this chapter are restricted to 0-degree wind direction, with results for additional wind directions presented in appendix E.

7.3.1. Wind induced forces

The directions of the forces are shown in Figure 102. The mean and peak forces obtained at various wind speeds are discussed in this section. Figure 105 presents the wind induced mean forces on loadcell 2 (messenger wire) and loadcell 4 (catenary wire) at 0 degrees wind direction, for increasing wind speeds. It may be noted that the 'y' and 'z' components of the forces correspond to the 'drag' and 'cable tensions' respectively, while the 'x' component represents the uplift forces.

Data show that the along wind forces (Fy), cable tension (Fz) and lift (Fx) increase with increasing wind speed at loadcell 2 (messenger wire), while these components experienced minimal change with increasing wind speeds on loadcell 4 (catenary). The highest along wind force of 228 lb was found at loadcell 2 at 150 mph. This shows that the messenger wire experiences higher tension and drag than the catenary wire for increasing wind speeds.

Similar observations were made for loadcell 5 (messenger) and loadcell 1 (catenary) as shown in Figure 106. For instance, Fz (cable tension) and Fy (drag) increase with increasing wind speed on loadcell 5 (messenger wire), while minimal change in these components for various wind speeds were observed on loadcell 1 (catenary). Fx on loadcell 5 also increases with increasing wind speed of up to 130 mph, beyond which it drops slightly.

The peak forces at 0 degrees wind direction for loadcell 2 and loadcell 4 are shown Figure 107. The highest magnitude of peak forces is reported since these values are critical to the wind design of traffic signals. The peak forces of Fx, Fy and Fz increase with increasing wind speeds up to 130 mph, beyond which the peaks are somewhat reduced on loadcell 2 (messenger); similar

trends were observed for Fy and Fz on loadcell 4 (catenary). It may be noted that the 'positive direction' of 'Fx' component on loadcells 2 and 4 is 'downwards' (see Figure 102). The peak tension forces (Fz) experienced by the messenger wire were higher than the catenary wire at a given wind speed. Results for additional wind directions are presented in appendix E. Figure 108 presents peak forces for loadcell 5 (messenger) and loadcell 1 (catenary). The peak drag (Fy) and peak tensions (Fz) on loadcell 5 (messenger) were found to be higher in magnitude at a given wind speed than those measured on loadcell 1 (catenary).

Figure 109 (a) presents the 'total' mean drag and lift forces on the traffic signals. Results show that the drag on the traffic signals increase with an increase in wind speed – highest values of 541 lb was obtained at 150 mph at 0 degrees wind direction. The lift forces increase initially with increase in wind speed, although beyond 100 mph a nearly constant force of 200 lb was obtained. The peak drag and lift are shown in Figure 109 (b). The peak drag and lift forces increase with increasing wind speed up to 130 mph, beyond which the peak drag and lift forces decrease slightly.

7.3.2. rms of accelerations

The root mean square (rms) of accelerations are presented in Figure 110. Accelerometers 4, 6 and 7 were located on the 3-section signal, while accelerometers 2, 3 and 5 were located on the 5-section signal (see Figure 103 and Figure 104). In general, the rms of accelerations obtained from all the accelerometers increase gradually with an increase in wind speed from 40 mph to 100 mph. Beyond 100 mph, the sensors were removed to avoid damage due to violent oscillation.

7.3.3. Inclinations of the traffic signals

Figure 111 shows the inclinations (mean and maximum) obtained from various inclinometers at 0 degrees wind direction. It may be noted that for inclinometer 1, '1-1' refers to the component of inclination perpendicular to the wind, while '1-2' refers to the component of inclination in the direction of wind. The highest mean inclination in the along wind direction of 41 degrees was measured on inclinometer 2 attached to the 3-section signal. The values of mean inclinations were smaller for components of inclination perpendicular to the wind in the wind speed range of

0-70 mph. Beyond 70 mph, an erratic movement of the traffic signals (aerodynamic flutter) was observed, with a wide range of inclinations.

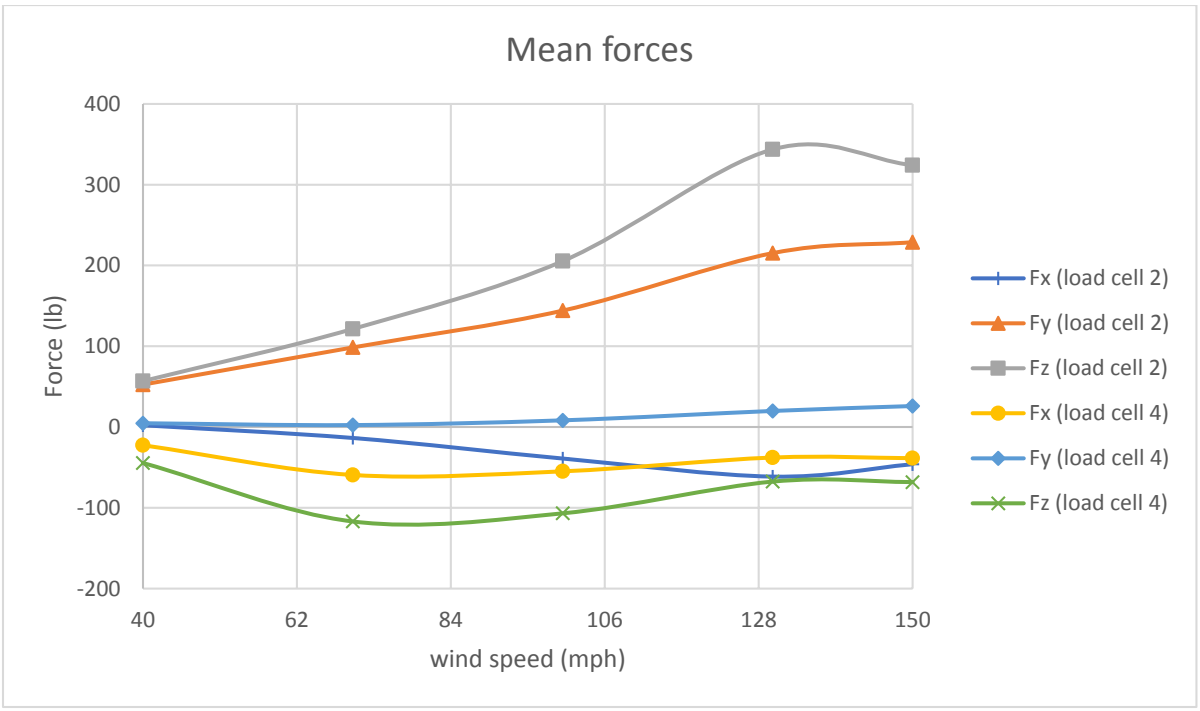

Figure 105: Mean forces on loadcells 2 (messenger wire) and 4 (catenary wire) at 0 degrees wind direction

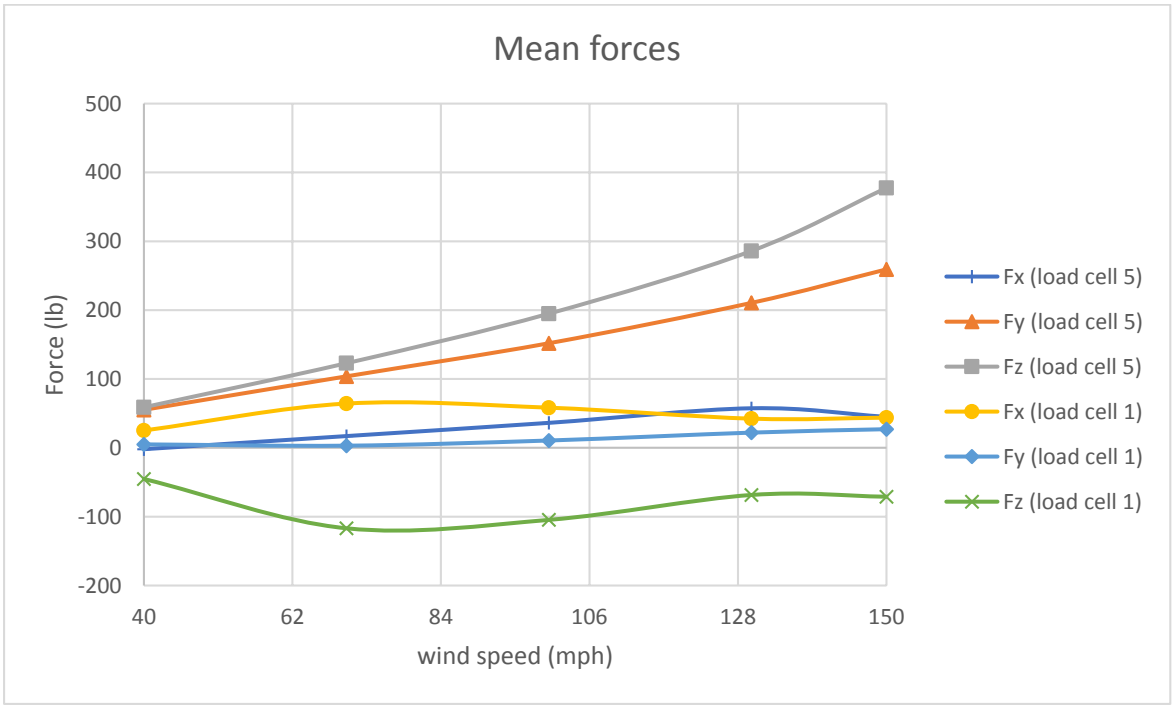

Figure 106: Mean forces on loadcells 1 (catenary wire) and 5 (messenger wire) at 0 degrees wind direction

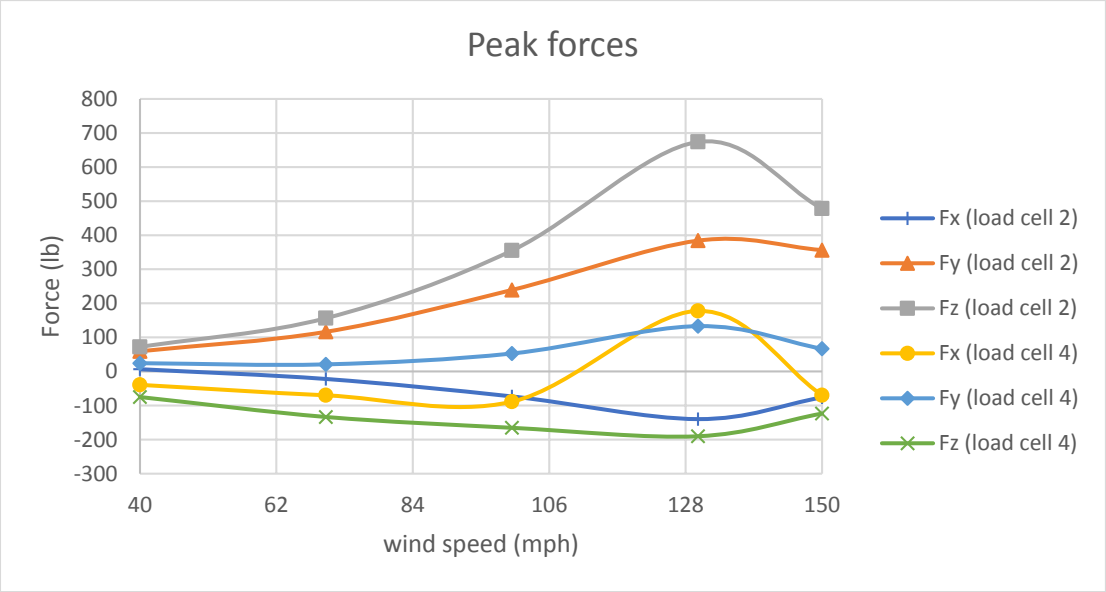

Figure 107: Peak forces at 0 degrees wind direction on loadcells 2 (messenger wire) and 4 (catenary wire)

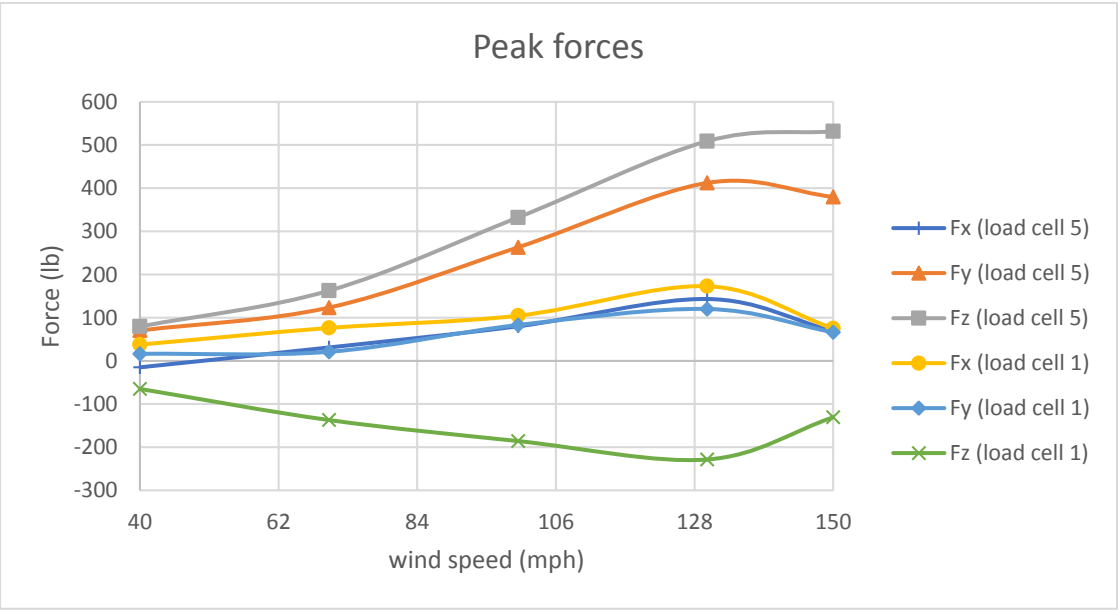

Figure 108: Peak forces at 0 degrees wind direction on loadcells 1 (catenary wire) and 5 (messenger wire)

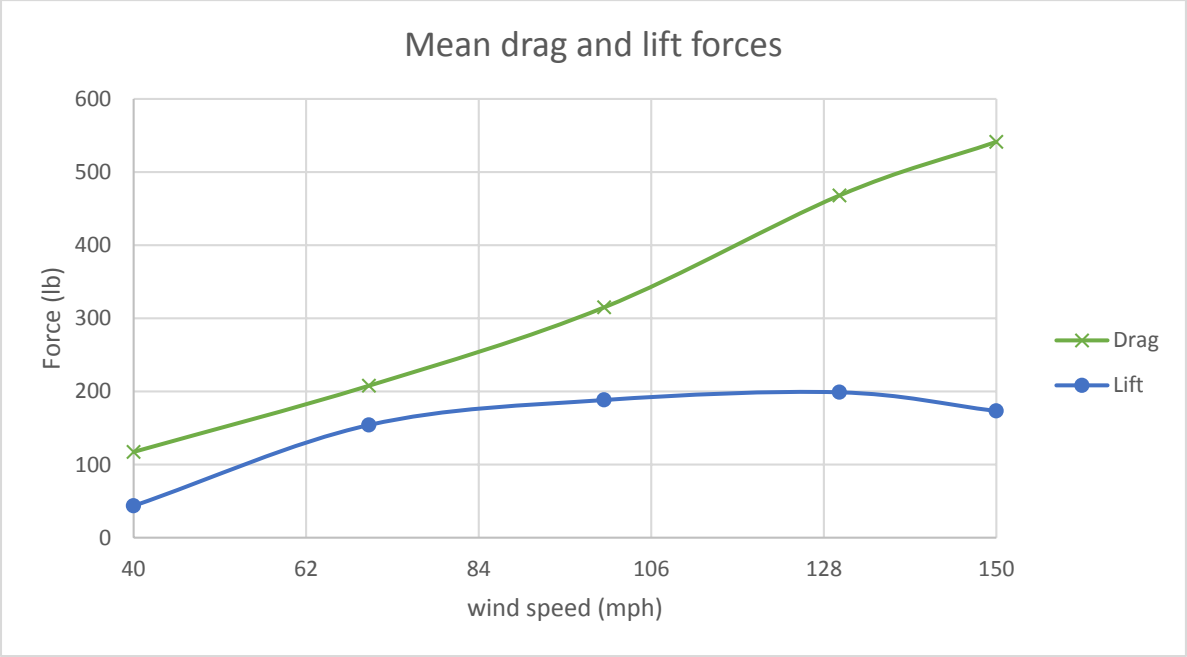

a)

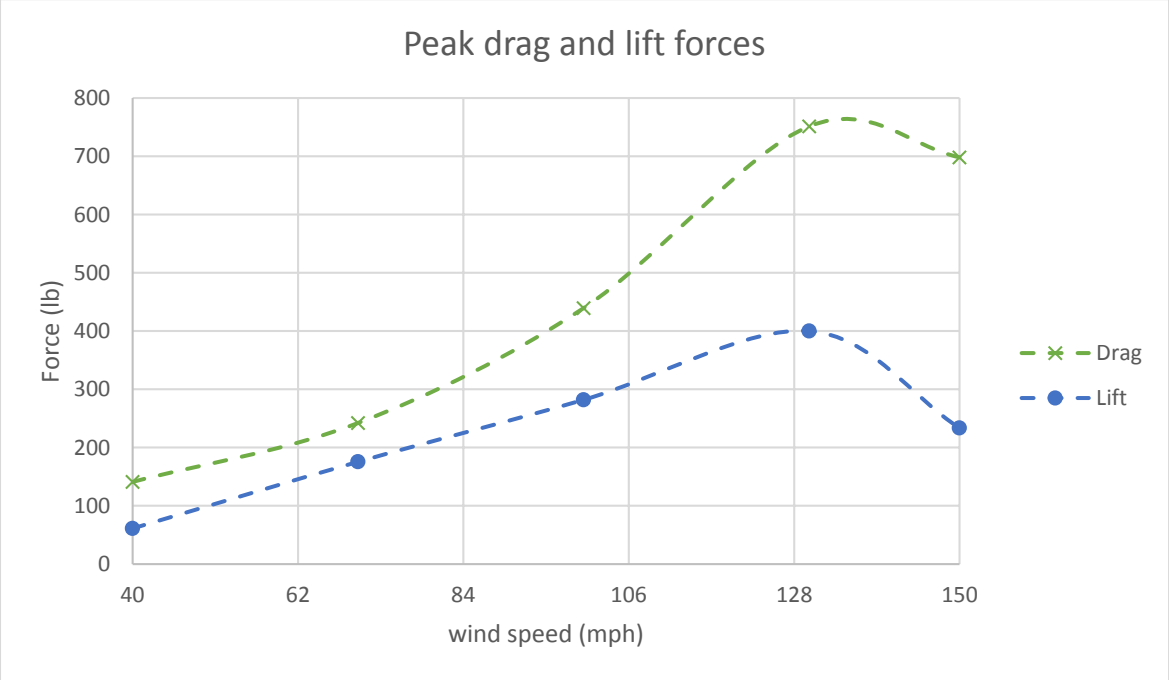

b)

Figure 109: Drag (Fy) and lift (Fx) forces on the traffic signals at 0 degrees: a) Mean; b) Peak

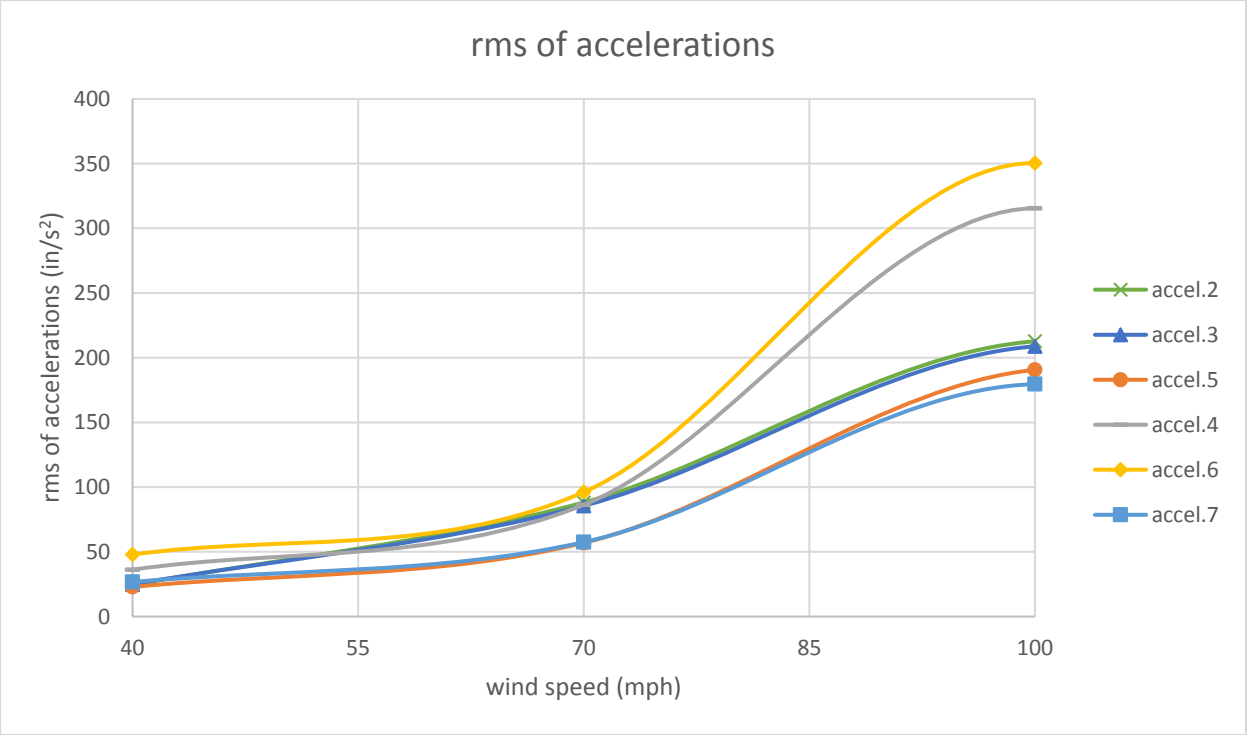

Figure 110: rms of accelerations on the 3-section and 5-section signals at 0 degrees

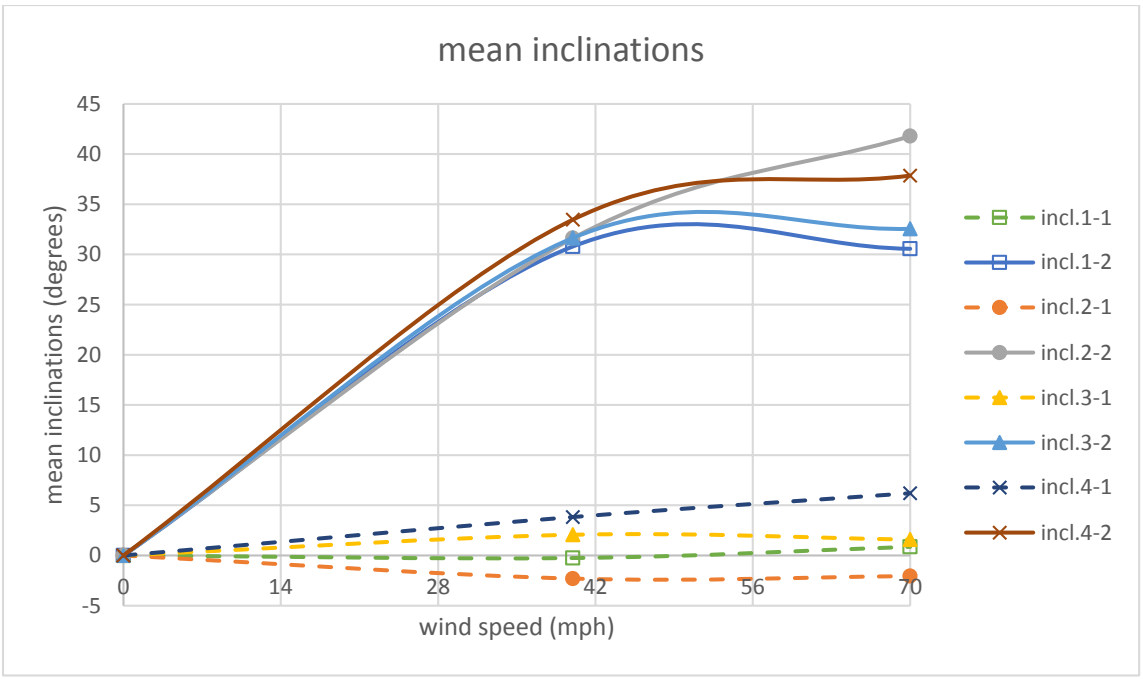

a)

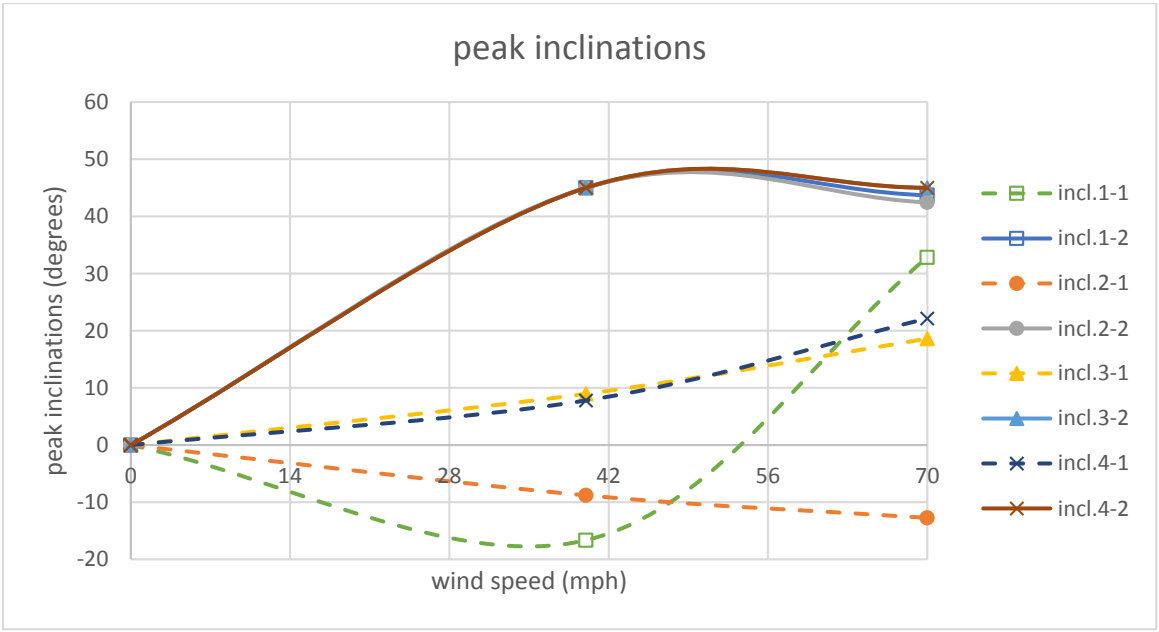

b)

Figure 111: Inclinations obtained at 0 deg from inclinometers: a) mean; b) peak

7.4. Performance of traffic signals during the tests

This test utilized two 3-section and one 5-section aluminum traffic signals installed in a span wire configuration connected to the catenary and messenger wires by means of an **"adjustable hanger assembly with cable dampener, reinforced disconnect hanger and aluminum signal housing" (vendor: Pelco Products)**.

From the onset and throughout the full range of wind speeds there was flexible bending of the cable dampener portion of the Pelco hanger assembly. Once the wind subside the cable dampener fully recovered from its bent position. The Pelco adjustable hanger assembly with cable dampener exhibited no damage and recovered from its' bent position at the end of the test. Pelco adjustable hanger assembly after completion of test is shown in Figure 112.

Traffic signals demonstrated an aerodynamic flutter commencing at 100 mph and above. At this point, portions of the 5-section traffic signal upper back plate began to loosen and bend. After the test, it was observed that the 5-section traffic signal showed rotation from the disconnect box. At 130 mph a large portion of the back plates from all three traffic signals had loosened and were windblown and visors began to detach. At 150 mph there were no back plates attached to the signals and visors began to come loose and blow away. Figure 113 shows the traffic signals after the completion of the full range of wind speed test.

The reinforced disconnect boxes for the 5-section and 3-section traffic signals exhibited no visible damage after the full range of wind speed test. Disconnect boxes after the completion of the test are shown in Figure 114 and Figure 115. A summary of the observed damages is as follows:

- Damage to signal hanger: Flexible bending of the cable portion. No permanent visual damage observed.
- Damage to disconnect hanger (box): No permanent visual damage observed.
- Damage to signal housing assembly: Damage to visors and back plate. No other permanent visual damage observed.

Figure 112: Pelco adjustable hanger assembly with cable dampener after full range test

Figure 113: Traffic signals after full range of wind speed test

Figure 114: Disconnect box for 3-section traffic signal after test

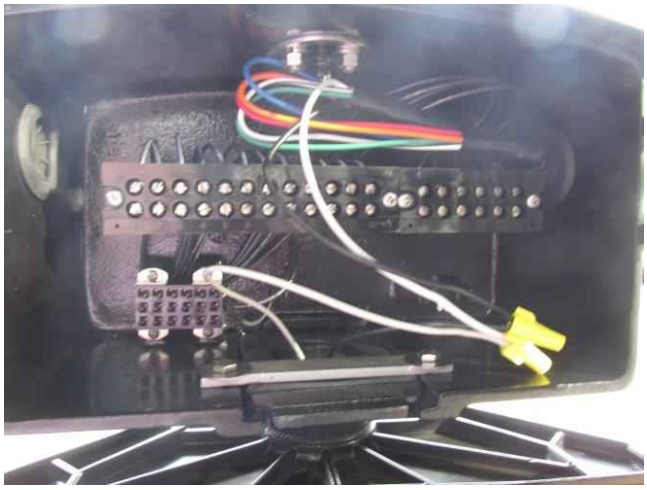

Figure 115: Disconnect box for 5-section traffic signal after test

7.5. Conclusions

This chapter summarizes the results of a test conducted at WOW Research Facility at FIU for a span wire traffic signal assemble consisting of two 3-section and a 5-section traffic signal, connected using an **"adjustable hanger assembly with cable dampener, reinforced disconnect hanger and aluminum signal housing" (vendor: Pelco Products)**. Wind speeds were varied from 40 to 150 mph and wind directions were varied from 0 to 180 degrees. The various instruments used for this test include: loadcells to measure forces, accelerometers to measure accelerations and inclinometers to measure the inclinations. This study reports the data for different wind directions, in terms of: wind induced forces (drag (y-component), lift (x-component) and cable tension (z-component)), rms of accelerations and inclinations. Results for 0 degrees wind direction indicate that the total mean drag and the total mean lift on the traffic signals increase with increasing wind speeds; similar trends were observed for peak drag/lift. The along wind forces and cable tensions increased with increasing wind speed. At any given wind speed, the messenger wire experiences higher tensions and drag compared to the catenary wire. The rms of accelerations increased with increasing wind speed from 40 mph to 100 mph. Similar observations were made for other wind directions (see appendix E). In the range of 40 to 70 mph for 0 degrees wind direction, the highest mean inclinations in the along wind direction was found to be 41 degrees. At 100 mph, the traffic signals experienced erratic motion (aerodynamic flutter). A slight rotation of the 5-section signal from the disconnect box was noticed and back plates began to disconnect and bend. There was no visible failure observed in the adjustable hanger assembly. Traffic signal housings did not suffer any detectable damage other than LED lights loosening. Fragments of back plates became unfastened at 100 mph and were blown away at 130 mph. Some visors began to detach at 130 mph and flew away at 150 mph.

Chapter 8 - Task 1a: FULL SCALE TESTING - Case 7

"Tri-Stud Adjustable Hanger with Aluminum Signal Housings, Base Configuration (145lb spring system)" - Test Date: 11/20/2015

8.1. Introduction

In the first tasks of the current project a 'base' configuration was identified consisting of a 21.9 ft long section with two 3-section and one 5-section traffic signals (Task 1a – Cases 1 and 2). As a continuation of the study, FDOT tested the span wire traffic signal configurations connected to the catenary and messenger wires via a "**tri-stud adjustable hanger" (also known as base configuration)** assembly. The tests were carried out at wind directions ranging from 0 to 180 degrees and wind speeds ranging from 40 to 130 mph. The instruments consisted of loadcells to measure wind loads, accelerometers to measure accelerations, and inclinometers to measure the inclinations of the traffic signals.

This chapter presents the results from the tests conducted on the traffic signal assembly with the "**tri-stud adjustable hanger" (also known as base configuration)** connection at the WOW. Additional results are presented in appendix F.

8.2. Experimental methodology

8.2.1. Test Setup

The 3-3-5 assembly was mounted on a short-span rig (described in Chapter 1) by means of a "**tri-stud adjustable hanger" (also known as base configuration).** Figure 116 and Figure 117 show the traffic signal assembly as well as the tri-stud adjustable hanger (also known as base aluminum eagle hanger) assembly. All the signals were made of aluminum and included louvered back plates and visors. The test protocol is presented in Table 13. Table 14 shows the list of components used for this signal assembly.

8.2.2. Instrumentation

The directions of the x, y and z components for each loadcell are shown in Figure 118. Loadcells number 2 and 5 were located at either end of the messenger cable and loadcells number 1 and 4 located at either end of the catenary cable.

Tri-axial accelerometers were installed in the traffic signals to measure accelerations. There was one accelerometer placed on the center top of the signal, Accel5, another placed on the bottom right side, Accel002, and a third placed on the bottom left side, Accel003 for the 5-section signal as shown in Figure 119. Accelerometer Accel007, was installed on the top center, accelerometer Accel004, was installed on the bottom left side and accelerometer Accel006, was installed on the bottom right side of the 3-section signal as shown in Figure 120.

There was one inclinometer installed on the top center of the signal, Inc4, and another on the bottom center of the signal, Inc3, for the 5-section signal as shown in Figure 119. Inclinometer, Inc2, was installed on the top center and inclinometer, Inc1, was installed on the bottom center of the of the 3-section signal as shown Figure 120.

Wind speeds in three component directions (u,v,w) were also recorded by the Wall of Wind velocity sensors.

8.2.3. Test Method

The test set up was first tested for ‘no wind’ conditions, and the values of the various ‘quantities’ (forces, accelerations and inclinations) obtained were later deducted from quantities obtained for different wind speeds (also known as “zero drift removal” process).

Although erratic behavior, such as aerodynamic fluttering, may not cause an initial failure of the signal equipment, it may lead to additional testing to confirm this behavior will not cause failure of the equipment when experienced for long-term.

Table 13: Test protocol (Task 1a: Case 7)

Wind Speed (mph)	Wind Direction	Total Duration (min)
40	0, 45, 80, 100, 135, 180	6
70	0, 45, 80, 100, 135, 180	6
100	0, 45, 80, 100, 135, 180	6
130	0, 45	2
TOTAL		**20**

Table 14: Signal assembly components (Task 1a: Case 7)

Component	Manufacturer
Span wire clamp	Pelco
Adjustable hanger	Pelco
Extension bar	Pelco
Messenger clamp	Pelco
Disconnect Hanger	Pelco
Signal Assembly	McCain
Backplate	TCS
Visor	McCain
LED Modules	GE - Dialight - Duralight

Figure 116: Picture showing a portion of the test rig frame with the tri-stud adjustable hanger system

a)

b)

Figure 117: Tri-stud adjustable hanger (also known as base configuration) connection: a) signal setup for the test; b) view of the connection

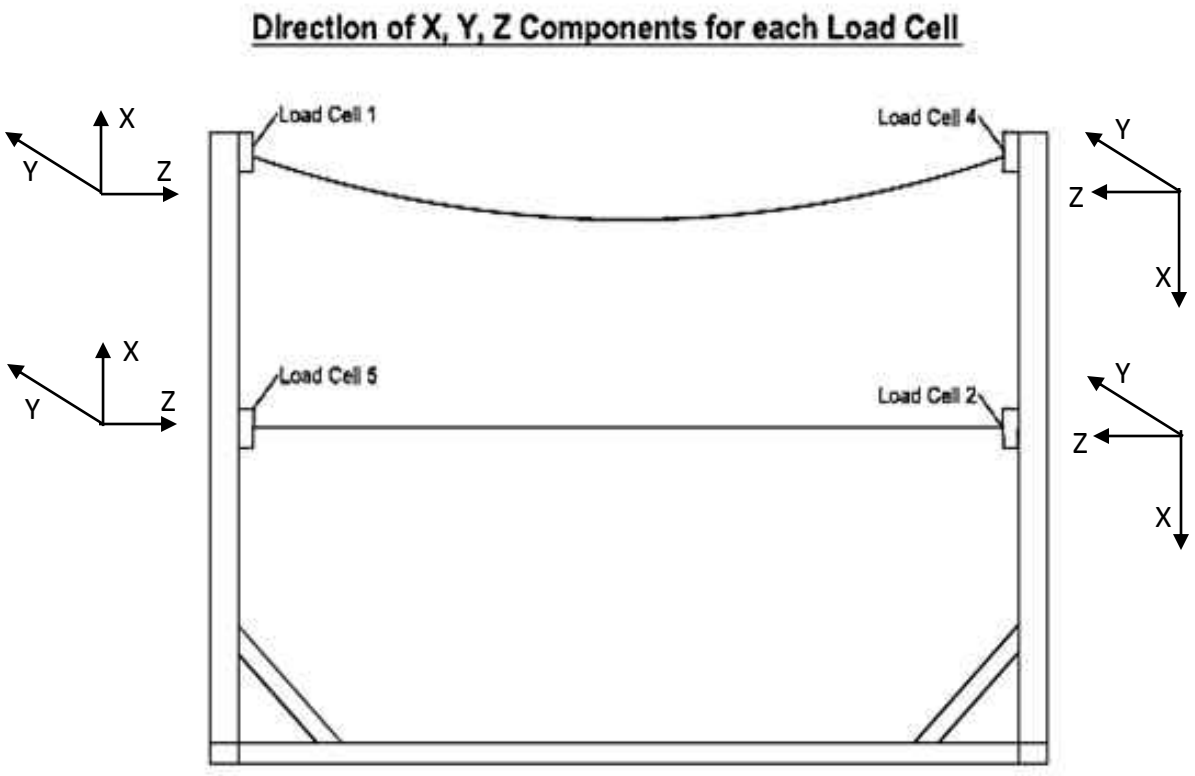

Figure 118: Direction of x, y, z components for each loadcell (direction of each axis shown represents 'positive direction')

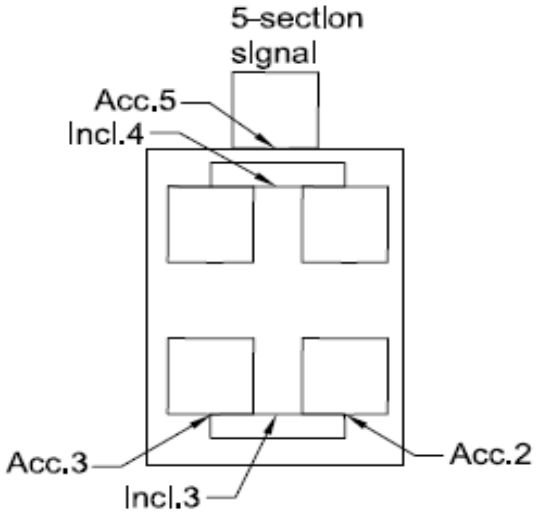

Figure 119: Location of accelerometers and inclinometers in 5-section signal for case 1

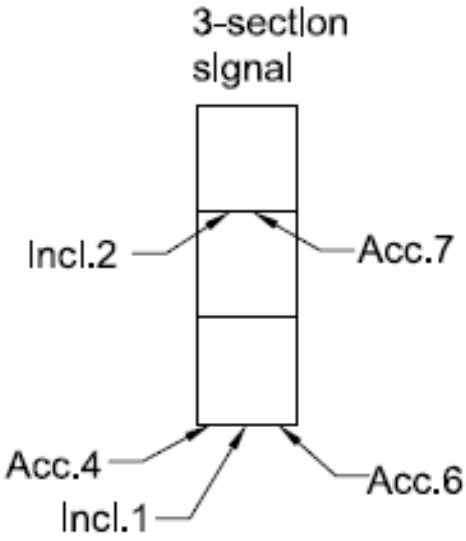

Figure 120: Location of accelerometers and inclinometers in 3-section signal for case 1

8.3. Results and discussion

The tests at the WOW were performed in the presence of the representatives from the Florida Department of Transportation (FDOT) Traffic Engineering and Operations Office and Traffic Engineering Research Lab (TERL), installation technicians from Horsepower Electric Inc. and members of the WOW technical team. The results in this chapter are restricted to 0-degree wind direction, with results for additional wind directions presented in appendix F.

8.3.1. Wind induced forces

The directions of the forces are shown in Figure 118. The mean and peak forces obtained at various wind speeds are discussed in this section. Figure 121 presents the wind induced mean forces on loadcell 2 (messenger wire) and loadcell 4 (catenary wire) at 0 degrees wind direction, for increasing wind speeds. It may be noted that the 'y' and 'z' components of the forces correspond to the 'drag' and 'cable tensions' respectively, while the 'x' component represents the uplift forces.

Data show that the along wind forces (Fy) and cable tensions (Fz) increase with increasing wind speed at loadcell 2 (messenger wire), while Fy and Fz at loadcell 4 (catenary wire) experiences minimal change with increasing wind speeds. The highest along wind force of 219 lb and highest cable tension of 296 lb were found at loadcell 2 at 130 mph. Similarly, the lift (Fx) increases with increasing wind speed on loadcell 2 (messenger), while loadcell 4 (catenary) experienced minimal change in the lift forces.

Similar observations were made for loadcell 5 (messenger) and loadcell 1 (catenary) as shown in Figure 122. For instance, Fz (cable tension) and Fy (drag) increase with increasing wind speed on loadcell 5 (messenger wire). Fx on loadcell 5 also increases initially but drops slightly beyond 100 mph. Fy and Fz increase slightly beyond 100 mph on loadcell 1 (catenary). In general, the messenger wire experienced higher drag and cable tensions than the catenary wire for a given wind speed.

The peak forces at 0 degrees wind direction for loadcell 2 and loadcell 4 are shown in Figure 123. The highest magnitude of peak forces is reported, since these values are critical to the safe wind design of span wire traffic signals. The peak forces of Fx, Fy and Fz increase sharply beyond

100 mph. Figure 124 presents results for loadcell 5 (messenger) and loadcell 1 (catenary). In general, Fy (drag) and Fz (cable tensions) on loadcells 1 and 5 increase with increasing wind speeds. The highest values of tension on loadcell 5 (messenger) and loadcell 1 (catenary) were found to be 662 lb and 430 lb, respectively at 130 mph. Results for additional wind directions are presented in appendix F.

Figure 125 (a) presents the 'total' mean drag and lift forces on the traffic signals. Results show that the drag on the traffic signals increase with an increase in wind speed – highest values of 432 lb was obtained at 130 mph at 0 degrees wind direction. The lift forces also increase with increase in wind speed, although beyond 100 mph the lift force drops slightly. The peak drag and lift also increase with increasing wind speeds, as shown in Figure 125 (b).

8.3.2. rms of accelerations

The root mean square (rms) of accelerations are presented in Figure 126. Accelerometers 4, 6 and 7 were located on the 3-scetion signal, while accelerometers 2, 3 and 5 were located on the 5-section signal (see Figure 119 and Figure 120). In general, the rms of accelerations obtained from all the accelerometers increase gradually with an increase in wind speed from 40 mph to 100 mph. Beyond 100 mph the sensors were removed to avoid any possible damage caused by excessive vibration.

8.3.3. Inclinations of the traffic signals

Figure 127 shows the inclinations (mean and maximum) obtained from inclinometers 1, 2 and 4 at 0 degrees wind direction. It may be noted that for inclinometer 1, '1-1' refers to the component of inclination perpendicular to the wind, while '1-2' refers to the component of inclination in the direction of wind. The highest mean inclination of 33 degrees and highest peak inclination of 45 degrees were obtained at wind speed of 70 mph. The values of inclinations were negligible for components of inclination perpendicular to the wind for wind speed range of 40-70 mph. Beyond 70 mph, an erratic movement of the traffic signals was observed, with a wide range of inclinations.

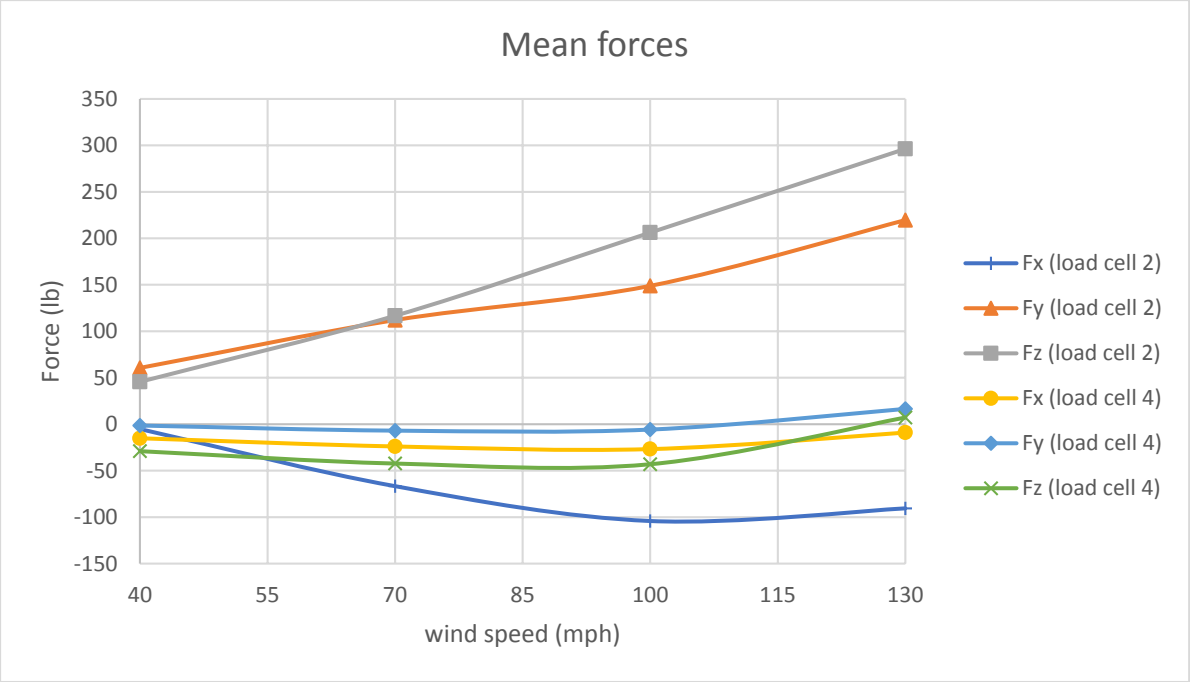

Figure 121: Mean forces on loadcells 2 (messenger wire) and 4 (catenary wire) at 0 degrees wind direction

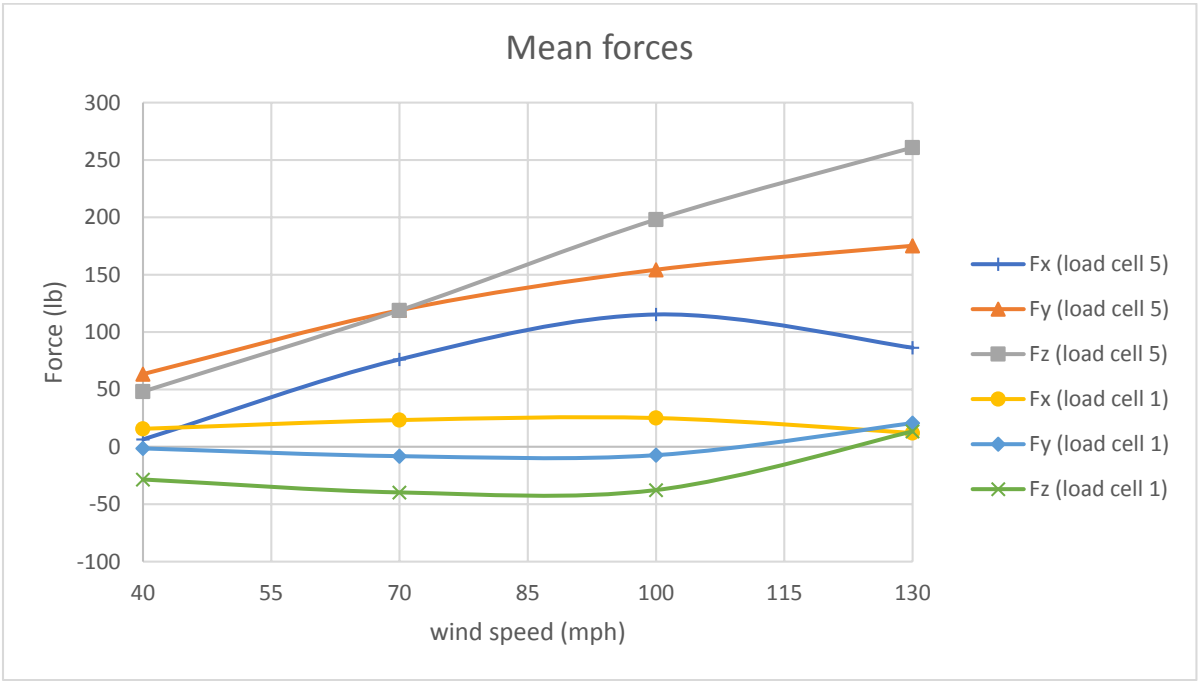

Figure 122: Mean forces on loadcells 1 (catenary wire) and 5 (messenger wire) at 0 degrees wind direction

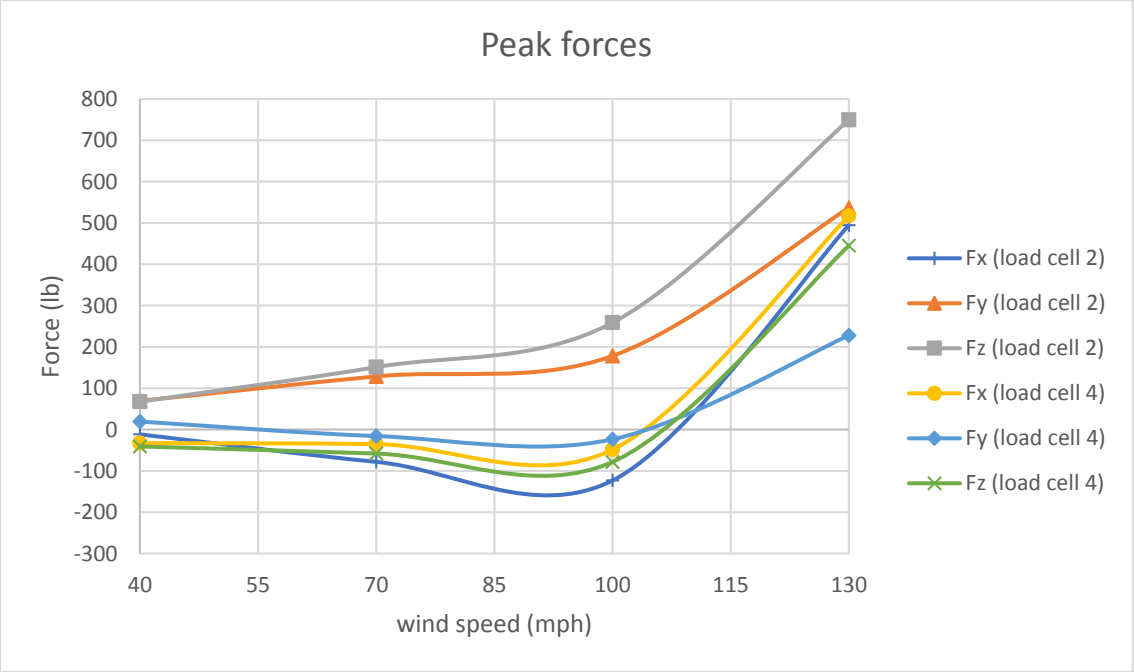

Figure 123: Peak forces at 0 degrees wind direction on loadcells 2 (messenger wire) and 4 (catenary wire)

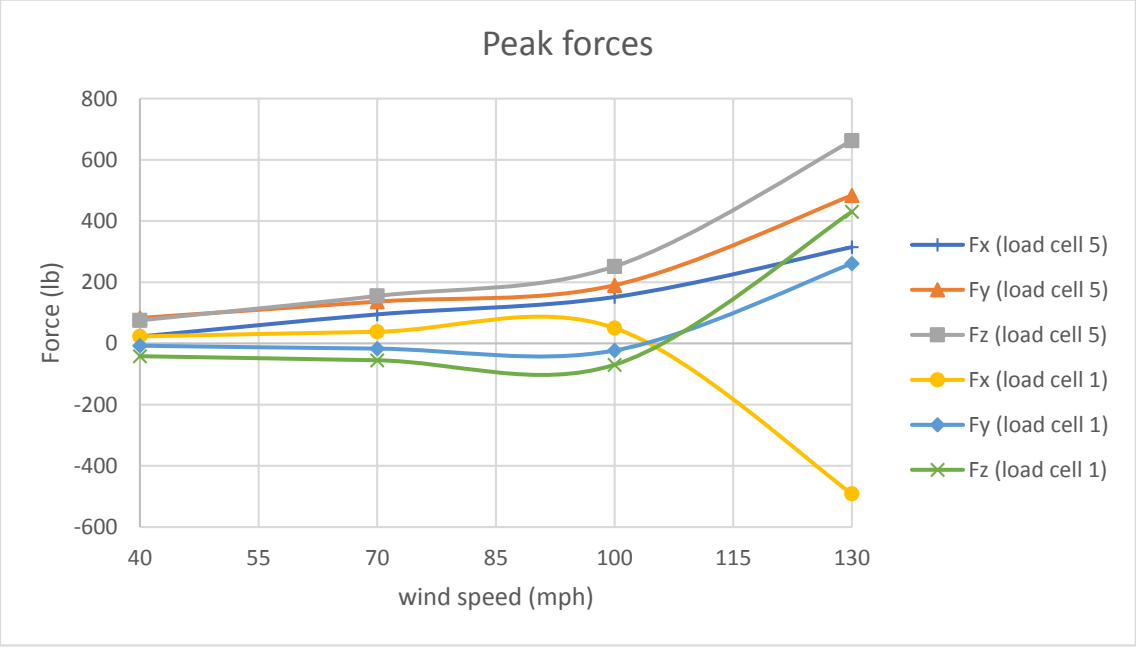

Figure 124: Peak forces at 0 degrees wind direction on loadcells 1 (catenary wire) and 5 (messenger wire)

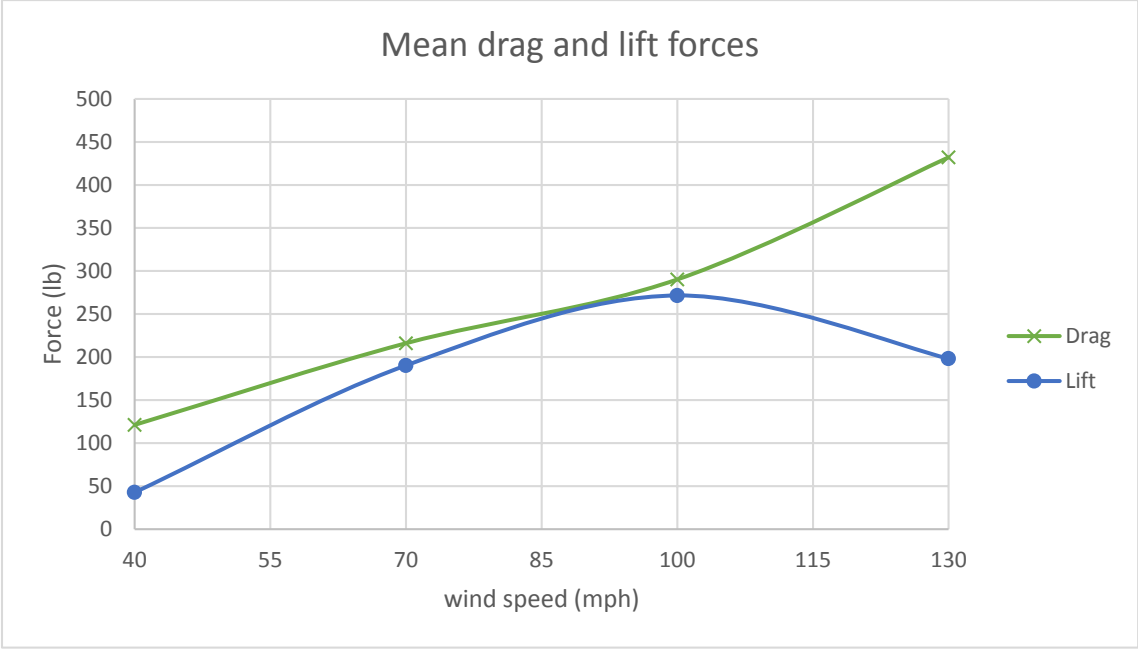

a)

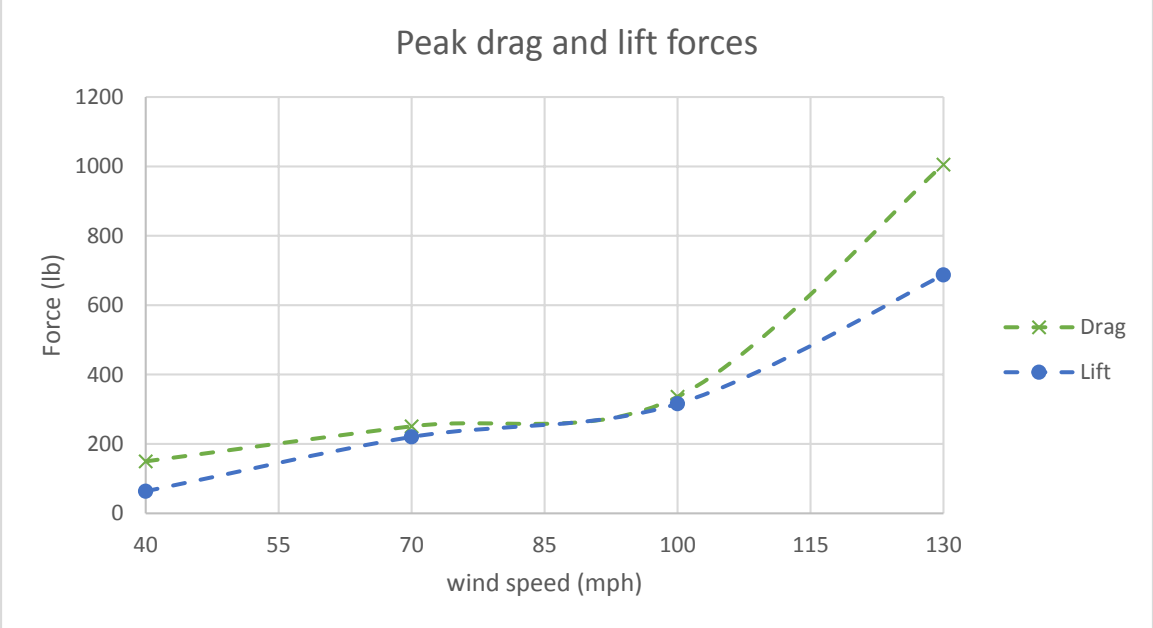

b)

Figure 125: Drag (Fy) and lift (Fx) forces on the traffic signals at 0 degrees: a) Mean; b) Peak

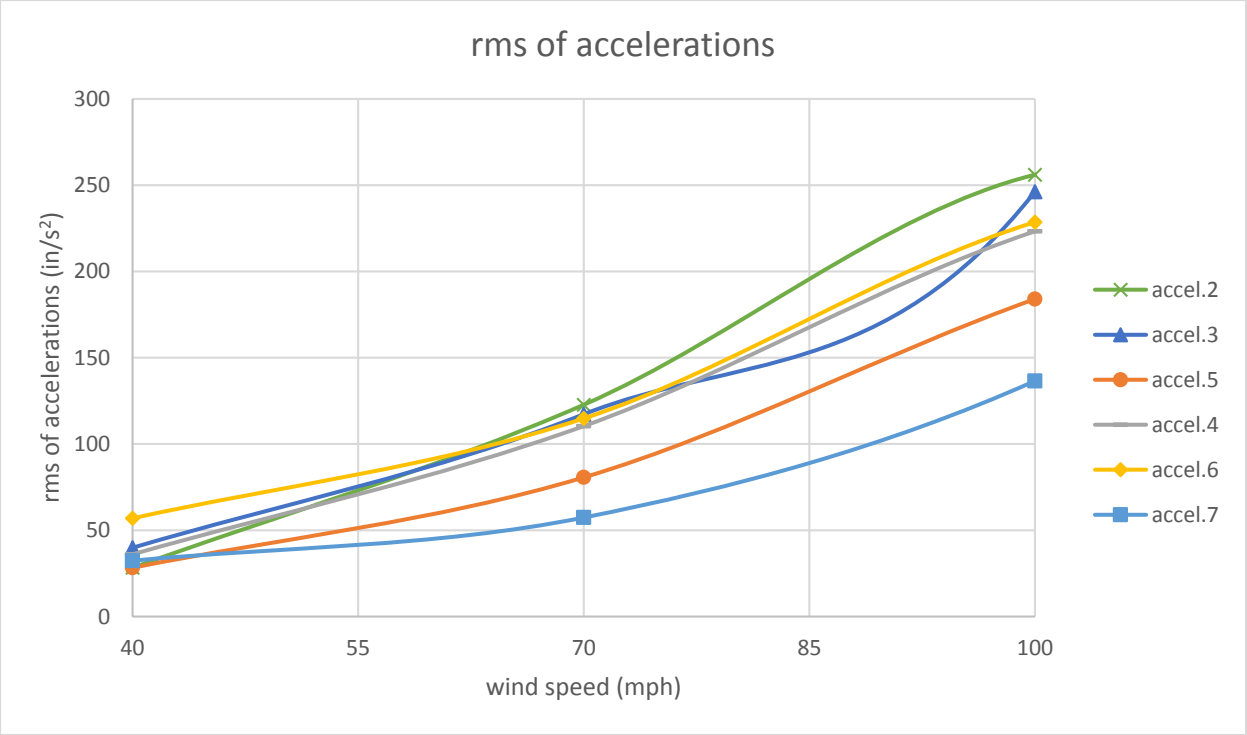

Figure 126: rms of accelerations on the 3-section and 5-section signals at 0 degrees

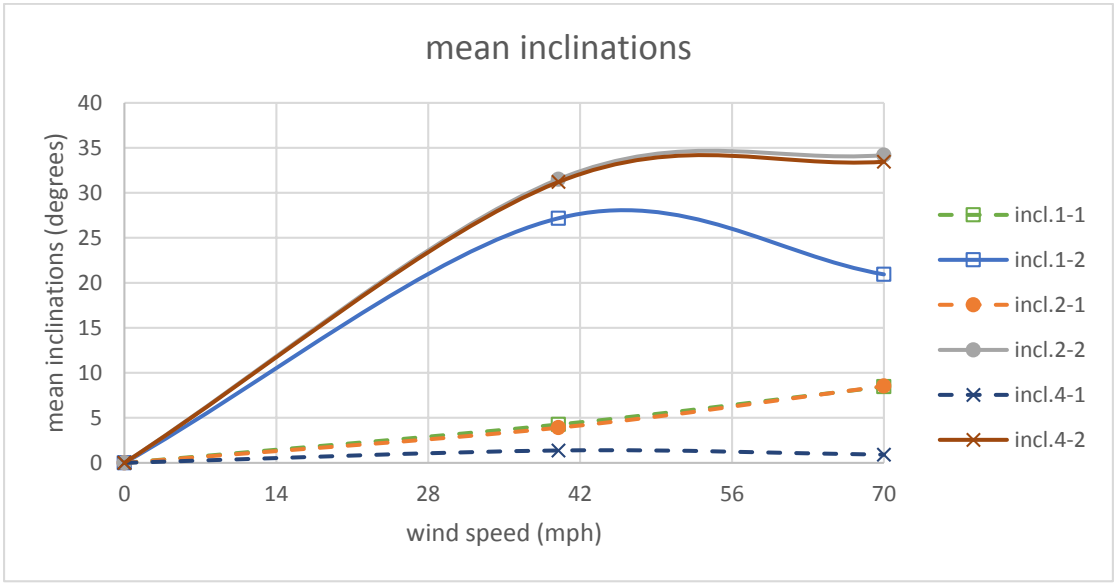

a)

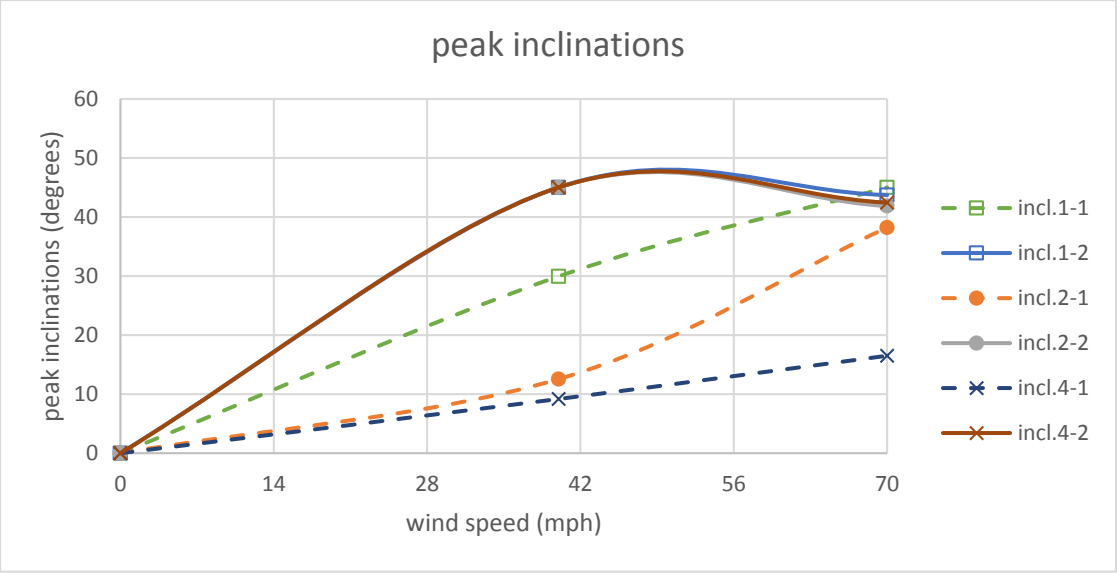

b)

Figure 127: Inclinations obtained at 0 deg for inclinometers 1 and 3

8.4. Performance of traffic signals during the tests

This test utilized two 3-section and one 5-section aluminum traffic signals installed in a span wire configuration connected to the catenary and messenger wires by means of a "**tri-stud adjustable hanger" (also known as base configuration)** assembly.

Commencing the test at 40 mph there was no visible evidence of damage to any section of the signal assembly throughout the full range of wind directions. Continuing through to 70 mph there was also no visible indication of damage to any segment of the signal assembly other than slight flexure of the tri-stud adjustable hangers. All back plates and visors were intact. Progressing to 100 mph, through all wind directions, there was no visible signs of damage to the traffic signals, back plates or visors. There was higher degree of flexure observed on the tri-stud adjustable hanger assemblies. There was a permanent bend remaining on all tri-stud adjustable hangers, particularly on the one connected to the 5-section signal, at the end of the 100-mph test through all wind directions. All back plates and visors remained intact.

At 130 mph there was more flexure in the tri-stud hangers. One tri-stud hanger extension bar broke and the other two experienced severe and permanent bend. Flutter instability was first observed and was severe. Upper segments of back plates became detached. Visors remained intact. Ultimately lower portion of the 5-section signal severed and flew away. Lower portion of 5-section signal that severed is shown in Figure 128. Figure 129 shows the traffic signals after the completion of 130 mph wind speed test. The disconnect boxes for the 5-section and 3-section traffic signals displayed no visible damage at the end of 130 mph wind speed test as shown in Figure 130 and Figure 131 respectively. A summary of the observed damages is as follows:

- Damage to signal hanger: One tri-stud hanger extension bar broke and the other two experienced severe and permanent bend.
- Damage to disconnect hanger (box): No permanent visual damage observed.
- Damage to signal housing assembly: Damage to visors and back plate. Lower portion of the 5-section signal severed and flew away.

Figure 128: Lower portion of 5-section signal that severed

Figure 129: Traffic signals after completion of test

Figure 130: Disconnect box for 5-section signal with no visible damage (all wiring removed)

Figure 131: Disconnect box for 3-section signal with no visible damage (all wiring removed)

8.5. Conclusions

This chapter summarizes the results of a test conducted at WOW at FIU for a span wire traffic signal assemble consisting of two 3-section and a 5-section traffic signal, connected using a "**tri-stud adjustable hanger" (also known as base configuration)**. Wind speeds were varied from 40 to 130 mph and wind directions were varied from 0 to 180 degrees. The various instruments used for this test include: loadcells to measure forces, accelerometers to measure accelerations and inclinometers to measure the inclinations. This study reports the data for different wind directions, in terms of: wind induced forces (drag (y-component), lift (x-component) and cable tension (z-component)), rms of accelerations and inclinations. Results for 0 degrees wind direction indicate that the mean and peak drag and lift on the traffic signals increase with increasing wind speeds. The cable tensions (mean and peak) increase in the messenger wire with increase in wind speed from 40 to 130 mph. At any given wind speed, the messenger wire experiences higher tensions and drag compared to the catenary wire. The rms of accelerations increased with increasing wind speed from 40 mph to 100 mph. Similar observations were made for other wind directions (see appendix F). In the range of 40 to 70 mph for 0 degrees wind direction, the highest mean inclination of 33 degrees was recorded in the along wind direction. Damage was witnessed at wind direction of 0 degrees and wind speed of 100 mph in the form of bending of the tri-stud 5-section signal adjustable hanger. Bending was found to be permanent at the end of this wind speed cycle. Beyond 100 mph, a slight erratic movement of the signals was first observed (aerodynamic flutter). However, a violent and clearly seen flutter was observed beyond 130 mph. At this speed there was severe and permanent curvature on the tri-stud adjustable hanger and the upper portions of back plates were loosened even though visors were still attached. Ultimately towards the end of this test cycle the lower portion of the 5-section signal housing severed from the rest of the signal and the tri-stud hanger extension bar broke.

Chapter 9 - Task 1a: FULL SCALE TESTING - Case 8

"Adjustable Hanger Assembly with Cable Dampener, Reinforced Disconnect Hanger and a Polycarbonate Signal Housing" (vendor: Pelco Products) - Test Date: 11/18/2015

9.1. Introduction

In the first tasks of the current project a 'base' configuration was identified consisting of a 21.9 ft long section with two 3-section and one 5-section traffic signals (Task 1a – Cases 1 and 2). As a continuation of the study, FDOT tested the span wire traffic signal configurations connected to the catenary and messenger wires via a**n "adjustable hanger assembly with cable dampener, reinforced disconnect hanger and a polycarbonate signal housing" (vendor: Pelco Products)**. The tests were carried out at wind directions ranging from 0 to 180 degrees and wind speeds ranging from 40 to 150 mph. The instruments consisted of loadcells to measure wind forces, accelerometers to measure accelerations, and inclinometers to measure the inclinations of the traffic signals.

This chapter presents the results from the tests conducted on the traffic signal assembly with the **"adjustable hanger assembly with cable dampener, reinforced disconnect hanger and a polycarbonate signal housing" (vendor: Pelco Products)** at the WOW. Additional results are presented in appendix G.

9.2. Experimental methodology

9.2.1. Test Setup

The 3-3-5 signal assembly was mounted on a short-span rig (described in Chapter 1) by means of an "adjustable hanger assembly with cable dampener, reinforced disconnect hanger and a polycarbonate signal housing" (vendor: Pelco Products). Figure 132 and Figure 133 shows a portion of the traffic signal assembly and the connection. All the signals were made of aluminum and included louvered back plates and visors. The test protocol is presented in Table 15. Table 16 shows the list of components used for this signal assembly.

9.2.2. Instrumentation

The directions of the x, y and z components for each loadcell are shown in Figure 134. Loadcells number 2 and 5 were located at either end of the messenger cable and loadcells number 1 and 4 located at either end of the catenary cable.

Tri-axial accelerometers were installed in the traffic signals to measure accelerations. There was one accelerometer placed on the center top of the signal, Accel5, another placed on the bottom right side, Accel002, and a third placed on the bottom left side, Accel003 for the 5-section signal as shown in Figure 135. Accelerometer Accel007, was installed on the top center, accelerometer Accel004, was installed on the bottom left side and accelerometer Accel006, was installed on the bottom right side of the 3-section signal as shown in Figure 136.

There was one inclinometer installed on the top center of the signal, Inc4, and another on the bottom center of the signal, Inc3, for the 5-section signal as shown in Figure 135. Inclinometer, Inc2, was installed on the top center and inclinometer, Inc1, was installed on the bottom center of the of the 3-section signal as shown Figure 136.

Wind speeds in three component directions (u,v,w) were also recorded by the Wall of Wind velocity sensors.

9.2.3. Test Method

The test set up was first tested for ‘zero wind’ conditions, and the values of the various ‘quantities’ (forces, accelerations and inclinations) obtained were later deducted from quantities obtained for different wind speeds (also known as “zero drift removal” process).

Although erratic behavior, such as aerodynamic fluttering, may not cause an initial failure of the signal equipment, it may lead to additional testing to confirm this behavior will not cause failure of the equipment when experienced for long-term.

Table 15: Test protocol (Task 1a: Case 8)

Wind Speed (mph)	Wind Direction	Total Duration (min)
40	0, 45, 80, 100, 135, 180	6
70	0, 45, 80, 100, 135, 180	6
100	0, 45, 80, 100, 135, 180	6
130	0, 45, 80, 100, 135, 180	6
150	0, 45, 80, 100, 135, 180	6
TOTAL		**30**

Table 16: Signal assembly components (Task 1a: Case 8)

Component	Manufacturer
Span wire clamp	Pelco
Adjustable hanger	Pelco
Extension bar	Pelco
Messenger clamp	Pelco
Disconnect Hanger	Pelco
Signal Assembly	Pelco
Backplate	Pelco
Visor	Pelco
LED Modules	GE - Dialight - Duralight

Figure 132: Picture of a part of the test rig frame with the 3-section signal and the adjustable hanger assembly

a)

b)

Figure 133: Traffic signal set up: a) portion of the messenger wire with the 3-section signal; b) enlarged picture of the adjustable hanger assembly connection

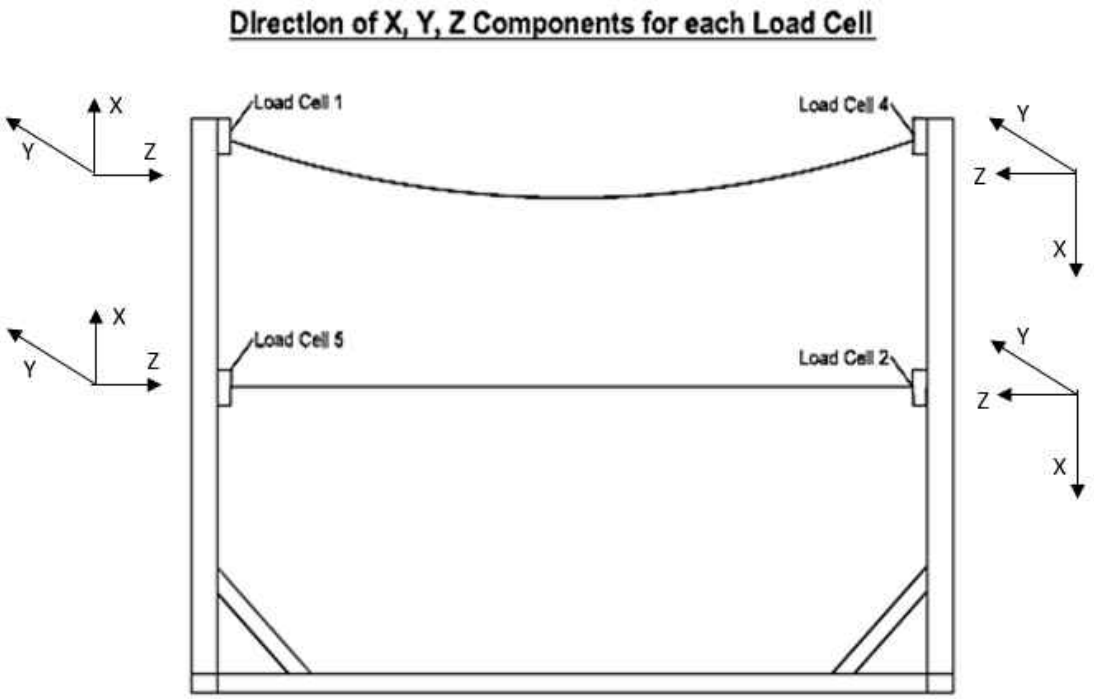

Figure 134: Direction of x, y, z components for each loadcell (direction of each axis shown represents 'positive direction')

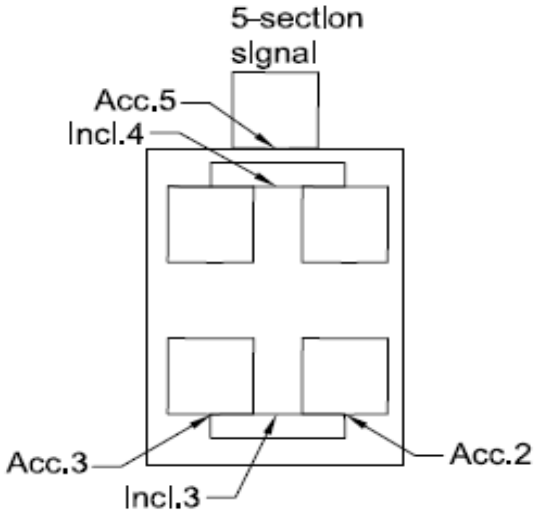

Figure 135: Location of accelerometers and inclinometers in 5-section signal

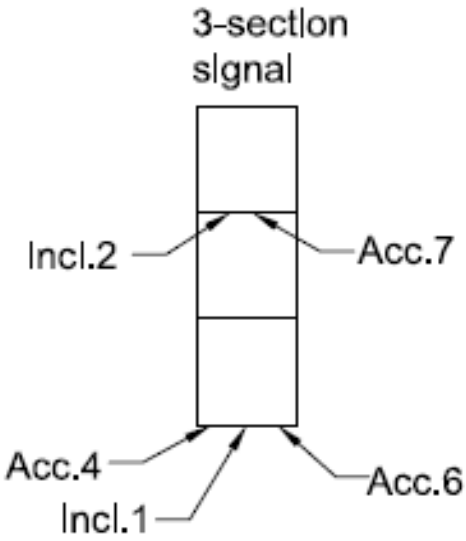

Figure 136: Location of accelerometers and inclinometers in 3-section signal

9.3. Results and discussion

The tests at the WOW were performed in the presence of the representatives from the Florida Department of Transportation (FDOT) Traffic Engineering and Operations Office and Traffic Engineering Research Lab (TERL), installation technicians from Horsepower Electric Inc. and members of the WOW technical team. The results in this chapter are restricted to 0-degree wind direction, with results for additional wind directions presented in appendix G.

9.3.1. Wind induced forces

The directions of the forces are shown in Figure 134. The mean and peak forces obtained at various wind speeds are discussed in this section. Figure 137 presents the wind induced mean forces on loadcell 2 (messenger wire) and loadcell 4 (catenary wire) at 0 degrees wind direction, for increasing wind speeds. It may be noted that the 'y' and 'z' components of the forces correspond to the 'drag' and 'cable tensions' respectively, while the 'x' component represents the uplift forces.

Data show that the along wind forces (Fy) increase with increasing wind speed at loadcell 2 (messenger wire), while Fy at loadcell 4 (catenary wire) experiences minimal change with increasing wind speeds. The highest along wind force of 171 lb was found at loadcell 2 at 150 mph. Similarly, the tension on loadcell 2 (Fz) increases in magnitude with increase in wind speed, although negligible change in tension on loadcell 4 for increasing wind speed was observed. This shows that the messenger wire experiences higher tension and drag than the catenary wire for increasing wind speeds. The uplift forces (Fx) on loadcell 2 (messenger wire) increases in magnitude with increase in wind speed. However only a marginal increase in Fx on loadcell 4 (catenary wire) with increasing wind speed was observed.

Similar observations were made for loadcell 5 (messenger) and loadcell 1 (catenary) as shown in Figure 138. For instance, Fz (cable tension) and Fy (drag) increase with increasing wind speed on loadcell 5 (messenger wire), while Fz and Fy experienced a slight increase for increasing wind speed on loadcell 1 (catenary).

The peak forces at 0 degrees wind direction for loadcell 2 and loadcell 4 are shown in Figure 139. The highest magnitude of the peak forces is reported for a given wind speed, since these are

required for the safe wind design of the traffic signals. The peak forces of Fx, Fy and Fz on loadcell 2 increase with increasing wind speeds up to 130 mph, beyond which the forces in all the three components drop. The magnitudes of the peak forces in the catenary wire were smaller than the messenger wire in the speed range of 0-70 mph. It may be noted that the 'positive direction' of 'Fx' component on loadcells 2 and 4 is 'downwards' (see Figure 134). Figure 140 presents results for loadcell 5 (messenger) and loadcell 1 (catenary). Fx (lift), Fy (drag) and Fz (cable tensions) on loadcell 5 (messenger) increase with increasing wind speeds up to 130 mph, following which the magnitudes of the forces drop. Results for additional wind directions are presented in appendix G.

Figure 141 (a) presents the 'total' mean drag and lift forces on the traffic signals. Results show that the drag and lift on the traffic signals increase with an increase in wind speed – highest mean drag of 370 lb and mean lift of 149 lb was obtained at 150 mph at 0 degrees wind direction. The peak drag and lift increase with increasing wind speed up to 100 mph, beyond which the magnitudes of the drag and lift forces decrease as shown in Figure 141 (b).

9.3.2. rms of accelerations

The root mean square (rms) of accelerations are presented in Figure 142. Accelerometers 4, 6 and 7 were located on the 3-section signal, while accelerometers 2, 3 and 5 were located on the 5-section signal (see Figure 135 and Figure 136). In general, the rms of accelerations obtained from all the accelerometers increase gradually with an increase in wind speed. Beyond 100 mph the sensors were disconnected to avoid damage.

9.3.3. Inclinations of the traffic signals

Figure 143 shows the inclinations (mean and maximum) obtained from various inclinometers at 0 degrees wind direction. It may be noted that for inclinometer 1, '1-1' refers to the component of inclination perpendicular to the wind, while '1-2' refers to the component of inclination in the direction of wind. The highest mean inclination of 38 degrees and highest peak inclination of 45 degrees was observed at wind speed of 40 mph. The values of inclinations were negligible for mean components of inclination perpendicular to the wind. Beyond 70 mph, an erratic

movement of the traffic signals (aerodynamic flutter) was observed, resulting in a wide range of inclinations.

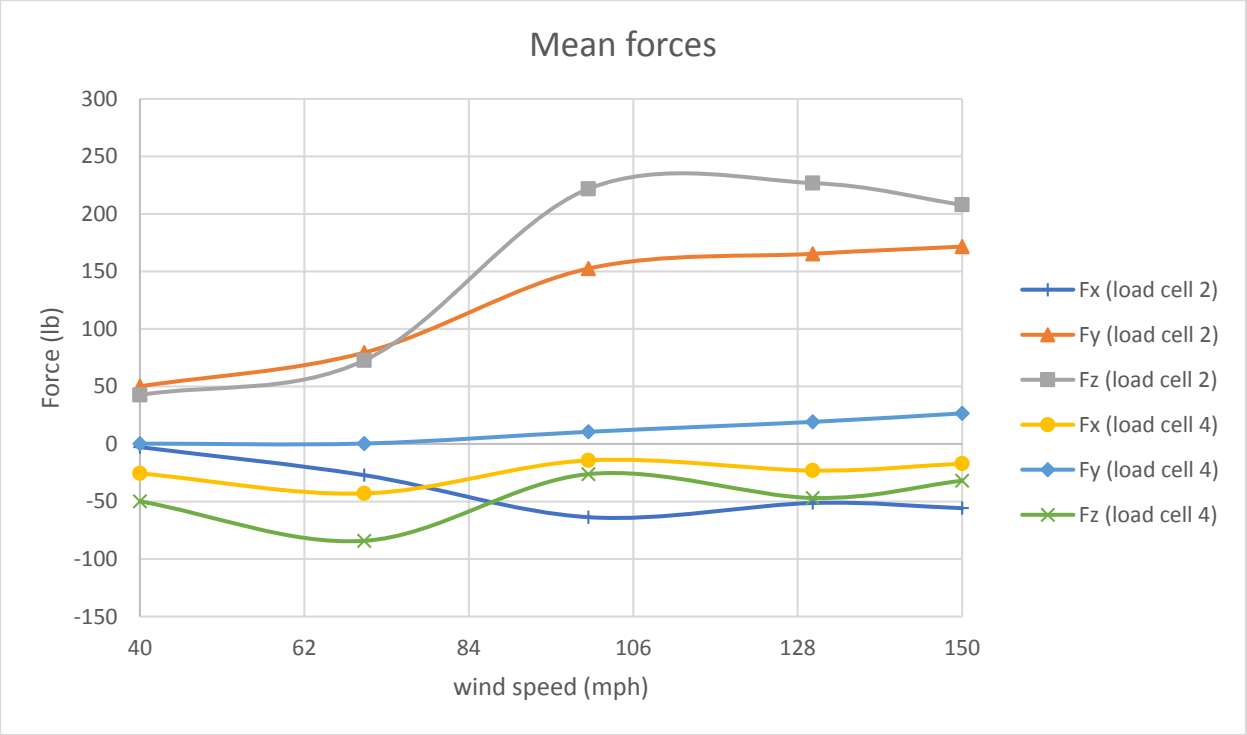

Figure 137: Mean forces on loadcells 2 (messenger wire) and 4 (catenary wire) at 0 degrees wind direction

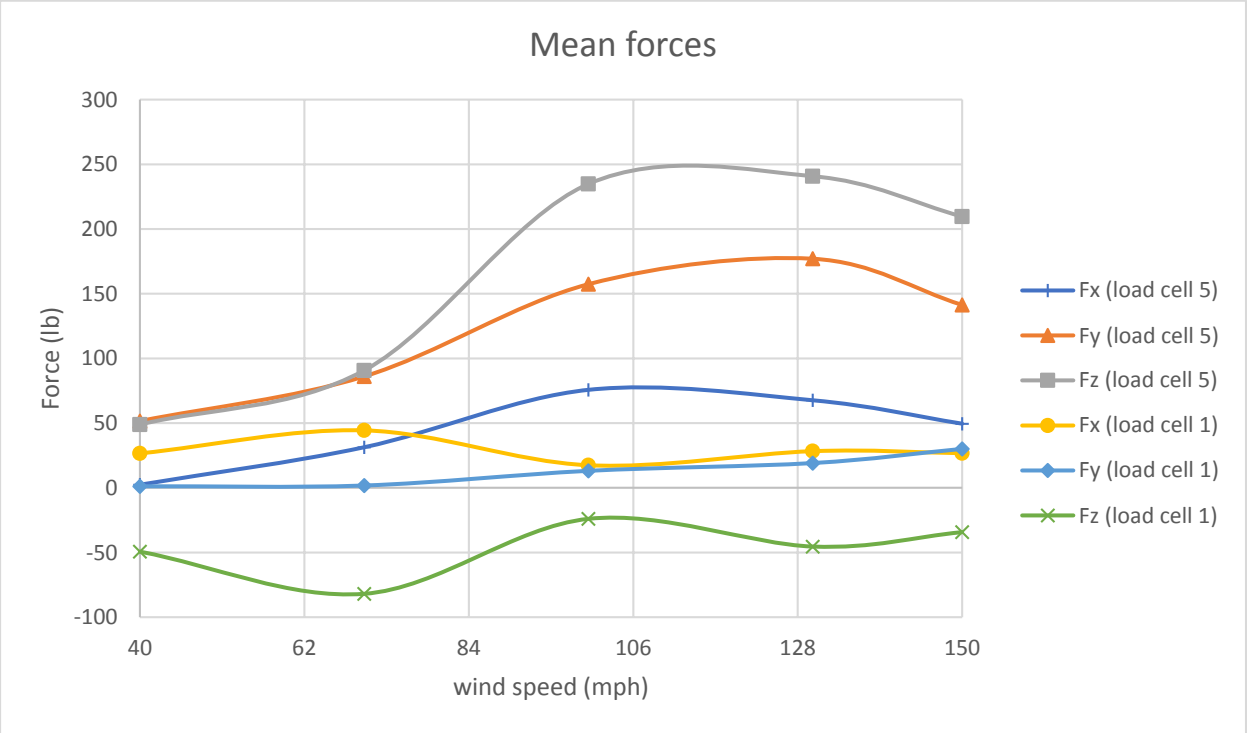

Figure 138: Mean forces on loadcells 1 (catenary wire) and 5 (messenger wire) at 0 degrees wind direction

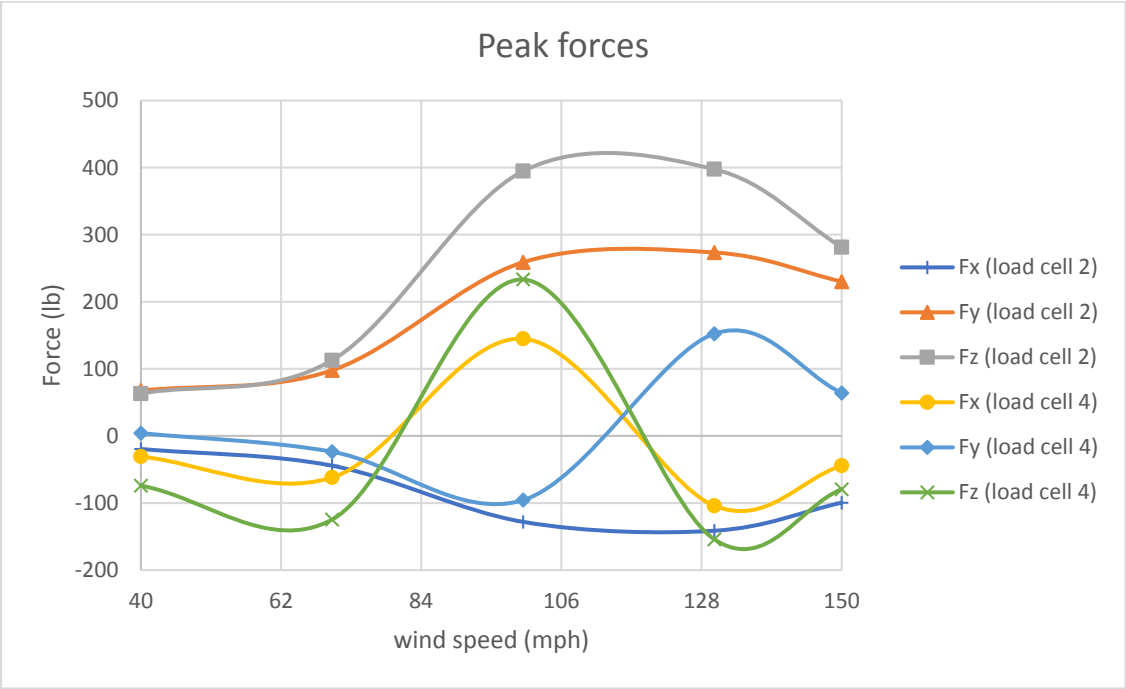

Figure 139: Peak forces at 0 degrees wind direction on loadcells 2 (messenger wire) and 4 (catenary wire)

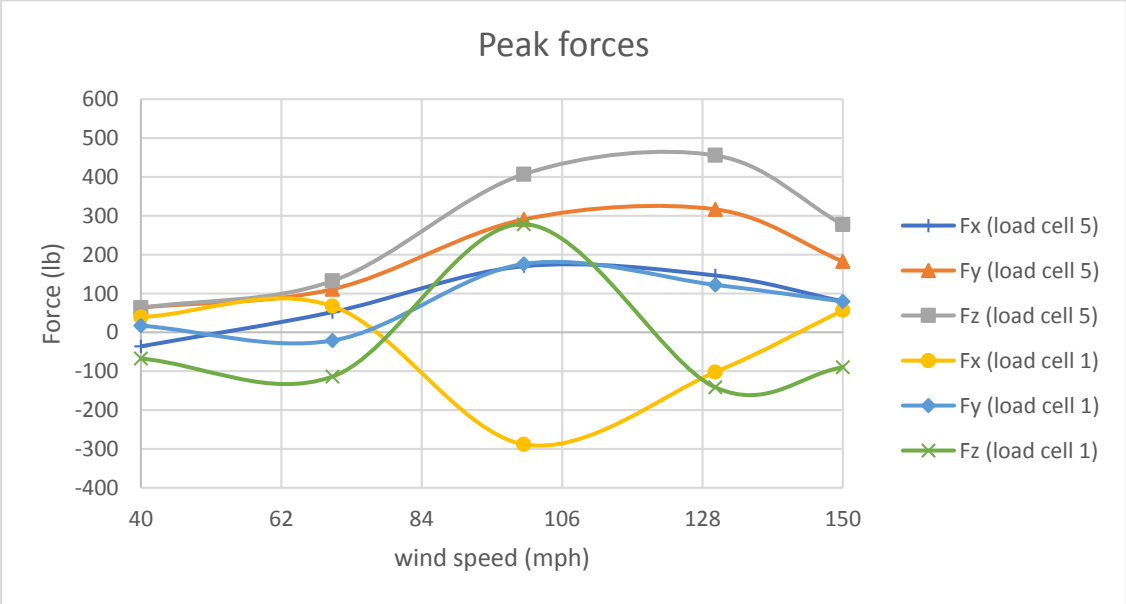

Figure 140: Peak forces at 0 degrees wind direction on loadcells 1 (catenary wire) and 5 (messenger wire)

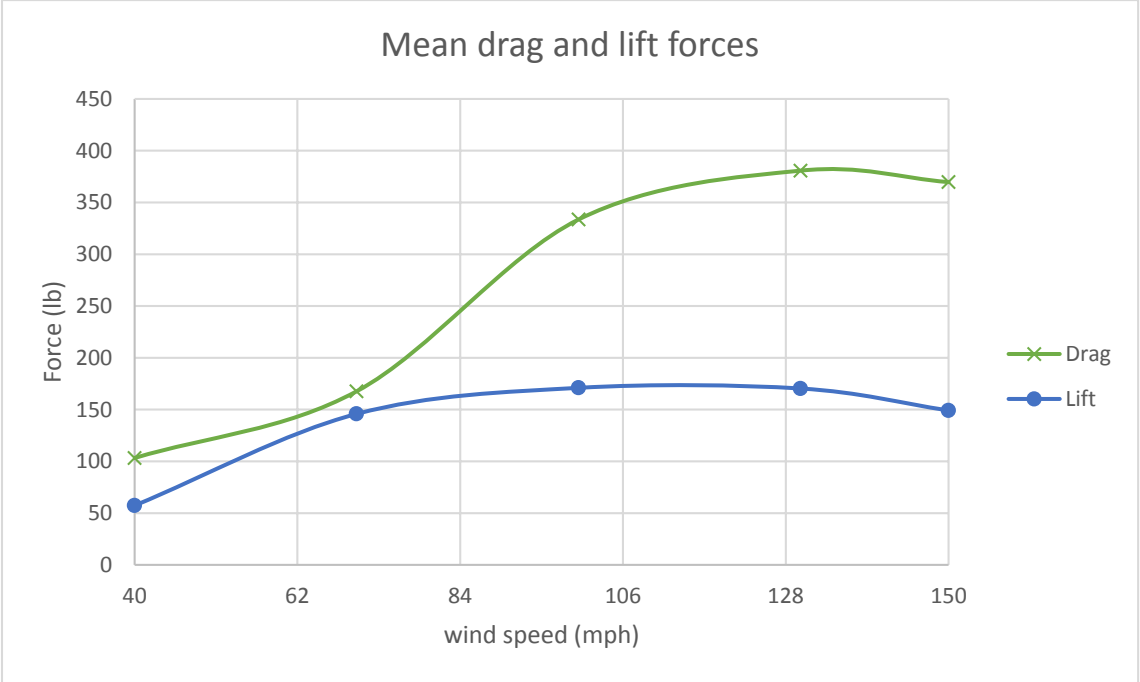

a)

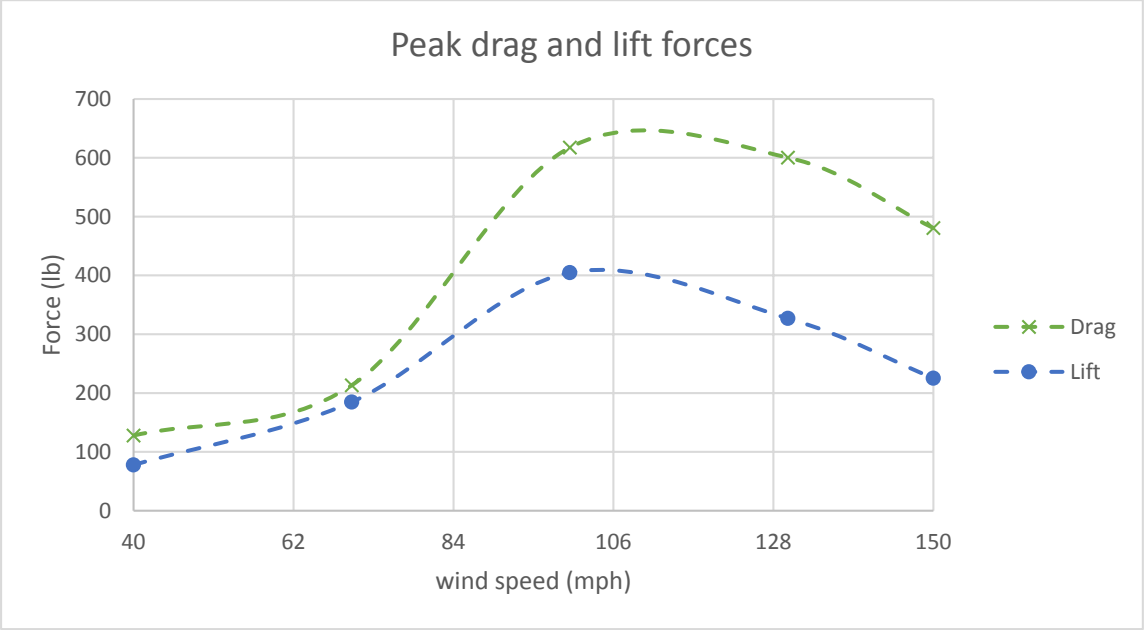

b)

Figure 141: Drag (Fy) and lift (Fx) forces on the traffic signals at 0 degrees: a) Mean; b) Peak

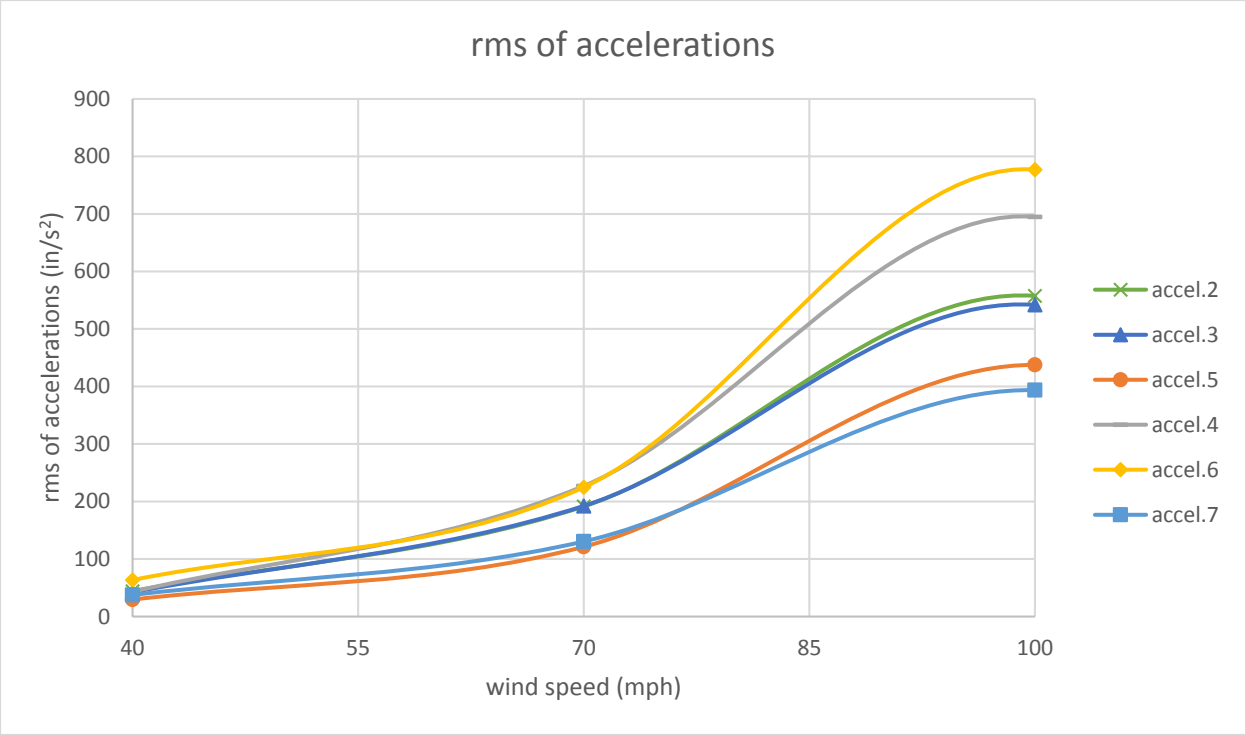

Figure 142: rms of accelerations on the 3-section and 5-section signals at 0 degrees

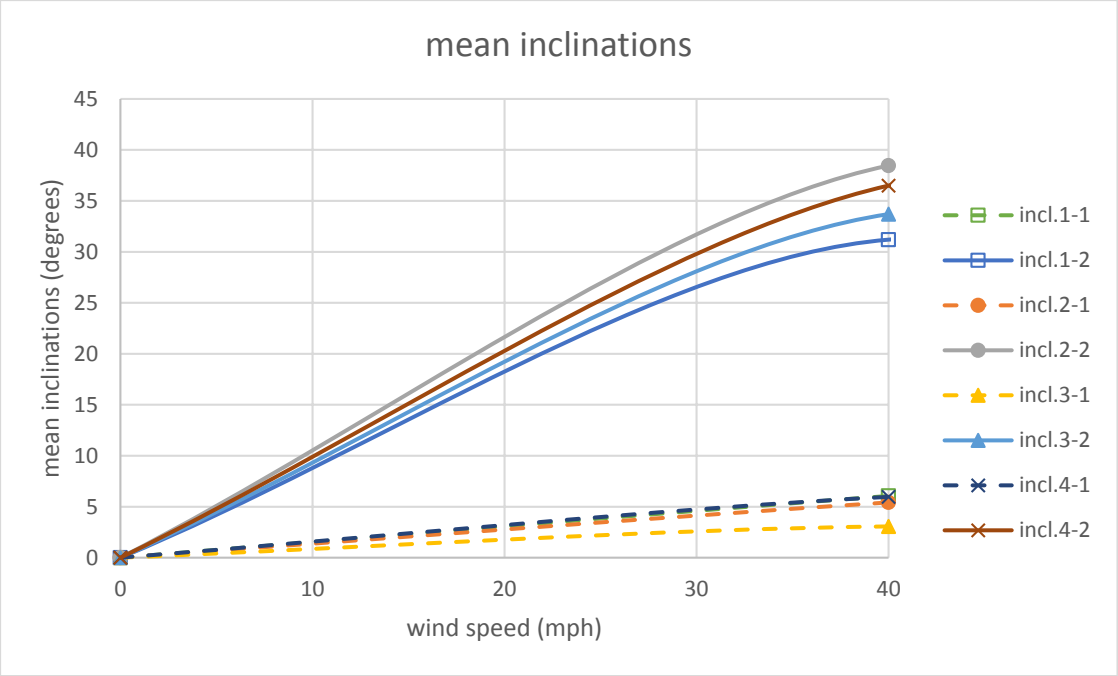

a)

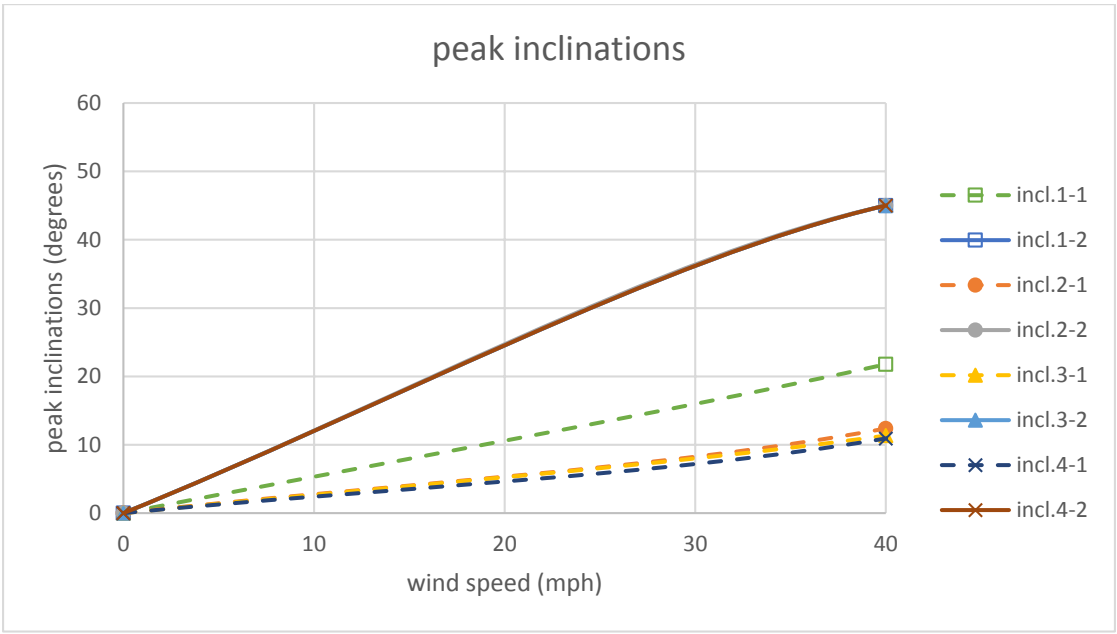

b)

Figure 143: Inclinations obtained from inclinometers at 0 deg: a) mean; b) peak

9.4. Performance of traffic signals during the tests

This test utilized two 3-section and one 5-section traffic signals span installed in a wire configuration connected to the catenary and messenger wires by means of an **"adjustable hanger assembly with cable dampener, reinforced disconnect hanger and a polycarbonate signal housing" (vendor: Pelco Products)**.

From the onset and throughout the full range of wind speeds there was flexible bending of the cable dampener portion of the adjustable hanger assembly. Once the wind subside the cable dampener fully recovered from its bent position. The adjustable hanger assembly with cable dampener exhibited no damage and recovered from its' bent position at the end of the test. The adjustable hanger assembly after completion of test is shown in Figure 144.

Traffic signals demonstrated significant aerodynamic flutter at 100 mph and above. At 120 mph the top portion of the polycarbonate 3-section traffic signal cracked at the base of the disconnect box and the entire signal was blown away by the high-speed winds and this same scenario occurred to the polycarbonate 5-section traffic signal at 130 mph. At that point most of the back plate for the 5-section signal was still attached and most of the back plate for the 3-section signal was missing. At approximately 150 mph there was only the outer 3-section polycarbonate traffic signal still attached to the messenger and catenary wire by the end of the full test cycle. Figure 145 and Figure 146 shows the 5-section polycarbonate and 3-section polycarbonate traffic signals after the completion of the full test cycle, respectively.

The reinforced disconnect box exhibited no visible damage after the full range of wind speed test. Disconnect box after the completion of the test is shown in Figure 147. A summary of the observed damages is as follows:

- Damage to signal hanger: Flexible bending of the cable portion. No permanent visual damage observed.
- Damage to disconnect hanger (box): No permanent visual damage observed.
- Damage to signal housing assembly: Top portion of the polycarbonate 3 and 5-section traffic signal cracked at the base of the disconnect box and the entire signal was blown away.

Figure 144: Pelco adjustable hanger assembly after test completion

Figure 145: 5-section polycarbonate signal after completion of full test cycle

Figure 146: 3-section polycarbonate signal after completion of full test cycle

Figure 147: Disconnect box after completion of test and broken top portion of signal assembly

9.5. Conclusions

This chapter summarizes the results of a test conducted at WOW at FIU for a span wire traffic signal assembly consisting of two 3-section and a 5-section traffic signal, connected using an **"adjustable hanger assembly with cable dampener, reinforced disconnect hanger and a polycarbonate signal housing" (vendor: Pelco Products)**. Wind speeds were varied from 40 to 150 mph and wind directions were varied from 0 to 180 degrees. The various instruments used for this test include: loadcells to measure forces, accelerometers to measure accelerations and inclinometers to measure the inclinations. This study reports the data for different wind directions, in terms of: wind induced forces (drag (y-component), lift (x-component) and cable tension (z-component)), rms of accelerations and inclinations. Results for 0 degrees wind direction indicate that along wind forces (drag) and cable tensions increase in the messenger wire with increase in wind speed. The lift on the messenger wire also increases with increasing wind speeds. The catenary wire experiences only a minor increase of all three components of wind forces with increase in wind speed. At any given wind speed the messenger wire experiences higher tension forces than the catenary wire. The rms of accelerations increased with increasing wind speed from 40 mph to 100 mph. Similar observations were made for other wind directions (see appendix G). The magnitudes of the peak forces (Fx, Fy and Fz) increased with increasing wind speeds from 40 to 150 mph, especially on the messenger wire. The highest mean inclination of 38 degrees and highest peak inclination of 45 degrees was obtained at 40 mph. At 100 mph and above, an erratic movement of the signals was observed (aerodynamic flutter). A failure was observed at 120 mph, whereby the top segment of the polycarbonate 3-section traffic signal fractured at the base of the disconnect box and the entire signal flew away. Similarly, this was observed with the polycarbonate 5-section traffic signal at 130 mph.

Chapter 10 - Task 1a: FULL SCALE TESTING - Case 9

"Steel Cable Hanger Assembly with Reinforced Disconnect Hanger and with Polycarbonate Signal Housing" (vendor: Engineered Castings) - Test Date: 3/2/2016

10.1. Introduction

In the first tasks of the current project a 'base' configuration was identified consisting of a 21.9 ft. long section with two 3-section and one 5-section traffic signals (Task 1a – Cases 1 and 2). As a continuation of the study, FDOT tested the span wire traffic signal configurations connected to the catenary and messenger wires via a **"steel cable hanger assembly with reinforced disconnect hanger and with polycarbonate signal housing" (vendor: Engineered Castings).** The tests were carried out at wind directions ranging from 0 to 180 degrees and wind speeds ranging from 40 to 150 mph. The instruments consisted of loadcells to measure wind forces, accelerometers to measure accelerations, and inclinometers to measure the inclinations of the traffic signals.

This chapter presents the results from the tests conducted on the traffic signal assembly using a **"steel cable hanger assembly with reinforced disconnect hanger and with polycarbonate signal housing" (vendor: Engineered Castings)** at the WOW. Additional results are presented in appendix H.

10.2. Experimental methodology

10.2.1. Test Setup

The 3-3-5 signal assembly was installed on a short-span rig (described in Chapter 1) by means of a "steel cable hanger assembly with reinforced disconnect hanger and with polycarbonate signal housing" (vendor: Engineered Castings). Figure 148 and Figure 149 shows the traffic signal assembly as well as the steel cable hanger assembly. Signals were made of either aluminum or polycarbonate and included louvered back plates and visors. The test protocol is presented in Table 17. Table 18 shows the list of components utilized for this signal assembly.

10.2.2. Instrumentation

The directions of the x, y, z components for each loadcell are shown in Figure 150. Loadcells number 2 and 5 were located at either end of the messenger cable and loadcells number 1 and 4 located at either end of the catenary cable.

Tri-axial accelerometers were installed in the traffic signals to measure accelerations. There was one accelerometer placed on the center top of the signal, Accel005, another placed on the bottom right side, Accel002, and a third placed on the bottom left side, Accel003 for the 5-section signal as shown in Figure 151. Accelerometer Accel007, was installed on the top center, accelerometer Accel004, was installed on the bottom left side and accelerometer Accel006, was installed on the bottom right side of the 3-section signal as shown in Figure 152.

There was one inclinometer installed on the top center of the signal, Inc4, and another on the bottom center of the signal, Inc3, for the 5-section signal as shown in Figure 151. Inclinometer, Inc2, was installed on the top center and inclinometer, Inc1, was installed on the bottom center of the of the 3-section signal as shown Figure 152.

Wind speeds in three component directions (u, v, w) were also recorded by the Wall of Wind velocity sensors.

10.2.3. Test Method

The test set up was first tested for ‘zero wind’ conditions, and the values of the various ‘quantities’ (forces, accelerations and inclinations) obtained were later deducted from quantities obtained for different wind speeds (also known as “zero drift removal” process).

Although erratic behavior, such as aerodynamic fluttering, may not cause an initial failure of the signal equipment, it may lead to additional testing to confirm this behavior will not cause failure of the equipment when experienced for long-term.

Table 17: Test protocol (Task 1a: Case 9)

Wind Speed (mph)	Wind Direction	Total Duration (min)
40	0, 45, 80, 100, 135, 180	6
70	0, 45, 80, 100, 135, 180	6
100	0, 45, 80, 100, 135, 180	6
130	0, 45, 80, 100, 135, 180	6
150	0, 45, 80, 100, 135, 180	6
TOTAL		**30**

Table 18: Signal assembly components (Task 1a: Case 9)

Component	Manufacturer
Span wire clamp	Pelco
Adjustable hanger	Pelco
Extension bar	No extension bar
Messenger clamp	Pelco
Disconnect Hanger	Engineered Castings
Signal Assembly	McCain
Backplate	TCS
Visor	McCain
LED Modules	GE - Dialight - Duralight

Figure 148: Picture of test rig frame with the signals and the steel cable hanger assembly

a)

b)

Figure 149: Traffic signal set up: a) 3-section signal showing the steel cable hanger assembly with reinforced disconnect hanger (vendor: Engineered Castings); b) traffic signal assembly facing the wind

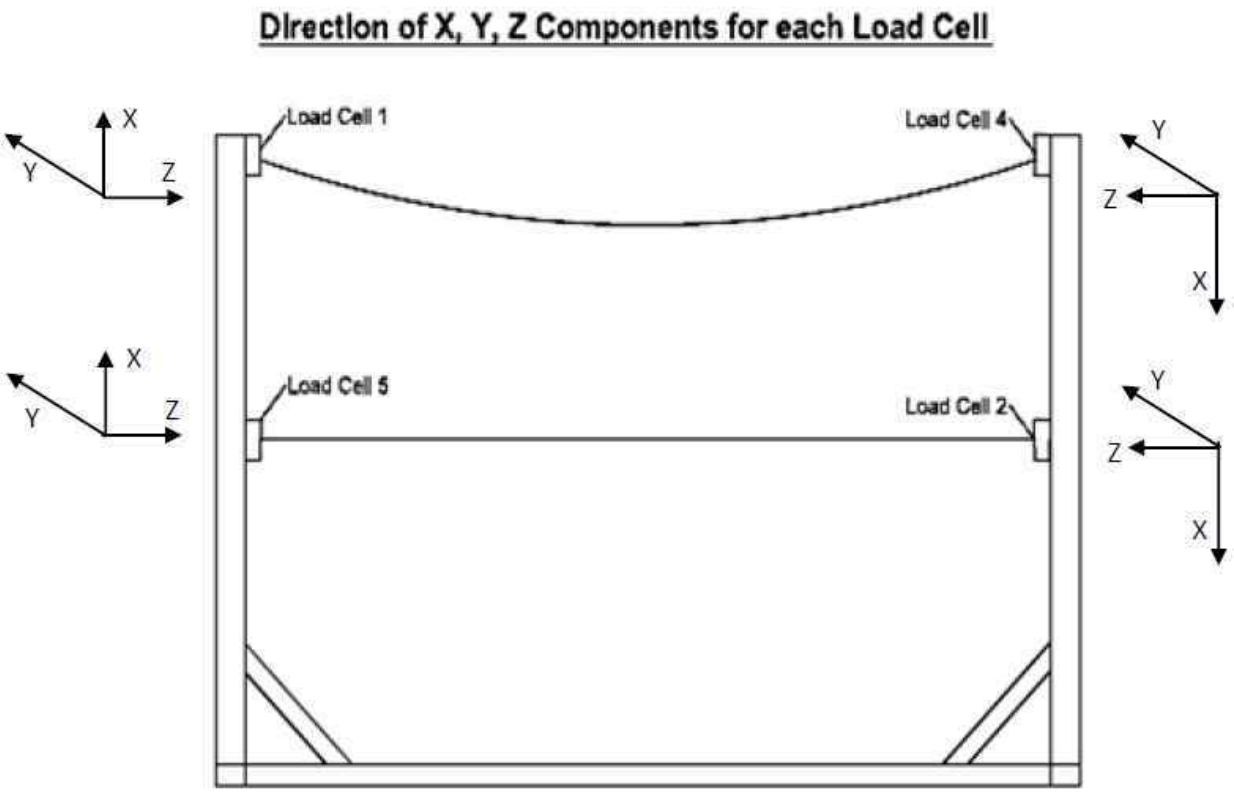

Figure 150: Direction of x, y, z components for each loadcell (direction of each axis shown represents 'positive direction')

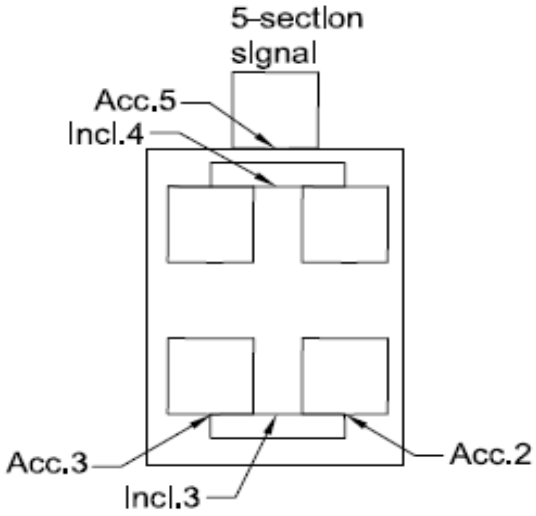

Figure 151: Location of accelerometers and inclinometers in 5-section signal

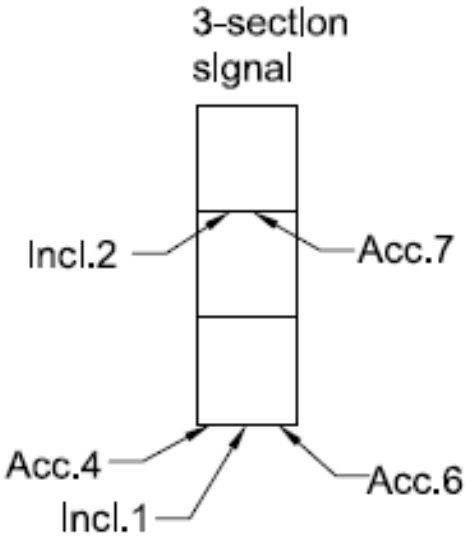

Figure 152: Location of accelerometers and inclinometers in 3-section signal

10.3. Results and discussion

The tests at the WOW were performed in the presence of the representatives from the Florida Department of Transportation (FDOT) Traffic Engineering and Operations Office and Traffic Engineering Research Lab (TERL), installation technicians from Horsepower Electric Inc., manufacturer and distributer of the steel cable hanger assembly with reinforced disconnect hanger and members of the WOW technical team. The results in this chapter are restricted to 0-degree wind direction, with results for additional wind directions presented in appendix H.

10.3.1. Wind induced forces

The directions of the forces are shown in Figure 150. The mean and peak forces obtained at various wind speeds are discussed in this section. Figure 153 presents the wind induced mean forces on loadcell 2 (messenger wire) and loadcell 4 (catenary wire) at 0-degrees wind direction, for increasing wind speeds. It may be noted that the 'y' and 'z' components of the forces correspond to the 'drag' and 'cable tensions' respectively, while the 'x' component represents the uplift forces.

Data show that the along wind forces (Fy) increase with increasing wind speed at loadcell 2 (messenger wire), while Fy at loadcell 4 (catenary wire) experiences minimal increase with increasing wind speeds. The highest along wind force of 163 lbs. was found at loadcell 2 at 150 mph. Similarly, the tension on loadcell 2 (Fz) increases with an increase in wind speed, although a slight increase in tension on loadcell 4 (catenary wire) for increasing wind speed was observed, followed by a small decrease starting at 70 mph wind speed. This shows that the messenger wire experiences higher tension and drag than the catenary wire for increasing wind speed. The uplift forces (Fx) on loadcell 2 (messenger wire) slightly increases in magnitude with increase in wind speed. An increase in uplift forces Fx on loadcell 4 (catenary wire) with increasing wind speed was observed up to 70 mph. Afterwards it began to decrease.

Similar observations were made for loadcell 5 (messenger) and loadcell 1 (catenary) as shown in Figure 154. For instance, Fz (cable tension) and Fy (drag) increase with increasing wind speed on loadcell 5 (messenger wire). Fx on loadcell 5 increases as wind speed increases up to 70 mph, afterwards it begins to slightly decrease.

The peak forces at 0-degrees wind direction for loadcell 2 and loadcell 4 are shown in Figure 155. The peak forces of Fz on loadcell 2 generally increase with increasing wind speeds up to 150 mph. The peak forces of Fz on loadcell 4 increase for 40 mph to 70 mph wind speed range, afterwards it begins to decrease. The peak forces of Fy on loadcell 2 generally increase with an increase in wind speed. The peak forces of Fy on loadcell 4 increase with increasing wind speeds up to 100 mph, thereafter showing a decreasing trend. It may be noted that the 'positive direction' of 'Fx' component on loadcells 2 and 4 is 'downwards' (see Figure 150). The magnitude of the peak force Fx on loadcell 2 increases with an increase in wind speed from 40 mph to 100 mph, afterwards it decreases in magnitude. Similarly, Fx on loadcell 4 increases for 40 mph to 70 mph wind speed range, following a decrease in magnitude. Figure 156 presents result for loadcell 5 (messenger) and loadcell 1 (catenary). Fz (cable tension) on loadcell 5 increases with increasing wind speeds from 40 mph to 100 mph. At 100 mph it commences to decrease with a slight upturn at 150 mph. Fz on loadcell 1 experiences an increase up to 70 mph wind speed but after begins to decrease. In fact, similar trends were observed for Fy on loadcells 5 and 1. Fx (lift) on loadcell 5 (messenger) and loadcell 1 (catenary) increase for increasing wind speeds to 100 mph wind speed but thereafter exhibiting a decrease. Results for additional wind directions are presented in appendix H.

Figure 157 (a) presents the 'total' mean drag and lift forces on the traffic signals. Results show that the drag on the traffic signals increase with an increase in wind speed– a value of 334 lbs. was obtained at 150 mph at 0-degrees wind direction. Lift forces increase between 40 mph and 70 mph wind speed and thereafter begins to decrease. The peak drag and lift are shown in Figure 157 (b). The peak drag increases with increasing wind speeds with a slight dip at 130 mph wind speed, but the peak lift increases with increasing wind speeds to 100 mph but afterwards displays a decrease in magnitude.

10.3.2. rms of accelerations

The root mean squares (rms) of accelerations are presented in Figure 158. Accelerometers 4, 6 and 7 were located on the 3-section signal, while accelerometers 2, 3 and 5 were located on the 5-section signal (see Figure 151 and Figure 152). In general, the rms of accelerations obtained

from all the accelerometers increase gradually with an increase in wind speed up to 100 mph wind speed. Thereafter the sensors were removed to avoid damage caused by excessive vibration.

10.3.3. Inclinations of the traffic signals

Figure 159 shows the inclinations (mean and maximum) obtained from inclinometer 1 (3-section) and inclinometer 3 (5-section) at 0-degrees wind direction. It may be noted that for inclinometer 1, '1-1' refers to the component of inclination perpendicular to the wind, while '1-2' refers to the component of inclination in the direction of wind. For inclinometers 1 and 3, the mean components '1-2' and '3-2' are generally in the range of 27 to 39 degrees for 40-70 mph wind speed range. Similarly, the maximum value of about 48 degrees was obtained at a wind speed of 70 mph for the inclinometer component 3-2. The values of inclinations were negligible for 1-1 and 3-1 components in the wind speed range of 40-70 mph. At 70 mph, an erratic movement of the traffic signals (aerodynamic flutter) was observed.

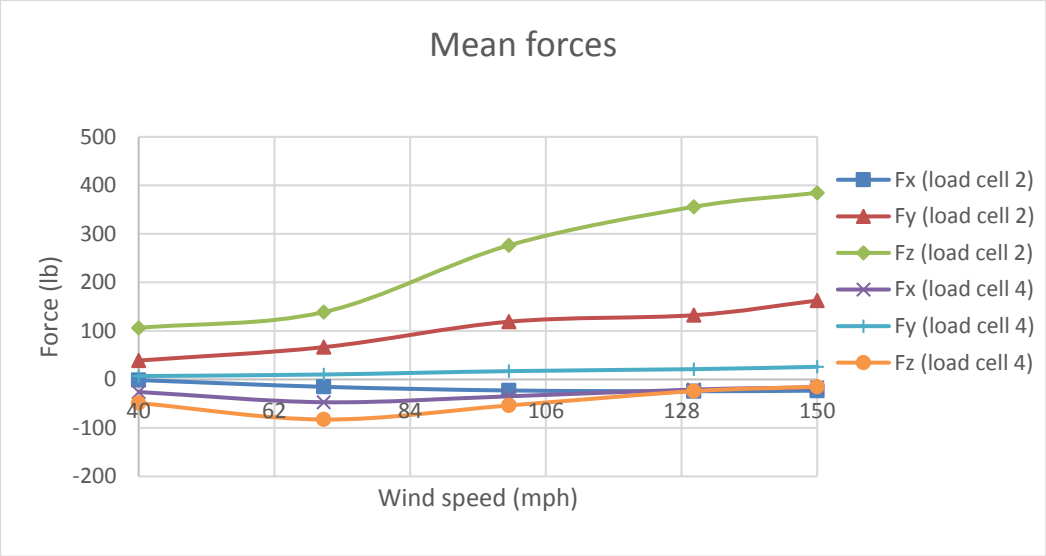

Figure 153: Mean forces on loadcells 2 (messenger wire) and 4 (catenary wire) at 0-degrees wind direction

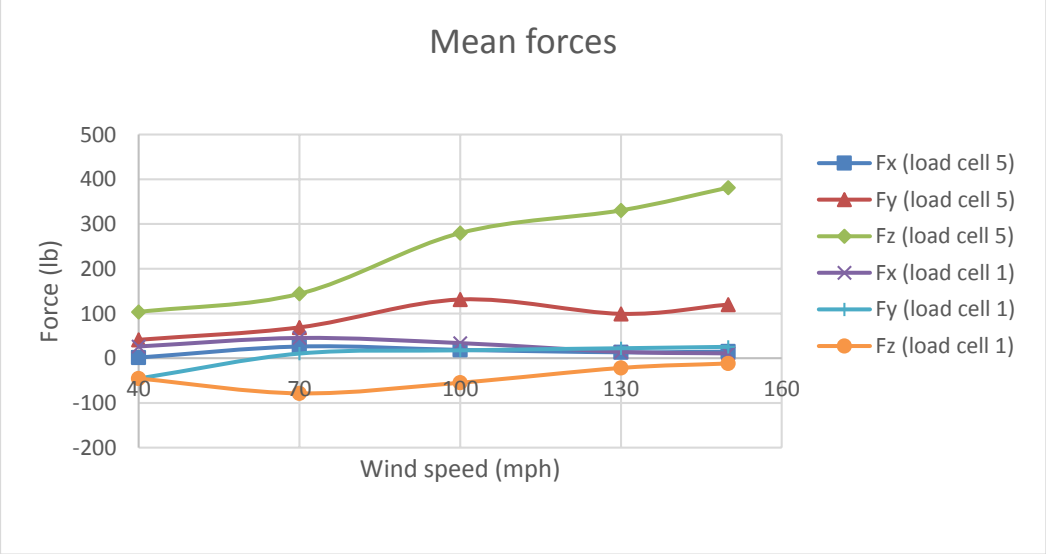

Figure 154: Mean forces on loadcells 1 (catenary wire) and 5 (messenger wire) at 0-degrees wind direction

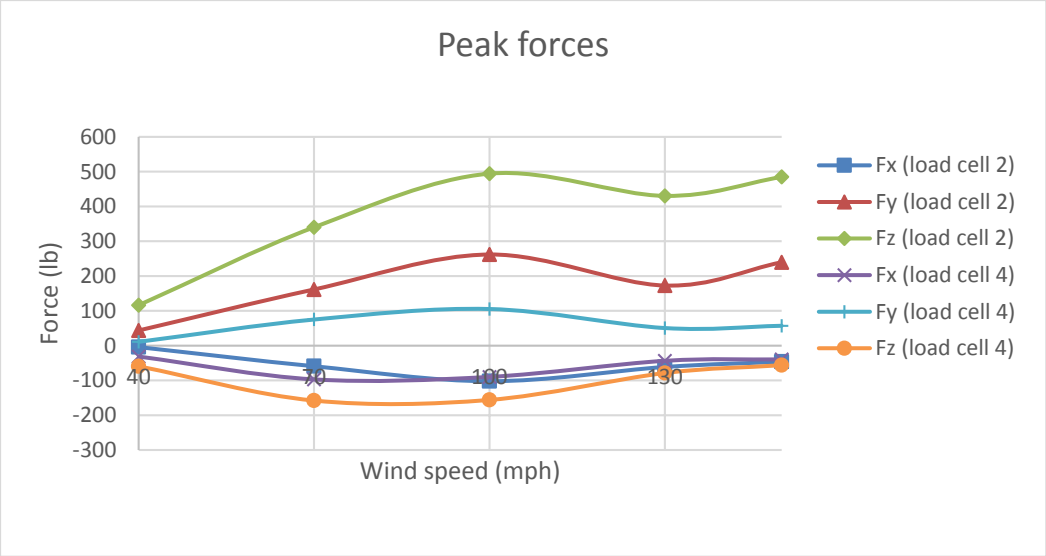

Figure 155: Peak forces at 0-degrees wind direction on loadcells 2 (messenger wire) and 4 (catenary wire)

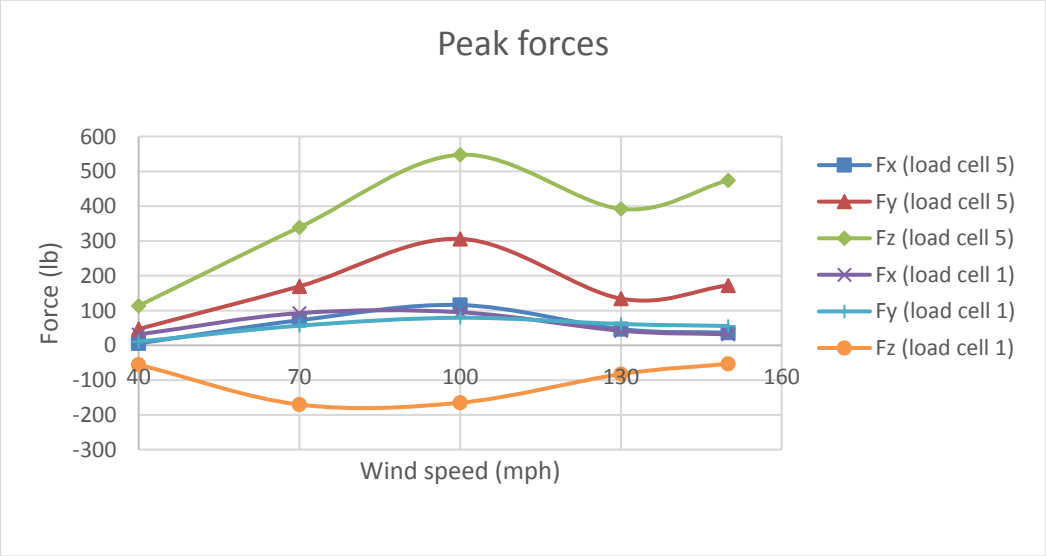

Figure 156: Peak forces at 0-degrees wind direction on loadcells 1 (catenary wire) and 5 (messenger wire)

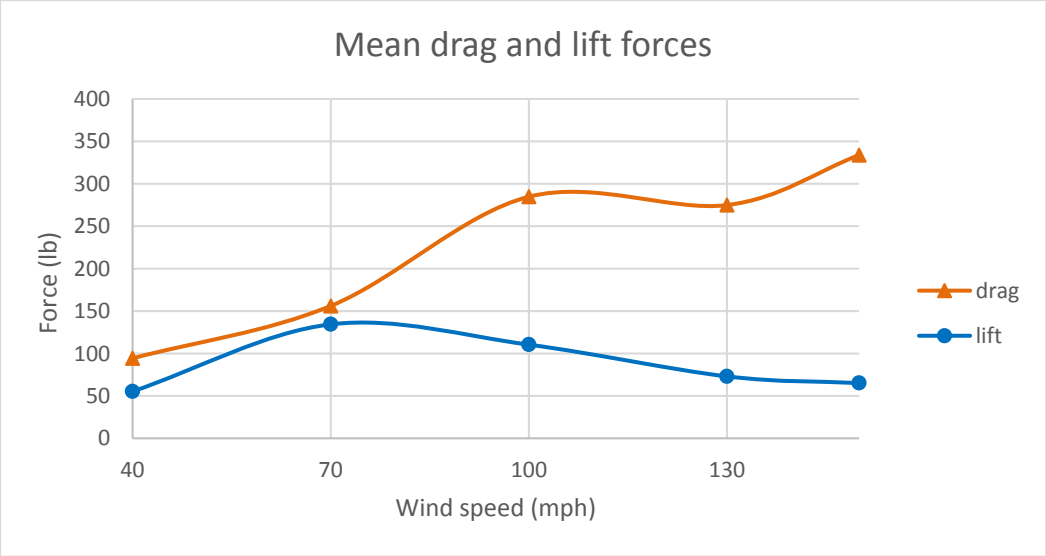

a)

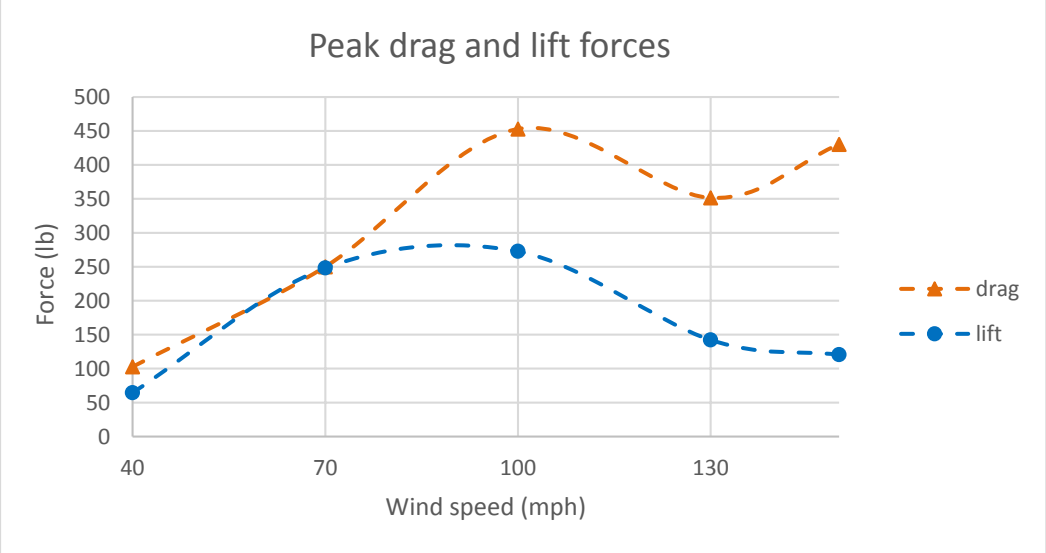

b)

Figure 157: Drag (Fy) and lift (Fx) forces on the traffic signals at 0-degrees: a) Mean; b) Peak

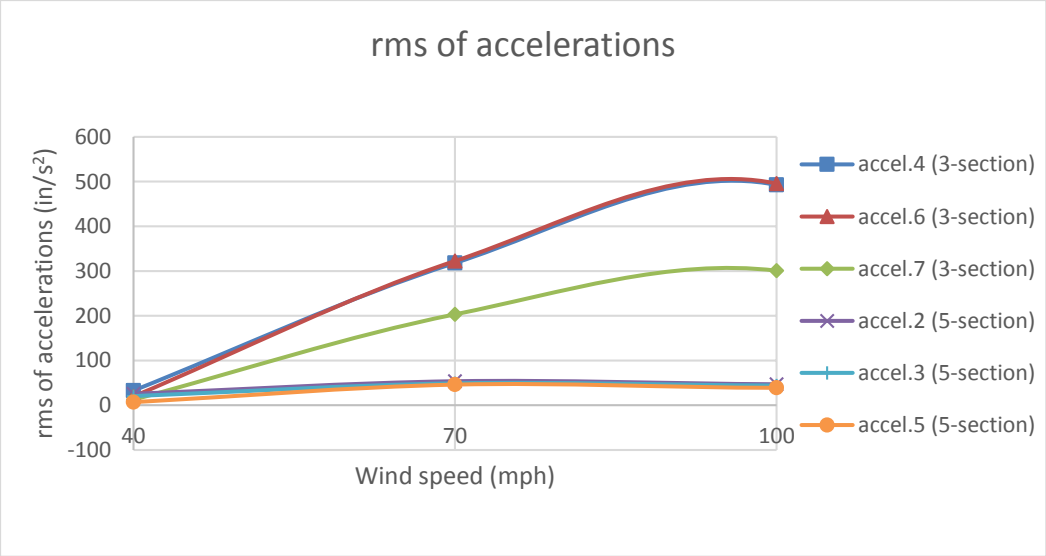

Figure 158: rms of accelerations on the 3-section and 5-section signals at 0-degrees

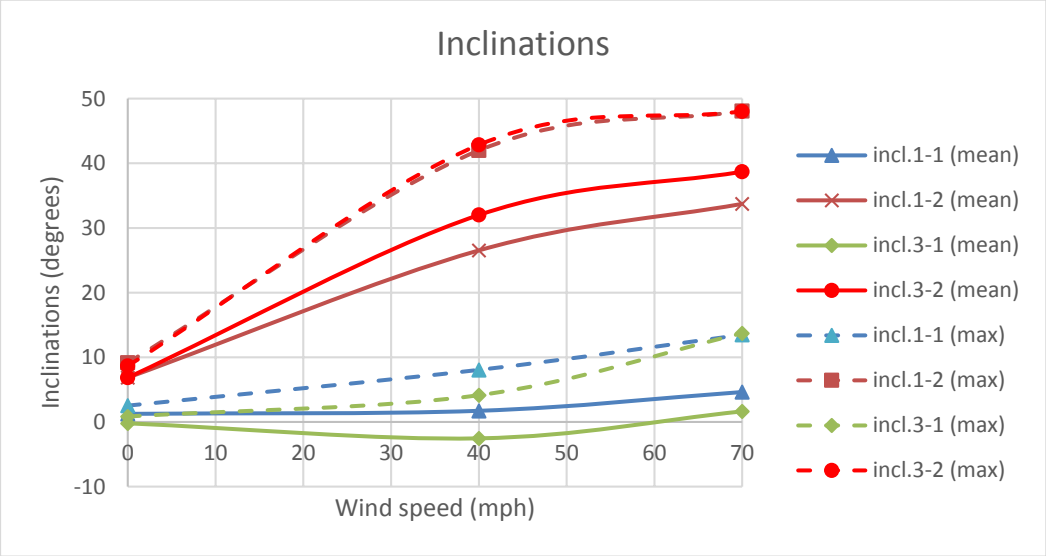

Figure 159: Inclinations (mean and max) obtained at 0-degrees from inclinometers 1 and 3

10.4. Performance of traffic signals during the tests

This test utilized two 3-section and one 5-section polycarbonate traffic signals span wire configuration connected to the catenary and messenger wires by means of a **"steel cable hanger assembly with reinforced disconnect hanger and with polycarbonate signal housing" (vendor: Engineered Castings)**.

At 40 mph, and all wind directions, there was no damage observed to any of the traffic signals nor hanger assemblies. Starting at 70 mph and 0-degrees traffic signals began to exhibit aerodynamic instability (flutter). At 45-degrees one visor from the 5-section signal detached and drifted away. At 80-degrees the 5-section signal pivoted about its longitudinal axis at the junction of the disconnect box and the upper LED signal. At 135-degrees, violent motion of the 5-section signal took place where the center 3-section signal was struck. Also, top portion of the 5-section signal back plate was bent backwards. It was later observed that the aluminum messenger clamp for the 5-section signal exhibited a hairline crack, as shown in Figure 160. **It may be noted that at 70 mph and 0-degrees strong aerodynamic instability (flutter) occurred, especially in the 5-section signal, therefore a decision was made to remove sensor equipment from the 5-section signal for fear of damaging equipment.**

At 100 mph and 0-degree wind direction, strong aerodynamic instability continued to be observed. Powerful rotation of the 5-section signal was observed, resulting in collisions with the center 3-section signal. The top LED visor for the 5-section was seen to detach and fly away. Also, the back plate for the 5-section signal became detached and drifted away. At one point during 100-degree wind direction the 5-section signal skipped over the messenger wire. At 180-degrees the 5-section polycarbonate signal cracked at the upper portion just underneath the disconnect box and drifted away. The cracked 5-section signal is shown in Figure 161. The disconnect box with a piece of the 5-section signal is shown in Figure 162. **It may be noted that at the end of the 100-mph wind speed test sensor equipment for the outer 3-section signal was removed for fear of damaging equipment.**

It was observed at 130 mph wind speed and 0-degrees, back plates for both 3-section signals began to detach. Aerodynamic flutter continued to occur for both 3-section signals as well. At 135-degrees the entire back plate for the center 3-section signal loosened and flew away. At 150

mph and 180-degrees wind direction, the remaining back plate for the outer 3-section signal detached and drifted away. Both 3-section signals remained with all its visors at the end of the wind speed test. Neither 3-section signal disconnect box had no observed damage. The outer 3-section signal disconnect box with no observed damage is shown in Figure 163. The three steel cable hanger assemblies after the wind speed test was conducted are shown in Figure 164. The 5-section signal steel cable hanger exhibits a bend near the messenger cable clamp.

A summary of the observed damages is as follows:

- Damage to signal hanger: The 5-section signal steel cable hanger exhibits a bend near the messenger cable clamp.
- Damage to disconnect hanger (box): No permanent visual damage observed.
- Damage to signal housing assembly: Damage to visors and back plate. Aluminum messenger clamp for the 5-section signal exhibited a hairline crack. The 5-section polycarbonate signal cracked at the upper portion just underneath the disconnect box and drifted away

Figure 160: Hairline crack on 5-section signal messenger clamp

Figure 161: 5-section polycarbonate signal cracked at the top

Figure 162: Disconnect box with a piece of the 5-section signal

Figure 163: Outer 3-section signal disconnect box with no observed damage (wiring was removed)

(a) *(b)* *(c)*

Figure 164: Steel cable hanger assemblies after tests were conducted

(a) Center 3-section signal hanger, (b) Outer 3-section signal hanger, (c) 5-section signal hanger

10.5. Conclusions

This chapter summarizes the results of a test conducted at WOW at FIU for a span wire traffic signal assembly consisting of two 3-section and a 5-section traffic signal, connected using a **"steel cable hanger assembly with reinforced disconnect hanger and with polycarbonate signal housing" (vendor: Engineered Castings)**. Wind speeds were varied from 40 to 150 mph and wind directions were varied from 0 to 180 degrees. The various instruments used for this test include: loadcells to measure forces, accelerometers to measure accelerations and inclinometers to measure the inclinations. This study reports the data for different wind directions, in terms of: wind induced forces (drag (y-component), lift (x-component) and cable tension (z-component)), rms of accelerations and inclinations. Results for 0-degrees wind direction indicate that along wind forces (drag) and cable tensions generally increase in the messenger wire with increase in wind speed. The lift on the messenger wire increases only marginally with increasing wind speeds at 0 degrees. The catenary wire experiences only negligible changes of the lift (Fx) and drag (Fy) components of wind forces but an increase of the tension (Fz) force up to 70 mph, thereafter decreasing.

At any given wind speed, the messenger wire experiences higher tension forces than the catenary wire. Similar observations were made for other wind directions (see appendix H). In general, the rms of accelerations increased with increasing wind speeds. In the range of 40 to 70 mph for 0-degrees wind direction, the mean inclinations in the along wind direction varied from 27 to 39 degrees, with a maximum value of about 48 degrees observed at 70 mph for inclinometer component 3-2. At 70 mph, an erratic movement of the signals was observed (aerodynamic flutter). A failure was observed at 100 mph and 180-degrees, whereby the 5-section polycarbonate signal fractured at the top of the signal right under the disconnect box and flew away. It was also noticed that the aluminum messenger clamp for the 5-section signal showed a hairline crack.

Chapter 11 - Task 1a: FULL SCALE TESTING - Case 10

"Adjustable Hanger Assembly with Solid (non-louvered) Backplates" - Test Date: 04/13/2017

11.1. Introduction

In the first tasks of the current project a 'base' configuration was identified consisting of a 21.9 ft long section with two 3-section and one 5-section traffic signals. As a continuation of the study, FDOT tested the span wire traffic signal configurations connected to the catenary and messenger wires via an **"Adjustable Hanger Assembly with Solid (non-louvered) Backplates."** The tests were carried out at wind directions ranging from 0 to 180 degrees and wind speeds ranging from 40 to 100 mph. The instruments consisted of loadcells to measure forces, accelerometers to measure accelerations, and inclinometers to measure the inclinations of the traffic signals.

This chapter presents the results from the tests conducted on the traffic signal assembly with the **"Adjustable Hanger Assembly with Solid (non-louvered)"** at the WOW. Additional results are presented in appendix I.

11.2. Experimental Methodology

11.2.1. Test Setup

The 3-section signal assembly was mounted on a reinforced short-span rig (described in Chapter 1) by means of an **"Adjustable Hanger Assembly with Solid (non-louvered)."** Figure 165 to Figure 167 show the traffic signal assembly as well as the **"Adjustable Hanger Assembly with Solid (non-louvered) Backplates"** assembly. The signal was made of aluminum and included solid backplates and visors.

The test protocol is presented in Table 19. The tests were conducted for longer durations, with wind speeds being varied from 40 to 100 mph, for wind directions of 0-180 degrees. The different components utilized for this particular test are shown in Table 20.

11.2.2. Instrumentation

The directions of the x, y and z components for each loadcell are shown Figure 168. Loadcells number 4 and 5 were located at either end of the messenger cable and loadcells number 1 and 2 located at either end of the catenary cable.

Tri-axial accelerometers were installed in the traffic signal to measure accelerations. Accelerometer Accel007, was installed on the top center, accelerometer Accel004, was installed on the bottom left side and accelerometer Accel006, was installed on the bottom right side of the 3-section signal as shown in Figure 169.

Inclinometer, Inc2, was installed on the top center and inclinometer, Inc1, was installed on the bottom center of the of the 3-section signal as shown Figure 169.

11.2.3. Test Method

The test set up was first tested for 'no wind' conditions and baselines for the various instruments were acquired (also known as "zero drift removal" process) before each test. The signal assembly was tested at wind speeds ranging from 40 to 100 mph at wind angles of attack ranging from 0 to 180 degrees, as shown in Table 19**.**

Table 19: Test protocol (Task 1a: Case 10)

Wind Speed (mph)	Wind Direction (degrees)	Total Duration (min)
40	0, 45, 80, 100, 135, 180	3.1
70	0, 45, 80, 100, 135, 180	3.1
100	0, 45, 80, 100, 135, 180	3.1
	TOTAL	**9.3**

Table 20: Signal assembly components (Task 1a: Case 10)

Standard Part	Manufacturer
Span wire clamp	Pelco
Adjustable hanger	Pelco
Extension bar	Pelco
Messenger clamp	Pelco
Disconnect Hanger	Pelco
Signal Assembly	McCain
Backplate	Pelco
Visor	McCain
LED Modules	GE - Dialight - Duralight

Figure 165: Test rig

Figure 166: Signal assembly installed on test rig (before testing)

a)

b)

Figure 167: a) Signal Setup for the test; b) Magnified view of the connection

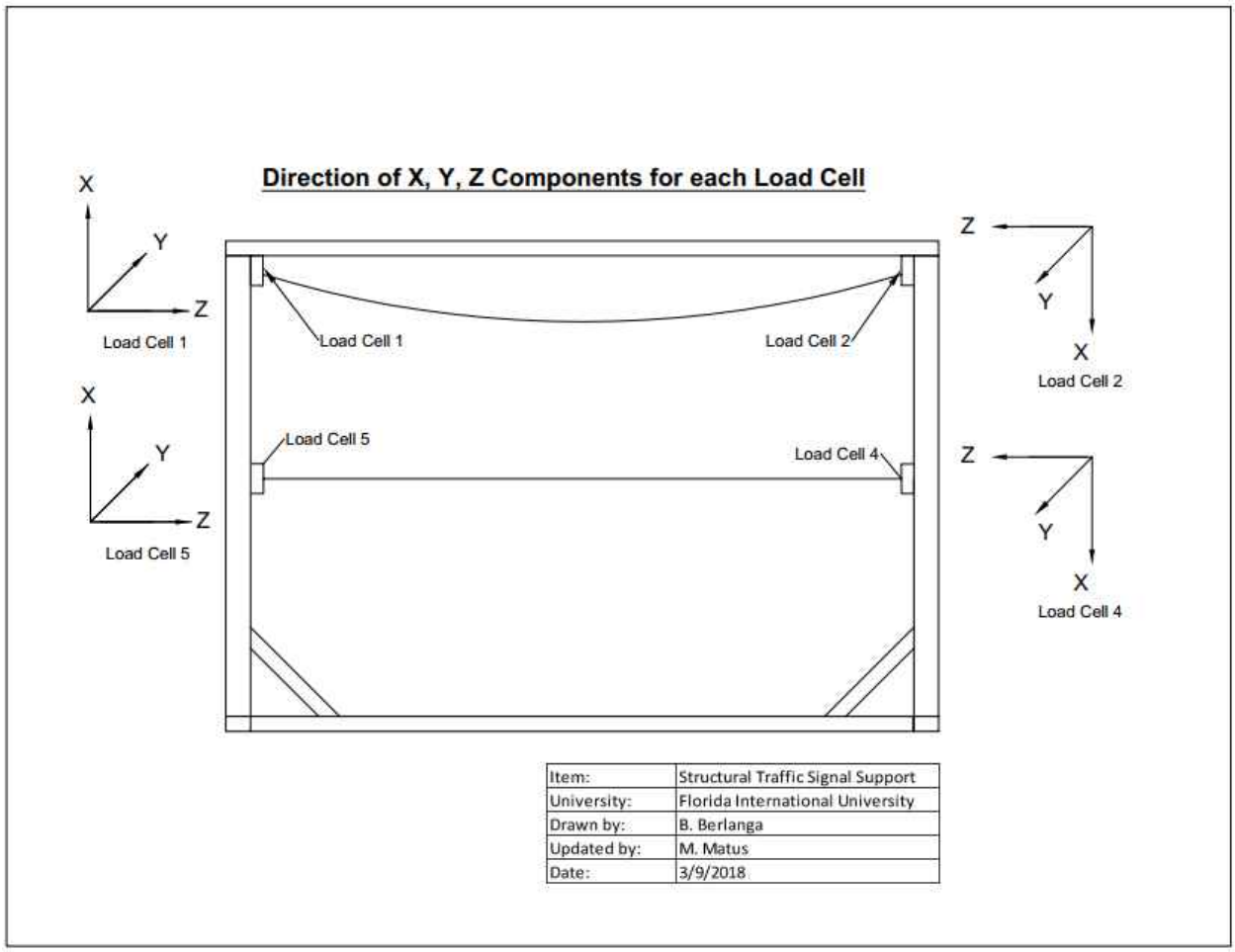

Figure 168: Direction of x,y,z components for each loadcell (direction of each axis shown represents 'positive direction')

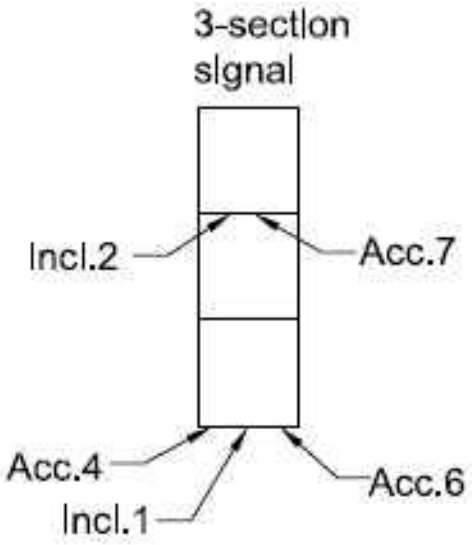

Figure 169: Location of accelerometers and inclinometers in 3-section signal

11.3. Results and Discussion

The tests at the WOW were performed in the presence of installation technicians from Horsepower Electric Inc. and members of the WOW technical team. The results in this chapter are restricted to 0-degree wind direction, with results for additional wind directions presented in appendix I.

11.3.1. Wind induced forces

The directions of the forces are shown in Figure 168. The mean and peak forces obtained at various wind speeds are discussed in this section. Figure 170 presents the wind induced mean forces on loadcell 2 (catenary wire) and loadcell 4 (messenger wire) at 0 degrees wind direction, for increasing wind speeds. It may be noted that the 'y' and 'z' components of the forces correspond to the 'drag' and 'cable tensions' respectively, while the 'x' component represents the uplift forces.

Data show that the along wind forces (Fy) increased with increasing wind speed at loadcell 4 (messenger wire), while Fy at loadcell 2 (catenary wire) experienced minimal change with increasing wind speeds. The highest along wind force of 67 lb was found at loadcell 4 at 100 mph. Similarly, the tension on loadcell 4 (Fz) increases in magnitude from 131 lb at 40 mph to 308 lb at 100 mph. This shows that the messenger wire experienced higher tension and drag than the catenary wire for increasing wind speeds. The uplift forces (Fx) on loadcell 4 (messenger wire) increased in magnitude with increase in wind speed. However negligible change in Fx on loadcell 2 (catenary wire) with increasing wind speed was observed.

Similar observations were made for loadcell 5 (messenger wire) and loadcell 1 (catenary wire) as shown in Figure 171. For instance, Fz (cable tension) and Fy (drag) increase with increasing wind speed on loadcell 5 (messenger wire). Fx on loadcell 5 increases marginally.

The peak forces at 0 degrees wind direction for loadcell 2 (catenary wire) and loadcell 4 (messenger wire) are shown in Figure 3-3. The peak forces of Fy and Fz increase with increasing wind speeds. The magnitudes of the peaks on loadcell 2 increase marginally for Fx with increasing wind speeds. Figure 175 presents peak results for loadcell 5 (messenger wire) and loadcell 1 (catenary wire). Fz (cable tensions) on loadcells 1 and 5 increase with increasing wind speeds –

highest values of 87 lb on loadcell 5 and 25 lb on loadcell 1 at wind speed of 100 mph was observed.

The peaks of Fy (drag) on loadcell 5 increases gradually with higher wind speeds, although the magnitudes of the peaks at loadcell 1 do not change markedly for a change in wind speed. Peak of Fx (lift) on loadcell 5 (messenger) and loadcell 1 (catenary) do not change significantly despite a change in wind speed. Results for additional wind directions are presented in appendix I. Figure 176 (a) presents the 'total' mean drag and lift forces on the traffic signals. Results show that the drag on the traffic signals increase with an increase in wind speed – highest value of 156 lb was obtained at 100 mph at 0 degrees wind direction. The peak drag and lift are shown in Figure 176 (b). The peak lift at 100 mph attains a value of 149 lb. However, the peak drag increases initially with increasing wind speed, and attains the highest value of 213 lb at 100 mph.

It needs to be noted that the sign convention of the x component of all loadcells was configured so that the weight of the lights is a positive reading while a lift force pushing the lights up is a negative reading. With the sign convention, it can be seen that the lift forces increased as wind speed increased. Mean forces of Louvered backplate case are shown in Figure 172 and Figure 173.

11.3.2. rms of accelerations

The root mean square (rms) of accelerations are presented in Figure 177. Accelerometers 4, 6 and 7 were located on the 3-section signal, as shown in Figure 169. Overall, the rms of accelerations obtained from all the accelerometers experienced an increase from wind speed of 40 mph to 100 mph.

11.3.3. Inclinations of the traffic signals

Figure 178 shows the inclinations (mean and peak) obtained from inclinometer 2. It may be noted that for inclinometer 2, '2-1' refers to the component of inclination parallel to the wind, while '2-2' refers to the component of inclination perpendicular to the direction of wind. For inclinometer 2, the mean components '2-1' are generally in the range of 13 to 53 degrees for 40-100 mph wind speed range. Inclinations of the louvered backplate case are presented in Figure 179.

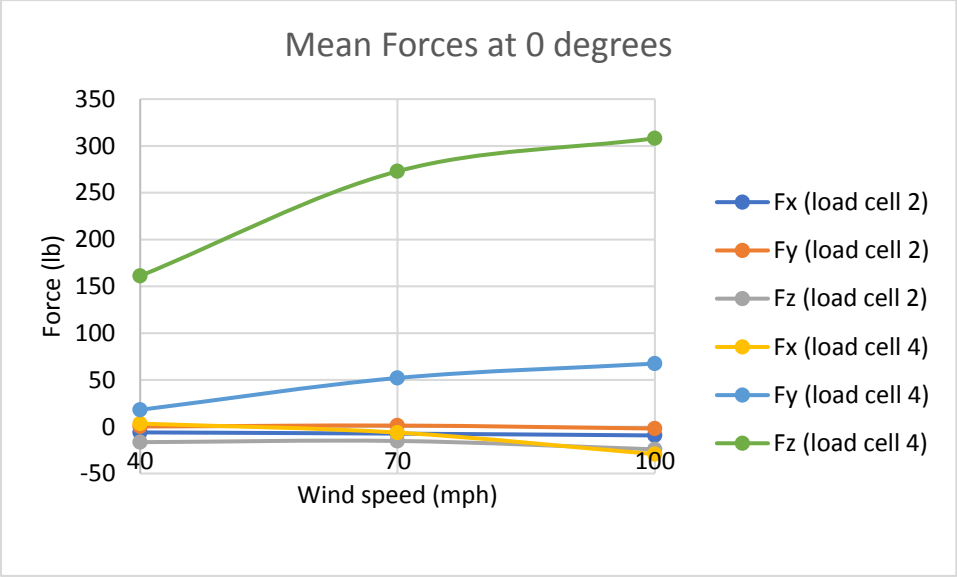

Figure 170: Mean Forces on loadcells 2 (catenary wire) and 4 (messenger wire) at 0 degrees wind direction

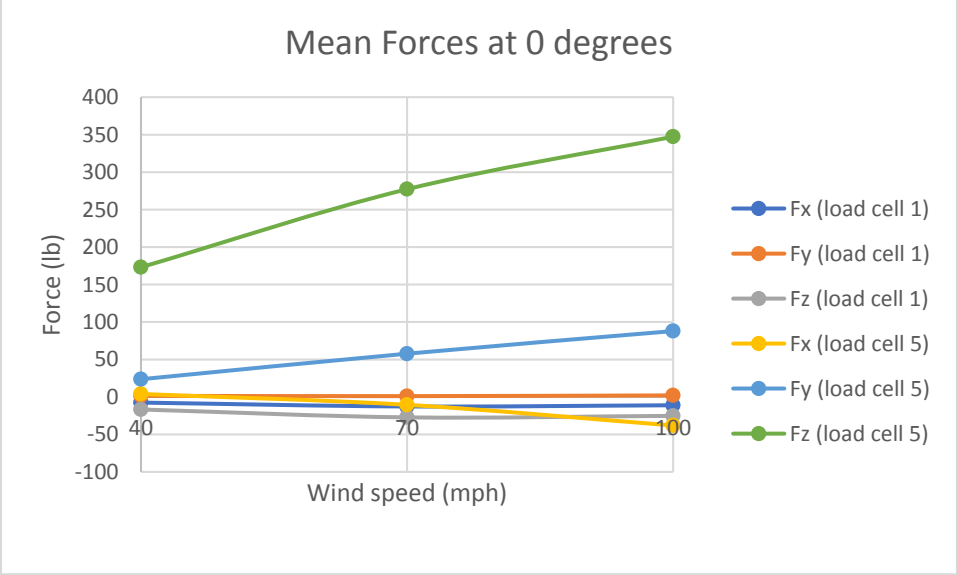

Figure 171: Mean Forces on loadcells 1 (catenary wire) and 5 (messenger wire) at 0 degrees wind direction

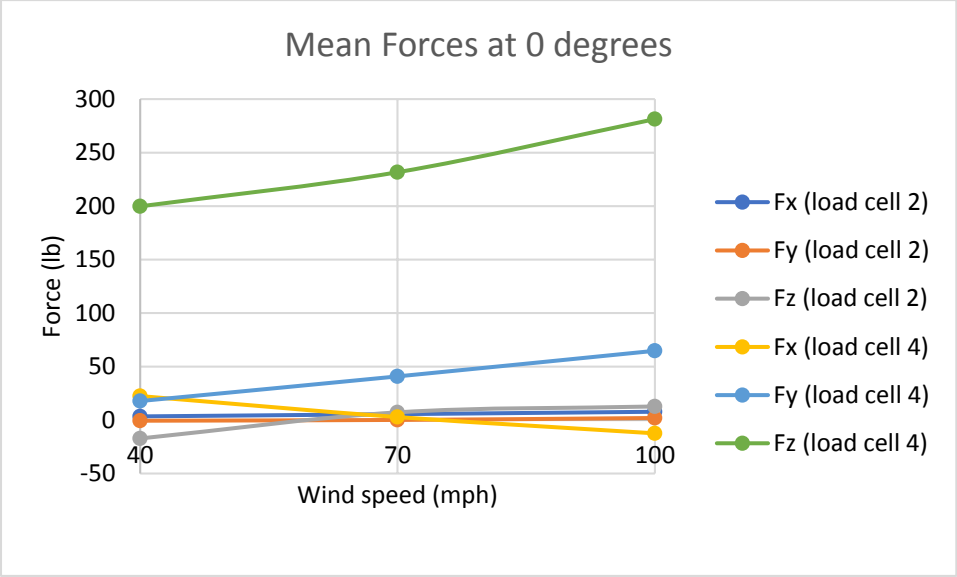

Figure 172: Louvered case mean forces on loadcells 2(catenary wire) and 4 (messenger wire) at 0 degrees wind direction

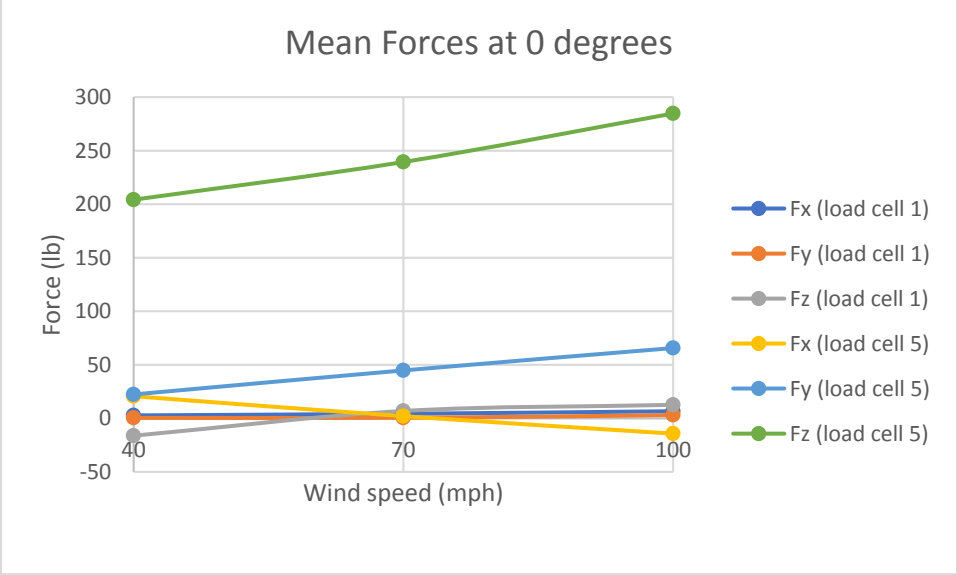

Figure 173: Louvered case mean forces on loadcells 1 (catenary wire) and 5 (messenger wire) at 0 degrees wind direction

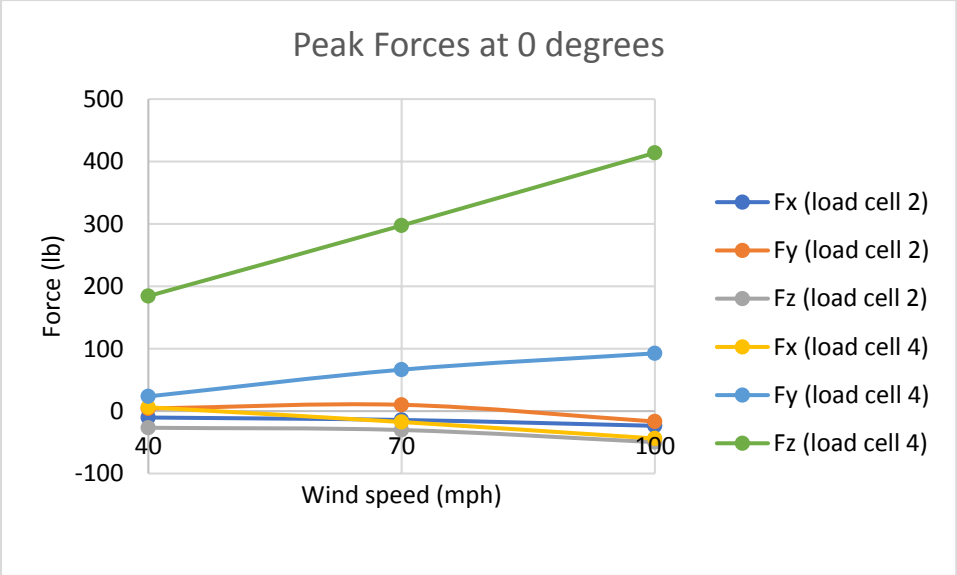

Figure 174: : Peak Forces on loadcells 2 (catenary wire) and 4 (messenger wire) at 0 degrees wind direction

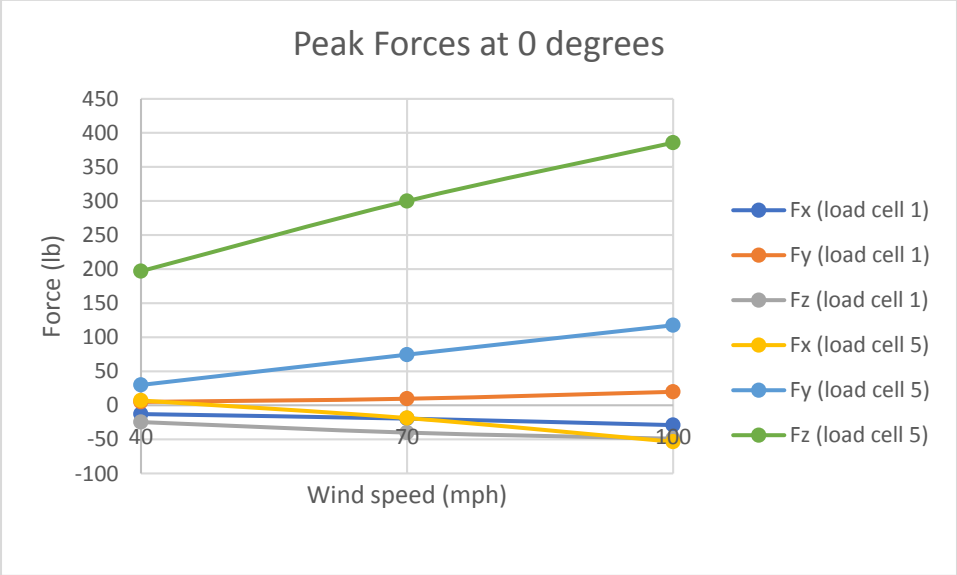

Figure 175: : Peak Forces on loadcells 1 (catenary wire) and 5 (messenger wire) at 0 degrees wind direction

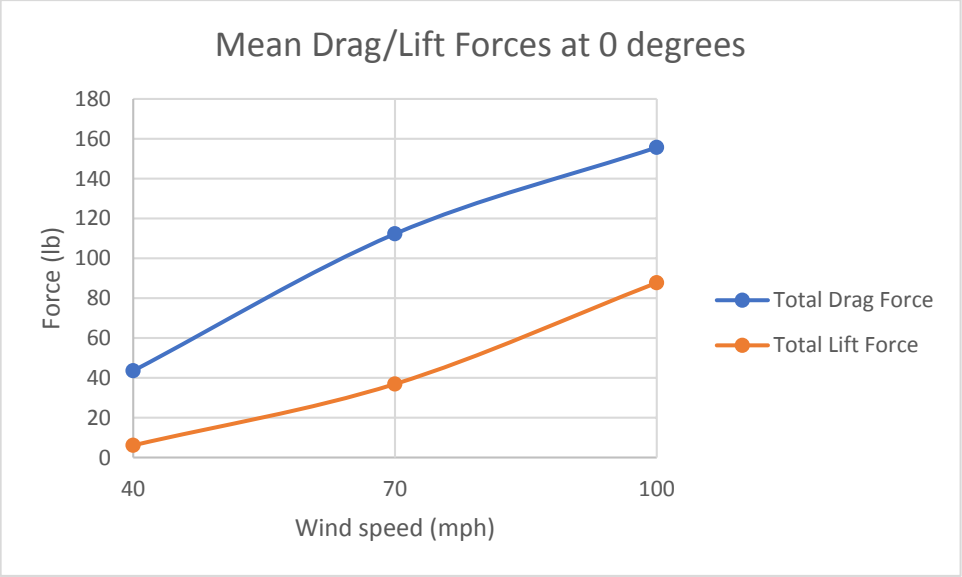

a)

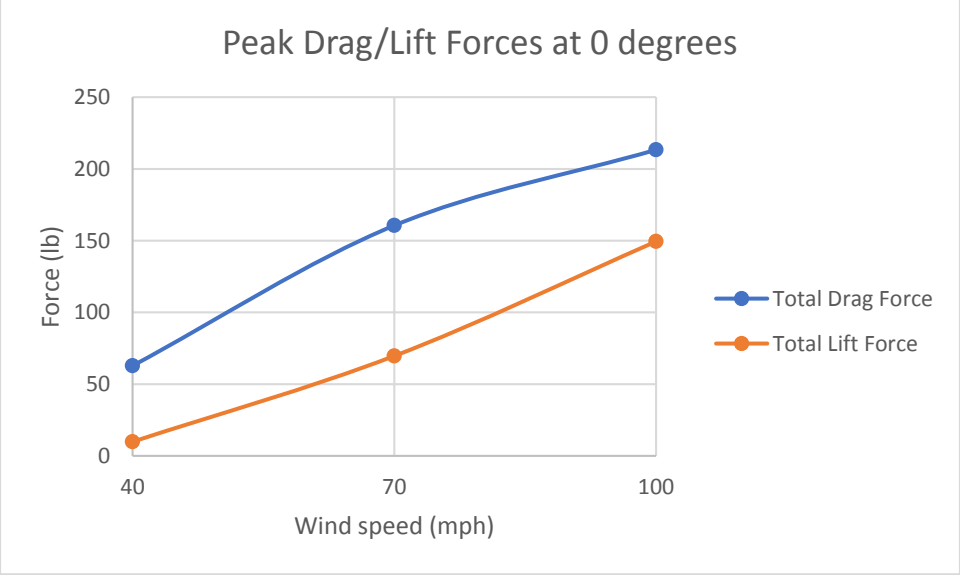

b)

Figure 176: Drag (Fy) and lift (Fx) forces on the traffic signal at 0 degrees: a) Mean; b) Peak

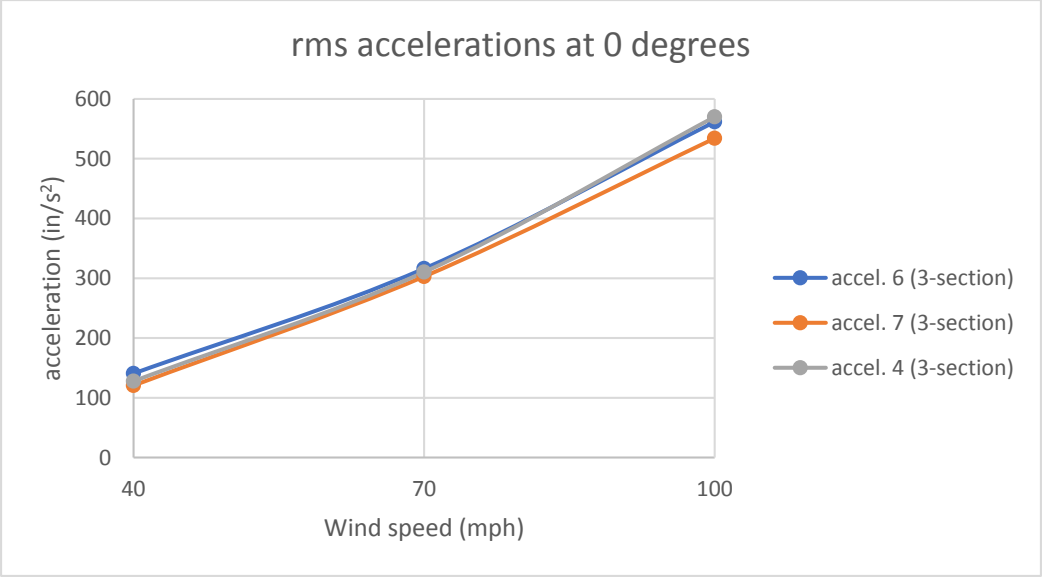

Figure 177: rms of accelerations on the 3-section and 5-section signals at 0 degrees

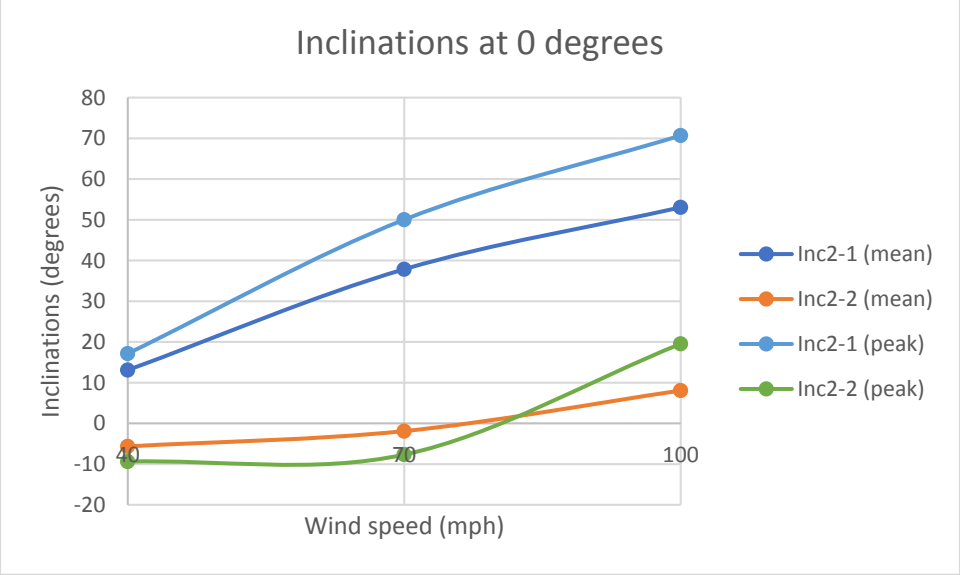

Figure 178: Inclinations (mean and max) obtained at 0 degrees for inclinometer 2

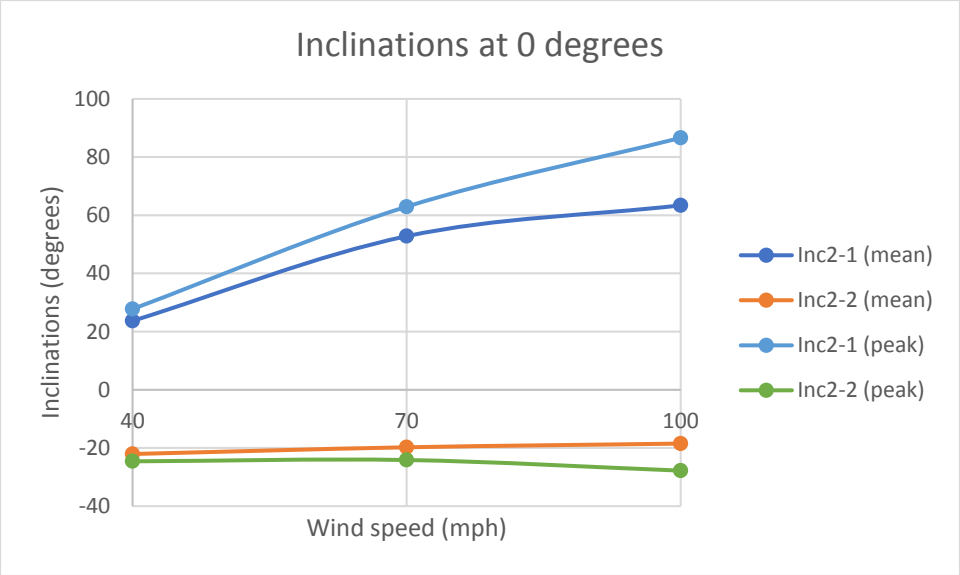

Figure 179: Louvered backplate case (mean and max) inclinations obtained at 0 degrees wind angle of attack

11.4. Performance of traffic signals during the tests

This test utilized a 3-section aluminum traffic signal installed in a test rig span-wire configuration connected to the catenary and messenger wires by means of an "**Adjustable Hanger Assembly with Solid (non-louvered) Backplates."**

Starting the test at 40 mph and progressing to 70 mph there were no major observations other than minor inclinations.

When reaching 100 mph and at 100 degrees, 3-section signal slid from the hanger-clamp to messenger wire connection causing the hanger to break at the disconnect-box to hanger connection, as shown in Figure 180. After the test was finished, it was found that the hanger was sheared, as shown in Figure 181, and that the top right backplate got disconnected from its anchorage point. No damages were observed in the disconnect box, wires nor visors.

Figure 180: Signal Assembly After Test

Figure 181: Sheared Hanger Connection

11.5. Conclusions

This chapter summarizes the results of a test conducted at WOW at FIU for a span wire traffic signal assembly consisting of a 3-section traffic signal with non-louvered backplate, connected using a **"Adjustable Hanger Assembly with Solid (non-louvered) Backplates."** The various instruments used for this test included: loadcells to measure forces, accelerometers to measure accelerations and inclinometers to measure the inclinations.

The signal assembly showed no damage during the 40 mph and 70 mph. When wind speed was increased to 100 mph and for the wind direction of 100 degrees, the traffic signal assembly slid from the messenger wire clamp and the hanger broke at the disconnect-box to hanger point. The disconnect box showed no damage and the solid back plate was detached at the two top anchorage points.

Chapter 12 - Task 1a: FULL SCALE TESTING - Case 11

"Tri-Stud Adjustable Hanger with Aluminum Signal Housings, Base Configuration" (145lb spring system) - Test Date: 11/16/2015

12.1. Introduction

In the first tasks of the current project a 'base' configuration was identified consisting of a 21.9 ft long section with two 3-section and one 5-section traffic signals (Task 1a – Cases 1 and 2). As a continuation of the study, FDOT tested the span wire traffic signal configurations connected to the catenary and messenger wires via **"tri-stud adjustable hanger" (also known as base configuration)**. **It should be noted that this base condition case was conducted using 145 lbs spring connected to the messenger wire. Following tests (i.e. after 11/16/2015) were conducted using 100 lbs spring connected to the messenger wire per FDOT request**. The tests were carried out at wind directions ranging from 0 to 180 degrees and wind speeds ranging from 40 to 150 mph. The instruments consisted of loadcells to measure wind forces, accelerometers to measure accelerations, and inclinometers to measure the inclinations of the traffic signals.

This chapter presents the results from the tests conducted on the traffic signal assembly with the **"tri-stud adjustable hanger" (also known as base configuration)** at the WOW. Additional results are presented in appendix J.

12.2. Experimental methodology

12.2.1. Test Setup

The 3-3-5 signal assembly was mounted on a short-span rig (described in Chapter 1) by means of a **"tri-stud adjustable hanger" (also known as base configuration).** This signal assembly was installed using springs of 145 lb (all other tests performed after 11/16/2015 used 100 lb springs). Figure 182 and Figure 183 show the traffic signal assembly. All the signals were made of aluminum and included louvered back plates and visors. The test protocol is presented in Table 21. Table 22 shows the list of components used for this signal assembly.

12.2.2. Instrumentation

The directions of the x, y and z components for each loadcell are shown in Figure 184. Loadcells number 2 and 5 were located at either end of the messenger cable and loadcells number 1 and 4 located at either end of the catenary cable.

Tri-axial accelerometers were installed in the traffic signals to measure accelerations. There was one accelerometer placed on the center top of the signal, Accel5, another placed on the bottom right side, Accel002, and a third placed on the bottom left side, Accel003 for the 5-section signal as shown in Figure 185. Accelerometer Accel007, was installed on the top center, accelerometer Accel004, was installed on the bottom left side and accelerometer Accel006, was installed on the bottom right side of the 3-section signal as shown in Figure 186.

There was one inclinometer installed on the top center of the signal, Inc4, and another on the bottom center of the signal, Inc3, for the 5-section signal as shown in Figure 185. Inclinometer, Inc2, was installed on the top center and inclinometer, Inc1, was installed on the bottom center of the of the 3-section signal as shown Figure 186.

Wind speeds in three component directions (u,v,w) were also recorded by the Wall of Wind velocity sensors.

12.2.3. Test Method

The test set up was first tested for ‘zero wind’ conditions, and the values of the various ‘quantities’ (forces, accelerations and inclinations) obtained were later deducted from quantities obtained for different wind speeds (also known as “zero drift removal” process).

Although erratic behavior, such as aerodynamic fluttering, may not cause an initial failure of the signal equipment, it may lead to additional testing to confirm this behavior will not cause failure of the equipment when experienced for long-term.

Table 21: Test protocol (Task 1a: Case 11)

Wind Speed (mph)	Wind Direction	Total Duration (min)
40	0, 45, 80, 100, 135, 180	6
70	0, 45, 80, 100, 135, 180	6
100	0, 45, 80, 100, 135, 180	6
110	0	1
120	0	1
130	0, 45, 80, 100, 135, 180	6
TOTAL		**26**

Table 22: Signal assembly components (Task 1a: Case 11)

Component	Manufacturer
Span wire clamp	Pelco
Adjustable hanger	Pelco
Extension bar	Pelco
Messenger clamp	Pelco
Disconnect Hanger	Pelco
Signal Assembly	McCain
Backplate	TCS
Visor	McCain
LED Modules	GE - Dialight - Duralight

Figure 182: Picture of test rig frame with the signals and the "tri-stud adjustable hanger" (also known as base configuration)

a)

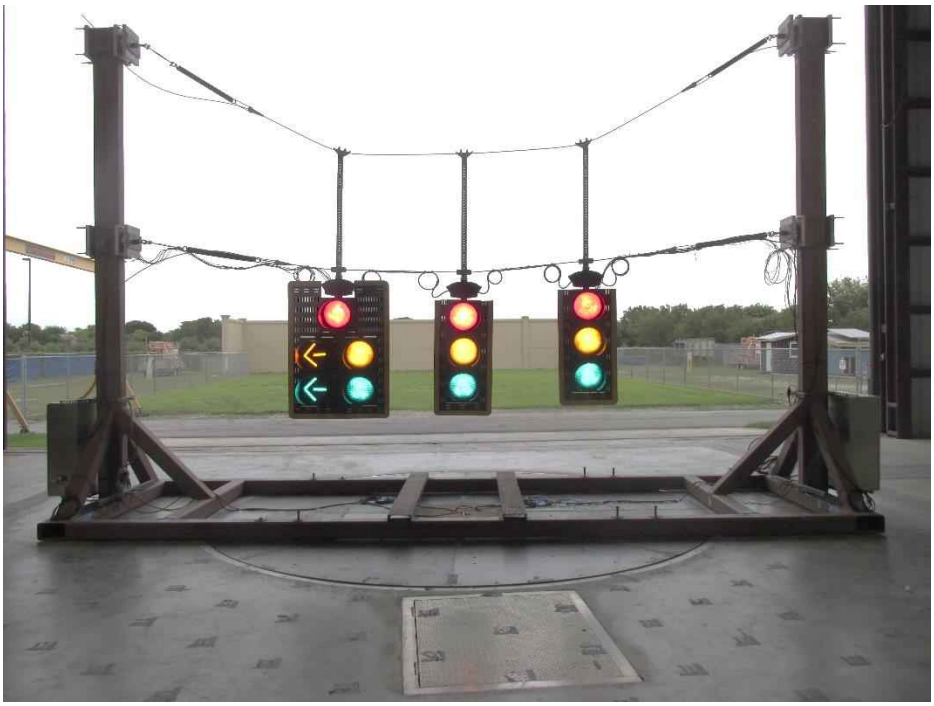

b)

Figure 183: Traffic signal set up: a) portion of the catenary and messenger wires with the loadcells attached; b) traffic signal assembly facing the wind

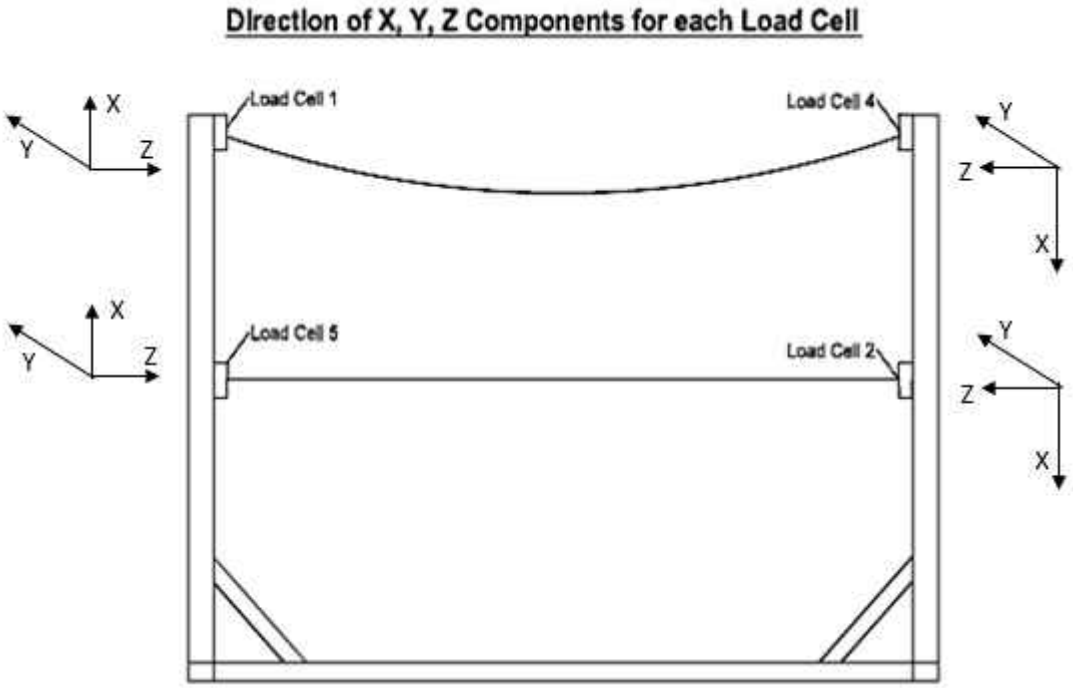

Figure 184: Direction of x, y, z components for each loadcell (direction of each axis shown represents 'positive direction')

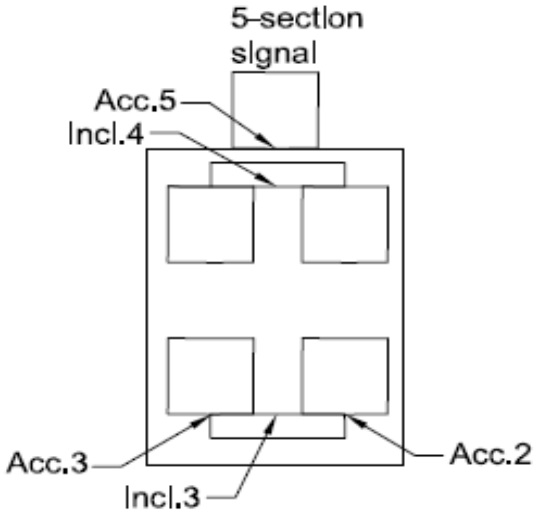

Figure 185: Location of accelerometers and inclinometers in 5-section signal

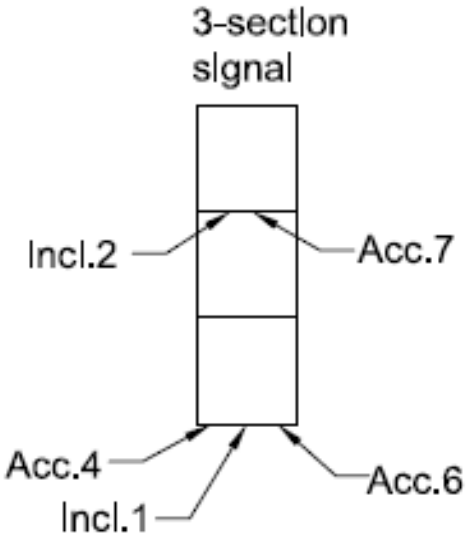

Figure 186: Location of accelerometers and inclinometers in 3-section signal

12.3. Results and discussion

The tests at the WOW were performed in the presence of the representatives from the Florida Department of Transportation (FDOT) Traffic Engineering and Operations Office and Traffic Engineering Research Lab (TERL), installation technicians from Horsepower Electric Inc. and members of the WOW technical team. The results in this chapter are restricted to 0-degree wind direction, with results for additional wind directions presented in appendix J.

12.3.1. Wind induced forces

The directions of the forces are shown in Figure 184. The mean and peak forces obtained at various wind speeds are discussed in this section. Figure 187 presents the wind induced mean forces on loadcell 2 (messenger wire) and loadcell 4 (catenary wire) at 0 degrees wind direction, for increasing wind speeds. It may be noted that the 'y' and 'z' components of the forces correspond to the 'drag' and 'cable tensions' respectively, while the 'x' component represents the uplift forces.

Data show that the along wind forces (Fy) increase with increasing wind speed at loadcell 2 (messenger wire), while Fy at loadcell 4 (catenary wire) experiences minimal change with increasing wind speeds. The highest along wind force of 255 lb was found at loadcell 2 at 130 mph. Similarly, the tension on loadcell 2 (Fz) increases in magnitude with increase in wind speed, although negligible change in tension on loadcell 4 for increasing wind speed was observed. This shows that the messenger wire experiences higher tension and drag than the catenary wire for increasing wind speeds. The uplift forces (Fx) on loadcell 2 (messenger wire) increases in magnitude with increase in wind speed. However negligible change in Fx on loadcell 4 (catenary wire) with increasing wind speed was observed.

Similar observations were made for loadcell 5 (messenger) and loadcell 1 (catenary) as shown in Figure 188. For instance, Fz (cable tension) and Fy (drag) increase with increasing wind speed on loadcell 5 (messenger wire). Fx on loadcell 5 also increases initially, but remains nearly constant beyond 100 mph.

The peak forces at 0 degrees wind direction for loadcell 2 and loadcell 4 are shown in Figure 189. The peak forces of Fx, Fy and Fz on loadcell 2 increase with increasing wind speeds up to 130

mph, while the forces on loadcell 4 experience negligible change for increasing wind speeds. It may be noted that the 'positive direction' of 'Fx' component on loadcells 2 and 4 is 'downwards' (see Figure 184). Figure 190 presents results for loadcell 5 (messenger) and loadcell 1 (catenary). Fx, Fy and Fz on loadcell 5 increase with increasing wind speed, while negligible changes in Fx, Fy and Fz for increasing wind speeds were observed on loadcell 1 (catenary). Results for additional wind directions are presented in appendix J.

Figure 191 (a) presents the 'total' mean drag and lift forces on the traffic signals. Results show that the drag and lift on the traffic signals increase with an increase in wind speed – highest mean drag of 520 lb and highest mean lift of 342 lb was obtained at 130 mph at 0 degrees wind direction. Similar trends were observed for peak drag and lift forces as shown in Figure 191 (b).

12.3.2. rms of accelerations

The root mean square (rms) of accelerations are presented in Figure 192. Accelerometers 4, 6 and 7 were located on the 3-scetion signal, while accelerometers 2, 3 and 5 were located on the 5-section signal (see Figure 185 and Figure 186). In general, the rms of accelerations obtained from all the accelerometers increase gradually with an increase in wind speed, although there is a slight drop in the rms values for accelerometers 2, 5 and 3 at 110 mph.

12.3.3. Inclinations of the traffic signals

Figure 193 a) shows the mean inclinations while Figure 193 b) shows the peak inclinations for inclinometers 1 and 3 for wind direction of 0 degrees. It may be noted that for inclinometer 1, '1-1' refers to the component of inclination perpendicular to the wind, while '1-2' refers to the component of inclination in the direction of wind. Mean and peak components of '3-2' (in the direction of wind) from inclinometer 3 were found to be 26 degrees and 43 degrees, respectively at wind speed of 70 mph.

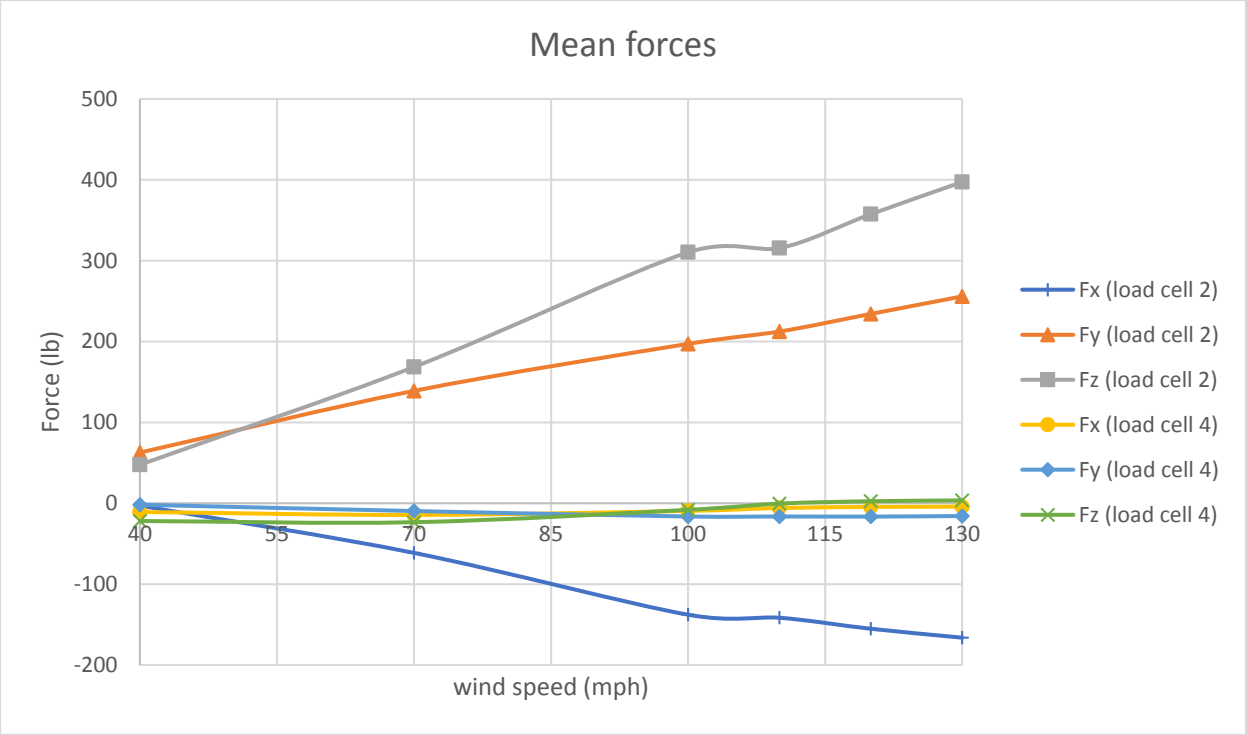

Figure 187: Mean forces on loadcells 2 (messenger wire) and 4 (catenary wire) at 0 degrees wind direction

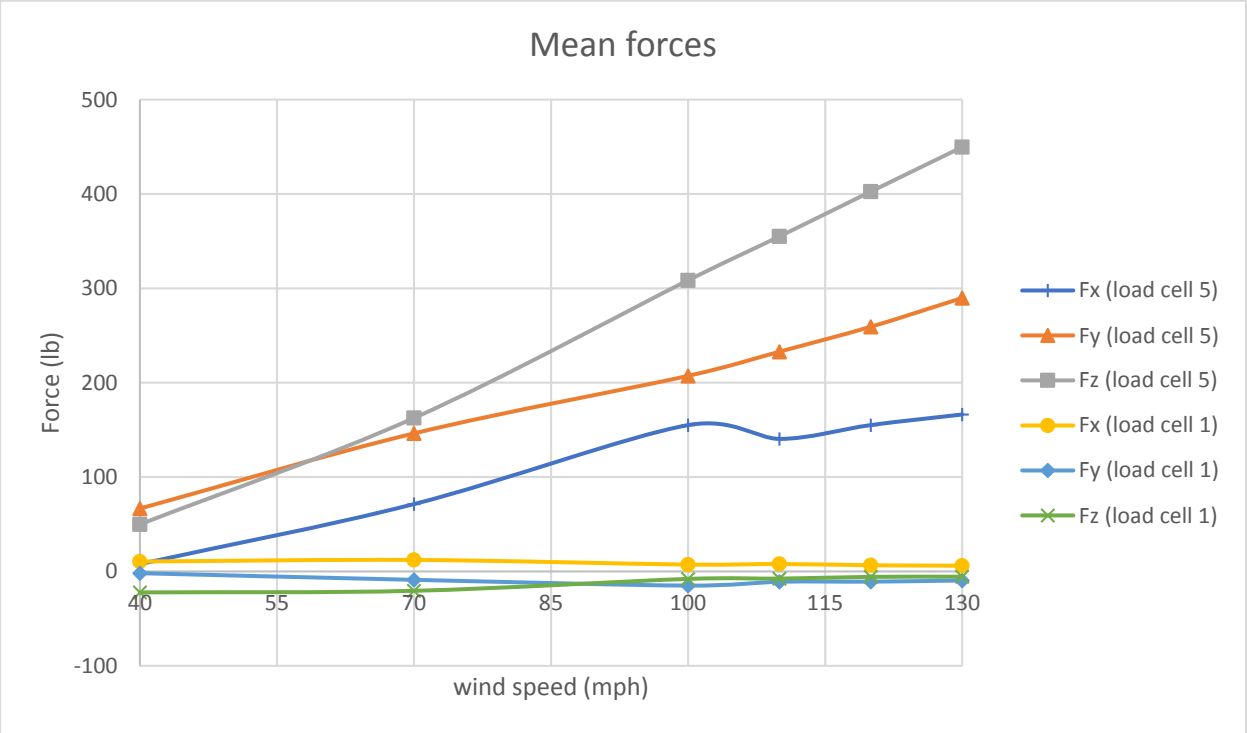

Figure 188: Mean forces on loadcells 1 (catenary wire) and 5 (messenger wire) at 0 degrees wind direction

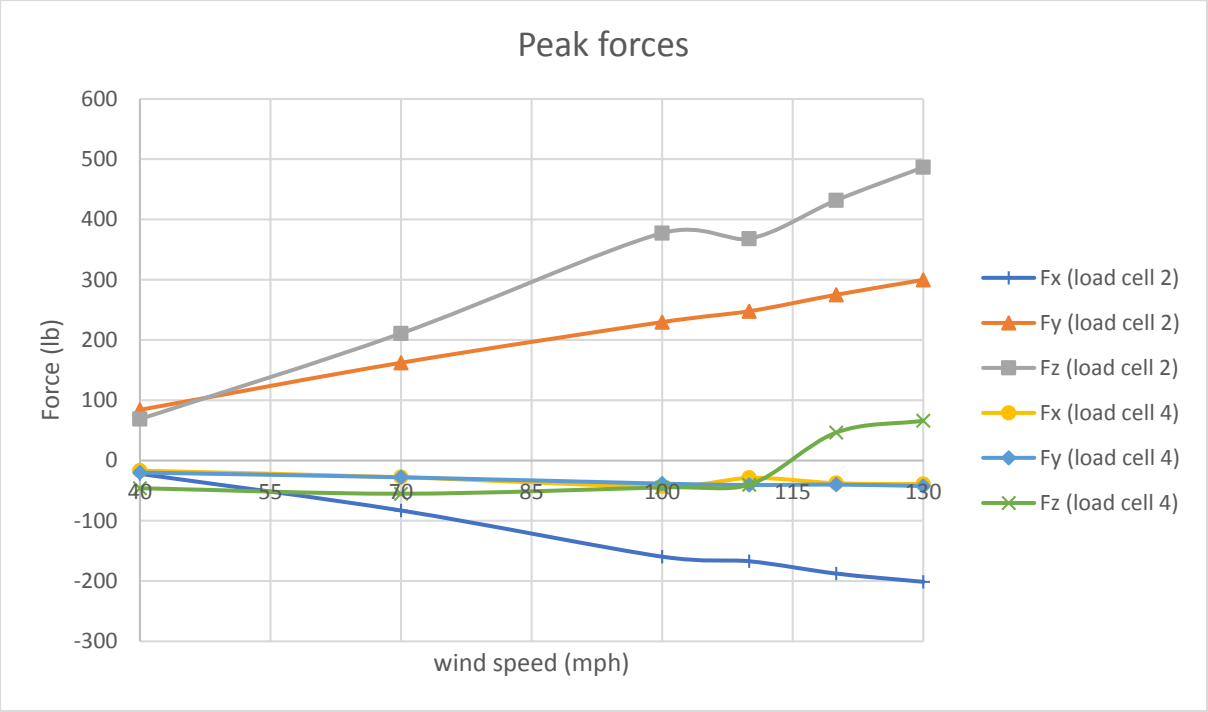

Figure 189: Peak forces at 0 degrees wind direction on loadcells 2 (messenger wire) and 4 (catenary wire)

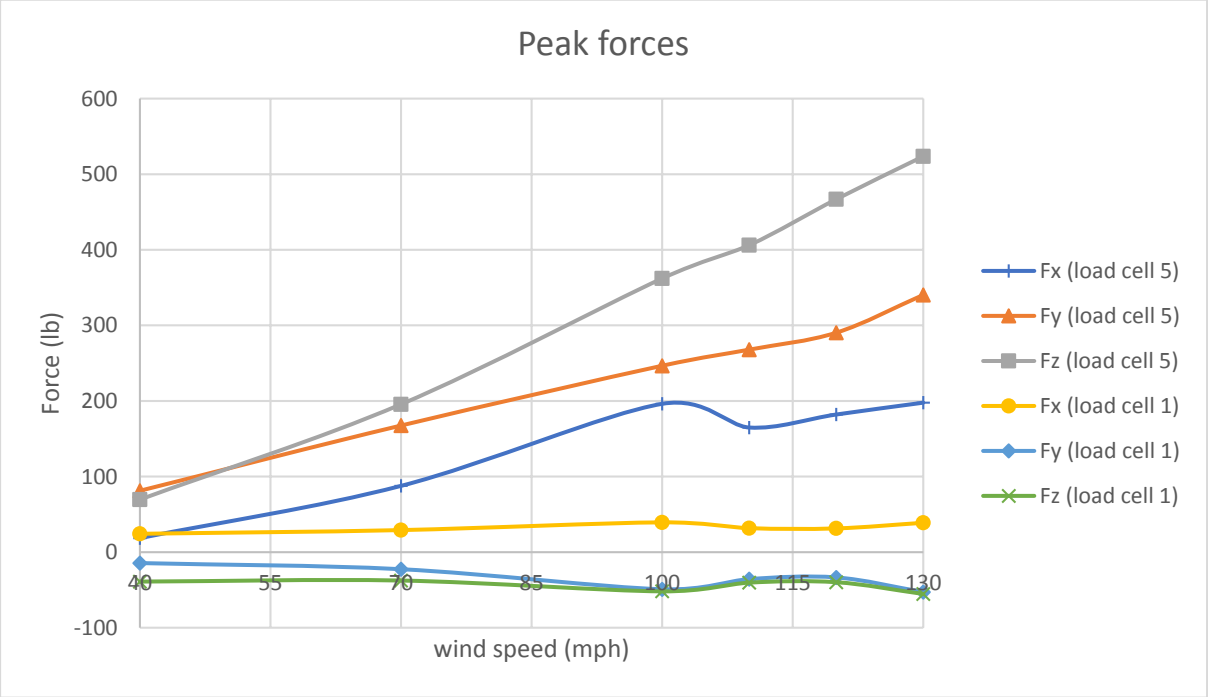

Figure 190: Peak forces at 0 degrees wind direction on loadcells 1 (catenary wire) and 5 (messenger wire)

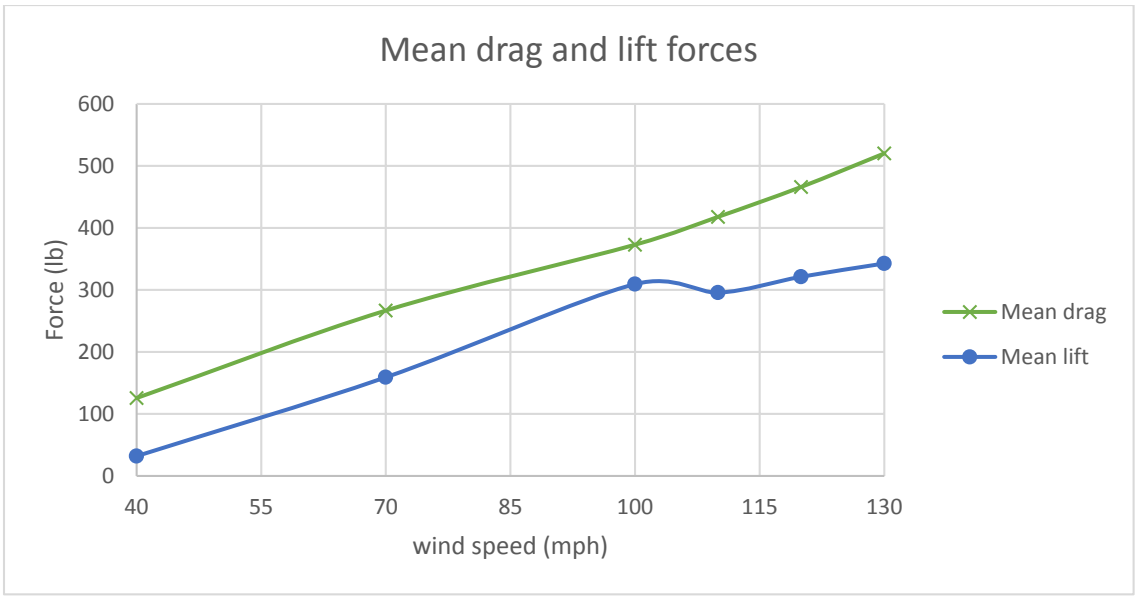

a)

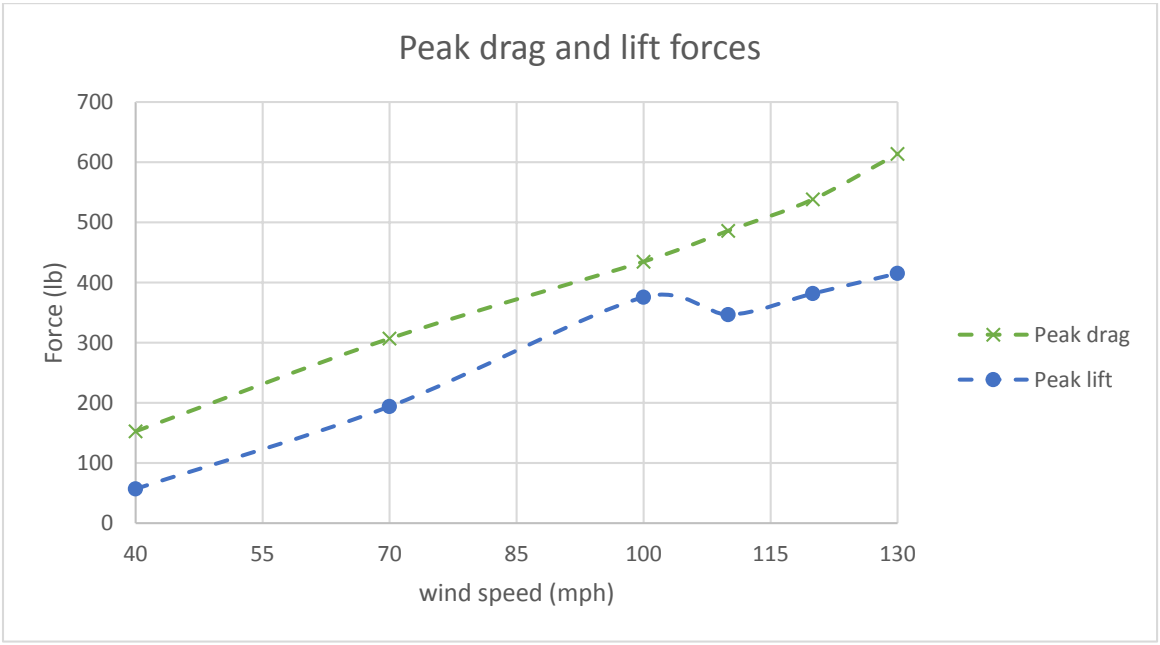

b)

Figure 191: Drag (Fy) and lift (Fx) forces on the traffic signals at 0 degrees: a) Mean; b) Peak

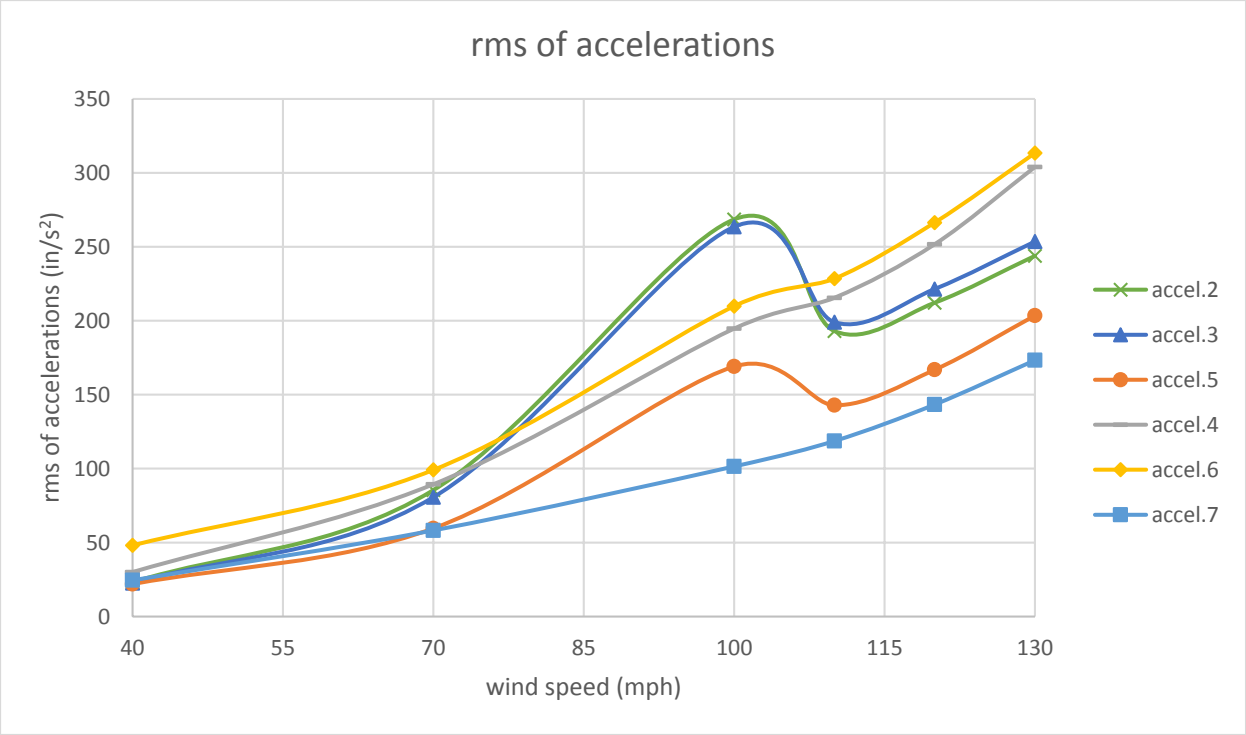

Figure 192: rms of accelerations on the 3-section and 5-section signals at 0 degrees

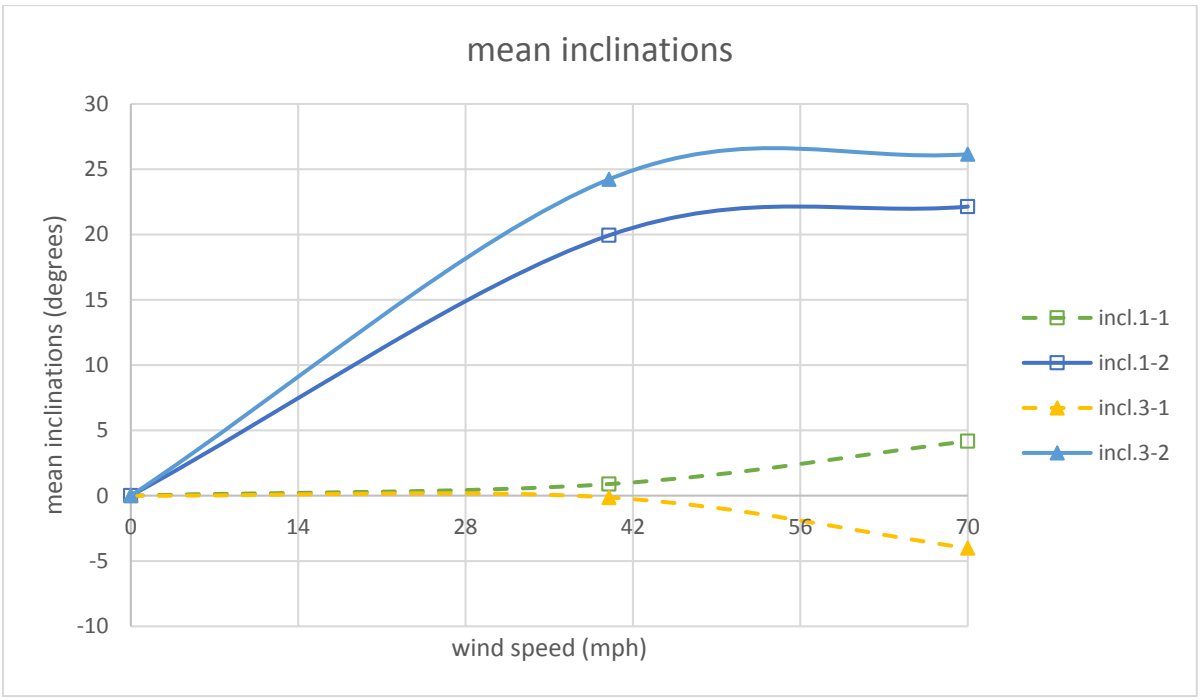

a)

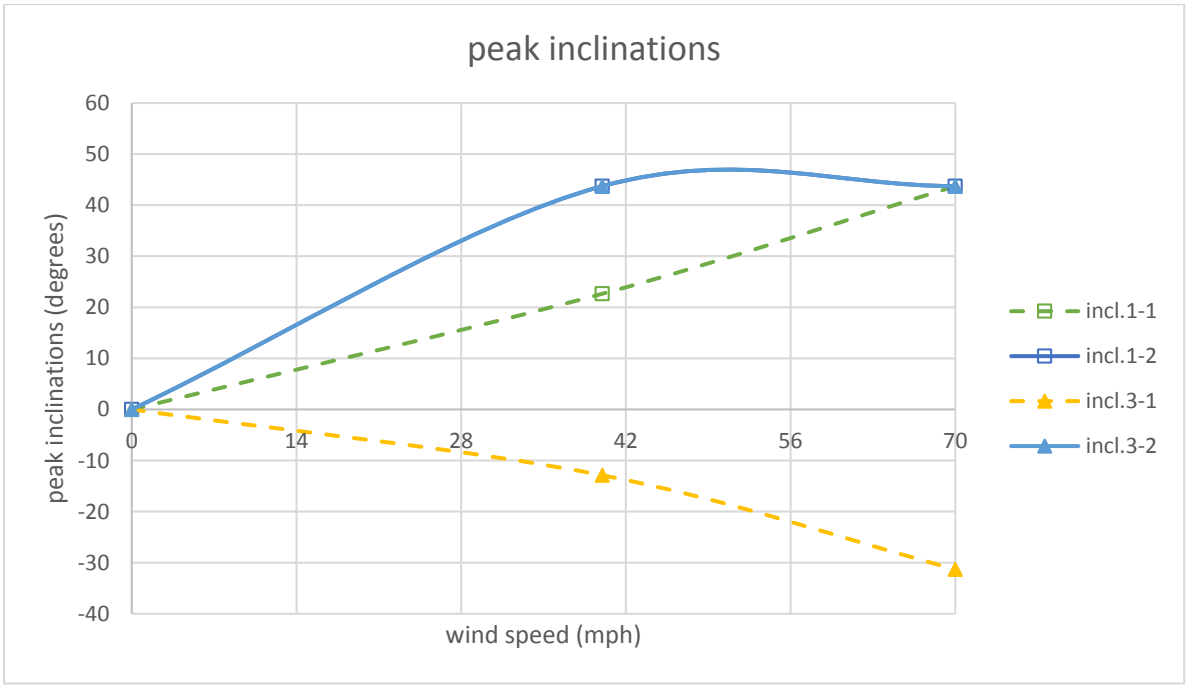

b)

Figure 193: Inclinations obtained from inclinometers 1 and 3 at 0-deg: a) mean; b) peak

12.4. Performance of traffic signals during the tests

This test utilized two 3-section and one 5-section aluminum traffic signals installed in a span wire configuration connected to the catenary and messenger wires by means of a **"tri-stud adjustable hanger" (also known as base configuration)**.

Commencing the test at 40 mph there was no visible evidence of damage to any section of the signal assembly throughout the full range of wind directions. Continuing through to 70 mph there was also no visible indication of damage to any segment of the signal assembly. All back plates and visors were intact. Progressing to 100 mph wind speed and through all wind directions, there was no visible signs of damage to the traffic signals, back plates or visors and there was no visible flexure observed on the tri-stud adjustable hanger assemblies. At 130 mph the upper two segments of the 5-section back plates became detached and were bent. Also, the upper left-hand visor was missing. Back plates for both 3-section signals were intact and visors remained intact other than the center visor for the outer signal. Once wind speed was taken at 150 mph, the bracket connected to the top of the 5-section traffic signal disconnect box fractured.

Figure 194 shows fractured bracket connected to the top of the 5-section signal disconnect box. Back plates for both 3-section signals were intact and most of the 5-section signal back plates were missing. All visors for both 3-section signals were missing and two visors for the 5-section signal were missing. Figure 195 and Figure 196 show the 3-section and 5-section signal after the full test, respectively. The disconnect boxes were observed and they had no visible damage as shown in Figure 197. A summary of the observed damages is as follows:

- Damage to signal hanger: Slight bending of tri-stud adjustable hanger for 3-section signals and fracture of tri-stud adjustable hanger for 5-section signal.
- Damage to disconnect hanger (box): No permanent visual damage observed.
- Damage to signal housing assembly: Damage to visors and back plate. No other permanent visual damage observed.

Figure 194: Fractured bracket connected to the top of the 5-section signal disconnect box

Figure 195: 3-section signal after full test

Figure 196: 5-section signal after full test

Figure 197: Disconnect box after full test (wiring was removed)

12.5. Conclusions

This chapter summarizes the results of a test conducted at WOW at FIU for a span wire traffic signal assembly consisting of two 3-section and a 5-section traffic signal, connected using a **"tri-stud adjustable hanger" (also known as base configuration)**. Wind speeds were varied from 40 to 150 mph and wind directions were varied from 0 to 180 degrees. The various instruments used for this test include: loadcells to measure forces, accelerometers to measure accelerations and inclinometers to measure the inclinations. This study reports the data for different wind directions, in terms of: wind induced forces (drag (y-component), lift (x-component) and cable tension (z-component)), rms of accelerations and inclinations. Results for 0 degrees wind direction indicate that along wind forces (drag) and cable tensions increase in the messenger wire with increase in wind speed. The lift on the messenger wire also increases with increasing wind speeds. The catenary wire experiences only a minor increase of all three components of wind forces with increase in wind speed. At any given wind speed the messenger wire experiences higher tension forces than the catenary wire. The rms of accelerations increased with increasing wind speed; similar observations were made for other wind directions (see appendix J). The magnitudes of the peak forces (Fx, Fy and Fz) increased with increasing wind speeds from 40 to 130 mph, especially on the messenger wire. In the range of 40 to 70 mph for 0 degrees wind direction, the highest mean inclination in the along wind direction was found to be 26 degrees. At 150 mph, the 5-section traffic signal bracket connected to the top of the disconnect box was severed.

Chapter 13 - Task 1b: 1:10 SCALE MODEL TESTING

Test Date: 01/29/2018 - 02/01/2018

13.1. Introduction

This project consisted of designing and testing an aeroelastic model consisting of two 3-section and one 5-section traffic signals. This model is a smaller version of a previously tested full-scale prototype at WOW. Mean wind speeds up to 80 mph (full-scale) were applied to the test specimen. The main objective of this experimental program was to investigate the buffeting response of this particular configuration and compare the aeroelastic model to its full-scale equivalent. This is because testing at a length scale of 1:10 allows a better representation of the wind turbulence spectrum and consequently more accurate evaluation of the wind-induced dynamic response of the structure.

13.2. Experimental Methodology

13.2.1. Prototype Description

The full-scale long-span traffic signal specimen was constructed from the following components:

- 2 columns at the ends of the span standing at a height of 28’.
- 2 cables (catenary and messenger) spanning a horizontal distance of 72.6’ (full scale) between their rig supports.
- 3 hangers that hold both catenary and messenger wires together. One hanger is located at the mid-span point and the other two hangers are located at 4.5’ from the left and right-hand sides of the center point.
- 3 traffic signals that hang from the messenger wire at their hanger support locations. Weights and dimensions of signals are summarized in Table 23.

The columns of the full-scale long span test set up are made of HSS ASTM A500 Grade B steel sections set 72 ft apart. The messenger and catenary cables are made of steel seven-wire strands with a (3/8)” diameter, meeting the properties described in Class A Zinc Coating ASTM A475

standard [7]. The catenary was tensioned to provide a 5% sag of the horizontal span length; i.e. 3.5’ at mid-span. The messenger was tensioned with an axial force of 240 lbs. As for the hangers, they are made of 535 Almag aluminum alloy whereas the extension bar is made of aluminum alloy with 6061-T6 designation. The rest of the assembly components in question are summarized in Table 24 below. Some pictures and sketches of the test specimen are illustrated in Figure 198, Figure 199 and Figure 200. Please note that the full-scale tests used columns that were 16’ high. However, for the aeroelastic tests, it was decided that a 28’ would better resemble an actual field set up used on intersections in the state of Florida.

13.2.2. Laws of Similitude

A relatively large length scale of 1:10 is chosen for the current experiment. Froude number scaling, which characterizes the ratio between the inertial forces of the fluid and the gravitational and elastic forces of the structure, is preserved. This is achieved by linking the velocity scale to the square root of the length scale; i.e., velocity scale is $1{:}\sqrt{10}$. To preserve the overall dynamic behavior of the building, certain parameters need to be considered. Similitude in dynamic behavior requires similar distribution of masses and stiffness along the prototype and model. If a general quantity Q_P has been measured on the prototype, Equation 1 can be used for calculating the model quantity Q_M:

$$Q_M = Q_P \times \lambda_Q \qquad \text{Equation 1}$$

where λ_Q is the physical property scale factor.

The relationships between the model and prototype quantities strongly depends on the materials used for the construction of the model. In this project, prototype materials are used for the construction of the aeroelastic models to preserve the structural damping of the system components. However, due to mass and stiffness scaling constrains, some elements required a change of materials. Table 25 summarizes the adopted scaling factors for different physical properties.

13.3. Design of Aeroelastic Model

13.3.1. Cables Design

To reproduce the dynamic behavior of cables, the elastic stiffness *EA*, the distributed weight *w* per unit length and the diameter *D* should be accurately scaled. From data on the prototype 3/8" span-wire stretch behavior, the value of elastic stiffness *EA* was deduced to be in the range of 1.24 x 10^6 lbs. to 1.81 x 10^6 lbs., depending on tension. For the range of tension varying between 0 and 2000 lbs., a typical value of 1.48 x 10^6 lbs. was selected This value was used in the project and was scaled down according to the appropriate scaling factor for the elastic stiffness. A stainless-steel wire with diameter of 0.010" was selected to satisfy the elastic stiffness scaling. To maintain the weight and the drag scaling requirements, non-structural elements were added along the span of the wire in order to maintain both the scaled distributed weight and average diameter of the wires over the entire horizontal span. Concerning the drag coefficient requirements, the following Equation 2 should be satisfied:

$$C_{D_M} \times D_M = C_{D_P} \times D_P \times \lambda_L \qquad \text{Equation 2}$$

where C_{D_M} is the drag coefficient for the model, D_M is the diameter of the cables in the model, C_{D_P} is the drag coefficient for the prototype, D_P is the drag coefficient for the prototype and λ_L is the scaling factor for the length. Although the chosen wires satisfy the scaling requirements for *EA*, it partially compensate for *D* and *w*. This explains the need to add non-structural elements which compensate for the lack in both *w* and *D* without contributing to the *EA*. The chosen non-structural elements for this project are made of Water-Resistant Neoprene Foam Rods having a diameter of (3/8)", a length of 0.9" and a unit weight of 35 lbs/ft^3. Based on the calculations, a total of 7 foam rods were hung on each wire, with approximately 1 foam element every 1' of cable length. Figure 201 shows a schematic depicting the actual shape and location of the foam elements on the length of the cables in the reduced scale model. By satisfying the three parameters, *EA*, *w*, and *D*, the frequency and mode shapes of the prototype signal system are reproduced at the reduced scale. More details about design validation are discussed later in this chapter.

13.3.2. Columns, Hangers and Traffic Lights Design

The column sections were modeled using aluminum solid rectangular sections having the following dimensions: 1" by 0.75" to represent the flexural stiffness of the column along its height. The scaled column height is 2.8'. The hangers are modeled using aluminum sheets with dimensions of 0.12" by 0.02" to maintain their elastic stiffness *EI* and the distributed weight *w.* The scaled hanger length is 0.2'.

As mentioned earlier, two configurations of traffic signals were attached to the messenger cable (3 section and 5 section). The shape and actual dimensions of the 3-section signals were measured, drawn and designed using the commercial software SAP2000 Section Designer. This enabled a correct simulation of the aerodynamics related to the traffic signals. For the 5-section signal, the same cross-section as the 3-section signal was used. However, the mass was adjusted to reflect the heavier weight of the 5-section signal. Figure 202 shows the actual shape of the cross-section drawn using SAP2000 Section Designer.

For the reduced-scale signals, the exact dimensions of the full-scale counterparts were scaled down and carefully drawn on SOLIDWORKS, considering all the meticulous details. Then, an in-house 3D printer, using resin that hardens with time, was utilized to produce the signals. Figure 203 shows an actual image depicting the signals printed and painted.

13.3.3. Numerical Model

Modal analyses were performed using the Finite Element Commercial Software SAP2000. First, modal analysis for the prototype was performed using the geometric and mass properties described earlier. The mode shapes and frequencies of the prototype were identified and provided in Table 26.

A second, modal analysis was performed on the designed aeroelastic model while utilizing the scaled down structural, geometric and mass properties obtained and mentioned in the previous section. The columns were modeled using straight rigid frames with fixed supports at the ground level. The hangers were modeled using frame elements and were attached to both messenger and catenary cables at the desired locations. The wires were modeled using cable elements and were divided into equal segments in order to assign the loads and hangers on the

joints. The hangers are clamped to both cables. The traffic signals were modeled as solid sections, with the same properties, shape and dimensions described earlier. Figure 204 shows a 3D view of the prototype model constructed on SAP2000 software. More information about the mode shapes and frequencies are provided in the Results and Discussions section.

13.3.4. Design Validation

Table 26 and Figure 205 to Figure 210 provide an insight about the modal behavior of the prototype and the corresponding behavior resulting by adopting the selected sections in the aeroelastic model. The first 3 modes of vibration for each prototype and model are presented in Figure 205 through Figure 210.

A good match is found between the prototype and the model mode shapes and frequencies. The first mode of vibration, demonstrated in Figure 205 (prototype) and Figure 206 (model), shows a rotation of the three signals with respect to their topmost support. The second mode of vibration, presented in Figure 207 (prototype) and Figure 208 (model), shows a torsional mode around the vertical axis at mid-span. As for the third mode, shown in Figure 209 and Figure 210, a similar trend of vibration is observed as the one described in mode 2, but with the signals behaving in a different rotational pattern.

Table 26 shows a good match between targeted frequencies (prototype frequency x frequency scaling factor) and the obtained frequencies where a maximum error of 6% is found for the first two modes. The mode shape of the third mode agrees with a difference in frequencies of about 20%. The overall agreement encouraged the research team at FIU to proceed to the construction and testing phases with the selected sections.

13.4. Instrumentation and Testing Protocol

The model was instrumented with three 3-axis accelerometers, one mounted on each traffic signal. In addition, two cobra probes were used above the height of the model (2’ height) to record the time histories of the velocities at a sampling rate of 2,500 Hz. Furthermore, two loadcells were mounted beneath each column of the specimen. These loadcells are able to capture the change in tension forces experienced by the messenger cable. Figure 211 shows the assembled aeroelastic model. Figure 212 shows a sketch of the instrumentation used.

Open terrain exposure was adopted and the model was tested at 10%, 13%, 17% and 20% throttle ratios of the full wind speed capability at the WOW. The throttle percentages correspond to 15, 20, 25 and 30 mph wind speed at small-scale (47, 63, 79 and 95 mph at full-scale according to the adopted velocity scale). The model was installed on the WOW turntable and the angles chosen for testing ranged between 0^o and 180^o at 15^o increments where 0^o angle of attack represents wind approaching perpendicular to the signals. The duration of each angle exposure was one minute and data was sampled at 520 Hz.

It should also be mentioned that three test cases were investigated in this project. Each test differed from the previous one by varying the amount of tension in the messenger cable. The test cases consist of the following:

- T1: Increased messenger cable tension (125% of the standard tension)
- T2: Standard messenger cable tension (240 lbs. full-scale)
- T3: Reduced messenger cable tension (75% of the standard tension)

The results obtained and the observations made in the three cases are discussed in the next section of this chapter. Last but not least, Figure 213 shows the mean wind speed and turbulence intensity profiles at WOW. By definition, turbulence is the fluctuating velocity component of the flow. Near ground level, the wind is highly turbulent. As height increases, the wind speed also goes up whereas the turbulence intensity goes down. The turbulence intensity I_u is given by Equation 3 below:

$$\mathrm{I}_u = \frac{\sigma_u}{\bar{u}} \qquad \text{Equation 3}$$

Where σ_u and $\bar{u}$ are the standard deviation and mean of the wind speed time history, respectively.

Table 23: Weights and dimensions of signals (Task 1b: 1:10 Scale Model)

Signal	3-section signal	5-section signal
Quantity Used	2	1
Weight (lbs.)	76	94
Height (in)	45.5	54.25
Width (in)	23.5	40
Thickness (in)	0.06 to 7	0.06 to 7

Table 24: Long-span full-scale signal assembly components (Task 1b: 1:10 Scale Model)

Standard Part	**Manufacturer**
Span-wire clamp	Pelco (standard)
Adjustable hanger	Pelco (standard)
Extension bar	Pelco (standard)
Messenger clamp	Pelco
Disconnect hanger	Pelco (standard)
Signal assembly	McCain
Backplate	McCain
Visor	McCain
LED modules	GE - Dialight - Duralight

Table 25: Scale factors (Task 1b: 1:10 Scale Model)

Parameter	Relationship	Scale Factor
Length	$\lambda_L = \frac{L_M}{L_P}$	$\frac{1}{10}$
Velocity	$\lambda_\vartheta = \frac{\vartheta_M}{\vartheta_P} = \sqrt{\lambda_L}$	$\sqrt{\frac{1}{10}}$
Mass	$\lambda_M = \lambda_P \times {\lambda_L}^3$	$(\frac{1}{10})^3 = \frac{1}{1{,}000}$
Mass Moment of Inertia	$\lambda_I = \lambda_M \times {\lambda_L}^2$	$\frac{1}{1{,}000} \times (\frac{1}{10})^2 = \frac{1}{100{,}000}$
Time	$\lambda_T = \frac{T_M}{T_P} = \frac{\lambda_L}{\sqrt{\lambda_L}} = \sqrt{\lambda_L}$	$\sqrt{\frac{1}{10}}$
Frequency	$\lambda_f = \frac{f_M}{f_P} = \frac{1}{\lambda_T} = \frac{1}{\sqrt{\lambda_L}}$	$\sqrt{10}$
Acceleration	$\lambda_a = \frac{a_M}{a_P} = \frac{\lambda_\vartheta}{\lambda_T} = 1$	1
Damping	$\lambda_\zeta = \frac{\zeta_M}{\zeta_P} = 1$	1
Elastic Stiffness (EI)	$\lambda_{EI} = \frac{EI_M}{EI_P}$	$\frac{1}{100{,}000}$
Elastic Stiffness (EA)	$\lambda_{EA} = \frac{EA_M}{EA_P}$	$\frac{1}{1{,}000}$
Force	$\lambda_F = \frac{F_M}{F_P} = {\lambda_\vartheta}^2 \times {\lambda_L}^2 = {\lambda_L}^3$	$(\frac{1}{10})^3 = \frac{1}{1{,}000}$
Bending and Torsional Moment	$\lambda_{BM} = \frac{BM_M}{BM_P} = {\lambda_\vartheta}^2 \times {\lambda_L}^3$	$\frac{1}{10{,}000}$

Table 26: Results of the modal analysis for the full-scale and reduced-scale models (Task 1b: 1:10 Scale Model)

Mode No.	Mode Description in the Full-Scale Model	Mode Description in the Reduced Scale Model	Full Scale Frequency f (Hz)	Target Frequency f (Hz)	Reduced Scale Frequency f (Hz)	Percentage Difference (%)
1	Displacement in the Transverse Direction	Displacement in the Transverse Direction	0.37	1.17	1.11	5.05
2	Opposite Rotations of all Traffic Signals about their Supports	Opposite Rotations of all Traffic Signals about their Supports	0.49	1.56	1.65	5.84
3	Opposite Rotations of all Traffic Signals about their Supports	Opposite Rotations of all Traffic Signals about their Supports	0.55	1.75	2.10	19.8

Figure 198: Column rig (full-scale, long-span)

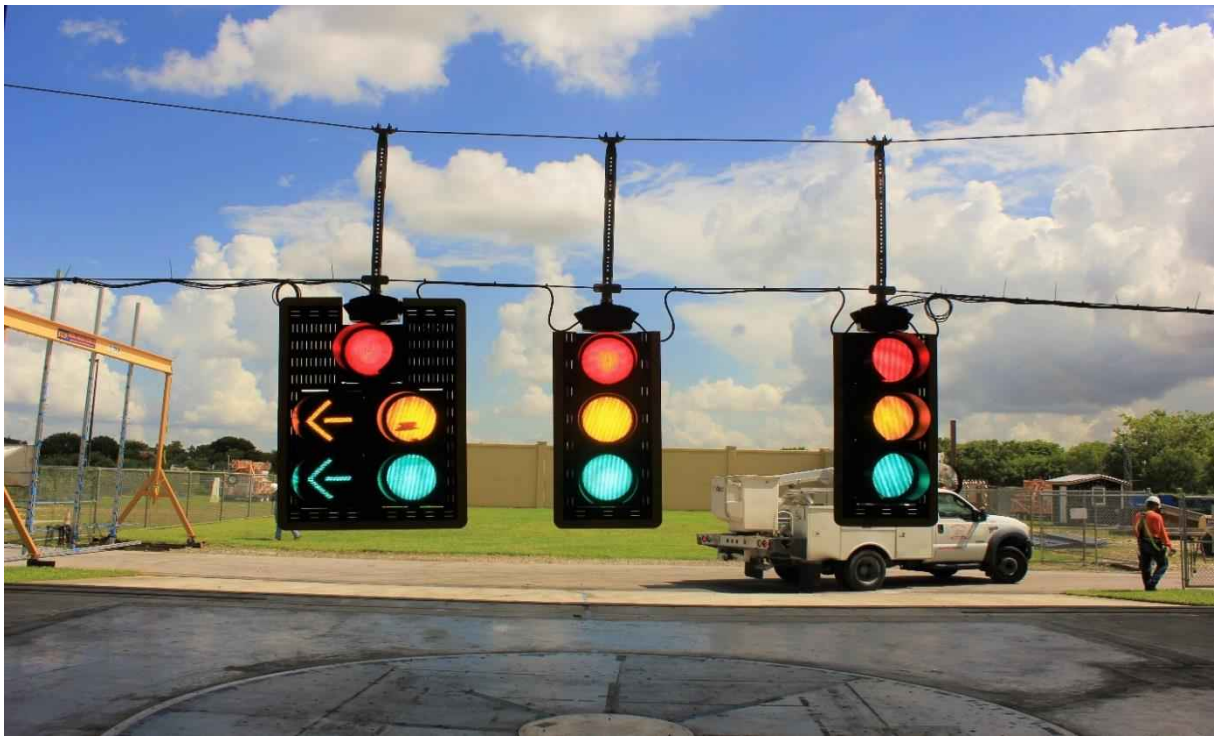

Figure 199: Traffic signals, hangers and span-wire

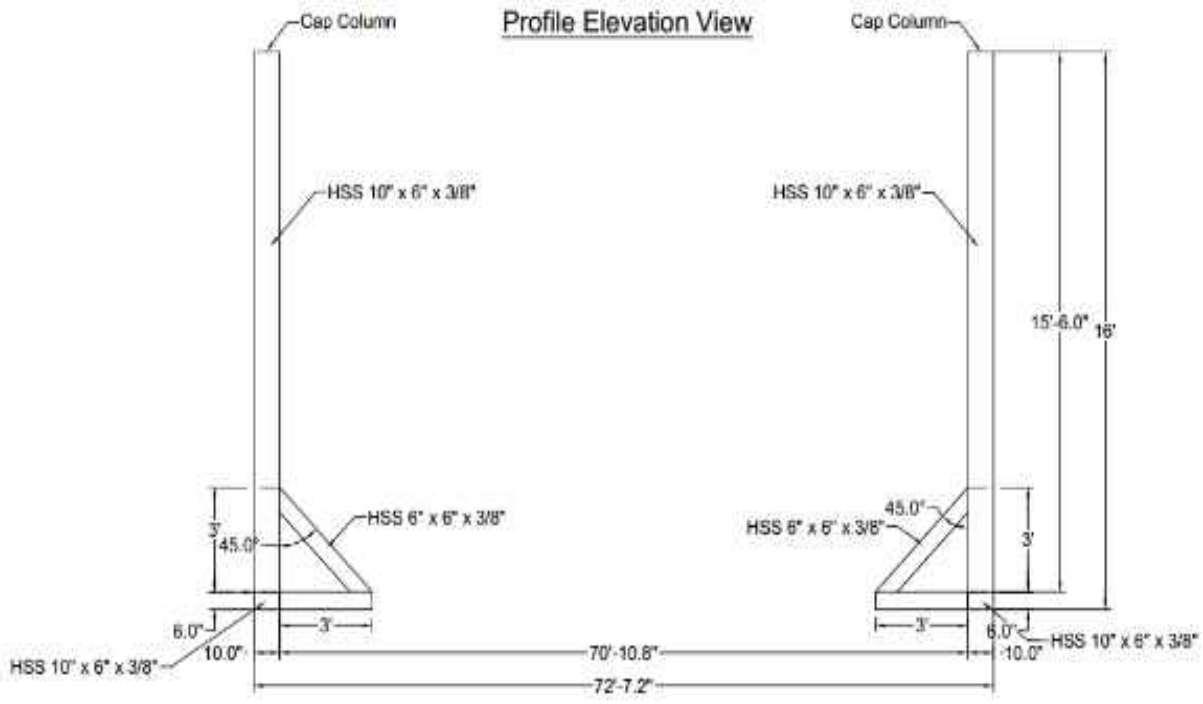

Figure 200: Profile view of full-scale long-span specimen

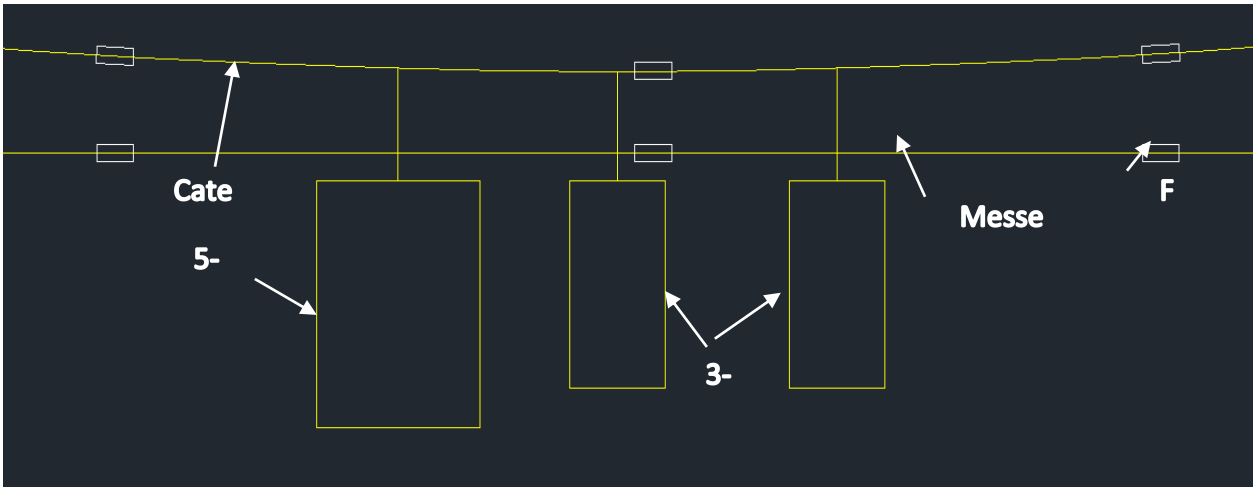

Figure 201: Placement of non-structural elements

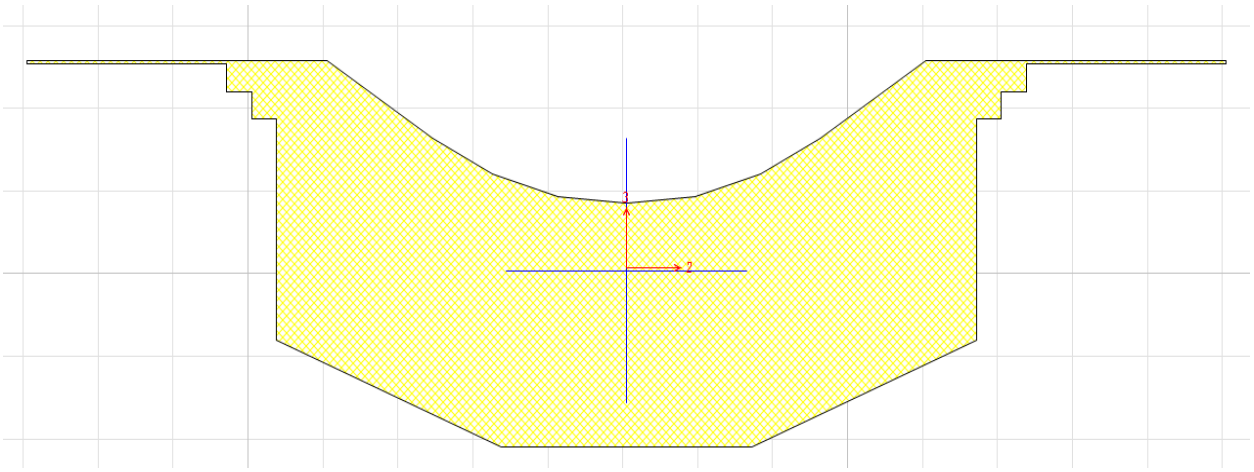

Figure 202: Cross-section shape of traffic signal

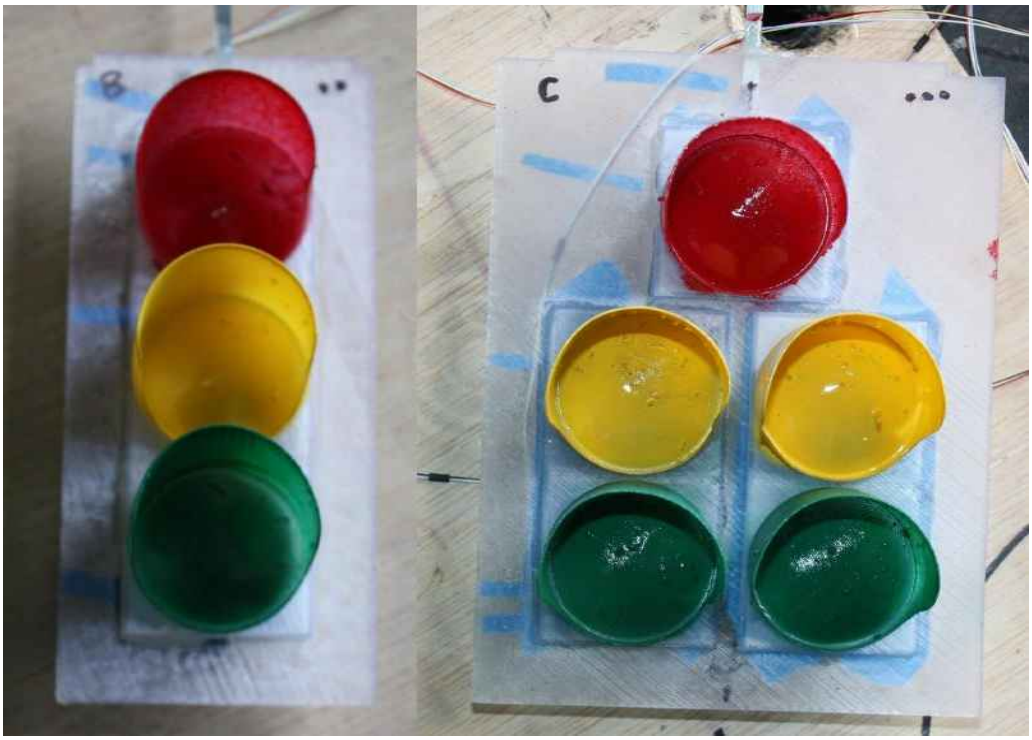

Figure 203: 3D printed signals (3 section and 5 section)

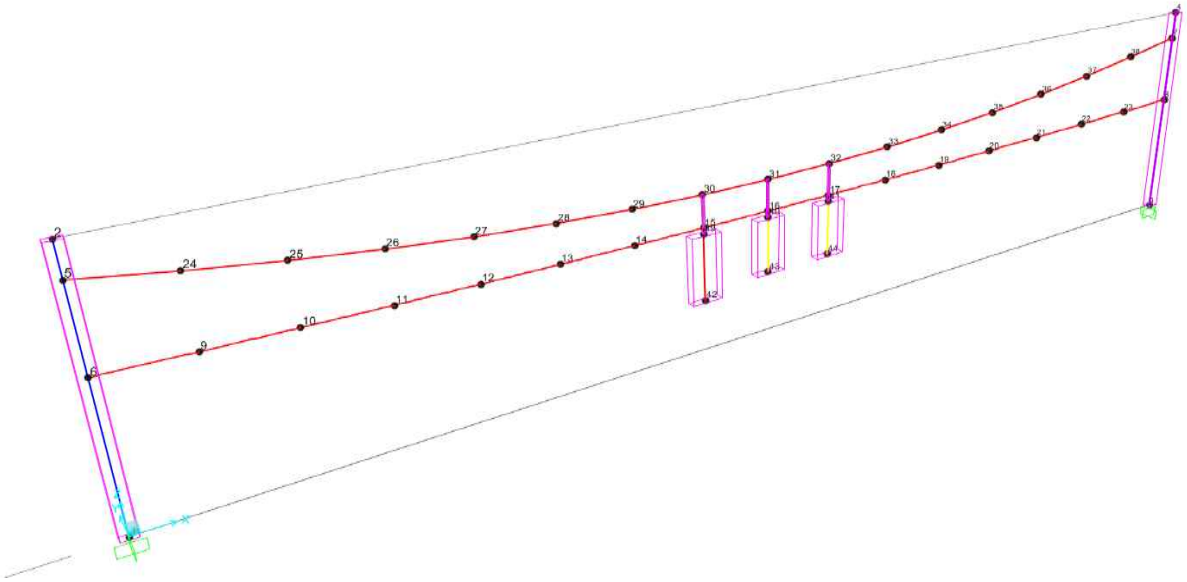

Figure 204: 3D view of the prototype model on SAP2000

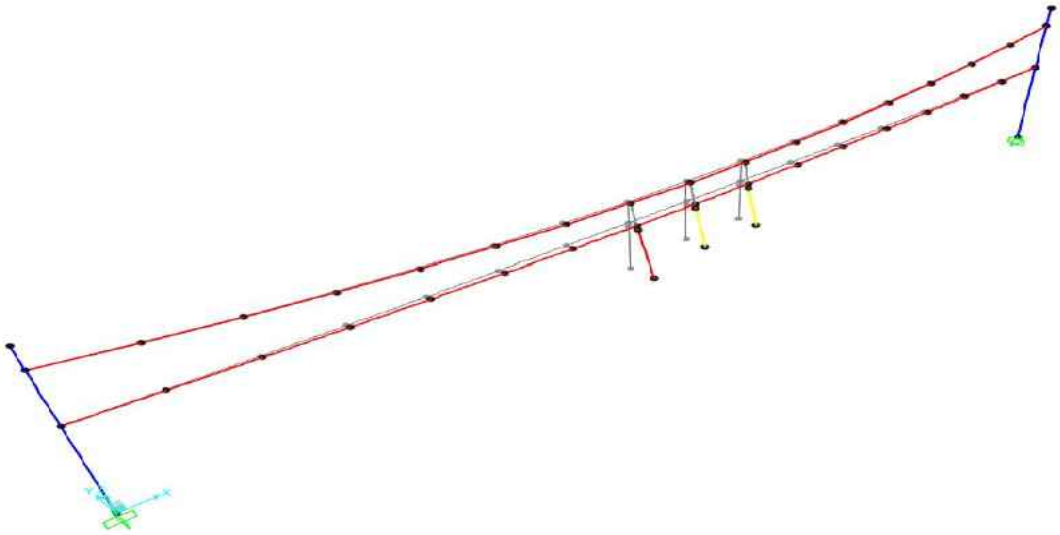

Figure 205: Mode shape 1 for full-scale model with a frequency f = 0.37 Hz

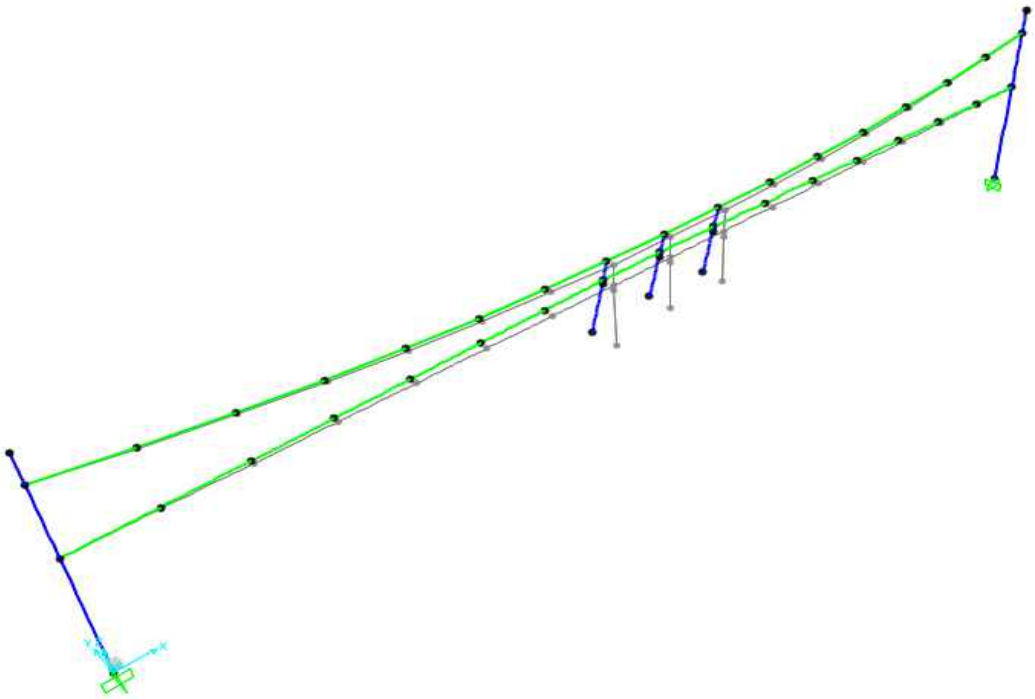

Figure 206: Mode shape 1 for reduced-scale model with a frequency f =1.11 Hz

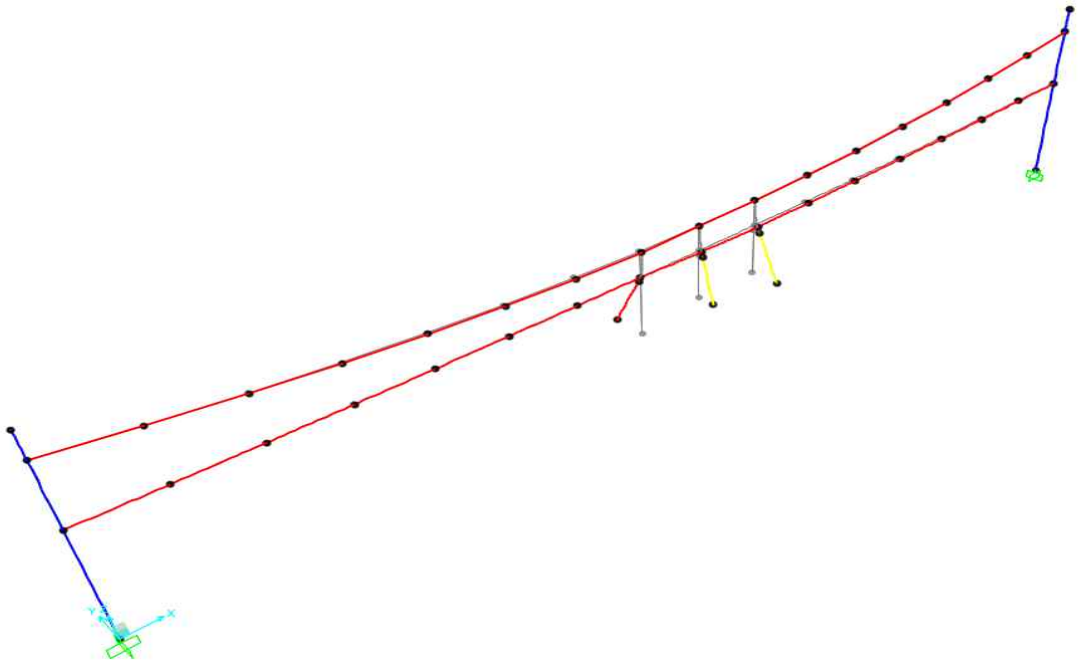

Figure 207: Mode shape 2 for full-scale model with a frequency f = 0.49 Hz

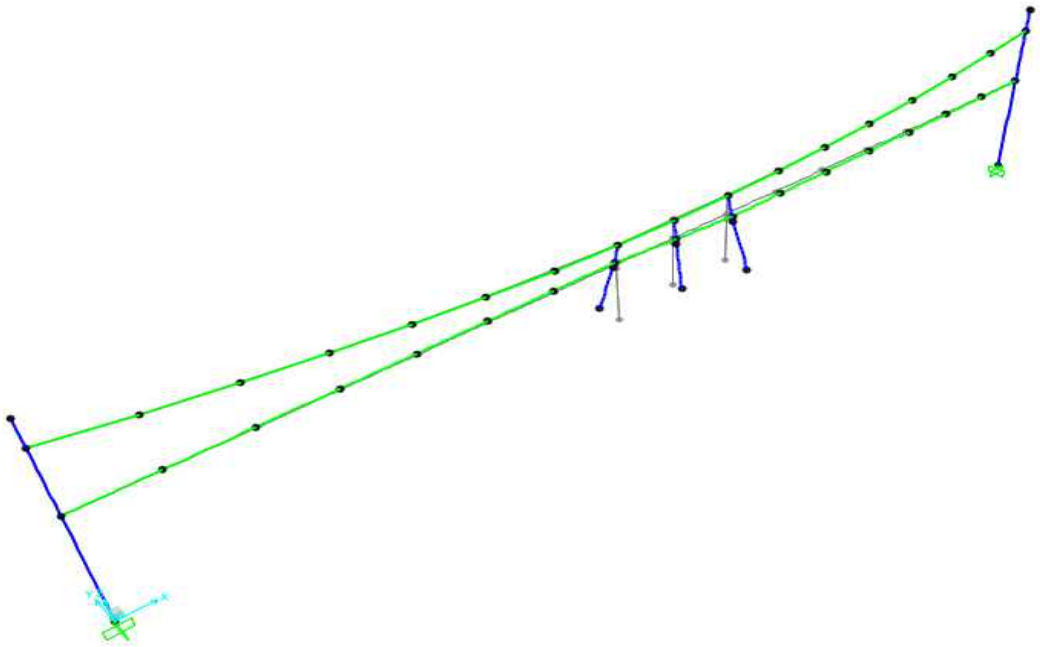

Figure 208: Mode shape 2 for reduced-scale model with a frequency f = 1.65 Hz

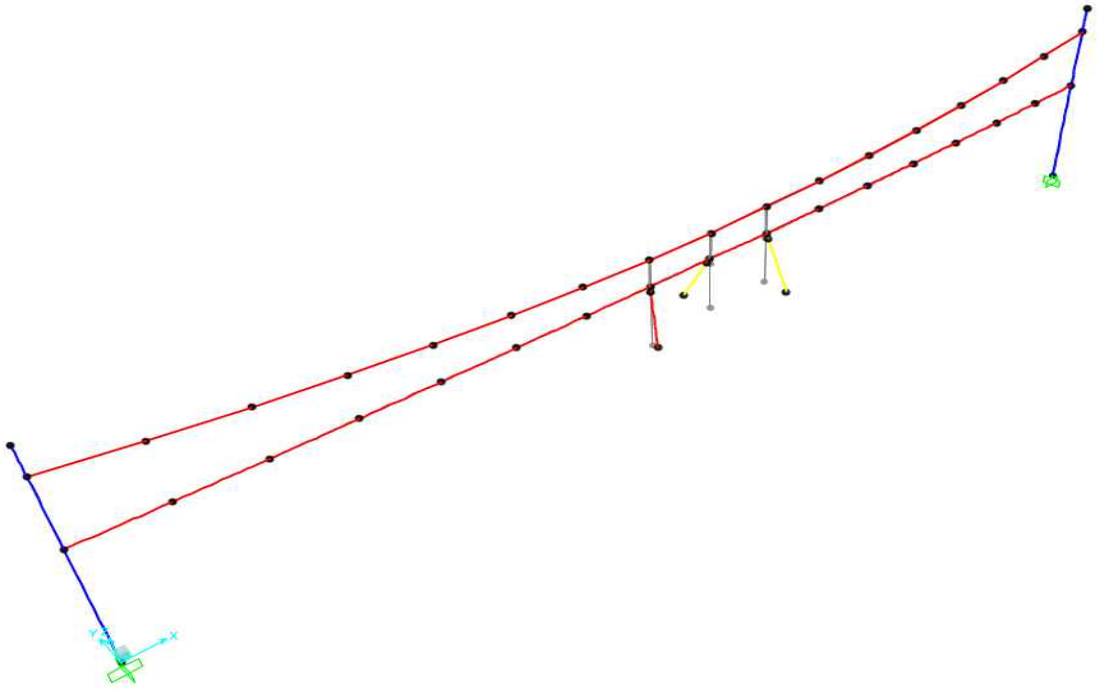

Figure 209: Mode shape 3 for full-scale model with a frequency f = 0.55 Hz

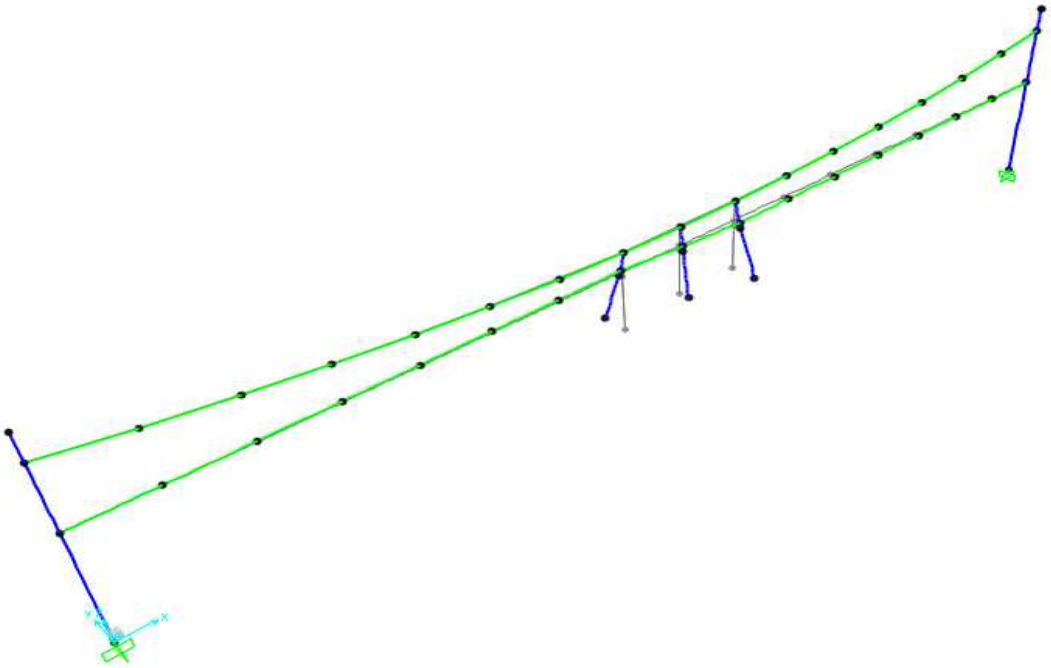

Figure 210: Mode shape 3 for reduced-scale model with a frequency f = 2.10 Hz

Figure 211: Actual instrumented model before testing

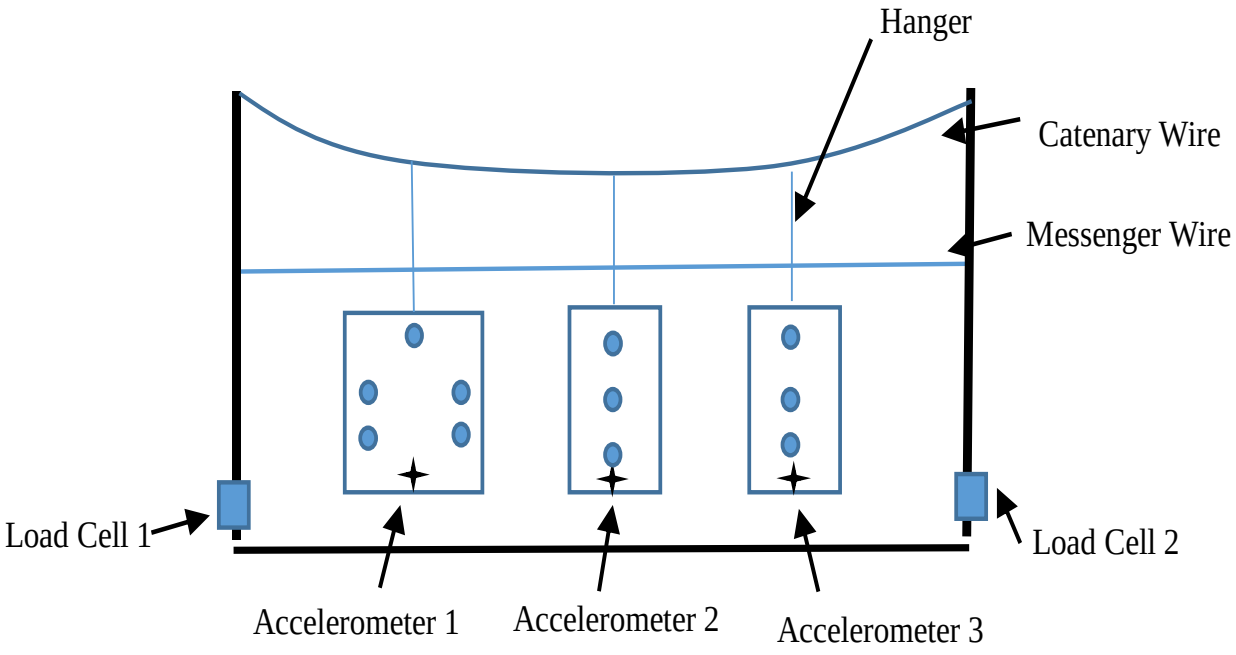

Figure 212: Sketch of instrumented model

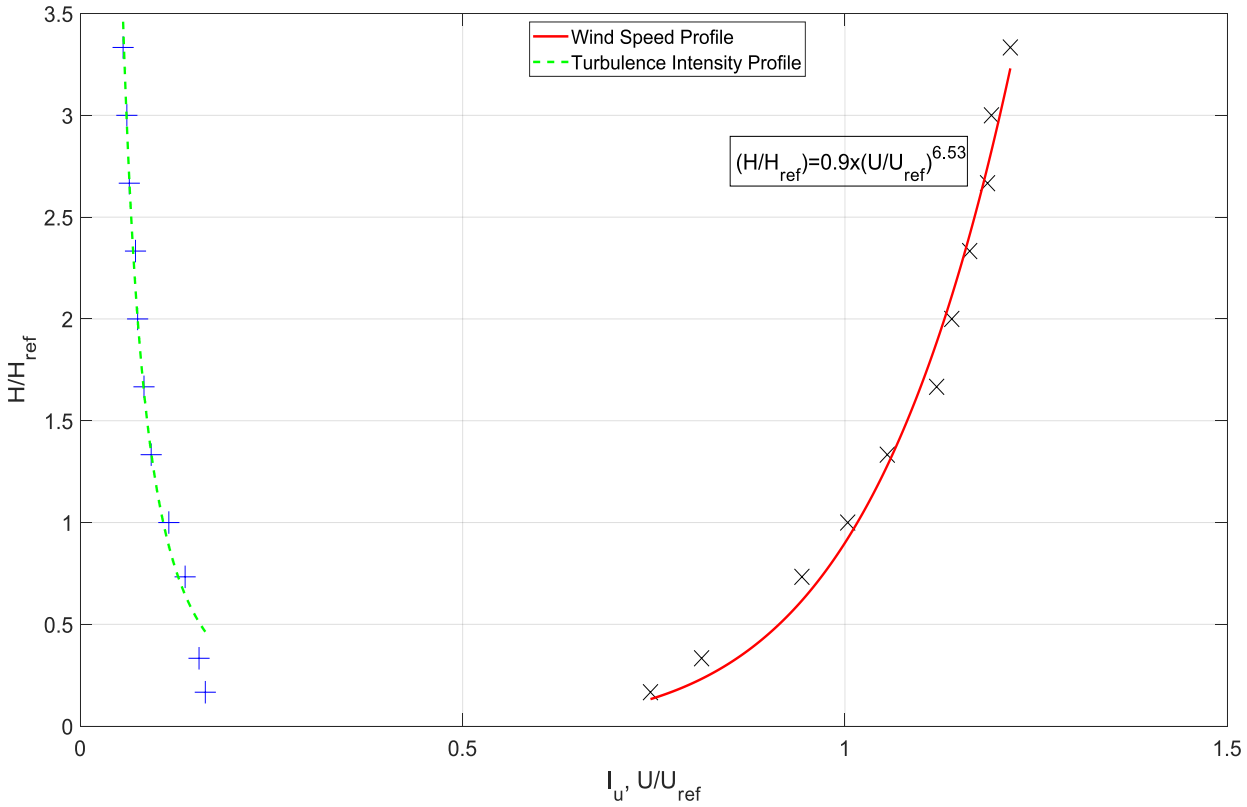

Figure 213: Wind speed and turbulence intensity profiles at WOW

13.5. Results of Aeroelastic Tests

In this section, free vibration test done prior to the actual wind testing to validate the design and assemblage of the model is reported. Then, the aerodynamic instabilities observed during the testing of the aeroelastic models are presented. In addition, wind-induced accelerations are presented along with mean tension forces in the messenger wire.

13.5.1. Free Vibrations Tests based on Accelerations

The free vibrations test consisted of using a straight rod to manually push back all three traffic signals and let them oscillate freely until they go back to their initial position while measuring their instantaneous accelerations. From the captured acceleration time histories, the fluctuating response and the corresponding frequencies can be obtained using a Fast Fourier Transform application. Figure 214 and Figure 215 below depict the time history captured of the 5-section traffic signal along with its respective power spectral density plot during the free vibrations test. Please note that the PSD plot of Figure 215 shows the full-scale frequencies obtained from the aeroelastic model.

From Figure 215, the first spike, which defines the lowest natural frequency of the system or the frequency of the first mode of vibration, occurs around 0.4 Hz (seen in the data box above first spike). By comparing that value to the target frequency for mode shape 1 available in Table 26 (0.37 Hz), it can be concluded that the tension in the messenger is nearly equal to the target one and that the model was correctly designed to mimic the behavior of the full-scale specimen.

13.5.2. Observations during Testing

As mentioned in the testing protocol, the model was subjected to wind speeds ranging between 48 and 80 mph (full-scale) and at angles of attack ranging between 0^o and 180^o at 15^o increments. During the entirety of the test time, some aerodynamic instabilities were observed, specially from oncoming cornering winds at different angles of attack. Figure 216 through Figure 220 show samples of the observed behavior of the traffic signals.

According to Figure 216, at 0^o angle of attack and 30 mph, all three signals rotated and tilted backwards due to oncoming winds, depicting the first mode of vibration discussed in the previous

section. Please note that there was an offset in the column placement on the turntable by around +8^{o}, which explains the use of a 352^{o} angle in Figure 216, instead of a 360^{o} or 0^{o}.

At 25 mph (90^{o} and 135^{o}) and at 30 mph (45^{o}), more aerodynamic instabilities were observed in the form of single-degree-of-freedom (SDOF) fluttering. SDOF fluttering is a type of wind-induced vibration. By observing the 5-section signal in Figure 217, Figure 218 and Figure 219, SDOF fluttering can be observed in the form of torsional vibration of the signal around its vertical axis at different wind speeds. Among some of the other observations made by the WOW team is the possible occurrence of mode shape 3 during the tests at 90^{o} angle of attack due to cross wind effects. Mode shape 3, as defined by the modal analysis conducted on SAP2000 in the previous section, is characterized by the opposite rotation of traffic signals with respect to their top supports. This can be clearly noted in Figure 220 where the middle signal is moving forward and the other two are tilting backwards.

13.5.3. Mean Tensions in the Messenger Cable

In this section, the increase in mean tension forces due to oncoming wind forces at 0^{o} experienced by the messenger wire are reported. As discussed earlier in the testing protocol, three cases were conducted in this investigation: T1 or 125% messenger tension case (300 lbs.), T2 or standard messenger tension case (240 lbs.) and T3 or 75% messenger tension case (180 lbs.). Figure 221 shows the original captured tensions in the messenger cable. To assess the effect of the pre-tensioning of the wires on the wind-induced tensions, the ratio of the change in tension forces divided by the initial tension of the messenger cable is calculated and depicted Figure 222. Please note that all values in the graphs pertain to the aeroelastic model, scaled up by a factor of 1,000 (force scale) to depict the full-scale values, as shown by the relevant scaling factor for forces in Table 25. Please note that all wind speeds are reported at mean signal height.

It can be concluded from Figure 221 and Figure 222 that the increase in messenger tension is directly proportional to the increase in wind speed in a linear manner. On a different note, T3, which represents the case with 75% messenger standard tension, experienced the highest mean tension forces at 0^{o} angle of attack, for wind speeds higher than 38 mph. Forces reached as high as 1,200 lbs. for a wind speed of 63 mph at model height. Similarly, T1, which represents the case with 125% messenger standard tension, experienced the least mean tension forces at the same

angle of attack. Forces reached a maximum of 750 lbs. for a wind speed of 63 mph at model height.

13.5.4. RMS of Accelerations

This section discusses the RMS of the accelerations experienced by the aeroelastic model. As previously discussed, 3 accelerometers were installed on the specimen, one on the backplate bottom of each traffic signal. Figure 223 shows the change in RMS of accelerations with the increase in oncoming wind speeds at 0^o angle of attack. Please note that series 'A' in Figure 223 pertain to the 5-section signal whereas B and C belong to each of the 3-section signal. Please note that all figures are reproduced at mean signal height.

Once again, it can be seen that the RMS of accelerations experienced by the system in general tends to linearly increase with the increase in oncoming wind speeds. Both 3-section signals B and C have approximately the same behavior whereas 5-section signal A tends to show higher values for the same wind speeds. A maximum value of around 120 in/s^2 is reached for a wind speed of 63 mph.

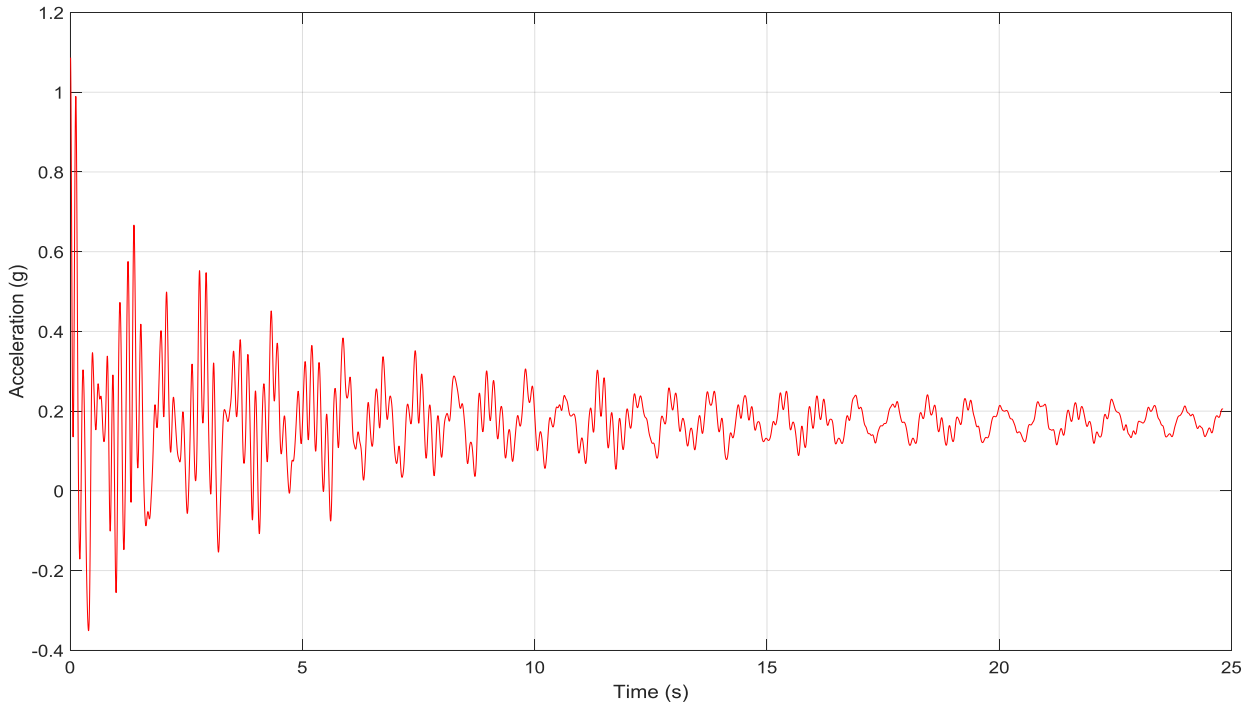

Figure 214: Time history of 5-section signal

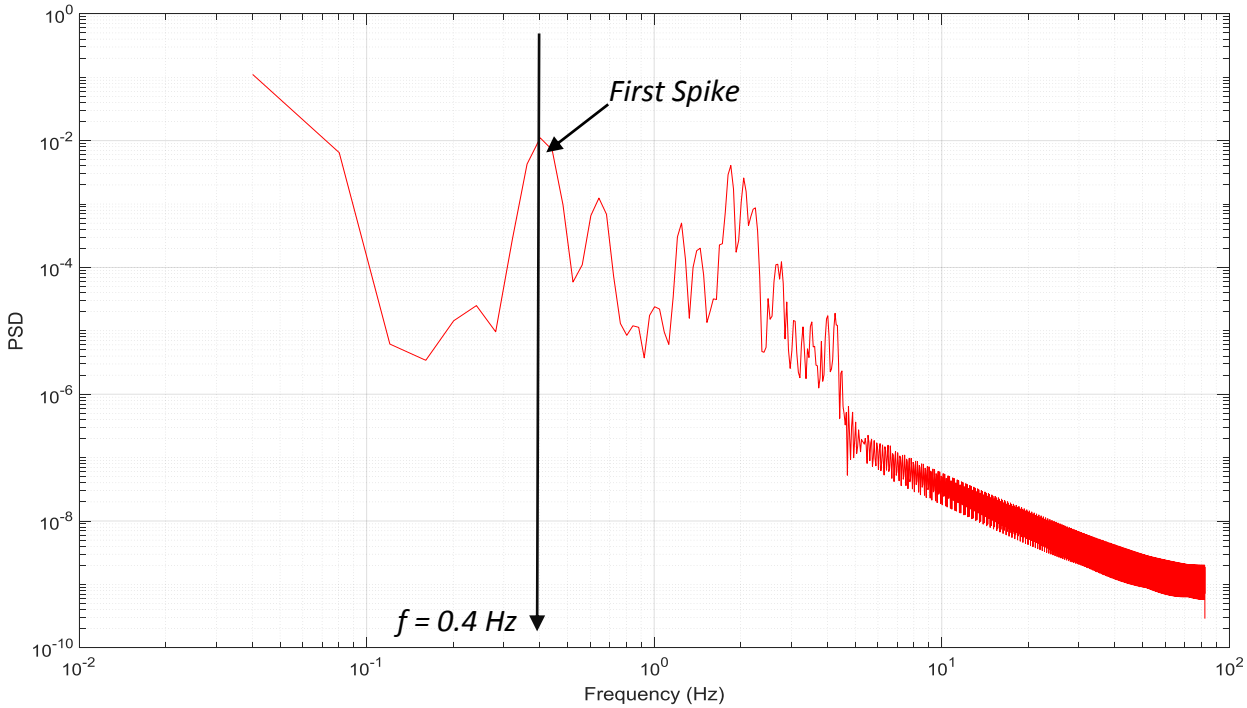

Figure 215: PSD of 5-section signal

Figure 216: Backward tilting of traffic signals

Figure 217: Aerodynamic instabilities at angle 45°

Figure 218: Fluttering at 90^{o} angle of attack

Figure 219: Fluttering at 135^{o} angle of attack

Figure 220: Possible occurrence of mode shape 3

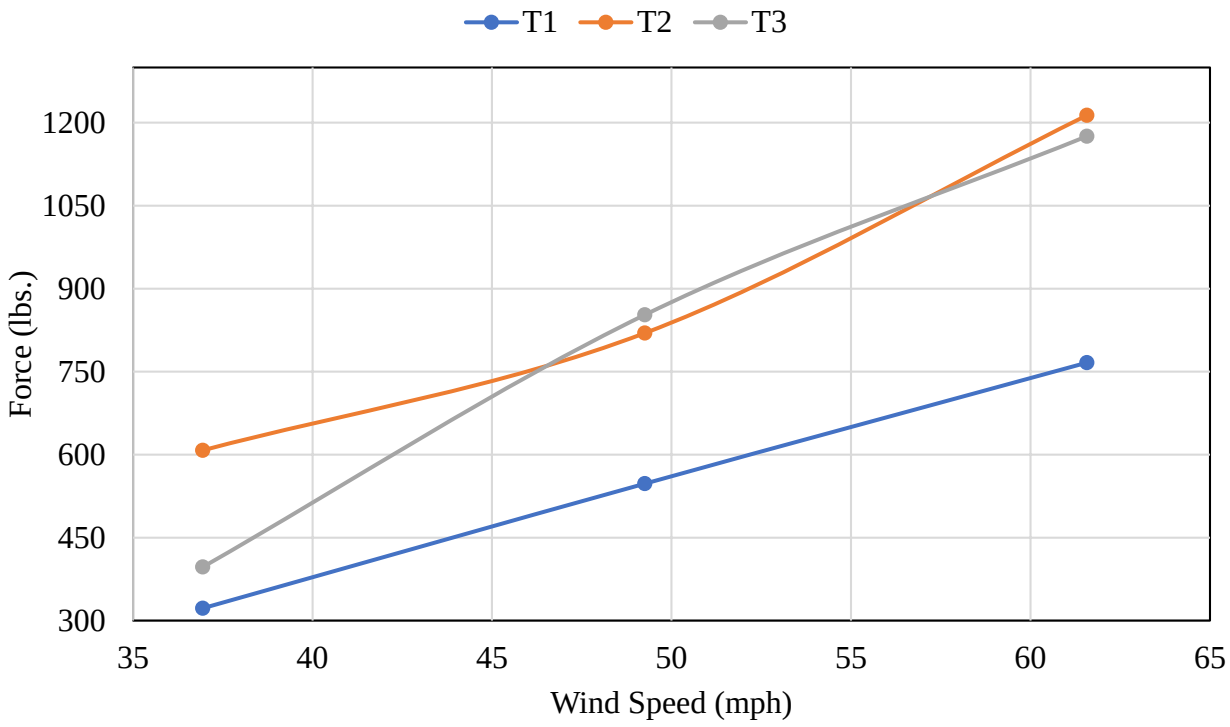

Figure 221: Messenger mean tension forces

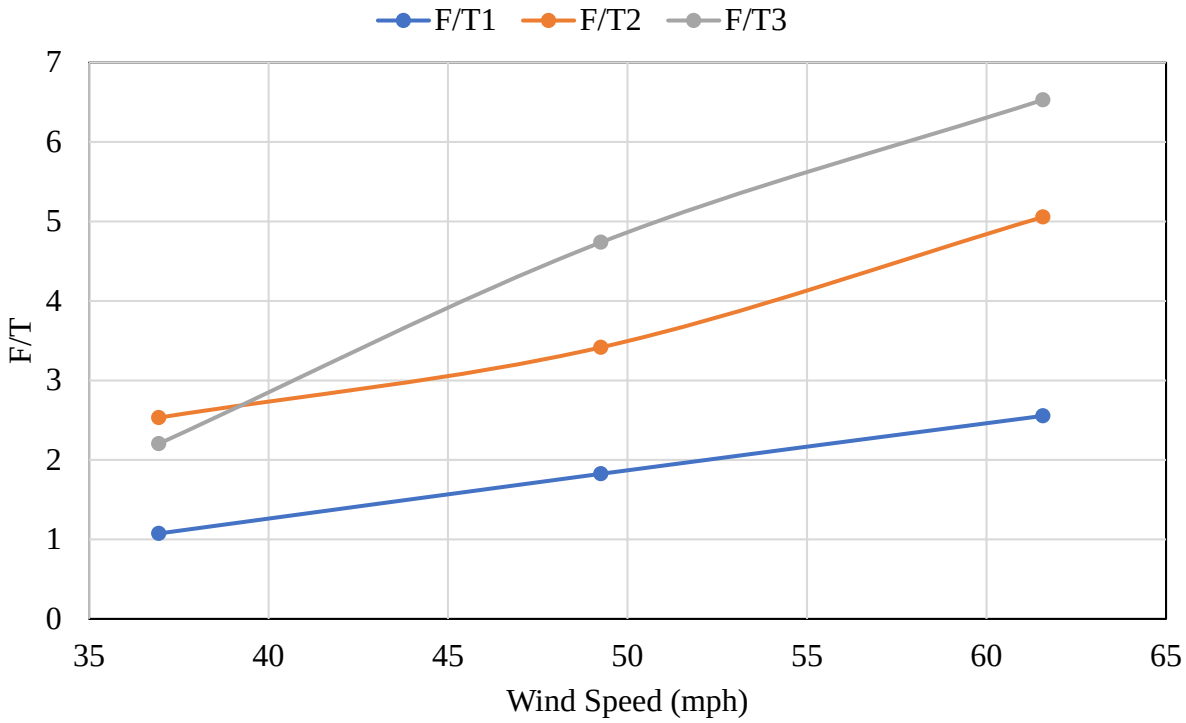

Figure 222: Ratio of change in tension to initial tension (messenger wire)

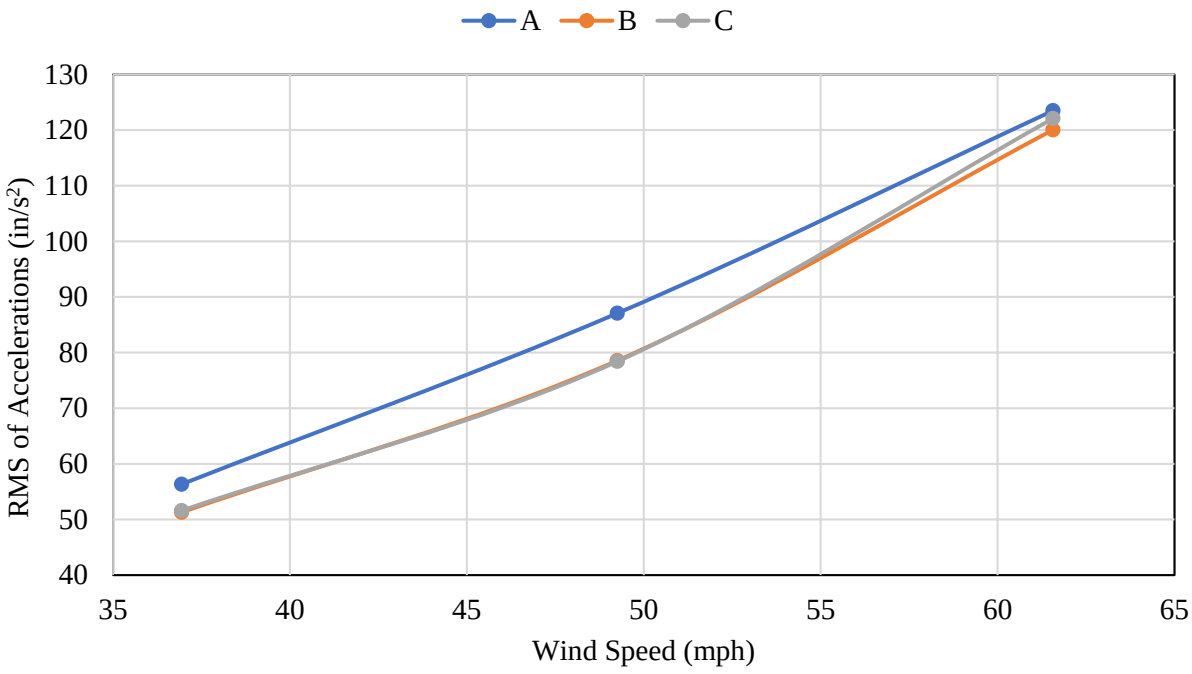

Figure 223: RMS of accelerations at 0° angle of attack

13.6. Comparison of Aeroelastic and Full-Scale Specimens

The objective of this section is to investigate how the aeroelastic results obtained in the current experimental program compare with previous full-scale specimen investigations conducted at WOW. In the past, full-scale specimens having the same traffic signal configurations were constructed and tested at WOW. A long-span version of the specimen was first investigated before constructing a short-span model, with springs as end connections between the messenger wire and the column rig. The role of the springs is to mimic the behavior of the long-span version. Since the short-span version of the specimen was rigorously tested at several wind speeds, it was decided that it would best to compare it to the aeroelastic model. Once again, the accelerations of the traffic signals and the mean tensions in the messenger cable will be compared against each other.

13.6.1. Power Spectral Density of Longitudinal Turbulence Fluctuations

Before going into the comparisons, it is worthwhile to note that both tests used the same spires and roughness elements that are installed in the configuration box in front of the fans at the WOW. Due to the big difference in model heights (2.8' for aeroelastic model compared to 16' for short-span full-scale model), the surface roughness z_o at the mean height of the traffic signals might have been rougher for the aeroelastic model. Figure 224 shows the normalized power spectral density of longitudinal turbulence fluctuations for the aeroelastic model.

According to Figure 224, the full-scale spectrum that matches the aeroelastic model tested at WOW has a surface roughness z_o of around 0.1 m. Since no cobra probes have been used in the long- or short-span models, it is impossible to compare the value of the surface roughness to the one for the full-scale tests. However, based on previous full-scale tests conducted at WOW having almost the same height, the surface roughness ranged between 0.03 to 0.06 m. This number is much smaller than the one obtained for the aeroelastic tests. This indicates that the aeroelastic model testing might have been rougher, i.e. more turbulent, than the full-scale one, which might contribute to divergences in the dynamic response comparisons that will follow. A rougher surface also indicates more fluctuations and possibly higher observed peaks for the aeroelastic

model. For the aeroelastic tests, the equivalent full-scale parameters such as the turbulence intensity I_u and the integral length scale ${}^{x}Lu$ were about 20.3% and 59.8 m, respectively.

13.6.2. Accelerations of Traffic Lights

This section compares the accelerations obtained for both aeroelastic and full-scale short-span models. Figure 225 shows all six RMS accelerations collected for both models at 0^{o} angle of attack. Please note that FS and SS in the series' names stand for full-scale short-span and small-scale aeroelastic models respectively. In addition, signal A represents the 5-section signal whereas signals B and C belong to the 3-section signals. As it can be observed, the aeroelastic results show higher numbers than the short-span ones for the same approaching wind speed at the height of the traffic signals. The RMS of the accelerations experienced by the aeroelastic model are around 15-40% higher than the ones felt by the short-span model, for the same wind speeds. However, as previously stated, both models show an approximately linear proportionality relationship between accelerations and oncoming wind speeds. In the aeroelastic model tests, the power spectrum of turbulence at the model natural frequencies was higher than in the full-scale tests, and at a level that gave a good indication of the resonant response caused by turbulence buffeting from the approaching turbulence, whereas the full-scale tests tended to be dominated by the effects of signature turbulence from the signals themselves.

13.6.3. Mean Tensions in Messenger Cable

This section compares the force over tension ratios (e.g. normalized tensions) obtained for both aeroelastic and full-scale short-span models. Figure 226 shows all six *F/T* collected for both models at 0^{o} angle of attack. Please note that FS and SS in the series' names stand for full-scale short-span and small-scale aeroelastic models, respectively. In addition, T1, T2 and T3 represent the high-, standard- and low-tension cases. From Figure 226, the short-span results show higher numbers than the aeroelastic ones for the same approaching wind speed. The effect of initial tension on accelerations is shown to be relatively small.

13.6.4. Dynamic Amplification Factor

In this last section, it was decided that decomposing the dynamic response of the system into peak, mean, background and resonance responses would be useful to assess the buffeting

response of the traffic signal. It is expected that the 1:10 aeroelastic model will experience higher dynamic response compared to the short-span full-scale model due to more of the low frequency end of the turbulence spectrum being present in the small scale aeroelastic tests.

A MATLAB® code was developed to analyze the time histories captured for peak tensions and accelerations. The ultimate goal of this numerical code is to separate the resonance from the fluctuating response and to try and come up with a Dynamic Amplification Factor (DAF) that can help in better estimating the wind-induced stresses in span-wire traffic signals. According to Elawady et al. [10], a DAF is calculated using Equation 4:

$$DAF = \frac{\text{Maximum peak response}}{Maximum\ quasi-static\ response} \qquad \textit{Equation 4}$$

where maximum quasi-static response is the summation of the mean response and the absolute maximum of the background response.

Figure 227 and Figure 228 show one sample of the processed power spectral density (PSD) plots obtained when decomposing the resonance of the acceleration of one traffic signal measured from both models. Similar plots are accomplished for the accelerations and wire tensions at different wind speeds and angles for both aeroelastic and short-span models. Consequently, DAF values for tension forces and accelerations are calculated for both models and are summarized in Table 27 and Table 28.

By observing Tables 5 and 6, it can be noted that the DAF for the aeroelastic model is higher than the one for full-scale short-span for all values of approaching wind speeds. DAF for tensions is higher by around 30% and by around 20% for accelerations. Please note that only two accelerometers were used in the short-span full-scale test, hence the non-availability of values for signal B. The main reason for the higher dynamic response at 1:10 scale, is that more low frequency turbulence is present in the small-scale than in the full-scale. Furthermore, the only aerodynamic instabilities observed in the full scale short-span model at the tested wind speeds were related to mode shape 1, or the backward tilting of all three signals. Other aerodynamic instabilities surfaced at much higher wind speeds. This might explain why the full-scale short-span model's DAF is approximately equal to 1 (e.g. static response) for wind speeds up to 67 mph for tensions, as depicted in Table 6. Last but not least, the first fluctuating frequency that appears

in Figure 227 for the aeroelastic model is around 0.08 Hz, which is significantly less than that depicted in Figure 228 for the full-scale model, which is 0.22 Hz. This shift in the appearance of the first fluctuating frequency could offer another justification for the observed discrepancy in DAF values for both models.

Table 27: Dynamic amplification factors for aeroelastic model (Task 1b: 1:10 Scale Model)

Wind Speed (mph)	Dynamic Amplification Factor (DAF) for:			
	Tensions in Messenger Cable	Accelerations		
		Signal A	Signal B	Signal C
37	1	1.33	1.44	1.46
49	1.35	1.56	1.44	1.44
62	1.34	1.25	1.39	1.42

Table 28: Dynamic amplification factors for short-span full-scale model (Task 1b: 1:10 Scale Model)

Wind Speed (mph)	Dynamic Amplification Factor (DAF) for:			
	Tensions in Messenger Cable	Accelerations		
		Signal A	Signal B	Signal C
27	1.01	1.31	N/A	1.21
41	1.02	1.32	N/A	1.27
54	1.03	1.20	N/A	1.17
68	1.03	1.17	N/A	1.22

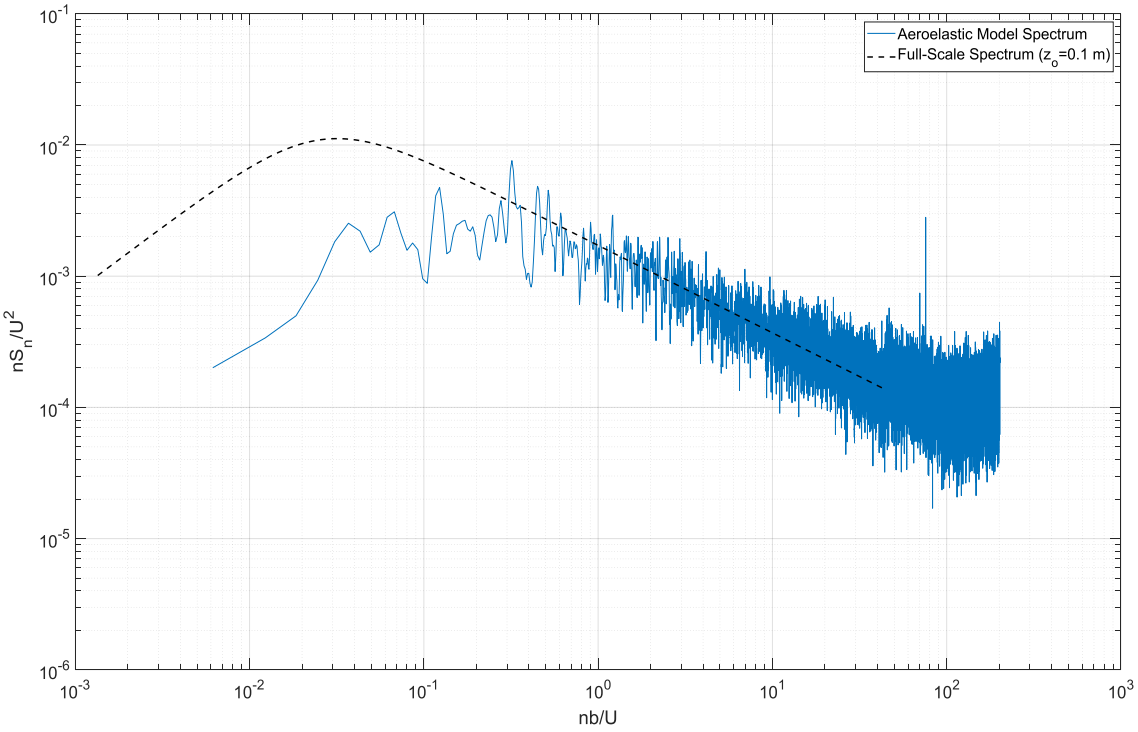

Figure 224: Normalized power spectral density of longitudinal turbulence fluctuations

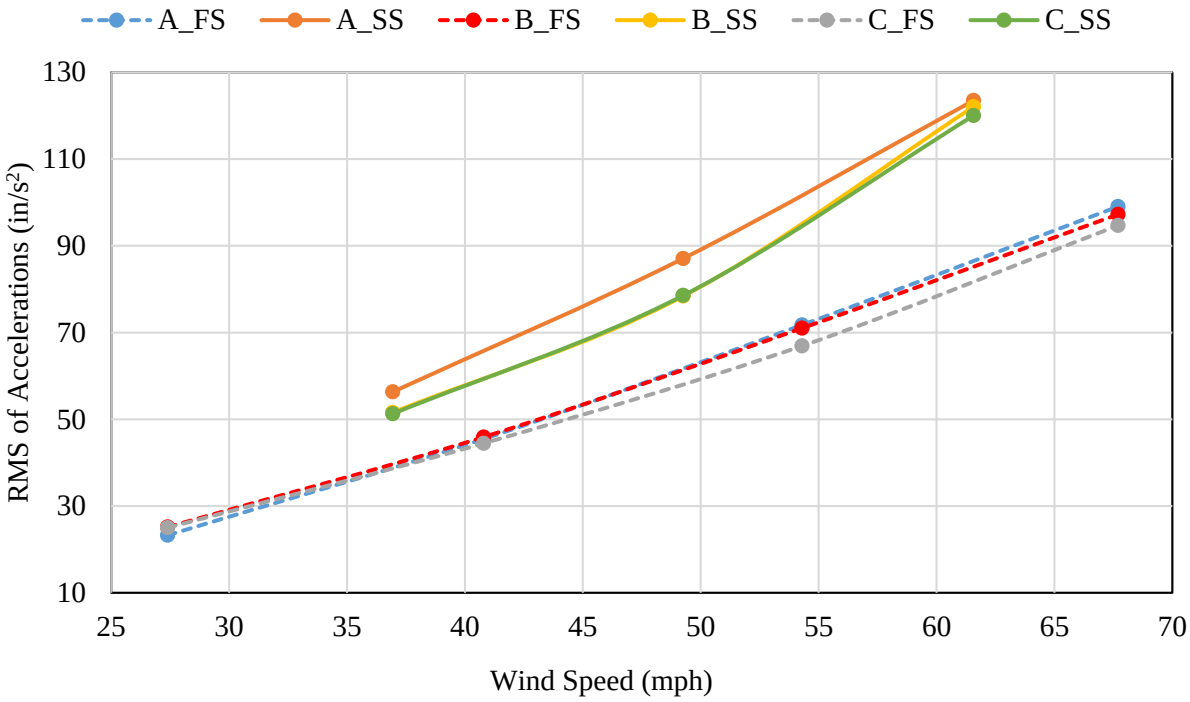

Figure 225: RMS of accelerations for both models (FS: full-scale short-span; SS : small-scale aeroelastic)

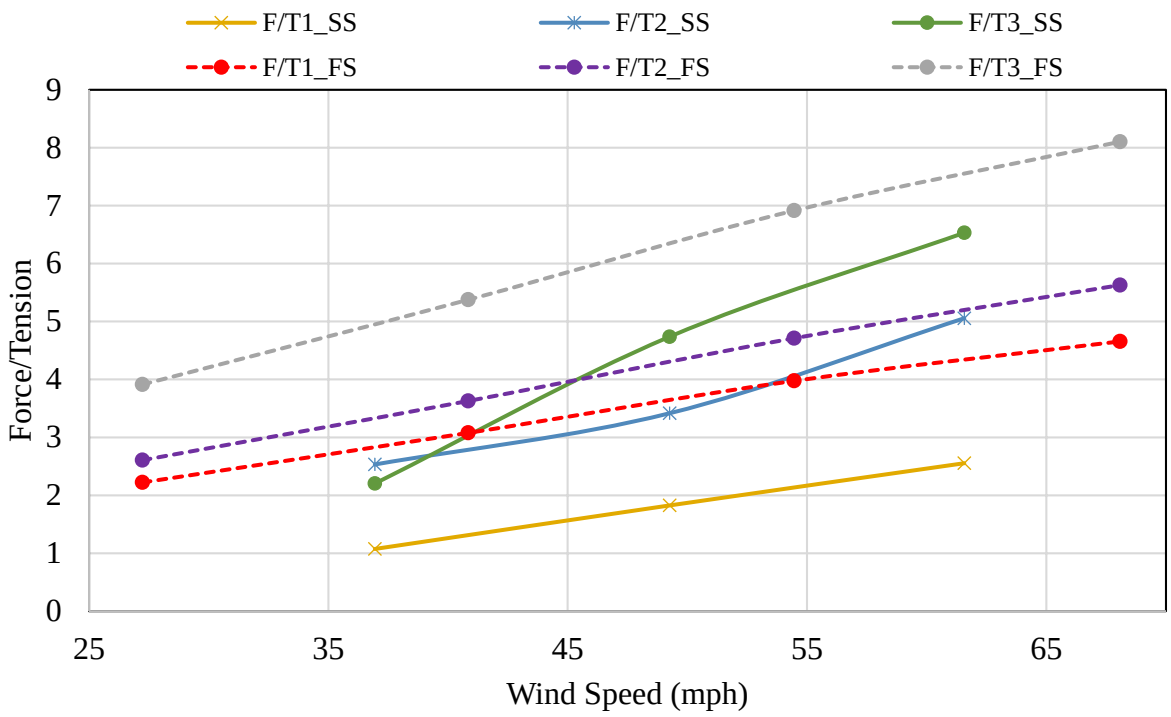

Figure 226: Ratio of change in tension to initial tension for both models

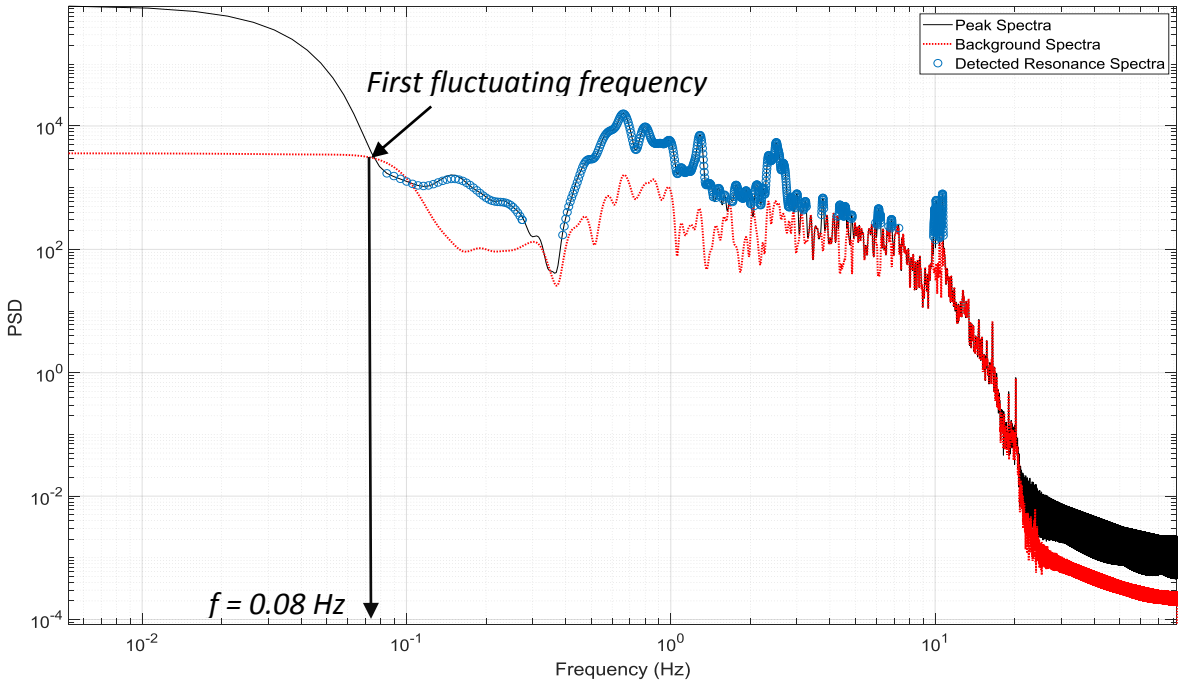

Figure 227: Decomposition of resonance for acceleration of signal A at 10% throttle at 0º (aeroelastic model)

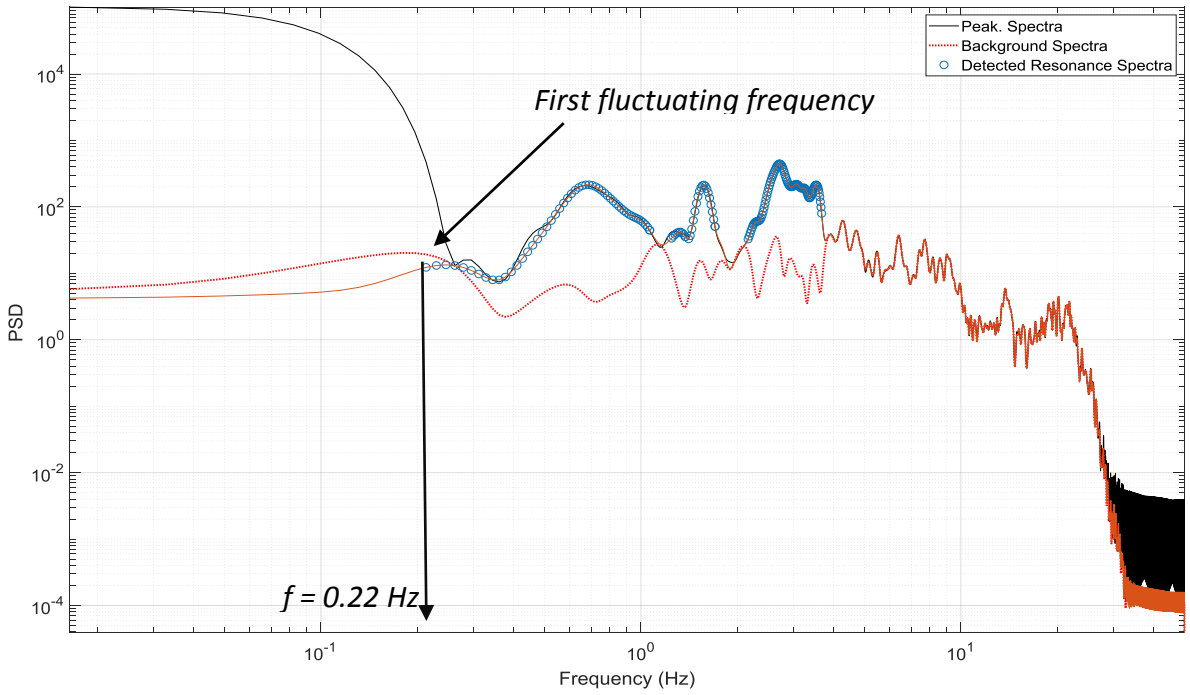

Figure 228: Decomposition of resonance for acceleration of signal A at 10% throttle at 0º (short-span full-scale model)

13.7. Recommendations

Based on the findings of this task the following can be recommended:

- Taking into consideration the results of the DAF obtained from the resonance decomposition of both models, all static forces used in the design of span-wire traffic signals can be multiplied by a factor of 1.3 to account for dynamic effects.
- More dynamic analysis is required to investigate the aeroelasticity of the system. The missing low frequency part of the turbulence spectrum needs to be accounted for in addition to obtaining the aerodynamic damping ζ_a and force and moment coefficients C_F and C_M among others.

13.8. Conclusions

This chapter summarizes the results of an aeroelastic test conducted at WOW for a span-wire traffic signal assembly consisting of a 5-section and two 3-section traffic signals. The model was designed based on previous full-scale experiments of the same model and was first verified using a Finite Element software SAP2000. Then, a SDOF loadcell was used along with three accelerometers.

Results have shown that the aeroelastic model started experiencing aerodynamic instabilities such as fluttering at wind speeds as low as 60 mph (full-scale) at cornering winds, mainly 45^o. In addition, acceleration and mean tension force results were compared with a short-span full-scale specimen. The aeroelastic model showed higher accelerations for the same wind speeds whereas a good agreement between the aeroelastic and the short-span full-scale models was observed in the mean tension exhibited in the messenger cable. Last but not least, a resonance decomposition was attempted on both models and a Dynamic Amplification Factor DAF was calculated. DAF results showed that the aeroelastic model exhibited higher numbers (30 to 35%) than the full-scale short-span one for both accelerations and tension forces.

Chapter 14 - Task 2: Development of Certification Test Parameters and Methodology

Test Date: 2/12/2018 – 2/16/2018

14.1. Introduction

A 'base' configuration consisting of a 21.9 ft long span wire test rig with two 3-section and one 5-section traffic signals was identified in previous tests during Task 1a of the current research project (BDV29 TWO 977-20) and also during a companion research project, (BDV29 TWO 977-27). In these tests an erratic behavior in the form of galloping and/or flutter were observed which resulted in different types of damages on different components of the span-wire assembly. It must be noted that the data collection procedures were compromised by the highly unstable behavior of the traffic signals and did not allow us to extract information that can be generalized and potentially utilized as part of the development of certification test parameters and a methodology. The parametric testing approach discussed in this chapter was performed up to wind speeds that did not initiate any aerodynamic instability and reliable data was recorded that could be generalized for the better design of the span-wire system. The forces that the system would undergo can be estimated by incorporating the force coefficients found during the tests into a theoretical/scientific approach that utilizes coefficients and a wind time history of a chosen extreme wind event.

This chapter presents qualitative observations and quantitative results from the tests conducted on the traffic signal assembly tested during Task 1a and during the companion research project (BDV29 TWO 977-27). Section 14.2 presents the experimental methodology, followed by the results and discussion in section 14.3. Section 14.4 discusses the methodology for a product certification method that could potentially be used for enhancing the resiliency of the span-wire assembly under wind induced forces. Finally, section 14.5 presents recommendations based on common failures observed during the previously conducted tests.

14.2. Experimental Methodology

14.2.1. Test Setup

A 3/8-inch diameter catenary cable was connected to an eyebolt on both ends of the test rig span. The eyebolt was welded to the top plate of the loadcell which was attached to the test rig column. The catenary cable was configured to represent 5% sag in the field, per FDOT Standard Specifications for Road and Bridge Construction, Section 634-3. Therefore, four times the sag ratio was required for the catenary wire used on the test rig to maintain the same lateral stiffness, which resulted in a sag length of 4 ft in the rig. The center of the circular loadcell at both ends of the messenger cable was located approximately 7 ft below the top catenary loadcells. The messenger cable was tensioned to approximately 80 Ibs per FDOT Standard Specifications for Road and Bridge Construction, Section 634-3, 3/8-inch diameter messenger wires are to be installed with wire tension of 340 Ibs/100 ft, linearly prorating cable tensions for other lengths. For this task, different tests with different components were tested to find the effect of wind induced forces on the different products provided by FDOT. The main focus of this task was to assess the overall response of the system with different hangers.

For parametric testing, the same reinforced test-rig as Task 1 was utilized, however, installation properties were modified to assess the behavior of the system with these modified parameters. The location of the loadcells for the parametric studies are shown in Figure 229. The assembly installed on the span-rig (which was modified one parameter at a time) is shown in Figure 230 to Figure 233. The first test performed had all parameters as per FDOT standards (i.e. sag ratio of 5%, messenger wire pretension of 80 lbs and clearance between messenger and catenary wire of 7 ft). The second test performed had all parameters as per FDOT standards but the sag ratio, which was modified to 7%. The third test performed had all parameters as per FDOT standards but the sag ratio, which was modified to 3%. The fourth test performed had all parameters as per FDOT standards but the messenger wire pre-tension, which was adjusted to 75% of the standard pre-tension. The fifth test performed had all parameters as per FDOT standards but the messenger wire pre-tension, which was adjusted to 125% of the standard messenger wire pre-tension. The sixth test performed consisted of keeping all parameters as per

FDOT standards but the clearance between catenary and messenger wire, which was set to 6.5 ft. The seventh case tested was configured to keep all parameters as per FDOT standards but the clearance between messenger and catenary wire, which was adjusted to be 6 ft. The last case was configured to keep all parameters as per FDOT standards but the messenger wire pre-tension, which was set to be un-tensioned. From this test, forces of drag and lift were calculated and from those, coefficients of drag and lift were calculated to be generalized to develop a method for product certification that could be potentially developed to certify that the different products used in span-wire traffic signals could survive the forces that the assembly would experience. The forces that the signal would undergo could be estimated by the use of a resultant coefficient (i.e. C_R). With these forces calculated during a wind time history of a chosen extreme wind event, a mechanical rig could be developed to test the assembly. It is important to notice that this approach would be valid when the signals do not experience an aerodynamic instability, as this instability produces an aerodynamic amplification that would make the assembly to no longer depend on the static aerodynamic coefficients used to develop the proposed product certification method.

The manufacturers of the components utilized for this round of tests (parametric study) are shown in Table 29. It must be noted that this assembly utilized a non-standard hanger (Pelco cable hanger) with the standard extension bar. This was due to the availability of the products sent by the provider and the available products stored at the WOW. The main focus of this round of tests was to assess the response of the assembly by changing the different parameters (sag ratio, messenger-wire pre-tension and distance between end-supports of catenary and messenger wires) of the assembly. All tests were run at wind speeds that would not induce any damage to any of the components of the assembly nor induce any type of aerodynamic instability. This was purposely done to compare the overall response of the different assemblies with all the components undamaged to avoid variances from case to case. In no case, the performance of the type of hanger was the main focus of this round of tests, for what the type of hanger used for this round of tests would serve the purpose of maintaining the connecting link between the catenary and messenger wire and the signal housing only.

Table 29: Signal assembly components (Task 2)

Component	Manufacturer
Span wire clamp	Pelco (cable hanger)
Adjustable hanger	Pelco (cable hanger)
Extension bar	Pelco (standard)
Messenger clamp	Pelco
Disconnect Hanger	Pelco (aluminum reinforced)
Signal Assembly	McCain (aluminum)
Backplates	Pelco (aluminum)
Visor	McCain (aluminum)
LED Modules	GE - Dialight - Duralight

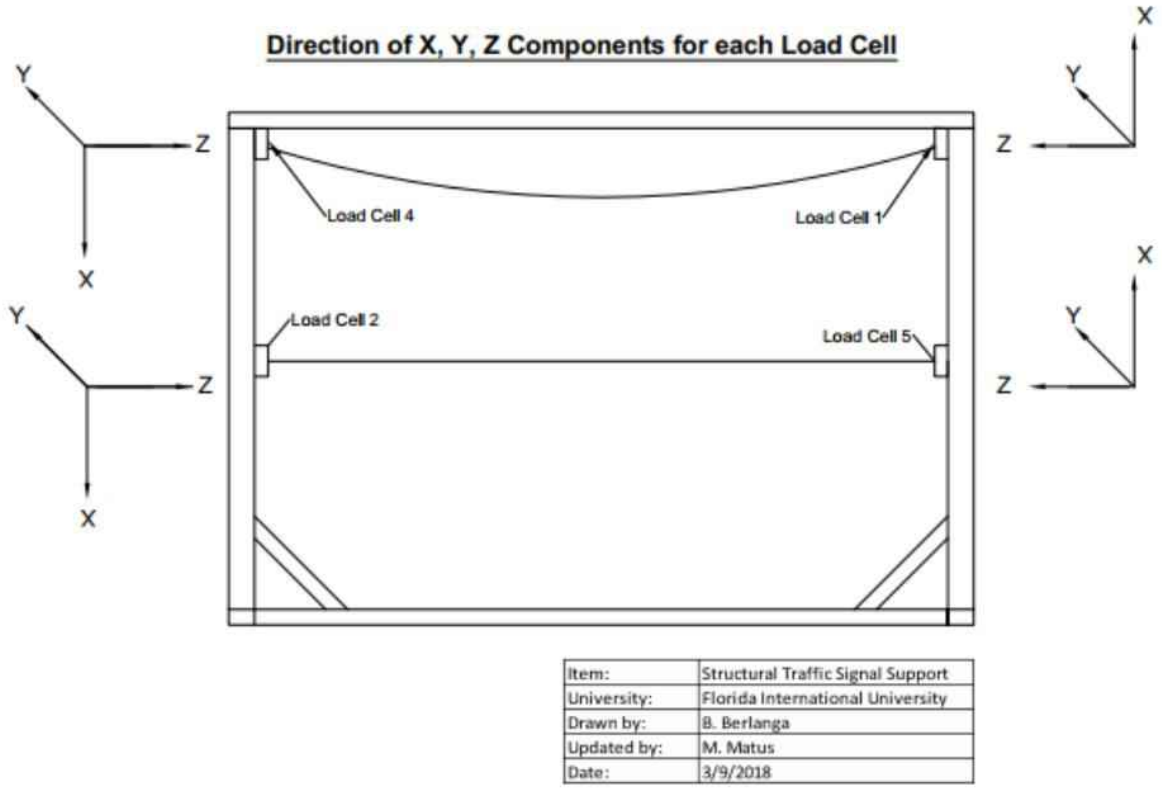

Figure 229: Direction of x, y, z components for each loadcell (direction of each axis shown represents 'positive direction')

Figure 230: Side vie of the test rig with the traffic lights

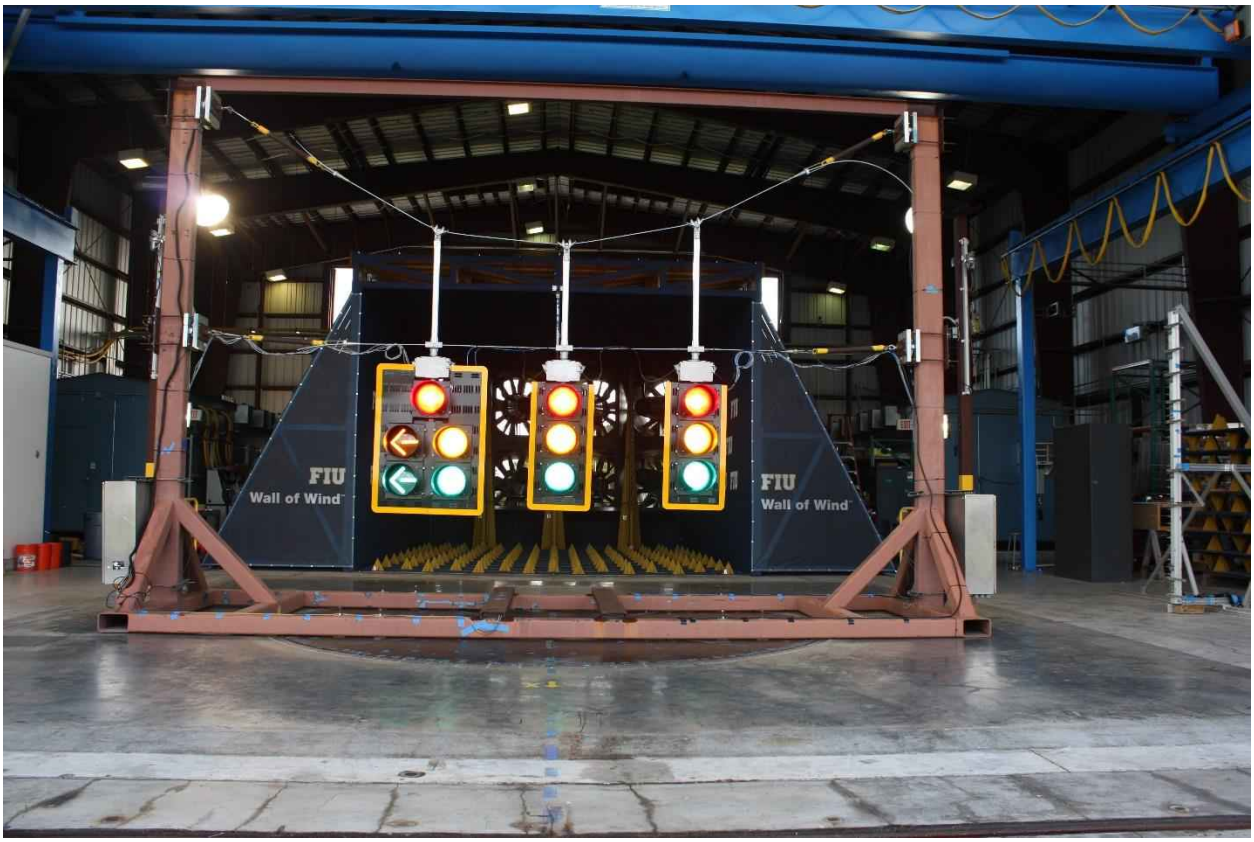

Figure 231: Signal assemblies installed on test rig (before testing)

Figure 232: Signal setup for test

Figure 233: Magnified view of the connection

14.3. Results and Discussion

The tests at the WOW were performed in the presence of the representatives from the Florida Department of Transportation (FDOT) Traffic Engineering and Operations Office, Traffic Engineering Research Lab (TERL), installation technicians from Horsepower Electric Inc. and members of the WOW technical team. The results in this chapter are restricted to 0-degree wind direction.

14.3.1. Wind induced forces

The directions of the forces are shown in Figure 229. The mean and peak forces obtained at various wind speeds are discussed in this section. For all cases, the drag forces (Fy) on the messenger wire were found to increase as wind speed was increased. At lower speeds, that is below 45 MPH, the drag forces of the messenger wire are similar and do not deviate noticeably from each other. However, when wind speed is higher than 45 MPH, the forces start to deviate from case to case. From all eight cases tested, the 3%-sag case resulted in somewhat higher values of drag forces (Fy), while the 7%-sag case was found to undergo the lowest drag forces (Fy) for both loadcells 2 and 5 – see Figure 234. The tension forces (Fz) of the messenger wire also increased as wind speed was increased. The un-tensioned messenger case was the worst case and the 7%-sag case was the case that resulted in lower messenger wire tension forces, see Figure 235. It should be noted that the different cases resulted in noticeable differences in mean tension forces even at lower wind speeds. The messenger wire lift forces (Fx) increased with increasing wind speed, as shown in Figure 236. As the convention of the weight and lift forces of the loadcells was positive downwards, an increase in the negative side of the curve indicates that the lift forces are increasing with increasing wind speeds. The lift force results indicate a relatively small absolute difference (about 10 lbs) between the various cases. Moreover, and in contrast to the previous results, the lift force values converge among the different cases at higher wind speeds.

The catenary wire drag forces (Fy) were found to be considerably lower than the messenger wire drag forces, Figure 237. As the wind speed was increased, some initial pre-tension was released, and the trends started becoming negative. Moreover, the signals create a pivot point

at the messenger wire and the catenary wire is pushed against the wind direction, thus going from positive to negative values. From all cases tested, it was found that the un-tensioned messenger case gave higher initial drag forces, which is justified, as the untensioned messenger wire does not produce a pivot at low wind speeds, producing the whole span wire system to be displaced along wind. It is noteworthy that for some cases, and at about 60 MPH, the drag forces increased at a higher rate. The tension forces of the catenary wire are shown in Figure 238. All cases follow a negative slope trend with the negative sign of the forces to indicate the loss of the initial tension exerted on the catenary wire due to the weight of the traffic signals. As wind speed increased, lift forces increased therefore the tension of the catenary wire decreased. The graphs show the rate at which the tension forces decreased as wind made the signals lift up. The 3%-sag case resulted in the worst absolute difference while the 7%-sag case showed the least tension. As expected, the wind speed increase resulted in an increase of the lift forces (Fx) of the catenary wire (Figure 239). It needs to be noted that the same sign convention of the messenger wire loadcells applies to the catenary loadcells, being upwards a positive convention, for the lift component. The findings indicate that there is not a considerable difference between the lift forces among the tested cases.

The maximum and minimum drag forces also increased with increasing wind speed, as seen in Figure 240. For the messenger wire forces, it was found that the worst maximum drag force was produced by the 3%-sag case, attaining a value of about 178 lbs at 75 MPH while the lowest maximum drag force was experienced by the 7%-sag case, attaining a value of approximately 150 lbs at 75 MPH.

The maximum and minimum tension forces of the messenger wire were also found to increase as wind speed was increased (Figure 241). The cases that were found to have experienced the highest tension forces of the messenger wire were the un-tensioned-messenger case, the 3%-sag and the 75%-messenger-tension case, attaining a value of about 520 lbs. This shows that for these three modifications, an increase in the maximum tensions experienced by the messenger wire should be expected. The lowest maximum tension was found during the 7%-sag case, which attained a value of about 450 lbs at 75 MPH, as seen in Figure 241. For the lift forces, it was found that as wind speed was increased, the lift forces started to increase making

the forces to go from a positive measurement (being the weight pointing downwards) to a negative measurement. This means that as wind speed was increased, signals started pulling the cables up, thus giving measures of negative values after weight was counteracted by the lift force. For the messenger wire, the critical minimum lift force was found to be about 49 lbs at 75 MPH in the un-tensioned messenger case, as shown in Figure 242.

As previously explained, the catenary wire drag forces are of very small magnitudes and they increase in the positive range until a pivot point is formed at the messenger-wire to hanger connection. After that, the rate of change is negative (the signals produced some type of lever that pushed the catenary wire against the wind direction, resulting in negative numbers). The maximum drag force for the catenary wire was found to be about 18 lbs while the lowest catenary wire drag force was produced in the 7%-sag case, as shown in Figure 243. Figure 244 shows the maximum and minimum rates at which the tension forces decreased, as previously explained. The lift forces showed an increase in magnitude as wind speed was increased and the maximum absolute value of lift force was found to be 90 lbs at 75 MPH with the 3%-sag case, as shown in Figure 245. The least critical maximum absolute lift force experienced by the catenary wire was during the 7%-sag case, attaining a value of 62 lbs at 75 MPH, as shown in Figure 245.

When comparing the mean forces to the maximum forces of the messenger tension forces (Figure 246), it can be seen that the maximum values are higher than the mean forces by about 50 lbs for all cases. At low speeds, the values are very similar and as wind speed was increased, the values between mean and maximum forces started to deviate.

14.3.2. Drag Coefficient

The drag coefficient is a non-dimensional quantity that is defined as the ratio of the drag force to the mean dynamic pressure times the reference area exposed to the wind field utilizing the following formula:

$$C_D = \frac{F_D}{\frac{1}{2}\rho V^2 A_{front}} \qquad \text{Equation 5}$$

In this equation, F_D is the total drag force, ρ is the air density, V is the mean wind speed at the traffic signal assembly, mean height and A is the total frontal area of the assembly. The total

frontal area is the sum of two 3-section signals and one 5-section signal plus coil springs, hangers, shackles and turn buckles. The summation of frontal area of the above listed items is 30.7 ft^2.

The resultant drag force for each case was calculated by adding all the contributions of the along wind forces of all loadcells, that is 2 loadcells measuring forces of the messenger wire and 2 loadcells measuring forces of the catenary wire. The drag force produced by the cables was neglected as the drag force generated by them is assumed to be relatively small [6].

As mentioned above, the velocities used to calculate the drag coefficients were the estimated velocities at the mean height of the traffic signal assembly. A reference wind speed was measured at 10.5 ft above the test floor near the exit of the flow management system of the WOW. The height from the surface of the turn table to the center of the traffic signals was calculated to be about 64 in. The mean height mean wind speed was then found applying the power law.

The drag coefficient of the traffic signal assembly had small changes for wind speeds between 30 and 45 MPH, as seen in Figure 247. At wind speeds greater than 45 MPH, the drag coefficient underwent a decrease, as wind speed was increased since the assembly becomes more aerodynamic as the signals incline due to the wind. After 45 MPH, the case resulting in higher drag coefficients was the 3%-sag case while the assembly that resulted in the lowest drag coefficients was the case with 7% sag.

14.3.3. Lift Coefficient

The lift coefficient expresses the ratio of the lift force to the force produced by the mean dynamic pressure over the effective area. To calculate the lift coefficient at different wind speeds and wind angles of attacks, the summation of all lift forces was found and then divided by the dynamic pressure multiplied by the frontal area of the traffic signals. The formula to calculate lift coefficient is as follows:

$$C_L = \frac{F_L}{\frac{1}{2}\rho V^2 A_{front}} \qquad \text{Equation 6}$$

where F_L is the lift force, ρ is the air density, V is the mean wind speed at the mean height of the traffic signals and A is the frontal view area of two 3-section signals, one 5-section signal, turn buckles and springs. The frontal view area was found to be 30.7 ft^2.

The resultant lift force for each case was found by adding all the contributions of x component of all loadcells measuring lift forces of messenger and catenary wires. The velocities used to calculate lift coefficients are the calculated velocities at the mean height of the traffic signal assembly. The mean wind speed at mean signal height was estimated utilizing the same approach as that described in the drag coefficient section.

The lift coefficient values of the traffic signal assembly were found to linearly increase up to 60 MPH after which they kept increasing at a much lower rate – see Figure 248. From all cases tested, it was found that for speeds less than 60 MPH, the case with 7% sag resulted in the highest lift coefficient value. After 60 MPH, the case with 7% sag lift coefficient showed a negative slope. At 75 MPH, the worst case was found to be the 3%-sag case with a value of 0.58 and the case that resulted in the lower lift coefficient t 75 MPH was the case with a 7% sag.

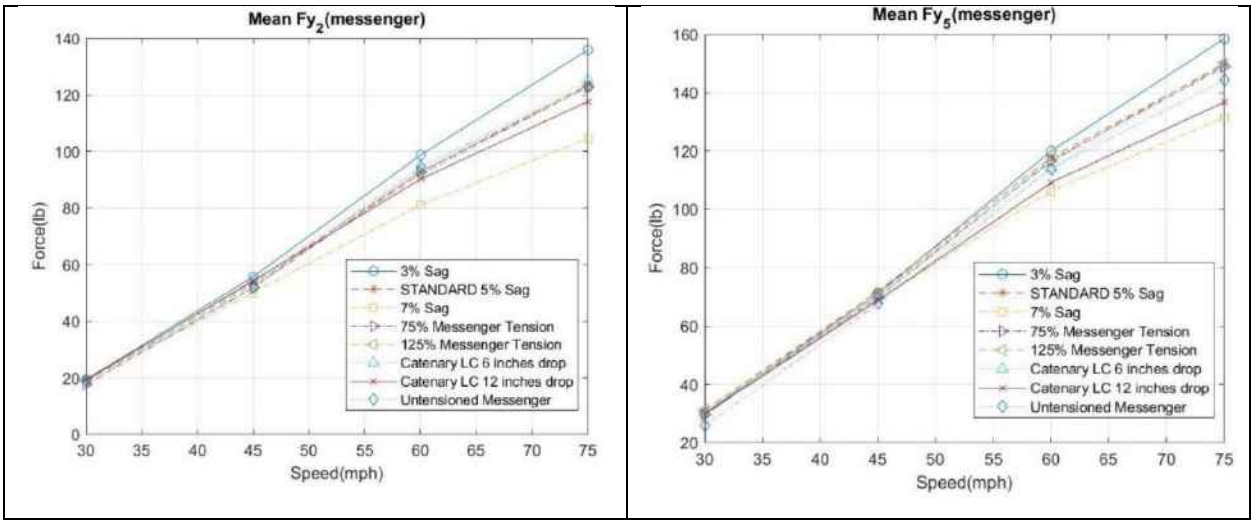

Figure 234: Mean messenger wire drag forces

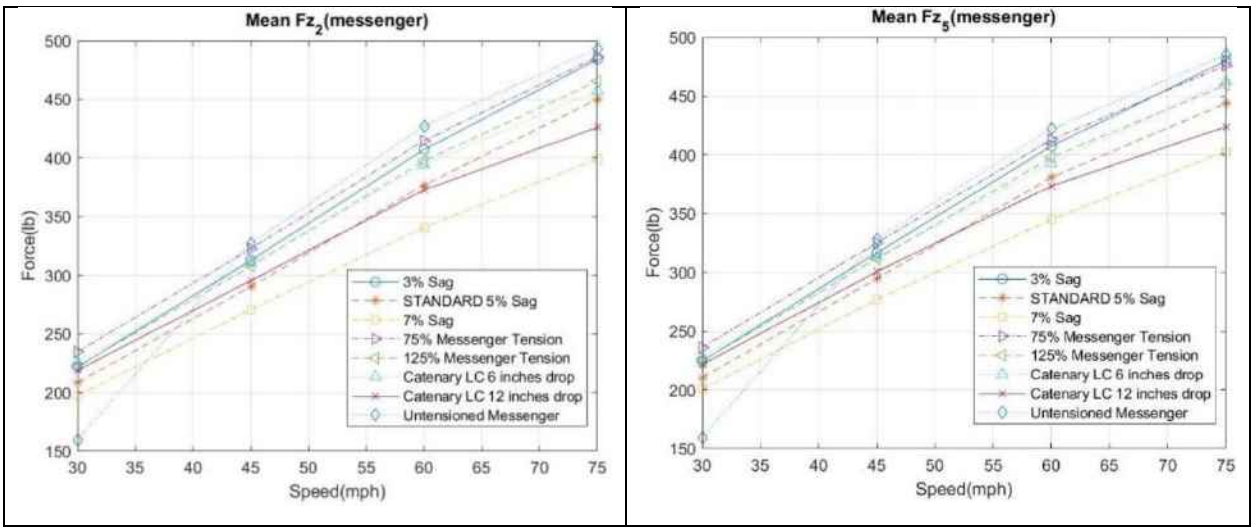

Figure 235: Mean messenger wire tension forces

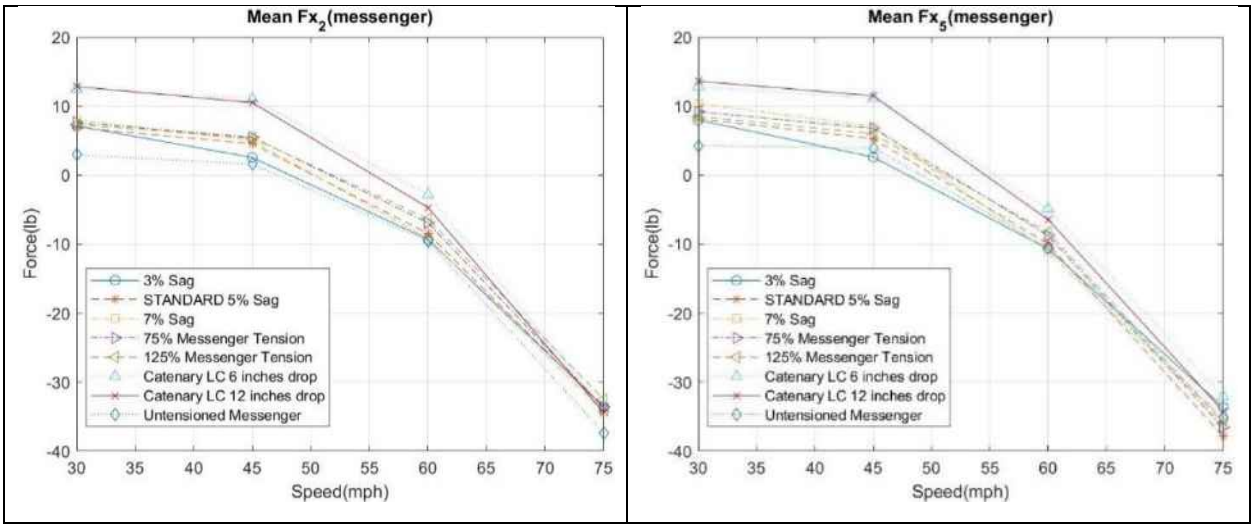

Figure 236: Mean messenger wire lift forces

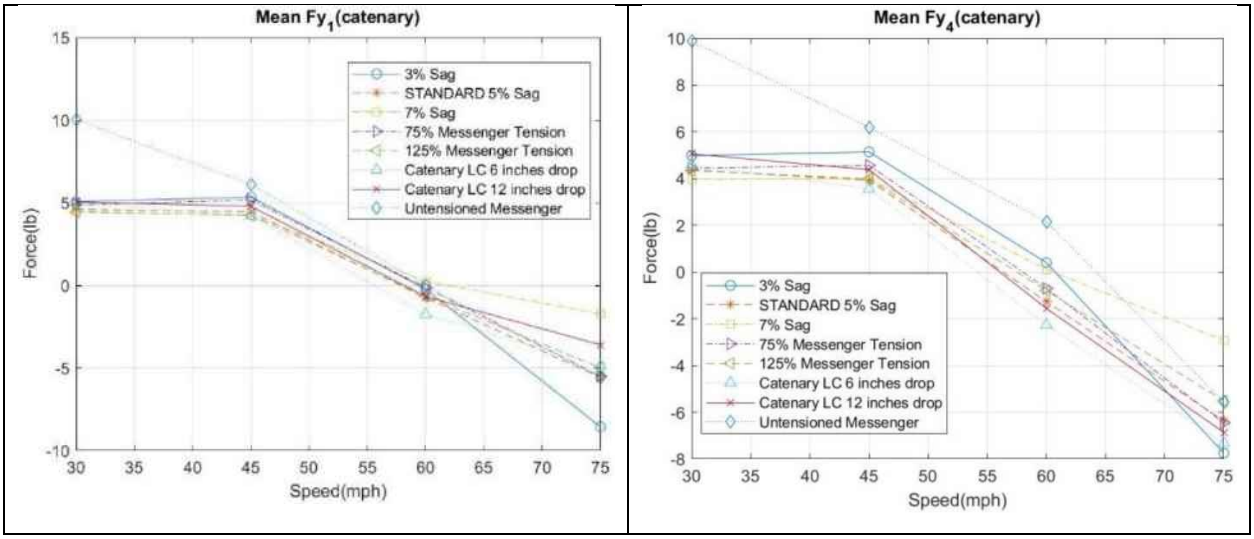

Figure 237: Mean catenary wire drag forces

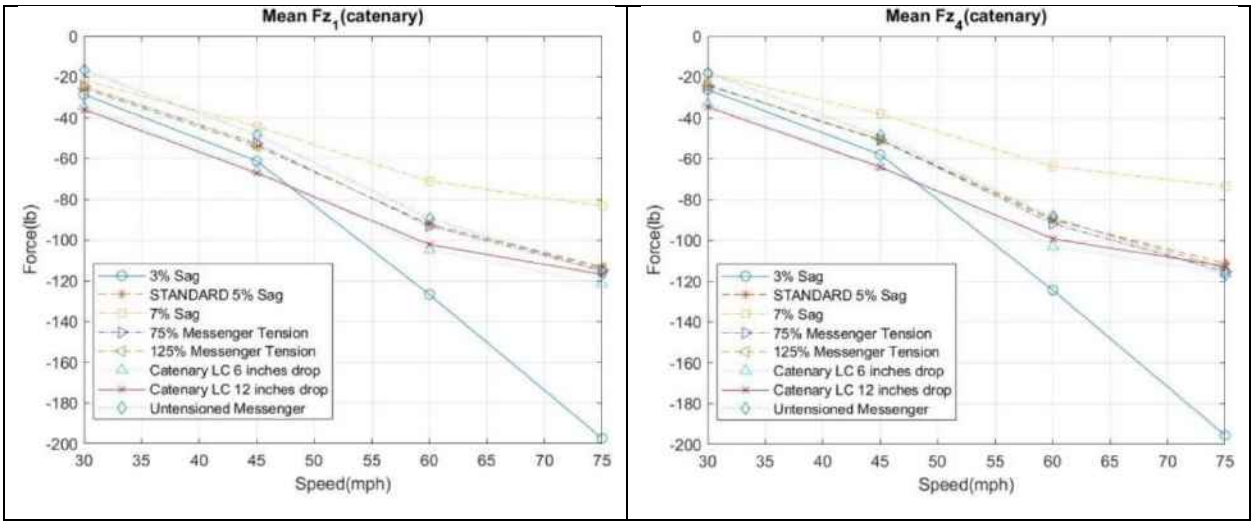

Figure 238: Mean catenary wire tension forces

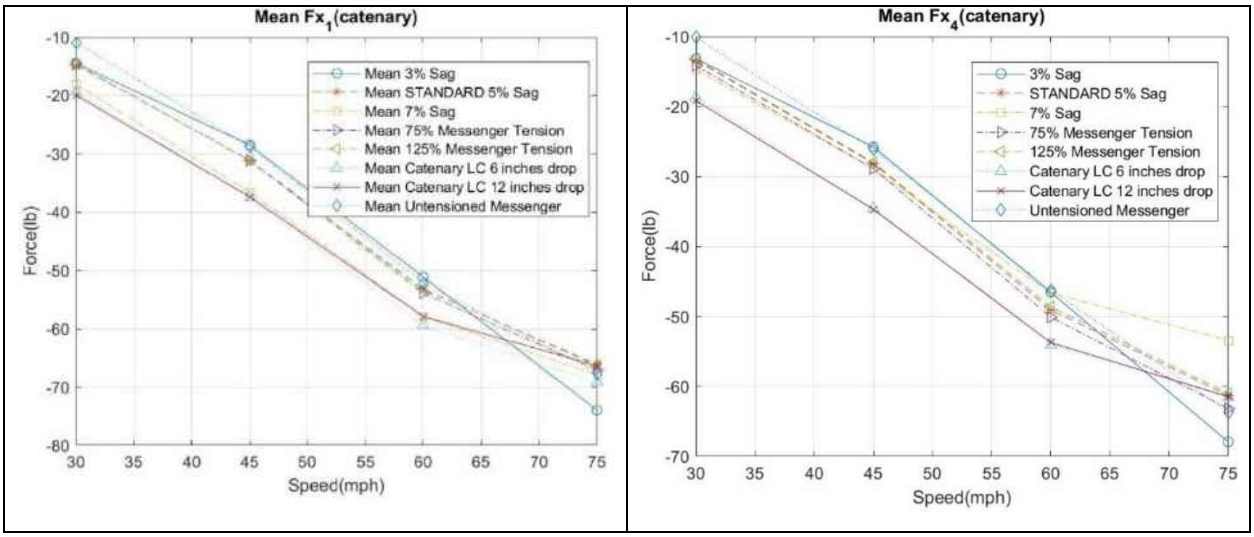

Figure 239: Mean catenary wire lift forces

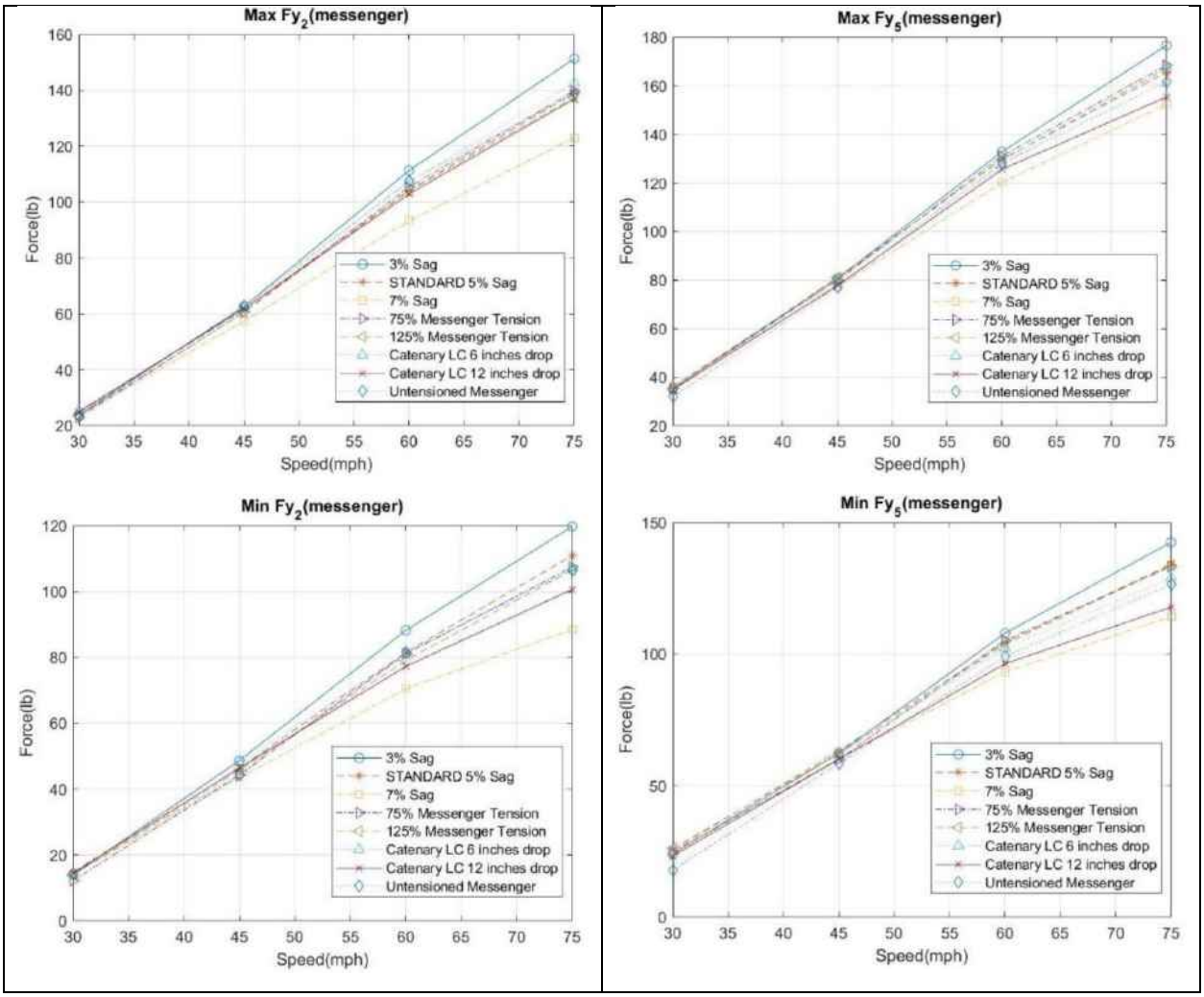

Figure 240: Maximum and minimum messenger wire drag forces

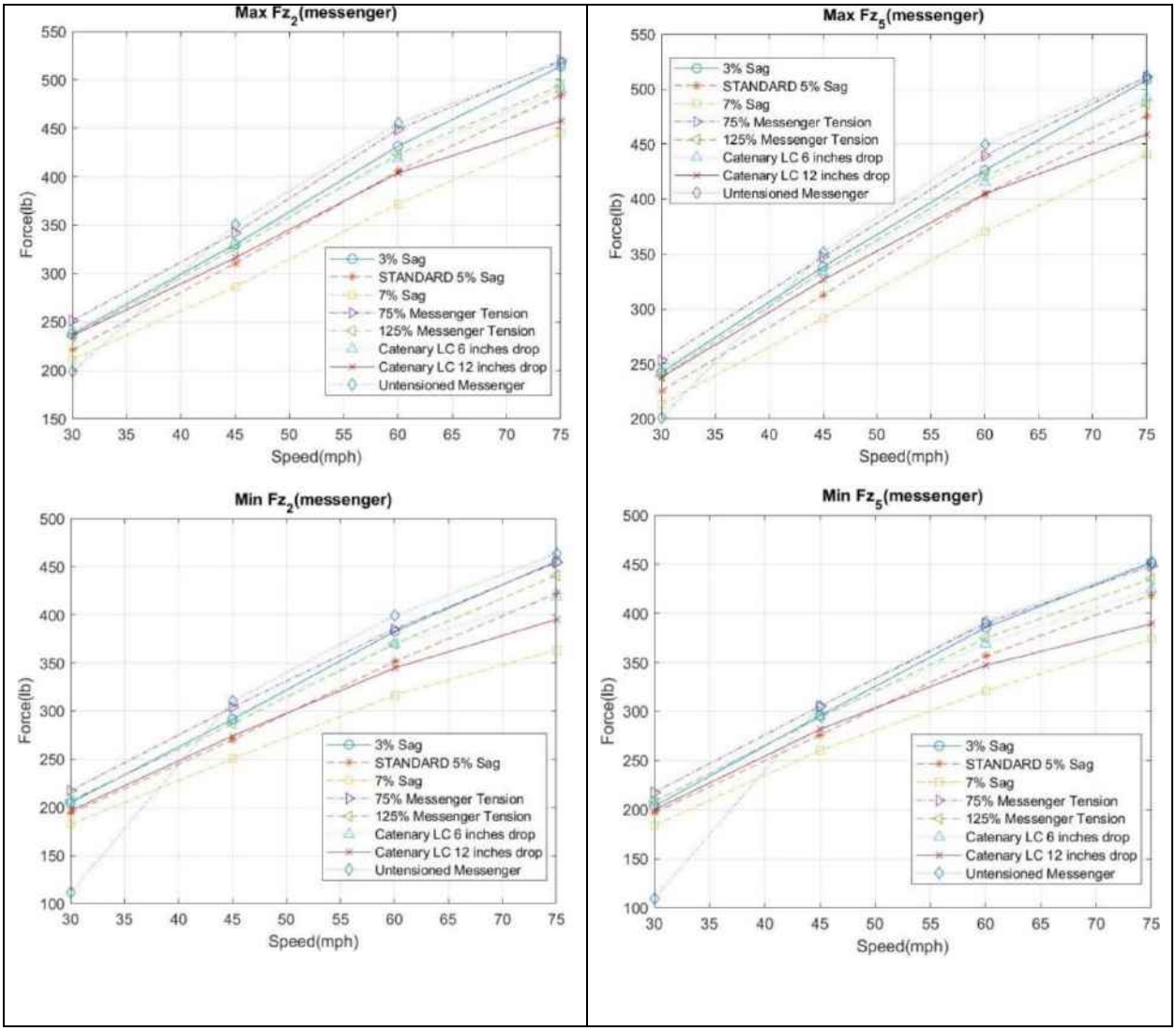

Figure 241: Maximum and minimum messenger wire tension forces

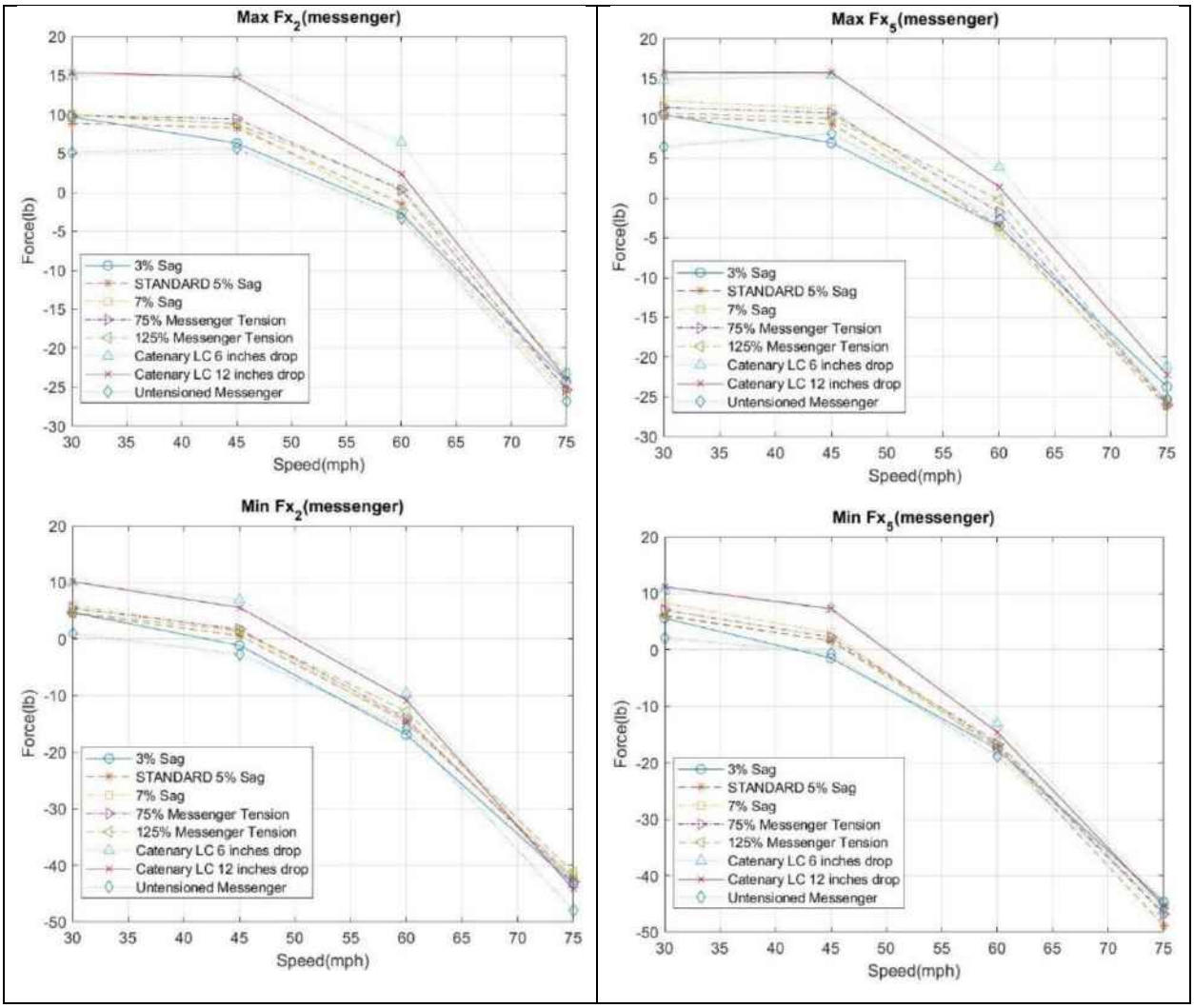

Figure 242: Maximum and minimum messenger lift forces

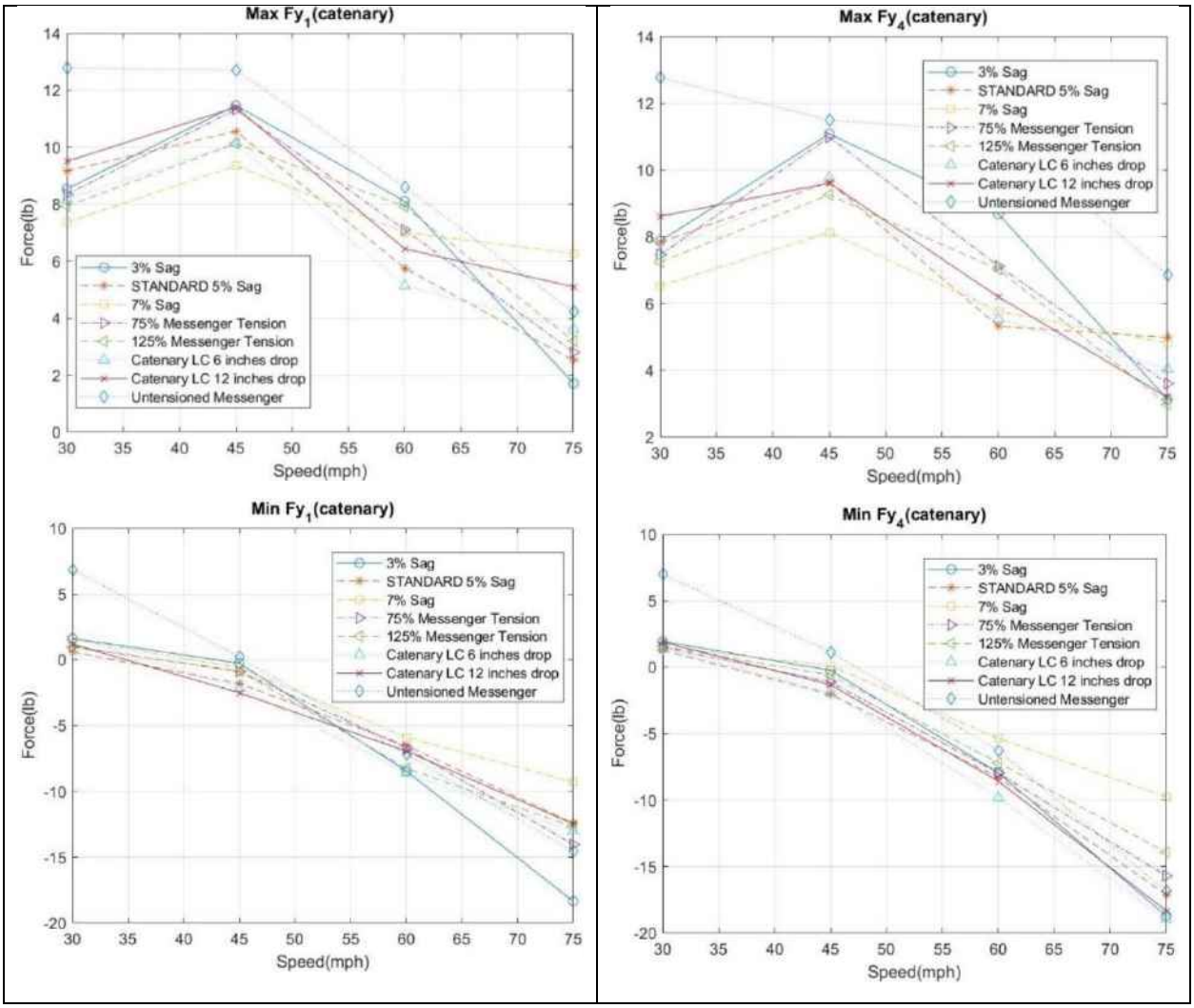

Figure 243: Maximum and minimum catenary drag forces

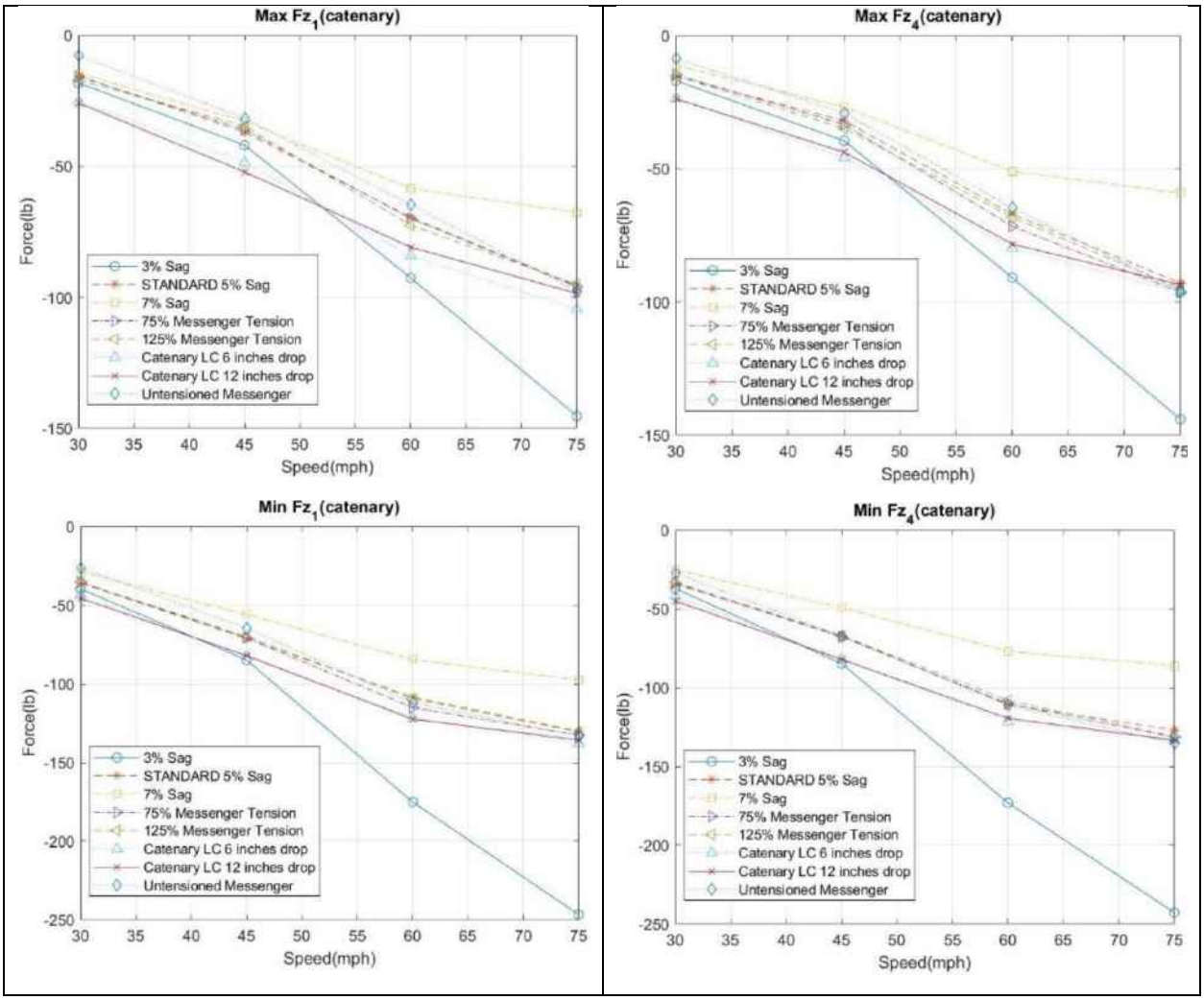

Figure 244: Maximum and minimum catenary tension forces

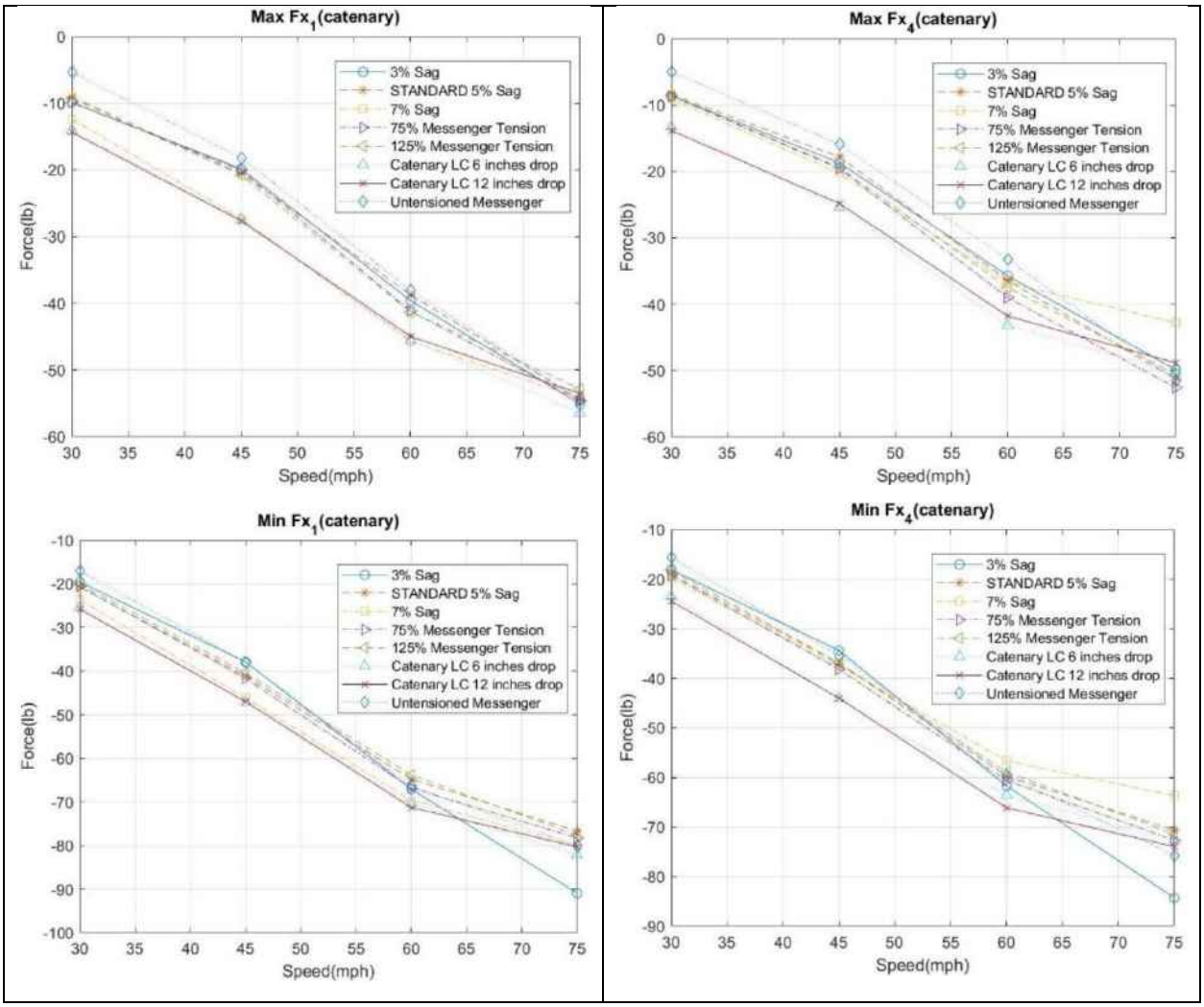

Figure 245: Maximum and minimum catenary lift forces

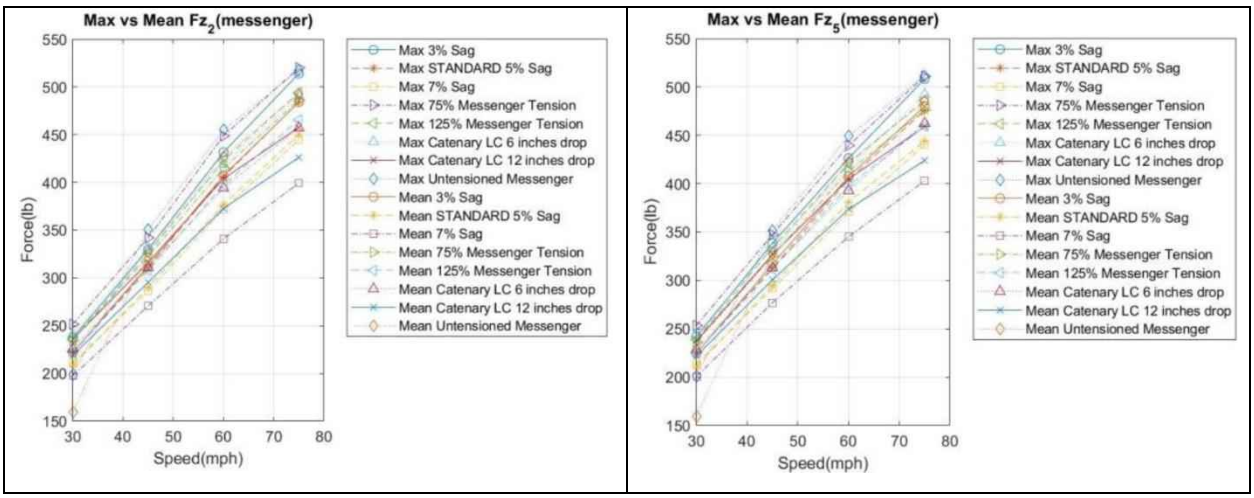

Figure 246: Maximum vs mean messenger wire tension forces

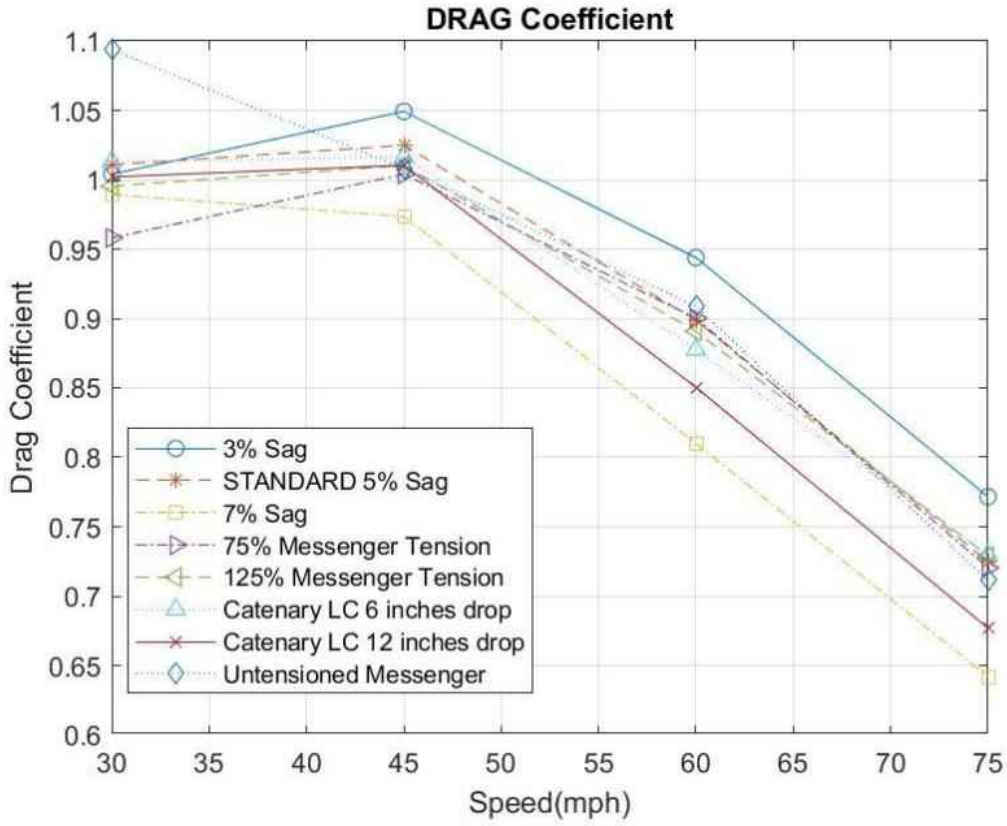

Figure 247: Drag coefficients vs wind speed

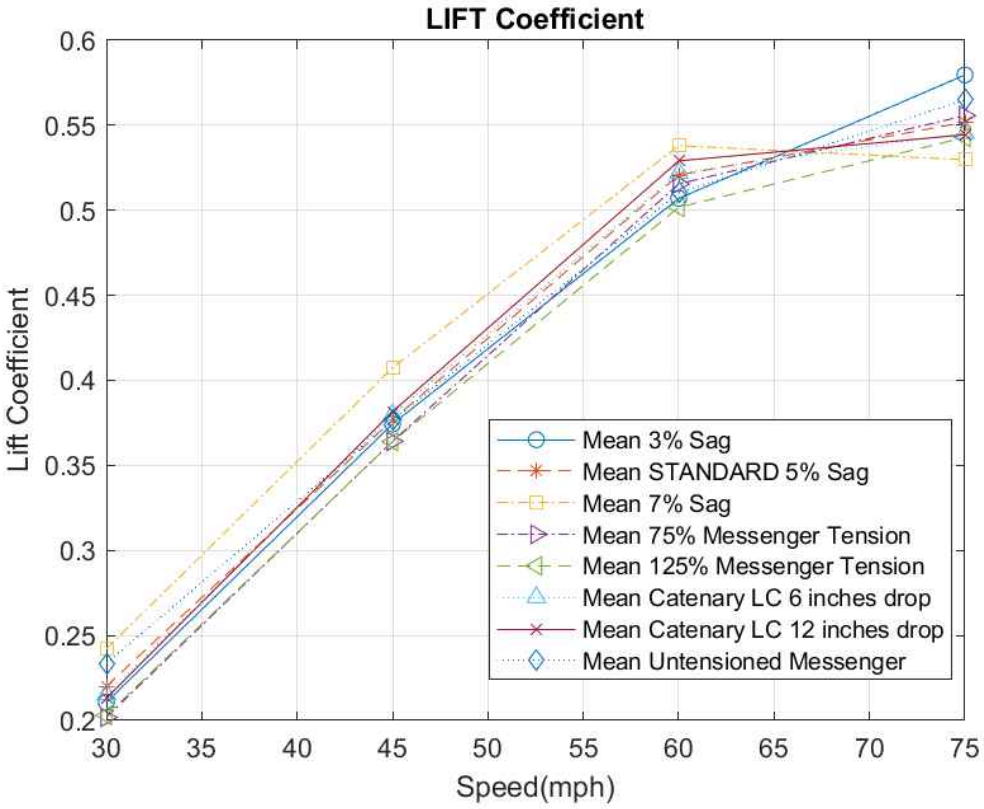

Figure 248: Lift coefficients vs wind speed

14.4. Methodology for Product Certification

Enhancing the survivability of the traffic signal assembly subjected to wind loads is crucial to avoid dangerous situations for the motorists during and after an extreme wind event. With the findings of previous and current tests, suggestions and a methodology for a better design of the different span-wire traffic signals can be achieved. During the many cases tested during task 1a and companion research project (BDV29 TWO 977-27), common failures where seen. During task 1, different assemblies were tested at wind speeds ranging from 30 to 150 mph. It was observed that, depending on the type of hanger, instabilities in the form of galloping developed at wind speeds as low as about 70 mph (~70 mph for flexible hangers and ~110 mph for rigid hangers), or when along wind inclinations of the traffic signals reached ~60 degrees or more. It must be noted that for the rigid hangers, the aerodynamic instability was triggered when the extension bar became severely bent making the signal to reach high angles of inclination. This aerodynamic instability lead to large amplitude oscillations making the forces put on the signals, hangers and support systems, to alleviate and no longer depend on the static aerodynamic coefficients. The qualitative failures observed during task 1 are as follow:

1. Excessive bending of the rigid extension bar which lead to initiation of aerodynamic instabilities. Typically, the extension bars became excessively bent at wind speeds of about 110 mph.
2. Failure of the adjustable hanger connection at the disconnect-box to adjustable-hanger point. It was seen that the brittleness of some components of the assembly is very important to prolong the survivability of the assembly. At this particular point, there is a concentration of stresses that makes this point susceptible to damages. It must be noted that the tri-stud failures were not seen when aluminum alloy 535 were used.
3. Shearing of the 72-tooth serrated edge at the disconnect-box to adjustable-hanger point and the disconnect-box to signal-housing point. This failure was primarily observed with the 5-section signal, making the 5-section signal more susceptible to damages under wind induced loads.

It needs to be noted that the same trends for the lift and drag forces were found during task 1a and companion research project (BDV29 TWO 977-27), where all the force measurements

were found to increase with increasing wind speed. During the parametric study and taking into consideration the above comment about aerodynamic instabilities, drag and lift coefficients were calculated. The parametric study was performed up to a wind speed which did not induce any aerodynamic instability to ensure reliability of data that could be generalized to explore a scientific approach and potentially develop a mechanical test rig for product certification. These coefficients are important as they can be used to theoretically estimate the forces that the assembly may experience at certain wind speeds or during a certain hurricane wind record. The forces that the assembly may undergo can be programmed to replicate wind forces of a chosen representative storm, keeping into consideration that this estimation would be reasonable up to the criteria above mentioned to avoid aerodynamic amplification due to instabilities, that is a wind speed of about 70 mph or an along wind inclination of the traffic signals of about 60 degrees. With this, the force in the cable would be estimated based on the static aerodynamic force coefficients (drag, lift and resultant coefficients), where the resultant coefficient C_R can be calculated with the following formula:

$$C_R = \sqrt{C_D^2 + C_L^2} \qquad \text{Equation 7}$$

With this coefficient and by keeping the right controlled parameters, the forces that the signals would experience during a storm could be estimated by utilizing the following formula:

$$F_R(t) = \frac{1}{2}\rho U^2(t) A C_R \qquad \text{Equation 8}$$

The development of a test time history of $F_R(t)$ has to have a representative time history of U(t). A time history of wind speed can be generated theoretically with some input parameters that are found in real extreme wind events. These parameters are mean wind speed (U), turbulence intensity (I_u) and turbulence integral scale (L_u). With all the information gathered from previous tests and theoretical approaches, a possible mechanical test rig could be developed to certify that the span-wire traffic assembly can survive the forces ($F_R(t)$) that would be produced by a chosen meteorological event of desire. It must be noted that the forces being produced

would be those experienced by the system when no aerodynamic instabilities develop, and it is important to emphasize that it would be very difficult to reproduce an aerodynamic instability with a mechanical rig as the origin of the forces is an aeroelastic interaction. Since the parametric study was a test performed to certain wind speeds to avoid aerodynamic instabilities, reliable data was found for resultant coefficient (CR) at different wind speeds (see Figure 249:).

The parametric study generated resultant force coefficients for several configurations. The results can be used either to select the optimal set up that will experience reduced forces or simply envelope the findings from all cases to generate critical resultant force coefficients at various wind speeds.

As the forces that the span-wire traffic signal assembly would undergo are directly proportional to the resultant coefficient, an assembly with a lower resultant coefficient would produce the assembly to experience lower forces, thus alleviating stresses from the different components that make up the span-wire traffic assembly. Figure 249: gives a good estimation of the different resultant coefficients of an assembly with modified parameters.

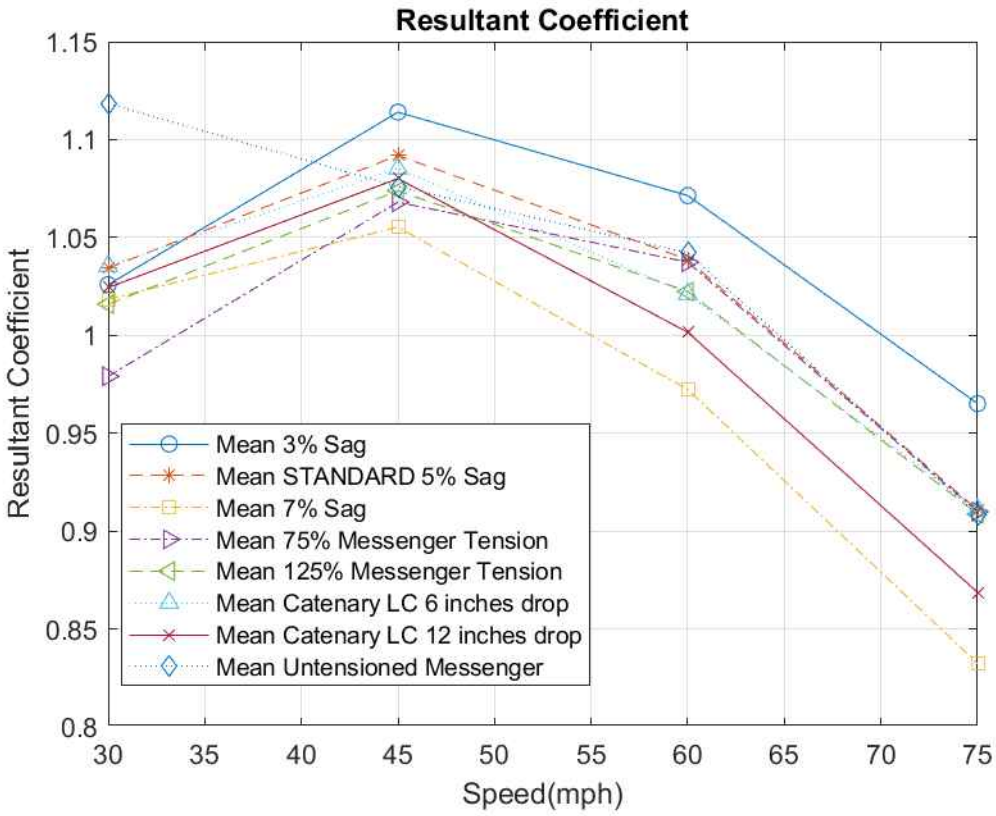

Figure 249: Resultant coefficient

14.5. Conclusions and Recommendations

Following the tests performed in project BDV29 TWO 977-20 and the companion project BDV29 TWO 977-27 the Wall of Wind and FDOT teams reviewed carefully the performances of the different assemblies tested and the following recommendations are provided:

1. It has been observed that depending on the rigidity of the hanger, the traffic signal assembly is more susceptible to aerodynamic instabilities in the form of galloping. Flexible hangers tend to undergo higher along-wind inclinations at lower wind speeds which would trigger this instability at lower wind speeds (about 70 mph) than a rigid hanger, while for the rigid hanger the instability appears when the extension bars severely bend (about 110 mph).
2. The 5-section signal has been found to be susceptible to damages regardless of the type of hanger used. This may be due to its increased weight as well as the increased surface area compared to the 3-section signal. It is recommended to find an alternative section to replace usage of 5-section signal.
3. A common failure observed was the serration of the 72-tooth edge connection between the adjustable-hanger and the disconnect-box and also between the disconnect-box to signal-housing point. A resilient connection at these points should be considered to enhance the survivability of the signal under wind induced loads. In discussions with FDOT, it was proposed to explore the possibility of using a device that could potentially remove the rotational degree of freedom of the adjustable-hanger to disconnect-box connection. Such component is currently available (i.e. octagon base) but for different types of traffic sign installations (see Figure 250 to Figure 252). This component would be connected to the back of the disconnect-box to restrain the stresses put on the 72-tooth connection. With regards to this issue, the following modifications can be made:
    - Top of signal:
        - Short-term: Add plate with tri-stud holes to inside top of signal to keep signal from turning.
        - Long-term: Change top of signal to accept the octagon tri-stud base.
    - Top of disconnect box:

- Short-term: Add plate to inside top of disconnect box with tri-stud holes to keep signal from turning.
- Long-term: Change top of disconnect box to accept the octagon tri-stud base.

1. The parameters (sag ratio, messenger wire pre-tension and distance between end supports of catenary and messenger wire) of the signal assembly affect the overall response of the span-wire system. Results from the parametric study showed that a sag ratio of 7% (of catenary wire) results in a better response at wind speeds up to 75 mph. It is recommended to test this configuration at higher wind speeds to verify the same behavior is observed at higher wind speeds when aerodynamic instabilities develop.
2. Use maximum overlap at tri-stud adjustable-hanger and extension-bar connection points (top and bottom portions/connections). At this connection points, use a minimum of 2 bolts per connection. The bolts should be spaced apart with one bolt-hole in between.
3. Use aluminum alloy 535 only (all adjustable hangers broken during the tests were not made of 535 aluminum alloy).
4. Consider installing safety wire between catenary and messenger wire to help holds the system up if hangers or extension bars break.
5. Consider a device that would limit the signal from tilting back more than the limit (~60-degrees) at which point aerodynamic instabilities develop. This solution might be carefully assessed before implementation due to the increased force coefficients at higher wind speeds.
6. After carefully reviewing the work done previously at University of Florida and the findings from the Wall of Wind testing, the certification general procedure that might be considered and implemented by FDOT should include:
    - Static flexural/tension testing of components (740 and 7400 per UF).
    - Dynamic test based on results given by WOW.
    - Twist/drop/sock/vibration test of the whole system (based on WOW data).

Figure 250: Octagon end and standard tri-stud adjustable hanger

Figure 251: Octagon end and insertion of standard tri-stud adjustable hanger

Figure 252: Connected octagon end with standard tri-stud adjustable hanger

Chapter 15 - Task 3: Exploration of Aerodynamic and Mechanical Mitigation Measures

Test Date: 06/18/2018 - 06/22/2018

15.1. Introduction

Previous experimental efforts (Tasks 1a and 2 of the current research project) examined the behavior of traffic signal assemblies using different hanger components. In the current task the research team at FIU identified three mitigation devices that could potentially enhance the overall response and survivability of the traffic signal assembly. A single 3-section signal was used as baseline case and three different mitigation devices were attached to the back or bottom of the signal housing, including a liquid damper, a fin and a metal box with an iron-ball inside it. From these mitigation devices, the following cases were identified and tested (the naming of the cases was created for simplicity):

1. "No-mitigation case" - signal without any mitigation device as a base for comparison purposes.
2. "Liquid-damper-with-2L case" - signal with liquid damper filled with two liters (2L) of water installed at the back of the signal housing.
3. "Liquid-damper-with-0L-case" – signal with liquid damper filled with zero liters (0L) of water installed at the back of the signal housing.
4. "Fin-at-top case" – signal with a flat plate (fin) installed at the top of the back of the signal housing.
5. "Fin-at-middle case" – signal with a flat plate (fin) installed at the middle of the back of the signal housing.
6. "Metal-box case" – signal with a hollow metal-box and iron-ball inside installed at the bottom of the signal housing.

All of the above configurations used a "Tri-stud Adjustable-hanger Assembly with Aluminum Housing." Notice that some configurations used different manufactures for some of the components. The tests were carried out at wind direction of 0 degree and wind speeds ranging

from 40 to 150 mph. The instruments consisted of loadcells to measure forces, accelerometers to measure accelerations, and inclinometers to measure the inclinations of the traffic signals.

This chapter presents the results from the tests conducted on the traffic signal assembly for all different cases.

15.2. Experimental Methodology

15.2.1. Test Setup

The 3-section signal was installed in the reinforced short-span rig (described in Chapter 1) by means of base configuration. The center of the circular loadcell at both ends of the messenger cable was located approximately 7 ft below the top catenary loadcells. The messenger cable was tensioned to approximately 80 Ibs per FDOT Standard Specifications for Road and Bridge Construction, Section 634-3, 3/8-inch diameter messenger wires are to be installed with wire tension of 340 Ibs/100 ft, linearly prorating cable tensions for other lengths.

The length between the catenary and messenger cables at the lowest point of the catenary cable where the hanger assemblies were installed was approximately 3 ft. Figure 253 to Figure 255 show the traffic signal assembly as well as the “Tri-stud Adjustable-hanger Assembly with Aluminum Housing and Backplates” assembly. The list of manufacturers for each component used in the different test cases is presented in Table 30. Figure 256 to Figure 265 show the assemblies of the different cases before testing (see cases 1-6 in section 1). The bottom of the signal was at approximately 4.5 ft above the concrete floor. The signal was made of aluminum and included louvered backplates and visors. The test protocol is presented in Table 31. The tests were conducted for wind speeds being varied from 40 to 150 mph, for wind direction of 0 degrees

15.2.2. Instrumentation

The directions of the x, y and z components for each loadcell are shown Figure 266. Loadcells number 4 and 2 were located at either end of the messenger cable and loadcells number 1 and 4 located at either end of the catenary cable.

Tri-axial accelerometers were installed in the traffic signal to measure accelerations. Accelerometer Accel007, was installed on the top center, accelerometer Accel004, was installed

on the bottom left side and accelerometer Accel006, was installed on the bottom right side of the 3-section signal as shown in Figure 267.

Inclinometer, Inc6, was installed on the top center and inclinometer, Inc5, was installed on the bottom center of the of the 3-section signal as shown Figure 267.

15.2.3. Test Method

The test set up was first tested for 'no wind' conditions and baselines for the various instruments were acquired (also known as "zero drift removal" process) before each test. The signal assembly was tested at wind speeds ranging from 40 mph to 150 mph at wind angles of attack of 0 degree, as shown in Table 31**.**

Table 30 shows the manufacturers of each component utilized for each assembly. It must be noted that during the tests, it was observed that the Pelco tri-stud adjustable-hanger underwent failure at the bottom tri-stud adjustable-hanger to extension bar connection. When this was observed, FDOT representatives requested to test with a different tri-stud adjustable-hanger manufacturer, which was Costcast. This adjustable-hanger showed a better performance as it behaved not as brittle as the Pelco adjustable-hanger. Instead of failing, this particular adjustable-hanger allowed for bending of the bottom part of the tri-stud adjustable-hanger to extension bar point instead of breaking.

Table 30: Manufacturer of components for each case (Task 3)

	Case			
Component	No Mitigation	Liquid Damper	Fin	Metal-box with iron-ball
Span wire clamp	Pelco	Pelco	Pelco/Costcast	Costcast
Adjustable-hanger	Pelco	Pelco	Pelco/Costcast	Costcast
Extension bar	Pelco (standard)	Pelco (standard)	Pelco (standard)	Pelco (standard)
Messenger clamp	Pelco	Pelco	Pelco/Costcast	Costcast
Disconnect Hanger	Pelco (aluminum reinforced)	Pelco (aluminum reinforced)	Pelco (standard)	Pelco (standard)
Signal Assembly	McCain	McCain	McCain	McCain
Backplate	Pelco	Pelco	Pelco	Pelco
Visor	McCain	McCain	McCain	McCain
LED Modules	GE - Dialight - Duralight	GE - Dialight - Duralight	GE - Dialight - Duralight	GE - Dialight - Duralight

Table 31: Test protocol (Task 2)

Wind Speed (mph)	Wind Direction (degrees)	Total Duration (min)
40	0	1
70	0	1
100	0	1
130	0	1
150	0	1
	TOTAL	5

Figure 253: Test rig

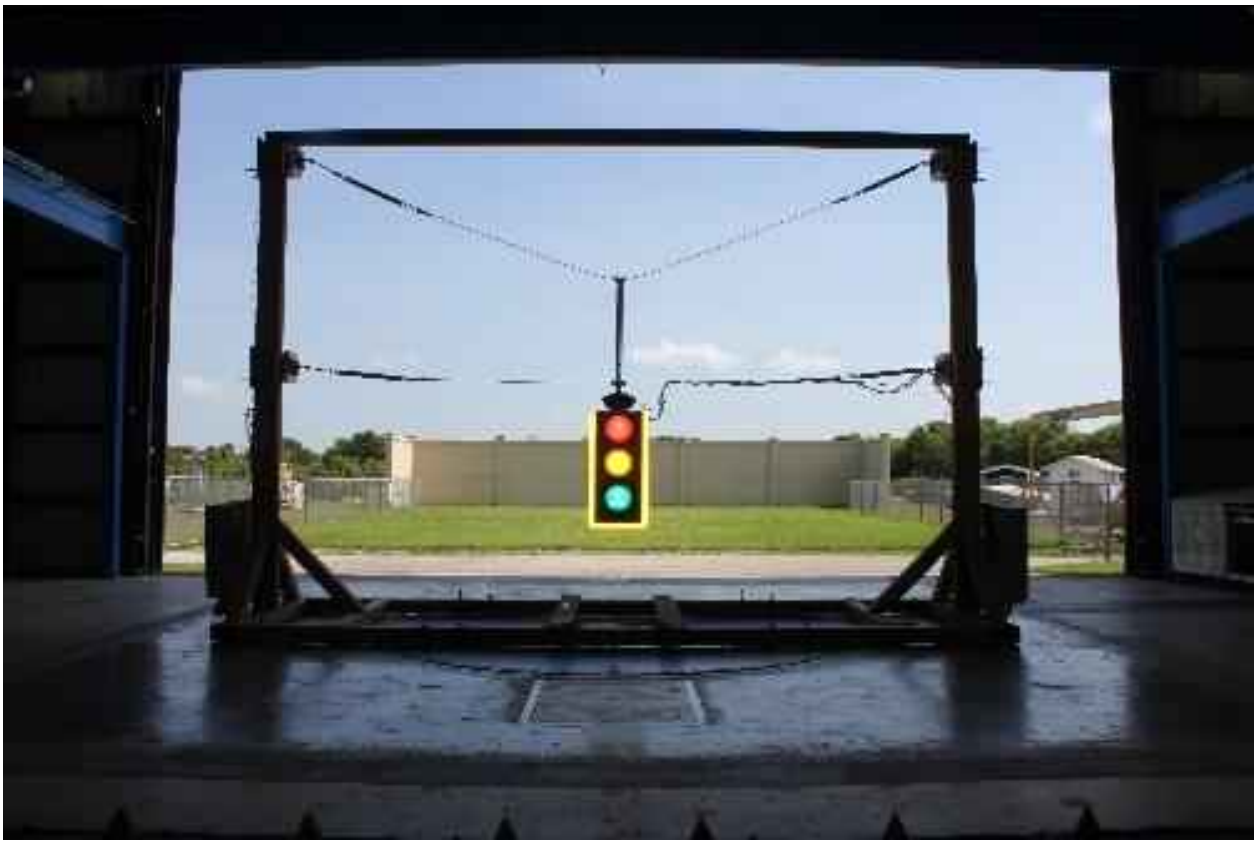

Figure 254: Signal setup for test

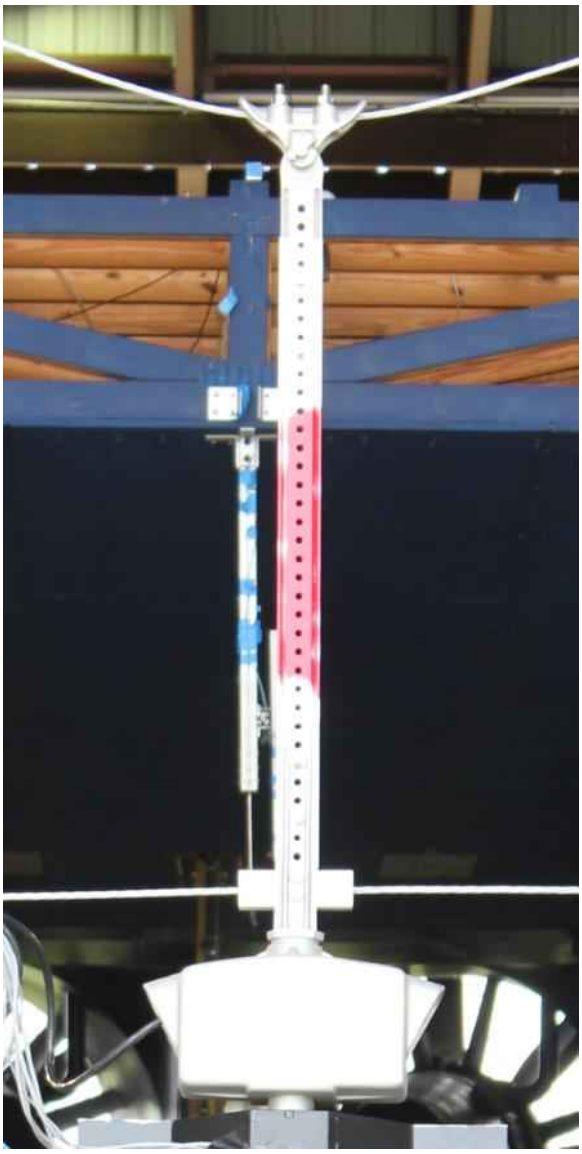

Figure 255: Magnified view of the connection

Figure 256: Signal assembly installed on test rig (before testing) with no mitigation device

Figure 257: Signal assembly installed on test rig (before testing) with liquid damper (with two liters of water)

Figure 258: Close up of liquid damper with 2 L installed in rear of signal housing

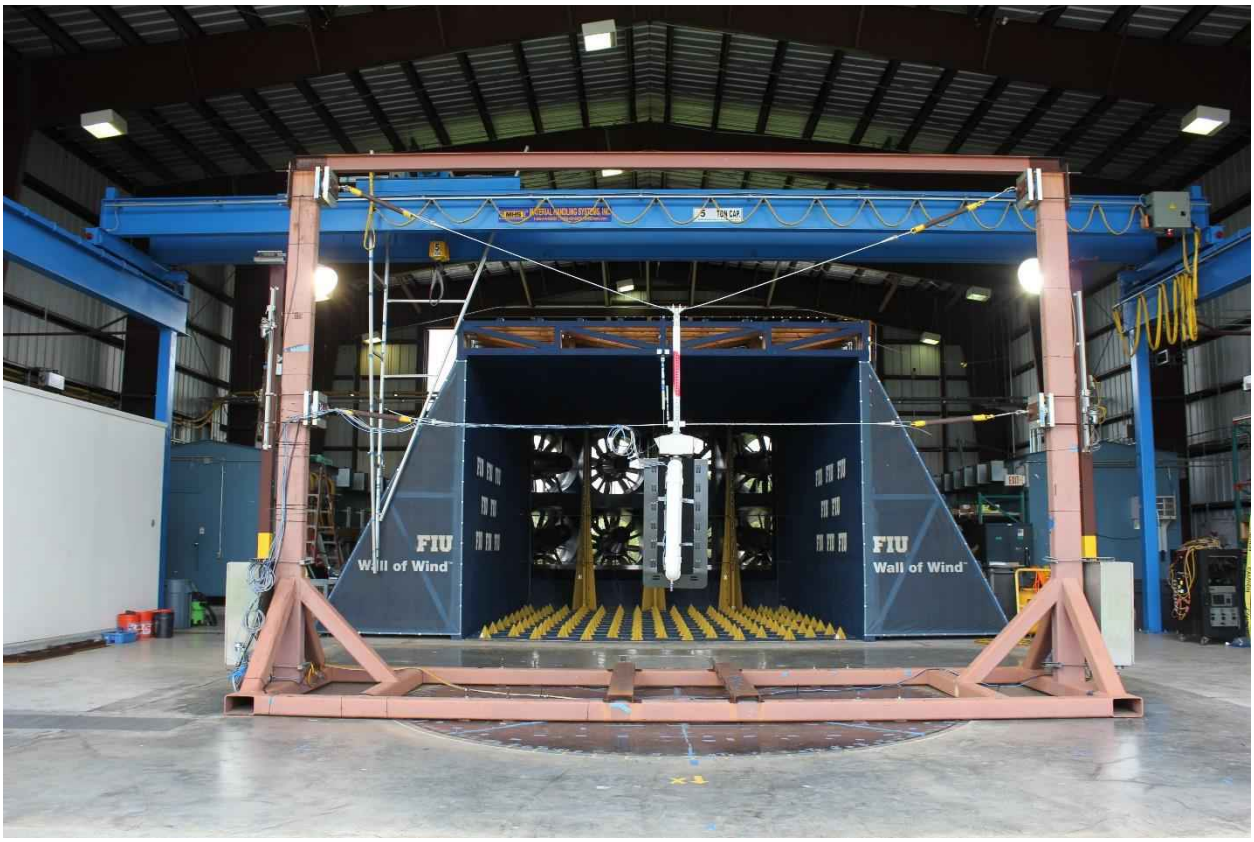

Figure 259: Signal assembly installed on test rig (before testing) with liquid damper (with zero liters of water)

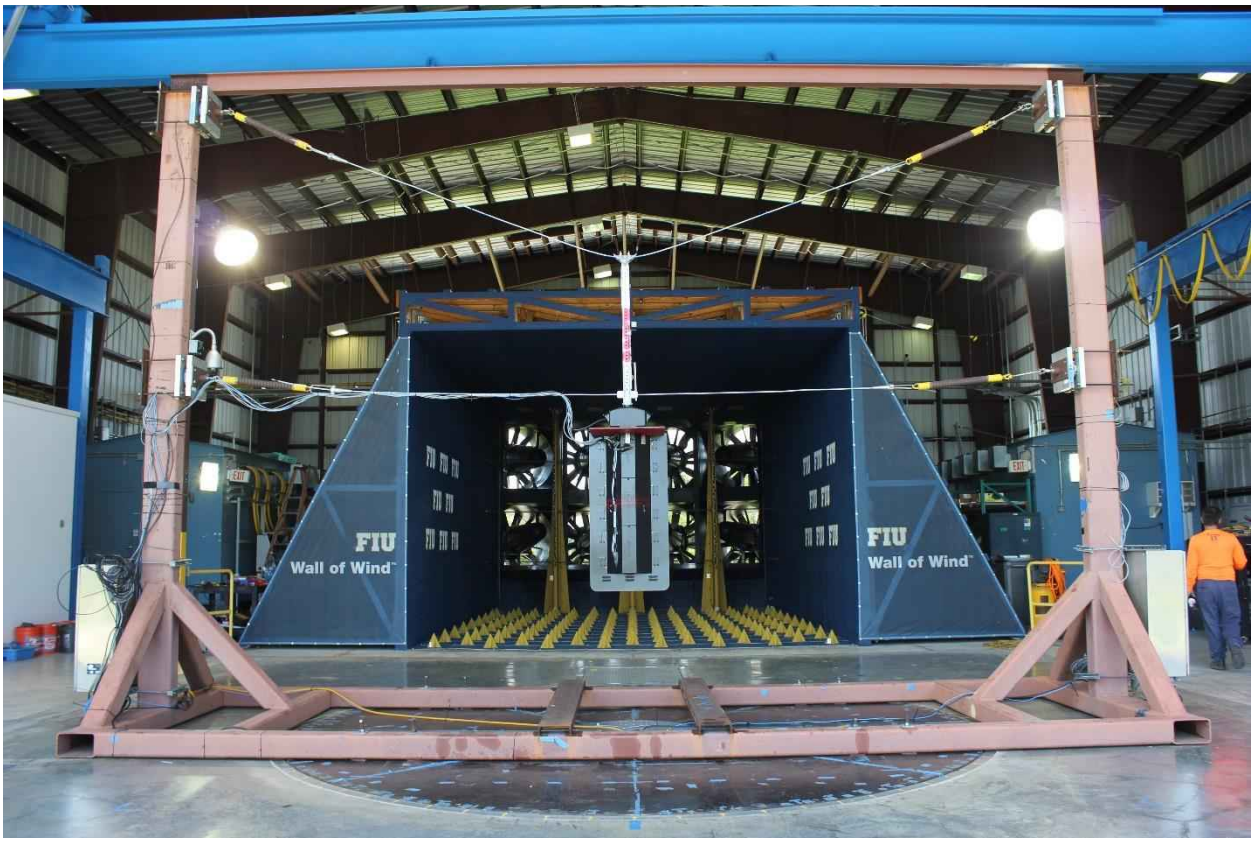

Figure 260: Signal assembly installed on test rig (before testing) with fin located at top of signal housing

Figure 261: Close up of fin located at top of signal housing

Figure 262: Signal assembly installed on test rig (before testing) with fin located at middle of signal housing

Figure 263: Close up of fin located at middle of signal housing

Figure 264: Signal assembly installed on test rig (before testing) with metal-box and iron-ball

Figure 265: Close up of metal-box with iron-ball located at bottom of signal housing

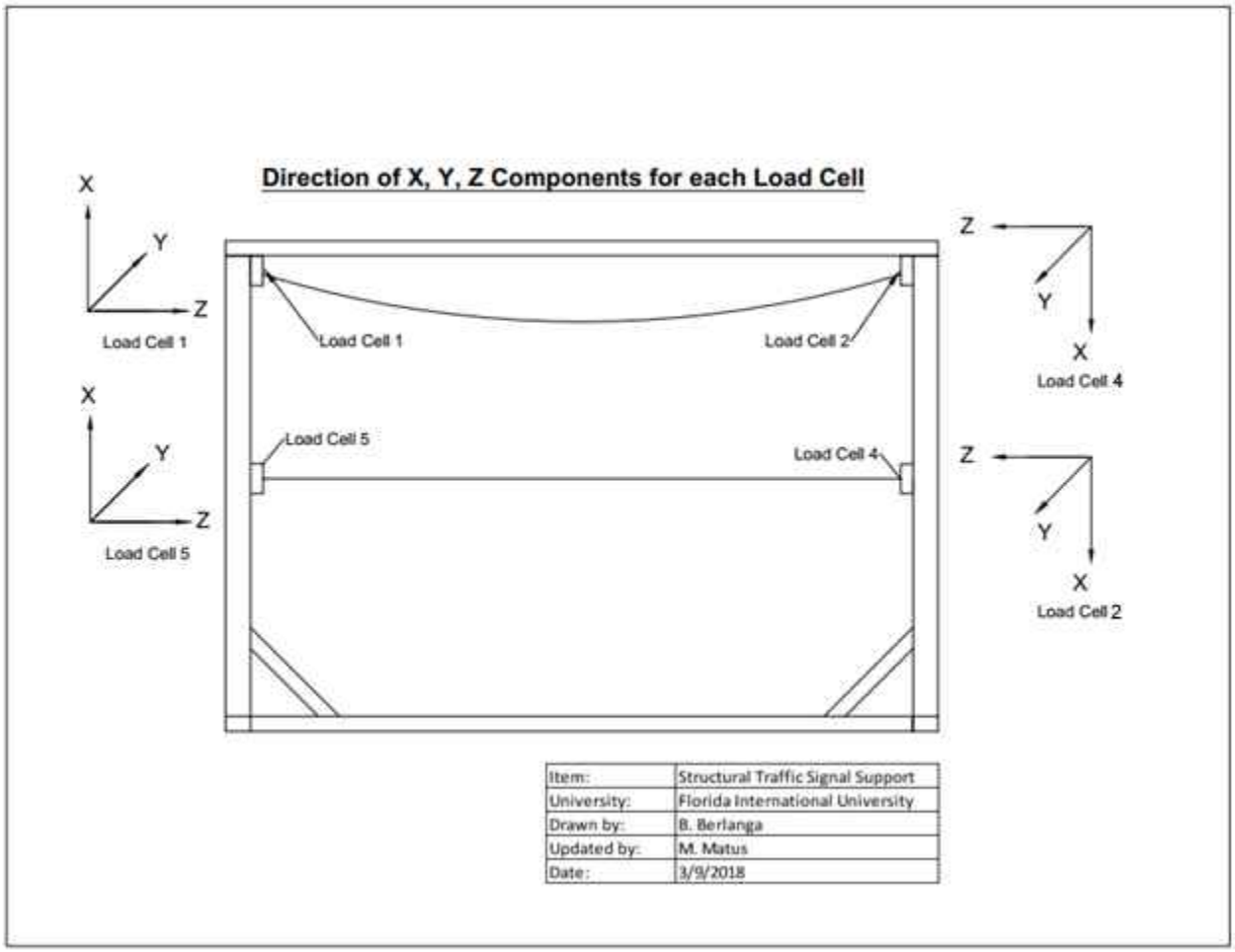

Figure 266: Direction of x,y,z components for each loadcell (direction of each axis shown represents 'positive direction')

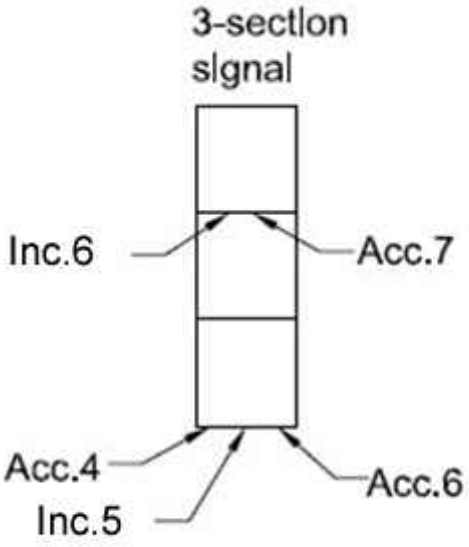

Figure 267: Location of accelerometers and inclinometers in 3-section signal

15.3. Results and Discussion

The tests at the WOW were performed in the presence of representatives from the Florida Department of Transportation (FDOT) Traffic Engineering and Operations Office and Traffic Engineering Research Lab (TERL), technicians from Horsepower Electric Inc. and members of the WOW technical team. The results in this chapter are restricted to 0-degree wind direction. It needs to be noted that the case with "no mitigation device" failed at 150 mph when the adjustable-hanger (Pelco) broke at the adjustable-hanger to extension bar connection point. For this reason, the readings at 150 mph of every figure for the "no mitigation case" might be erroneous and therefore should not be considered for comparison purposes.

15.3.1. Wind induced forces

The directions of the forces are shown in Figure 266. The mean and peak forces obtained at various wind speeds are discussed in this section. Figure 268 presents the total drag forces experienced by the different cases at 0 degrees wind direction, for increasing wind speeds. Data shows that the total drag force of the assembly increased with increasing wind speed. The highest along wind force of 275 lbs was found at 130 mph during the "Fin-at-top case" while lowest drag force was found during the "no-mitigation case" and resulted in a value of 210 lbs. Lift forces were found to increase with increasing speed, as shown in Figure 269:. The highest lift force experienced by the assembly was found during the "Liquid-damper-with-2L case" and it attained a value of about 122 lbs at 130 mph while the case that experienced the lowest lift force was the "fin-at-middle case" with a value of about 62 lbs. The same trend was found for the tension forces, where the forces were found to increase with increasing speed. The case that resulted in the highest messenger tension force was the "Liquid-damper-with-2L case" with a value of 405 lb at 130 mph. On the other hand, the cases that experienced the lowest tension force at 130 mph was the "Fin-at-middle case" and the "no-mitigation case" with a value of 375 lbs, see Figure 270.

For the maximum drag forces, it was found that the case with the highest maximum drag force was the "Fin-at-top case" and attained a value of 380 lbs at 130 mph while the case with the lowest drag force at 130 mph was the "no-mitigation case" and it attained a value of 310 lbs, see Figure 271. The maximum and minimum lift forces at 130 mph were found during the "Liquid-

damper-with-2L case" and "Fin-at-top", respectively and the values were found to be 200 lbs and 130 lbs, as shown in Figure 272. The values for the maximum and minimum tension forces experienced by the messenger wire were found to be 450 lbs and 410 lbs during the "Liquid-damper-with-2L case" and the "Fin-at-middle case" respectively, see Figure 273.

15.3.2. rms of accelerations

The root mean square (rms) of accelerations are presented in Figure 274 to Figure 276. Accelerometers 4, 6 and 7 were located on the 3-section signal, as shown in Figure 267. Overall, the rms of accelerations obtained from all the accelerometers experienced an increase from wind speed of 40 mph to 150 mph. The accelerometers that showed higher readings were the accelerometers located at the bottom of the signal. The case that was found to have the highest rms of accelerations was the "Fin-at-top case" and attained a value of 580 in/s^2 at 130 mph. The case that experienced the lowest rms of accelerations was the "metal-box case" and attained a value of 310 in/s2 at 130 mph, Figure 274.

15.3.3. Inclinations of the traffic signals

Figure 277 shows the mean inclinations experienced by the signal assembly. The inclinations were found to increase with increasing wind speed up to 130 mph. At 150 mph, there were aerodynamic instabilities and failures that may have influenced the readings of the inclinations. The case that resulted in the highest inclination among all cases was the "Liquid-damper-with-2L case" and attained a value of 61 degrees at 130 mph. The cases that resulted in lower inclinations at 130 mph were the "no-mitigation case," "metal-box case" and "fin-at-middle" cases and attained a value of 58 degrees. The highest maximum inclination was found to be 81 degrees at 130 mph during the "fin-at-top" case while the lowest maximum inclination was found to be 71 degrees during the "metal-box" case at 130 mph, see Figure 278.

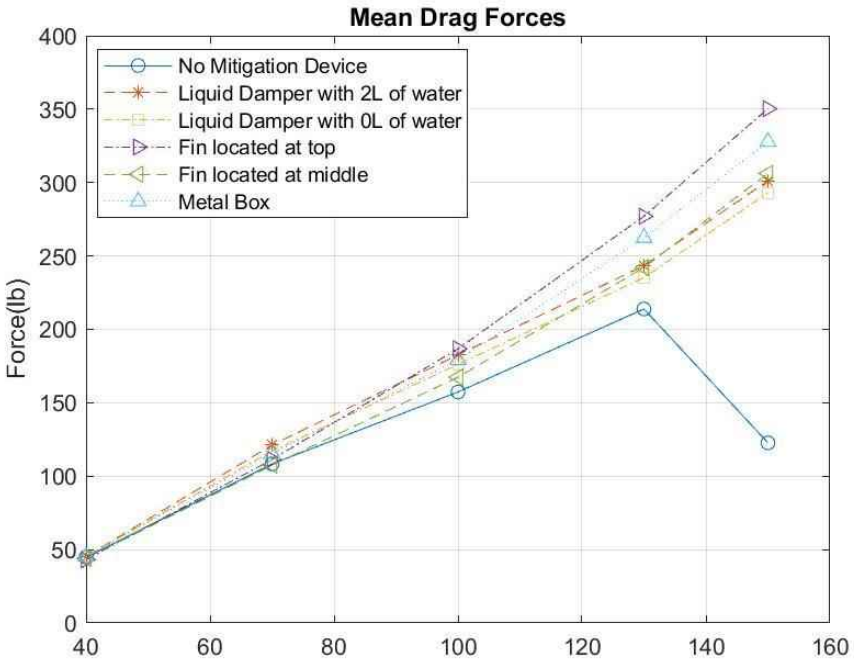

Figure 268: Mean drag forces

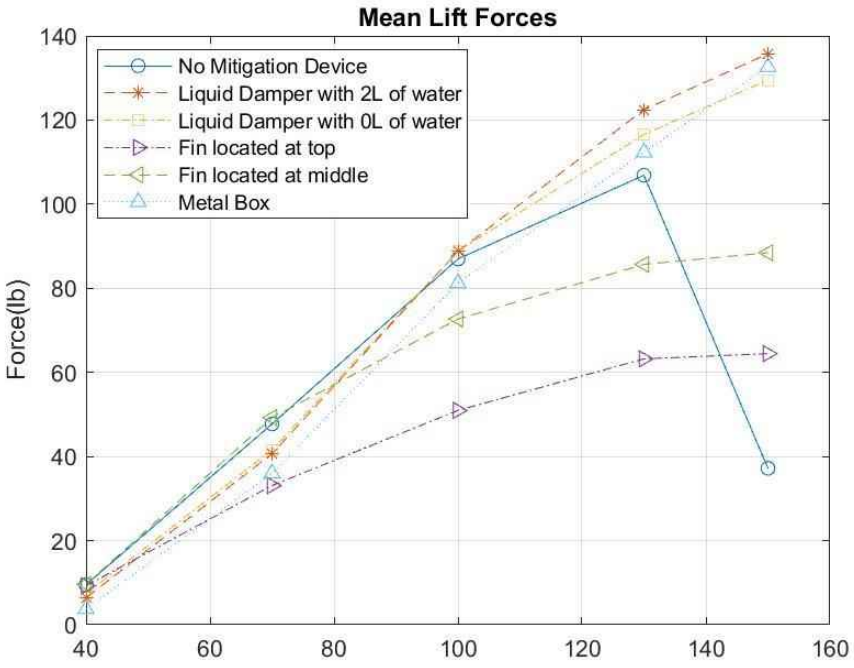

Figure 269: Mean lift forces

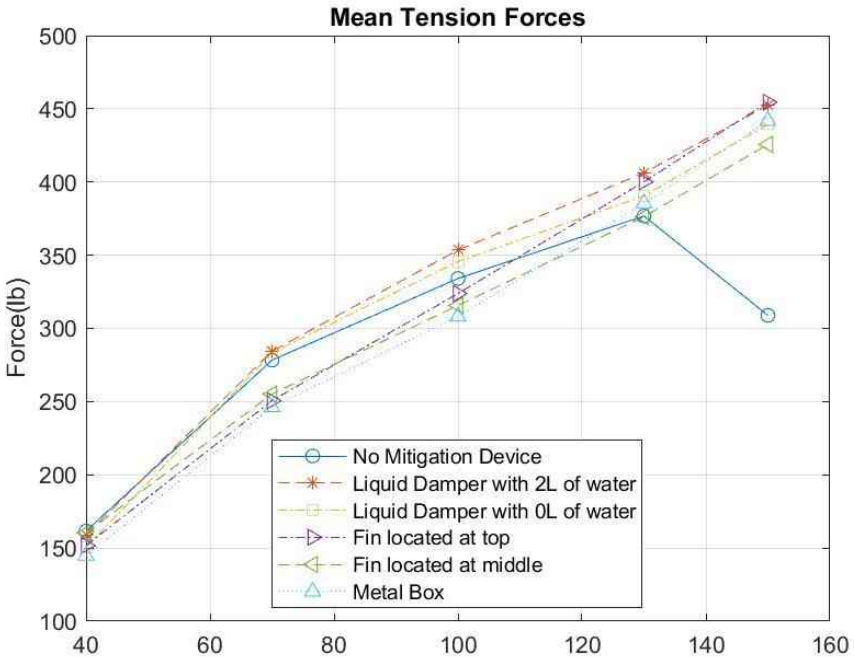

Figure 270: Mean tension forces

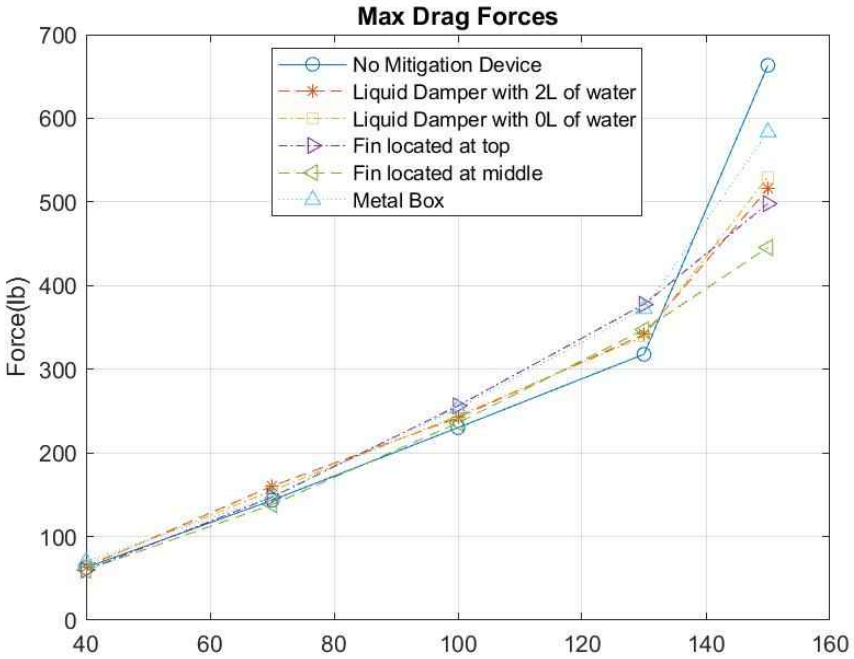

Figure 271: Maximum drag forces

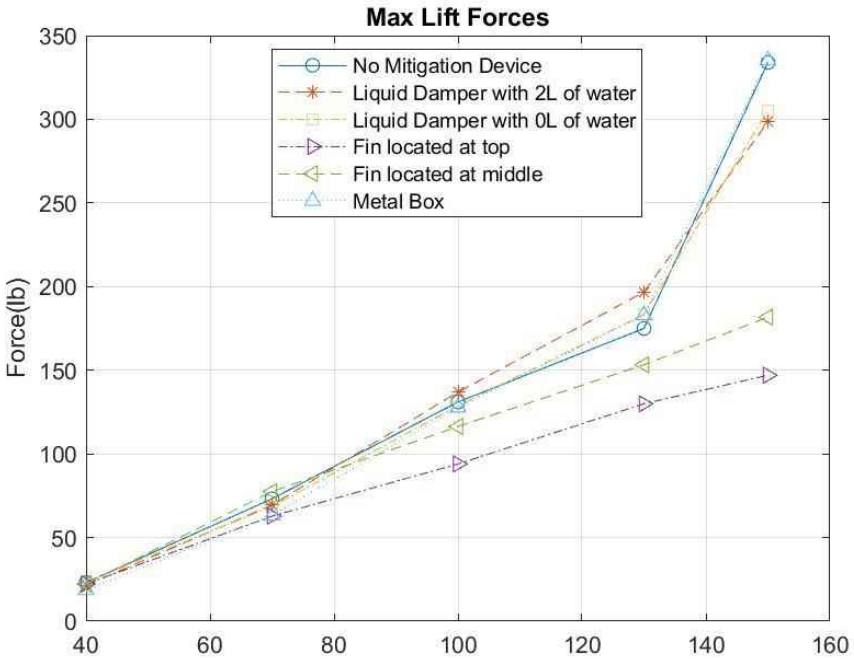

Figure 272: Maximum lift forces

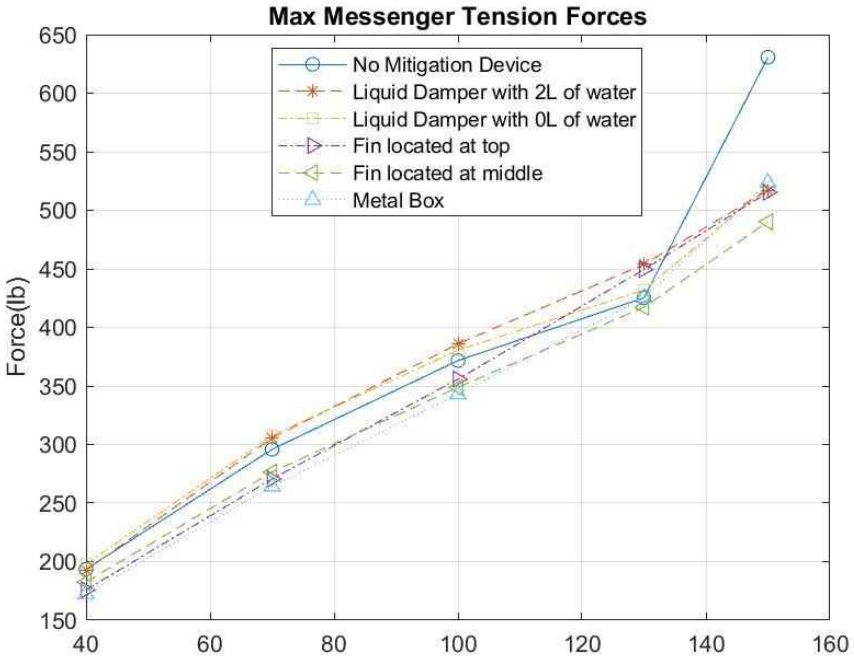

Figure 273: Maximum tension forces

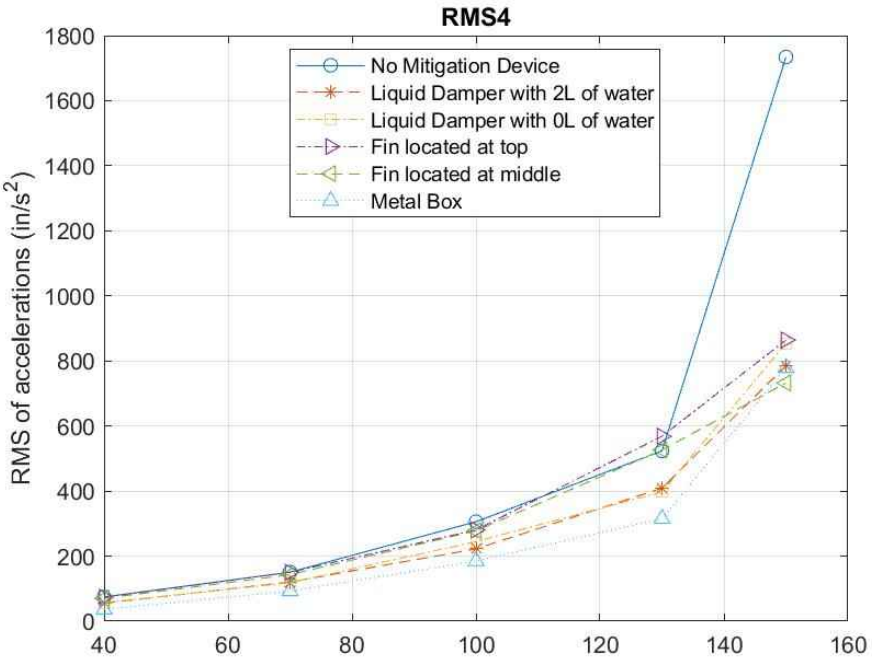

Figure 274: Root mean square of accelerations acc4 (bottom of signal)

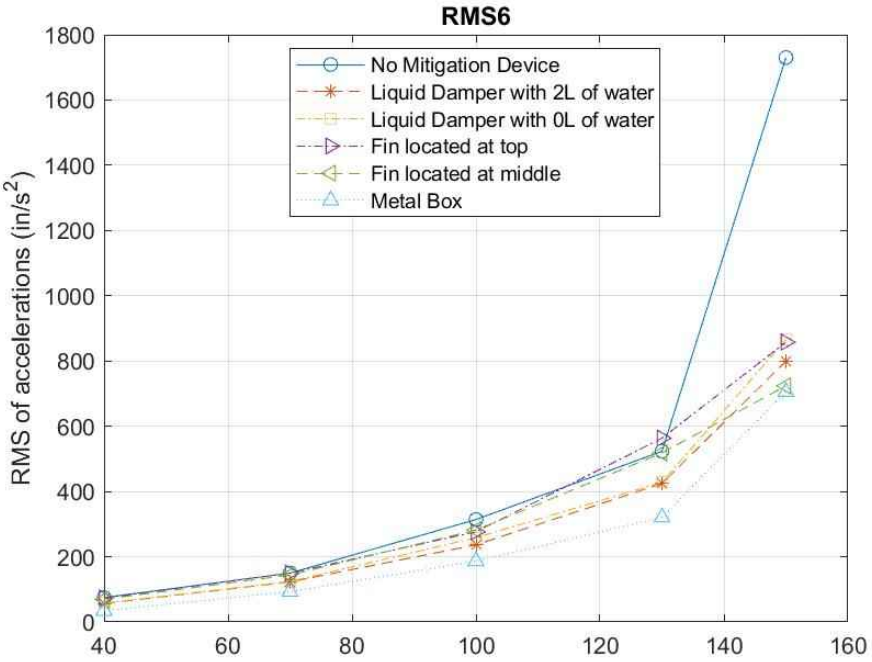

Figure 275: Root mean square of accelerations acc6 (bottom of signal)

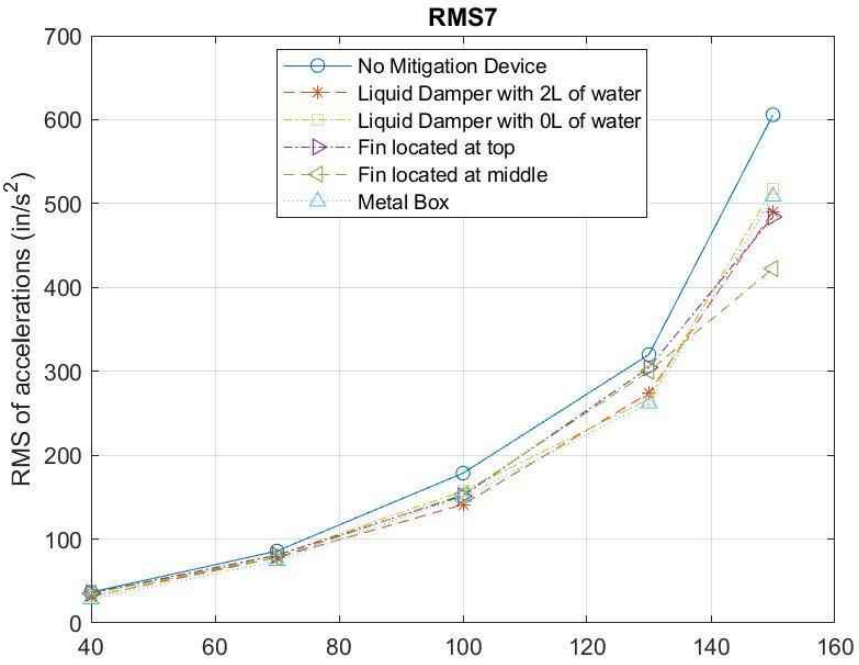

Figure 276: Root mean square of accelerations acc7 (top of signal)

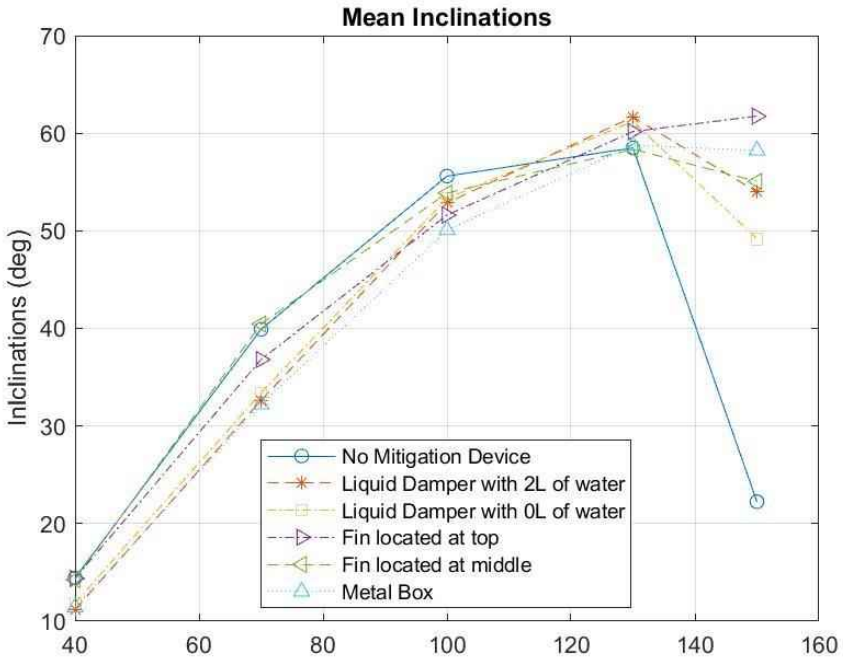

Figure 277: Mean inclinations

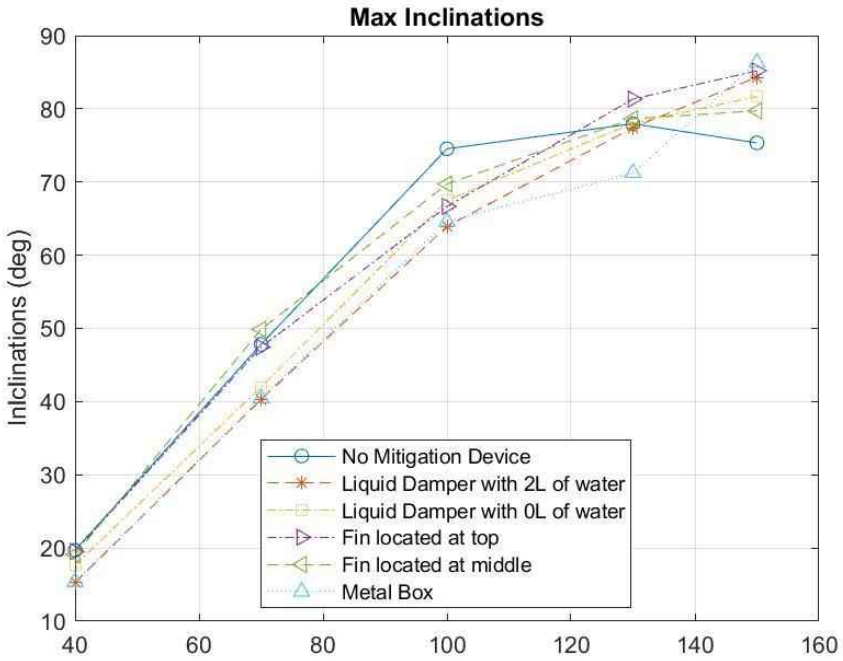

Figure 278: Maximum inclinations

15.4. Performance of traffic signals during the tests

This test utilized a 3-section aluminum traffic signal installed in a test rig span-wire configuration connected to the catenary and messenger wires by means of a "Tri-stud Adjustable-hanger Assembly with Aluminum Housing and Backplates." Notice that some test cases were installed with different components of different manufacturers. Please refer to Table 30.

No-mitigation case performance

The assembly showed no damage before 130 mph, at which point the extension bar started to bend. At 150 mph, the assembly started to show aerodynamic instability and after ~2 seconds, failure of the tri-stud hanger at the extension bar connection point occurred, Figure 279.

Liquid Damper with two liters (2L) of water

The assembly showed no damage before 130 mph, at which point the extension bar started to bend. The assembly showed no aerodynamic instability until the extension bar underwent severe bending (Figure 280) and the assembly started to gallop at 150 mph.

Liquid Damper with zero liters (0L) of water

The assembly showed no damage before 130 mph, at which point the lower portion of the extension bar started to bend. The assembly showed no aerodynamic instability until the extension bar bent severely (Figure 281) and aerodynamic instability was noticed at 150 mph.

Fin located at top

The assembly showed no damage before 130 mph, at which point the extension bar showed some bending (Figure 282). The assembly showed no aerodynamic instability through 150 mph.

Fin located at middle

The assembly showed no damage before 130 mph, at which point slight galloping was noticed. This galloping was seen to increase when the wind speed reached 150 mph, however, the signal stabilized when the inclination increased. The bending of the extension bar is considerably lower than other cases, Figure 283.

Iron ball in metal box

The assembly showed no damages during all wind speeds other than severe bending of the extension bar which started at about 130 mph. An aerodynamic instability was seen during the 150-mph wind speed, see Figure 284.

Figure 279: "No-mitigation case" failure of adjustable-hanger at 150 mph at 0 degrees

Figure 280: "Liquid-damper-with-2L case" after 150 mph at 0 degrees

Figure 281: "Liquid-damper-with-0L case" after 150 mph at 0 degrees

Figure 282: "Fin-at-top case" after 150 mph at 0 degrees

Figure 283: "Fin-at-middle case" after 150 mph at 0 degrees

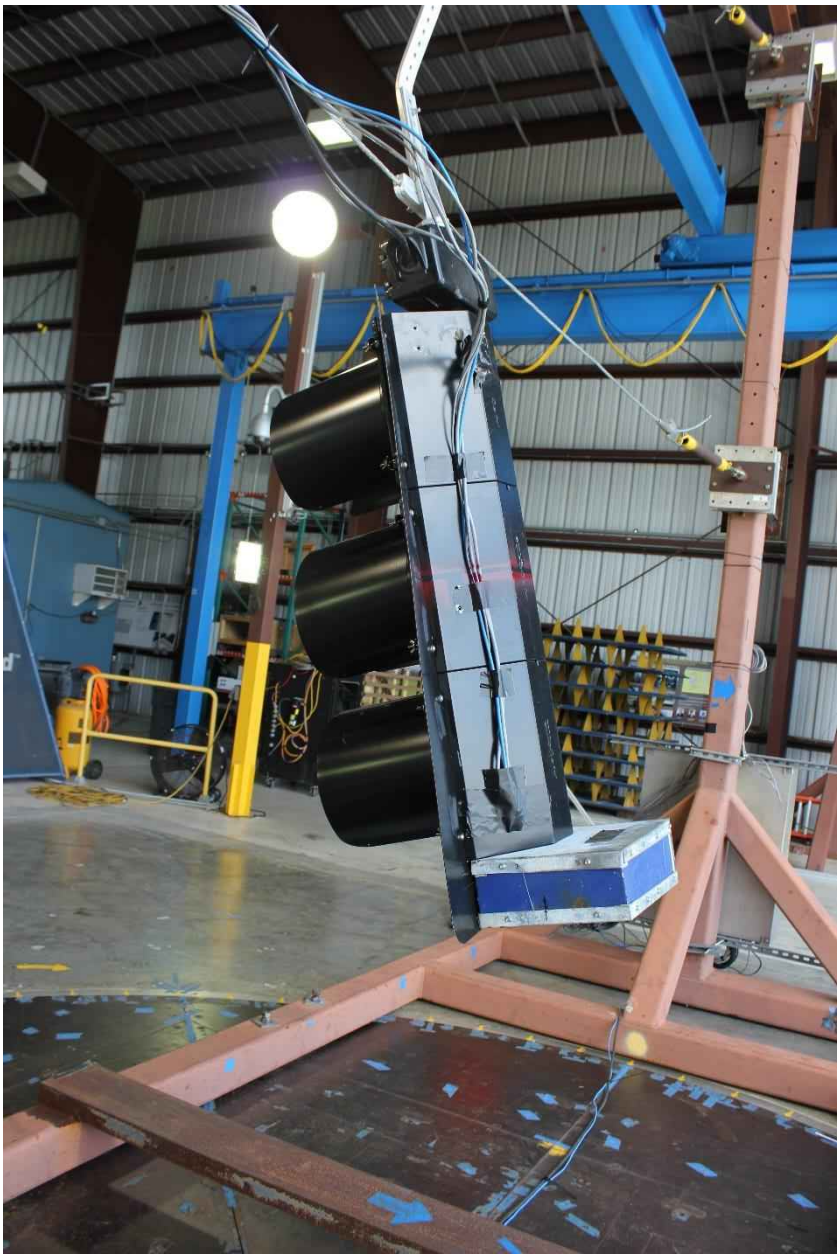

Figure 284: "Metal-box case" after 150 mph at 0 degrees

15.5. Conclusions and Recommendations

This chapter summarizes the results of a test conducted at WOW at FIU for a span wire traffic signal assembly consisting of a 3-section traffic signal, connected using an "Tri-stud Adjustable-hanger Assembly with Aluminum Signal Housing." The various instruments used for this test included: loadcells to measure forces, accelerometers to measure accelerations and inclinometers to measure the inclinations.

Results have shown that although the tested mitigation devices have produced different responses in terms of drag, lift and tension forces, RMS of accelerations and inclinations, the trends among all cases are similar. The case that resulted in lower lift and tension forces and inclinations was the "fin-at-middle case" while the cases resulting in lower drag forces and RMS of accelerations were the "No-mitigation case" and the "Metal-box case." Table 32 summarizes the highest and lowest mean results obtained at 130 mph at 0-degree wind angle of attack for: drag, lift and tension forces and the RMS of accelerations and inclinations.

When reviewing the above results, it is recommended to consider a device that would limit the signal from tilting back more than the limit (~60-degrees) at which point aerodynamic instabilities develop. When a sturdier adjustable-hanger is utilized (aluminum alloy 535), then the concentration of stresses is shifted to the extension bar and it bends, triggering aerodynamic instabilities. When a fin was installed at the back of the signal housing of the traffic signals, the bending of the extension bar was considerably lower than other cases, thus avoiding the appearance of aerodynamic instabilities due to the lower inclinations induced on the traffic signals. This mitigation device is ideal since it contains neither movable nor mechanical parts and the retrofitting of this device is relatively easy. It must be noted that the results of this mitigation device should be tested at angles of 180 degrees to see the response of the signal when the wind is hitting the back of the traffic signal.

Table 32: Summary of findings for the examined mitigation solutions

Parameter	Case with highest values	Case with lowest values
Mean Drag Forces	275 lbs. Fin-at-top case	210 lbs. No-mitigation case
Mean Lift Forces	122 lbs. Liquid-damper-with-2L case	62 lbs. Fin-at-middle case
Mean Tension Forces	405 lbs. Liquid-damper-with-2L case	375 lbs. Fin-at-middle case
RMS of Accelerations	580 in/s^2 Fin-at-top	310 in/s^2 Metal-box case
Mean Along-wind Inclinations	61 degrees Liquid-damper-with-2L case	58 degrees Metal-box, Fin-at-middle and No-mitigation cases

Chapter 16 - Task 4: Feasibility Study for an FDOT Test Apparatus

16.1. Introduction

Span wire traffic signals have been tested at the Wall of Wind (WOW) at Florida International University (FIU). From these tests (BDV29 TWO 977-20 and companion research project BDV29 TWO 977-27), wind forces on the signals can be enveloped. However, some signals were found to undergo an aeroelastic instability in the form of galloping which is not possible to replicate on a purely mechanical rig. It appears that the aeroelastic instability occurs when the signal along wind inclination reaches 60 degrees or more. If the signal inclinations remain at lower angles than 60 degrees, then the forces are more predictable since they are mainly determined by the static aerodynamic force coefficients such as drag coefficient (C_D), lift coefficient (C_L) and resultant coefficient (C_R). It must be noted that if an aerodynamic instability occurs, it leads to large amplitude oscillations and the forces put on the signals, hangers and support systems like wires, clamps and poles, become greatly magnified by these oscillations, no longer depending on the static aerodynamic coefficients. The resulting forces on the system can be determined by the WOW tests where the wind is present, but it will be difficult to replicate in a purely mechanical rig because the origin of the forces is an aeroelastic interaction.

16.2. Proposed Methodology

A mechanical test rig may be achievable if the blow back angle does not exceed about 60 degrees of along wind inclination. The simplest rig, which uses a single cable and actuator to impose forces on the signal, could be as depicted schematically in Figure 285. In this rig a complete span-wire system would be assembled including end posts, catenary wire, messenger wire, hanger system, connections and signal. A cable would be attached to the back of the signal housing and taken over a pulley attached to a rigid frame at some distance, e.g. 30 ft, from the signal. From the pulley the cable would be connected to an actuator system with force range large enough to encompass the anticipated range of aerodynamic forces (e.g. 1000 lbs) and stroke of the order three ft. If necessary, a leverage system would be used to lessen the stroke

requirements for the actuator. The pulley and actuator would be attached to a rigid frame. The force exerted by the actuator would be commanded by software to go through a sequence of fluctuations corresponding to a design storm. The number of cycles and magnitude of force fluctuations would be based on the von Karman spectrum of wind which has been found to match field measurements in strong wind storms. The design storm of selected strength, e.g. a Category 1 or Category 2 hurricane, would be selected based on discussions with FDOT. More precise rigs could be envisaged involving more complex arrangements, but, for the present we continue with the simplest concept. The force F would be programmed to replicate wind forces during a representative storm. Every storm is different, but a standard storm could be selected which could form the basis for comparing the performance of different systems (signal attachments, hangers, clamps etc.). Note however that if the signal system deflects such that the angle theta becomes more than 60 degrees, then instability is indicated, and the test would no longer be valid. In this case, when aerodynamic instabilities develop, WOW tests would be needed to assess the performance of the system.

16.2.1. Normal Force

The force F in the cable would be estimated based on the static aerodynamic force coefficients. If we assume as a conservative approximation, that the normal force coefficient stays constant out to 60 degrees, which is roughly true as shown in Figure 286., then we could take C_N= 1.2 to 1.3. The normal force F_N then becomes $F_N=0.5\rho U^2 AC_N$.

We will assume that the cable force in the rig is representative of the normal force. If we have the initial angle of the cable at 30 degrees to the horizontal, the normal component will be about 86% of the cable force. When the signal angle reaches 30 degrees, the normal force will be equal to the cable force. When the signal reaches 60 degrees, the normal component will be about 86% of the cable force again. Since the test is simply a means of comparing signal systems, this level of approximation is acceptable. With these approximations, in terms of mean speed $\overline{U}$ and speed fluctuations u the cable force would then be:

Equation 9

$$F = \frac{1}{2}\rho(\overline{U}+u)^2 AC_N \approx \frac{1}{2}\rho(\overline{U}^2 + 2u\overline{U})AC_N$$

In this expression u is function of time but $\overline{U}$ remains constant over periods of about an hour. In a storm, $\overline{U}$ will gradually increase over a few hours, reach a peak, and then decrease over a few hours. The test could be set to run with constant mean force for each hour of storm:

$$\bar{F} = \frac{1}{2}\rho\overline{U}^2 AC_N \qquad \textit{Equation 10}$$

plus a fluctuating superimposed force:

$$f = \frac{1}{2}\rho(\overline{U}+u)^2 AC_N \approx \rho u(t)\overline{U}AC_N = \rho\overline{U}^2 AC_N \frac{u}{\overline{U}}(t) \qquad \textit{Equation 11}$$

So that:

$$F = \bar{F} + f(t) \qquad \textit{Equation 12}$$

The test could be set to run for a 7-hour storm with seven values of $\overline{U}$ each run for one hour. At the same time force fluctuations would be imposed to approximate those caused by wind speed fluctuations $u(t)$. The programing of $u(t)$ would be based on the power spectrum of turbulence for the mean speed $\overline{U}$ and turbulence intensity $I = \sigma_u/\overline{U}$.

16.2.2. Resultant Force

In the above explanation, the normal force was used to set the force in the cable pulling on the signal. It would be preferable to use the resultant force and its corresponding force coefficient C_R since it is the resultant that is best simulated by a cable. The resultant coefficient C_R is calculated as the resultant of the drag (C_D) and lift (C_L) coefficients with the following formula:

$$C_R = \sqrt{C_D^2 + C_L^2} \qquad \textit{Equation 13}$$

The resultant force is aligned at an angle to the horizontal given by

$$\alpha = \arctan\left(\frac{C_L}{C_D}\right) \qquad \textit{Equation 14}$$

From Task 2 results performed at the WOW, measurements of C_D and C_L (shown in Figure 286) were recorded and utilized to calculate C_R and are plotted in Figure 287. A simple approach would be to set C_R to a constant value which is roughly true for blow back angles up to about 50 degrees but the angle α changes as the blow back angle changes. For this, α could be set to an initial

guessed value α_0, apply a mean force given by the desired wind speed and assumed C_R. Then measure the mean blow back angle θ, and then calculate a revised value α which can be called α_1. Then move the top end of the forcing cable up to achieve the value of α_1. The value of θ can then be remeasured if necessary and a further iteration carried out.

The resultant force then becomes:

$$F_R(t) = \frac{1}{2}\rho U^2(t) A C_R \qquad \textit{Equation 15}$$

To develop a test time history of $\boldsymbol{F_R(t)}$, a presentative time history of wind velocity $\boldsymbol{U(t)}$ needs to be developed, which is done in the next section.

16.2.3. Time History of Wind Speed

To a first approximation it is reasonable to not try to vary $\boldsymbol{\alpha}$ as a function of time but to leave it set at the mean value determined from the measurement of $\boldsymbol{\theta}$ when the mean value of $\boldsymbol{F_R}$ is applied.

The wind velocity $\boldsymbol{U(t)}$ at any instant is made up of a mean value $\boldsymbol{\overline{U}}$, that is constant for a period of about an hour, and a fluctuating component $\boldsymbol{u(t)}$ that is a function of time $\boldsymbol{t}$:

$$\boldsymbol{U(t) = \overline{U} + u(t)} \qquad \textit{Equation 16}$$

The fluctuating part can be expressed as a Fourier series:

$$\boldsymbol{u(t) = a_1 \sin(\Delta\omega t + \phi_1) + a_2 \sin(2\Delta\omega t + \phi_2) + a_3 \sin(3\Delta\omega t + \phi_3) + \cdots + a_n \sin(n\,\Delta\omega t + \phi_n)}$$

or:

$$\boldsymbol{u(t) = \sum_{i=1}^{n} a_i \sin(i\Delta\omega t + \phi_i)} \qquad \textit{Equation 17}$$

In this expression $\boldsymbol{\Delta\omega}$is the increment in circular frequency and is related to increment in frequency $\boldsymbol{\Delta f}$ in Hertz by $\boldsymbol{\Delta\omega = 2\pi\Delta f}$. And, $\boldsymbol{\phi_i}$ = phase angle for the i^{th} term.

The mean square of fluctuating velocity fluctuations can be shown to be:

$$\boldsymbol{\sigma_u^2 = \overline{u^2} = \sum_{i=1}^{n} \frac{a_i^2}{2}} \qquad \textit{Equation 18}$$

The non-dimensional spectrum of wind speed $\boldsymbol{S_u(f)}$, is well described by the von Karman expression:

$$S(f) = \frac{4\sigma_u^2 \left(\frac{L_u}{\bar{U}}\right)}{\left(1 + 70.78\left(\frac{fL_u}{\bar{U}}\right)^2\right)^{5/6}} \qquad \textit{Equation 19}$$

Where L_u is the integral turbulence scale, which is a measure of the average size of turbulence eddies.

Integrating this spectrum over all frequencies results in σ_u^2:

$$\sigma_u^2 = \int_0^\infty S(f)\, df \qquad \textit{Equation 20}$$

Note that this integral can also be expressed as:

$$\sigma_u^2 = \int_0^\infty fS(f)\, dln(f) \qquad \textit{Equation 21}$$

Which can be useful since the important range of f for turbulence can spread over several decades. Using the von Karman expression this becomes:

$$\sigma_u^2 = \int_0^\infty \frac{4\sigma_u^2 \left(\frac{fL_u}{\bar{U}}\right)}{\left(1 + 70.78\left(\frac{fL_u}{\bar{U}}\right)^2\right)^{5/6}} dln\left(\frac{fL_u}{\bar{U}}\right) \qquad \textit{Equation 22}$$

For an interval $\Delta \ln\left(\frac{fL_u}{\bar{U}}\right) = \Delta\eta$ centered on η_i:

$$\frac{\Delta\sigma_i^2}{\sigma^2} = \int_{\eta_i - \Delta\eta}^{\eta_i + \Delta\eta} \frac{4\left(\frac{fL_u}{\bar{U}}\right)}{\left(1 + 70.78\left(\frac{fL_u}{\bar{U}}\right)^2\right)^{5/6}} dln\left(\frac{fL_u}{\bar{U}}\right) \qquad \textit{Equation 23}$$

This then provides a way of determining the coefficients a_i in Equation 5 for each interval of frequency:

$$a_i = \sqrt{2} I_u \bar{U} \sqrt{\frac{\Delta\sigma_i^2}{\sigma_u^2}} \qquad \textit{Equation 24}$$

where the values of $\sqrt{\frac{\Delta\sigma_i^2}{\sigma_u^2}}$ are evaluated numerically using Equation 15.

As an example, a time history of wind speed has been generated for the following parameters:

- *Mean wind speed* $\bar{U} = 30$ *m/s*
- *Turbulence intensity* $I_u = 0.2$
- *Turbulence integral scale* $L_u = 25$ *m*

The results are shown in Figure 288.

Each storm is different, but a category of hurricane could be selected, and a storm duration estimated. For example, if the eyewall is 15 miles across and it travels at 5 mph forward speed then the duration for the storm peak is probably about 2 to 3 hours. A representative test might be 2 hours at highest mean speed and then 2 hours either side at mean speed reduced to say 80 % of the peak. At each mean speed the associated fluctuations due to turbulence would be simulated via fluctuations in F_R calculated using Equation 7 along with the predetermined velocity time history. Alternatively, the test could be set up so that it has more speed intervals: e.g. one hour at each speed, building up and then dying down. As a recommendation, a test could be run as follows:

- 1 hour at 70% peak speed
- 1 hour at 80%
- 1 hour at 90%
- 1 hour at 100%
- 1 hour at 90%
- 1 hour at 80%
- 1 hour at 70%

16.2.4. Torsional Loads

Torsion loads could be simulated by offsetting the point of attachment of the cable to say 5% of the width of the signal.

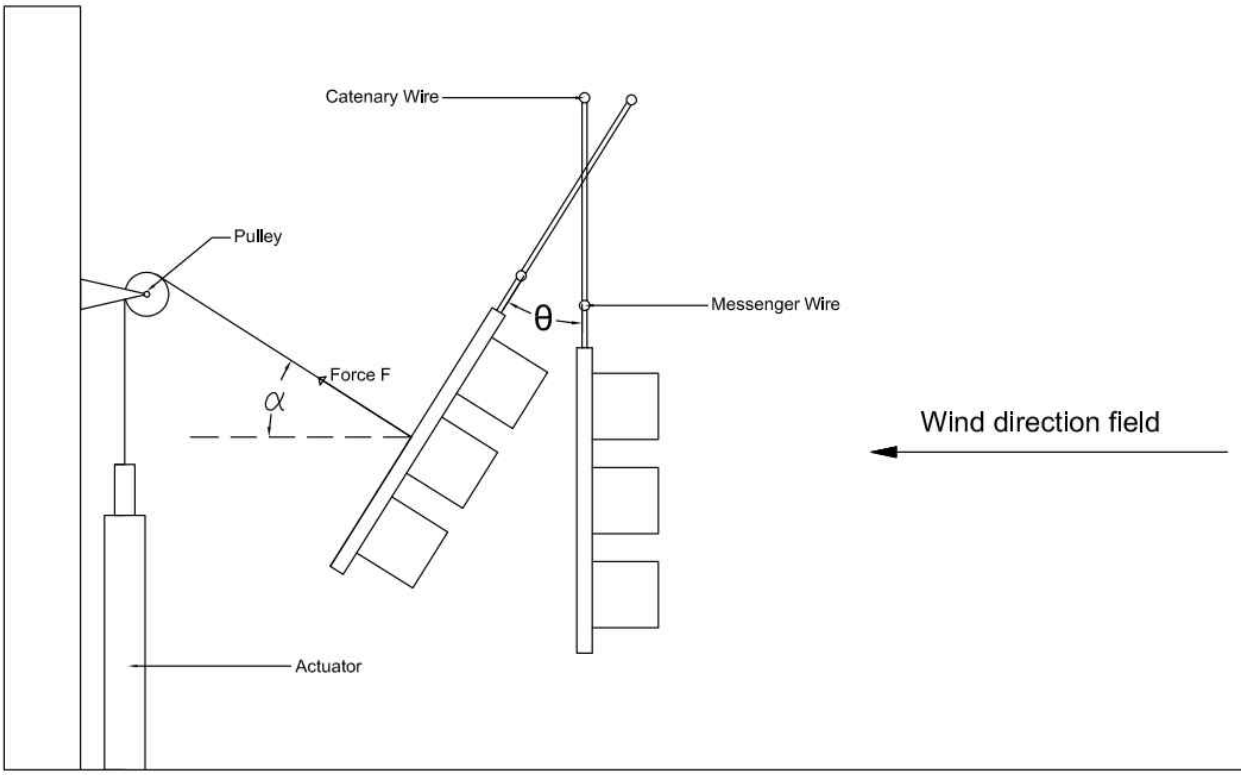

Figure 285: Simple test rig

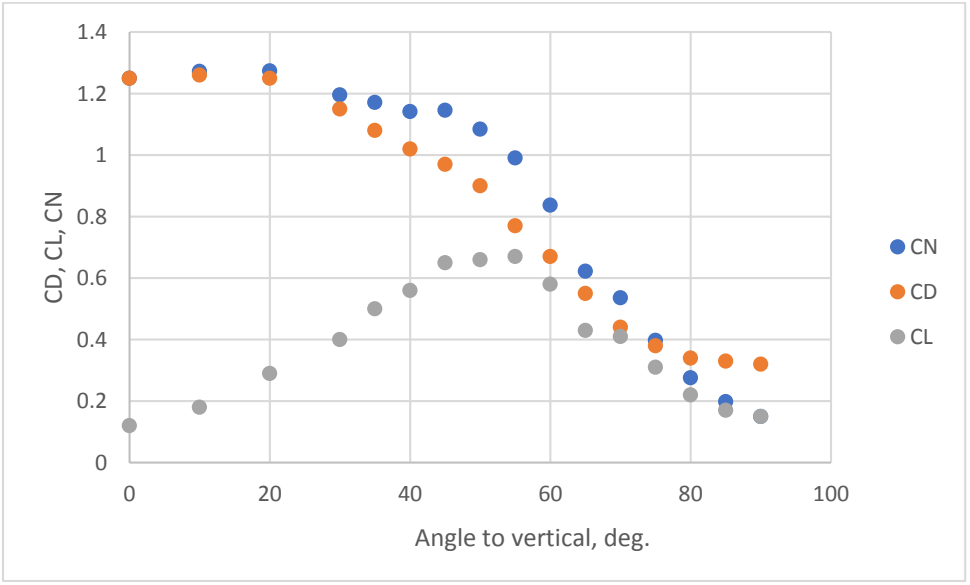

Figure 286: Variation of aerodynamic force coefficients with blow back angle

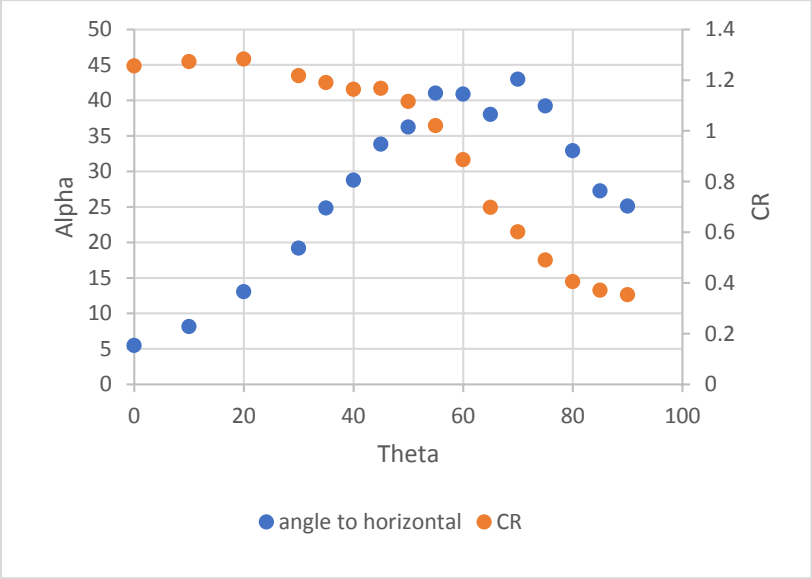

Figure 287: WOW data for resultant force coefficient and angle to horizontal of resultant

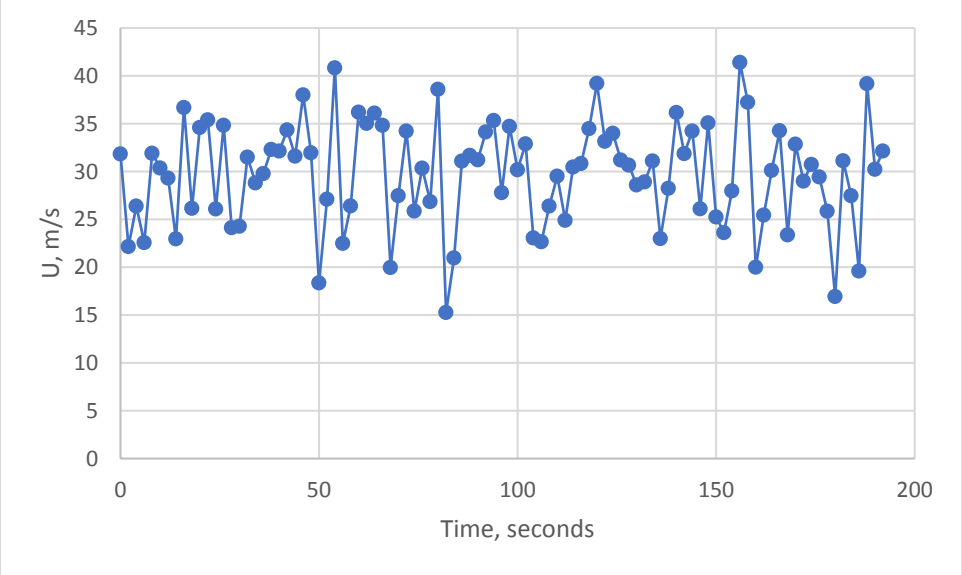

Figure 288: Wind velocity time history

16.3. Conclusions

A mechanical test rig can be constructed but it must be noted that it would have limitations. In previous tests, span-wire systems were found to undergo aerodynamic instabilities when the angle of inclination of the traffic signals reached 60 degrees or more. These aerodynamic instabilities produced large amplitude oscillations and the forces put on the signals and its components become greatly magnified. Resulting forces on the system when galloping or flutters occurs, can only be determined with appropriate boundary layer wind tunnel tests. Considering the experience gained during this lengthy and thorough experimental research project, it is concluded that it is not feasible to replicate this behavior in a purely mechanical rig because the origin of the forces is an aeroelastic interaction. Nevertheless, a mechanical rig is achievable if the blow back angle does not exceed about 60 degrees. A feasible and simplified test rig that can be developed consists of one cable connected to an actuator that would go through a pulley that would then be connected to the back side of the signal. This actuator would impose forces on the signal to replicate the forces that would be found during a representative storm chosen. The methodology developed in this task will estimate the forces produced by the storm. These forces will be used as input to program the actuator to replicate the induced hurricane wind forces. It is clear that every storm is different, but a standard representative storm could be selected to form the basis for comparing the performance of different systems and components. This mechanical rig would serve to experimentally test components to certify the survivability and resiliency during and after a hurricane event, thus enhancing the safety of the motorists utilizing the different transportation facilities that contain span-wire traffic signals.

Chapter 17 - Overview of Conclusions, Findings, and Recommendations

This section summarizes conclusions, findings and recommendations from the current project BDV29 TWO 977-20 and its companion project BDV29 TWO 977-27.

17.1. Full-scale Tests

- It has been observed that depending on the rigidity of the hanger, the traffic signal assembly is more susceptible to aerodynamic instabilities in the form of galloping. Flexible hangers have a tendency to undergo higher along-wind inclinations at lower wind speeds which would trigger this instability at lower wind speeds (about 70 mph) than a rigid hanger, while for the rigid hanger the instability appears when the extension bars severely bend (about 110 mph).
- The 5-section signal has been found to be susceptible to damage regardless of the type of hanger used. This may be due to its increased weight as well as the increased surface area compared to the 3-section signal. It is recommended to find an alternative section to replace usage of 5-section signal.
- A common failure observed was with the 72-tooth serrated edge connection between the adjustable-hanger and the disconnect-box and also between the disconnect-box to signal-housing point. The failure mode with this connection point was the serrated edge would shear, allowing the connection to turn. A resilient connection at these points should be considered to enhance the survivability of the signal under wind induced loads. In discussions with FDOT, it was proposed to explore the possibility of using a device that could potentially remove the rotational degree of freedom of the adjustable-hanger to disconnect-box connection. Such component is currently available (i.e. octagon base) but for different types of traffic sign installations and can be connected to the back of the disconnect-box to restrain the stresses put on the 72-tooth connection. With regards to this issue, modifications should be made to the connection to prevent this failure mode.
- The parameters (sag ratio, messenger wire pre-tension and distance between end supports of catenary and messenger wire) of the signal assembly affect the overall response of the span-wire system. Results from the parametric study showed that a sag ratio of 7% (of

catenary wire) results in a better response at wind speeds up to 75 mph. It is recommended to test this configuration at higher wind speeds to verify the same behavior is observed at higher wind speeds when aerodynamic instabilities develop.

- Due to improved performance, use maximum overlap at tri-stud adjustable-hanger and extension-bar connection points (top and bottom portions/connections). At these connection points, use a minimum of 2 bolts per connection. The bolts should be spaced apart with one unused bolt-hole in between.
- Due to its outstanding performance during testing, continue to use Florida DOT specified aluminum alloy 535 (note that all tri-stud adjustable hangers broken during testing were not made of 535 aluminum alloy),
- Avoid using a thicker extension bar. A thicker bar was tested with the standard adjustable hanger and while it didn't break, it placed more strain on the rest of the assembly.
- Consider installing safety wire between catenary and messenger wire to help hold the system up if hangers or extension bars break.
- Consider a device that would limit the signal from tilting back more than the limit (~60-degrees) at which point aerodynamic instabilities develop. This solution might be carefully assessed before implementation due to the increased force coefficients at higher wind speeds.
- After carefully reviewing the work done previously at University of Florida and the findings from the Wall of Wind testing, the certification general procedure that might be considered and implemented by FDOT should include:
    - Perform static flexural/tension testing of components (740 and 7400 per UF).
    - Perform mechanical test on signal assembly based on the results of the feasibility study. This would cover up to the 60 degree blow back angle.
    - Perform dynamic test to cover instabilities above the 60 degree blow back angle (will require further research).

17.2. Small-scale Aeroelastic Tests

- Results have shown that the aeroelastic model started experiencing aerodynamic instabilities such as fluttering at wind speeds as low as 60 mph (full-scale) at cornering winds, mainly 45°.
- Taking into consideration the results of the DAF obtained from the resonance decomposition of both models, all static forces used in the design of span-wire traffic signals can be multiplied by a factor of 1.3 to account for dynamic effects.
- More dynamic analysis is required to investigate the aeroelasticity of the system. The missing low frequency part of the turbulence spectrum needs to be accounted for in addition to obtaining the aerodynamic damping ζ_a and force and moment coefficients C_F and C_M among others.

17.3. Full-scale Mitigation Tests

- It is recommended to consider a device that would limit the signal from tilting back more than the limit (~60-degrees) at which point aerodynamic instabilities develop.
- When a sturdier adjustable-hanger is utilized (aluminum alloy 535), then the concentration of stresses is shifted to the extension bar and it bends, triggering aerodynamic instabilities.
- When a fin was installed at the back of the signal housing of the traffic signals, the bending of the extension bar was considerably lower than other cases, thus avoiding the appearance of aerodynamic instabilities due to the lower inclinations induced on the traffic signals. This mitigation device is ideal since it contains neither movable nor mechanical parts and the retrofitting of this device is relatively easy. It must be noted that the results of this mitigation device should be tested at angles of 180 degrees to see the response of the signal when the wind is hitting the back of the traffic signal.

17.4. Feasibility Study for a Test Apparatus

- Considering the experience gained during this lengthy and thorough experimental research project, it is concluded that it is not feasible to replicate the aerodynamic instabilities (i.e. galloping and/or flutter) in a purely mechanical rig because the origin of the forces is an aeroelastic interaction.

- A mechanical test rig is achievable if the blow back angle does not exceed about 60 degrees. A feasible and simplified test rig that can be developed consists of one cable connected to an actuator that would go through a pulley that would then be connected to the back side of the signal. This actuator would impose forces on the signal to replicate the forces that would be found during a representative storm chosen.

References

[1] State of Florida Department of Transportation (FDOT). (January 2015). Standard Specifications for Road and Bridge Construction, FDOT, Tallahassee, FL.

[2] Cook, R.A., Masters, F., & Rigdon, J.L. (2012). "Evaluation of Dual Cable Signal Support Systems with Pivotal Hanger Assemblies." FDOT Contract No. BDK75 977-37, University of Florida, Department of Civil and Coastal Engineering, Gainesville, FL.

[3] Zisis, I., Irwin, P., Berlanga, B., Chowdhury, A.G., Hajra, B. (2016) "Assessing the performance of vehicular traffic signal assemblies during hurricane force winds", Proceedings of the 1st International Conference on Natural Hazards and Infrastructure, June 28-30, Chania, Greece.

[4] Aly, A. M., Chowdhury, A. G., Bitsuamlak, G. (2011) "Wind profile management and blockage assessment for a new 12-fan Wall of Wind facility at FIU", Wind & Structures, 14(4), 285-300.

[5] Chowdhury, A.G., Zisis, I., Irwin, P., Bitsuamlak, G.T., Pinelli, J.P., Hajra, B., Moravej, M. (2016) "Large Scale Experimentation using the 12-Fan Wall of Wind to Assess and Mitigate Hurricane Wind and Rain Impacts on Buildings and Infrastructure Systems", Journal of Structural Engineering (ASCE)-Special Issue: Recent advances in assessment and mitigation of multiple hazards for structures and infrastructures, DOI: 10.1061/(ASCE)ST.1943-541X.0001785.

[6] Zisis, I., Irwin, P., Chowdhury, A. G., Matus, M., BDV29 TWO 977-27 FDOT Interim Report_Task 2-Case 5, December 2017.

[7] ASTM Standard A475, 2003 (2014). Standard Specification for Zinc-Coated Steel Wire Strand. ASTM International, West Conshohocken, PA, DOI: 10.1520

[8] ASTM Standard A500/A500M, 2018. Standard Specification for Cold-Formed Welded and Seamless Carbon Steel Structural Tubing in Rounds and Shapes. ASTM International, West Conshohocken, PA, DOI: 10.1520

[9] CSI, 2018. SAP2000 Integrated Software for Structural Analysis and Design. Computers and Structures Inc., Berkeley, California

[10] Elawady, A., Aboshosha, H., El Damatty, A., Bitsuamlak, G., Hangan, H. and Elatar A., 2017. Aero-elastic testing of multi-spanned transmission line subjected to downbursts. Journal of Wind Engineering & Industrial Aerodynamics, 169, 194-216

[11] Irwin, P., Zisis, I., Berlanga, B., Hajra, B. and Chowdhury, A., 2016. Wind Testing of Span-Wire Traffic Signal Systems. Resilient Infrastructure, London, NDM-519, 1-10

[12] Kaczinski, MR., Dexter, RJ., and Van Dien, JP., 1998. Fatigue-resistant design of cantilevered signal, sign and light supports. Transportation Research Board, NCHRP Report 412, National Research Council

[13] MATLAB® and Statistics Toolbox, Release 2018b, the MathWorks, Inc., Natick, Massachusetts, United States

[14] Matus, M., 2018. Experimental Investigation of Wind-Induced Response of Span-Wire Traffic Signal Systems. FIU Electronic Theses and Dissertations

[15] McDonald J. R., Mehta, K. C., Oler, W. and Pulipaka N., 1995. Wind load effects on signs, luminaires and traffic signal structures. Department of Transportation, Report 1303-1F, Texas, USA

[16] Sivarao, Subramanian, S. K., Esro, M. and Anand, T. J. S., 2010. Electrical & Mechanical Fault Alert Traffic Light System Using Wireless Technology. International Journal of Mechanical & Mechatronics Engineering IJMME-IJENS, Vol:10, No:04

[17] Xu Xie, Ziaozhang Li and Yonggang Shen, “Static and Dynamic Characteristics of a Long-span Cable-stayed Bridge with CFRP Cables”, June 2014.

APPENDIX A – Stiffness of Span Wire Systems and Use of Springs in a Test Rig of Shorter Span

Force Relationships for Messenger Wire

1. Consider a wire tensioned between two anchor points as shown in **Error! Reference source not found.**. This can be thought of as the messenger wire. If a force F_n is applied normal to its span (either vertically or horizontally) at the point of attachment of the signal/hanger system, the balance of forces in the normal direction is given by

$$F_n = T_a \sin\theta_a + T_b \sin\theta_b \qquad \textit{Equation A 1}$$

In the direction parallel to the span it is

$$T_a \cos\theta_a = T_b \cos\theta_b \qquad \textit{Equation A 2}$$

where θ_a and θ_b are the deflection angles of the wire as shown in **Error! Reference source not found.**. T_a and T_b are tensions in the wire either side of the point of application of the force which is defined by the part span lengths L_a and L_b. The total span length is $L = L_a + L_b$.

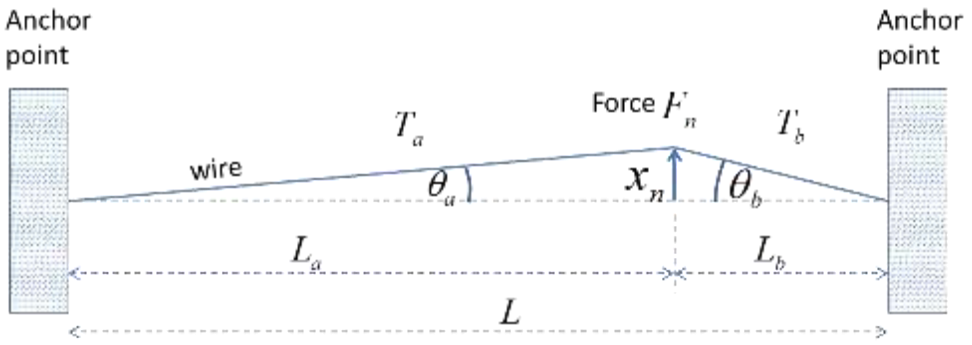

Figure A 1 Deflection of wire due to application of a force normal to the span

The deflection angles are related to the deflection distance x_n by

$$\sin\theta_a = \frac{x_n}{\sqrt{L_a^2 + x_n^2}} \quad , \quad \sin\theta_b = \frac{x_n}{\sqrt{L_b^2 + x_n^2}} \qquad \textit{Equation A 3}$$

For small deflections (e.g. $\frac{x_n}{L_a}, \frac{x_n}{L_b} < 0.1$) these can be simplified to within ½% accuracy by

$$\sin\theta_a = \frac{x_n}{L_a} \quad , \quad \sin\theta_b = \frac{x_n}{L_b} \qquad \textit{Equation A 4}$$

Also, for small deflections, $\cos\theta_a \approx \cos\theta_b \approx 1.0$, which implies that to good approximation

$$T_a = T_b \qquad \textit{Equation A 5}$$

So for further analysis we will simply use the symbol T, rather than distinguishing between T_a and T_b, and the balance of forces as given by Equation 1 may be written for small deflections as

$$F_n = T\left(\frac{L}{L_a L_b}\right)x_n \qquad \textit{Equation A 6}$$

If the wire were to be replaced by a spring of stiffness k_n in the normal direction the relationship between force and deflection would be

$$F_n = k_n x_n \qquad \textit{Equation A 7}$$

From this we see that the wire behaves like a spring aligned normal to the span and that its stiffness is

$$k_n = T\left(\frac{L}{L_a L_b}\right) \qquad \textit{Equation A 8}$$

If the point of application of the force is at mid-span then this reduces to

$$k_n = 4\frac{T}{L} \qquad \textit{Equation A 9}$$

Wire Tension and Effect of Wire Extension

When the normal force is applied to the wire, if the end anchors are absolutely rigid, then the wire must extend in order to deflect. If it extends then there must be a corresponding increase

in tension. The extended length after application of the force F_n is $L(1+\varepsilon)$, where $\varepsilon =$ strain in the wire. By geometry we have:

$$L(1+\varepsilon) = \left(L_a^2 + x_n^2\right)^{1/2} + \left(L_b^2 + x_n^2\right)^{1/2} \qquad \text{Equation A 10}$$

For small deflections (e.g. $\frac{x_n}{L_a} < 0.1$) the right-hand side of this equation may be simplified using the truncated binomial expression, resulting in:

$$\begin{aligned} L(1+\varepsilon) &= L_a\left(1+\frac{1}{2}\left(\frac{x_n}{L_a}\right)^2\right) + L_b\left(1+\frac{1}{2}\left(\frac{x_n}{L_b}\right)^2\right) \\ &= L + \frac{1}{2}x_n^2\left[\frac{1}{L_a}+\frac{1}{L_b}\right] = L\left(1+\frac{1}{2}\left[\frac{L^2}{L_aL_b}\right]\left(\frac{x_n}{L}\right)^2\right) \end{aligned} \qquad \text{Equation A 11}$$

From this relationship we see that the strain in the wire is

$$\varepsilon = \frac{1}{2}\left[\frac{L^2}{L_aL_b}\right]\left(\frac{x_n}{L}\right)^2 \qquad \text{Equation A 12}$$

The strain is related to the change in the wire tension ΔT by

$$\Delta T = EA\varepsilon \qquad \text{Equation A 13}$$

From this is follows that the total tension is

$$T = T_0 + \Delta T = T_0 + EA\frac{1}{2}\left[\frac{L^2}{L_aL_b}\right]\left(\frac{x_n}{L}\right)^2 \qquad \text{Equation A 14}$$

where $T_0 =$ initial wire tension before application of the normal force F_n. Combining this with Equation 6 we deduce that the relationship between normal force F_n and deflection x_n is

$$F_n = \frac{T_0}{L}\left(\frac{L^2}{L_aL_b}\right)x_n + \frac{1}{2}\frac{EA}{L^3}\left[\frac{L^4}{L_a^2L_b^2}\right]x_n^3 \qquad \text{Equation A 15}$$

For the case where the force is applied at mid-span this becomes

$$F_n = 4\frac{T_0}{L}x_n + 8\frac{EA}{L^3}x_n^3 \qquad \textit{Equation A 16}$$

This relationship shows that the Force/Deflection relationship is non-linear. As an example, suppose we have 3/8" diameter wire, for which the value of $EA = 0.81\times10^6$ lb is estimated, and that the span is $L = 84$ ft. For 3/8" diameter wire FDOT specifies that $T_0 = \frac{L}{100}\times 340 = 286$ lb. Therefore, for this case Equation 16 tells us that at mid span

$$F_n = 13.6\,x_n + 10.9\,x_n^3\,lb \qquad \textit{Equation A 17}$$

where x_n is in ft. So, for 1 ft deflection the force is 24.5 lb, nearly half of which comes from the second non-linear term. Note that if the span were 50 ft, not 84 ft, the force relationship would be

$$F_n = 22.9\,x_n + 51.8\,x_n^3 \qquad \textit{Equation A 18}$$

For 1 ft deflection the force is 74.7 lb, which is about three times as much as for 84 ft span and most of the force is contributed by the non-linear second term.

It appears that in practice the initial tension on the messenger wire is often set by the contractor to a much higher value than specified by FDOT. If $T_0 = 800$ lb for example, then the force for 1 ft deflection on an 84 ft span becomes 49 lb and on a 50 span becomes 115.8 lb. Thus, by tensioning to higher than FDOT specifications the system is considerably stiffened which almost certainly helps to improve aerodynamic stability of the signals but would increase stresses and forces at connections to the end anchors.

Note that the above derivation of the force-versus-deflection relationship is developed from first principles but has been checked by comparing results with those of Irvine (1974), and Inglis (1963), and found to agree.

Test Rig Using Springs

In designing a test rig for full scale testing it is desirable to use a shorter span than in the field because this facilitates rotating the entire rig within the wind field of the test facility so as to explore the effect of various wind directions relative to the span. However, it is important in doing this that the span-wire possesses the same deflection versus force relationship as the field span. This can be achieved as follows for the case where the force is applied at mid-span in both the field and on the rig. In the field, the mid-span position for signals provides the least system stiffness, so it might be regarded as the most conservative case to examine (see next section for discussion of other positions), and in the rig at the Wall of Wind the signals are always set up so that they are symmetrically disposed about mid-span.

In Equation 16 we see that the coefficient of x_n in the first term on the right-hand side is $4\frac{T_0}{L}$. We want this coefficient to be the same on the rig as in the field. This will be achieved if we set the initial tension in the rig such that

$$T_{0,RIG} = \frac{L_{RIG}}{L_{FIELD}} T_{0,FIELD} \qquad \textit{Equation A 19}$$

where subscripts *RIG* and *FIELD* denote the rig and field quantities respectively.

The coefficient of the second term in Equation 16 is $8\frac{EA}{L^3}$ and we need to devise a way of achieving an "effective" EA value, AE_{eff}, in the rig so that

$$EA_{eff} = \left(\frac{L_{RIG}}{L_{FIELD}} \right)^3 EA_{FIELD} \qquad \textit{Equation A 20}$$

If we insert springs near each end of the wire as shown in **Error! Reference source not found.**, in t he rig the extension of the wire plus springs when the tension is increased by ΔT is

$$\delta L = \frac{L_{wire}\Delta T}{EA_{RIG}} + 2\frac{\Delta T}{k} \qquad \text{Equation A 21}$$

where L_{wire} is the length of the wire in the rig after subtracting the length occupied by the springs.

We want δL to be the same as would occur without springs but with a rig wire that has an effective EA value given by Equation 20. Therefore, from Equations 20 and 21

$$\frac{L_{wire}\Delta T}{EA_{RIG}} + 2\frac{\Delta T}{k} = \frac{L_{RIG}\Delta T}{EA_{eff}} = \frac{L_{RIG}\Delta T}{\left(\frac{L_{RIG}}{L_{FIELD}}\right)^3 EA_{FIELD}} \qquad \textit{Equation A 22}$$

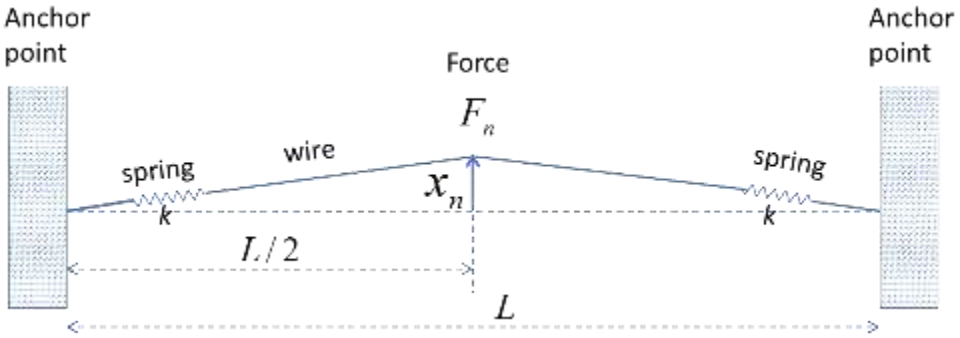

Figure A 2: Use of springs to represent longer span

From this equation it can be deduced that the required spring stiffness is:

$$k = \frac{2\left(\frac{L_{RIG}}{L_{FIELD}}\right)^3 \frac{EA_{FIELD}}{L_{RIG}}}{1-\left(\frac{L_{RIG}}{L_{FIELD}}\right)^3 \frac{EA_{FIELD}L_{WIRE}}{EA_{RIG}L_{RIG}}} \qquad \textit{Equation A 23}$$

In typical rig set ups the same diameter wire is used in the rig as in the field, so that $EA_{FIELD}/EA_{RIG} = 1$. Also, the factor $(L_{RIG}/L_{FIELD})^3$ in the WOW test rig is typically 1/64 or smaller and L_{WIRE}/L_{RIG} is less than 1.0. These facts combine to make the denominator in Equation 23 very close to 1.0. Therefore, for practical purposes the following simpler relationship can often be used to reasonable engineering accuracy

$$k \approx 2\left(\frac{L_{RIG}}{L_{FIELD}}\right)^3 \frac{EA_{FIELD}}{L_{RIG}} \qquad \textit{Equation A 24}$$

Case of Signal Positions Away from Mid-Span

When the signal in the field is not at mid-span, instead of using Equation 16 for the force versus deflection relationship, we need to use Equation 15. However, we would still typically mount the signal at mid-span on the rig. In this case, to match the first term on the right-hand side of Equation 15 we need to have

$$T_{0RIG} = T_{0FIELD} \frac{L_{RIG}}{L_{FIELD}} P \qquad \textit{Equation A 25}$$

where the position factor P is given by

$$P = \left(\frac{L_{FIELD}^2}{4 L_{a,FIELD} L_{b,FIELD}} \right) \qquad \textit{Equation A 26}$$

Error! Reference source not found. shows a plot of the position factor versus L_a / L, (note that EMBED Equation.3 $L_a + L_b = L$).

For the rig to match the second term on the right-hand side of Equation 15 we need it to have an effective EA value such that

$$EA_{eff} = EA_{FIELD} \left(\frac{L_{RIG}}{L_{FIELD}} \right)^3 P^2 \qquad \text{Equation A 27}$$

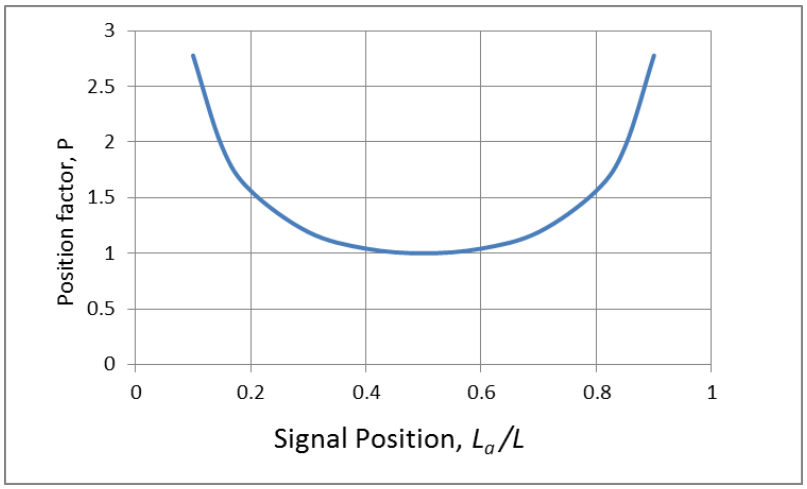

Figure A 3: Position factor as a function of signal position

Then using the same logic as before of matching the extension due to the required effective value EA_{eff} with that due to EA_{RIG} plus the springs, we have

$$\frac{L_{wire}\Delta T}{EA_{RIG}} + 2\frac{\Delta T}{k} = \frac{L_{RIG}\Delta T}{EA_{eff}} = \frac{L_{RIG}\Delta T}{\left(\frac{L_{RIG}}{L_{FIELD}}\right)^3 P^2 EA_{FIELD}} \qquad \textit{Equation A 28}$$

Thus, the expression for the required spring stiffness in the rig is

$$k = \frac{2\left(\frac{L_{RIG}}{L_{FIELD}}\right)^3 P^2 \frac{EA_{FIELD}}{L_{RIG}}}{1-\left(\frac{L_{RIG}}{L_{FIELD}}\right)^3 P^2 \frac{EA_{FIELD}L_{WIRE}}{EA_{RIG}L_{RIG}}} \qquad \textit{Equation A 29}$$

Again, the second term in the denominator would typically be very small compared with 1.0 for the FIU test rig, so to reasonable engineering approximation we have

$$k \approx 2\left(\frac{L_{RIG}}{L_{FIELD}}\right)^3 P^2 \frac{EA_{FIELD}}{L_{RIG}} \qquad \textit{Equation A 30}$$

From this expression we see that if the signals in the field are offset from the center of the span then the required spring stiffness will go up according the square of the position factor, i.e. P^2. The minimum value of P is 1.0 which occurs when the signal position is at mid-span. However, if

the signal is at the ¼ span position then $P = 4/3$ and P^2 =1.78, indicating a 78% increase in spring stiffness is required compared to the mid-span mounting position.

Treatment of Catenary Wire

In the case of the catenary wire is depicted in **Error! Reference source not found.** for the case w here the signal is mounted in the center. The initial tension T_0 is the result of the built in sag δ and the weight Mg , where M =mass of signal and g = gravitational acceleration. The balance of forces for small sag ratio δ / L may be written

$$Mg = T_0 . 4\frac{\delta}{L} \qquad \textit{Equation A 31}$$

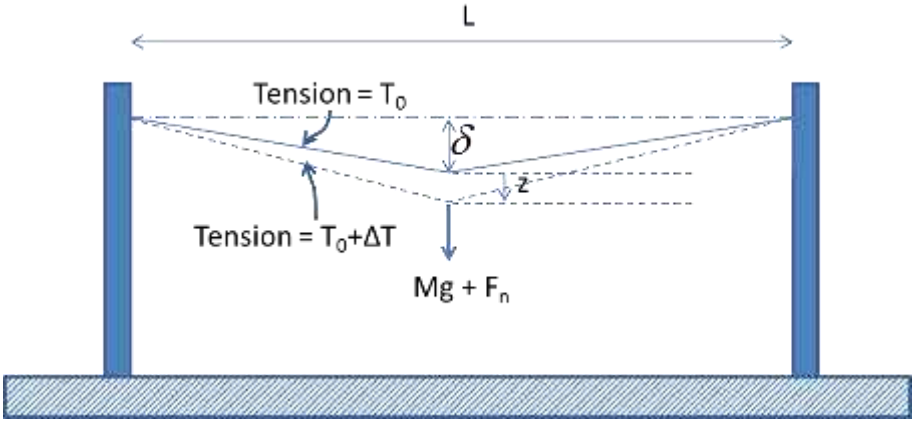

Figure A 4: Catenary deflections

When an additional force F_n acts vertically the balance of forces may be written for small sags and deflections as

$$Mg + F_n = (T_0 + \Delta T).4\frac{\delta + z}{L} \qquad \textit{Equation A 32}$$

where $\Delta T =$ additional tension and $z =$ additional deflection caused by application of force F_n. Subtracting Equation 31 from Equation 32 leads to

$$F_n = T_0 4\frac{\delta}{L} + \Delta T.4\frac{\delta + z}{L} \qquad \textit{Equation A 33}$$

The additional tension may be written in terms of the extra strain ε caused by application of F_n.

$$\Delta T = EA\varepsilon \qquad \text{Equation A 34}$$

where EA is the extensible stiffness per unit length of the catenary wire. The strain can be shown to be

$$\varepsilon = 4\frac{z\delta}{L^2} + 2\left(\frac{z}{L}\right)^2 \qquad \textit{Equation A 35}$$

Combining Equations 33 through 34 leads to the force versus deflection relationship for the catenary wire

$$F_n = 4\frac{T_0}{L}z + 8\frac{EA}{L^3}\left[z^3 + 3z^2\delta + 2z\delta^2\right] \qquad \textit{Equation A 36}$$

Therefore, on the rig we can obtain the same relationship between vertical force and deflection provided that we satisfy 2 criteria which are:

1. The sag distance δ is kept the same as in the field. This ensures both that $\frac{T_0}{L}$ is maintained the same as in the field and that the coefficients of z^2 and z in the square brackets in Equation 36 are kept the same as in the field.
2. The parameter $\frac{EA}{L^3}$ is kept the same as in the field, which can be achieved as described above for the messenger wire, by using springs to achieve an effective value of EA which is scaled down in proportion to L^3.

It can be seen that these are the same criteria as were found for correctly simulating the messenger wire behavior on a rig with shorter span L than in the field. Therefore, the same method for calculating the required spring stiffness for the messenger wire can be applied for vertical deflections of the catenary wire. Also, for small sag ratios it can be shown that the same springs used to simulate the vertical force-versus-deflection relationship of the catenary deflections give the correct relationship for the horizontal direction.

APPENDIX B – (Task 1a: FULL SCALE TESTING - CASE 3)

Results for total drag/lift forces on the traffic signals, and rms of accelerations for 45 degrees wind direction

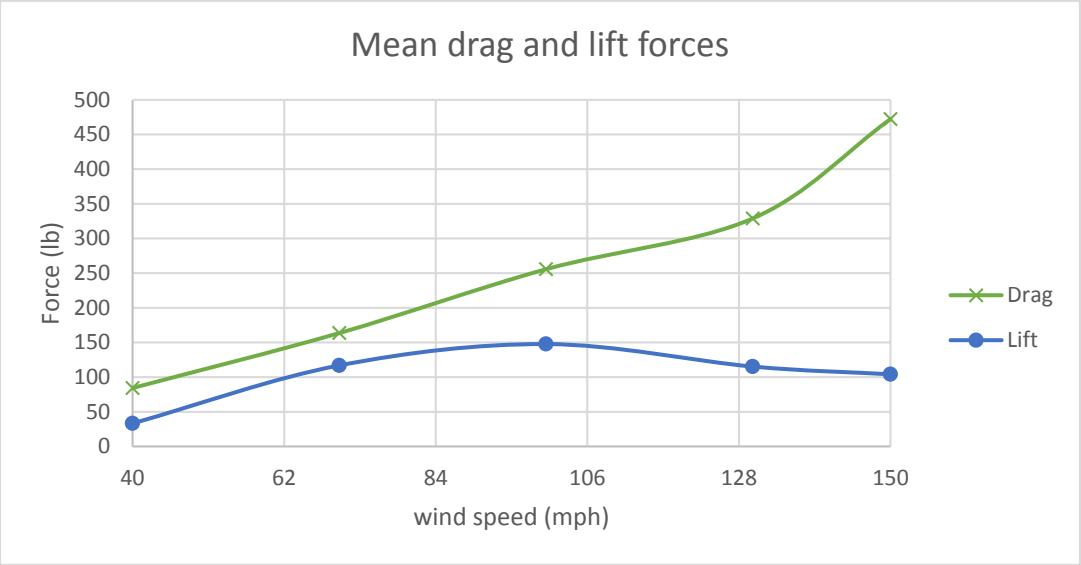

Figure B 1 Mean drag and mean lift forces at 45 degrees wind direction on the traffic signals

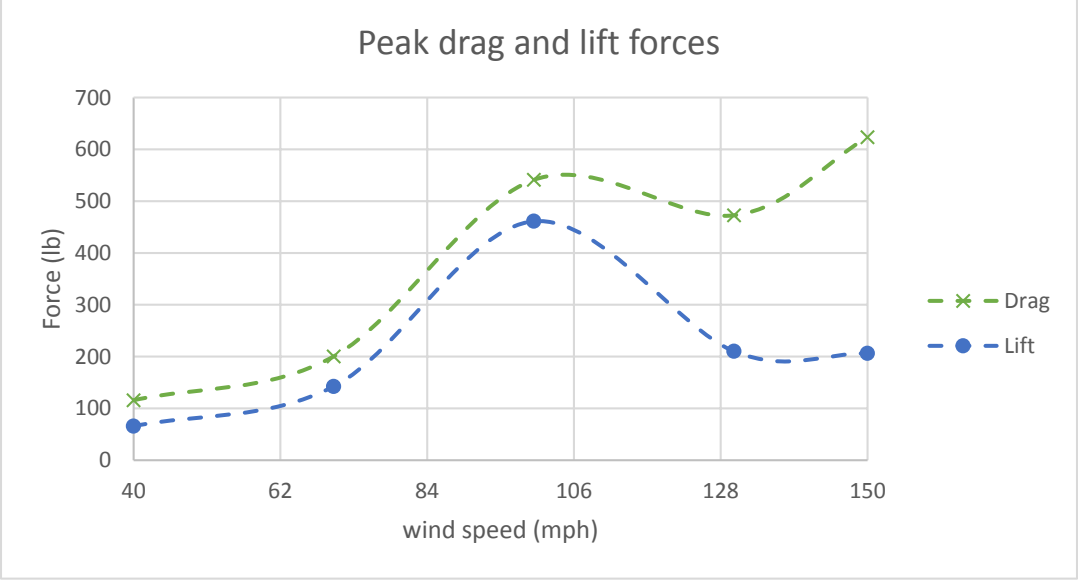

Figure B 2: Peak drag and peak lift forces at 45 degrees wind direction on the traffic signals

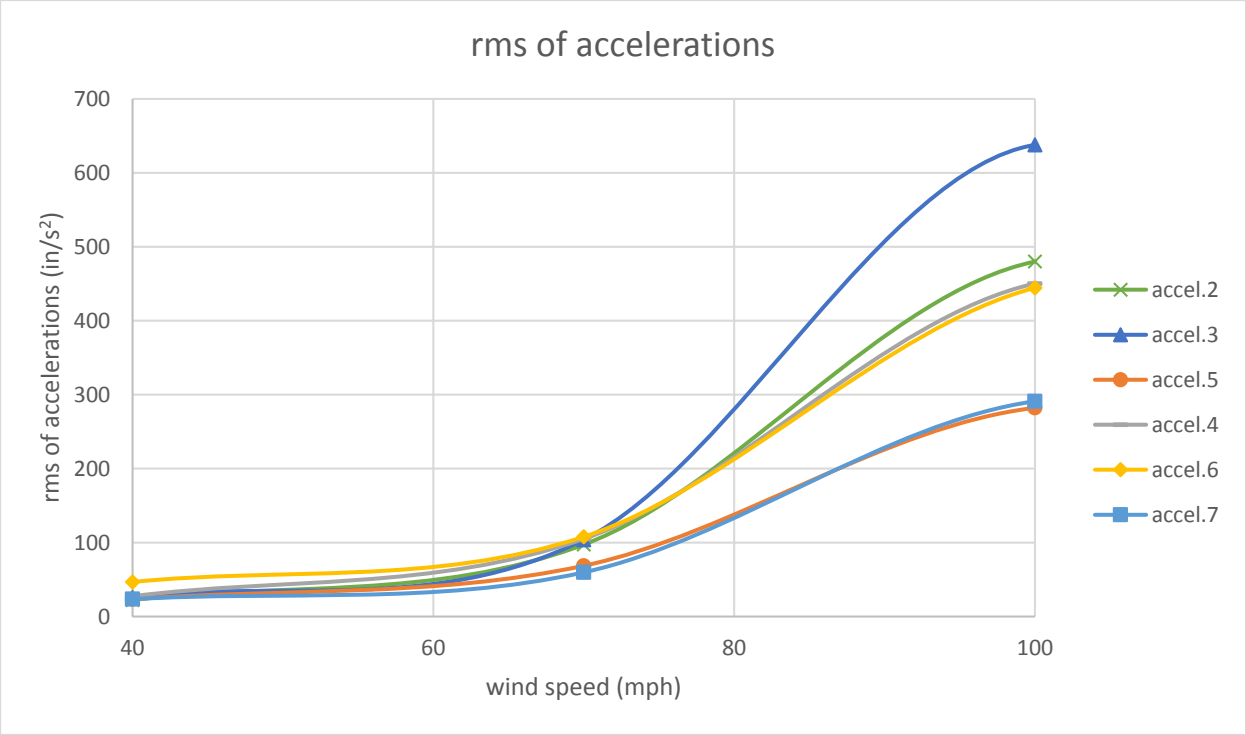

Figure B 3: rms of accelerations at 45 degrees wind direction for various wind speeds

Results for total drag/lift forces on the traffic signals, and rms of accelerations for 80 degrees wind direction

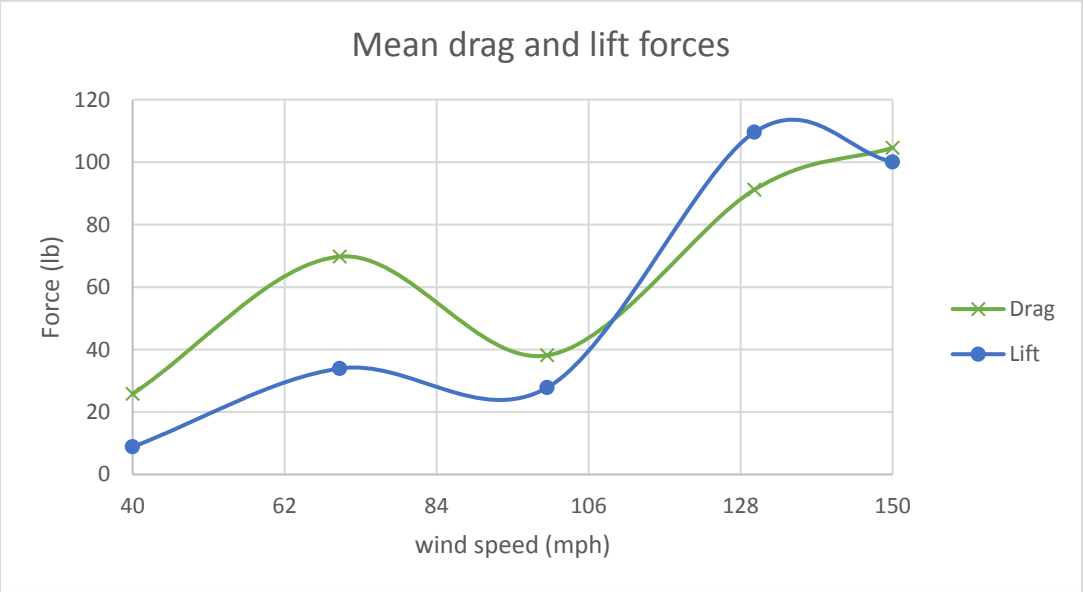

Figure B 4: Mean drag and mean lift forces at 80 degrees wind direction on the traffic signals

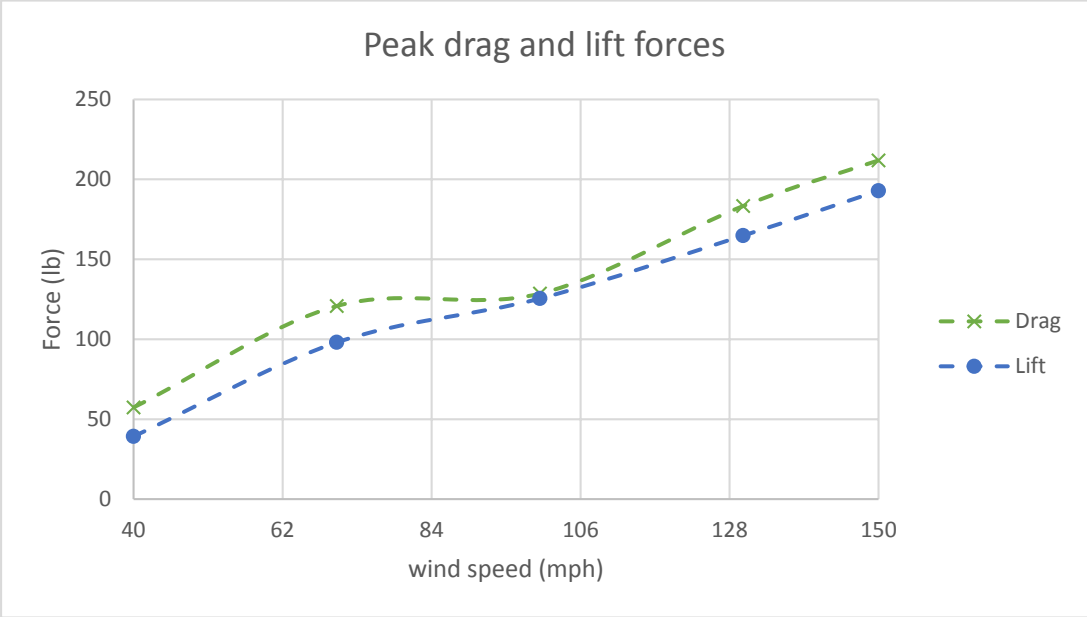

Figure B 5: Peak drag and peak lift forces at 80 degrees wind direction on the traffic signals

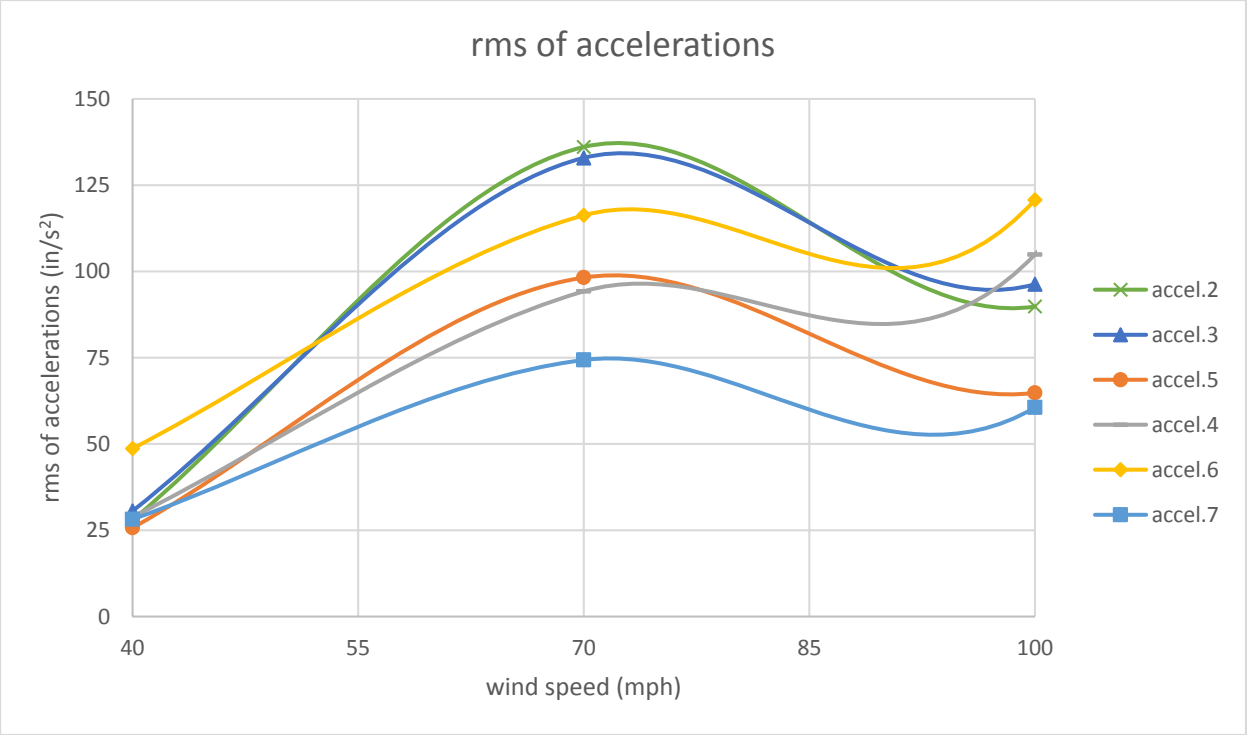

Figure B 6: rms of accelerations at 80 degrees wind direction for various wind speeds

Results for total drag/lift forces on the traffic signals, and rms of accelerations for 100 degrees wind direction

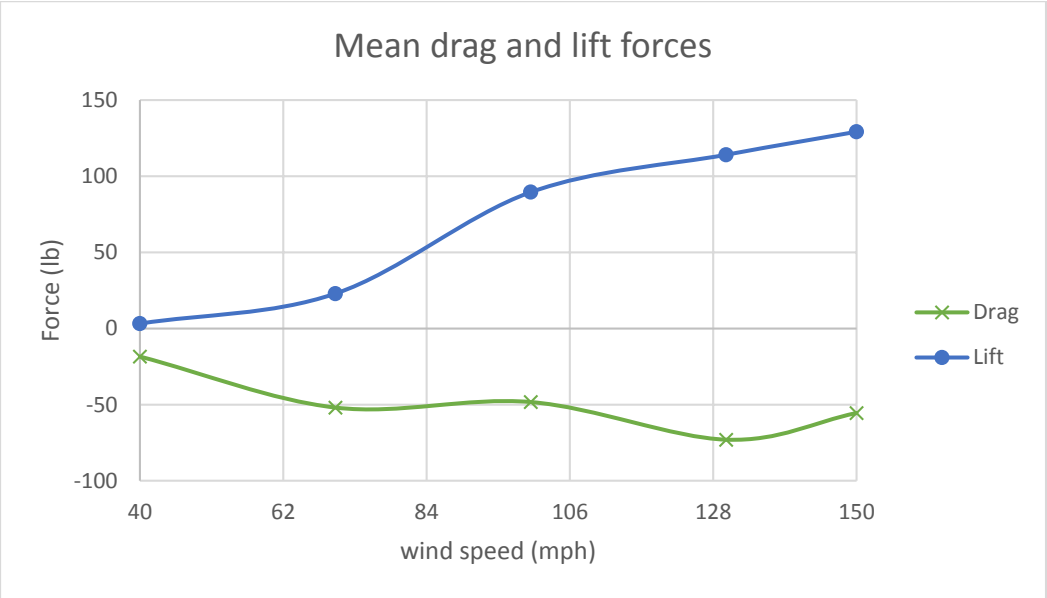

Figure B 7: Mean drag and mean lift forces at 100 degrees wind direction on the traffic signals

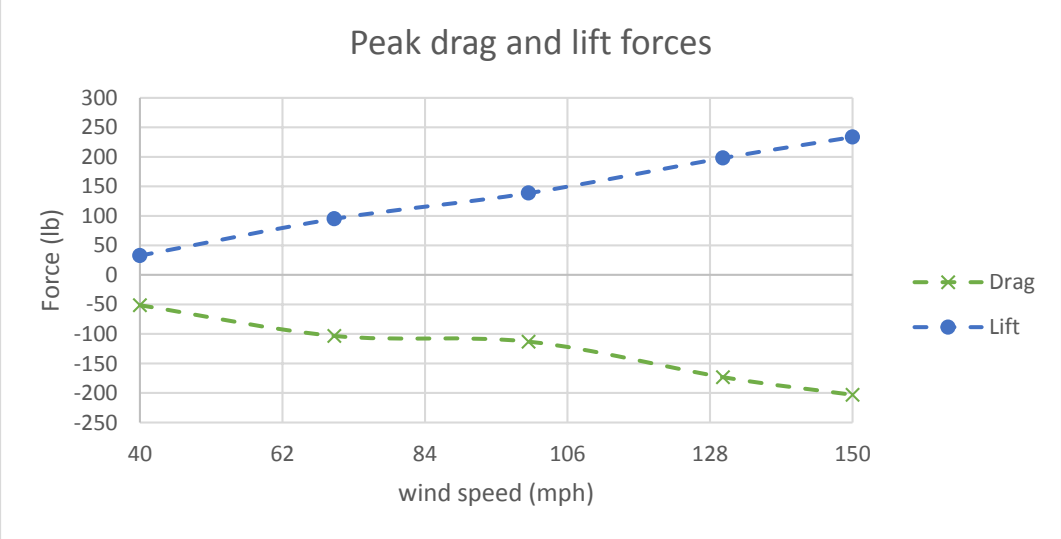

Figure B 8: Peak drag and peak lift forces at 100 degrees wind direction on the traffic signals

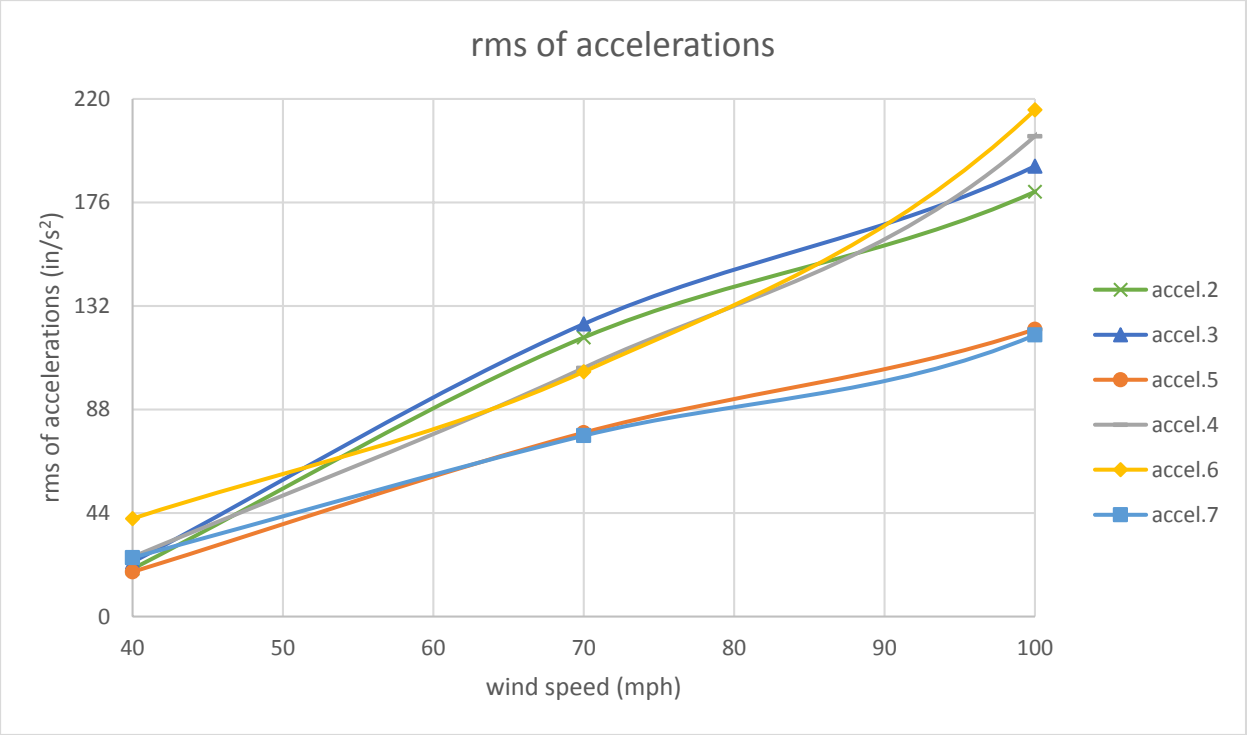

Figure B 9: rms of accelerations at 100 degrees wind direction for various wind speeds

Results for total drag/lift forces on the traffic signals, and rms of accelerations for 135 degrees wind direction

Figure B 10: Mean drag and mean lift forces at 135 degrees wind direction on the traffic signals

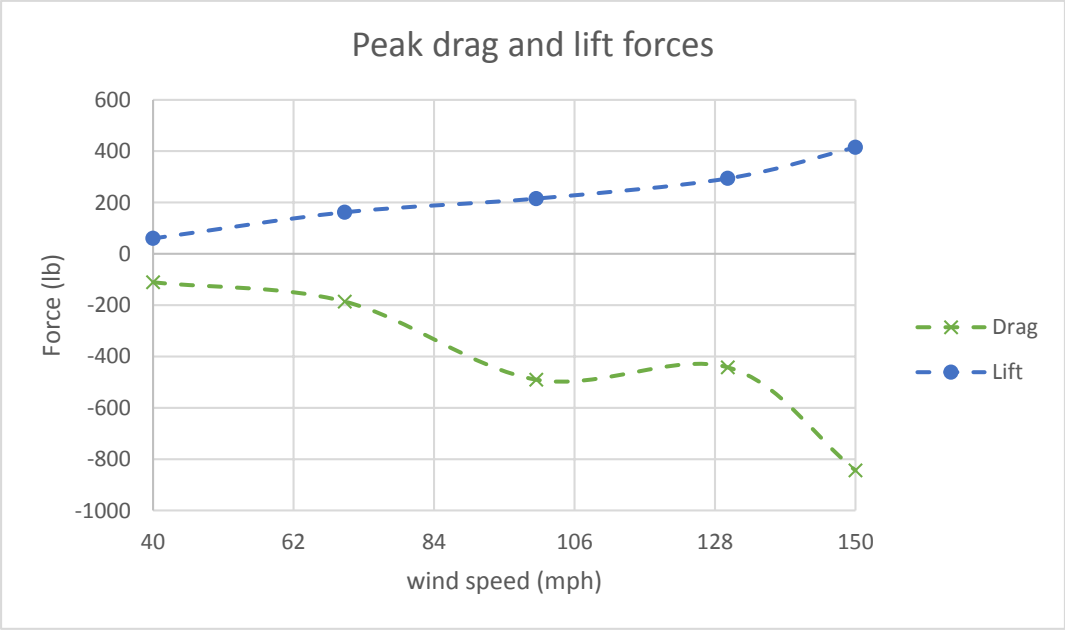

Figure B 11: Peak drag and peak lift forces at 135 degrees wind direction on the traffic signals

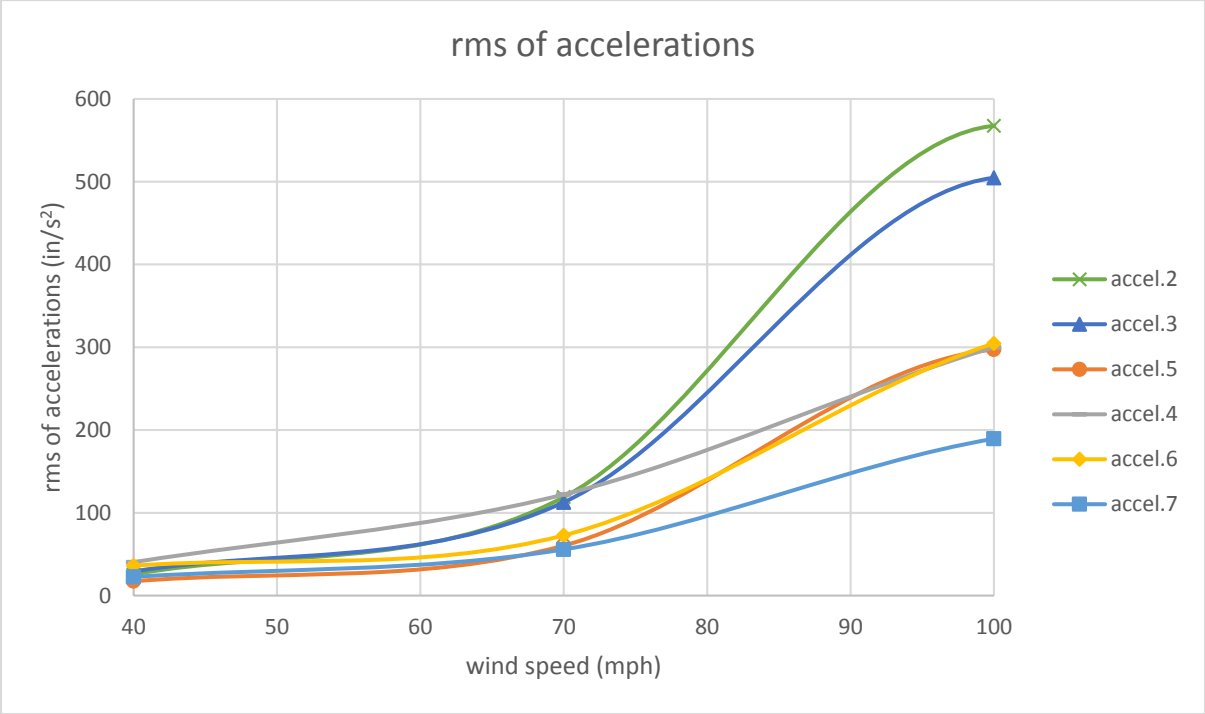

Figure B 12: rms of accelerations at 135 degrees wind direction for various wind speeds

Results for total drag/lift forces on the traffic signals, and rms of accelerations for 180 degrees wind direction

Figure B 13: Mean drag and mean lift forces at 180 degrees wind direction on the traffic signals

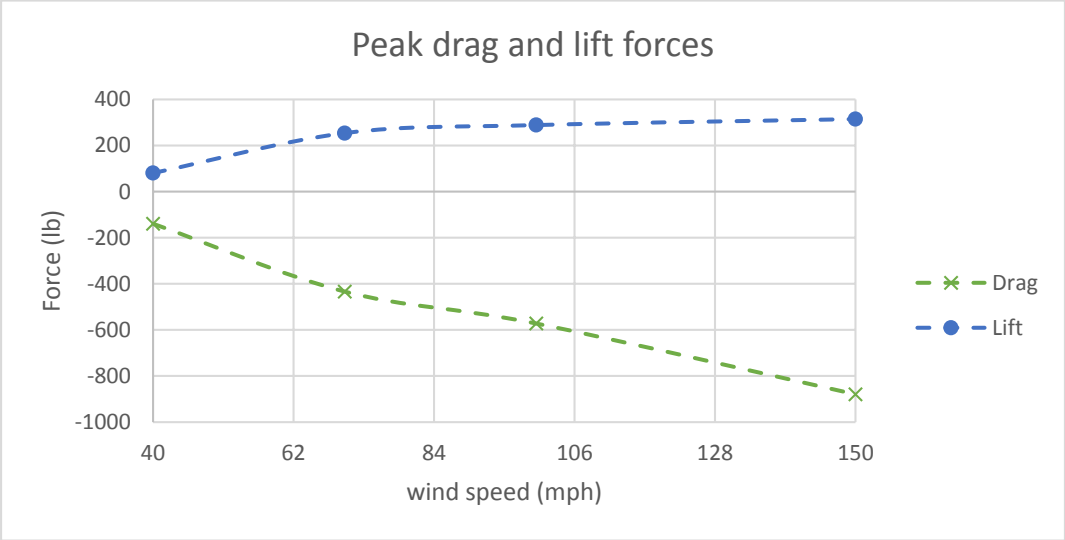

Figure B 14: Peak drag and peak lift forces at 180 degrees wind direction on the traffic signals

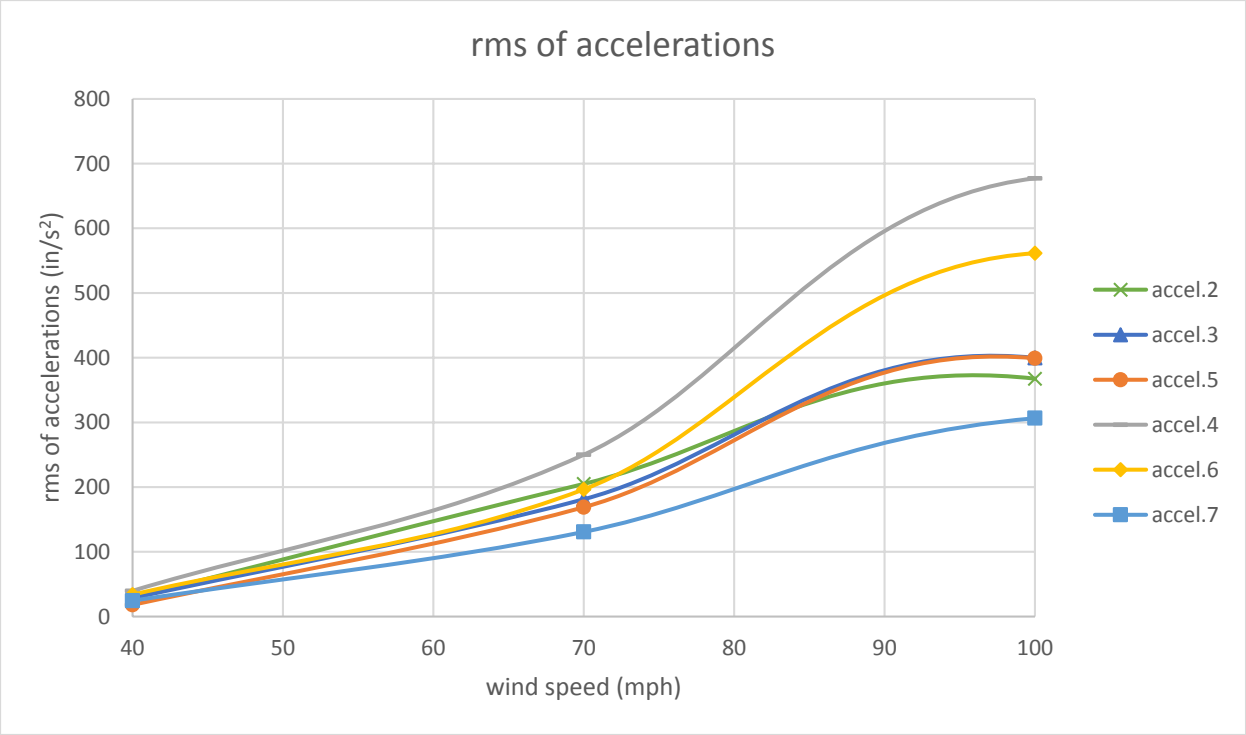

Figure B 15: rms of accelerations at 180 degrees wind direction for various wind speeds

APPENDIX C - (Task 1a: FULL SCALE TESTING - CASE 4)

Results for total drag/lift forces, and rms of accelerations for 45 degrees wind direction

Figure C 1: Mean drag and lift forces on the traffic signals at 45 degrees wind direction

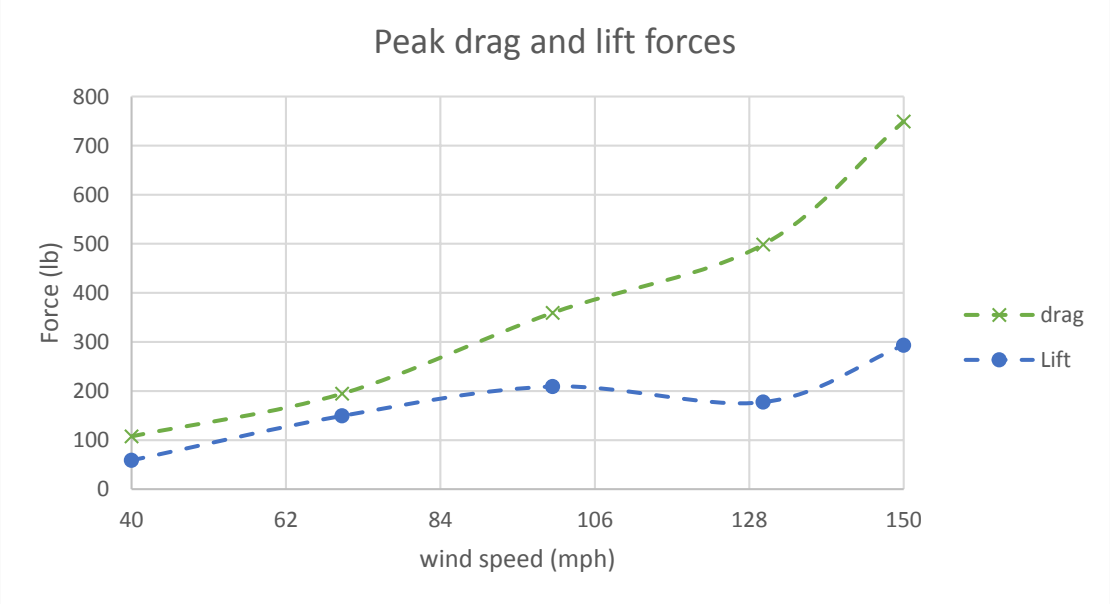

Figure C 2: Peak drag and lift forces on the traffic signals at 45 degrees wind direction

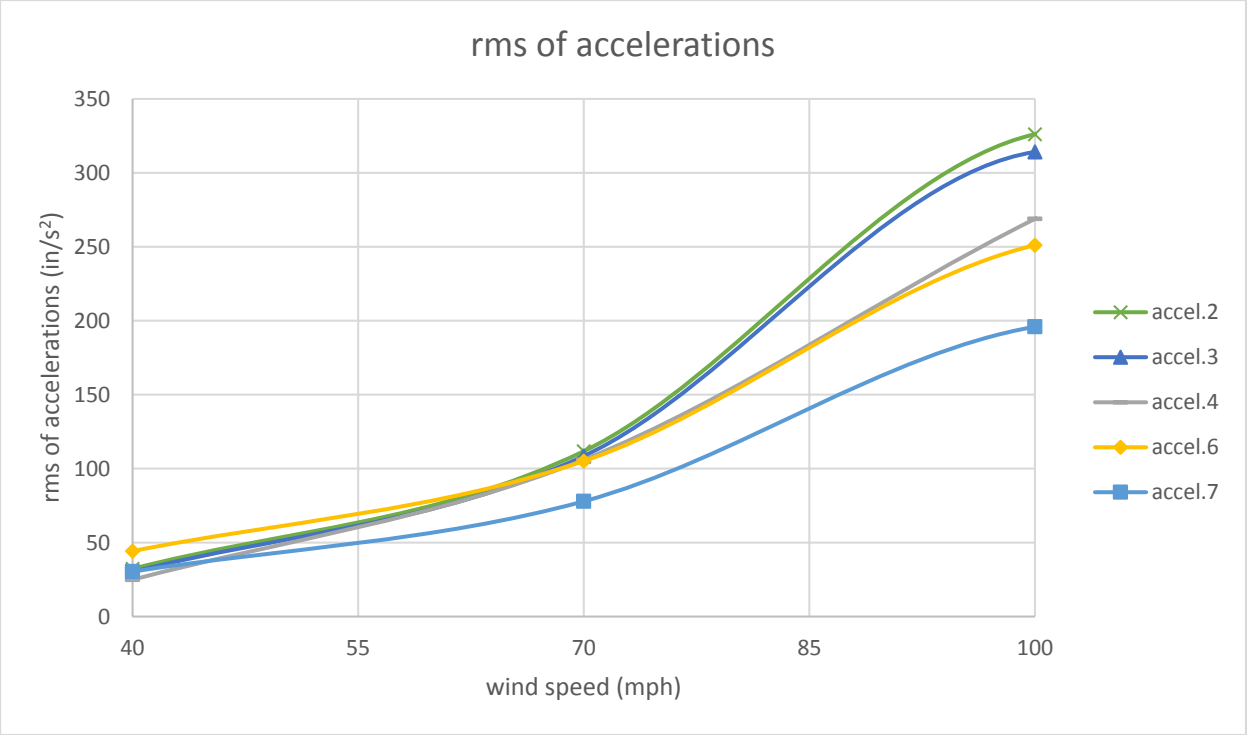

Figure C 3: rms of accelerations at 45 degrees wind direction for various wind speeds

Results for total drag/lift forces, and rms of accelerations for 80 degrees wind direction

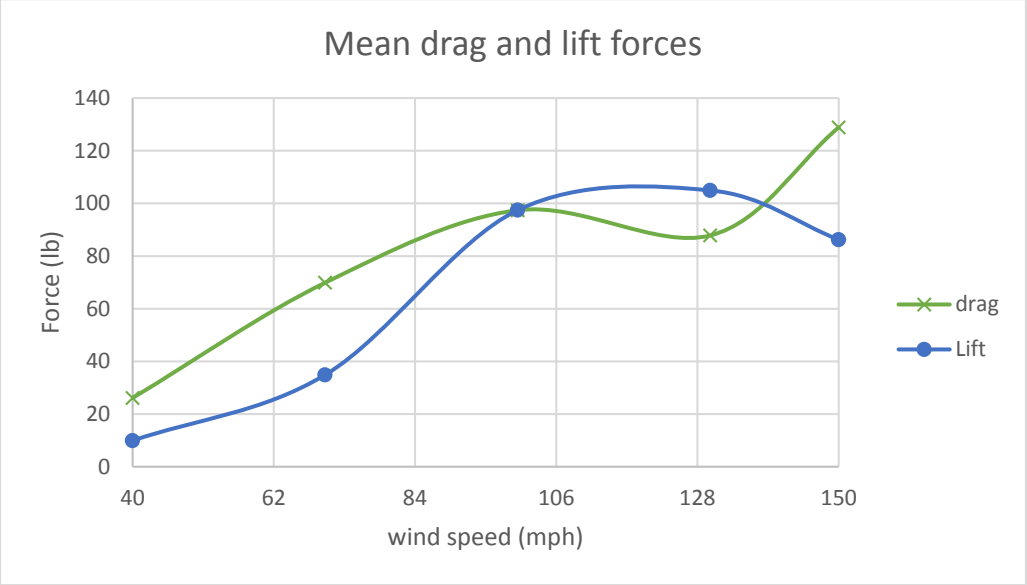

Figure C 4: Mean drag and lift forces on the traffic signals at 80 degrees wind direction

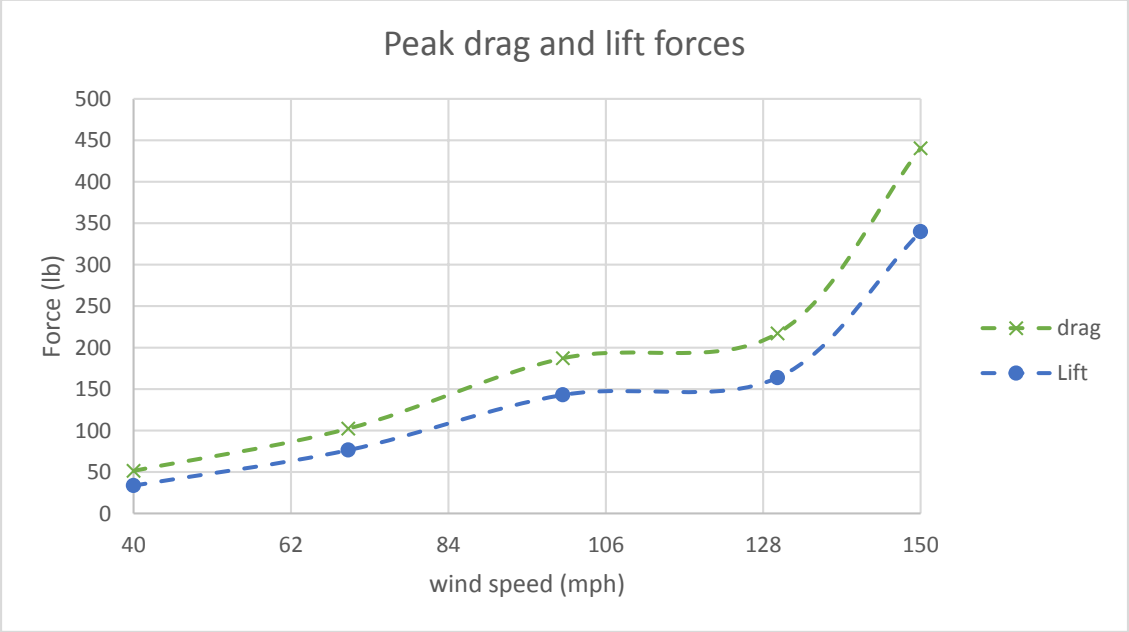

Figure C 5: Peak drag and lift forces on the traffic signals at 80 degrees wind direction

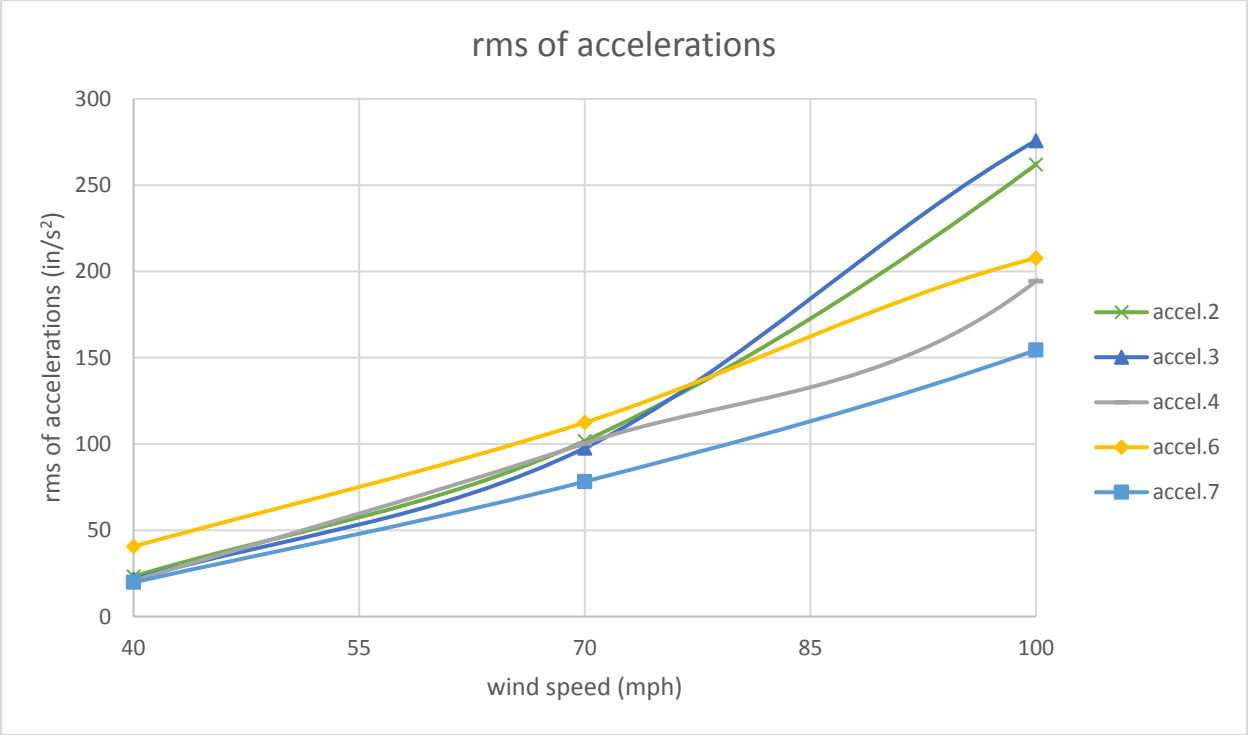

Figure C 6: rms of accelerations at 80 degrees wind direction for various wind speeds

Results for total drag/lift forces, and rms of accelerations for 100 degrees wind direction

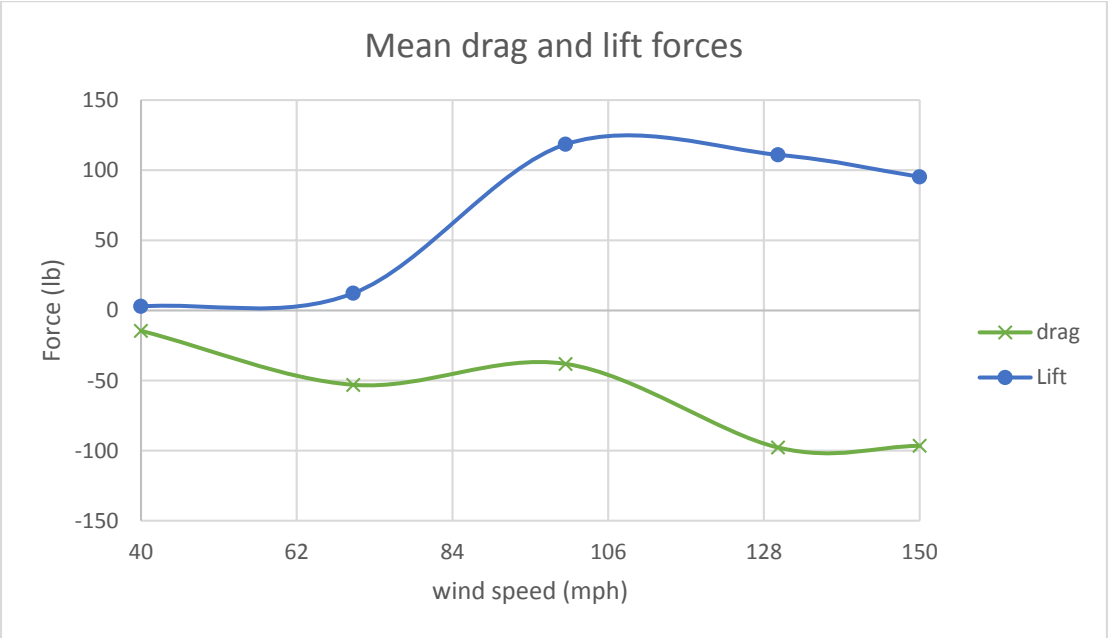

Figure C 7: Mean drag and lift forces on the traffic signals at 100 degrees wind direction

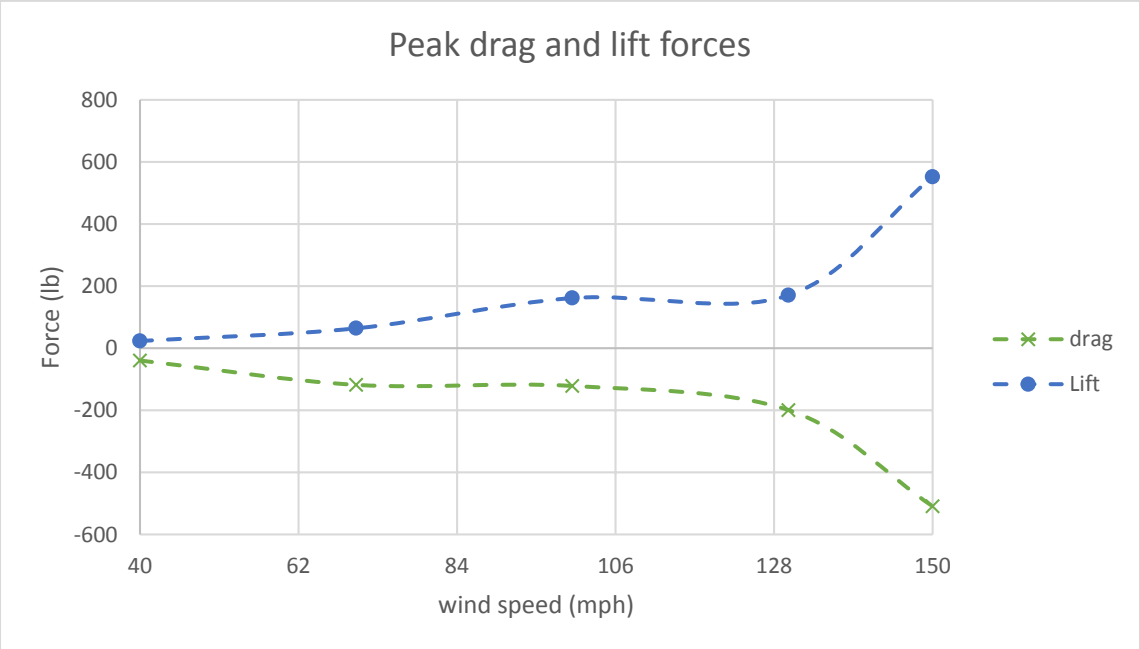

Figure C 8: Peak drag and lift forces on the traffic signals at 100 degrees wind direction

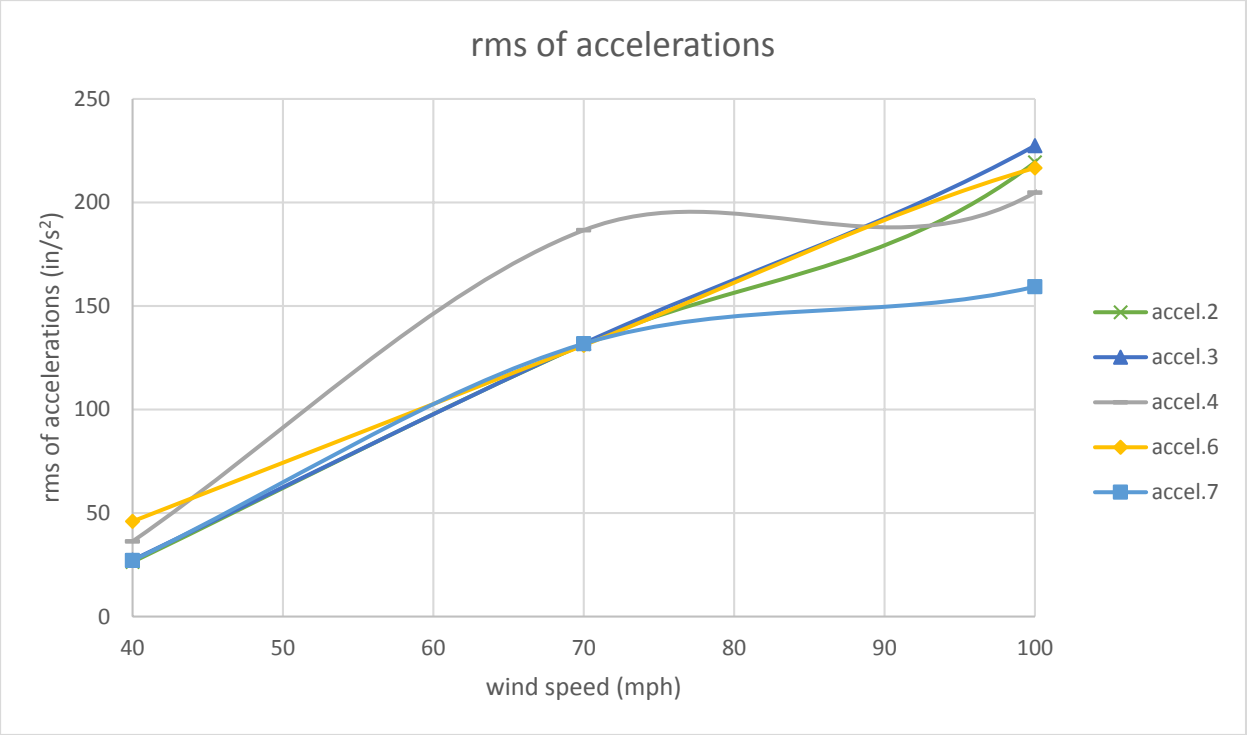

Figure C 9: rms of accelerations at 100 degrees wind direction for various wind speeds

Results for total drag/lift forces, and rms of accelerations for 135 degrees wind direction

Figure C 10: Mean drag and lift forces on the traffic signals at 135 degrees wind direction

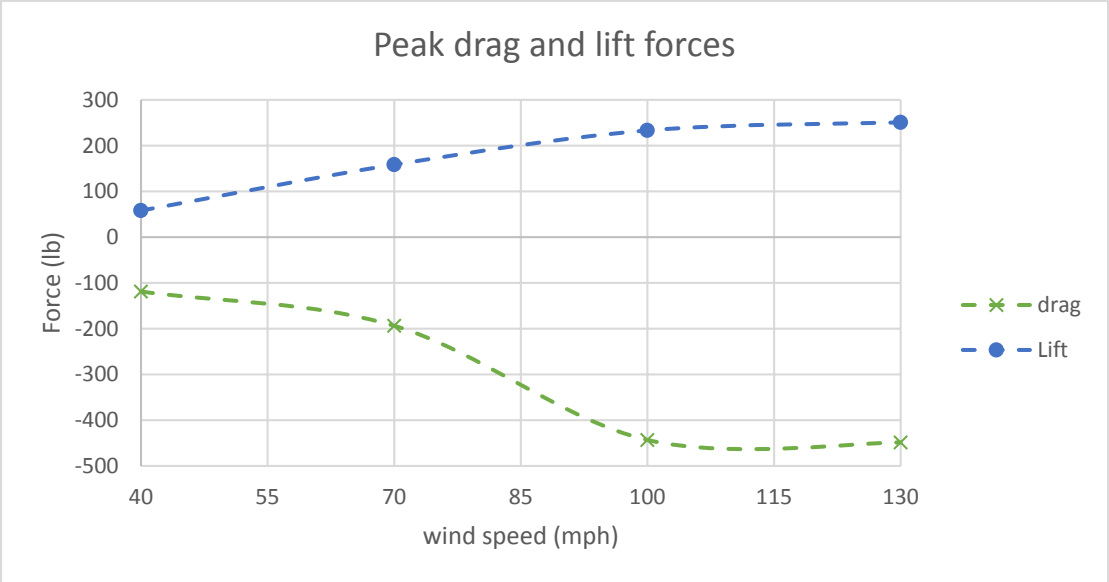

Figure C 11: Peak drag and lift forces at 135 degrees wind direction

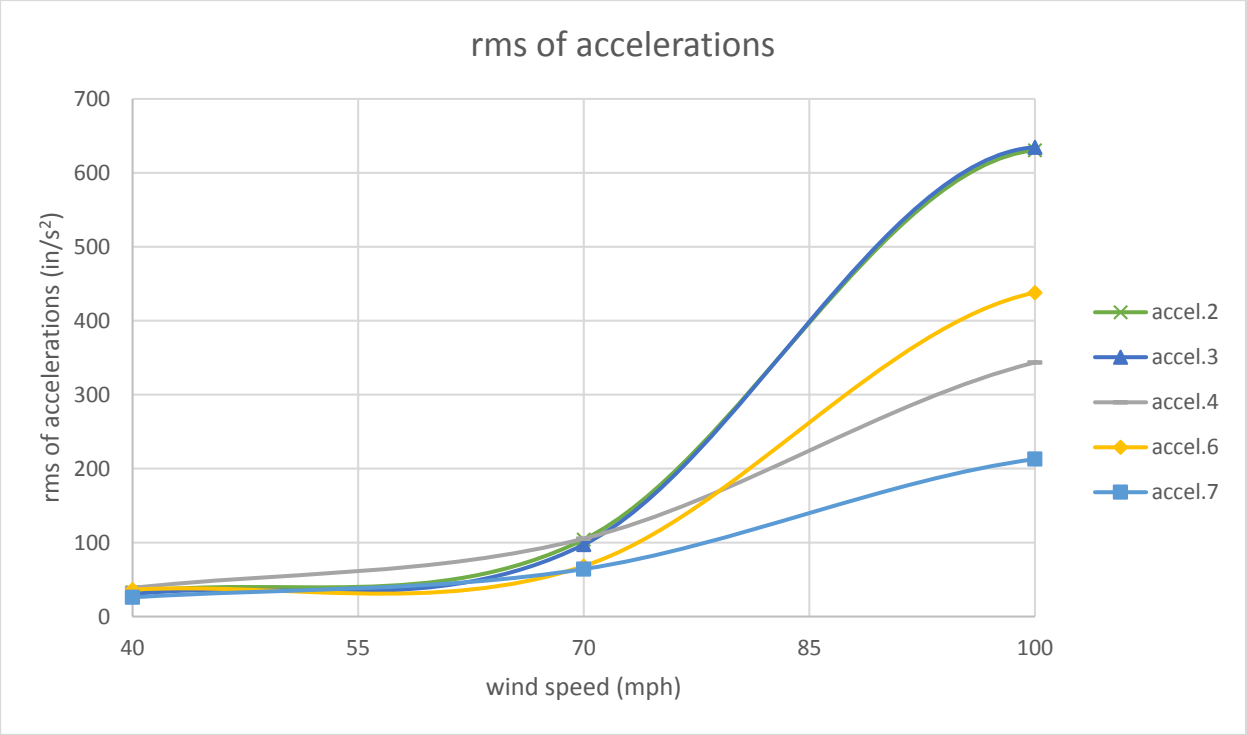

Figure C 12: rms of accelerations at 135 degrees wind direction for various wind speeds

Results for total drag/lift forces, and rms of accelerations for 180 degrees wind direction

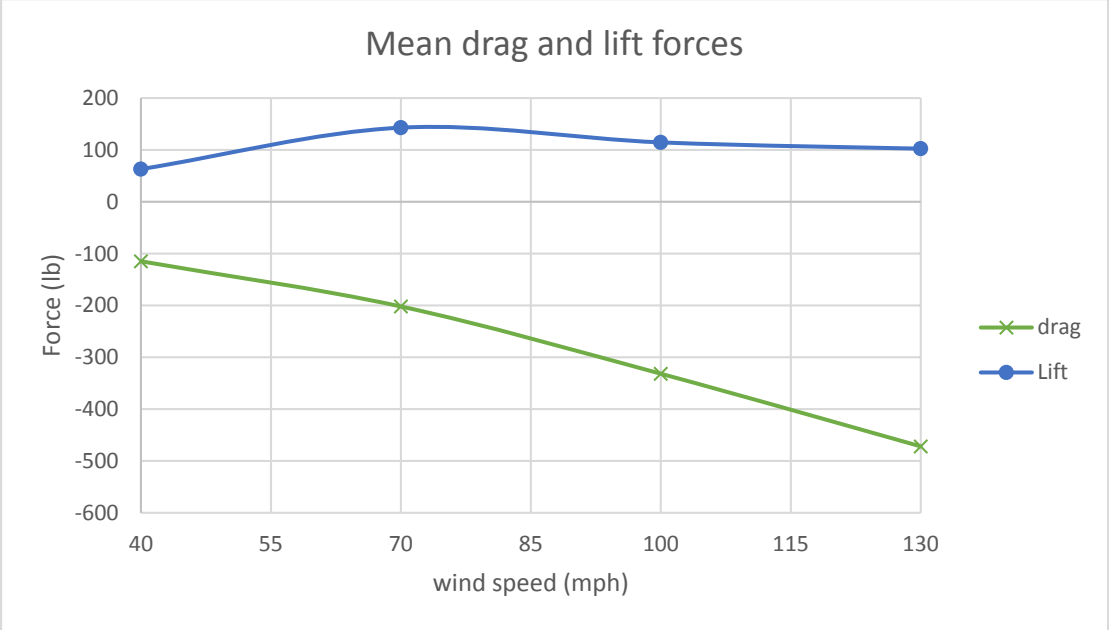

Figure C 13: Mean drag and lift forces on the traffic signals at 180 degrees wind direction

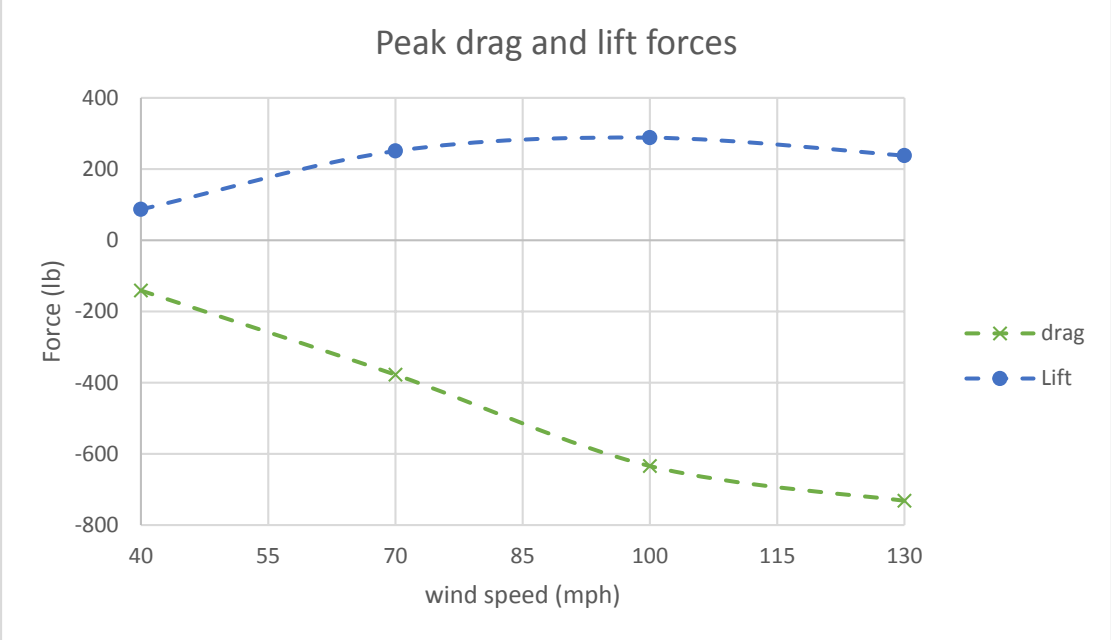

Figure C 14: Peak drag and lift forces on the traffic signals at 180 degrees wind direction

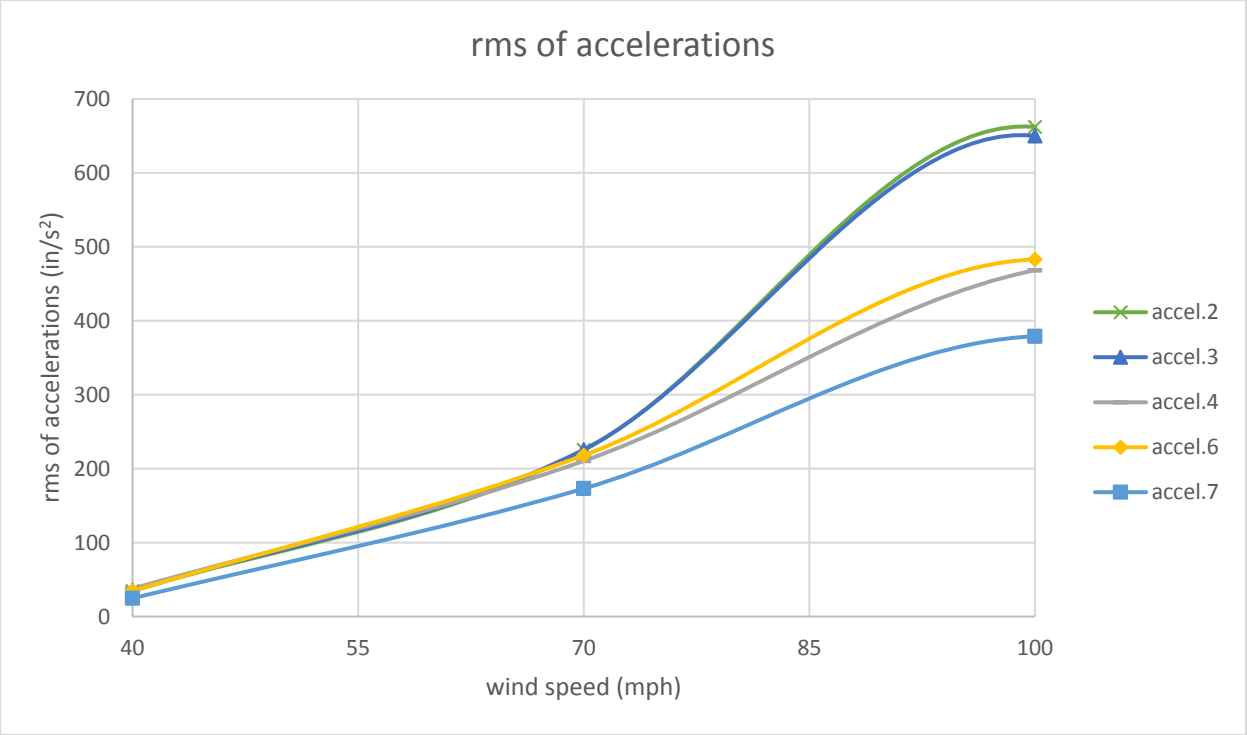

Figure C 15: rms of accelerations at 180 degrees wind direction for various wind speeds

APPENDIX D - (Task 1a: FULL SCALE TESTING - CASE 5)

Results for total drag/lift forces, and rms of accelerations for 45 degrees wind direction

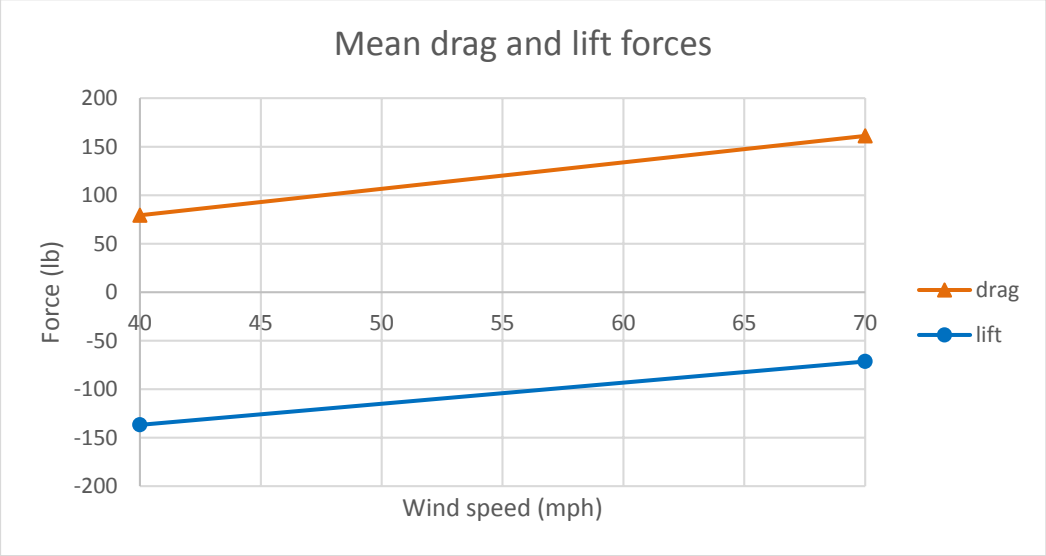

Figure D 1: Mean drag and lift forces on the traffic signals at 45 degrees wind direction

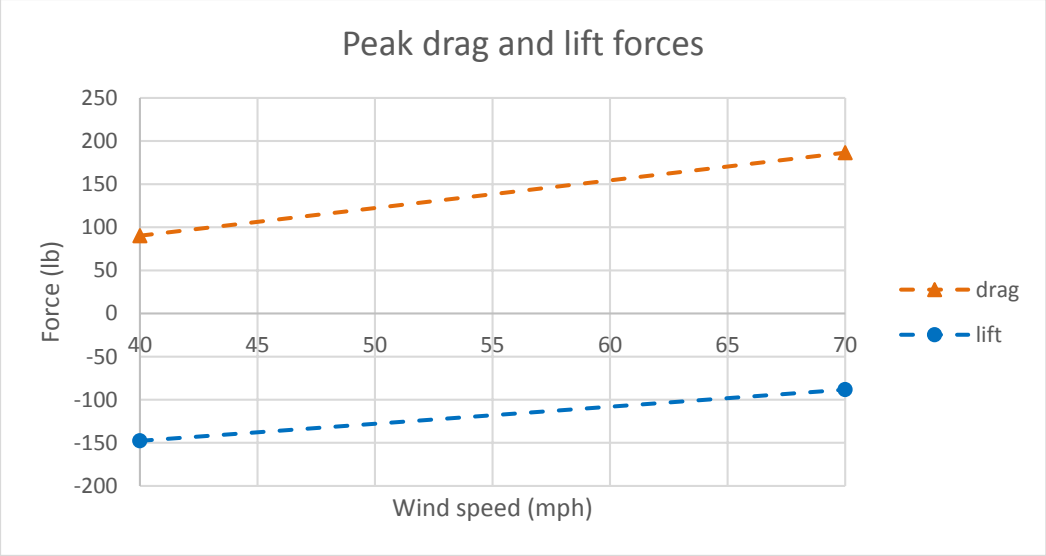

Figure D 2: Peak drag and lift forces on the traffic signals at 45 degrees wind direction

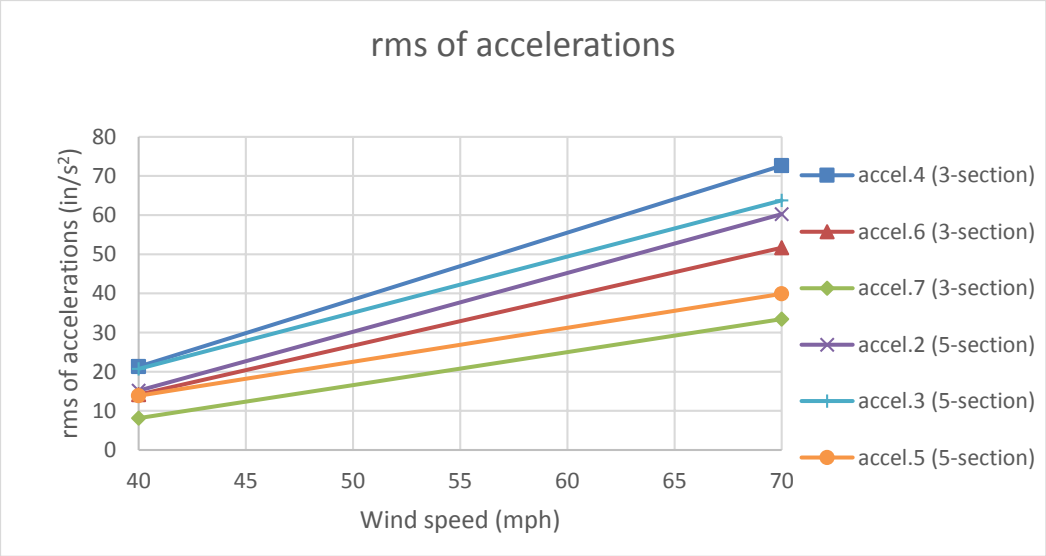

Figure D 3: rms of accelerations at 45 degrees wind direction for various wind speeds

Results for total drag/lift forces, and rms of accelerations for 80 degrees wind direction

Figure D 4: Mean drag and lift forces on the traffic signals at 80 degrees wind direction

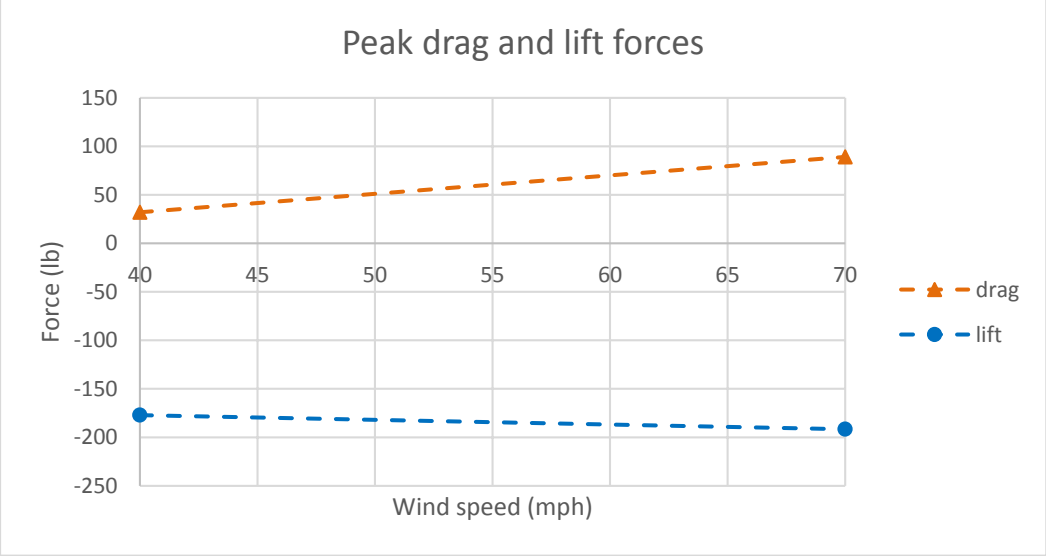

Figure D 5: Peak drag and lift forces on the traffic signals at 80 degrees wind direction

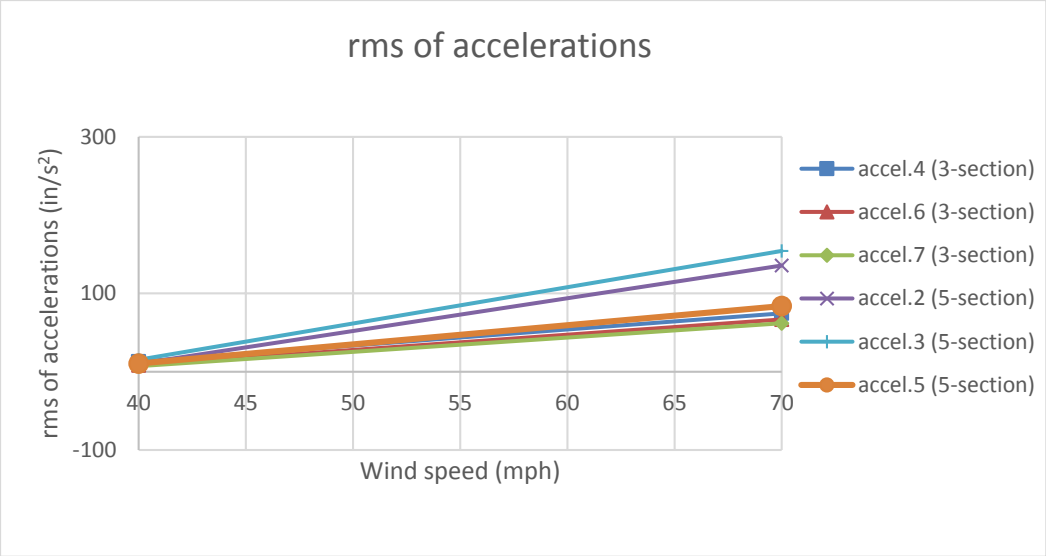

Figure D 6: rms of accelerations at 80 degrees wind direction for various wind speeds

Results for total drag/lift forces, and rms of accelerations for 100 degrees wind direction

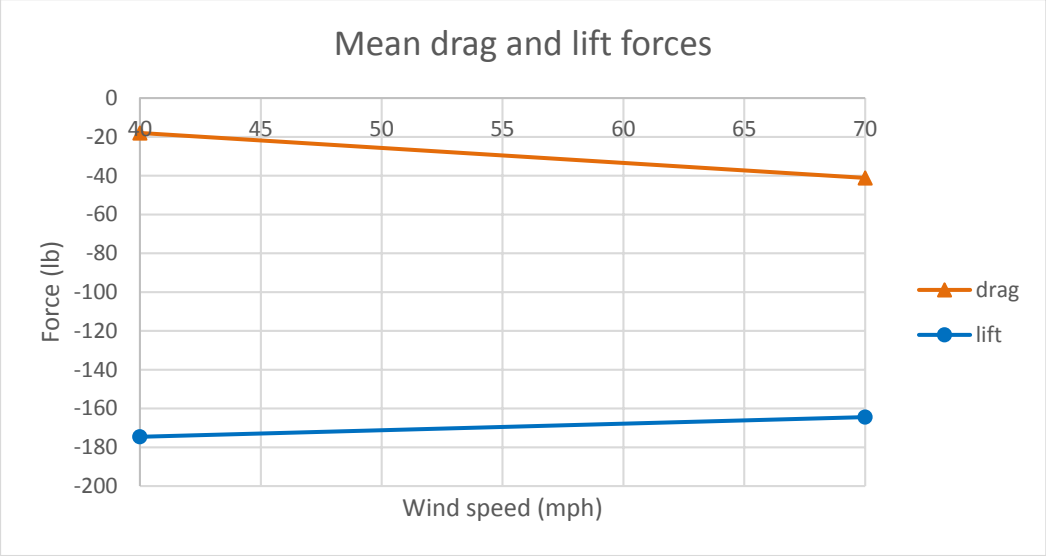

Figure D 7: Mean drag and lift forces on the traffic signals at 100 degrees wind direction

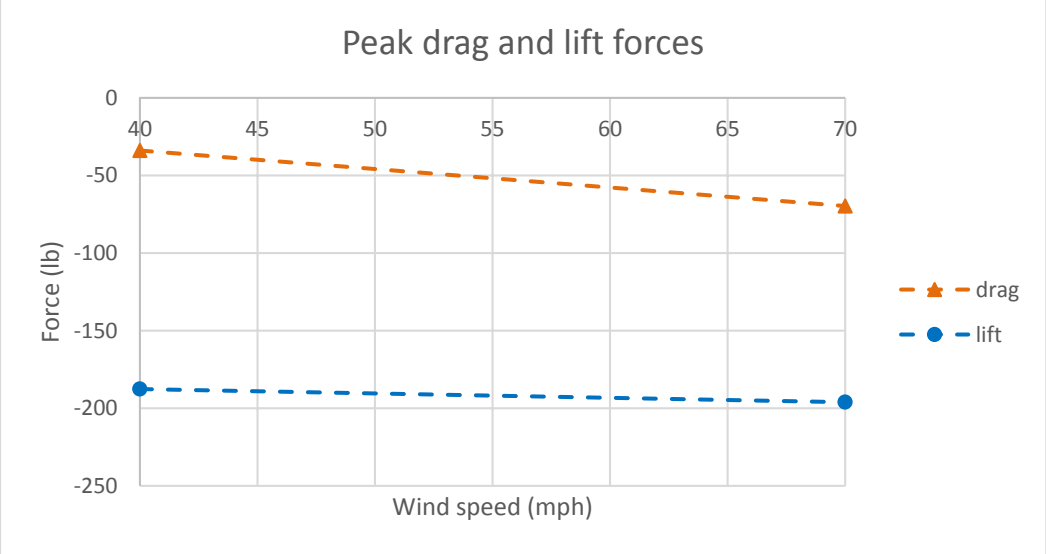

Figure D 8: Peak drag and lift forces on the traffic signals at 100 degrees wind direction

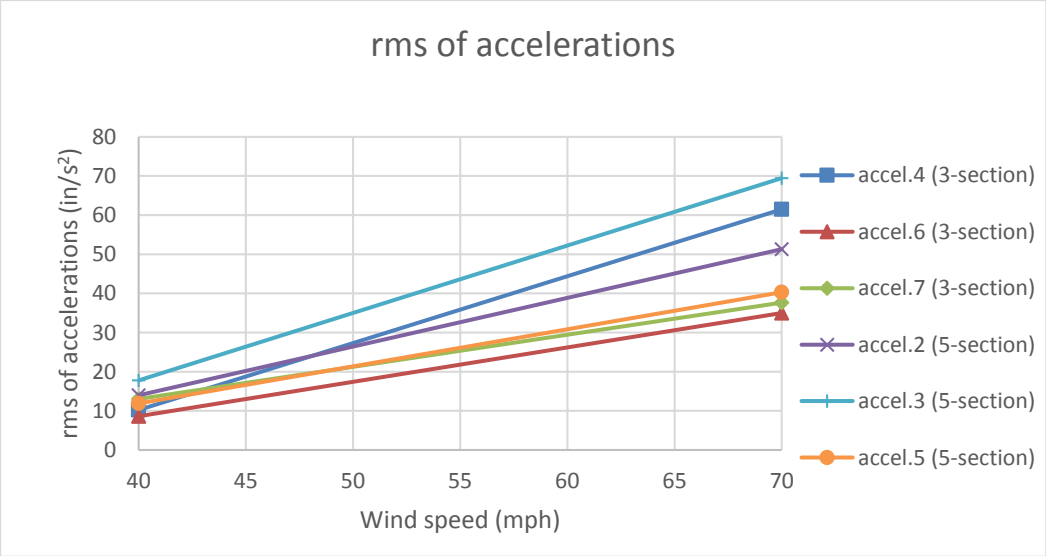

Figure D 9: rms of accelerations at 100 degrees wind direction for various wind speeds

Results for total drag/lift forces, and rms of accelerations for 135 degrees wind direction

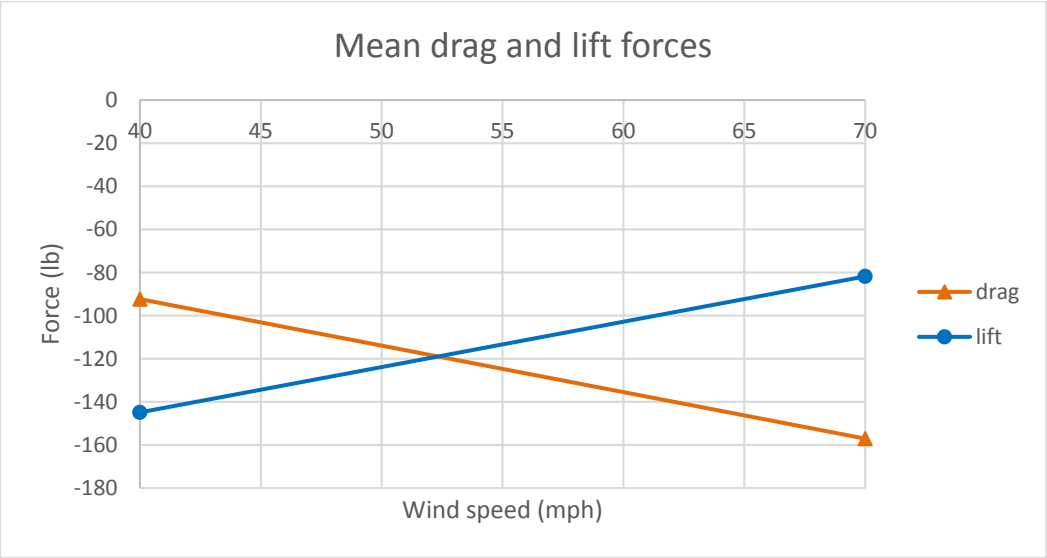

Figure D 10: Mean drag and lift forces on the traffic signals at 135 degrees wind direction

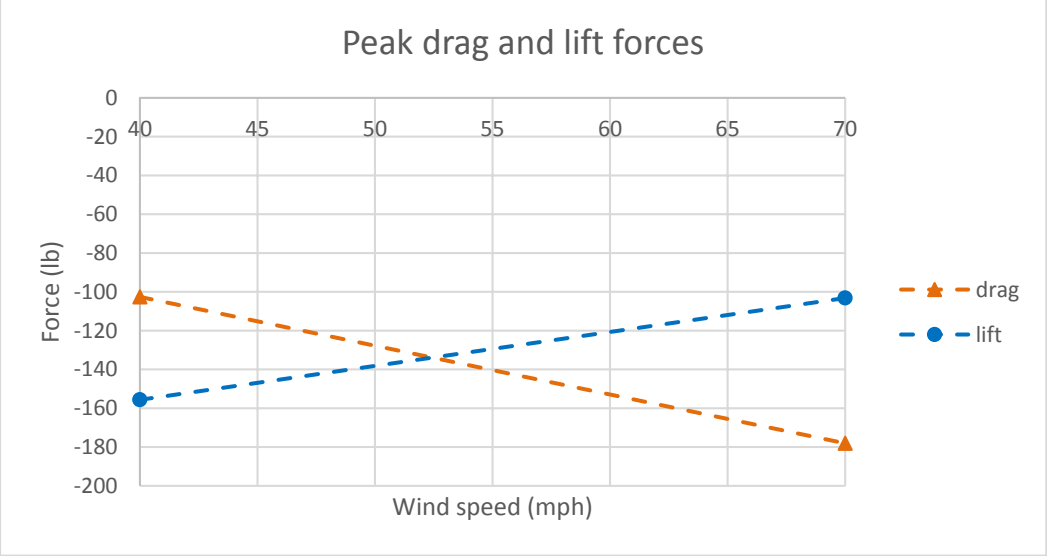

Figure D 11: Peak drag and lift forces on the traffic signals at 135 degrees wind direction

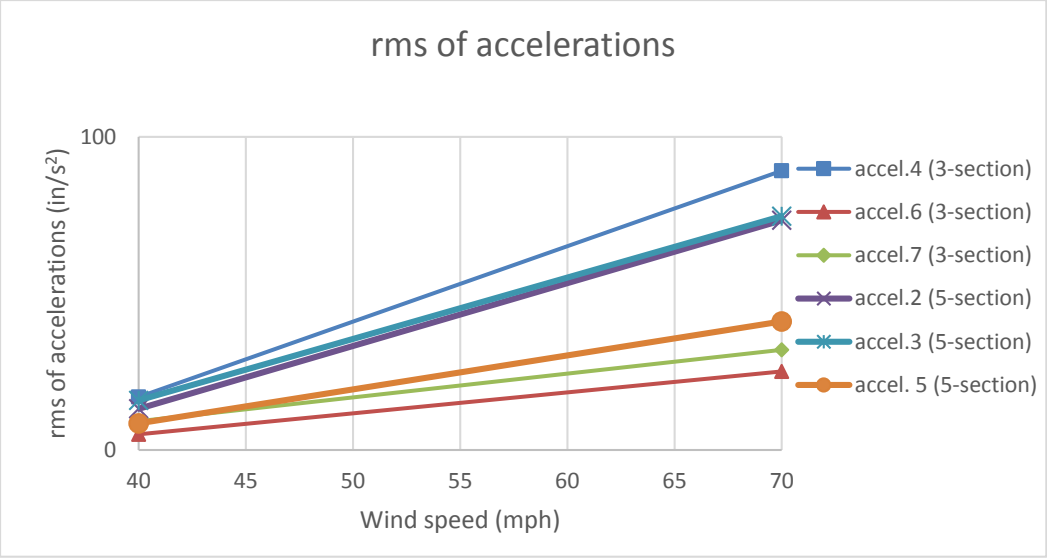

Figure D 12: rms of accelerations at 135 degrees wind direction for various wind speeds

Results for total drag/lift forces, and rms of accelerations for 180 degrees wind direction

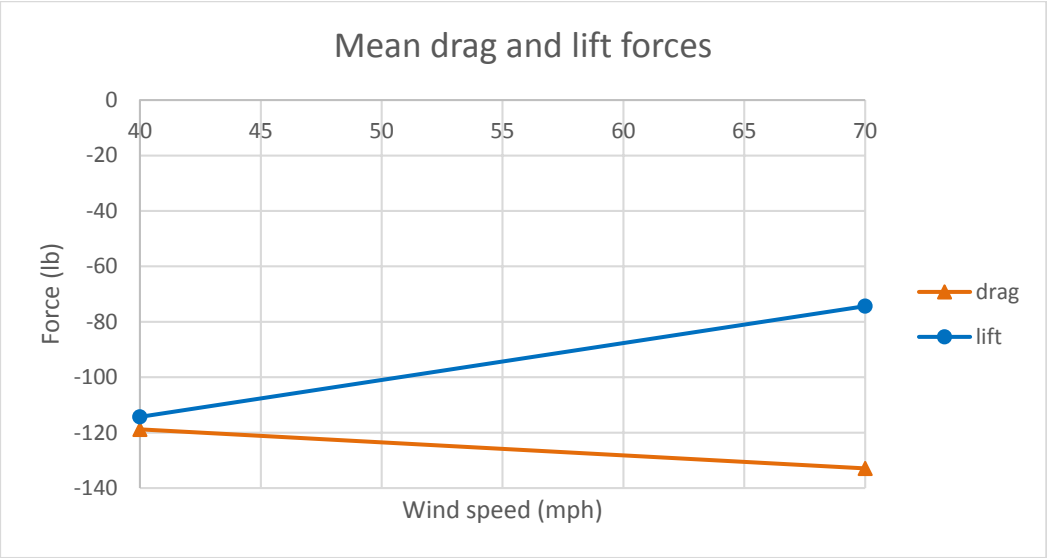

Figure D 13: Mean drag and lift forces on the traffic signals at 180 degrees wind direction

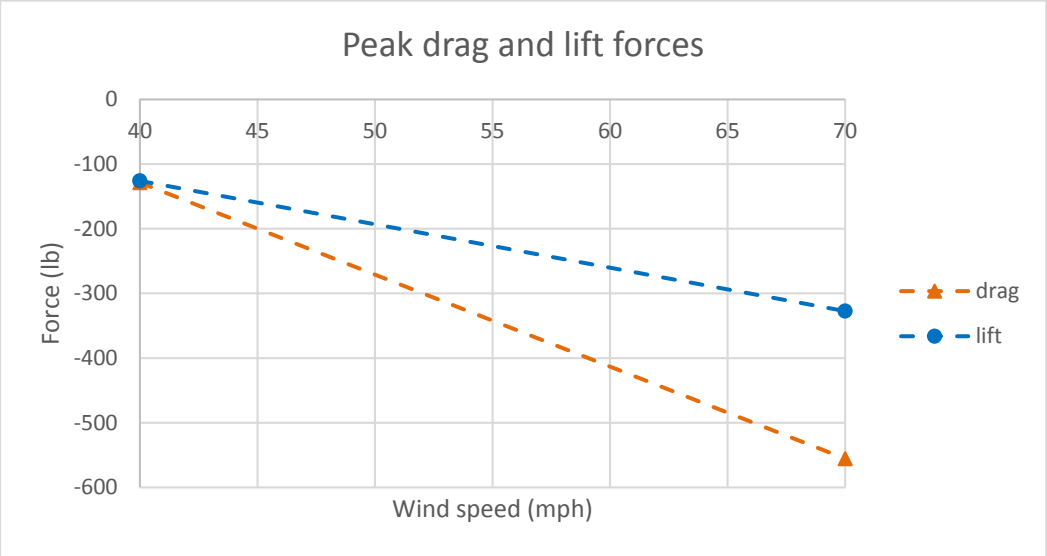

Figure D 14: Peak drag and lift forces on the traffic signals at 180 degrees wind direction

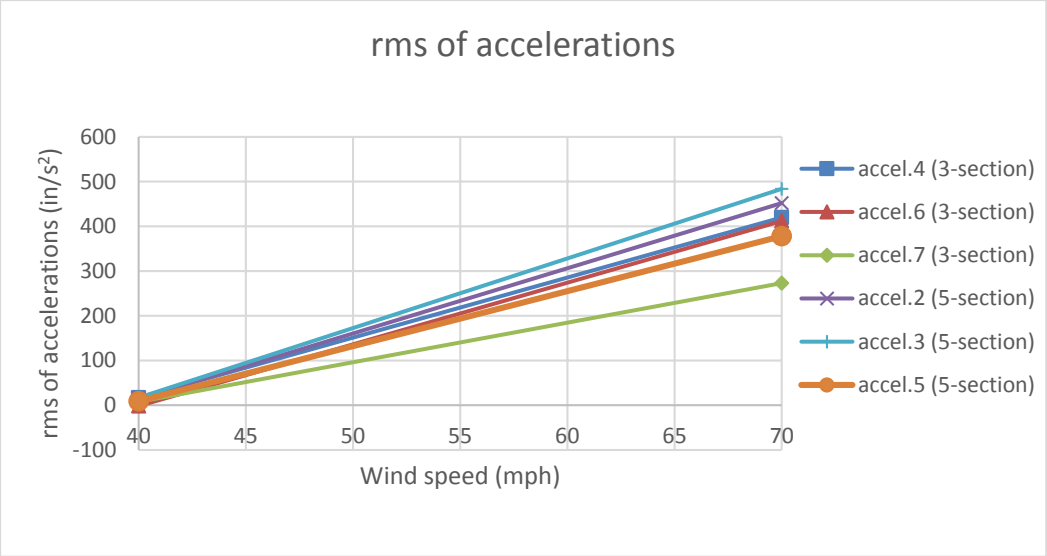

Figure D 15: rms of accelerations at 180 degrees wind direction for various wind speeds

APPENDIX E – (Task 1a: FULL SCALE TESTING - CASE 6)

Results for total drag/lift forces on the traffic signals, and rms of accelerations for 45 degrees wind direction

Figure E 1: Mean drag and lift forces on the traffic signals at 45 degrees wind direction

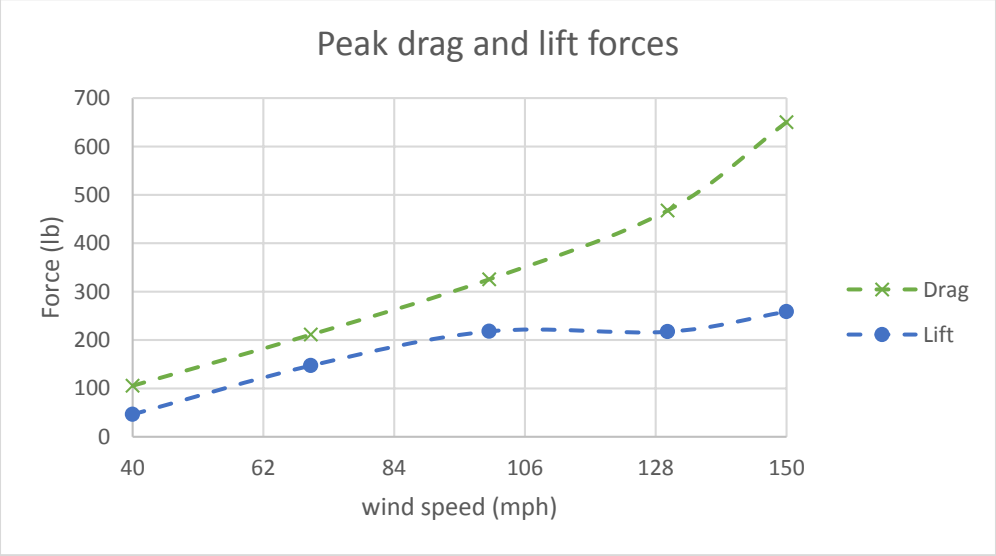

Figure E 2: Peak drag and lift forces on the traffic signals at 45 degrees wind direction

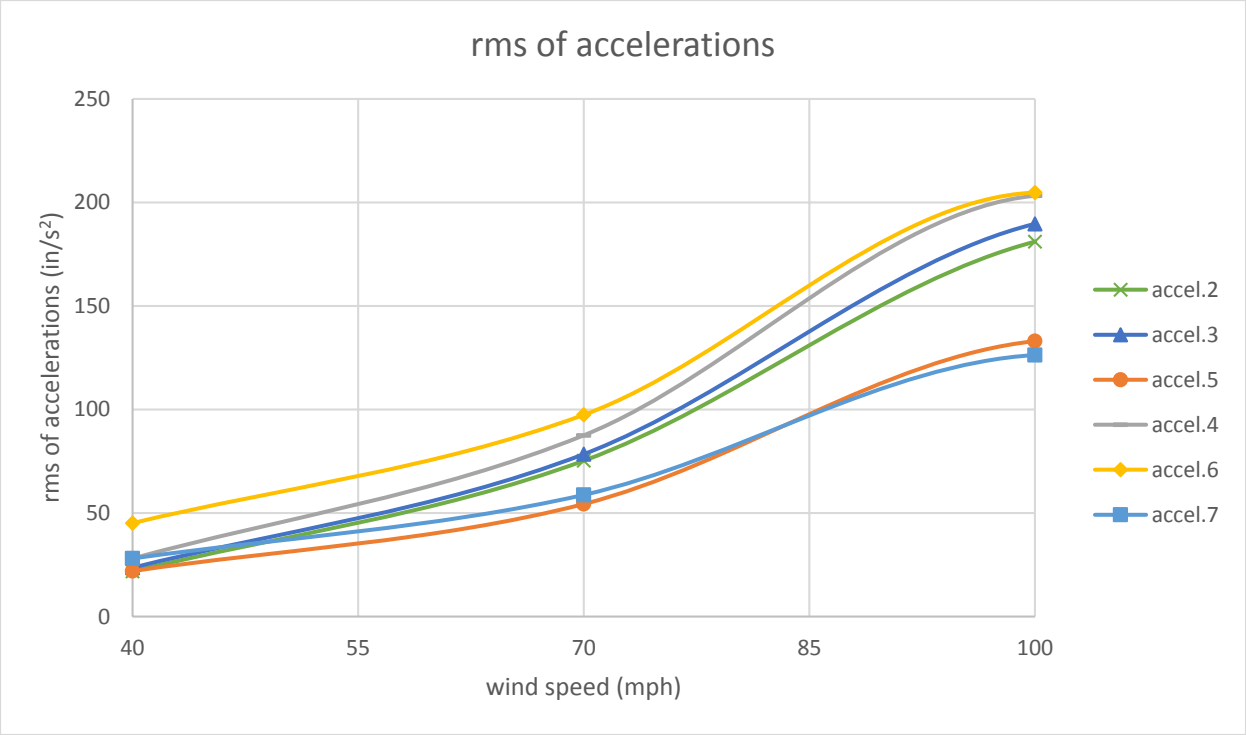

Figure E 3: rms of accelerations at 45 degrees wind direction for various wind speeds

Results for total drag/lift forces on the traffic signals, and rms of accelerations for 80 degrees wind direction

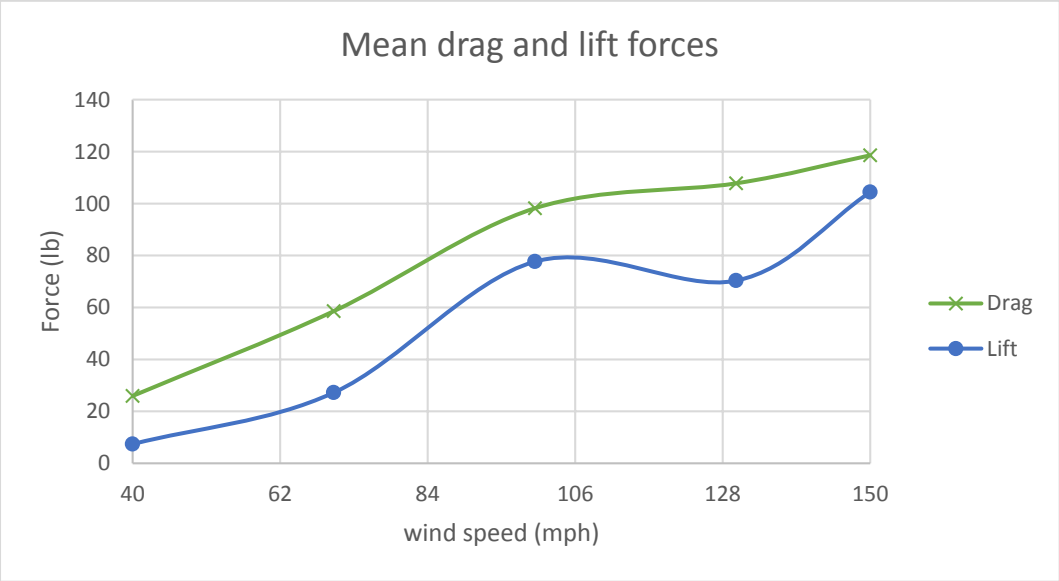

Figure E 4: Mean drag and lift forces on the traffic signals at 80 degrees wind direction

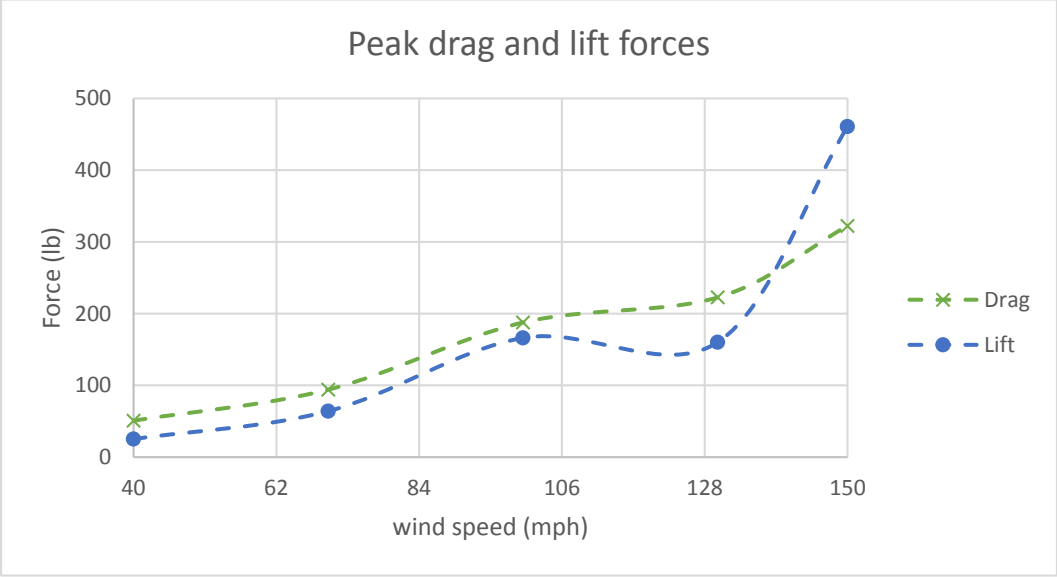

Figure E 5: Peak drag and lift forces on the traffic signals at 80 degrees wind direction

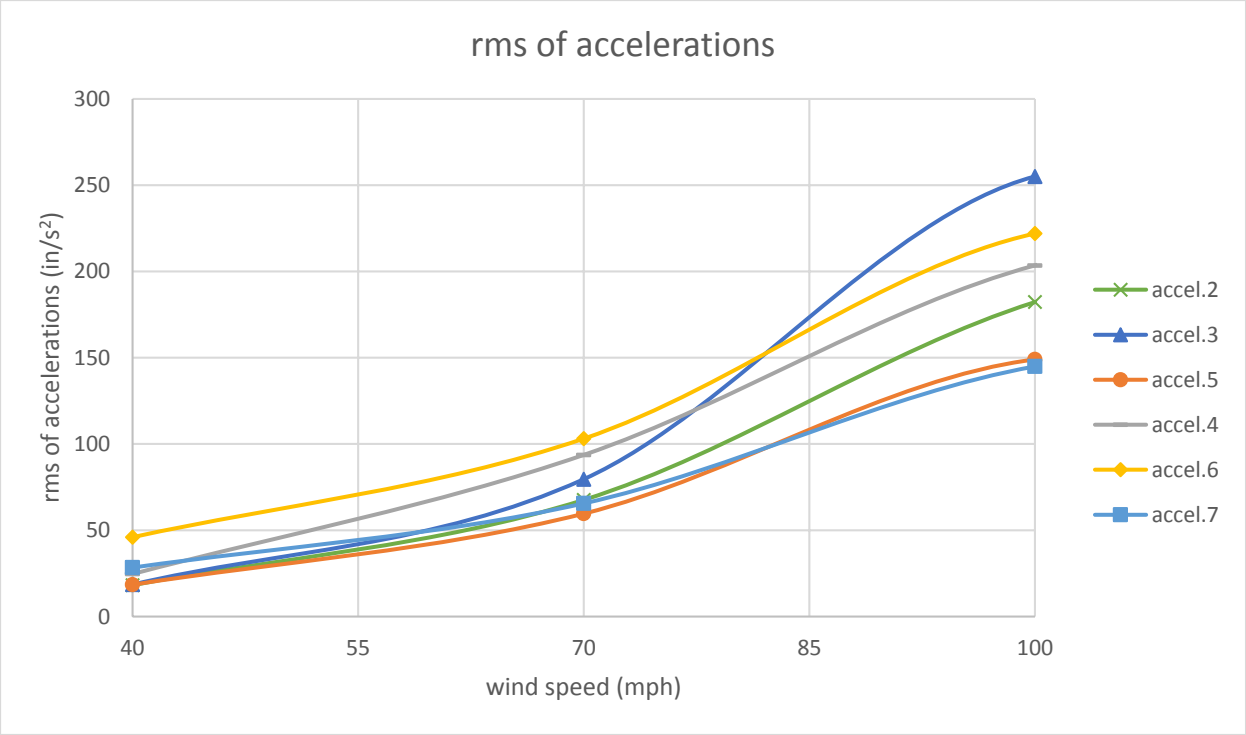

Figure E 6: rms of accelerations at 80 degrees wind direction for various wind speeds

Results for total drag/lift forces on the traffic signals, and rms of accelerations for 100 degrees wind direction

Figure E 7: Mean drag and lift forces on the traffic signals at 100 degrees wind direction

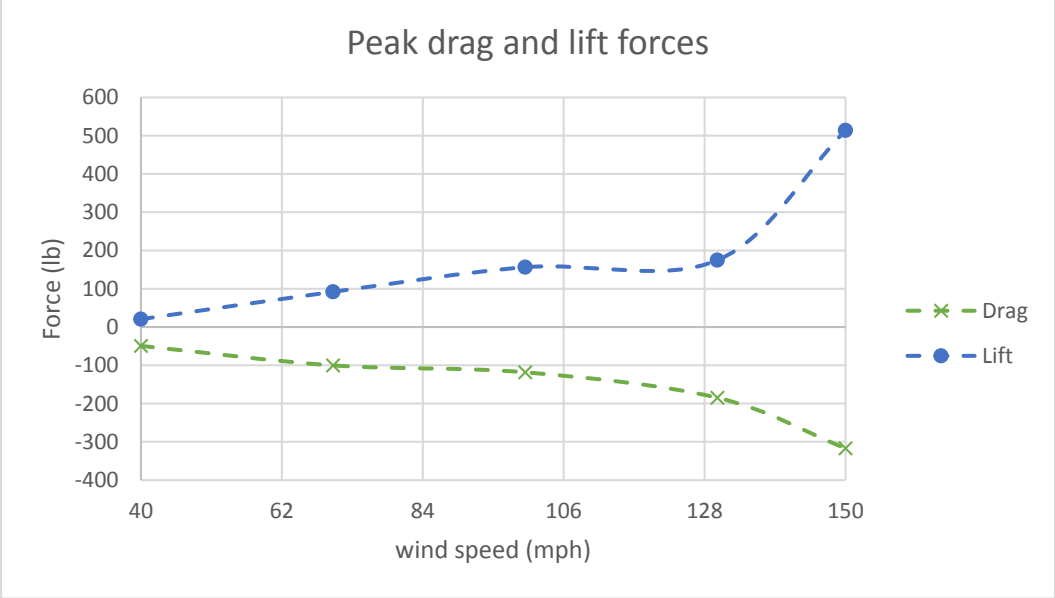

Figure E 8: Peak drag and lift forces on the traffic signals at 100 degrees wind direction

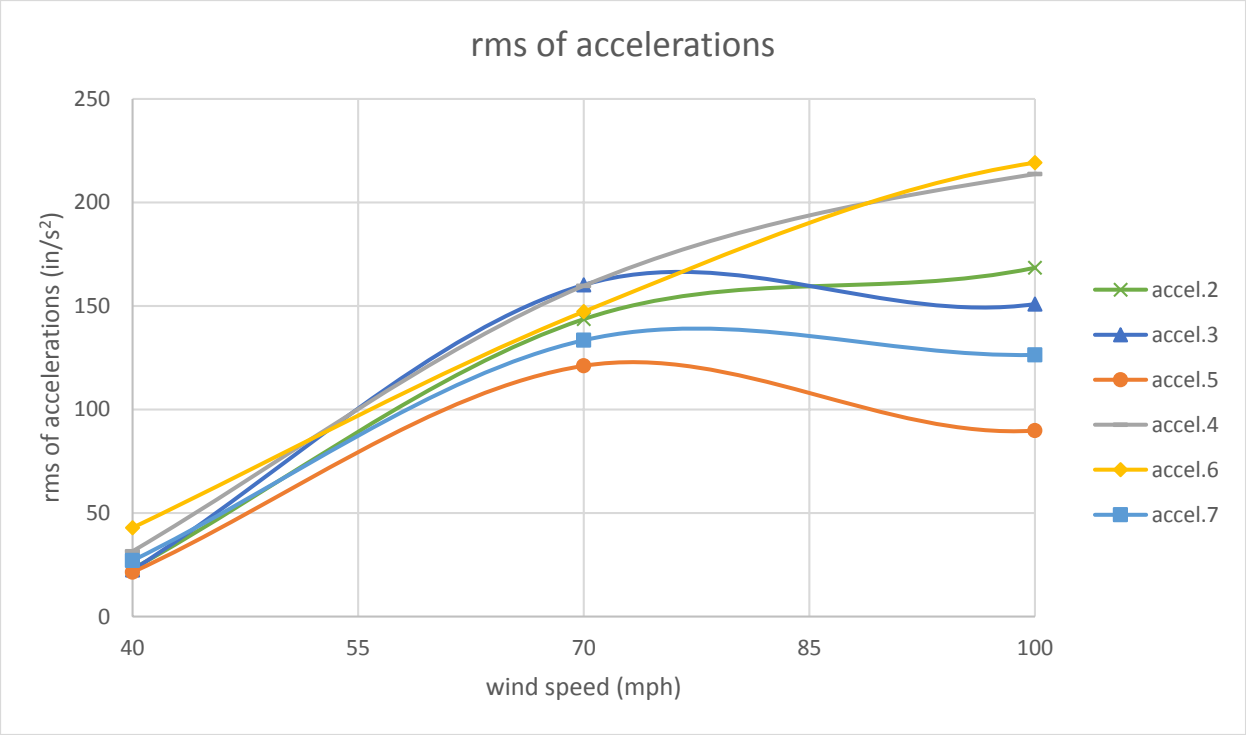

Figure E 9: rms of accelerations at 100 degrees wind direction for various wind speeds

Results for total drag/lift forces on the traffic signals, and rms of accelerations for 135 degrees wind direction

Figure E 10: Mean drag and lift forces on the traffic signals at 135 degrees wind direction

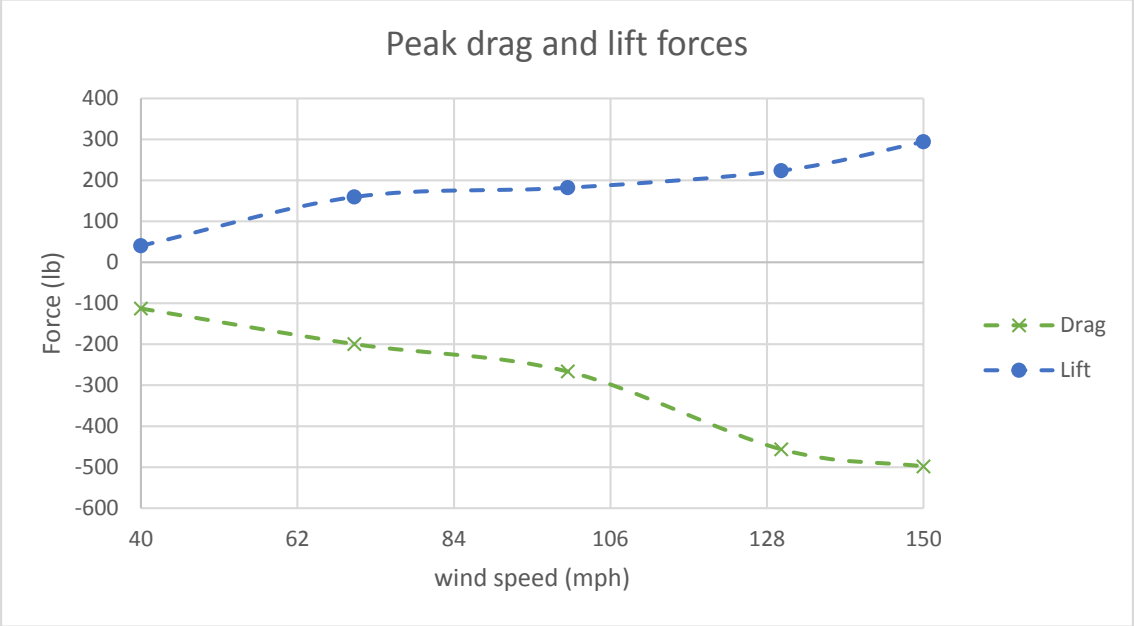

Figure E 11: Peak drag and lift forces on the traffic signals at 135 degrees wind direction

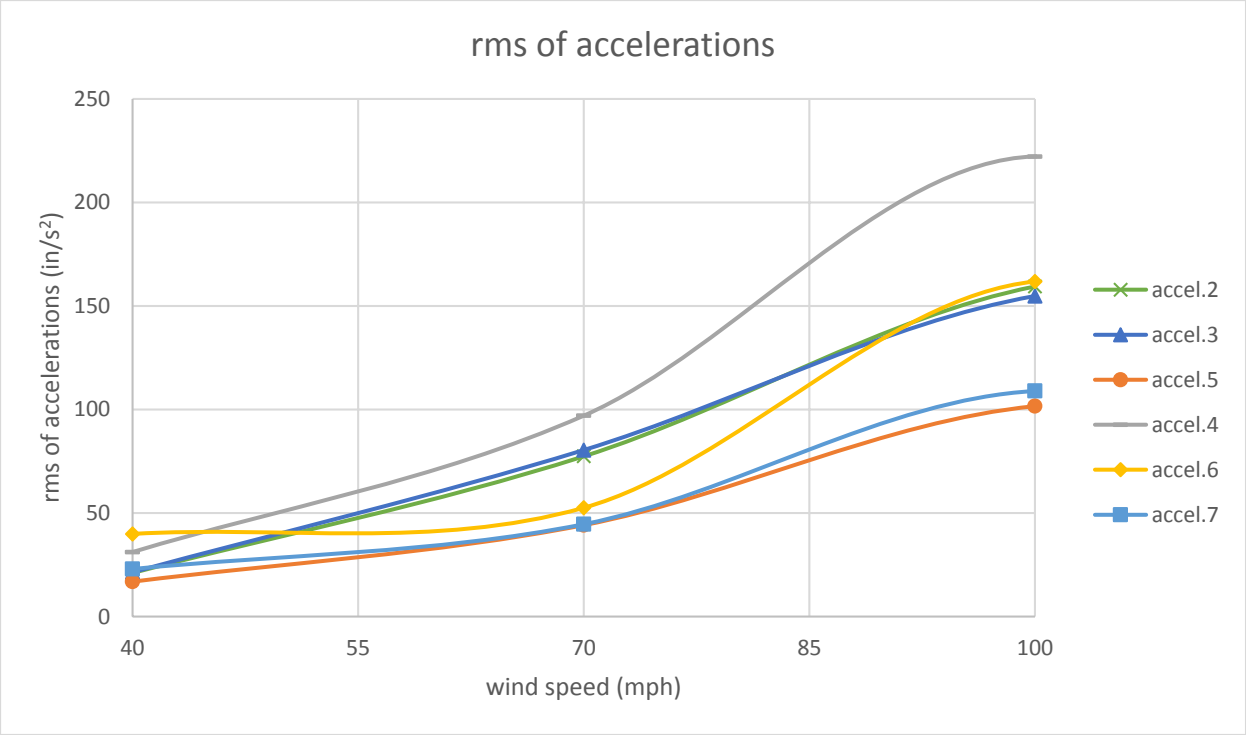

Figure E 12: rms of accelerations at 135 degrees wind direction for various wind speeds

Results for total drag/lift forces on the traffic signals, and rms of accelerations for 180 degrees wind direction

Figure E 13: Mean drag and lift forces on the traffic signals at 180 degrees wind direction

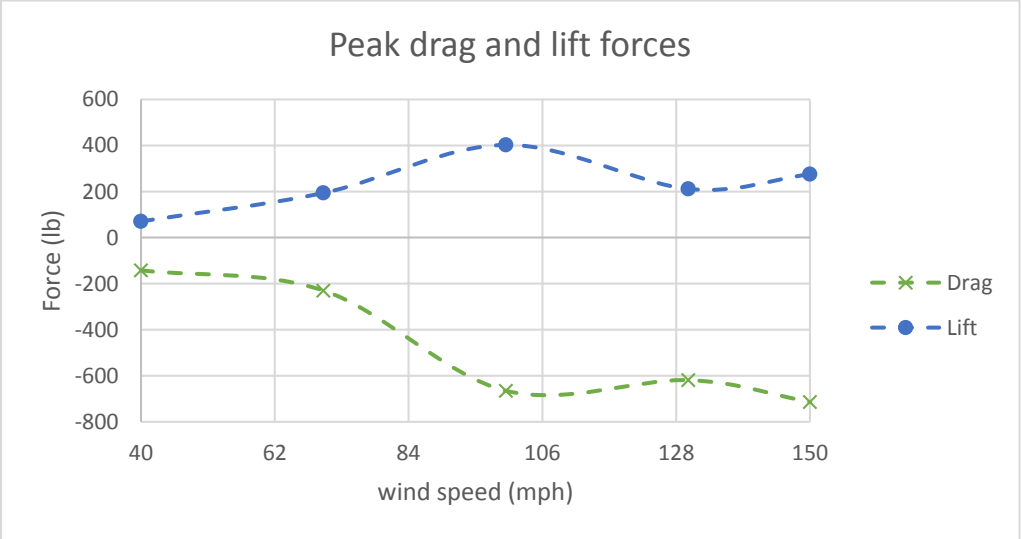

Figure E 14: Peak drag and lift forces on the traffic signals at 180 degrees wind direction

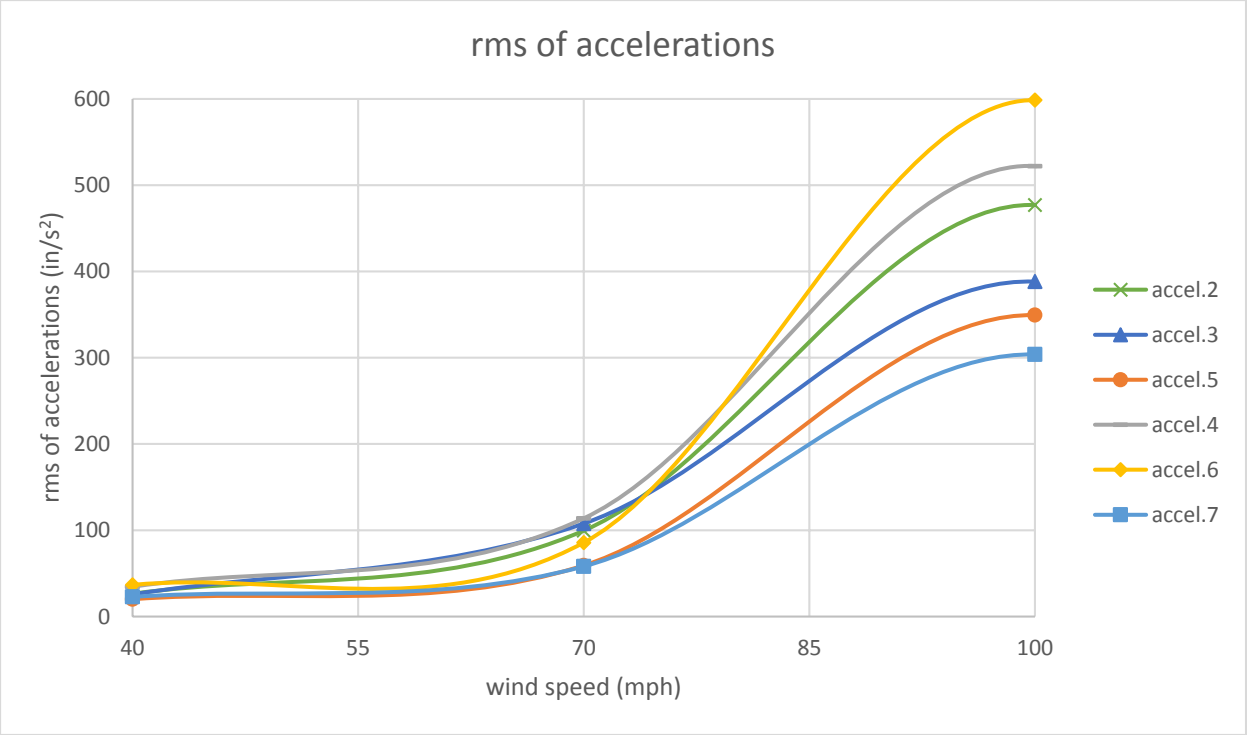

Figure E 15: rms of accelerations at 180 degrees wind direction for various wind speeds

APPENDIX F – (Task 1a: FULL SCALE TESTING - CASE 7)

Results for total drag/lift forces on the traffic signals, and rms of accelerations for 45 degrees wind direction

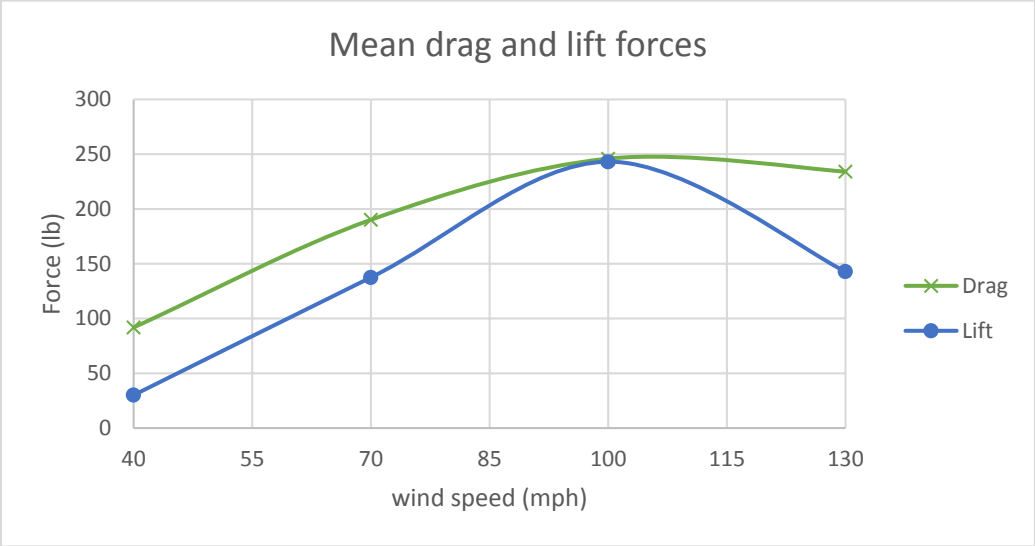

Figure F 1: Mean drag and lift forces on the traffic signals at 45 degrees wind direction

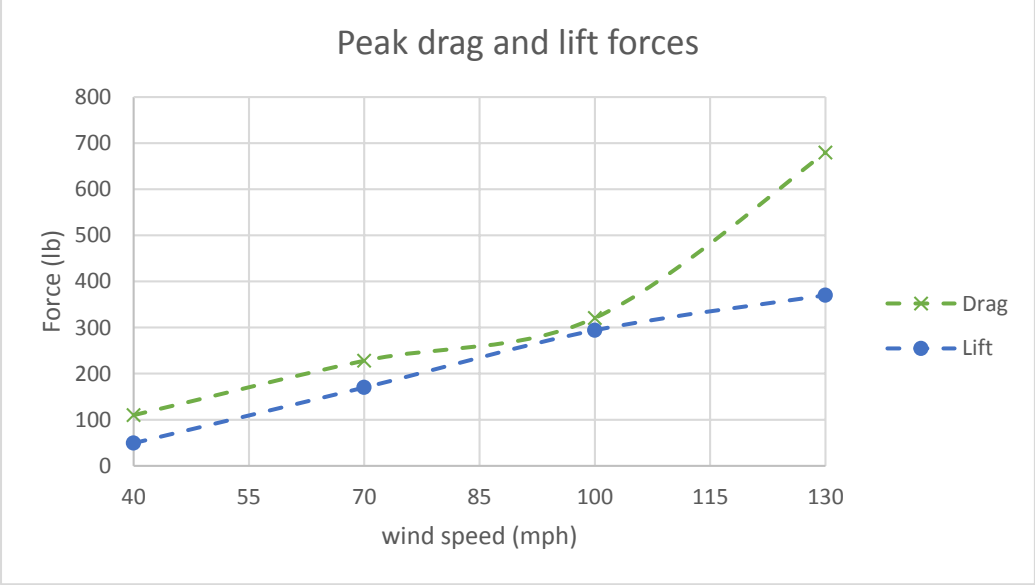

Figure F 2: Peak drag and lift forces on the traffic signals at 45 degrees wind direction

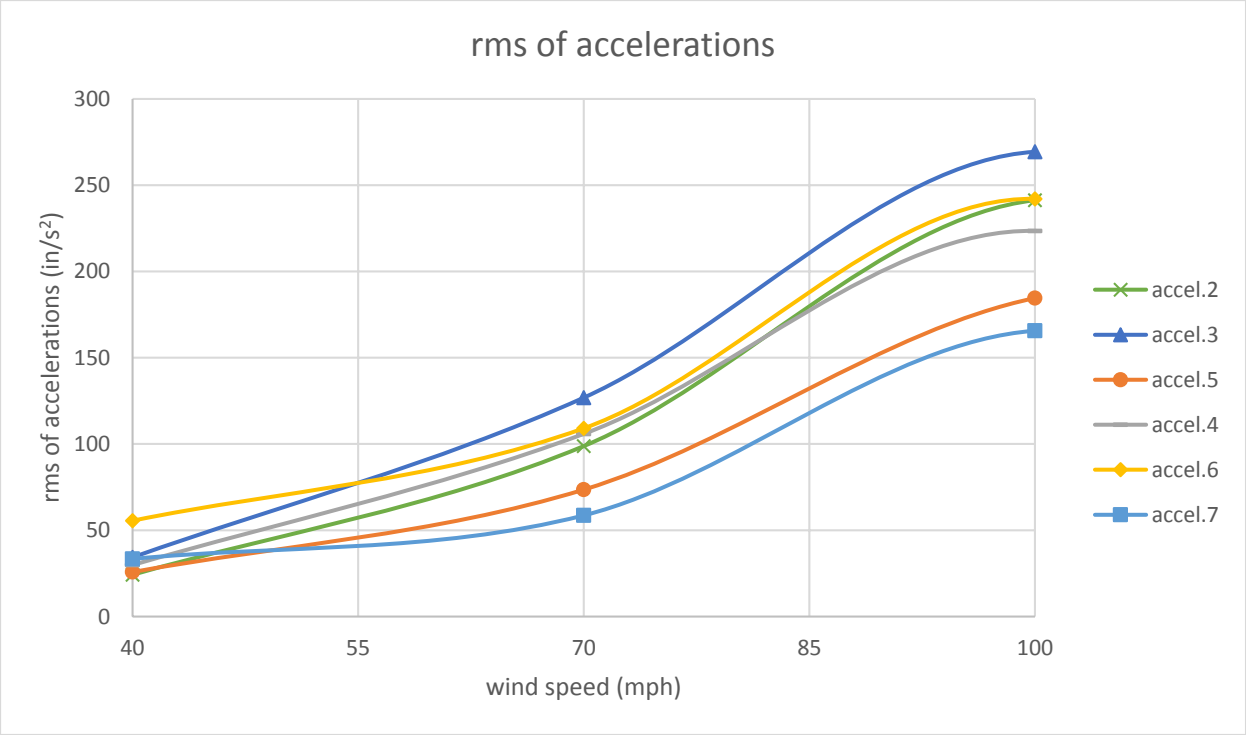

Figure F 3: rms of accelerations at 45 degrees wind direction for various wind speeds

Results for total drag/lift forces on the traffic signals, and rms of accelerations for 80 degrees wind direction

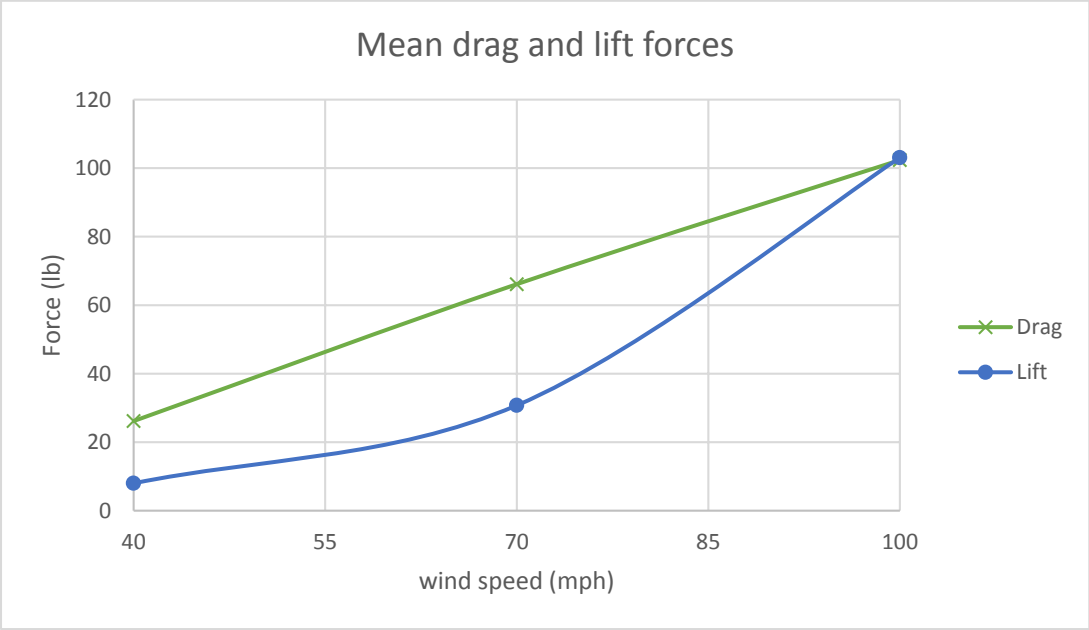

Figure F 4: Mean drag and lift forces on the traffic signals at 80 degrees wind direction

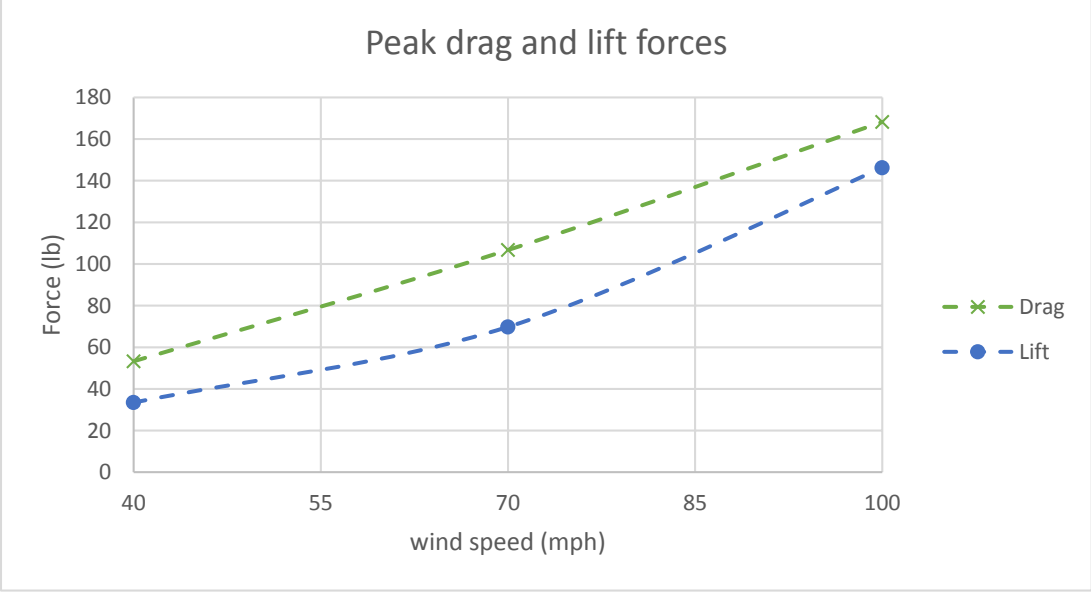

Figure F 5: Peak drag and lift forces on the traffic signals at 80 degrees wind direction

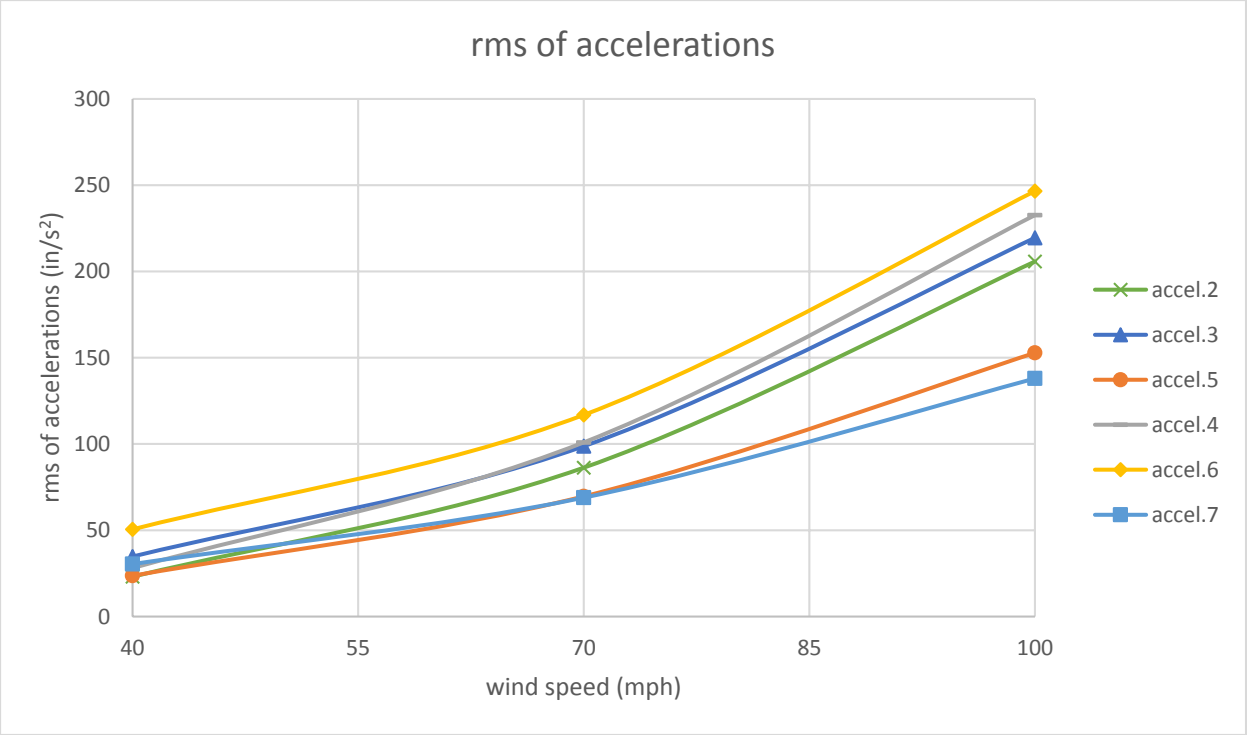

Figure F 6: rms of accelerations at 80 degrees wind direction for various wind speeds

Results for total drag/lift forces on the traffic signals, and rms of accelerations for 100 degrees wind direction

Figure F 7: Mean drag and lift forces on the traffic signals at 100 degrees wind direction

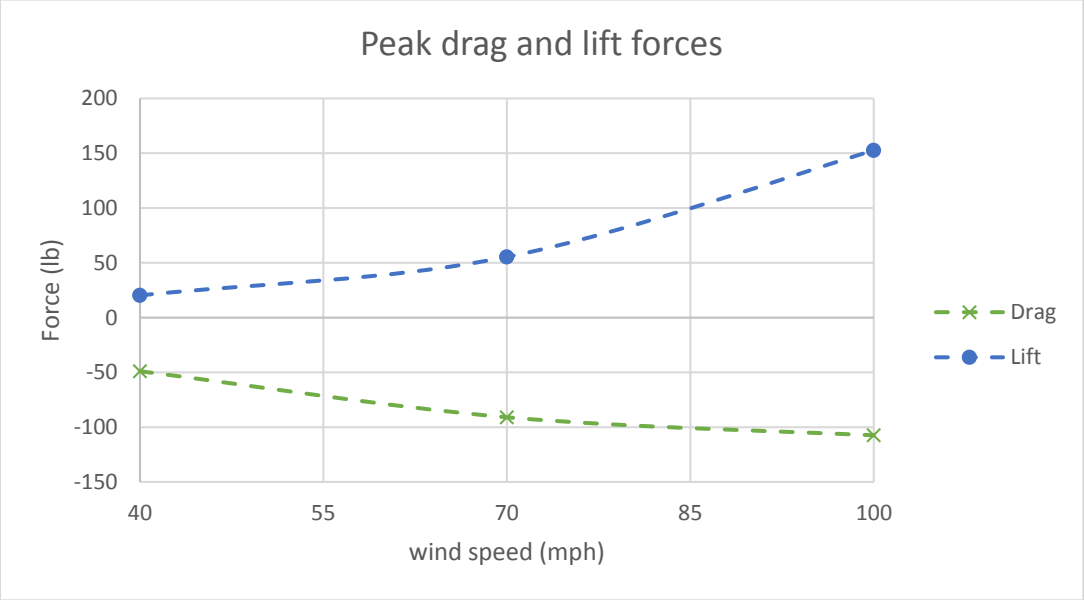

Figure F 8: Peak drag and lift forces on the traffic signals at 100 degrees wind direction

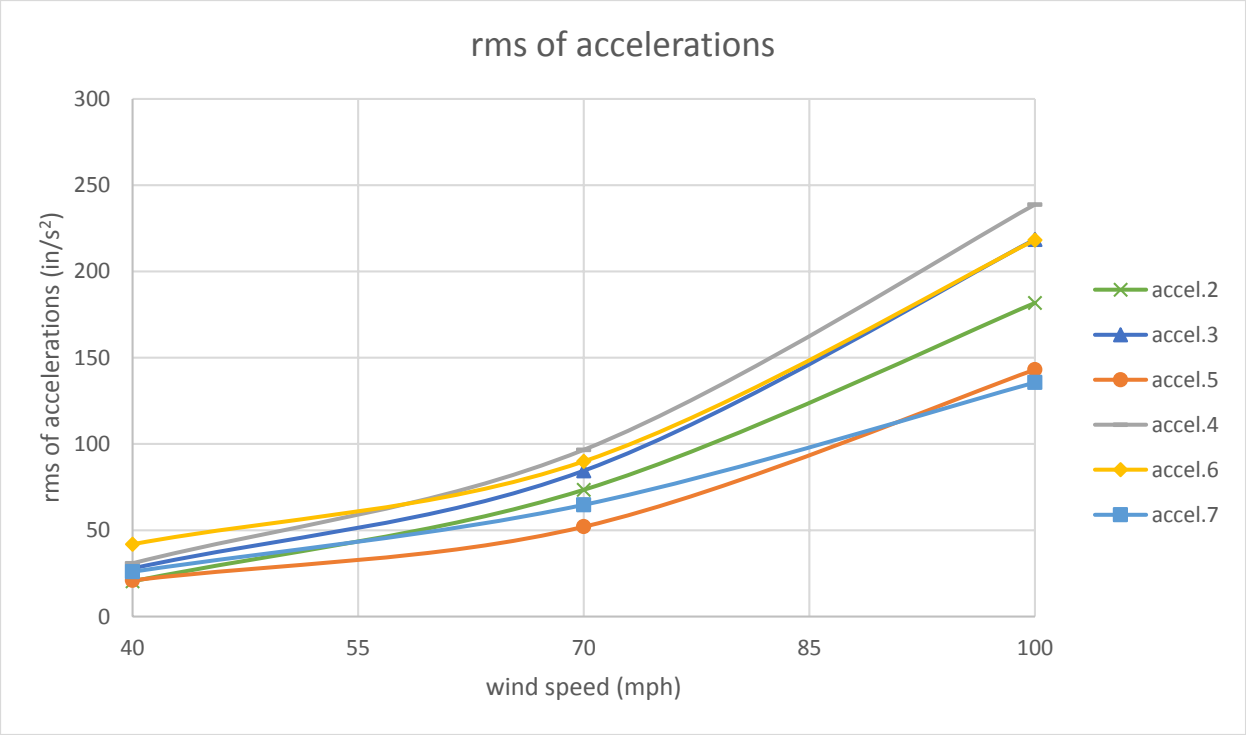

Figure F 9: rms of accelerations at 100 degrees wind direction for various wind speeds

Results for total drag/lift forces on the traffic signals, and rms of accelerations for 135 degrees wind direction

Figure F 10: Mean drag and lift forces on the traffic signals at 135 degrees wind direction

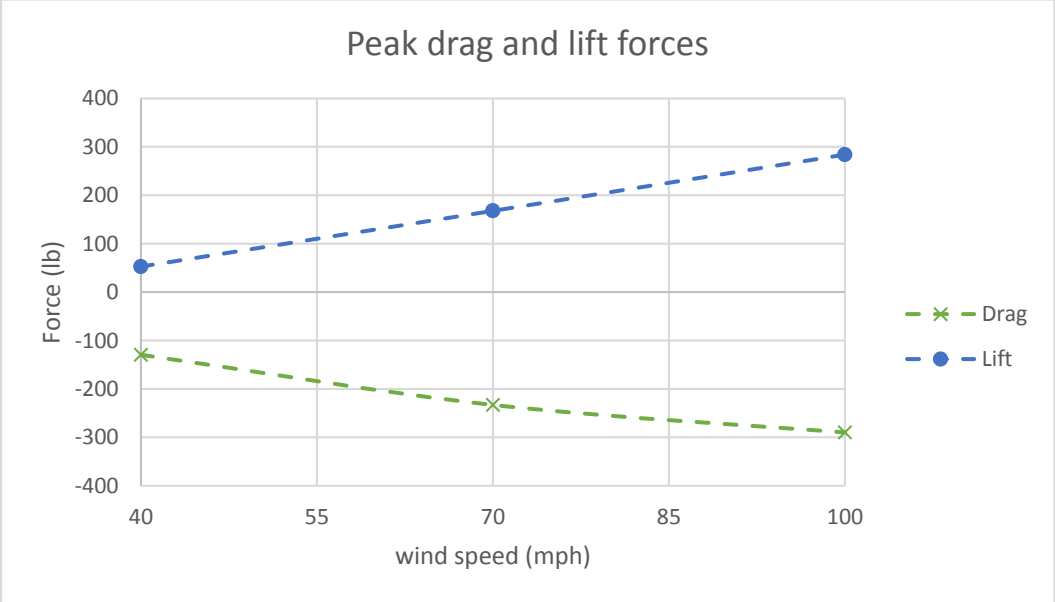

Figure F 11: Peak drag and lift forces on the traffic signals at 135 degrees wind direction

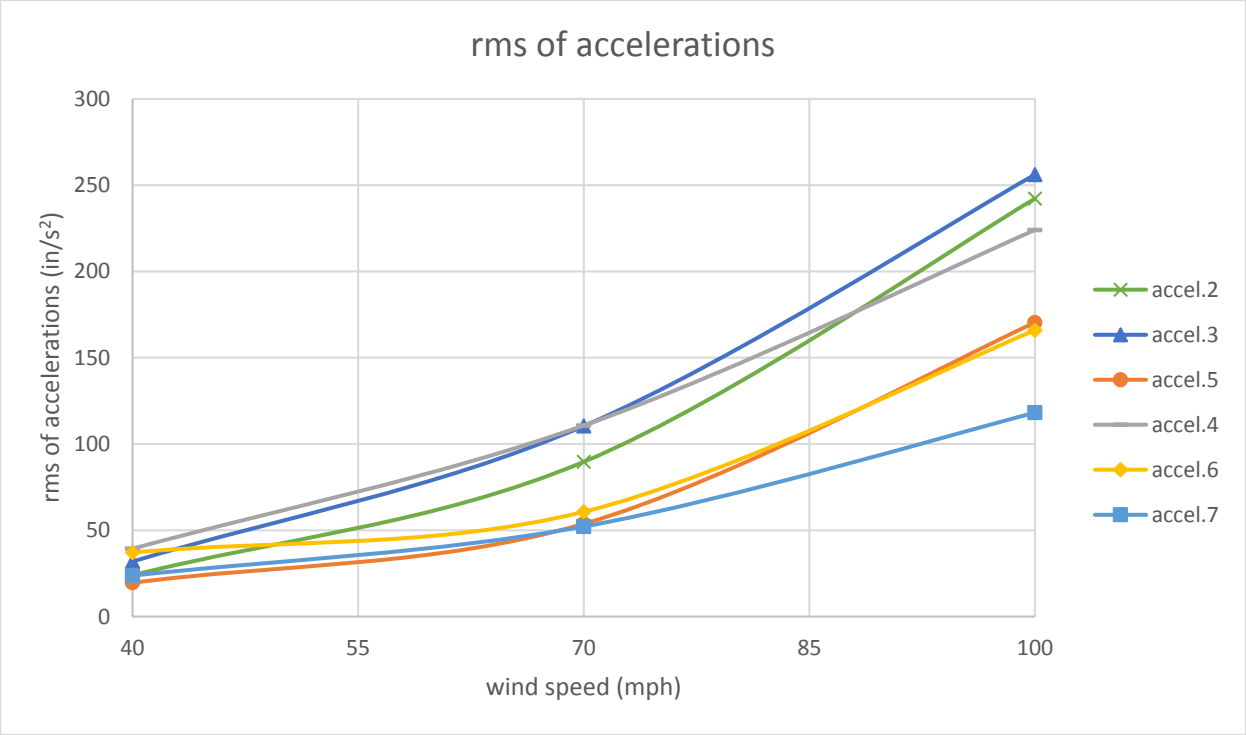

Figure F 12: rms of accelerations at 135 degrees wind direction for various wind speeds

Results for total drag/lift forces on the traffic signals, and rms of accelerations for 180 degrees wind direction

Figure F 13: Mean drag and lift forces on the traffic signals at 180 degrees wind direction

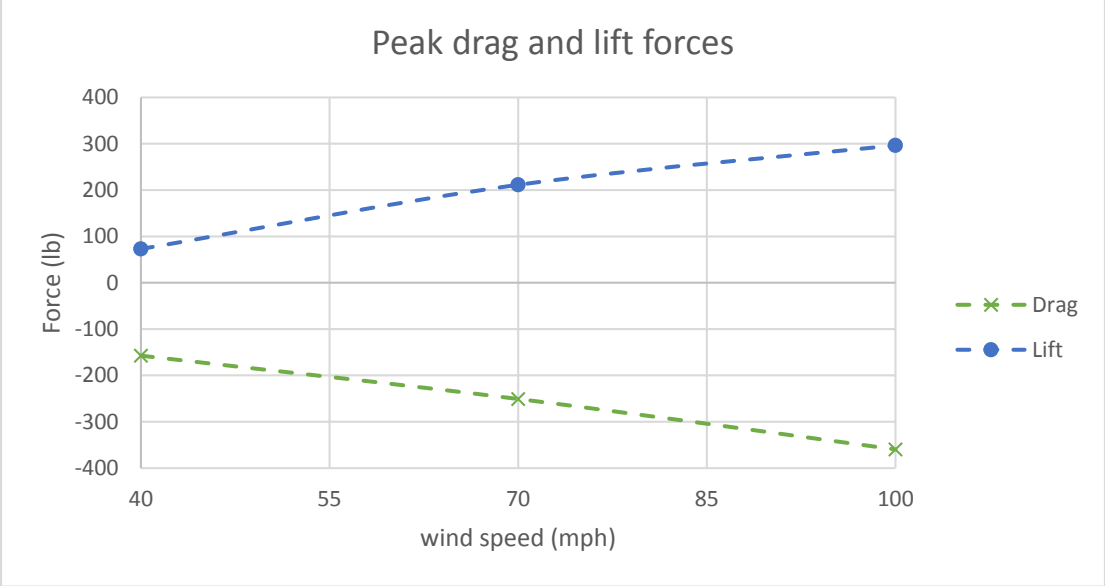

Figure F 14: Peak drag and lift forces on the traffic signals at 180 degrees wind direction

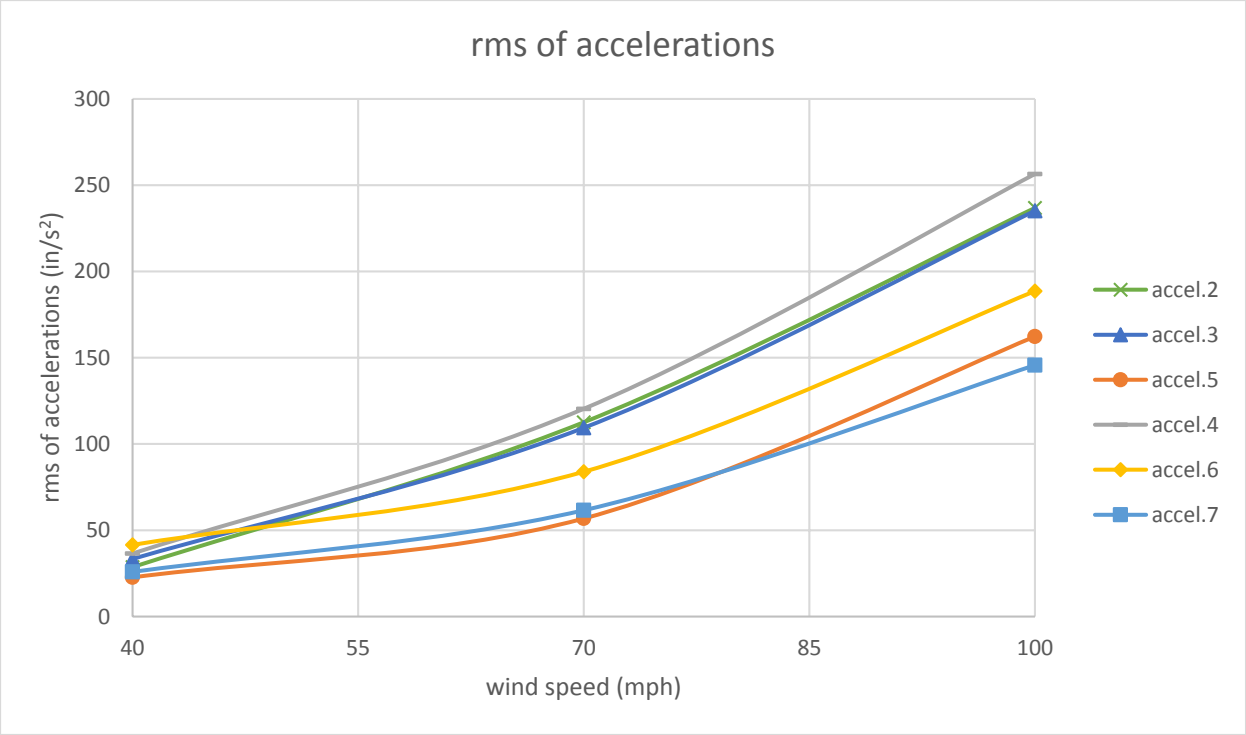

Figure F 15: rms of accelerations at 180 degrees wind direction for various wind speeds

APPENDIX G – (Task 1a: FULL SCALE TESTING - CASE 8)

Results for total drag/lift forces on the traffic signals, and rms of accelerations for 45 degrees wind direction

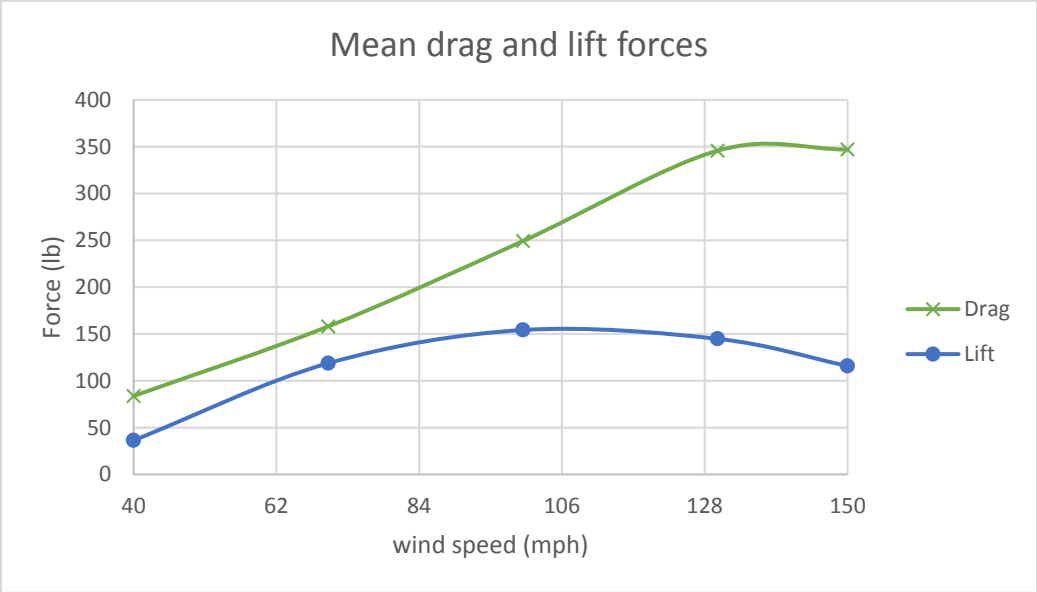

Figure G 1: Mean drag and lift forces on the traffic signals at 45 degrees wind direction

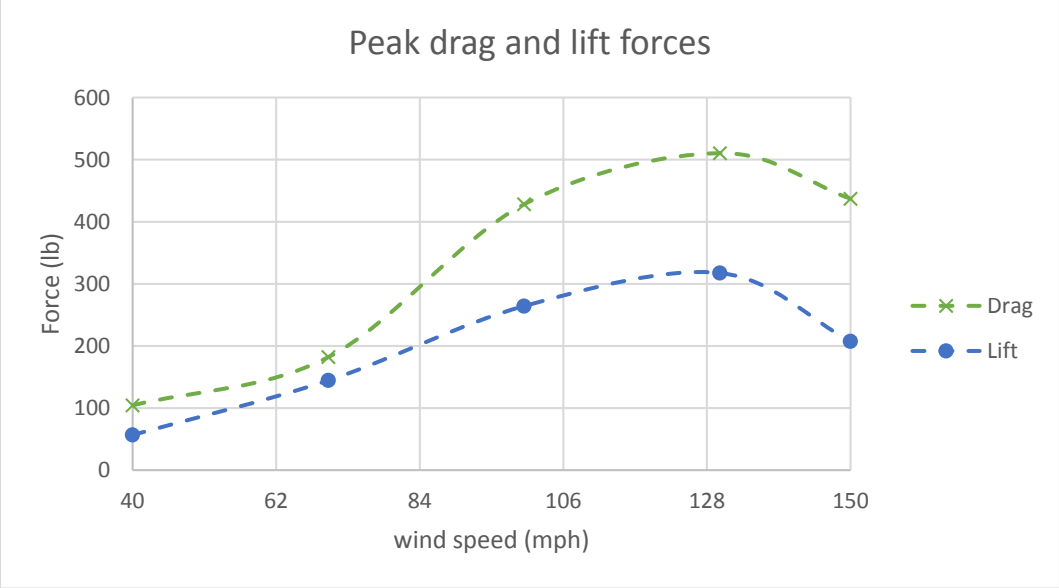

Figure G 2: Peak drag and lift forces on the traffic signals at 45 degrees wind direction

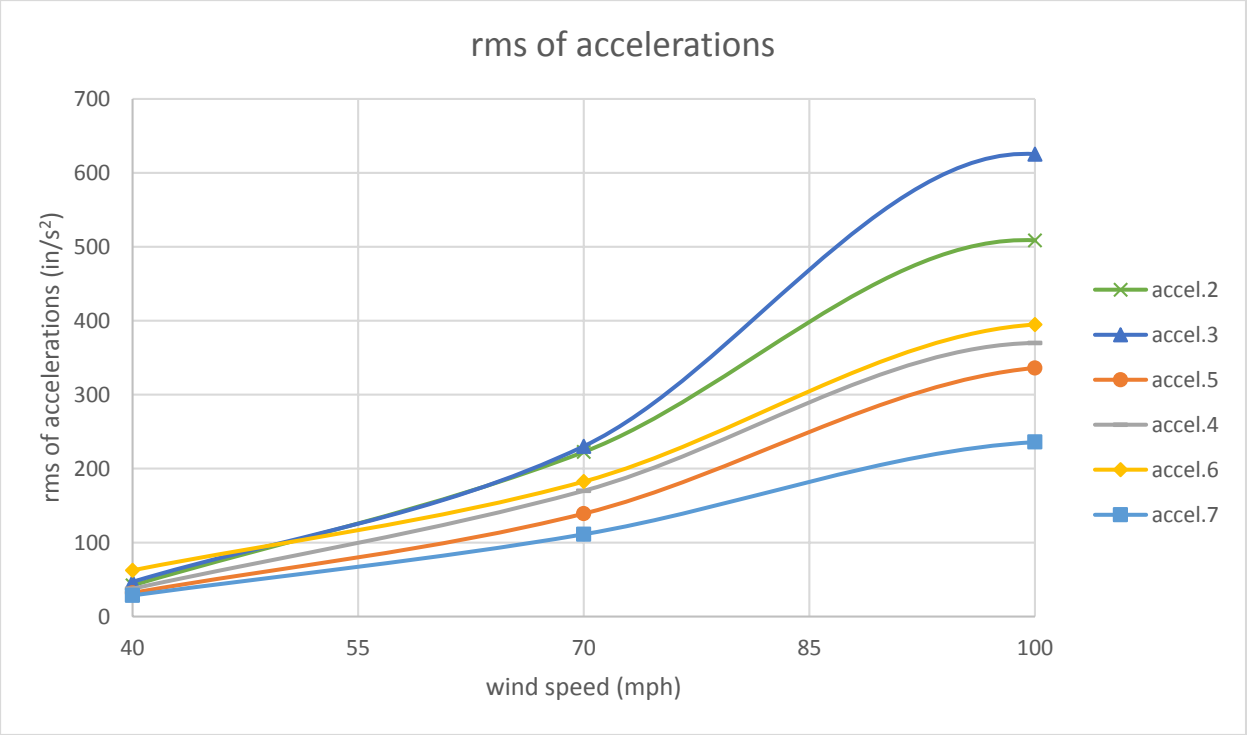

Figure G 3: rms of accelerations at 45 degrees wind direction for various wind speeds

Results for total drag/lift forces on the traffic signals, and rms of accelerations for 80 degrees wind direction

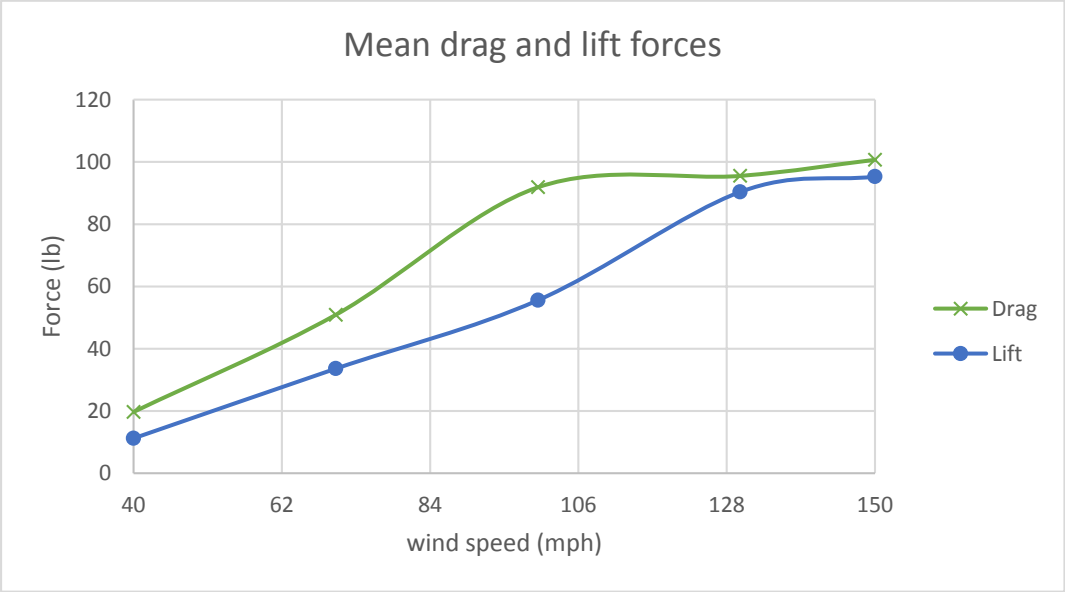

Figure G 4: Mean drag and lift forces on the traffic signals at 80 degrees wind direction

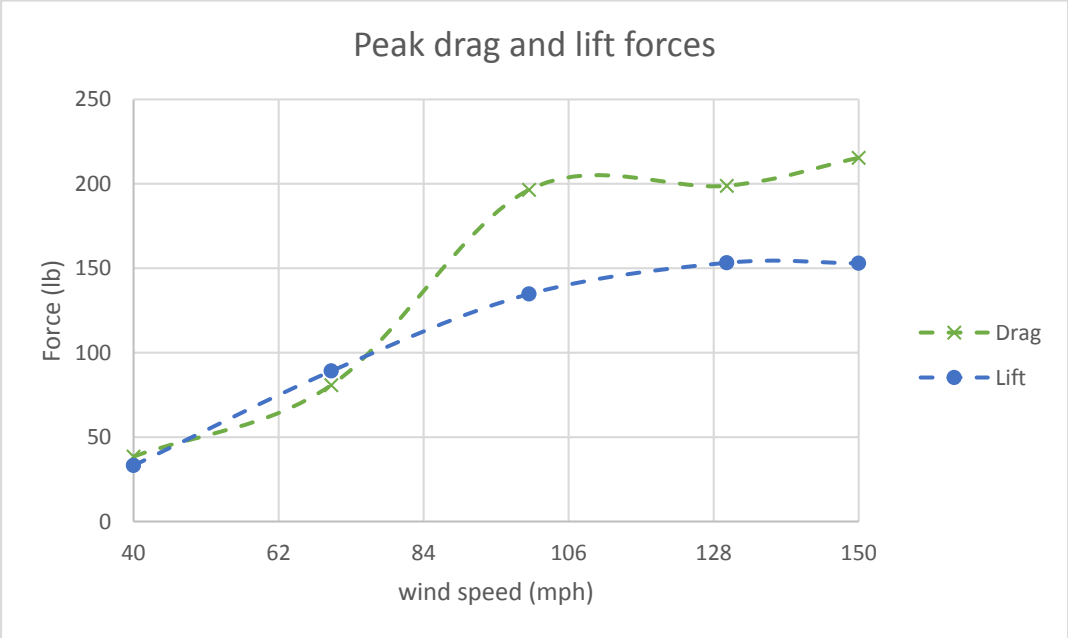

Figure G 5: Peak drag and lift forces on the traffic signals at 80 degrees wind direction

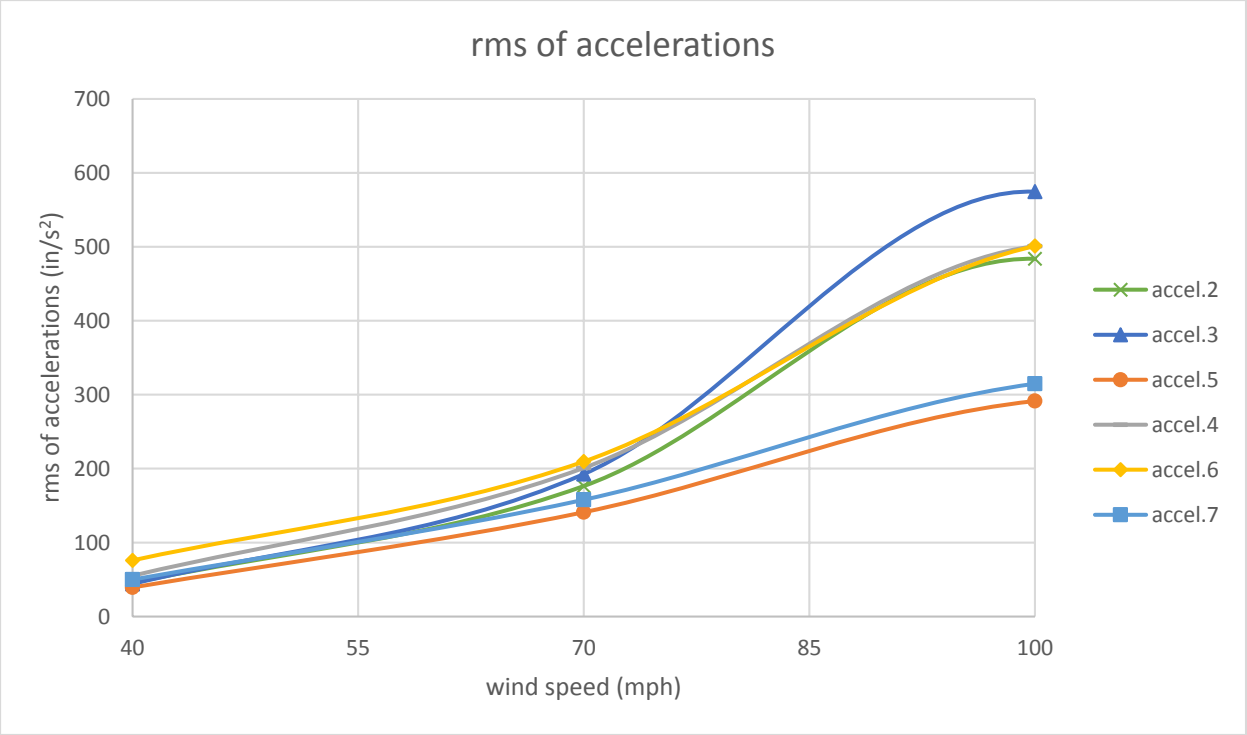

Figure G 6: rms of accelerations at 80 degrees wind direction for various wind speeds

Results for total drag/lift forces on the traffic signals, and rms of accelerations for 100 degrees wind direction

Figure G 7: Mean drag and lift forces on the traffic signals at 100 degrees wind direction

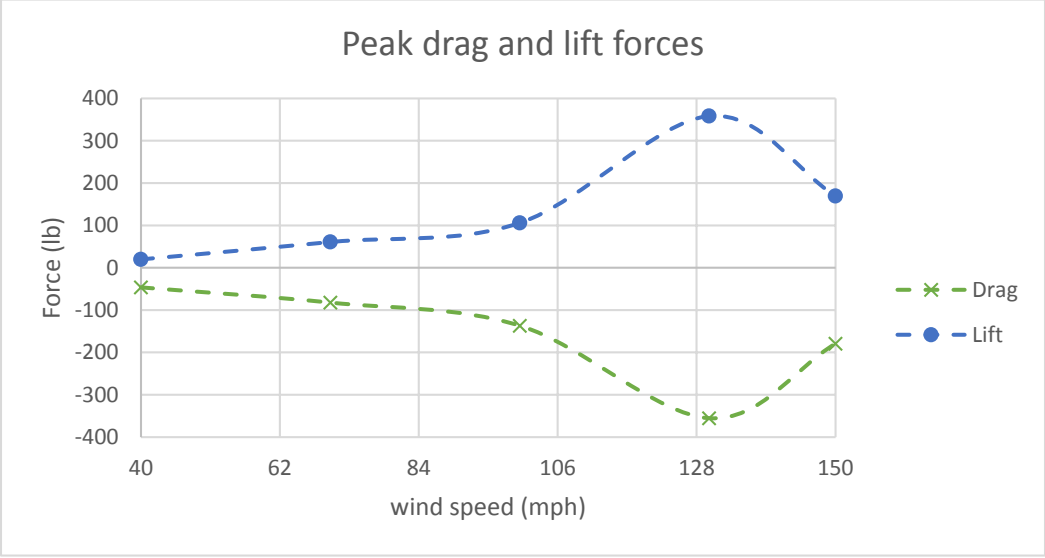

Figure G 8: Peak drag and lift forces on the traffic signals at 100 degrees wind direction

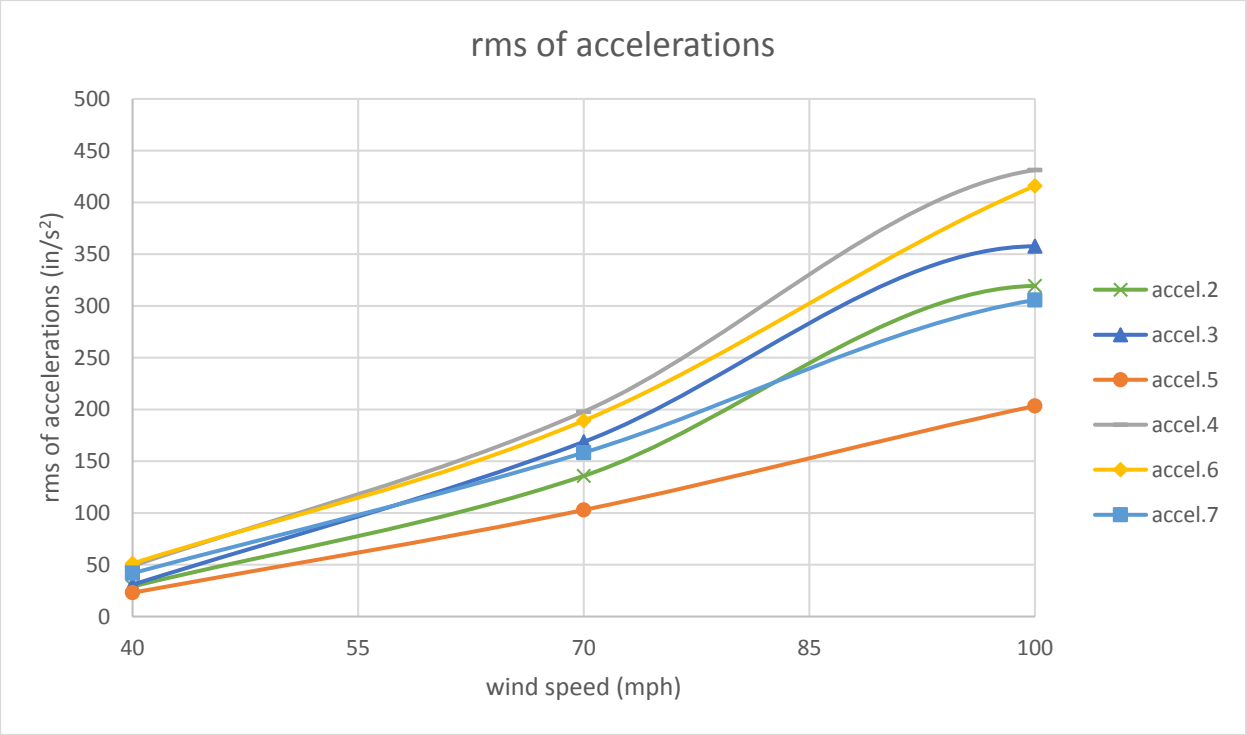

Figure G 9: rms of accelerations at 100 degrees wind direction for various wind speeds

Results for total drag/lift forces on the traffic signals, and rms of accelerations for 135 degrees wind direction

Figure G 10: Mean drag and lift forces on the traffic signals at 135 degrees wind direction

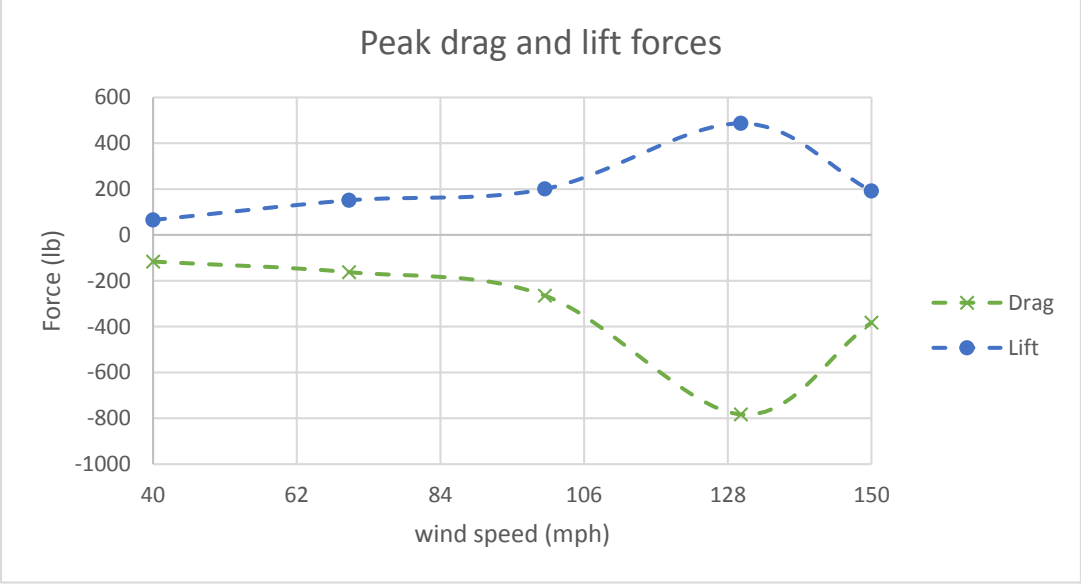

Figure G 11: Peak drag and lift forces on the traffic signals at 135 degrees wind direction

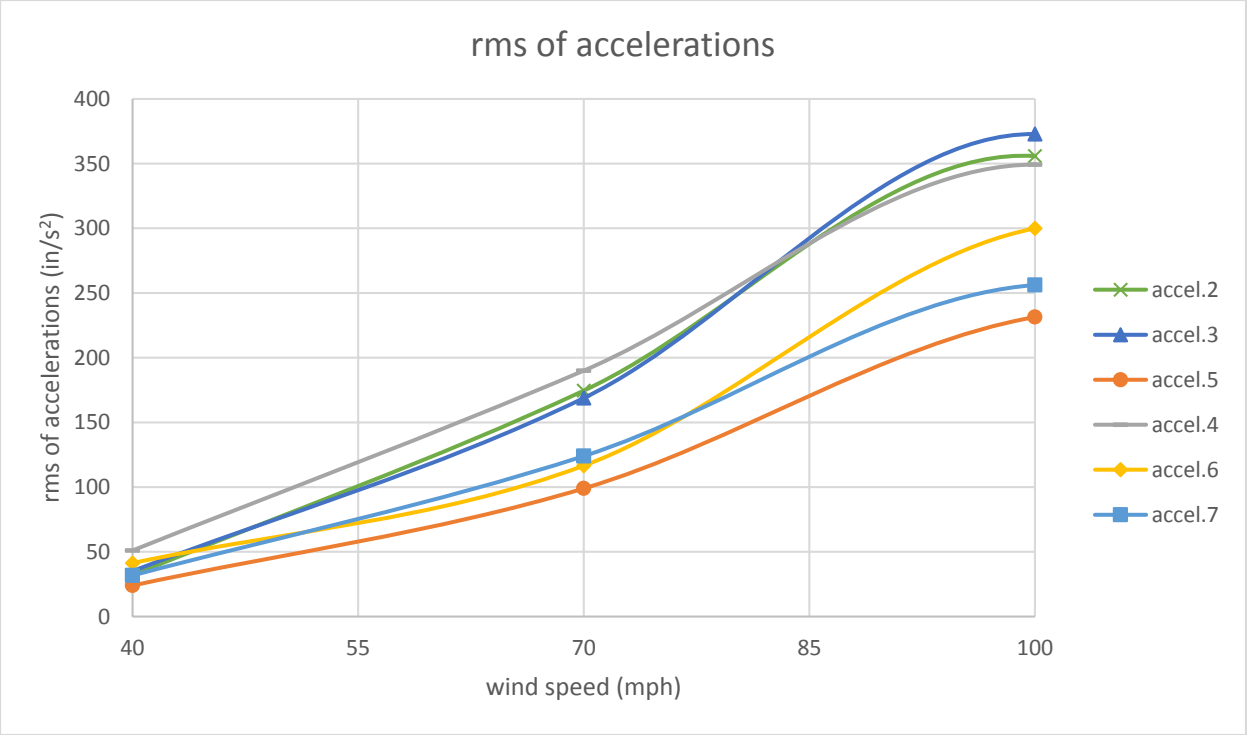

Figure G 12: rms of accelerations at 135 degrees wind direction for various wind speeds

Results for total drag/lift forces on the traffic signals, and rms of accelerations for 180 degrees wind direction

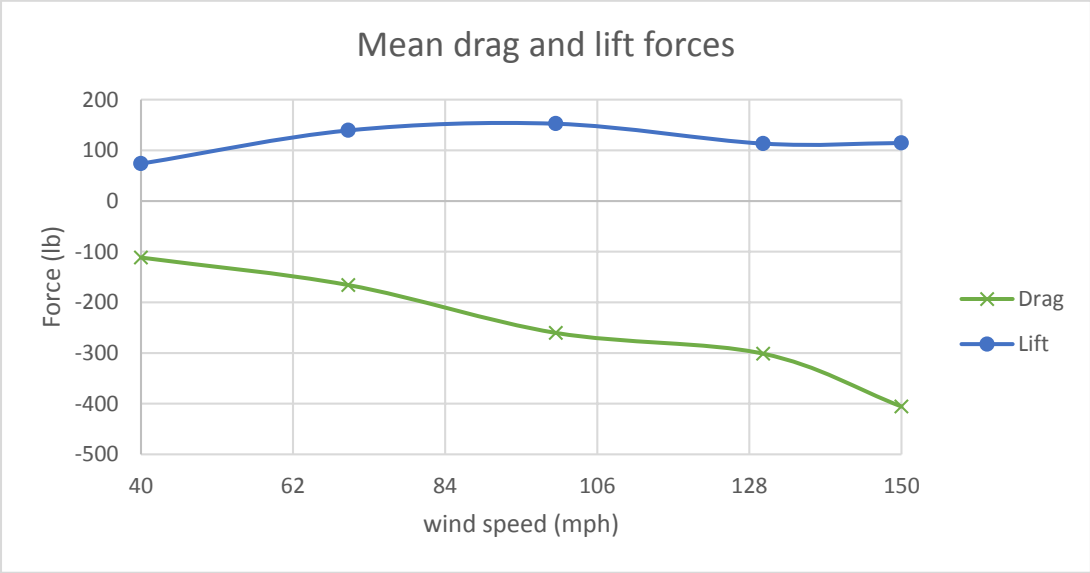

Figure G 13: Mean drag and lift forces on the traffic signals at 180 degrees wind direction

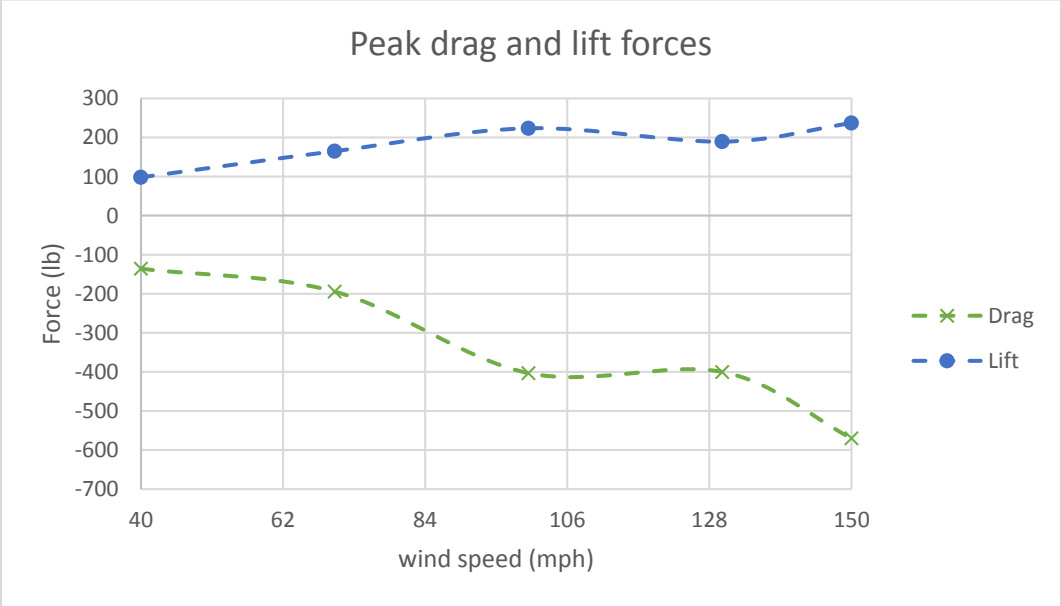

Figure G 14: Peak drag and lift forces on the traffic signals at 180 degrees wind direction

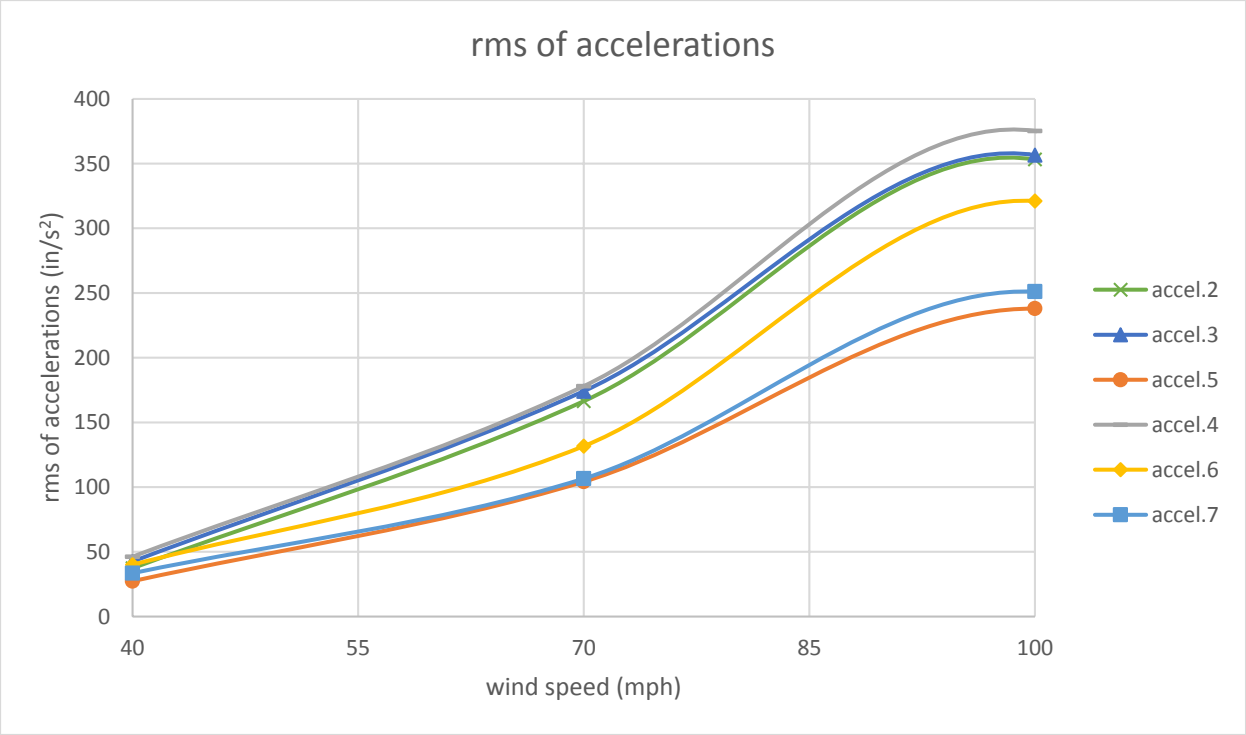

Figure G 15: rms of accelerations at 180 degrees wind direction for various wind speeds

APPENDIX H – (Task 1a: FULL SCALE TESTING - CASE 9)

Results for total drag/lift forces, and rms of accelerations for 45 degrees wind direction

Figure H 1: Mean drag and lift forces on the traffic signals at 45 degrees wind direction

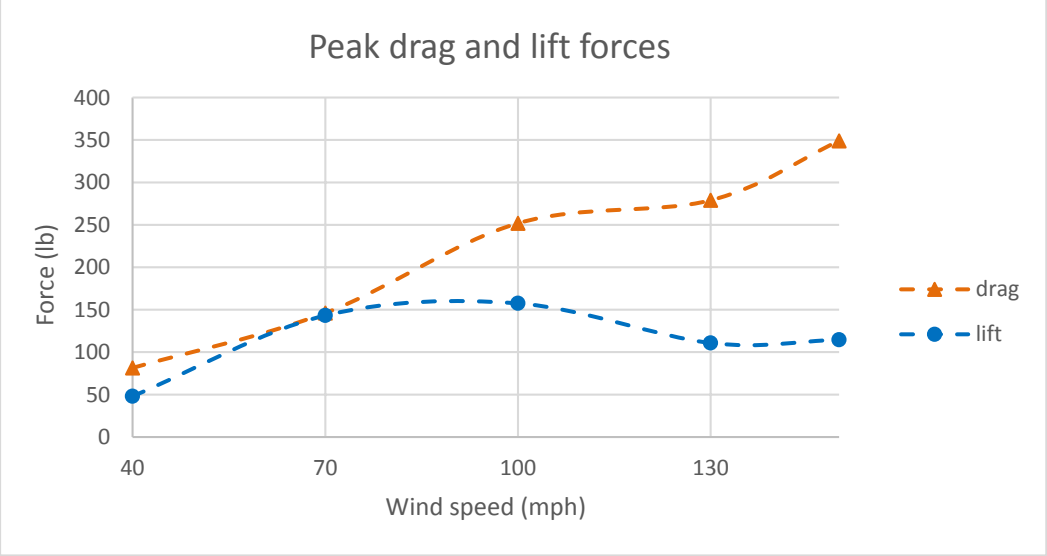

Figure H 2: Peak drag and lift forces on the traffic signals at 45 degrees wind direction

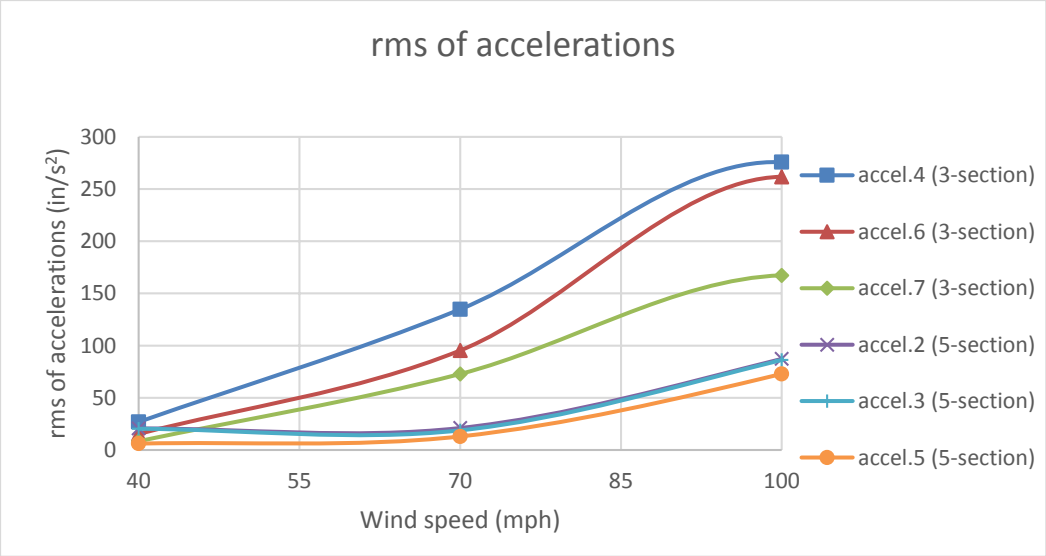

Figure H 3: rms of accelerations at 45 degrees wind direction for various wind speeds

Results for total drag/lift forces, and rms of accelerations for 80 degrees wind direction

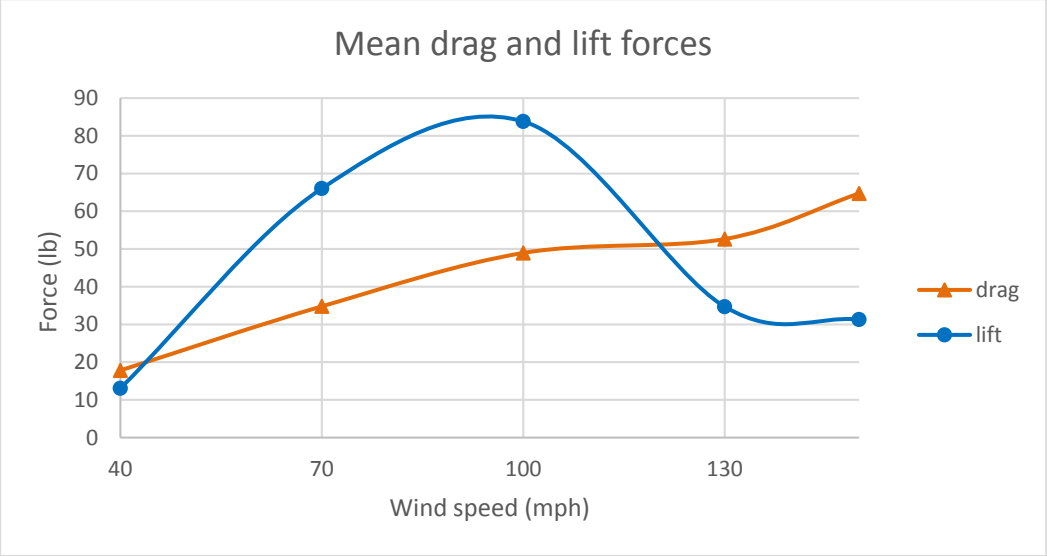

Figure H 4: Mean drag and lift forces on the traffic signals at 80 degrees wind direction

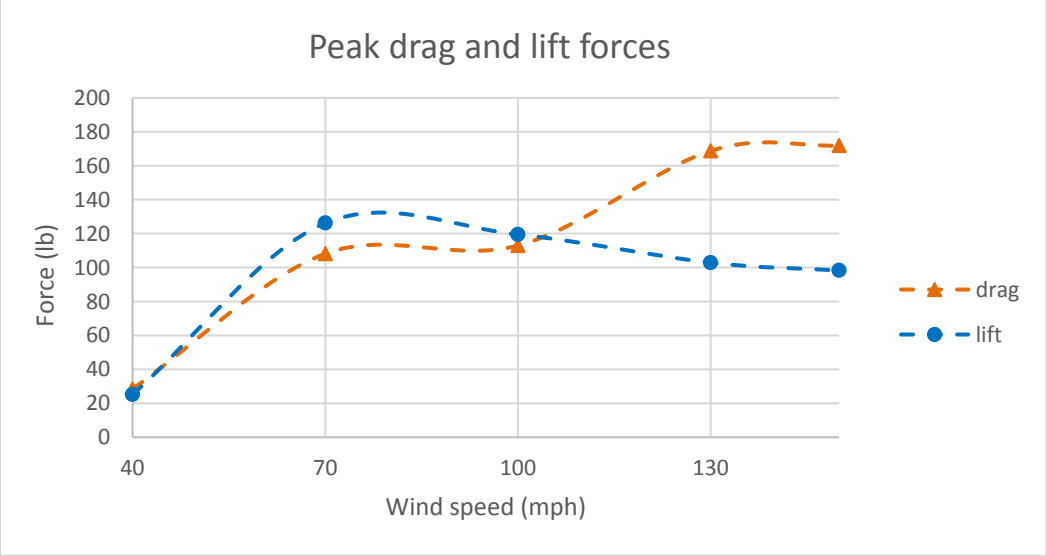

Figure H 5: Peak drag and lift forces on the traffic signals at 80 degrees wind direction

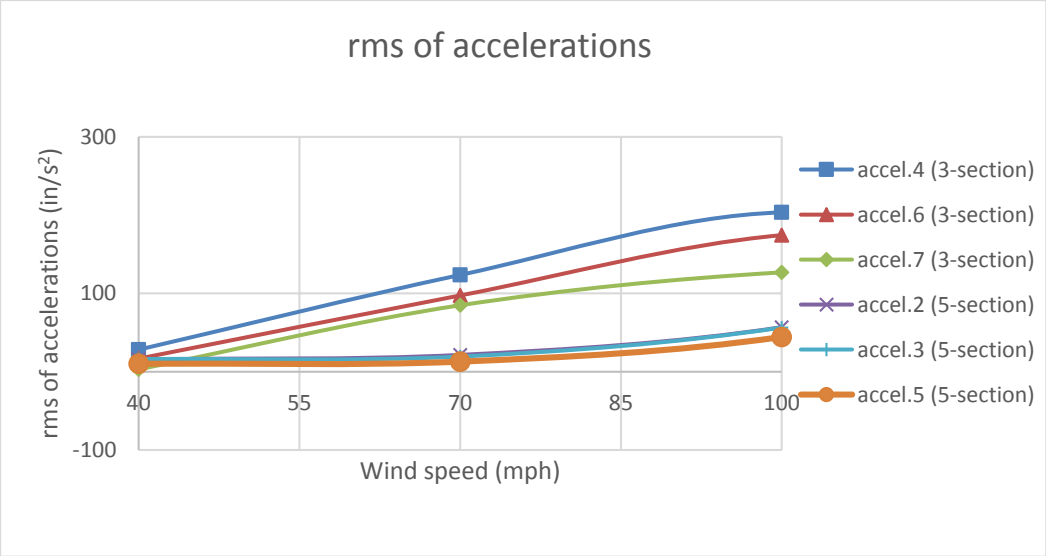

Figure H 6: rms of accelerations at 80 degrees wind direction for various wind speeds

Results for total drag/lift forces, and rms of accelerations for 100 degrees wind direction

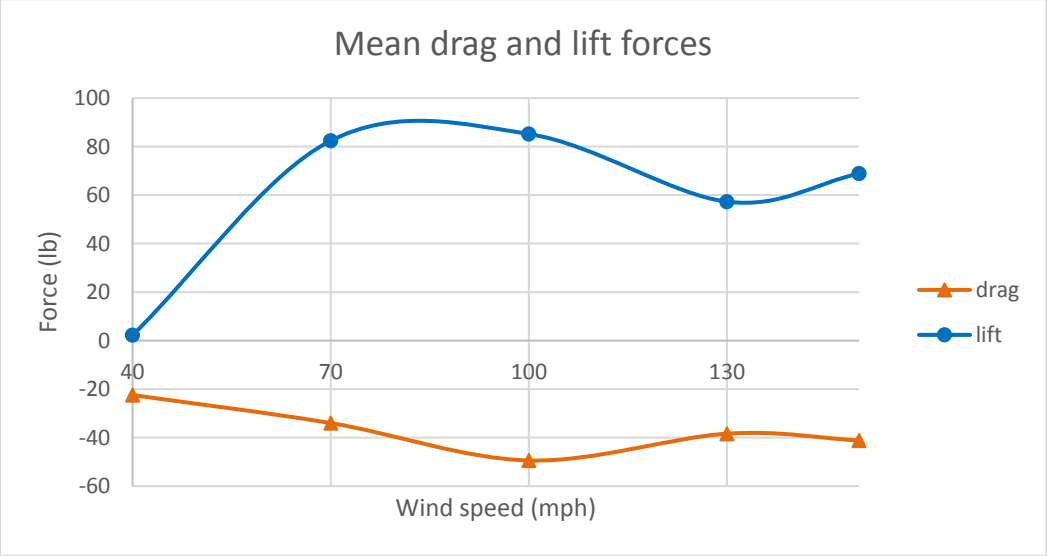

Figure H 7: Mean drag and lift forces on the traffic signals at 100 degrees wind direction

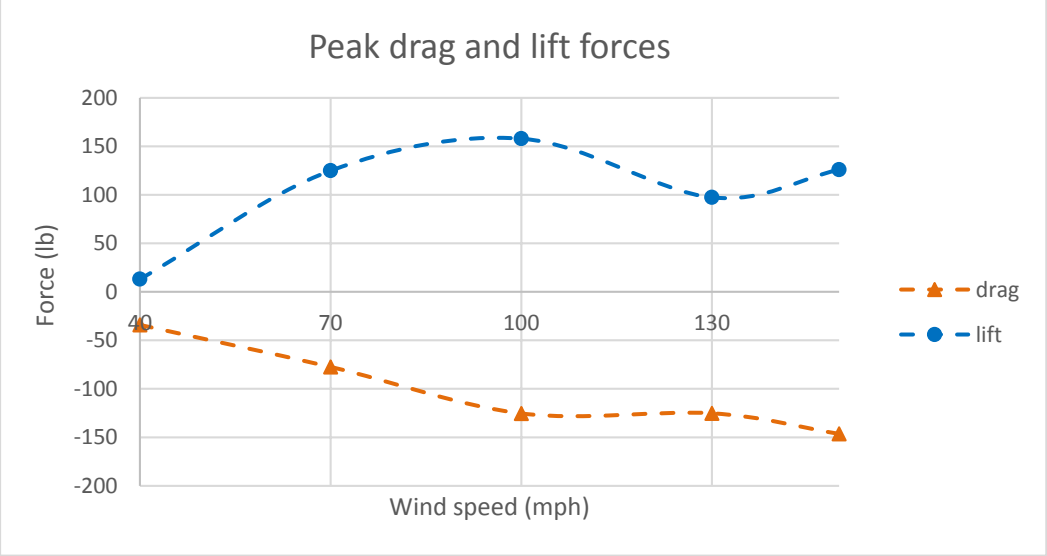

Figure H 8: Peak drag and lift forces on the traffic signals at 100 degrees wind direction

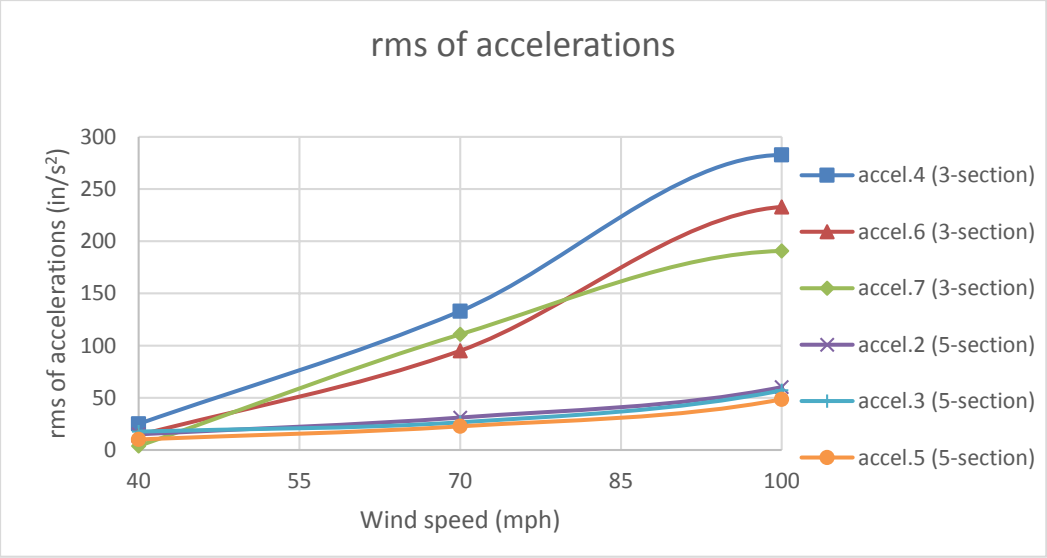

Figure H 9: rms of accelerations at 100 degrees wind direction for various wind speeds

Results for total drag/lift forces, and rms of accelerations for 135 degrees wind direction

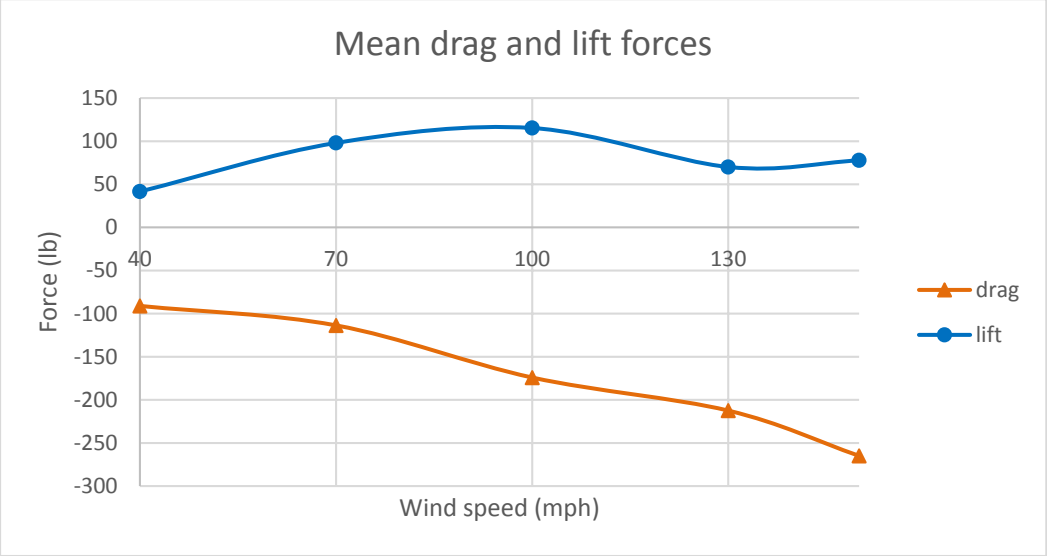

Figure H 10: Mean drag and lift forces on the traffic signals at 135 degrees wind direction

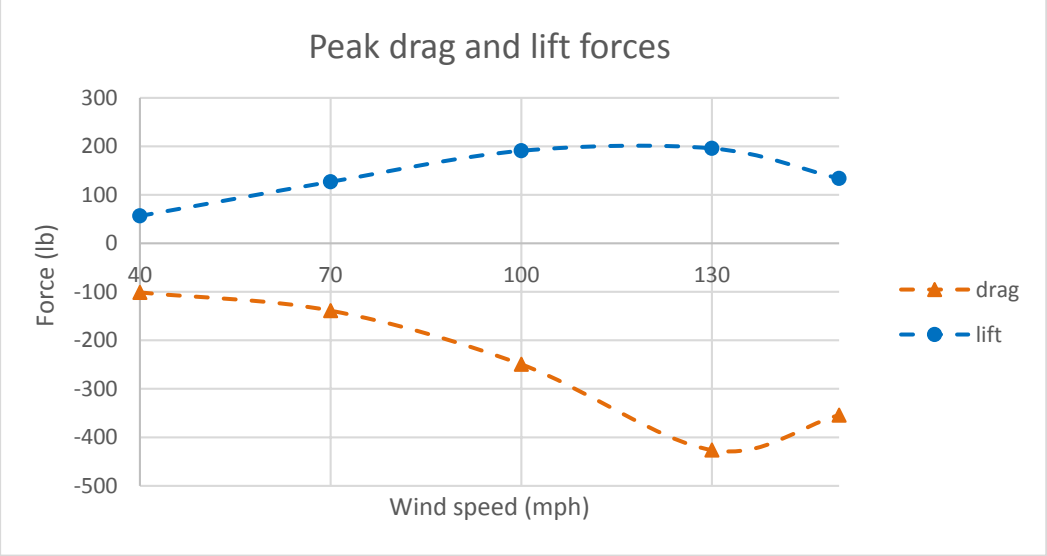

Figure H 11: Peak drag and lift forces on the traffic signals at 135 degrees wind direction

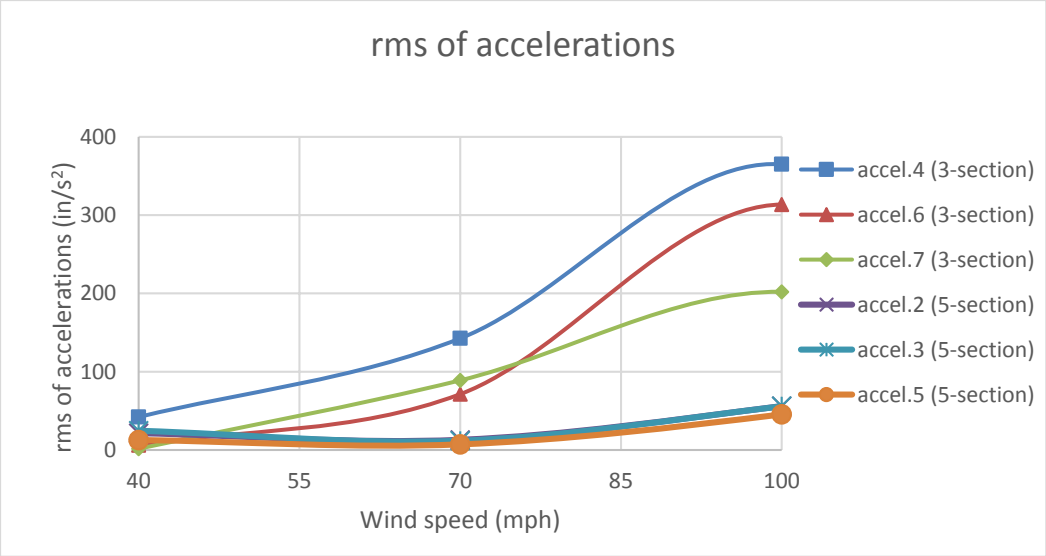

Figure H 12: rms of accelerations at 135 degrees wind direction for various wind speeds

Results for total drag/lift forces, and rms of accelerations for 180 degrees wind direction

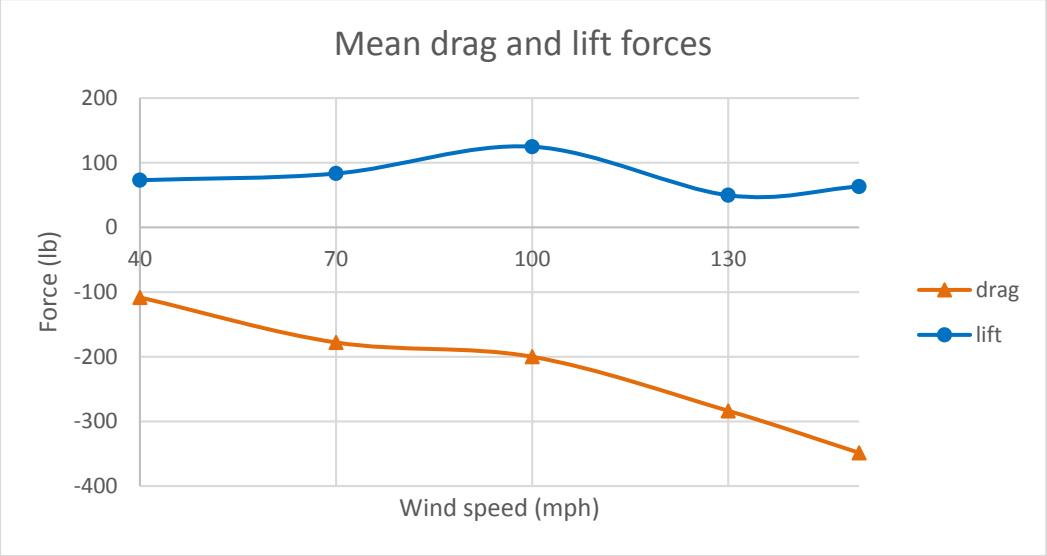

Figure H 13: Mean drag and lift forces on the traffic signals at 180 degrees wind direction

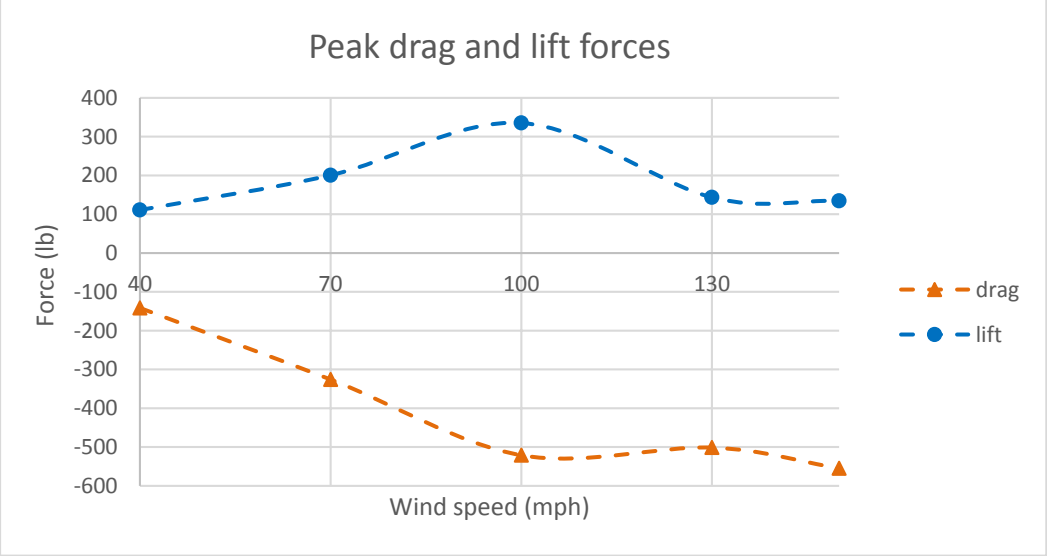

Figure H 14: Peak drag and lift forces on the traffic signals at 180 degrees wind direction

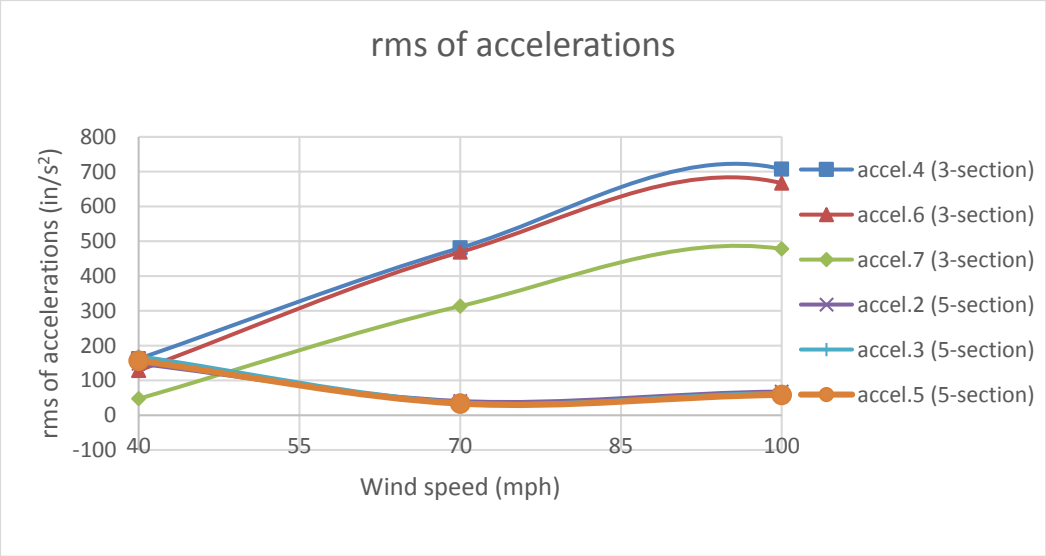

Figure H 15: rms of accelerations at 180 degrees wind direction for various wind speeds

APPENDIX I – (Comparison of solid (non-louvered) backplates and louvered backplates cases – CASE 10)

There were two configurations tested with only a 3-section signal. One configuration was assembled with louvered backplates while the other configuration was assembled with solid backplates. The main purpose of these two tests was to assess the overall response of the system with the different backplates and compare them. Results of the non-louvered (solid) backplate case are presented in this report and the results of the Louvered backplate case are presented in the report BDV29 TWO 977-27 (Task 2-Case 5) [6].

When comparing the results between the solid (non-louvered) and louvered backplates cases, it was found that the solid (non-louvered) backplates case experienced higher mean forces than the louvered backplates, where at 100 mph and at 0 degrees wind direction, the solid (non-louvered) case experienced a maximum mean Fz force of 347 lbs while the louvered backplates case had a maximum mean Fz force of 284.7 lbs, as shown in Figure 171 and Figure 173 . The overall response of both cases is similar, however, the louvered backplates case experienced less forces than the solid (non-louvered) backplates case while the opposite is seen for inclinations, where the solid (non-louvered) case experienced less mean inclinations than the louvered backplates case, as shown in Figure 178 and Figure 179, attaining values of 53 degrees and 63 degrees at 100 mph respectively. When looking at the peak inclinations (along wind), the solid (non-louvered) backplates case experienced a maximum inclination of 70 degrees while the louvered backplates case attained a maximum inclination of 86 degrees, at 100 mph and 0-degree wind direction. It needs to be noted that in the non-louvered backplate case, the clamp attached to the adjustable hanger to hold the messenger wire slipped and the adjustable hanger broke.

Results for Mean and peak forces, and rms of accelerations for 45 degrees wind direction

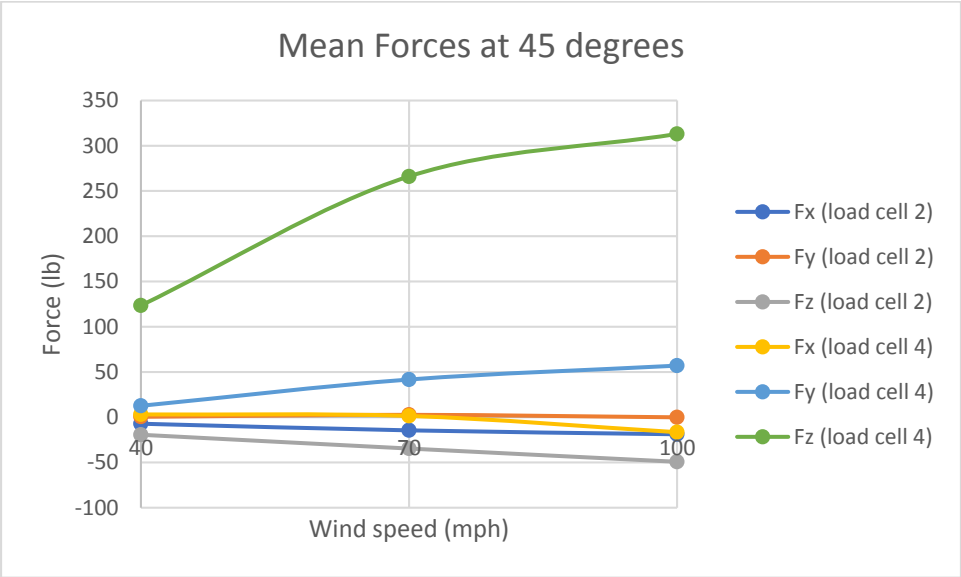

Figure I 1: Mean forces at 45 degrees wind direction on loadcells 2 (catenary wire) and 4 (messenger wire)

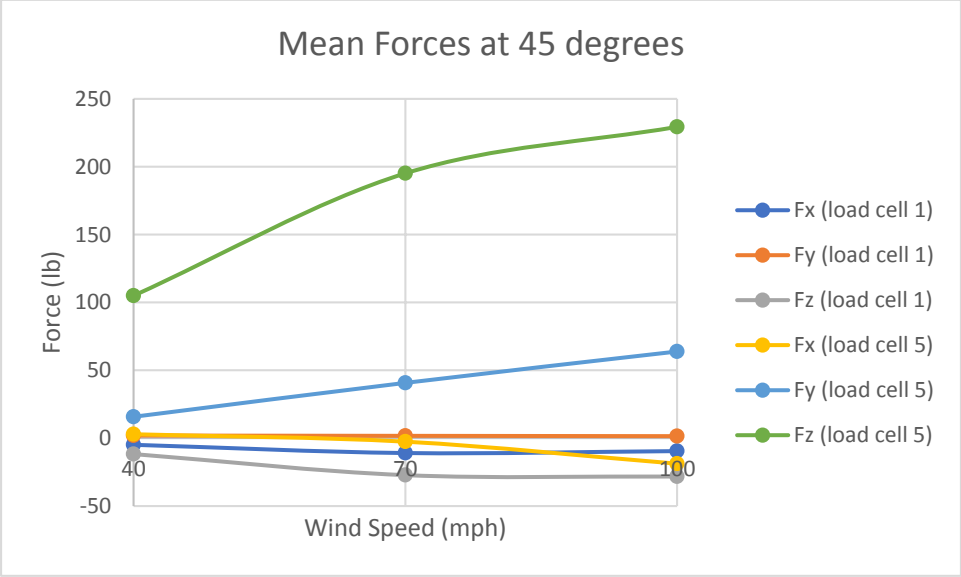

Figure I 2: Mean forces at 45 degrees wind direction on loadcells 1 (catenary wire) and 5 (messenger wire)

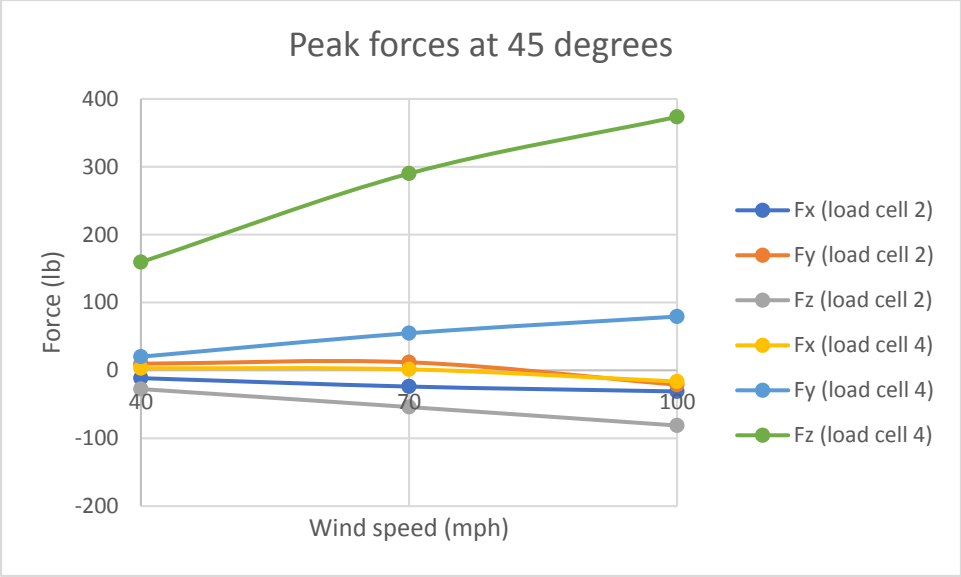

Figure I 3: Peak forces at 45 degrees wind direction on loadcells 2 (catenary wire) and 4 (messenger wire)

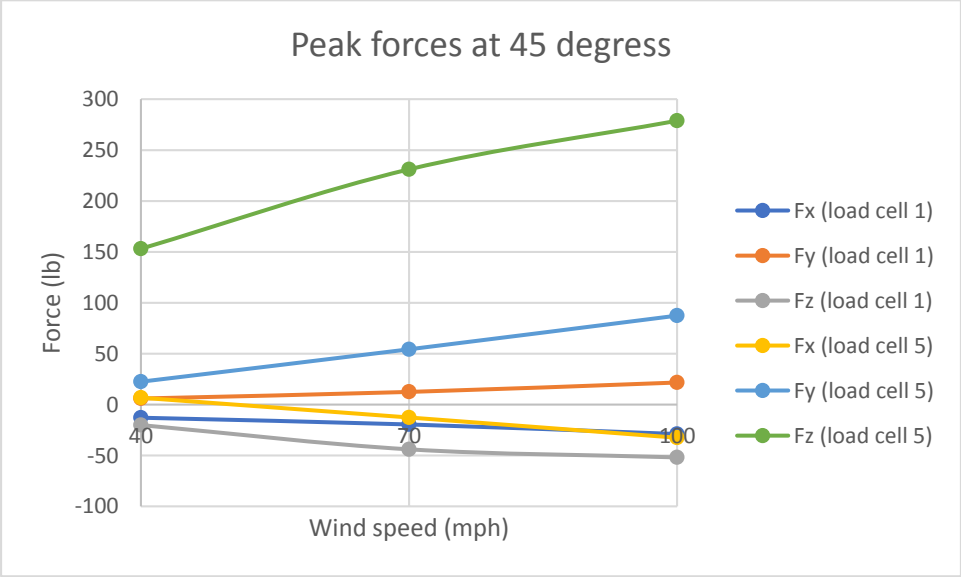

Figure I 4: Peak forces at 45 degrees wind direction on loadcells 1 (catenary wire) and 5 (messenger wire)

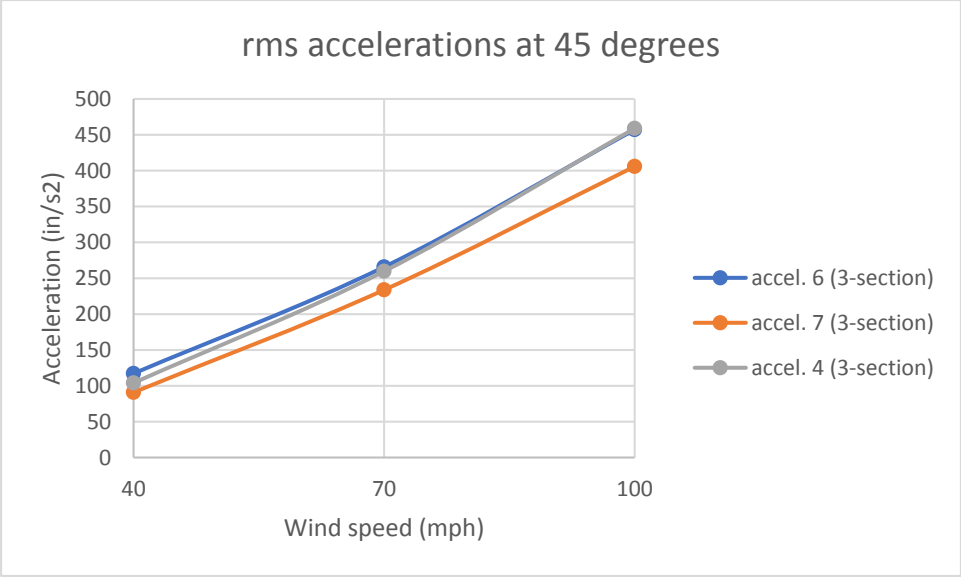

Figure I 5: rms of accelerations at 45 degrees wind direction for various wind speeds

Results for Mean and peak forces, and rms of accelerations for 80 degrees wind direction

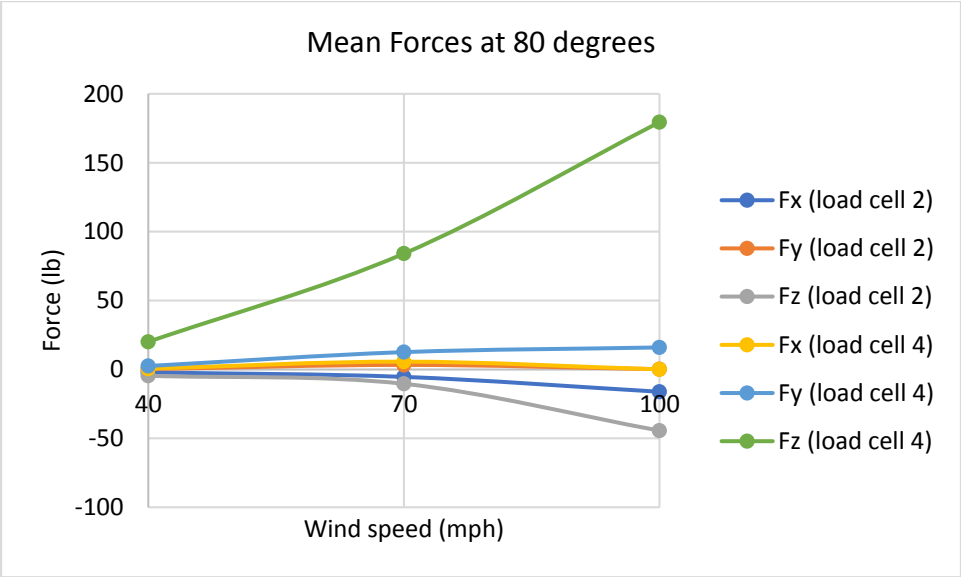

Figure I 6: Mean forces at 80 degrees wind direction on loadcells 2 (catenary wire) and 4 (messenger wire)

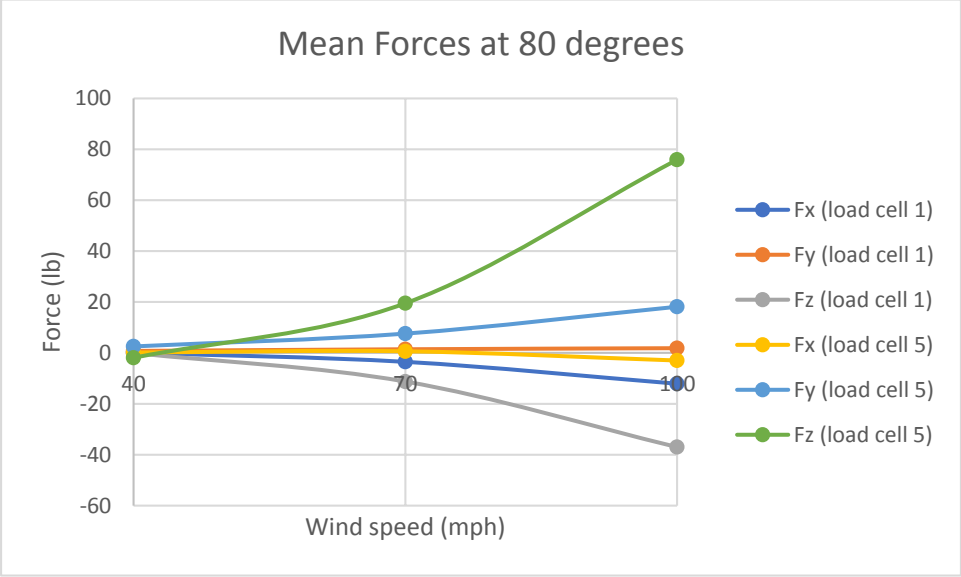

Figure I 7: Mean forces at 80 degrees wind direction on loadcells 1 (catenary wire) and 5 (messenger wire)

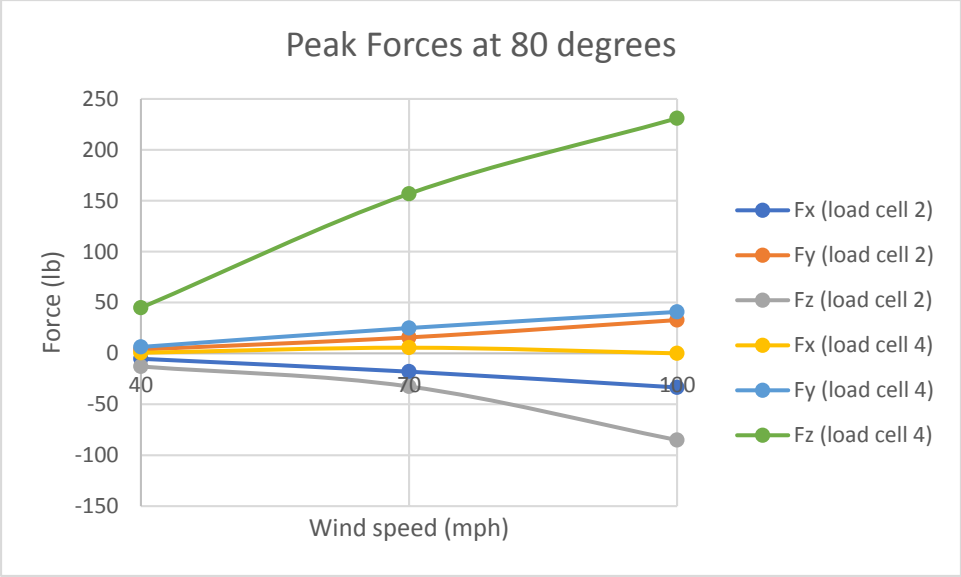

Figure I 8: Peak forces at 80 degrees wind direction on loadcells 2 (catenary wire) and 4 (messenger wire)

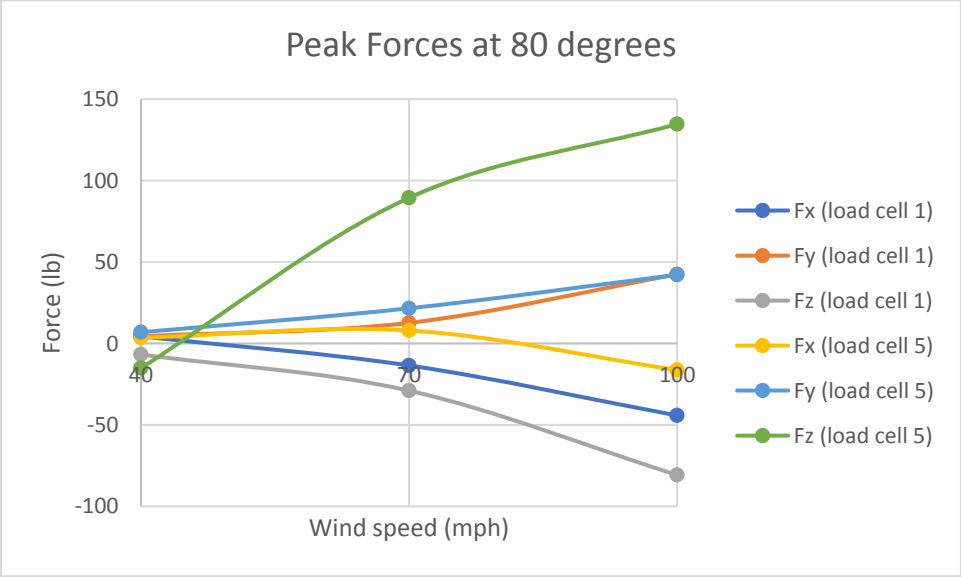

Figure I 9: Peak forces at 80 degrees wind direction on loadcells 1 (catenary wire) and 5 (messenger wire)

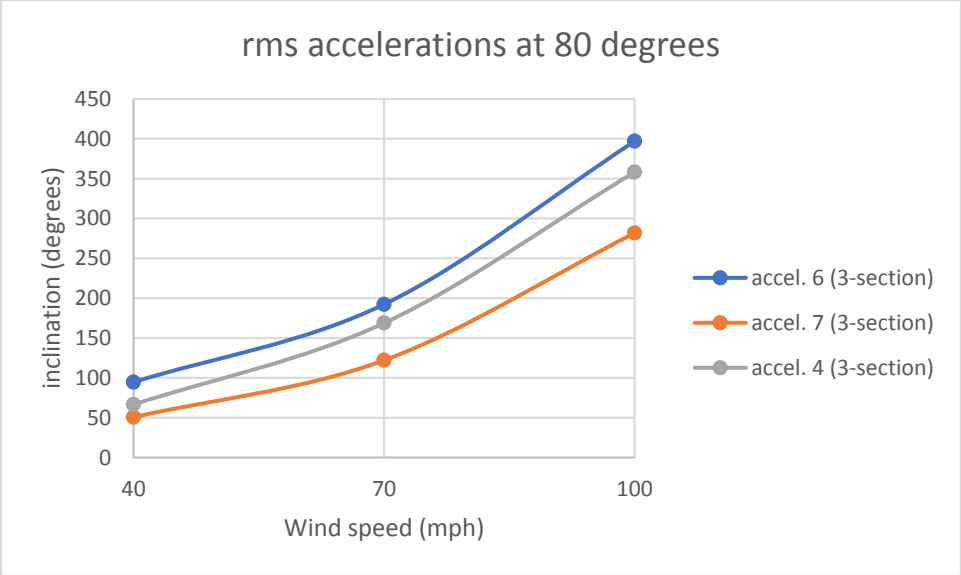

Figure I 10: rms of accelerations at 80 degrees wind direction for various wind speeds

Results for Mean and peak forces, and rms of accelerations for 100 degrees wind direction

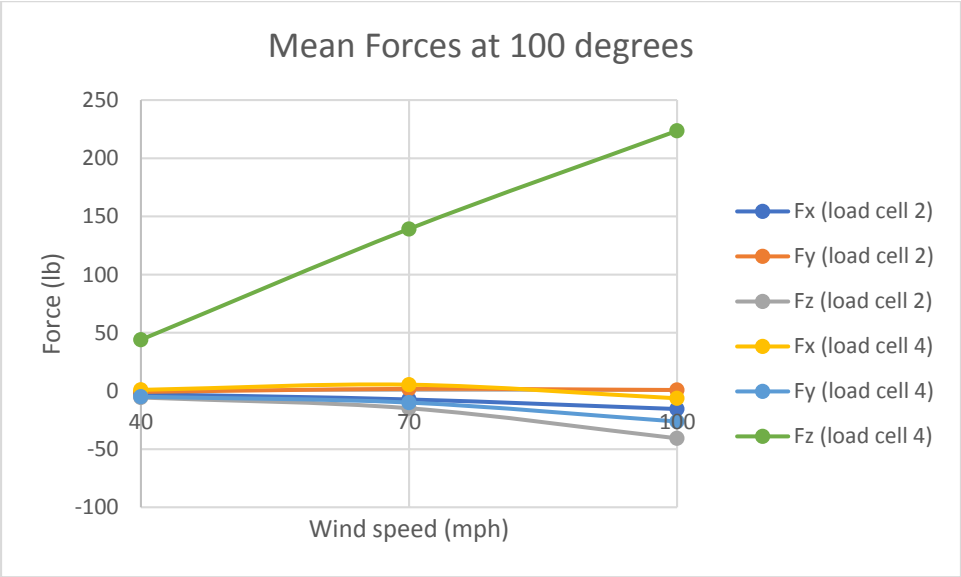

Figure I 11: Mean forces at 100 degrees wind direction on loadcells 2 (catenary wire) and 4 (messenger wire)

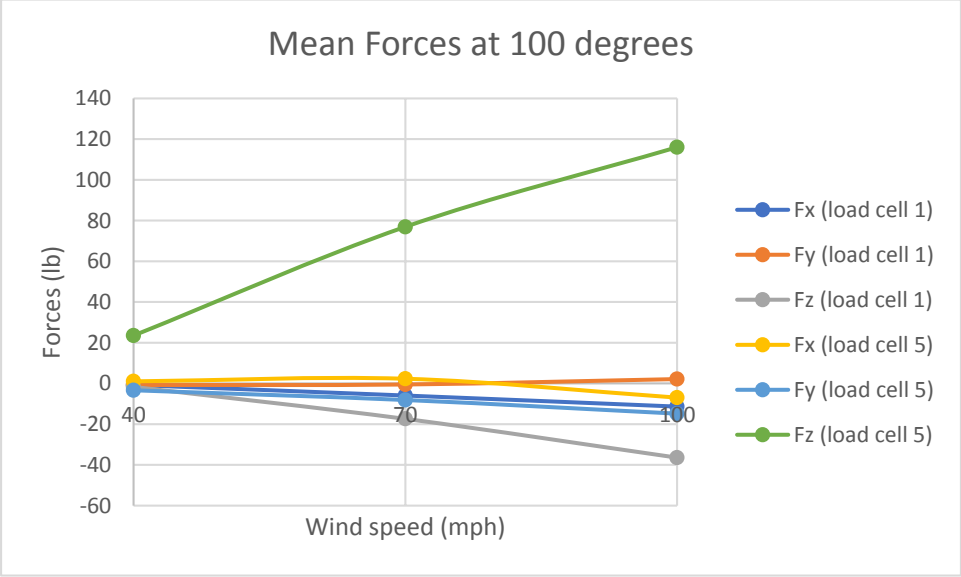

Figure I 12: Mean forces at 100 degrees wind direction on loadcells 1 (catenary wire) and 5 (messenger wire)

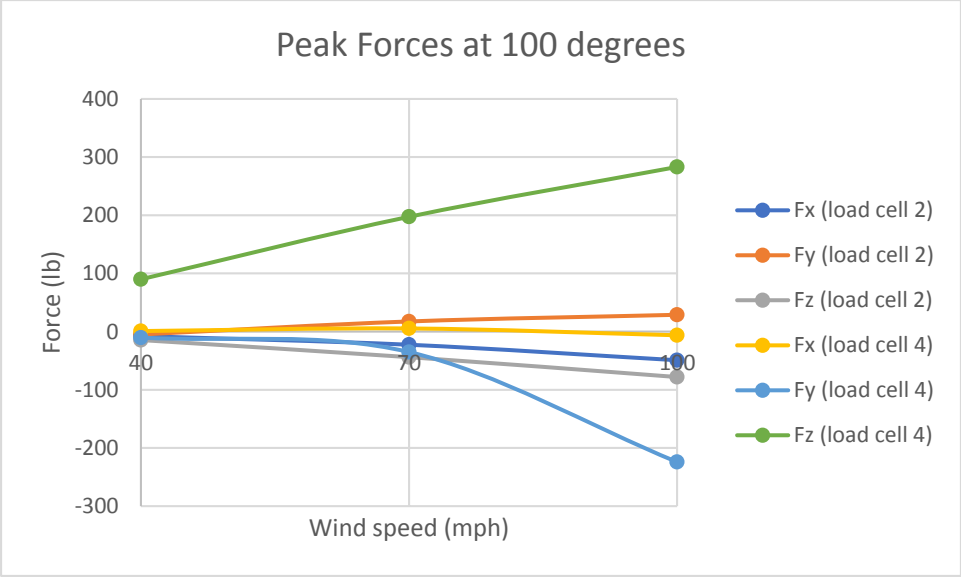

Figure I 13: Peak forces at 100 degrees wind direction on loadcells 2 (catenary wire) and 4 (messenger wire)

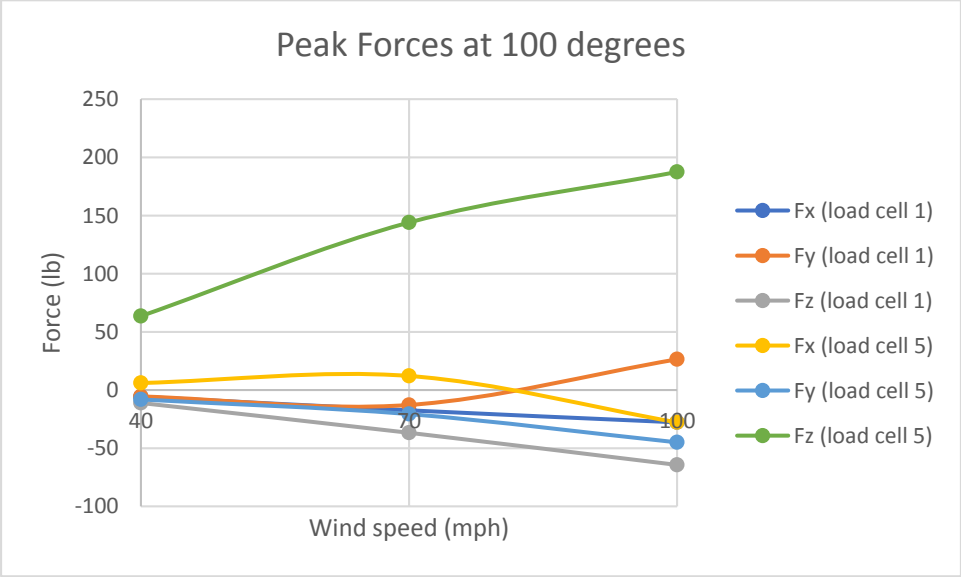

Figure I 14: Peak forces at 100 degrees wind direction on loadcells 1 (catenary wire) and 5 (messenger wire)

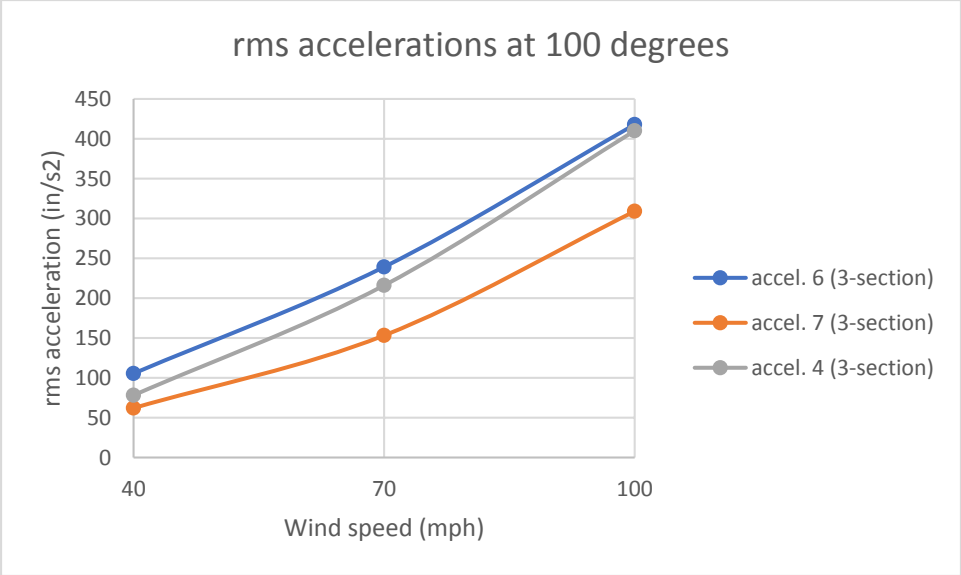

Figure I 15: rms of accelerations at 100 degrees wind direction for various wind speeds

Results for Mean and peak forces, and rms of accelerations for 135 degrees wind direction

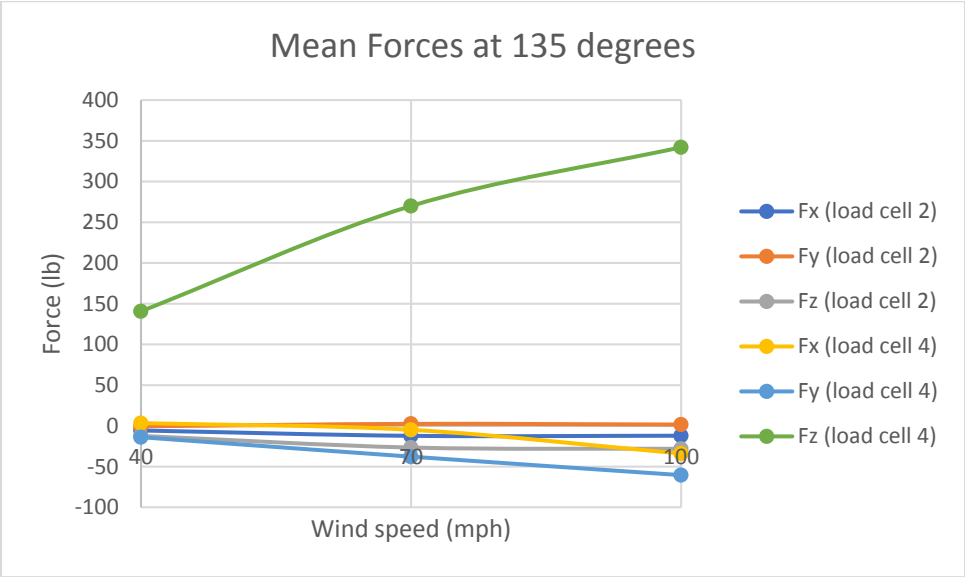

Figure I 16: Mean forces at 135 degrees wind direction on loadcells 2 (catenary wire) and 4 (messenger wire)

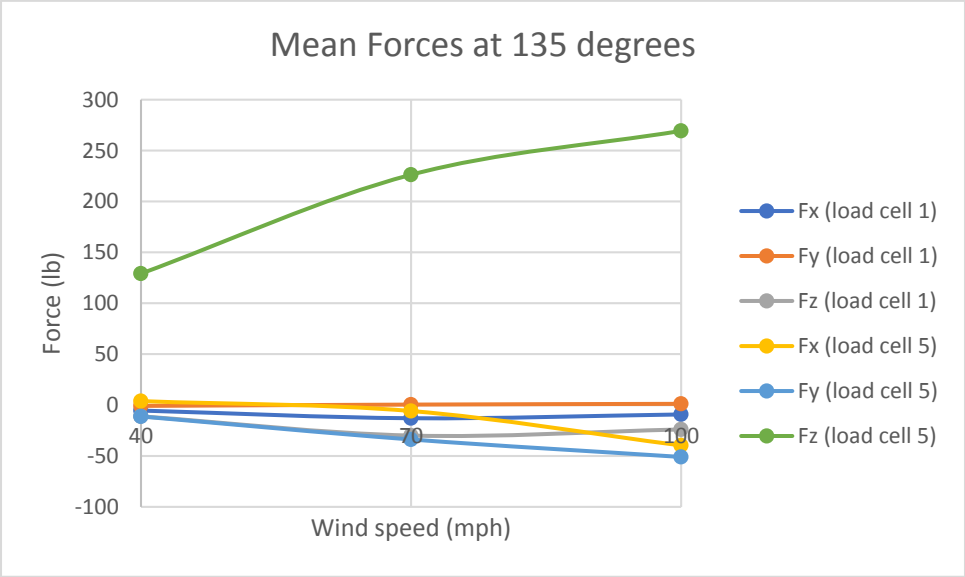

Figure I 17: Mean forces at 135 degrees wind direction on loadcells 1 (catenary wire) and 5 (messenger wire)

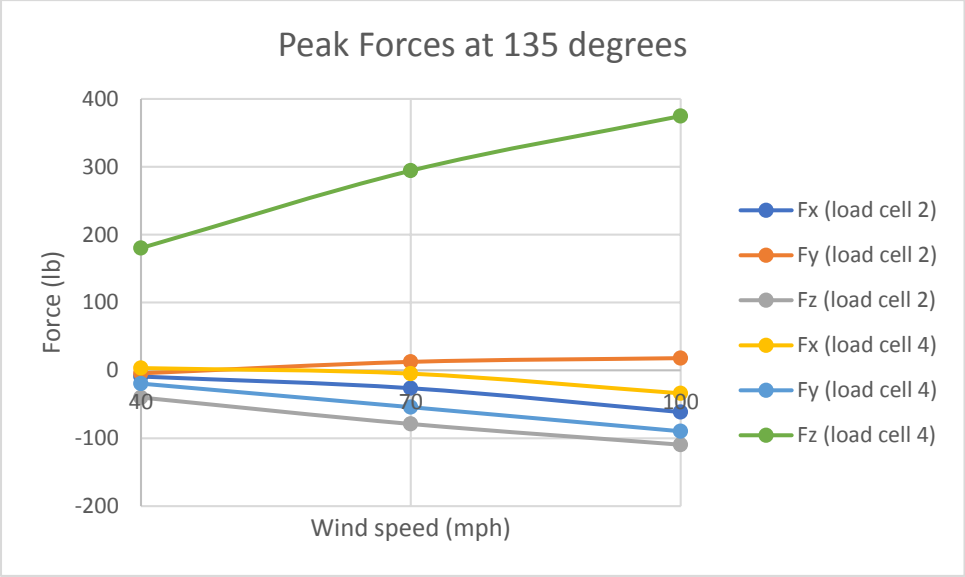

Figure I 18: Peak forces at 135 degrees wind direction on loadcells 2 (catenary wire) and 4 (messenger wire)

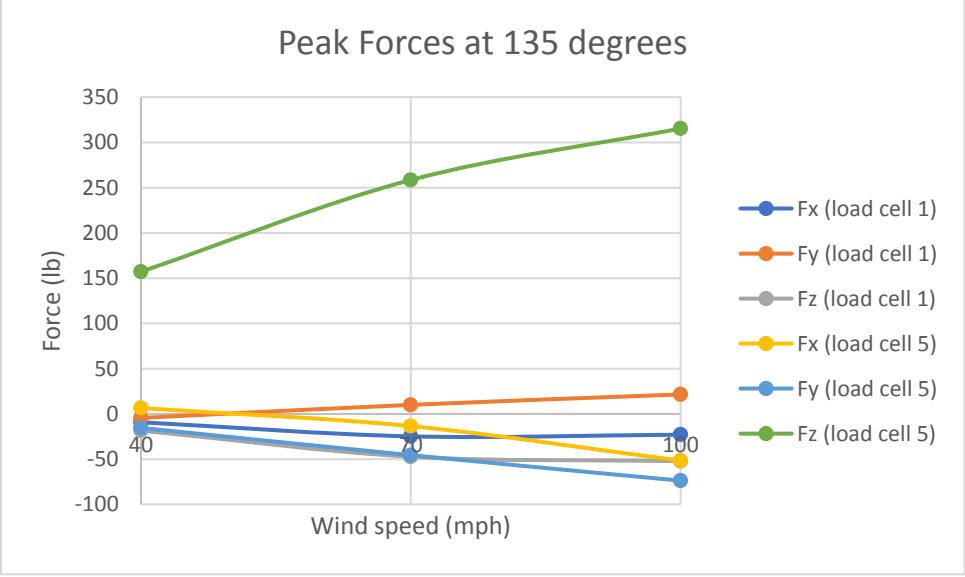

Figure I 19: Peak forces at 135 degrees wind direction on loadcells 1 (catenary wire) and 5 (messenger wire)

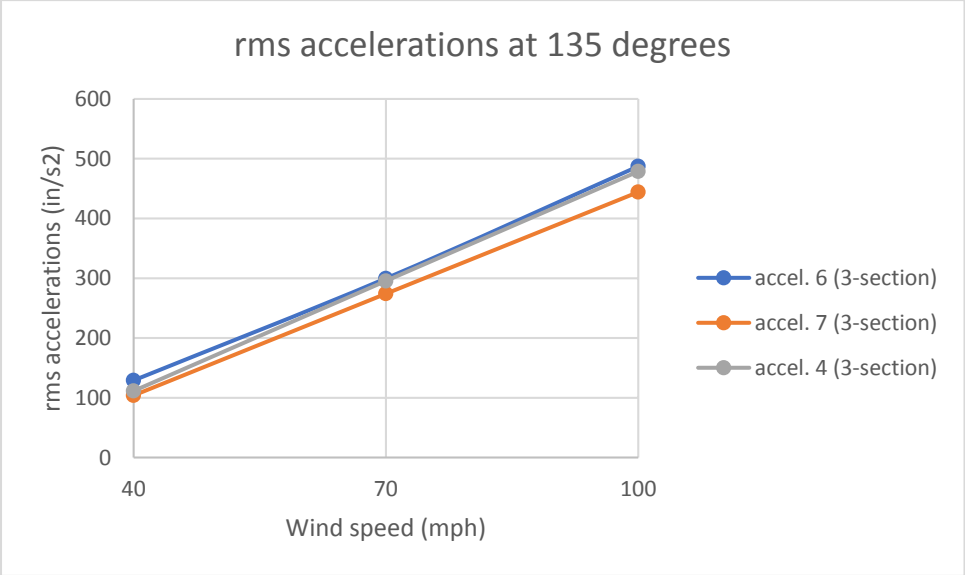

Figure I 20: rms of accelerations at 135 degrees wind direction for various wind speeds

Results for Mean and peak forces, and rms of accelerations for 180 degrees wind direction

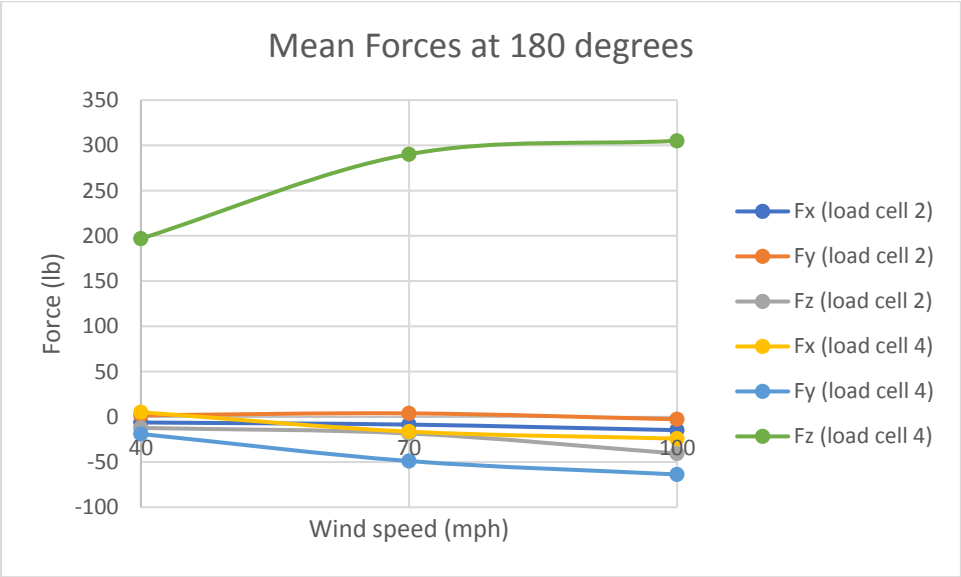

Figure I 21: Mean forces at 180 degrees wind direction on loadcells 2 (catenary wire) and 4 (messenger wire)

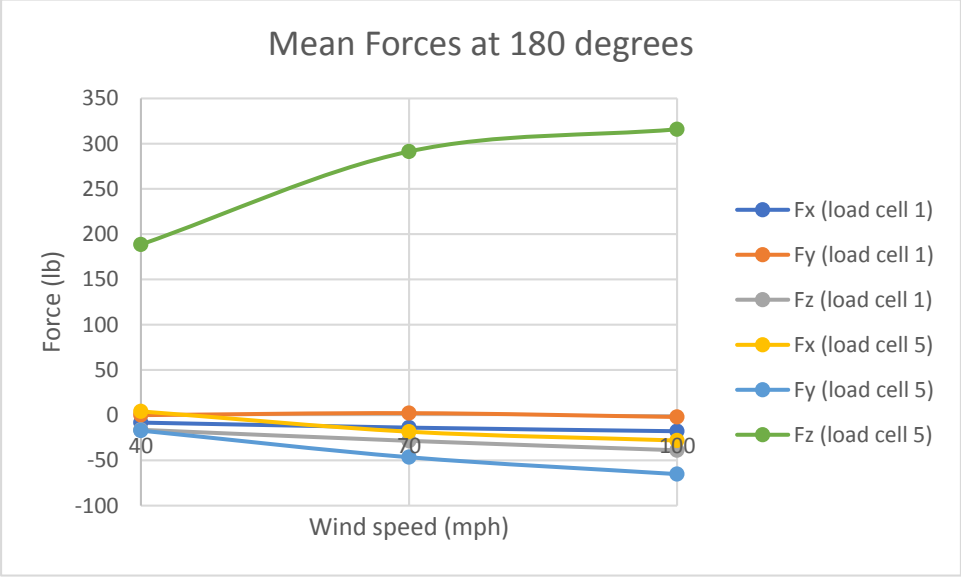

Figure I 22: Mean forces at 180 degrees wind direction on loadcells 1 (catenary wire) and 5 (messenger wire)

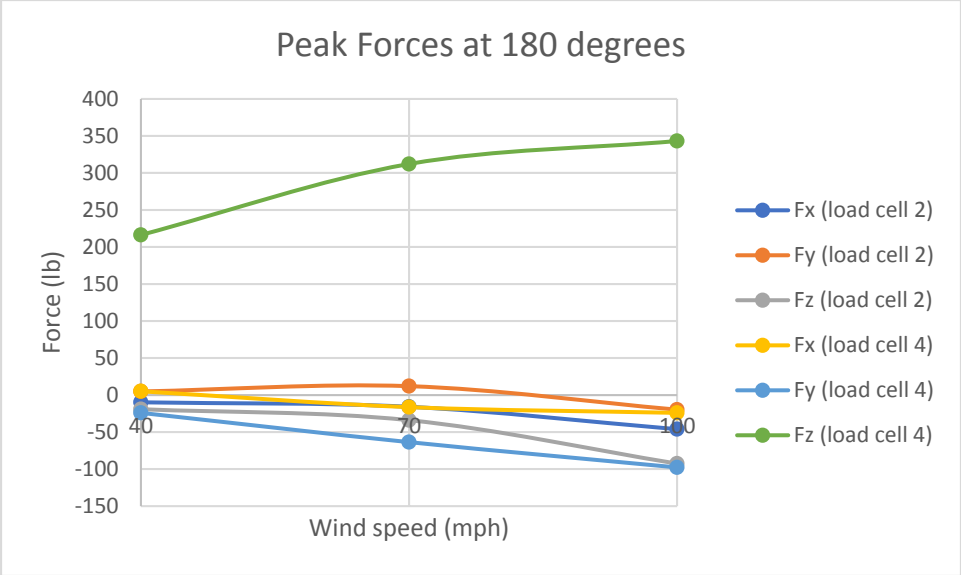

Figure I 23: Peak forces at 180 degrees wind direction on loadcells 2 (catenary wire) and 4 (messenger wire)

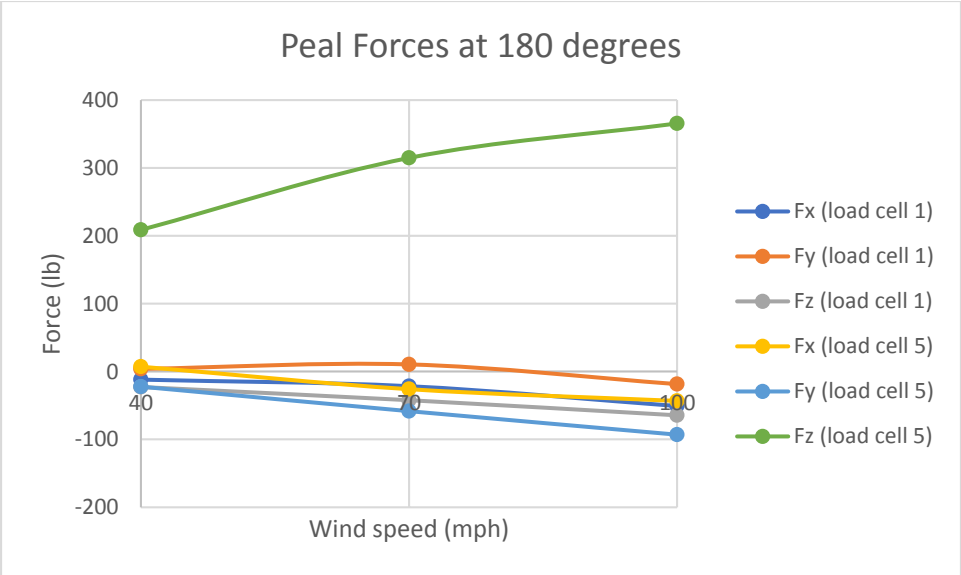

Figure I 24: Peak forces at 180 degrees wind direction on loadcells 1 (catenary wire) and 5 (messenger wire)

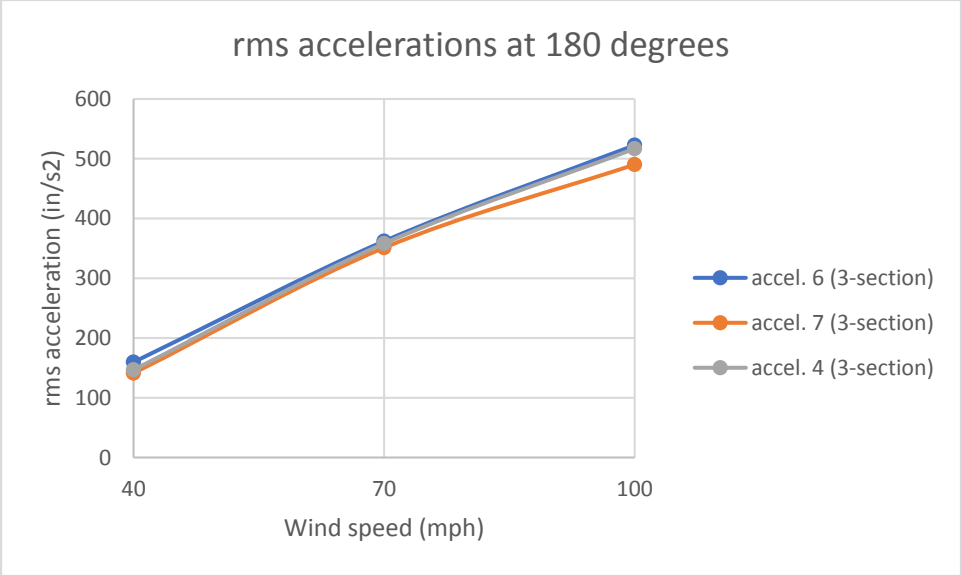

Figure I 25: rms of accelerations at 180 degrees wind direction for various wind speeds

APPENDIX J – (Task 1a: FULL SCALE TESTING - CASE 11)

Results for total drag/lift forces, and rms of accelerations for 45 degrees wind direction

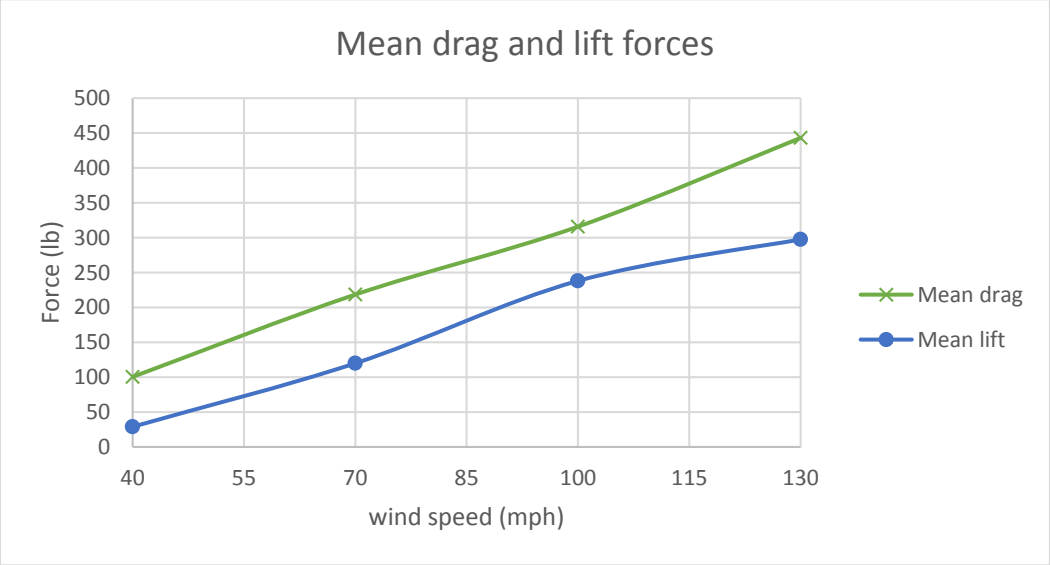

Figure J 1: Mean drag and mean lift forces on the traffic signals at 45 degrees wind direction

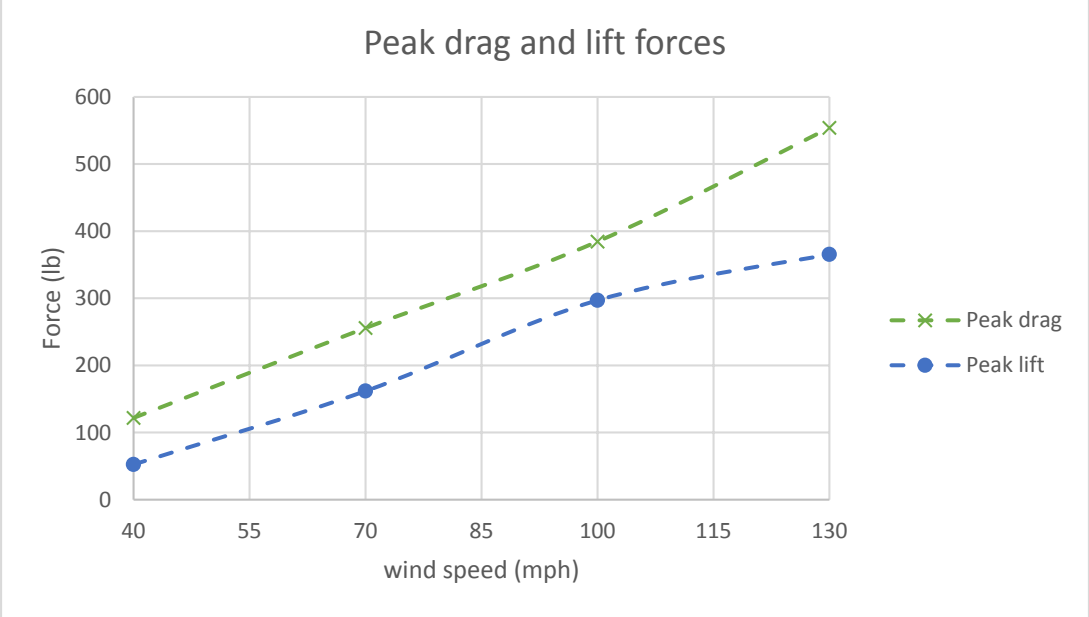

Figure J 2: Peak drag and peak lift forces on the traffic signals at 45 degrees wind direction

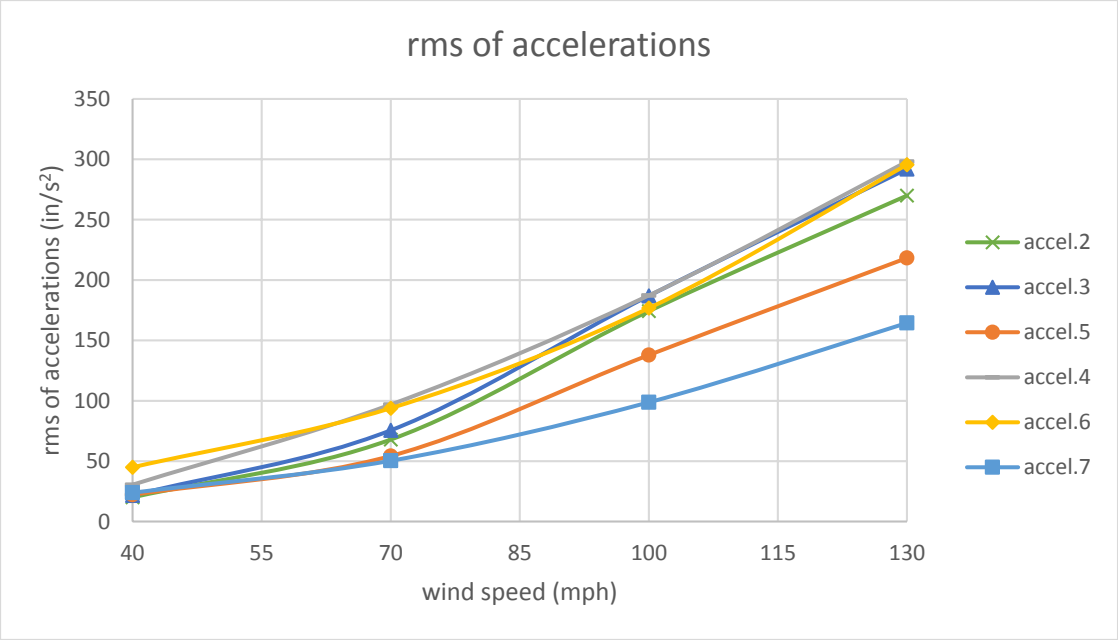

Figure J 3: rms of accelerations at 45 degrees wind direction for various wind speeds

Results for total drag/lift forces, and rms of accelerations for 80 degrees wind direction

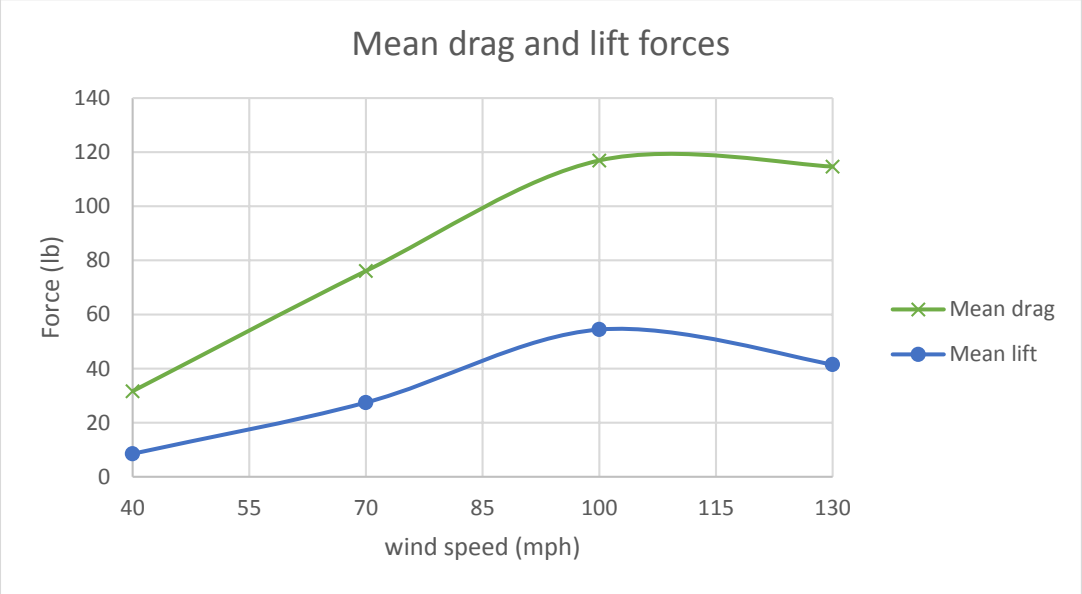

Figure J 4: Mean drag and mean lift forces on the traffic signals at 80 degrees wind direction

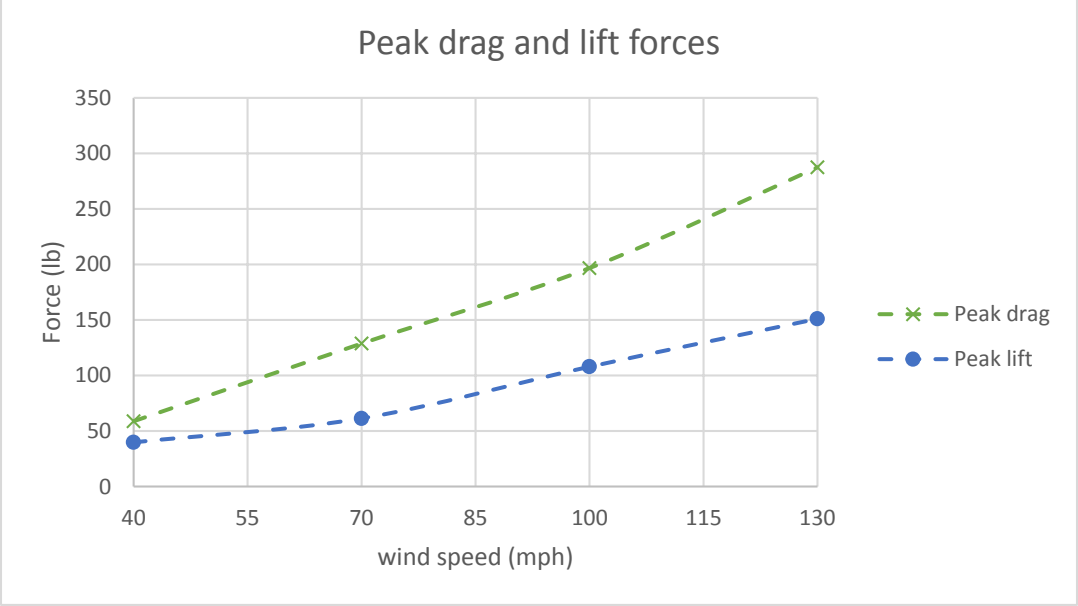

Figure J 5: Peak drag and peak lift forces on the traffic signals at 80 degrees wind direction

J 1-

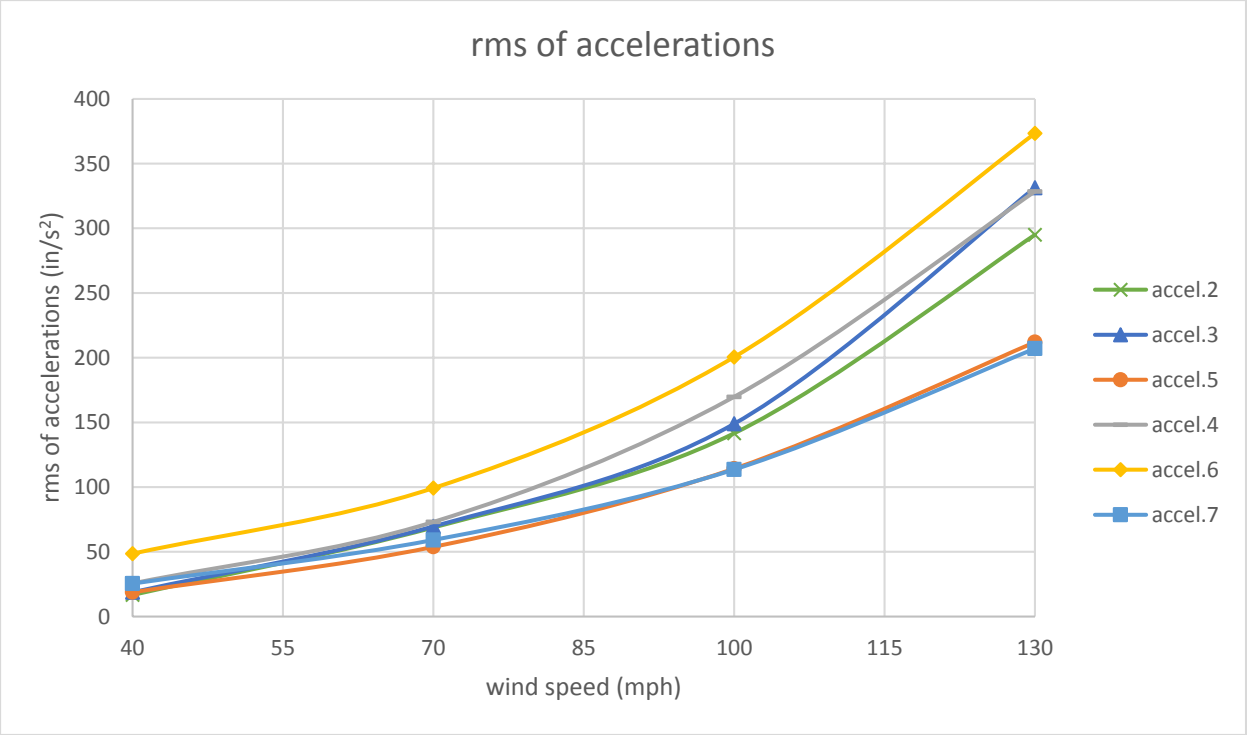

Figure J 6: rms of accelerations at 80 degrees wind direction for various wind speeds

Results for total drag/lift forces, and rms of accelerations for 100 degrees wind direction

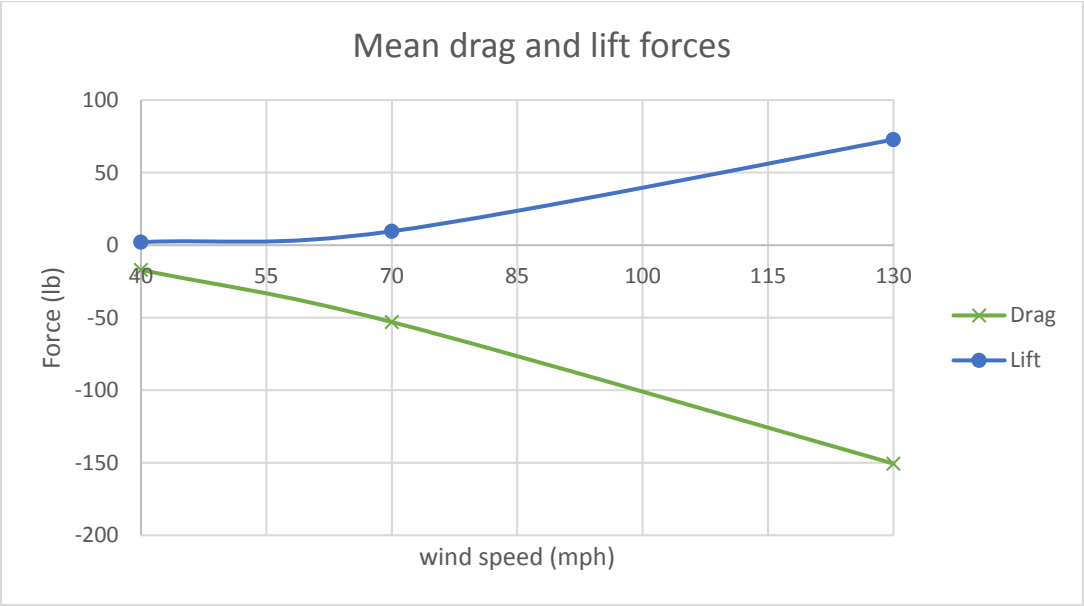

Figure J 7: Mean drag and mean lift forces on the traffic signals at 100 degrees wind direction

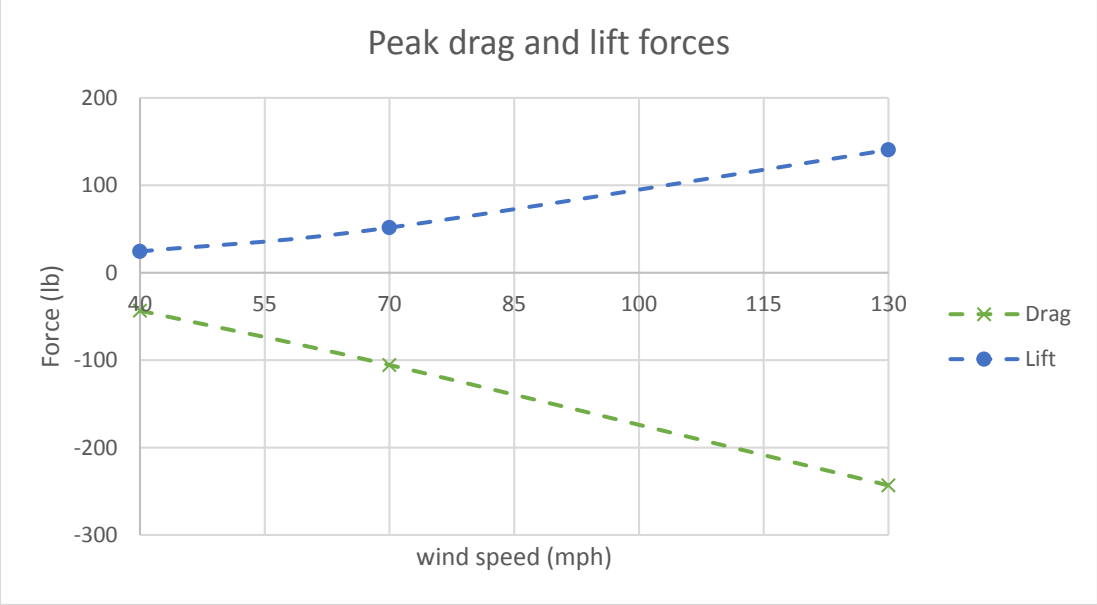

Figure J 8: Peak drag and peak lift forces on the traffic signals at 100 degrees wind direction

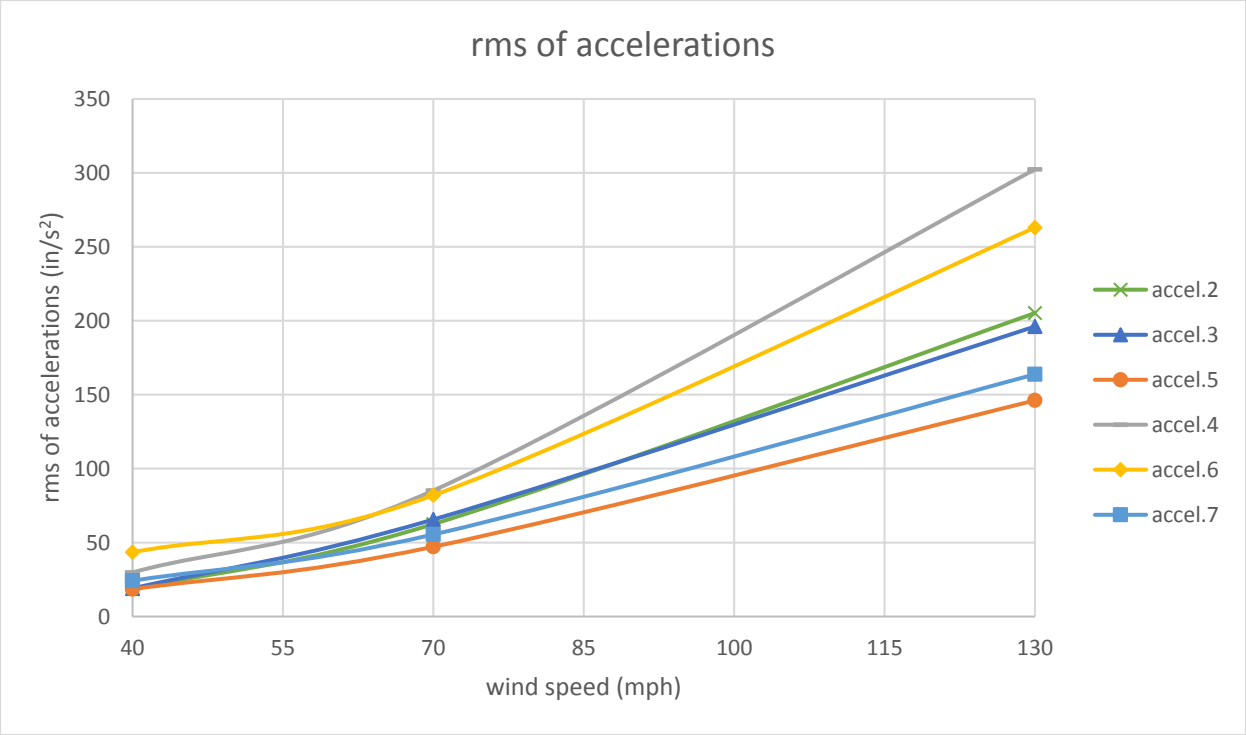

Figure J 9: rms of accelerations at 100 degrees wind direction for various wind speeds

Results for total drag/lift forces, and rms of accelerations for 135 degrees wind direction

Figure J 10: Mean drag and mean lift forces on the traffic signals at 135 degrees wind direction

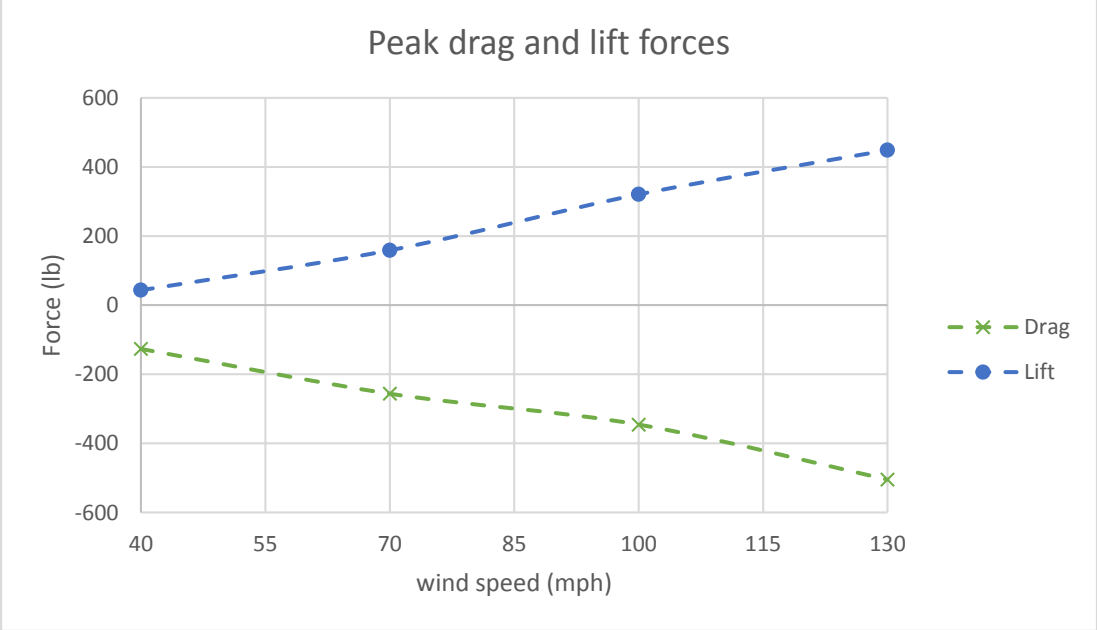

Figure J 11: Peak drag and peak lift forces on the traffic signals at 135 degrees wind direction

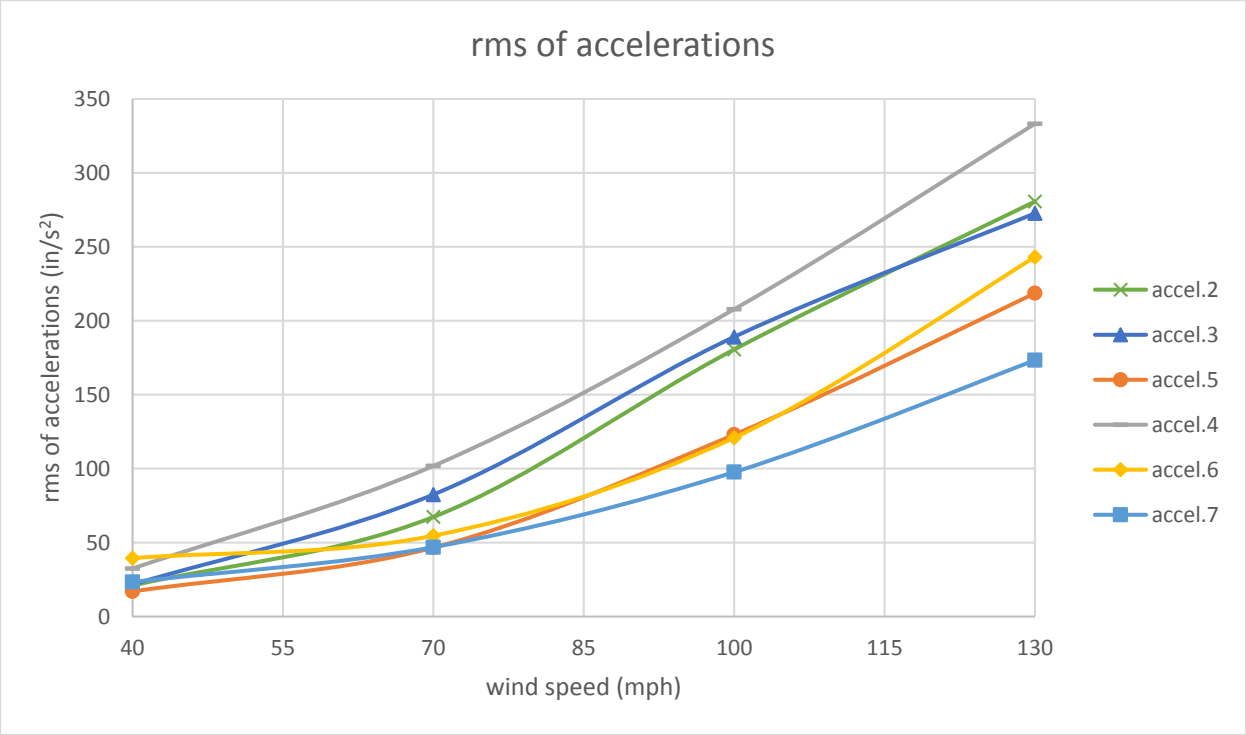

Figure J 12: rms of accelerations at 135 degrees wind direction for various wind speeds

Results for total drag/lift forces, and rms of accelerations for 180 degrees wind direction

Figure J 13: Mean drag and mean lift forces on the traffic signals at 180 degrees wind direction

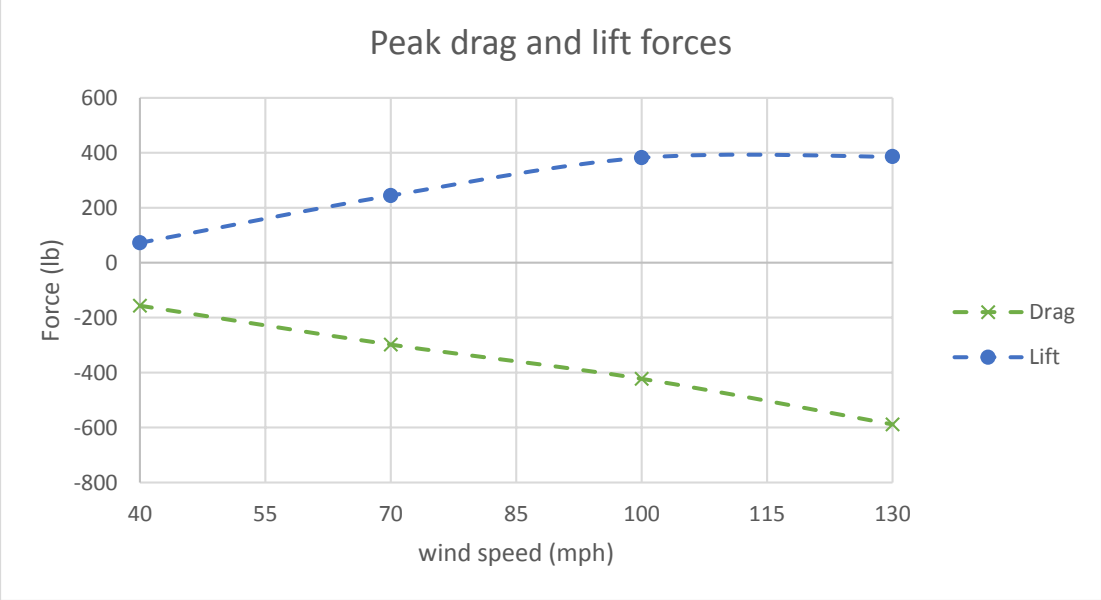

Figure J 14: Peak drag and peak lift forces on the traffic signals at 180 degrees wind direction

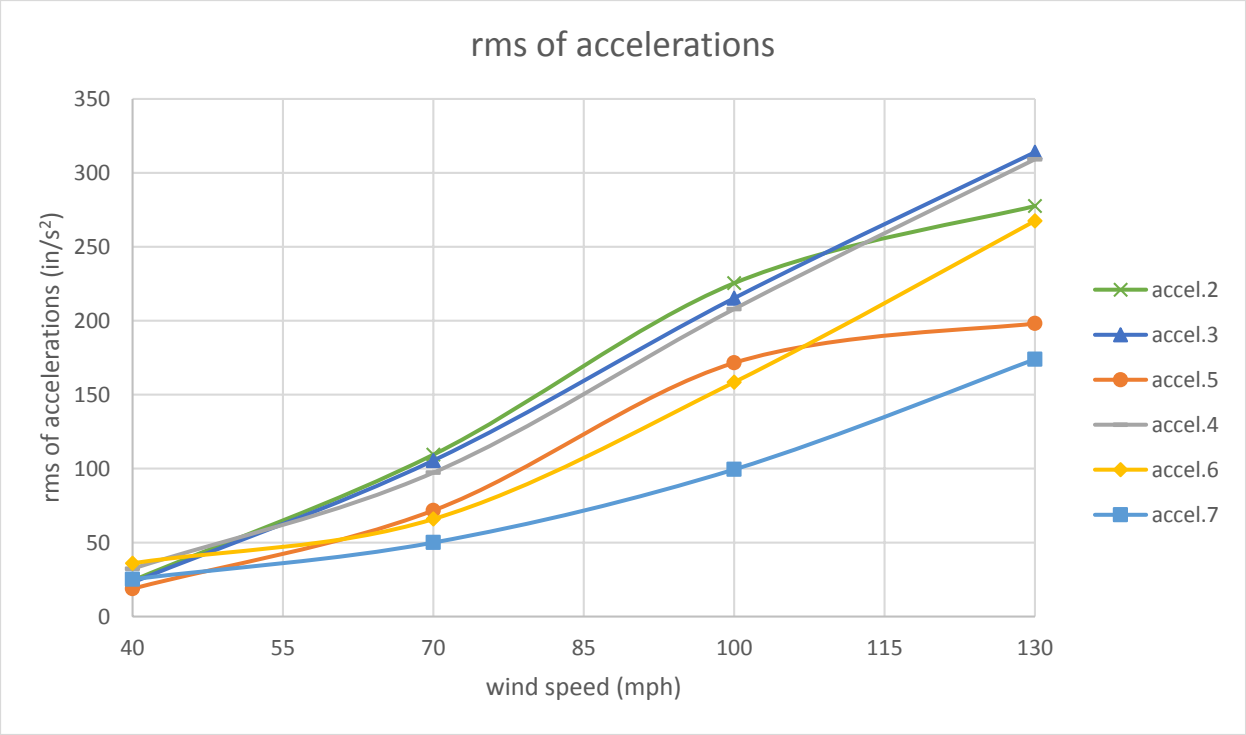

Figure J 15: rms of accelerations at 180 degrees wind direction for various wind speeds